
Gareth James • Daniela Witten • Trevor Hastie
Robert Tibshirani • Jonathan Taylor

An Introduction to Statistical Learning

with Applications in Python

First Printing: July 5, 2023

Contents

Preface	vii
1 Introduction	1
2 Statistical Learning	15
2.1 What Is Statistical Learning?	15
2.1.1 Why Estimate f ?	17
2.1.2 How Do We Estimate f ?	20
2.1.3 The Trade-Off Between Prediction Accuracy and Model Interpretability	23
2.1.4 Supervised Versus Unsupervised Learning	25
2.1.5 Regression Versus Classification Problems	27
2.2 Assessing Model Accuracy	27
2.2.1 Measuring the Quality of Fit	28
2.2.2 The Bias-Variance Trade-Off	31
2.2.3 The Classification Setting	34
2.3 Lab: Introduction to Python	40
2.3.1 Getting Started	40
2.3.2 Basic Commands	40
2.3.3 Introduction to Numerical Python	42
2.3.4 Graphics	48
2.3.5 Sequences and Slice Notation	51
2.3.6 Indexing Data	51
2.3.7 Loading Data	55
2.3.8 For Loops	59
2.3.9 Additional Graphical and Numerical Summaries .	61
2.4 Exercises	63
3 Linear Regression	69
3.1 Simple Linear Regression	70
3.1.1 Estimating the Coefficients	71
3.1.2 Assessing the Accuracy of the Coefficient Estimates	72
3.1.3 Assessing the Accuracy of the Model	77
3.2 Multiple Linear Regression	80
3.2.1 Estimating the Regression Coefficients	81

3.2.2	Some Important Questions	83
3.3	Other Considerations in the Regression Model	91
3.3.1	Qualitative Predictors	91
3.3.2	Extensions of the Linear Model	94
3.3.3	Potential Problems	100
3.4	The Marketing Plan	109
3.5	Comparison of Linear Regression with K -Nearest Neighbors	111
3.6	Lab: Linear Regression	116
3.6.1	Importing packages	116
3.6.2	Simple Linear Regression	117
3.6.3	Multiple Linear Regression	122
3.6.4	Multivariate Goodness of Fit	123
3.6.5	Interaction Terms	124
3.6.6	Non-linear Transformations of the Predictors	125
3.6.7	Qualitative Predictors	126
3.7	Exercises	127
4	Classification	135
4.1	An Overview of Classification	135
4.2	Why Not Linear Regression?	136
4.3	Logistic Regression	138
4.3.1	The Logistic Model	139
4.3.2	Estimating the Regression Coefficients	140
4.3.3	Making Predictions	141
4.3.4	Multiple Logistic Regression	142
4.3.5	Multinomial Logistic Regression	144
4.4	Generative Models for Classification	146
4.4.1	Linear Discriminant Analysis for $p = 1$	147
4.4.2	Linear Discriminant Analysis for $p > 1$	150
4.4.3	Quadratic Discriminant Analysis	156
4.4.4	Naive Bayes	158
4.5	A Comparison of Classification Methods	161
4.5.1	An Analytical Comparison	161
4.5.2	An Empirical Comparison	164
4.6	Generalized Linear Models	167
4.6.1	Linear Regression on the Bikeshare Data	167
4.6.2	Poisson Regression on the Bikeshare Data	169
4.6.3	Generalized Linear Models in Greater Generality .	172
4.7	Lab: Logistic Regression, LDA, QDA, and KNN	173
4.7.1	The Stock Market Data	173
4.7.2	Logistic Regression	174
4.7.3	Linear Discriminant Analysis	179
4.7.4	Quadratic Discriminant Analysis	181
4.7.5	Naive Bayes	182
4.7.6	K-Nearest Neighbors	183
4.7.7	Linear and Poisson Regression on the Bikeshare Data	188
4.8	Exercises	193

5 Resampling Methods	201
5.1 Cross-Validation	202
5.1.1 The Validation Set Approach	202
5.1.2 Leave-One-Out Cross-Validation	204
5.1.3 k -Fold Cross-Validation	206
5.1.4 Bias-Variance Trade-Off for k -Fold Cross-Validation	208
5.1.5 Cross-Validation on Classification Problems	209
5.2 The Bootstrap	212
5.3 Lab: Cross-Validation and the Bootstrap	215
5.3.1 The Validation Set Approach	216
5.3.2 Cross-Validation	217
5.3.3 The Bootstrap	220
5.4 Exercises	224
6 Linear Model Selection and Regularization	229
6.1 Subset Selection	231
6.1.1 Best Subset Selection	231
6.1.2 Stepwise Selection	233
6.1.3 Choosing the Optimal Model	235
6.2 Shrinkage Methods	240
6.2.1 Ridge Regression	240
6.2.2 The Lasso	244
6.2.3 Selecting the Tuning Parameter	252
6.3 Dimension Reduction Methods	253
6.3.1 Principal Components Regression	254
6.3.2 Partial Least Squares	260
6.4 Considerations in High Dimensions	262
6.4.1 High-Dimensional Data	262
6.4.2 What Goes Wrong in High Dimensions?	263
6.4.3 Regression in High Dimensions	265
6.4.4 Interpreting Results in High Dimensions	266
6.5 Lab: Linear Models and Regularization Methods	267
6.5.1 Subset Selection Methods	268
6.5.2 Ridge Regression and the Lasso	273
6.5.3 PCR and PLS Regression	280
6.6 Exercises	283
7 Moving Beyond Linearity	289
7.1 Polynomial Regression	290
7.2 Step Functions	292
7.3 Basis Functions	293
7.4 Regression Splines	294
7.4.1 Piecewise Polynomials	294
7.4.2 Constraints and Splines	296
7.4.3 The Spline Basis Representation	296
7.4.4 Choosing the Number and Locations of the Knots	297
7.4.5 Comparison to Polynomial Regression	299

7.5	Smoothing Splines	300
7.5.1	An Overview of Smoothing Splines	300
7.5.2	Choosing the Smoothing Parameter λ	301
7.6	Local Regression	303
7.7	Generalized Additive Models	305
7.7.1	GAMs for Regression Problems	306
7.7.2	GAMs for Classification Problems	308
7.8	Lab: Non-Linear Modeling	309
7.8.1	Polynomial Regression and Step Functions	310
7.8.2	Splines	315
7.8.3	Smoothing Splines and GAMs	317
7.8.4	Local Regression	324
7.9	Exercises	325
8	Tree-Based Methods	331
8.1	The Basics of Decision Trees	331
8.1.1	Regression Trees	331
8.1.2	Classification Trees	337
8.1.3	Trees Versus Linear Models	341
8.1.4	Advantages and Disadvantages of Trees	341
8.2	Bagging, Random Forests, Boosting, and Bayesian Additive Regression Trees	343
8.2.1	Bagging	343
8.2.2	Random Forests	346
8.2.3	Boosting	347
8.2.4	Bayesian Additive Regression Trees	350
8.2.5	Summary of Tree Ensemble Methods	353
8.3	Lab: Tree-Based Methods	354
8.3.1	Fitting Classification Trees	355
8.3.2	Fitting Regression Trees	358
8.3.3	Bagging and Random Forests	360
8.3.4	Boosting	361
8.3.5	Bayesian Additive Regression Trees	362
8.4	Exercises	363
9	Support Vector Machines	367
9.1	Maximal Margin Classifier	367
9.1.1	What Is a Hyperplane?	368
9.1.2	Classification Using a Separating Hyperplane	368
9.1.3	The Maximal Margin Classifier	370
9.1.4	Construction of the Maximal Margin Classifier	372
9.1.5	The Non-separable Case	372
9.2	Support Vector Classifiers	373
9.2.1	Overview of the Support Vector Classifier	373
9.2.2	Details of the Support Vector Classifier	374
9.3	Support Vector Machines	377
9.3.1	Classification with Non-Linear Decision Boundaries	378
9.3.2	The Support Vector Machine	379

9.3.3	An Application to the Heart Disease Data	382
9.4	SVMs with More than Two Classes	383
9.4.1	One-Versus-One Classification	384
9.4.2	One-Versus-All Classification	384
9.5	Relationship to Logistic Regression	384
9.6	Lab: Support Vector Machines	387
9.6.1	Support Vector Classifier	387
9.6.2	Support Vector Machine	390
9.6.3	ROC Curves	392
9.6.4	SVM with Multiple Classes	393
9.6.5	Application to Gene Expression Data	394
9.7	Exercises	395
10	Deep Learning	399
10.1	Single Layer Neural Networks	400
10.2	Multilayer Neural Networks	402
10.3	Convolutional Neural Networks	406
10.3.1	Convolution Layers	407
10.3.2	Pooling Layers	410
10.3.3	Architecture of a Convolutional Neural Network .	410
10.3.4	Data Augmentation	411
10.3.5	Results Using a Pretrained Classifier	412
10.4	Document Classification	413
10.5	Recurrent Neural Networks	416
10.5.1	Sequential Models for Document Classification .	418
10.5.2	Time Series Forecasting	420
10.5.3	Summary of RNNs	424
10.6	When to Use Deep Learning	425
10.7	Fitting a Neural Network	427
10.7.1	Backpropagation	428
10.7.2	Regularization and Stochastic Gradient Descent .	429
10.7.3	Dropout Learning	431
10.7.4	Network Tuning	431
10.8	Interpolation and Double Descent	432
10.9	Lab: Deep Learning	435
10.9.1	Single Layer Network on Hitters Data	437
10.9.2	Multilayer Network on the MNIST Digit Data .	444
10.9.3	Convolutional Neural Networks	448
10.9.4	Using Pretrained CNN Models	452
10.9.5	IMDB Document Classification	454
10.9.6	Recurrent Neural Networks	458
10.10	Exercises	465
11	Survival Analysis and Censored Data	469
11.1	Survival and Censoring Times	470
11.2	A Closer Look at Censoring	470
11.3	The Kaplan–Meier Survival Curve	472
11.4	The Log-Rank Test	474
11.5	Regression Models With a Survival Response	476

11.5.1	The Hazard Function	476
11.5.2	Proportional Hazards	478
11.5.3	Example: Brain Cancer Data	482
11.5.4	Example: Publication Data	482
11.6	Shrinkage for the Cox Model	484
11.7	Additional Topics	486
11.7.1	Area Under the Curve for Survival Analysis	486
11.7.2	Choice of Time Scale	487
11.7.3	Time-Dependent Covariates	488
11.7.4	Checking the Proportional Hazards Assumption	488
11.7.5	Survival Trees	488
11.8	Lab: Survival Analysis	489
11.8.1	Brain Cancer Data	489
11.8.2	Publication Data	493
11.8.3	Call Center Data	494
11.9	Exercises	498
12	Unsupervised Learning	503
12.1	The Challenge of Unsupervised Learning	503
12.2	Principal Components Analysis	504
12.2.1	What Are Principal Components?	505
12.2.2	Another Interpretation of Principal Components	508
12.2.3	The Proportion of Variance Explained	510
12.2.4	More on PCA	512
12.2.5	Other Uses for Principal Components	515
12.3	Missing Values and Matrix Completion	515
12.4	Clustering Methods	520
12.4.1	K -Means Clustering	521
12.4.2	Hierarchical Clustering	525
12.4.3	Practical Issues in Clustering	532
12.5	Lab: Unsupervised Learning	535
12.5.1	Principal Components Analysis	535
12.5.2	Matrix Completion	539
12.5.3	Clustering	542
12.5.4	NCI60 Data Example	546
12.6	Exercises	552
13	Multiple Testing	557
13.1	A Quick Review of Hypothesis Testing	558
13.1.1	Testing a Hypothesis	558
13.1.2	Type I and Type II Errors	562
13.2	The Challenge of Multiple Testing	563
13.3	The Family-Wise Error Rate	565
13.3.1	What is the Family-Wise Error Rate?	565
13.3.2	Approaches to Control the Family-Wise Error Rate	567
13.3.3	Trade-Off Between the FWER and Power	572
13.4	The False Discovery Rate	573
13.4.1	Intuition for the False Discovery Rate	573
13.4.2	The Benjamini–Hochberg Procedure	575

13.5 A Re-Sampling Approach to <i>p</i> -Values and False Discovery Rates	577
13.5.1 A Re-Sampling Approach to the <i>p</i> -Value	578
13.5.2 A Re-Sampling Approach to the False Discovery Rate	579
13.5.3 When Are Re-Sampling Approaches Useful?	581
13.6 Lab: Multiple Testing	583
13.6.1 Review of Hypothesis Tests	583
13.6.2 Family-Wise Error Rate	585
13.6.3 False Discovery Rate	588
13.6.4 A Re-Sampling Approach	590
13.7 Exercises	593
Index	597

3

Linear Regression



This chapter is about *linear regression*, a very simple approach for supervised learning. In particular, linear regression is a useful tool for predicting a quantitative response. It has been around for a long time and is the topic of innumerable textbooks. Though it may seem somewhat dull compared to some of the more modern statistical learning approaches described in later chapters of this book, linear regression is still a useful and widely used statistical learning method. Moreover, it serves as a good jumping-off point for newer approaches: as we will see in later chapters, many fancy statistical learning approaches can be seen as generalizations or extensions of linear regression. Consequently, the importance of having a good understanding of linear regression before studying more complex learning methods cannot be overstated. In this chapter, we review some of the key ideas underlying the linear regression model, as well as the least squares approach that is most commonly used to fit this model.

Recall the `Advertising` data from Chapter 2. Figure 2.1 displays `sales` (in thousands of units) for a particular product as a function of advertising budgets (in thousands of dollars) for `TV`, `radio`, and `newspaper` media. Suppose that in our role as statistical consultants we are asked to suggest, on the basis of this data, a marketing plan for next year that will result in high product sales. What information would be useful in order to provide such a recommendation? Here are a few important questions that we might seek to address:

1. *Is there a relationship between advertising budget and sales?*

Our first goal should be to determine whether the data provide evidence of an association between advertising expenditure and sales. If the evidence is weak, then one might argue that no money should be spent on advertising!

2. *How strong is the relationship between advertising budget and sales?*

Assuming that there is a relationship between advertising and sales, we would like to know the strength of this relationship. Does knowledge of the advertising budget provide a lot of information about product sales?

3. *Which media are associated with sales?*

Are all three media—TV, radio, and newspaper—associated with sales, or are just one or two of the media associated? To answer this question, we must find a way to separate out the individual contribution of each medium to sales when we have spent money on all three media.

4. *How large is the association between each medium and sales?*

For every dollar spent on advertising in a particular medium, by what amount will sales increase? How accurately can we predict this amount of increase?

5. *How accurately can we predict future sales?*

For any given level of television, radio, or newspaper advertising, what is our prediction for sales, and what is the accuracy of this prediction?

6. *Is the relationship linear?*

If there is approximately a straight-line relationship between advertising expenditure in the various media and sales, then linear regression is an appropriate tool. If not, then it may still be possible to transform the predictor or the response so that linear regression can be used.

7. *Is there synergy among the advertising media?*

Perhaps spending \$50,000 on television advertising and \$50,000 on radio advertising is associated with higher sales than allocating \$100,000 to either television or radio individually. In marketing, this is known as a *synergy* effect, while in statistics it is called an *interaction* effect.

synergy
interaction

It turns out that linear regression can be used to answer each of these questions. We will first discuss all of these questions in a general context, and then return to them in this specific context in Section 3.4.

3.1 Simple Linear Regression

Simple linear regression lives up to its name: it is a very straightforward approach for predicting a quantitative response Y on the basis of a single predictor variable X . It assumes that there is approximately a linear relationship between X and Y . Mathematically, we can write this linear relationship as

$$Y \approx \beta_0 + \beta_1 X. \quad (3.1)$$

simple linear
regression

You might read “ \approx ” as “*is approximately modeled as*”. We will sometimes describe (3.1) by saying that we are *regressing Y on X* (or *Y onto X*).

For example, X may represent **TV** advertising and Y may represent **sales**. Then we can regress **sales** onto **TV** by fitting the model

$$\text{sales} \approx \beta_0 + \beta_1 \times \text{TV}.$$

In Equation 3.1, β_0 and β_1 are two unknown constants that represent the *intercept* and *slope* terms in the linear model. Together, β_0 and β_1 are known as the model *coefficients* or *parameters*. Once we have used our training data to produce estimates $\hat{\beta}_0$ and $\hat{\beta}_1$ for the model coefficients, we can predict future sales on the basis of a particular value of TV advertising by computing

$$\hat{y} = \hat{\beta}_0 + \hat{\beta}_1 x, \quad (3.2)$$

intercept
slope
coefficient
parameter

where \hat{y} indicates a prediction of Y on the basis of $X = x$. Here we use a *hat* symbol, $\hat{}$, to denote the estimated value for an unknown parameter or coefficient, or to denote the predicted value of the response.

3.1.1 Estimating the Coefficients

In practice, β_0 and β_1 are unknown. So before we can use (3.1) to make predictions, we must use data to estimate the coefficients. Let

$$(x_1, y_1), (x_2, y_2), \dots, (x_n, y_n)$$

represent n observation pairs, each of which consists of a measurement of X and a measurement of Y . In the **Advertising** example, this data set consists of the TV advertising budget and product sales in $n = 200$ different markets. (Recall that the data are displayed in Figure 2.1.) Our goal is to obtain coefficient estimates $\hat{\beta}_0$ and $\hat{\beta}_1$ such that the linear model (3.1) fits the available data well—that is, so that $y_i \approx \hat{\beta}_0 + \hat{\beta}_1 x_i$ for $i = 1, \dots, n$. In other words, we want to find an intercept $\hat{\beta}_0$ and a slope $\hat{\beta}_1$ such that the resulting line is as close as possible to the $n = 200$ data points. There are a number of ways of measuring *closeness*. However, by far the most common approach involves minimizing the *least squares* criterion, and we take that approach in this chapter. Alternative approaches will be considered in Chapter 6.

least squares

Let $\hat{y}_i = \hat{\beta}_0 + \hat{\beta}_1 x_i$ be the prediction for Y based on the i th value of X . Then $e_i = y_i - \hat{y}_i$ represents the i th *residual*—this is the difference between the i th observed response value and the i th response value that is predicted by our linear model. We define the *residual sum of squares* (RSS) as

$$\text{RSS} = e_1^2 + e_2^2 + \dots + e_n^2,$$

residual

residual sum
of squares

or equivalently as

$$\text{RSS} = (y_1 - \hat{\beta}_0 - \hat{\beta}_1 x_1)^2 + (y_2 - \hat{\beta}_0 - \hat{\beta}_1 x_2)^2 + \dots + (y_n - \hat{\beta}_0 - \hat{\beta}_1 x_n)^2. \quad (3.3)$$

The least squares approach chooses $\hat{\beta}_0$ and $\hat{\beta}_1$ to minimize the RSS. Using some calculus, one can show that the minimizers are

$$\begin{aligned} \hat{\beta}_1 &= \frac{\sum_{i=1}^n (x_i - \bar{x})(y_i - \bar{y})}{\sum_{i=1}^n (x_i - \bar{x})^2}, \\ \hat{\beta}_0 &= \bar{y} - \hat{\beta}_1 \bar{x}, \end{aligned} \quad (3.4)$$

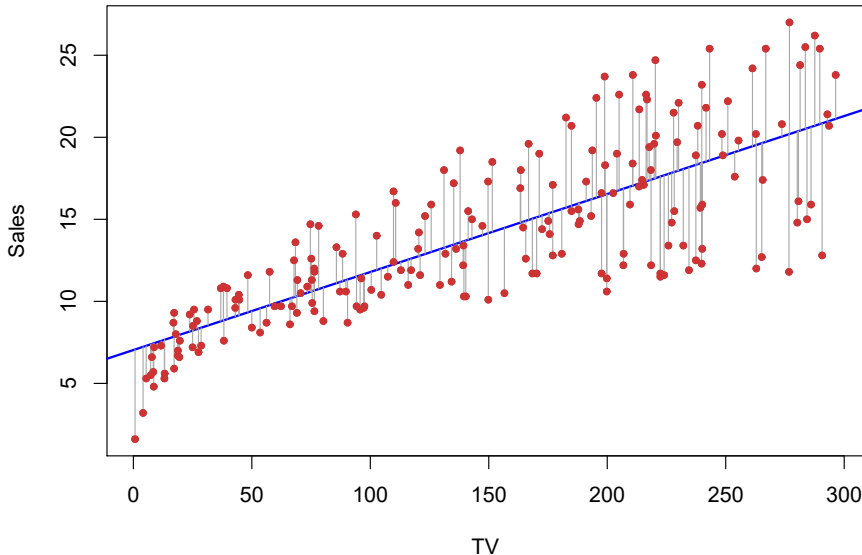


FIGURE 3.1. For the `Advertising` data, the least squares fit for the regression of `Sales` onto `TV` is shown. The fit is found by minimizing the residual sum of squares. Each grey line segment represents a residual. In this case a linear fit captures the essence of the relationship, although it overestimates the trend in the left of the plot.

where $\bar{y} \equiv \frac{1}{n} \sum_{i=1}^n y_i$ and $\bar{x} \equiv \frac{1}{n} \sum_{i=1}^n x_i$ are the sample means. In other words, (3.4) defines the *least squares coefficient estimates* for simple linear regression.

Figure 3.1 displays the simple linear regression fit to the `Advertising` data, where $\hat{\beta}_0 = 7.03$ and $\hat{\beta}_1 = 0.0475$. In other words, according to this approximation, an additional \$1,000 spent on TV advertising is associated with selling approximately 47.5 additional units of the product. In Figure 3.2, we have computed RSS for a number of values of β_0 and β_1 , using the advertising data with `sales` as the response and `TV` as the predictor. In each plot, the red dot represents the pair of least squares estimates $(\hat{\beta}_0, \hat{\beta}_1)$ given by (3.4). These values clearly minimize the RSS.

3.1.2 Assessing the Accuracy of the Coefficient Estimates

Recall from (2.1) that we assume that the *true* relationship between X and Y takes the form $Y = f(X) + \epsilon$ for some unknown function f , where ϵ is a mean-zero random error term. If f is to be approximated by a linear function, then we can write this relationship as

$$Y = \beta_0 + \beta_1 X + \epsilon. \quad (3.5)$$

Here β_0 is the intercept term—that is, the expected value of Y when $X = 0$, and β_1 is the slope—the average increase in Y associated with a one-unit increase in X . The error term is a catch-all for what we miss with this simple model: the true relationship is probably not linear, there may be other variables that cause variation in Y , and there may be measurement error. We typically assume that the error term is independent of X .

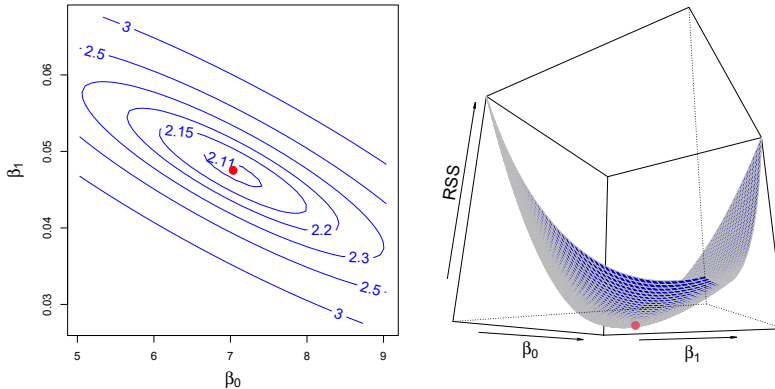


FIGURE 3.2. Contour and three-dimensional plots of the RSS on the `Advertising` data, using `sales` as the response and `TV` as the predictor. The red dots correspond to the least squares estimates $\hat{\beta}_0$ and $\hat{\beta}_1$, given by (3.4).

The model given by (3.5) defines the *population regression line*, which is the best linear approximation to the true relationship between X and Y .¹ The least squares regression coefficient estimates (3.4) characterize the *least squares line* (3.2). The left-hand panel of Figure 3.3 displays these two lines in a simple simulated example. We created 100 random X s, and generated 100 corresponding Y s from the model

$$Y = 2 + 3X + \epsilon, \quad (3.6)$$

where ϵ was generated from a normal distribution with mean zero. The red line in the left-hand panel of Figure 3.3 displays the *true* relationship, $f(X) = 2 + 3X$, while the blue line is the least squares estimate based on the observed data. The true relationship is generally not known for real data, but the least squares line can always be computed using the coefficient estimates given in (3.4). In other words, in real applications, we have access to a set of observations from which we can compute the least squares line; however, the population regression line is unobserved. In the right-hand panel of Figure 3.3 we have generated ten different data sets from the model given by (3.6) and plotted the corresponding ten least squares lines. Notice that different data sets generated from the same true model result in slightly different least squares lines, but the unobserved population regression line does not change.

At first glance, the difference between the population regression line and the least squares line may seem subtle and confusing. We only have one data set, and so what does it mean that two different lines describe the relationship between the predictor and the response? Fundamentally, the concept of these two lines is a natural extension of the standard statistical approach of using information from a sample to estimate characteristics of a large population. For example, suppose that we are interested in knowing

population
regression
line

least squares
line

¹The assumption of linearity is often a useful working model. However, despite what many textbooks might tell us, we seldom believe that the true relationship is linear.

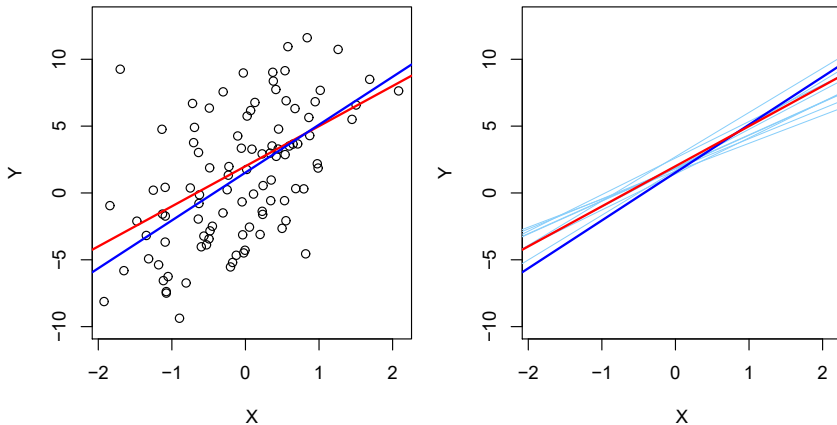


FIGURE 3.3. A simulated data set. Left: The red line represents the true relationship, $f(X) = 2 + 3X$, which is known as the population regression line. The blue line is the least squares line; it is the least squares estimate for $f(X)$ based on the observed data, shown in black. Right: The population regression line is again shown in red, and the least squares line in dark blue. In light blue, ten least squares lines are shown, each computed on the basis of a separate random set of observations. Each least squares line is different, but on average, the least squares lines are quite close to the population regression line.

the population mean μ of some random variable Y . Unfortunately, μ is unknown, but we do have access to n observations from Y , y_1, \dots, y_n , which we can use to estimate μ . A reasonable estimate is $\hat{\mu} = \bar{y}$, where $\bar{y} = \frac{1}{n} \sum_{i=1}^n y_i$ is the sample mean. The sample mean and the population mean are different, but in general the sample mean will provide a good estimate of the population mean. In the same way, the unknown coefficients β_0 and β_1 in linear regression define the population regression line. We seek to estimate these unknown coefficients using $\hat{\beta}_0$ and $\hat{\beta}_1$ given in (3.4). These coefficient estimates define the least squares line.

The analogy between linear regression and estimation of the mean of a random variable is an apt one based on the concept of *bias*. If we use the sample mean $\hat{\mu}$ to estimate μ , this estimate is *unbiased*, in the sense that on average, we expect $\hat{\mu}$ to equal μ . What exactly does this mean? It means that on the basis of one particular set of observations y_1, \dots, y_n , $\hat{\mu}$ might overestimate μ , and on the basis of another set of observations, $\hat{\mu}$ might underestimate μ . But if we could average a huge number of estimates of μ obtained from a huge number of sets of observations, then this average would *exactly* equal μ . Hence, an unbiased estimator does not *systematically* over- or under-estimate the true parameter. The property of unbiasedness holds for the least squares coefficient estimates given by (3.4) as well: if we estimate β_0 and β_1 on the basis of a particular data set, then our estimates won't be exactly equal to β_0 and β_1 . But if we could average the estimates obtained over a huge number of data sets, then the average of these estimates would be spot on! In fact, we can see from the right-hand panel of Figure 3.3 that the average of many least squares lines, each

bias
unbiased

estimated from a separate data set, is pretty close to the true population regression line.

We continue the analogy with the estimation of the population mean μ of a random variable Y . A natural question is as follows: how accurate is the sample mean $\hat{\mu}$ as an estimate of μ ? We have established that the average of $\hat{\mu}$'s over many data sets will be very close to μ , but that a single estimate $\hat{\mu}$ may be a substantial underestimate or overestimate of μ . How far off will that single estimate of $\hat{\mu}$ be? In general, we answer this question by computing the *standard error* of $\hat{\mu}$, written as $\text{SE}(\hat{\mu})$. We have the well-known formula

$$\text{Var}(\hat{\mu}) = \text{SE}(\hat{\mu})^2 = \frac{\sigma^2}{n}, \quad (3.7)$$

standard
error

where σ is the standard deviation of each of the realizations y_i of Y .² Roughly speaking, the standard error tells us the average amount that this estimate $\hat{\mu}$ differs from the actual value of μ . Equation 3.7 also tells us how this deviation shrinks with n —the more observations we have, the smaller the standard error of $\hat{\mu}$. In a similar vein, we can wonder how close $\hat{\beta}_0$ and $\hat{\beta}_1$ are to the true values β_0 and β_1 . To compute the standard errors associated with $\hat{\beta}_0$ and $\hat{\beta}_1$, we use the following formulas:

$$\text{SE}(\hat{\beta}_0)^2 = \sigma^2 \left[\frac{1}{n} + \frac{\bar{x}^2}{\sum_{i=1}^n (x_i - \bar{x})^2} \right], \quad \text{SE}(\hat{\beta}_1)^2 = \frac{\sigma^2}{\sum_{i=1}^n (x_i - \bar{x})^2}, \quad (3.8)$$

where $\sigma^2 = \text{Var}(\epsilon)$. For these formulas to be strictly valid, we need to assume that the errors ϵ_i for each observation have common variance σ^2 and are uncorrelated. This is clearly not true in Figure 3.1, but the formula still turns out to be a good approximation. Notice in the formula that $\text{SE}(\hat{\beta}_1)$ is smaller when the x_i are more spread out; intuitively we have more *leverage* to estimate a slope when this is the case. We also see that $\text{SE}(\hat{\beta}_0)$ would be the same as $\text{SE}(\hat{\mu})$ if \bar{x} were zero (in which case $\hat{\beta}_0$ would be equal to \bar{y}). In general, σ^2 is not known, but can be estimated from the data. This estimate of σ is known as the *residual standard error*, and is given by the formula $\text{RSE} = \sqrt{\text{RSS}/(n-2)}$. Strictly speaking, when σ^2 is estimated from the data we should write $\widehat{\text{SE}}(\hat{\beta}_1)$ to indicate that an estimate has been made, but for simplicity of notation we will drop this extra “hat”.

residual
standard
error

Standard errors can be used to compute *confidence intervals*. A 95% confidence interval is defined as a range of values such that with 95% probability, the range will contain the true unknown value of the parameter. The range is defined in terms of lower and upper limits computed from the sample of data. A 95% confidence interval has the following property: if we take repeated samples and construct the confidence interval for each sample, 95% of the intervals will contain the true unknown value of the parameter. For linear regression, the 95% confidence interval for β_1 approximately takes the form

$$\hat{\beta}_1 \pm 2 \cdot \text{SE}(\hat{\beta}_1). \quad (3.9)$$

confidence
interval

²This formula holds provided that the n observations are uncorrelated.

That is, there is approximately a 95 % chance that the interval

$$\left[\hat{\beta}_1 - 2 \cdot \text{SE}(\hat{\beta}_1), \hat{\beta}_1 + 2 \cdot \text{SE}(\hat{\beta}_1) \right] \quad (3.10)$$

will contain the true value of β_1 .³ Similarly, a confidence interval for β_0 approximately takes the form

$$\hat{\beta}_0 \pm 2 \cdot \text{SE}(\hat{\beta}_0). \quad (3.11)$$

In the case of the advertising data, the 95 % confidence interval for β_0 is [6,130, 7,935] and the 95 % confidence interval for β_1 is [0,042, 0,053]. Therefore, we can conclude that in the absence of any advertising, sales will, on average, fall somewhere between 6,130 and 7,935 units. Furthermore, for each \$1,000 increase in television advertising, there will be an average increase in sales of between 42 and 53 units.

Standard errors can also be used to perform *hypothesis tests* on the coefficients. The most common hypothesis test involves testing the *null hypothesis* of

$$H_0 : \text{There is no relationship between } X \text{ and } Y \quad (3.12)$$

versus the *alternative hypothesis*

$$H_a : \text{There is some relationship between } X \text{ and } Y. \quad (3.13)$$

Mathematically, this corresponds to testing

$$H_0 : \beta_1 = 0$$

versus

$$H_a : \beta_1 \neq 0,$$

since if $\beta_1 = 0$ then the model (3.5) reduces to $Y = \beta_0 + \epsilon$, and X is not associated with Y . To test the null hypothesis, we need to determine whether $\hat{\beta}_1$, our estimate for β_1 , is sufficiently far from zero that we can be confident that β_1 is non-zero. How far is far enough? This of course depends on the accuracy of $\hat{\beta}_1$ —that is, it depends on $\text{SE}(\hat{\beta}_1)$. If $\text{SE}(\hat{\beta}_1)$ is small, then even relatively small values of $\hat{\beta}_1$ may provide strong evidence that $\beta_1 \neq 0$, and hence that there is a relationship between X and Y . In contrast, if $\text{SE}(\hat{\beta}_1)$ is large, then $\hat{\beta}_1$ must be large in absolute value in order for us to reject the null hypothesis. In practice, we compute a *t-statistic*, given by

$$t = \frac{\hat{\beta}_1 - 0}{\text{SE}(\hat{\beta}_1)}, \quad (3.14)$$

³Approximately for several reasons. Equation 3.10 relies on the assumption that the errors are Gaussian. Also, the factor of 2 in front of the $\text{SE}(\hat{\beta}_1)$ term will vary slightly depending on the number of observations n in the linear regression. To be precise, rather than the number 2, (3.10) should contain the 97.5 % quantile of a *t*-distribution with $n - 2$ degrees of freedom. Details of how to compute the 95 % confidence interval precisely in R will be provided later in this chapter.

	Coefficient	Std. error	<i>t</i> -statistic	<i>p</i> -value
Intercept	7.0325	0.4578	15.36	< 0.0001
TV	0.0475	0.0027	17.67	< 0.0001

TABLE 3.1. For the **Advertising** data, coefficients of the least squares model for the regression of number of units sold on TV advertising budget. An increase of \$1,000 in the TV advertising budget is associated with an increase in sales by around 50 units. (Recall that the **sales** variable is in thousands of units, and the **TV** variable is in thousands of dollars.)

which measures the number of standard deviations that $\hat{\beta}_1$ is away from 0. If there really is no relationship between X and Y , then we expect that (3.14) will have a *t*-distribution with $n - 2$ degrees of freedom. The *t*-distribution has a bell shape and for values of n greater than approximately 30 it is quite similar to the standard normal distribution. Consequently, it is a simple matter to compute the probability of observing any number equal to $|t|$ or larger in absolute value, assuming $\beta_1 = 0$. We call this probability the *p-value*. Roughly speaking, we interpret the *p-value* as follows: a small *p-value* indicates that it is unlikely to observe such a substantial association between the predictor and the response due to chance, in the absence of any real association between the predictor and the response. Hence, if we see a small *p-value*, then we can infer that there is an association between the predictor and the response. We *reject the null hypothesis*—that is, we declare a relationship to exist between X and Y —if the *p-value* is small enough. Typical *p-value* cutoffs for rejecting the null hypothesis are 5% or 1%, although this topic will be explored in much greater detail in Chapter 13. When $n = 30$, these correspond to *t*-statistics (3.14) of around 2 and 2.75, respectively.

Table 3.1 provides details of the least squares model for the regression of number of units sold on TV advertising budget for the **Advertising** data. Notice that the coefficients for $\hat{\beta}_0$ and $\hat{\beta}_1$ are very large relative to their standard errors, so the *t*-statistics are also large; the probabilities of seeing such values if H_0 is true are virtually zero. Hence we can conclude that $\beta_0 \neq 0$ and $\beta_1 \neq 0$.⁴

3.1.3 Assessing the Accuracy of the Model

Once we have rejected the null hypothesis (3.12) in favor of the alternative hypothesis (3.13), it is natural to want to quantify *the extent to which the model fits the data*. The quality of a linear regression fit is typically assessed using two related quantities: the *residual standard error* (RSE) and the R^2 statistic.

⁴In Table 3.1, a small *p-value* for the intercept indicates that we can reject the null hypothesis that $\beta_0 = 0$, and a small *p-value* for **TV** indicates that we can reject the null hypothesis that $\beta_1 = 0$. Rejecting the latter null hypothesis allows us to conclude that there is a relationship between **TV** and **sales**. Rejecting the former allows us to conclude that in the absence of **TV** expenditure, **sales** are non-zero.

Quantity	Value
Residual standard error	3.26
R^2	0.612
F -statistic	312.1

TABLE 3.2. For the **Advertising** data, more information about the least squares model for the regression of number of units sold on TV advertising budget.

Table 3.2 displays the RSE, the R^2 statistic, and the F -statistic (to be described in Section 3.2.2) for the linear regression of number of units sold on TV advertising budget.

Residual Standard Error

Recall from the model (3.5) that associated with each observation is an error term ϵ . Due to the presence of these error terms, even if we knew the true regression line (i.e. even if β_0 and β_1 were known), we would not be able to perfectly predict Y from X . The RSE is an estimate of the standard deviation of ϵ . Roughly speaking, it is the average amount that the response will deviate from the true regression line. It is computed using the formula

$$\text{RSE} = \sqrt{\frac{1}{n-2} \text{RSS}} = \sqrt{\frac{1}{n-2} \sum_{i=1}^n (y_i - \hat{y}_i)^2}. \quad (3.15)$$

Note that RSS was defined in Section 3.1.1, and is given by the formula

$$\text{RSS} = \sum_{i=1}^n (y_i - \hat{y}_i)^2. \quad (3.16)$$

In the case of the advertising data, we see from the linear regression output in Table 3.2 that the RSE is 3.26. In other words, actual sales in each market deviate from the true regression line by approximately 3,260 units, on average. Another way to think about this is that even if the model were correct and the true values of the unknown coefficients β_0 and β_1 were known exactly, any prediction of sales on the basis of TV advertising would still be off by about 3,260 units on average. Of course, whether or not 3,260 units is an acceptable prediction error depends on the problem context. In the advertising data set, the mean value of **sales** over all markets is approximately 14,000 units, and so the percentage error is $3,260/14,000 = 23\%$.

The RSE is considered a measure of the *lack of fit* of the model (3.5) to the data. If the predictions obtained using the model are very close to the true outcome values—that is, if $\hat{y}_i \approx y_i$ for $i = 1, \dots, n$ —then (3.15) will be small, and we can conclude that the model fits the data very well. On the other hand, if \hat{y}_i is very far from y_i for one or more observations, then the RSE may be quite large, indicating that the model doesn't fit the data well.

R^2 Statistic

The RSE provides an absolute measure of lack of fit of the model (3.5) to the data. But since it is measured in the units of Y , it is not always

clear what constitutes a good RSE. The R^2 statistic provides an alternative measure of fit. It takes the form of a *proportion*—the proportion of variance explained—and so it always takes on a value between 0 and 1, and is independent of the scale of Y .

To calculate R^2 , we use the formula

$$R^2 = \frac{\text{TSS} - \text{RSS}}{\text{TSS}} = 1 - \frac{\text{RSS}}{\text{TSS}} \quad (3.17)$$

where $\text{TSS} = \sum(y_i - \bar{y})^2$ is the *total sum of squares*, and RSS is defined in (3.16). TSS measures the total variance in the response Y , and can be thought of as the amount of variability inherent in the response before the regression is performed. In contrast, RSS measures the amount of variability that is left unexplained after performing the regression. Hence, $\text{TSS} - \text{RSS}$ measures the amount of variability in the response that is explained (or removed) by performing the regression, and R^2 measures the *proportion of variability in Y that can be explained using X* . An R^2 statistic that is close to 1 indicates that a large proportion of the variability in the response is explained by the regression. A number near 0 indicates that the regression does not explain much of the variability in the response; this might occur because the linear model is wrong, or the error variance σ^2 is high, or both. In Table 3.2, the R^2 was 0.61, and so just under two-thirds of the variability in **sales** is explained by a linear regression on **TV**.

total sum of squares

The R^2 statistic (3.17) has an interpretational advantage over the RSE (3.15), since unlike the RSE, it always lies between 0 and 1. However, it can still be challenging to determine what is a *good* R^2 value, and in general, this will depend on the application. For instance, in certain problems in physics, we may know that the data truly comes from a linear model with a small residual error. In this case, we would expect to see an R^2 value that is extremely close to 1, and a substantially smaller R^2 value might indicate a serious problem with the experiment in which the data were generated. On the other hand, in typical applications in biology, psychology, marketing, and other domains, the linear model (3.5) is at best an extremely rough approximation to the data, and residual errors due to other unmeasured factors are often very large. In this setting, we would expect only a very small proportion of the variance in the response to be explained by the predictor, and an R^2 value well below 0.1 might be more realistic!

The R^2 statistic is a measure of the linear relationship between X and Y . Recall that *correlation*, defined as

$$\text{Cor}(X, Y) = \frac{\sum_{i=1}^n (x_i - \bar{x})(y_i - \bar{y})}{\sqrt{\sum_{i=1}^n (x_i - \bar{x})^2} \sqrt{\sum_{i=1}^n (y_i - \bar{y})^2}}, \quad (3.18)$$

correlation

is also a measure of the linear relationship between X and Y .⁵ This suggests that we might be able to use $r = \text{Cor}(X, Y)$ instead of R^2 in order to assess the fit of the linear model. In fact, it can be shown that in the simple

⁵We note that in fact, the right-hand side of (3.18) is the sample correlation; thus, it would be more correct to write $\widehat{\text{Cor}}(X, Y)$; however, we omit the “hat” for ease of notation.

Simple regression of sales on radio				
	Coefficient	Std. error	t-statistic	p-value
Intercept	9.312	0.563	16.54	< 0.0001
radio	0.203	0.020	9.92	< 0.0001

Simple regression of **sales** on **newspaper**

	Coefficient	Std. error	t-statistic	p-value
Intercept	12.351	0.621	19.88	< 0.0001
newspaper	0.055	0.017	3.30	0.00115

TABLE 3.3. More simple linear regression models for the **Advertising** data. Coefficients of the simple linear regression model for number of units sold on Top: radio advertising budget and Bottom: newspaper advertising budget. A \$1,000 increase in spending on radio advertising is associated with an average increase in sales by around 203 units, while the same increase in spending on newspaper advertising is associated with an average increase in sales by around 55 units. (Note that the **sales** variable is in thousands of units, and the **radio** and **newspaper** variables are in thousands of dollars.)

linear regression setting, $R^2 = r^2$. In other words, the squared correlation and the R^2 statistic are identical. However, in the next section we will discuss the multiple linear regression problem, in which we use several predictors simultaneously to predict the response. The concept of correlation between the predictors and the response does not extend automatically to this setting, since correlation quantifies the association between a single pair of variables rather than between a larger number of variables. We will see that R^2 fills this role.

3.2 Multiple Linear Regression

Simple linear regression is a useful approach for predicting a response on the basis of a single predictor variable. However, in practice we often have more than one predictor. For example, in the **Advertising** data, we have examined the relationship between sales and TV advertising. We also have data for the amount of money spent advertising on the radio and in newspapers, and we may want to know whether either of these two media is associated with sales. How can we extend our analysis of the advertising data in order to accommodate these two additional predictors?

One option is to run three separate simple linear regressions, each of which uses a different advertising medium as a predictor. For instance, we can fit a simple linear regression to predict sales on the basis of the amount spent on radio advertisements. Results are shown in Table 3.3 (top table). We find that a \$1,000 increase in spending on radio advertising is associated with an increase in sales of around 203 units. Table 3.3 (bottom table) contains the least squares coefficients for a simple linear regression of sales onto newspaper advertising budget. A \$1,000 increase in newspaper advertising budget is associated with an increase in sales of approximately 55 units.

However, the approach of fitting a separate simple linear regression model for each predictor is not entirely satisfactory. First of all, it is unclear how to make a single prediction of sales given the three advertising media budgets, since each of the budgets is associated with a separate regression equation. Second, each of the three regression equations ignores the other two media in forming estimates for the regression coefficients. We will see shortly that if the media budgets are correlated with each other in the 200 markets in our data set, then this can lead to very misleading estimates of the association between each media budget and sales.

Instead of fitting a separate simple linear regression model for each predictor, a better approach is to extend the simple linear regression model (3.5) so that it can directly accommodate multiple predictors. We can do this by giving each predictor a separate slope coefficient in a single model. In general, suppose that we have p distinct predictors. Then the multiple linear regression model takes the form

$$Y = \beta_0 + \beta_1 X_1 + \beta_2 X_2 + \cdots + \beta_p X_p + \epsilon, \quad (3.19)$$

where X_j represents the j th predictor and β_j quantifies the association between that variable and the response. We interpret β_j as the *average* effect on Y of a one unit increase in X_j , *holding all other predictors fixed*. In the advertising example, (3.19) becomes

$$\text{sales} = \beta_0 + \beta_1 \times \text{TV} + \beta_2 \times \text{radio} + \beta_3 \times \text{newspaper} + \epsilon. \quad (3.20)$$

3.2.1 Estimating the Regression Coefficients

As was the case in the simple linear regression setting, the regression coefficients $\beta_0, \beta_1, \dots, \beta_p$ in (3.19) are unknown, and must be estimated. Given estimates $\hat{\beta}_0, \hat{\beta}_1, \dots, \hat{\beta}_p$, we can make predictions using the formula

$$\hat{y} = \hat{\beta}_0 + \hat{\beta}_1 x_1 + \hat{\beta}_2 x_2 + \cdots + \hat{\beta}_p x_p. \quad (3.21)$$

The parameters are estimated using the same least squares approach that we saw in the context of simple linear regression. We choose $\beta_0, \beta_1, \dots, \beta_p$ to minimize the sum of squared residuals

$$\begin{aligned} \text{RSS} &= \sum_{i=1}^n (y_i - \hat{y}_i)^2 \\ &= \sum_{i=1}^n (y_i - \hat{\beta}_0 - \hat{\beta}_1 x_{i1} - \hat{\beta}_2 x_{i2} - \cdots - \hat{\beta}_p x_{ip})^2. \end{aligned} \quad (3.22)$$

The values $\hat{\beta}_0, \hat{\beta}_1, \dots, \hat{\beta}_p$ that minimize (3.22) are the multiple least squares regression coefficient estimates. Unlike the simple linear regression estimates given in (3.4), the multiple regression coefficient estimates have somewhat complicated forms that are most easily represented using matrix algebra. For this reason, we do not provide them here. Any statistical software package can be used to compute these coefficient estimates, and later in this chapter we will show how this can be done in R. Figure 3.4

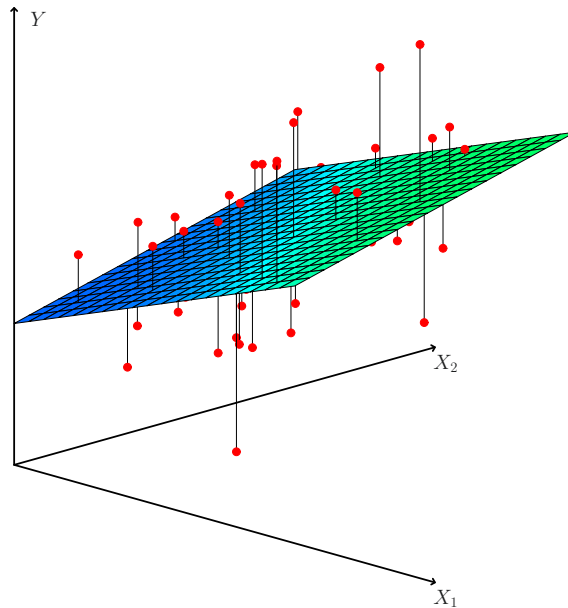


FIGURE 3.4. In a three-dimensional setting, with two predictors and one response, the least squares regression line becomes a plane. The plane is chosen to minimize the sum of the squared vertical distances between each observation (shown in red) and the plane.

illustrates an example of the least squares fit to a toy data set with $p = 2$ predictors.

Table 3.4 displays the multiple regression coefficient estimates when TV, radio, and newspaper advertising budgets are used to predict product sales using the [Advertising](#) data. We interpret these results as follows: for a given amount of TV and newspaper advertising, spending an additional \$1,000 on radio advertising is associated with approximately 189 units of additional sales. Comparing these coefficient estimates to those displayed in Tables 3.1 and 3.3, we notice that the multiple regression coefficient estimates for **TV** and **radio** are pretty similar to the simple linear regression coefficient estimates. However, while the **newspaper** regression coefficient estimate in Table 3.3 was significantly non-zero, the coefficient estimate for **newspaper** in the multiple regression model is close to zero, and the corresponding p -value is no longer significant, with a value around 0.86. This illustrates that the simple and multiple regression coefficients can be quite different. This difference stems from the fact that in the simple regression case, the slope term represents the average increase in product sales associated with a \$1,000 increase in newspaper advertising, ignoring other predictors such as **TV** and **radio**. By contrast, in the multiple regression setting, the coefficient for **newspaper** represents the average increase in product sales associated with increasing newspaper spending by \$1,000 while holding **TV** and **radio** fixed.

Does it make sense for the multiple regression to suggest no relationship between **sales** and **newspaper** while the simple linear regression implies the

	Coefficient	Std. error	<i>t</i> -statistic	<i>p</i> -value
Intercept	2.939	0.3119	9.42	< 0.0001
TV	0.046	0.0014	32.81	< 0.0001
radio	0.189	0.0086	21.89	< 0.0001
newspaper	-0.001	0.0059	-0.18	0.8599

TABLE 3.4. For the `Advertising` data, least squares coefficient estimates of the multiple linear regression of number of units sold on TV, radio, and newspaper advertising budgets.

	TV	radio	newspaper	sales
TV	1.0000	0.0548	0.0567	0.7822
radio		1.0000	0.3541	0.5762
newspaper			1.0000	0.2283
sales				1.0000

TABLE 3.5. Correlation matrix for TV, radio, newspaper, and sales for the `Advertising` data.

opposite? In fact it does. Consider the correlation matrix for the three predictor variables and response variable, displayed in Table 3.5. Notice that the correlation between `radio` and `newspaper` is 0.35. This indicates that markets with high newspaper advertising tend to also have high radio advertising. Now suppose that the multiple regression is correct and newspaper advertising is not associated with sales, but radio advertising is associated with sales. Then in markets where we spend more on radio our sales will tend to be higher, and as our correlation matrix shows, we also tend to spend more on newspaper advertising in those same markets. Hence, in a simple linear regression which only examines `sales` versus `newspaper`, we will observe that higher values of `newspaper` tend to be associated with higher values of `sales`, even though newspaper advertising is not directly associated with sales. So `newspaper` advertising is a surrogate for `radio` advertising; `newspaper` gets “credit” for the association between `radio` on `sales`.

This slightly counterintuitive result is very common in many real life situations. Consider an absurd example to illustrate the point. Running a regression of shark attacks versus ice cream sales for data collected at a given beach community over a period of time would show a positive relationship, similar to that seen between `sales` and `newspaper`. Of course no one has (yet) suggested that ice creams should be banned at beaches to reduce shark attacks. In reality, higher temperatures cause more people to visit the beach, which in turn results in more ice cream sales and more shark attacks. A multiple regression of shark attacks onto ice cream sales and temperature reveals that, as intuition implies, ice cream sales is no longer a significant predictor after adjusting for temperature.

3.2.2 Some Important Questions

When we perform multiple linear regression, we usually are interested in answering a few important questions.

1. Is at least one of the predictors X_1, X_2, \dots, X_p useful in predicting the response?
2. Do all the predictors help to explain Y , or is only a subset of the predictors useful?
3. How well does the model fit the data?
4. Given a set of predictor values, what response value should we predict, and how accurate is our prediction?

We now address each of these questions in turn.

One: Is There a Relationship Between the Response and Predictors?

Recall that in the simple linear regression setting, in order to determine whether there is a relationship between the response and the predictor we can simply check whether $\beta_1 = 0$. In the multiple regression setting with p predictors, we need to ask whether all of the regression coefficients are zero, i.e. whether $\beta_1 = \beta_2 = \dots = \beta_p = 0$. As in the simple linear regression setting, we use a hypothesis test to answer this question. We test the null hypothesis,

$$H_0 : \beta_1 = \beta_2 = \dots = \beta_p = 0$$

versus the alternative

$$H_a : \text{at least one } \beta_j \text{ is non-zero.}$$

This hypothesis test is performed by computing the *F-statistic*,

F-statistic

$$F = \frac{(\text{TSS} - \text{RSS})/p}{\text{RSS}/(n - p - 1)}, \quad (3.23)$$

where, as with simple linear regression, $\text{TSS} = \sum(y_i - \bar{y})^2$ and $\text{RSS} = \sum(y_i - \hat{y}_i)^2$. If the linear model assumptions are correct, one can show that

$$E\{\text{RSS}/(n - p - 1)\} = \sigma^2$$

and that, provided H_0 is true,

$$E\{(\text{TSS} - \text{RSS})/p\} = \sigma^2.$$

Hence, when there is no relationship between the response and predictors, one would expect the *F*-statistic to take on a value close to 1. On the other hand, if H_a is true, then $E\{(\text{TSS} - \text{RSS})/p\} > \sigma^2$, so we expect *F* to be greater than 1.

The *F*-statistic for the multiple linear regression model obtained by regressing **sales** onto **radio**, **TV**, and **newspaper** is shown in Table 3.6. In this example the *F*-statistic is 570. Since this is far larger than 1, it provides compelling evidence against the null hypothesis H_0 . In other words, the large *F*-statistic suggests that at least one of the advertising media must be related to **sales**. However, what if the *F*-statistic had been closer to 1? How large does the *F*-statistic need to be before we can reject H_0 and

Quantity	Value
Residual standard error	1.69
R^2	0.897
F -statistic	570

TABLE 3.6. More information about the least squares model for the regression of number of units sold on TV, newspaper, and radio advertising budgets in the **Advertising** data. Other information about this model was displayed in Table 3.4.

conclude that there is a relationship? It turns out that the answer depends on the values of n and p . When n is large, an F -statistic that is just a little larger than 1 might still provide evidence against H_0 . In contrast, a larger F -statistic is needed to reject H_0 if n is small. When H_0 is true and the errors ϵ_i have a normal distribution, the F -statistic follows an F -distribution.⁶ For any given value of n and p , any statistical software package can be used to compute the p -value associated with the F -statistic using this distribution. Based on this p -value, we can determine whether or not to reject H_0 . For the advertising data, the p -value associated with the F -statistic in Table 3.6 is essentially zero, so we have extremely strong evidence that at least one of the media is associated with increased **sales**.

In (3.23) we are testing H_0 that all the coefficients are zero. Sometimes we want to test that a particular subset of q of the coefficients are zero. This corresponds to a null hypothesis

$$H_0 : \beta_{p-q+1} = \beta_{p-q+2} = \cdots = \beta_p = 0,$$

where for convenience we have put the variables chosen for omission at the end of the list. In this case we fit a second model that uses all the variables *except* those last q . Suppose that the residual sum of squares for that model is RSS_0 . Then the appropriate F -statistic is

$$F = \frac{(\text{RSS}_0 - \text{RSS})/q}{\text{RSS}/(n - p - 1)}. \quad (3.24)$$

Notice that in Table 3.4, for each individual predictor a t -statistic and a p -value were reported. These provide information about whether each individual predictor is related to the response, after adjusting for the other predictors. It turns out that each of these is exactly equivalent⁷ to the F -test that omits that single variable from the model, leaving all the others in—i.e. $q=1$ in (3.24). So it reports the *partial effect* of adding that variable to the model. For instance, as we discussed earlier, these p -values indicate that **TV** and **radio** are related to **sales**, but that there is no evidence that **newspaper** is associated with **sales**, when **TV** and **radio** are held fixed.

Given these individual p -values for each variable, why do we need to look at the overall F -statistic? After all, it seems likely that if any one of the p -values for the individual variables is very small, then *at least one of the predictors is related to the response*. However, this logic is flawed, especially when the number of predictors p is large.

⁶Even if the errors are not normally-distributed, the F -statistic approximately follows an F -distribution provided that the sample size n is large.

⁷The square of each t -statistic is the corresponding F -statistic.

For instance, consider an example in which $p = 100$ and $H_0 : \beta_1 = \beta_2 = \dots = \beta_p = 0$ is true, so no variable is truly associated with the response. In this situation, about 5% of the p -values associated with each variable (of the type shown in Table 3.4) will be below 0.05 by chance. In other words, we expect to see approximately five *small* p -values even in the absence of any true association between the predictors and the response.⁸ In fact, it is likely that we will observe at least one p -value below 0.05 by chance! Hence, if we use the individual t -statistics and associated p -values in order to decide whether or not there is any association between the variables and the response, there is a very high chance that we will incorrectly conclude that there is a relationship. However, the F -statistic does not suffer from this problem because it adjusts for the number of predictors. Hence, if H_0 is true, there is only a 5% chance that the F -statistic will result in a p -value below 0.05, regardless of the number of predictors or the number of observations.

The approach of using an F -statistic to test for any association between the predictors and the response works when p is relatively small, and certainly small compared to n . However, sometimes we have a very large number of variables. If $p > n$ then there are more coefficients β_j to estimate than observations from which to estimate them. In this case we cannot even fit the multiple linear regression model using least squares, so the F -statistic cannot be used, and neither can most of the other concepts that we have seen so far in this chapter. When p is large, some of the approaches discussed in the next section, such as *forward selection*, can be used. This *high-dimensional* setting is discussed in greater detail in Chapter 6.

high-dimensional

Two: Deciding on Important Variables

As discussed in the previous section, the first step in a multiple regression analysis is to compute the F -statistic and to examine the associated p -value. If we conclude on the basis of that p -value that at least one of the predictors is related to the response, then it is natural to wonder *which* are the guilty ones! We could look at the individual p -values as in Table 3.4, but as discussed (and as further explored in Chapter 13), if p is large we are likely to make some false discoveries.

It is possible that all of the predictors are associated with the response, but it is more often the case that the response is only associated with a subset of the predictors. The task of determining which predictors are associated with the response, in order to fit a single model involving only those predictors, is referred to as *variable selection*. The variable selection problem is studied extensively in Chapter 6, and so here we will provide only a brief outline of some classical approaches.

variable selection

Ideally, we would like to perform variable selection by trying out a lot of different models, each containing a different subset of the predictors. For instance, if $p = 2$, then we can consider four models: (1) a model containing no variables, (2) a model containing X_1 only, (3) a model containing

⁸This is related to the important concept of *multiple testing*, which is the focus of Chapter 13.

X_2 only, and (4) a model containing both X_1 and X_2 . We can then select the *best* model out of all of the models that we have considered. How do we determine which model is best? Various statistics can be used to judge the quality of a model. These include *Mallow's C_p* , *Akaike information criterion* (AIC), *Bayesian information criterion* (BIC), and *adjusted R^2* . These are discussed in more detail in Chapter 6. We can also determine which model is best by plotting various model outputs, such as the residuals, in order to search for patterns.

Unfortunately, there are a total of 2^p models that contain subsets of p variables. This means that even for moderate p , trying out every possible subset of the predictors is infeasible. For instance, we saw that if $p = 2$, then there are $2^2 = 4$ models to consider. But if $p = 30$, then we must consider $2^{30} = 1,073,741,824$ models! This is not practical. Therefore, unless p is very small, we cannot consider all 2^p models, and instead we need an automated and efficient approach to choose a smaller set of models to consider. There are three classical approaches for this task:

- *Forward selection.* We begin with the *null model*—a model that contains an intercept but no predictors. We then fit p simple linear regressions and add to the null model the variable that results in the lowest RSS. We then add to that model the variable that results in the lowest RSS for the new two-variable model. This approach is continued until some stopping rule is satisfied.
- *Backward selection.* We start with all variables in the model, and remove the variable with the largest p -value—that is, the variable that is the least statistically significant. The new $(p - 1)$ -variable model is fit, and the variable with the largest p -value is removed. This procedure continues until a stopping rule is reached. For instance, we may stop when all remaining variables have a p -value below some threshold.
- *Mixed selection.* This is a combination of forward and backward selection. We start with no variables in the model, and as with forward selection, we add the variable that provides the best fit. We continue to add variables one-by-one. Of course, as we noted with the **Advertising** example, the p -values for variables can become larger as new predictors are added to the model. Hence, if at any point the p -value for one of the variables in the model rises above a certain threshold, then we remove that variable from the model. We continue to perform these forward and backward steps until all variables in the model have a sufficiently low p -value, and all variables outside the model would have a large p -value if added to the model.

Backward selection cannot be used if $p > n$, while forward selection can always be used. Forward selection is a greedy approach, and might include variables early that later become redundant. Mixed selection can remedy this.

Mallow's C_p
Akaike
information
criterion
Bayesian
information
criterion
adjusted R^2

forward
selection
null model

backward
selection

mixed
selection

Three: Model Fit

Two of the most common numerical measures of model fit are the RSE and R^2 , the fraction of variance explained. These quantities are computed and interpreted in the same fashion as for simple linear regression.

Recall that in simple regression, R^2 is the square of the correlation of the response and the variable. In multiple linear regression, it turns out that it equals $\text{Cor}(Y, \hat{Y})^2$, the square of the correlation between the response and the fitted linear model; in fact one property of the fitted linear model is that it maximizes this correlation among all possible linear models.

An R^2 value close to 1 indicates that the model explains a large portion of the variance in the response variable. As an example, we saw in Table 3.6 that for the `Advertising` data, the model that uses all three advertising media to predict `sales` has an R^2 of 0.8972. On the other hand, the model that uses only `TV` and `radio` to predict `sales` has an R^2 value of 0.89719. In other words, there is a *small* increase in R^2 if we include newspaper advertising in the model that already contains `TV` and `radio` advertising, even though we saw earlier that the p -value for newspaper advertising in Table 3.4 is not significant. It turns out that R^2 will always increase when more variables are added to the model, even if those variables are only weakly associated with the response. This is due to the fact that adding another variable always results in a decrease in the residual sum of squares on the training data (though not necessarily the testing data). Thus, the R^2 statistic, which is also computed on the training data, must increase. The fact that adding newspaper advertising to the model containing only `TV` and `radio` advertising leads to just a tiny increase in R^2 provides additional evidence that `newspaper` can be dropped from the model. Essentially, `newspaper` provides no real improvement in the model fit to the training samples, and its inclusion will likely lead to poor results on independent test samples due to overfitting.

By contrast, the model containing only `TV` as a predictor had an R^2 of 0.61 (Table 3.2). Adding `radio` to the model leads to a substantial improvement in R^2 . This implies that a model that uses `TV` and `radio` expenditures to predict `sales` is substantially better than one that uses only `TV` advertising. We could further quantify this improvement by looking at the p -value for the `radio` coefficient in a model that contains only `TV` and `radio` as predictors.

The model that contains only `TV` and `radio` as predictors has an RSE of 1.681, and the model that also contains `newspaper` as a predictor has an RSE of 1.686 (Table 3.6). In contrast, the model that contains only `TV` has an RSE of 3.26 (Table 3.2). This corroborates our previous conclusion that a model that uses `TV` and `radio` expenditures to predict `sales` is much more accurate (on the training data) than one that only uses `TV` spending. Furthermore, given that `TV` and `radio` expenditures are used as predictors, there is no point in also using `newspaper` spending as a predictor in the model. The observant reader may wonder how RSE can increase when `newspaper` is added to the model given that RSS must decrease. In general RSE is defined as

$$\text{RSE} = \sqrt{\frac{1}{n - p - 1} \text{RSS}}, \quad (3.25)$$

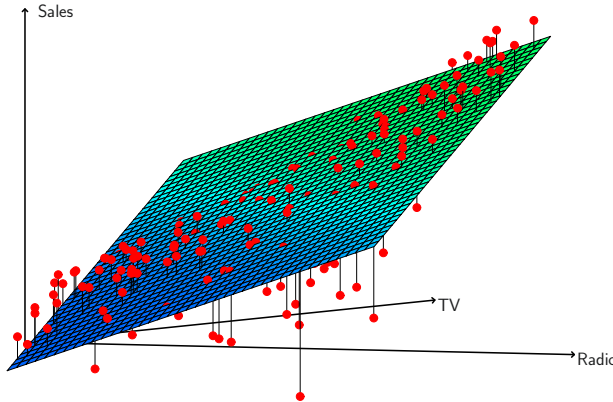


FIGURE 3.5. For the `Advertising` data, a linear regression fit to `sales` using `TV` and `radio` as predictors. From the pattern of the residuals, we can see that there is a pronounced non-linear relationship in the data. The positive residuals (those visible above the surface), tend to lie along the 45-degree line, where `TV` and `Radio` budgets are split evenly. The negative residuals (most not visible), tend to lie away from this line, where budgets are more lopsided.

which simplifies to (3.15) for a simple linear regression. Thus, models with more variables can have higher RSE if the decrease in RSS is small relative to the increase in p .

In addition to looking at the RSE and R^2 statistics just discussed, it can be useful to plot the data. Graphical summaries can reveal problems with a model that are not visible from numerical statistics. For example, Figure 3.5 displays a three-dimensional plot of `TV` and `radio` versus `sales`. We see that some observations lie above and some observations lie below the least squares regression plane. In particular, the linear model seems to overestimate `sales` for instances in which most of the advertising money was spent exclusively on either `TV` or `radio`. It underestimates `sales` for instances where the budget was split between the two media. This pronounced non-linear pattern suggests a *synergy* or *interaction* effect between the advertising media, whereby combining the media together results in a bigger boost to sales than using any single medium. In Section 3.3.2, we will discuss extending the linear model to accommodate such synergistic effects through the use of interaction terms.

interaction

Four: Predictions

Once we have fit the multiple regression model, it is straightforward to apply (3.21) in order to predict the response Y on the basis of a set of values for the predictors X_1, X_2, \dots, X_p . However, there are three sorts of uncertainty associated with this prediction.

1. The coefficient estimates $\hat{\beta}_0, \hat{\beta}_1, \dots, \hat{\beta}_p$ are estimates for $\beta_0, \beta_1, \dots, \beta_p$. That is, the *least squares plane*

$$\hat{Y} = \hat{\beta}_0 + \hat{\beta}_1 X_1 + \dots + \hat{\beta}_p X_p$$

is only an estimate for the *true population regression plane*

$$f(X) = \beta_0 + \beta_1 X_1 + \cdots + \beta_p X_p.$$

The inaccuracy in the coefficient estimates is related to the *reducible error* from Chapter 2. We can compute a *confidence interval* in order to determine how close \hat{Y} will be to $f(X)$.

2. Of course, in practice assuming a linear model for $f(X)$ is almost always an approximation of reality, so there is an additional source of potentially reducible error which we call *model bias*. So when we use a linear model, we are in fact estimating the best linear approximation to the true surface. However, here we will ignore this discrepancy, and operate as if the linear model were correct.
3. Even if we knew $f(X)$ —that is, even if we knew the true values for $\beta_0, \beta_1, \dots, \beta_p$ —the response value cannot be predicted perfectly because of the random error ϵ in the model (3.20). In Chapter 2, we referred to this as the *irreducible error*. How much will Y vary from \hat{Y} ? We use *prediction intervals* to answer this question. Prediction intervals are always wider than confidence intervals, because they incorporate both the error in the estimate for $f(X)$ (the reducible error) and the uncertainty as to how much an individual point will differ from the population regression plane (the irreducible error).

We use a *confidence interval* to quantify the uncertainty surrounding the *average sales* over a large number of cities. For example, given that \$100,000 is spent on **TV** advertising and \$20,000 is spent on **radio** advertising in each city, the 95 % confidence interval is [10,985, 11,528]. We interpret this to mean that 95 % of intervals of this form will contain the true value of $f(X)$.⁹ On the other hand, a *prediction interval* can be used to quantify the uncertainty surrounding **sales** for a *particular* city. Given that \$100,000 is spent on **TV** advertising and \$20,000 is spent on **radio** advertising in that city the 95 % prediction interval is [7,930, 14,580]. We interpret this to mean that 95 % of intervals of this form will contain the true value of Y for this city. Note that both intervals are centered at 11,256, but that the prediction interval is substantially wider than the confidence interval, reflecting the increased uncertainty about **sales** for a given city in comparison to the average **sales** over many locations.

confidence
interval

prediction
interval

⁹In other words, if we collect a large number of data sets like the **Advertising** data set, and we construct a confidence interval for the average **sales** on the basis of each data set (given \$100,000 in **TV** and \$20,000 in **radio** advertising), then 95 % of these confidence intervals will contain the true value of average **sales**.

3.3 Other Considerations in the Regression Model

3.3.1 Qualitative Predictors

In our discussion so far, we have assumed that all variables in our linear regression model are *quantitative*. But in practice, this is not necessarily the case; often some predictors are *qualitative*.

For example, the `Credit` data set displayed in Figure 3.6 records variables for a number of credit card holders. The response is `balance` (average credit card debt for each individual) and there are several quantitative predictors: `age`, `cards` (number of credit cards), `education` (years of education), `income` (in thousands of dollars), `limit` (credit limit), and `rating` (credit rating). Each panel of Figure 3.6 is a scatterplot for a pair of variables whose identities are given by the corresponding row and column labels. For example, the scatterplot directly to the right of the word “Balance” depicts `balance` versus `age`, while the plot directly to the right of “Age” corresponds to `age` versus `cards`. In addition to these quantitative variables, we also have four qualitative variables: `own` (house ownership), `student` (student status), `status` (marital status), and `region` (East, West or South).

Predictors with Only Two Levels

Suppose that we wish to investigate differences in credit card balance between those who own a house and those who don’t, ignoring the other variables for the moment. If a qualitative predictor (also known as a *factor*) only has two *levels*, or possible values, then incorporating it into a regression model is very simple. We simply create an indicator or *dummy variable* that takes on two possible numerical values.¹⁰ For example, based on the `own` variable, we can create a new variable that takes the form

$$x_i = \begin{cases} 1 & \text{if } i\text{th person owns a house} \\ 0 & \text{if } i\text{th person does not own a house,} \end{cases} \quad (3.26)$$

factor
level
dummy
variable

and use this variable as a predictor in the regression equation. This results in the model

$$y_i = \beta_0 + \beta_1 x_i + \epsilon_i = \begin{cases} \beta_0 + \beta_1 + \epsilon_i & \text{if } i\text{th person owns a house} \\ \beta_0 + \epsilon_i & \text{if } i\text{th person does not.} \end{cases} \quad (3.27)$$

Now β_0 can be interpreted as the average credit card balance among those who do not own, $\beta_0 + \beta_1$ as the average credit card balance among those who do own their house, and β_1 as the average difference in credit card balance between owners and non-owners.

Table 3.7 displays the coefficient estimates and other information associated with the model (3.27). The average credit card debt for non-owners is estimated to be \$509.80, whereas owners are estimated to carry \$19.73 in additional debt for a total of $\$509.80 + \$19.73 = \$529.53$. However, we

¹⁰In the machine learning community, the creation of dummy variables to handle qualitative predictors is known as “one-hot encoding”.

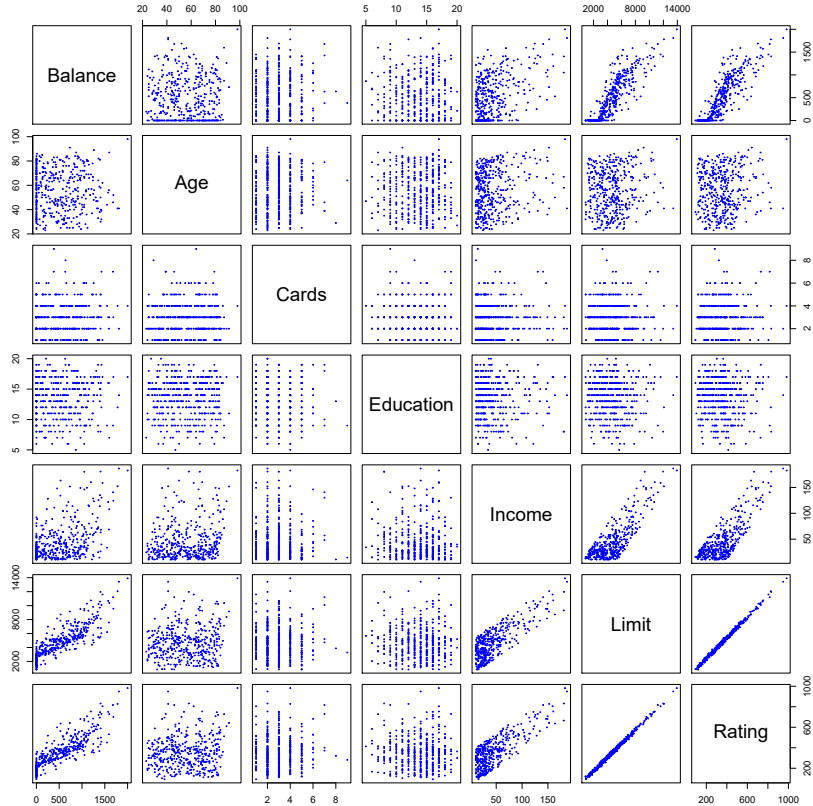


FIGURE 3.6. The Credit data set contains information about **balance**, **age**, **cards**, **education**, **income**, **limit**, and **rating** for a number of potential customers.

notice that the p -value for the dummy variable is very high. This indicates that there is no statistical evidence of a difference in average credit card balance based on house ownership.

The decision to code owners as 1 and non-owners as 0 in (3.27) is arbitrary, and has no effect on the regression fit, but does alter the interpretation of the coefficients. If we had coded non-owners as 1 and owners as 0, then the estimates for β_0 and β_1 would have been 529.53 and -19.73 , respectively, leading once again to a prediction of credit card debt of $\$529.53 - \$19.73 = \$509.80$ for non-owners and a prediction of $\$529.53$ for owners. Alternatively, instead of a 0/1 coding scheme, we could create a dummy variable

$$x_i = \begin{cases} 1 & \text{if } i\text{th person owns a house} \\ -1 & \text{if } i\text{th person does not own a house} \end{cases}$$

and use this variable in the regression equation. This results in the model

$$y_i = \beta_0 + \beta_1 x_i + \epsilon_i = \begin{cases} \beta_0 + \beta_1 + \epsilon_i & \text{if } i\text{th person owns a house} \\ \beta_0 - \beta_1 + \epsilon_i & \text{if } i\text{th person does not own a house.} \end{cases}$$

	Coefficient	Std. error	t-statistic	p-value
Intercept	509.80	33.13	15.389	< 0.0001
own [Yes]	19.73	46.05	0.429	0.6690

TABLE 3.7. Least squares coefficient estimates associated with the regression of `balance` onto `own` in the `Credit` data set. The linear model is given in (3.27). That is, ownership is encoded as a dummy variable, as in (3.26).

Now β_0 can be interpreted as the overall average credit card balance (ignoring the house ownership effect), and β_1 is the amount by which house owners and non-owners have credit card balances that are above and below the average, respectively.¹¹ In this example, the estimate for β_0 is \$519.665, halfway between the non-owner and owner averages of \$509.80 and \$529.53. The estimate for β_1 is \$9.865, which is half of \$19.73, the average difference between owners and non-owners. It is important to note that the final predictions for the credit balances of owners and non-owners will be identical regardless of the coding scheme used. The only difference is in the way that the coefficients are interpreted.

Qualitative Predictors with More than Two Levels

When a qualitative predictor has more than two levels, a single dummy variable cannot represent all possible values. In this situation, we can create additional dummy variables. For example, for the `region` variable we create two dummy variables. The first could be

$$x_{i1} = \begin{cases} 1 & \text{if } i\text{th person is from the South} \\ 0 & \text{if } i\text{th person is not from the South,} \end{cases} \quad (3.28)$$

and the second could be

$$x_{i2} = \begin{cases} 1 & \text{if } i\text{th person is from the West} \\ 0 & \text{if } i\text{th person is not from the West.} \end{cases} \quad (3.29)$$

Then both of these variables can be used in the regression equation, in order to obtain the model

$$y_i = \beta_0 + \beta_1 x_{i1} + \beta_2 x_{i2} + \epsilon_i = \begin{cases} \beta_0 + \beta_1 + \epsilon_i & \text{if } i\text{th person is from the South} \\ \beta_0 + \beta_2 + \epsilon_i & \text{if } i\text{th person is from the West} \\ \beta_0 + \epsilon_i & \text{if } i\text{th person is from the East.} \end{cases} \quad (3.30)$$

Now β_0 can be interpreted as the average credit card balance for individuals from the East, β_1 can be interpreted as the difference in the average balance between people from the South versus the East, and β_2 can be interpreted as the difference in the average balance between those from the West versus the East. There will always be one fewer dummy variable than the number of levels. The level with no dummy variable—East in this example—is known as the *baseline*.

baseline

¹¹Technically β_0 is half the sum of the average debt for house owners and the average debt for non-house owners. Hence, β_0 is exactly equal to the overall average only if the two groups have an equal number of members.

	Coefficient	Std. error	t-statistic	p-value
Intercept	531.00	46.32	11.464	< 0.0001
region[South]	-12.50	56.68	-0.221	0.8260
region[West]	-18.69	65.02	-0.287	0.7740

TABLE 3.8. Least squares coefficient estimates associated with the regression of `balance` onto `region` in the `Credit` data set. The linear model is given in (3.30). That is, `region` is encoded via two dummy variables (3.28) and (3.29).

From Table 3.8, we see that the estimated `balance` for the baseline, East, is \$531.00. It is estimated that those in the South will have \$18.69 less debt than those in the East, and that those in the West will have \$12.50 less debt than those in the East. However, the *p*-values associated with the coefficient estimates for the two dummy variables are very large, suggesting no statistical evidence of a real difference in average credit card balance between South and East or between West and East.¹² Once again, the level selected as the baseline category is arbitrary, and the final predictions for each group will be the same regardless of this choice. However, the coefficients and their *p*-values do depend on the choice of dummy variable coding. Rather than rely on the individual coefficients, we can use an *F*-test to test $H_0 : \beta_1 = \beta_2 = 0$; this does not depend on the coding. This *F*-test has a *p*-value of 0.96, indicating that we cannot reject the null hypothesis that there is no relationship between `balance` and `region`.

Using this dummy variable approach presents no difficulties when incorporating both quantitative and qualitative predictors. For example, to regress `balance` on both a quantitative variable such as `income` and a qualitative variable such as `student`, we must simply create a dummy variable for `student` and then fit a multiple regression model using `income` and the dummy variable as predictors for credit card balance.

There are many different ways of coding qualitative variables besides the dummy variable approach taken here. All of these approaches lead to equivalent model fits, but the coefficients are different and have different interpretations, and are designed to measure particular *contrasts*. This topic

contrast

3.3.2 Extensions of the Linear Model

The standard linear regression model (3.19) provides interpretable results and works quite well on many real-world problems. However, it makes several highly restrictive assumptions that are often violated in practice. Two of the most important assumptions state that the relationship between the predictors and response are *additive* and *linear*. The additivity assumption means that the association between a predictor X_j and the response Y does not depend on the values of the other predictors. The linearity assumption states that the change in the response Y associated with a one-unit change in X_j is constant, regardless of the value of X_j . In later chapters of this book, we examine a number of sophisticated methods that relax these two

additive
linear

¹²There could still in theory be a difference between South and West, although the data here does not suggest any difference.

assumptions. Here, we briefly examine some common classical approaches for extending the linear model.

Removing the Additive Assumption

In our previous analysis of the `Advertising` data, we concluded that both `TV` and `radio` seem to be associated with `sales`. The linear models that formed the basis for this conclusion assumed that the effect on `sales` of increasing one advertising medium is independent of the amount spent on the other media. For example, the linear model (3.20) states that the average increase in `sales` associated with a one-unit increase in `TV` is always β_1 , regardless of the amount spent on `radio`.

However, this simple model may be incorrect. Suppose that spending money on radio advertising actually increases the effectiveness of TV advertising, so that the slope term for `TV` should increase as `radio` increases. In this situation, given a fixed budget of \$100,000, spending half on `radio` and half on `TV` may increase `sales` more than allocating the entire amount to either `TV` or to `radio`. In marketing, this is known as a *synergy* effect, and in statistics it is referred to as an *interaction* effect. Figure 3.5 suggests that such an effect may be present in the advertising data. Notice that when levels of either `TV` or `radio` are low, then the true `sales` are lower than predicted by the linear model. But when advertising is split between the two media, then the model tends to underestimate `sales`.

Consider the standard linear regression model with two variables,

$$Y = \beta_0 + \beta_1 X_1 + \beta_2 X_2 + \epsilon.$$

According to this model, a one-unit increase in X_1 is associated with an average increase in Y of β_1 units. Notice that the presence of X_2 does not alter this statement—that is, regardless of the value of X_2 , a one-unit increase in X_1 is associated with a β_1 -unit increase in Y . One way of extending this model is to include a third predictor, called an *interaction term*, which is constructed by computing the product of X_1 and X_2 . This results in the model

$$Y = \beta_0 + \beta_1 X_1 + \beta_2 X_2 + \beta_3 X_1 X_2 + \epsilon. \quad (3.31)$$

How does inclusion of this interaction term relax the additive assumption? Notice that (3.31) can be rewritten as

$$\begin{aligned} Y &= \beta_0 + (\beta_1 + \beta_3 X_2) X_1 + \beta_2 X_2 + \epsilon \\ &= \beta_0 + \tilde{\beta}_1 X_1 + \beta_2 X_2 + \epsilon \end{aligned} \quad (3.32)$$

where $\tilde{\beta}_1 = \beta_1 + \beta_3 X_2$. Since $\tilde{\beta}_1$ is now a function of X_2 , the association between X_1 and Y is no longer constant: a change in the value of X_2 will change the association between X_1 and Y . A similar argument shows that a change in the value of X_1 changes the association between X_2 and Y .

For example, suppose that we are interested in studying the productivity of a factory. We wish to predict the number of `units` produced on the basis of the number of production `lines` and the total number of `workers`. It seems likely that the effect of increasing the number of production lines

	Coefficient	Std. error	<i>t</i> -statistic	<i>p</i> -value
Intercept	6.7502	0.248	27.23	< 0.0001
TV	0.0191	0.002	12.70	< 0.0001
radio	0.0289	0.009	3.24	0.0014
TV×radio	0.0011	0.000	20.73	< 0.0001

TABLE 3.9. For the *Advertising* data, least squares coefficient estimates associated with the regression of **sales** onto **TV** and **radio**, with an interaction term, as in (3.33).

will depend on the number of workers, since if no workers are available to operate the lines, then increasing the number of lines will not increase production. This suggests that it would be appropriate to include an interaction term between **lines** and **workers** in a linear model to predict **units**. Suppose that when we fit the model, we obtain

$$\begin{aligned} \text{units} &\approx 1.2 + 3.4 \times \text{lines} + 0.22 \times \text{workers} + 1.4 \times (\text{lines} \times \text{workers}) \\ &= 1.2 + (3.4 + 1.4 \times \text{workers}) \times \text{lines} + 0.22 \times \text{workers}. \end{aligned}$$

In other words, adding an additional line will increase the number of units produced by $3.4 + 1.4 \times \text{workers}$. Hence the more **workers** we have, the stronger will be the effect of **lines**.

We now return to the *Advertising* example. A linear model that uses **radio**, **TV**, and an interaction between the two to predict **sales** takes the form

$$\begin{aligned} \text{sales} &= \beta_0 + \beta_1 \times \text{TV} + \beta_2 \times \text{radio} + \beta_3 \times (\text{radio} \times \text{TV}) + \epsilon \\ &= \beta_0 + (\beta_1 + \beta_3 \times \text{radio}) \times \text{TV} + \beta_2 \times \text{radio} + \epsilon. \end{aligned} \quad (3.33)$$

We can interpret β_3 as the increase in the effectiveness of TV advertising associated with a one-unit increase in radio advertising (or vice-versa). The coefficients that result from fitting the model (3.33) are given in Table 3.9.

The results in Table 3.9 strongly suggest that the model that includes the interaction term is superior to the model that contains only *main effects*. The *p*-value for the interaction term, **TV**×**radio**, is extremely low, indicating that there is strong evidence for $H_a : \beta_3 \neq 0$. In other words, it is clear that the true relationship is not additive. The R^2 for the model (3.33) is 96.8 %, compared to only 89.7 % for the model that predicts **sales** using **TV** and **radio** without an interaction term. This means that $(96.8 - 89.7)/(100 - 89.7) = 69\%$ of the variability in **sales** that remains after fitting the additive model has been explained by the interaction term. The coefficient estimates in Table 3.9 suggest that an increase in TV advertising of \$1,000 is associated with increased sales of $(\hat{\beta}_1 + \hat{\beta}_3 \times \text{radio}) \times 1,000 = 19 + 1.1 \times \text{radio}$ units. And an increase in radio advertising of \$1,000 will be associated with an increase in sales of $(\hat{\beta}_2 + \hat{\beta}_3 \times \text{TV}) \times 1,000 = 29 + 1.1 \times \text{TV}$ units.

In this example, the *p*-values associated with **TV**, **radio**, and the interaction term all are statistically significant (Table 3.9), and so it is obvious that all three variables should be included in the model. However, it is sometimes the case that an interaction term has a very small *p*-value, but the associated main effects (in this case, **TV** and **radio**) do not. The *hierarchical principle* states that *if we include an interaction in a model, we*

main effect

hierarchical principle

should also include the main effects, even if the *p*-values associated with their coefficients are not significant. In other words, if the interaction between X_1 and X_2 seems important, then we should include both X_1 and X_2 in the model even if their coefficient estimates have large *p*-values. The rationale for this principle is that if $X_1 \times X_2$ is related to the response, then whether or not the coefficients of X_1 or X_2 are exactly zero is of little interest. Also $X_1 \times X_2$ is typically correlated with X_1 and X_2 , and so leaving them out tends to alter the meaning of the interaction.

In the previous example, we considered an interaction between `TV` and `radio`, both of which are quantitative variables. However, the concept of interactions applies just as well to qualitative variables, or to a combination of quantitative and qualitative variables. In fact, an interaction between a qualitative variable and a quantitative variable has a particularly nice interpretation. Consider the `Credit` data set from Section 3.3.1, and suppose that we wish to predict `balance` using the `income` (quantitative) and `student` (qualitative) variables. In the absence of an interaction term, the model takes the form

$$\begin{aligned} \text{balance}_i &\approx \beta_0 + \beta_1 \times \text{income}_i + \begin{cases} \beta_2 & \text{if } i\text{th person is a student} \\ 0 & \text{if } i\text{th person is not a student} \end{cases} \\ &= \beta_1 \times \text{income}_i + \begin{cases} \beta_0 + \beta_2 & \text{if } i\text{th person is a student} \\ \beta_0 & \text{if } i\text{th person is not a student.} \end{cases} \end{aligned} \quad (3.34)$$

Notice that this amounts to fitting two parallel lines to the data, one for students and one for non-students. The lines for students and non-students have different intercepts, $\beta_0 + \beta_2$ versus β_0 , but the same slope, β_1 . This is illustrated in the left-hand panel of Figure 3.7. The fact that the lines are parallel means that the average effect on `balance` of a one-unit increase in `income` does not depend on whether or not the individual is a student. This represents a potentially serious limitation of the model, since in fact a change in `income` may have a very different effect on the credit card balance of a student versus a non-student.

This limitation can be addressed by adding an interaction variable, created by multiplying `income` with the dummy variable for `student`. Our model now becomes

$$\begin{aligned} \text{balance}_i &\approx \beta_0 + \beta_1 \times \text{income}_i + \begin{cases} \beta_2 + \beta_3 \times \text{income}_i & \text{if student} \\ 0 & \text{if not student} \end{cases} \\ &= \begin{cases} (\beta_0 + \beta_2) + (\beta_1 + \beta_3) \times \text{income}_i & \text{if student} \\ \beta_0 + \beta_1 \times \text{income}_i & \text{if not student.} \end{cases} \end{aligned} \quad (3.35)$$

Once again, we have two different regression lines for the students and the non-students. But now those regression lines have different intercepts, $\beta_0 + \beta_2$ versus β_0 , as well as different slopes, $\beta_1 + \beta_3$ versus β_1 . This allows for the possibility that changes in income may affect the credit card balances of students and non-students differently. The right-hand panel of Figure 3.7

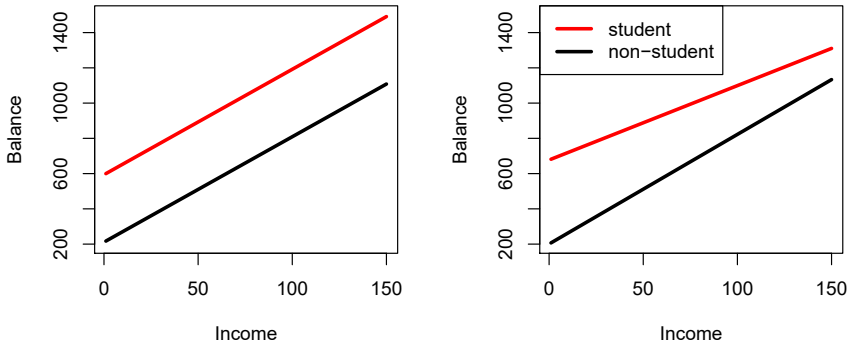


FIGURE 3.7. For the `Credit` data, the least squares lines are shown for prediction of `balance` from `income` for students and non-students. Left: The model (3.34) was fit. There is no interaction between `income` and `student`. Right: The model (3.35) was fit. There is an interaction term between `income` and `student`.

shows the estimated relationships between `income` and `balance` for students and non-students in the model (3.35). We note that the slope for students is lower than the slope for non-students. This suggests that increases in income are associated with smaller increases in credit card balance among students as compared to non-students.

Non-linear Relationships

As discussed previously, the linear regression model (3.19) assumes a linear relationship between the response and predictors. But in some cases, the true relationship between the response and the predictors may be non-linear. Here we present a very simple way to directly extend the linear model to accommodate non-linear relationships, using *polynomial regression*. In later chapters, we will present more complex approaches for performing non-linear fits in more general settings.

polynomial regression

Consider Figure 3.8, in which the `mpg` (gas mileage in miles per gallon) versus `horsepower` is shown for a number of cars in the `Auto` data set. The orange line represents the linear regression fit. There is a pronounced relationship between `mpg` and `horsepower`, but it seems clear that this relationship is in fact non-linear: the data suggest a curved relationship. A simple approach for incorporating non-linear associations in a linear model is to include transformed versions of the predictors. For example, the points in Figure 3.8 seem to have a *quadratic* shape, suggesting that a model of the form

$$\text{mpg} = \beta_0 + \beta_1 \times \text{horsepower} + \beta_2 \times \text{horsepower}^2 + \epsilon \quad (3.36)$$

quadratic

may provide a better fit. Equation 3.36 involves predicting `mpg` using a non-linear function of `horsepower`. *But it is still a linear model!* That is, (3.36) is simply a multiple linear regression model with $X_1 = \text{horsepower}$ and $X_2 = \text{horsepower}^2$. So we can use standard linear regression software to estimate β_0 , β_1 , and β_2 in order to produce a non-linear fit. The blue curve in Figure 3.8 shows the resulting quadratic fit to the data. The quadratic

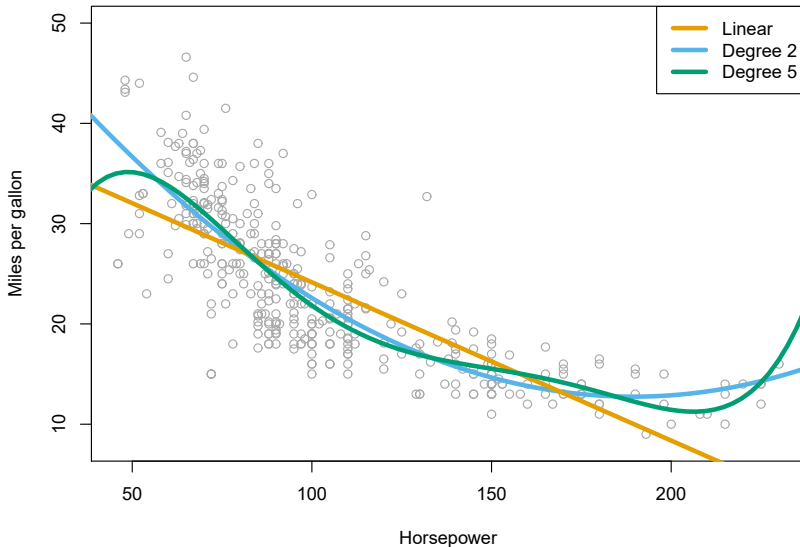


FIGURE 3.8. The `Auto` data set. For a number of cars, `mpg` and `horsepower` are shown. The linear regression fit is shown in orange. The linear regression fit for a model that includes `horsepower`² is shown as a blue curve. The linear regression fit for a model that includes all polynomials of `horsepower` up to fifth-degree is shown in green.

	Coefficient	Std. error	t-statistic	p-value
<code>Intercept</code>	56.9001	1.8004	31.6	< 0.0001
<code>horsepower</code>	-0.4662	0.0311	-15.0	< 0.0001
<code>horsepower</code> ²	0.0012	0.0001	10.1	< 0.0001

TABLE 3.10. For the `Auto` data set, least squares coefficient estimates associated with the regression of `mpg` onto `horsepower` and `horsepower`².

fit appears to be substantially better than the fit obtained when just the linear term is included. The R^2 of the quadratic fit is 0.688, compared to 0.606 for the linear fit, and the p -value in Table 3.10 for the quadratic term is highly significant.

If including `horsepower`² led to such a big improvement in the model, why not include `horsepower`³, `horsepower`⁴, or even `horsepower`⁵? The green curve in Figure 3.8 displays the fit that results from including all polynomials up to fifth degree in the model (3.36). The resulting fit seems unnecessarily wiggly—that is, it is unclear that including the additional terms really has led to a better fit to the data.

The approach that we have just described for extending the linear model to accommodate non-linear relationships is known as *polynomial regression*, since we have included polynomial functions of the predictors in the regression model. We further explore this approach and other non-linear extensions of the linear model in Chapter 7.

3.3.3 Potential Problems

When we fit a linear regression model to a particular data set, many problems may occur. Most common among these are the following:

1. *Non-linearity of the response-predictor relationships.*
2. *Correlation of error terms.*
3. *Non-constant variance of error terms.*
4. *Outliers.*
5. *High-leverage points.*
6. *Collinearity.*

In practice, identifying and overcoming these problems is as much an art as a science. Many pages in countless books have been written on this topic. Since the linear regression model is not our primary focus here, we will provide only a brief summary of some key points.

1. Non-linearity of the Data

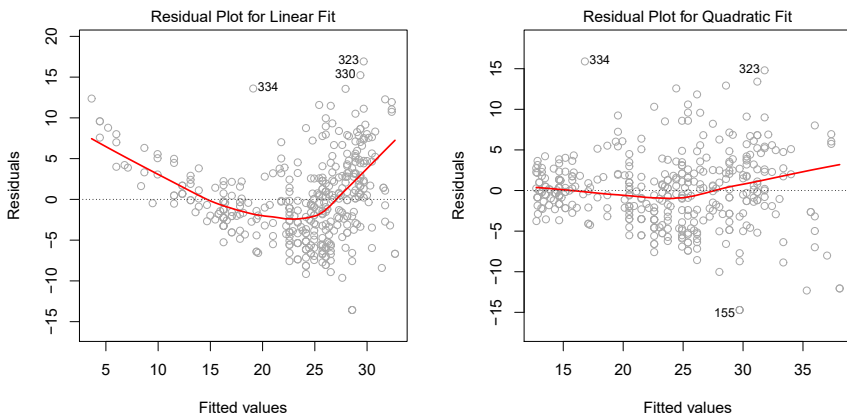


FIGURE 3.9. Plots of residuals versus predicted (or fitted) values for the `Auto` data set. In each plot, the red line is a smooth fit to the residuals, intended to make it easier to identify a trend. Left: A linear regression of `mpg` on `horsepower`. A strong pattern in the residuals indicates non-linearity in the data. Right: A linear regression of `mpg` on `horsepower` and `horsepower`². There is little pattern in the residuals.

The linear regression model assumes that there is a straight-line relationship between the predictors and the response. If the true relationship is far from linear, then virtually all of the conclusions that we draw from the fit are suspect. In addition, the prediction accuracy of the model can be significantly reduced.

Residual plots are a useful graphical tool for identifying non-linearity. Given a simple linear regression model, we can plot the residuals, $e_i =$

residual plot

$y_i - \hat{y}_i$, versus the predictor x_i . In the case of a multiple regression model, since there are multiple predictors, we instead plot the residuals versus the predicted (or *fitted*) values \hat{y}_i . Ideally, the residual plot will show no discernible pattern. The presence of a pattern may indicate a problem with some aspect of the linear model.

The left panel of Figure 3.9 displays a residual plot from the linear regression of `mpg` onto `horsepower` on the `Auto` data set that was illustrated in Figure 3.8. The red line is a smooth fit to the residuals, which is displayed in order to make it easier to identify any trends. The residuals exhibit a clear U-shape, which provides a strong indication of non-linearity in the data. In contrast, the right-hand panel of Figure 3.9 displays the residual plot that results from the model (3.36), which contains a quadratic term. There appears to be little pattern in the residuals, suggesting that the quadratic term improves the fit to the data.

If the residual plot indicates that there are non-linear associations in the data, then a simple approach is to use non-linear transformations of the predictors, such as $\log X$, \sqrt{X} , and X^2 , in the regression model. In the later chapters of this book, we will discuss other more advanced non-linear approaches for addressing this issue.

2. Correlation of Error Terms

An important assumption of the linear regression model is that the error terms, $\epsilon_1, \epsilon_2, \dots, \epsilon_n$, are uncorrelated. What does this mean? For instance, if the errors are uncorrelated, then the fact that ϵ_i is positive provides little or no information about the sign of ϵ_{i+1} . The standard errors that are computed for the estimated regression coefficients or the fitted values are based on the assumption of uncorrelated error terms. If in fact there is correlation among the error terms, then the estimated standard errors will tend to underestimate the true standard errors. As a result, confidence and prediction intervals will be narrower than they should be. For example, a 95% confidence interval may in reality have a much lower probability than 0.95 of containing the true value of the parameter. In addition, *p*-values associated with the model will be lower than they should be; this could cause us to erroneously conclude that a parameter is statistically significant. In short, if the error terms are correlated, we may have an unwarranted sense of confidence in our model.

As an extreme example, suppose we accidentally doubled our data, leading to observations and error terms identical in pairs. If we ignored this, our standard error calculations would be as if we had a sample of size $2n$, when in fact we have only n samples. Our estimated parameters would be the same for the $2n$ samples as for the n samples, but the confidence intervals would be narrower by a factor of $\sqrt{2}$!

Why might correlations among the error terms occur? Such correlations frequently occur in the context of *time series* data, which consists of observations for which measurements are obtained at discrete points in time. In many cases, observations that are obtained at adjacent time points will have positively correlated errors. In order to determine if this is the case for a given data set, we can plot the residuals from our model as a function of time. If the errors are uncorrelated, then there should be no discernible pat-

time series

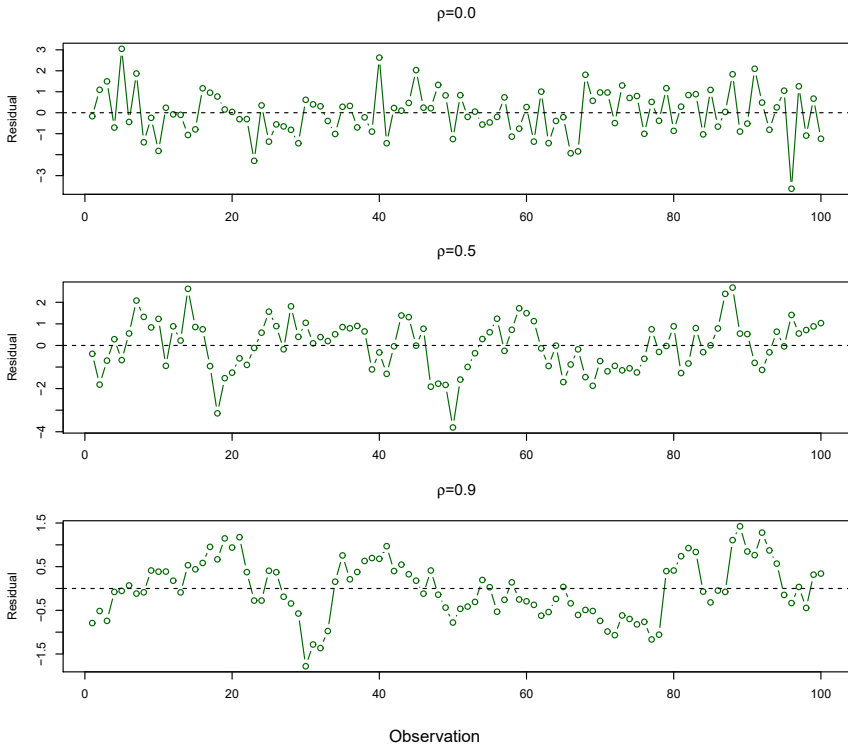


FIGURE 3.10. Plots of residuals from simulated time series data sets generated with differing levels of correlation ρ between error terms for adjacent time points.

tern. On the other hand, if the error terms are positively correlated, then we may see *tracking* in the residuals—that is, adjacent residuals may have similar values. Figure 3.10 provides an illustration. In the top panel, we see the residuals from a linear regression fit to data generated with uncorrelated errors. There is no evidence of a time-related trend in the residuals. In contrast, the residuals in the bottom panel are from a data set in which adjacent errors had a correlation of 0.9. Now there is a clear pattern in the residuals—adjacent residuals tend to take on similar values. Finally, the center panel illustrates a more moderate case in which the residuals had a correlation of 0.5. There is still evidence of tracking, but the pattern is less clear.

tracking

Many methods have been developed to properly take account of correlations in the error terms in time series data. Correlation among the error terms can also occur outside of time series data. For instance, consider a study in which individuals' heights are predicted from their weights. The assumption of uncorrelated errors could be violated if some of the individuals in the study are members of the same family, eat the same diet, or have been exposed to the same environmental factors. In general, the assumption of uncorrelated errors is extremely important for linear regression as well as for other statistical methods, and good experimental design is crucial in order to mitigate the risk of such correlations.

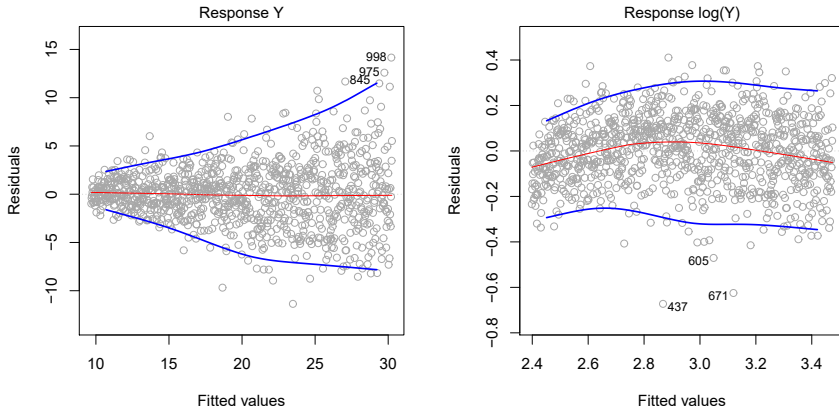


FIGURE 3.11. Residual plots. In each plot, the red line is a smooth fit to the residuals, intended to make it easier to identify a trend. The blue lines track the outer quantiles of the residuals, and emphasize patterns. Left: The funnel shape indicates heteroscedasticity. Right: The response has been log transformed, and there is now no evidence of heteroscedasticity.

3. Non-constant Variance of Error Terms

Another important assumption of the linear regression model is that the error terms have a constant variance, $\text{Var}(\epsilon_i) = \sigma^2$. The standard errors, confidence intervals, and hypothesis tests associated with the linear model rely upon this assumption.

Unfortunately, it is often the case that the variances of the error terms are non-constant. For instance, the variances of the error terms may increase with the value of the response. One can identify non-constant variances in the errors, or *heteroscedasticity*, from the presence of a *funnel shape* in the residual plot. An example is shown in the left-hand panel of Figure 3.11, in which the magnitude of the residuals tends to increase with the fitted values. When faced with this problem, one possible solution is to transform the response Y using a concave function such as $\log Y$ or \sqrt{Y} . Such a transformation results in a greater amount of shrinkage of the larger responses, leading to a reduction in heteroscedasticity. The right-hand panel of Figure 3.11 displays the residual plot after transforming the response using $\log Y$. The residuals now appear to have constant variance, though there is some evidence of a slight non-linear relationship in the data.

Sometimes we have a good idea of the variance of each response. For example, the i th response could be an average of n_i raw observations. If each of these raw observations is uncorrelated with variance σ^2 , then their average has variance $\sigma_i^2 = \sigma^2/n_i$. In this case a simple remedy is to fit our model by *weighted least squares*, with weights proportional to the inverse variances—i.e. $w_i = n_i$ in this case. Most linear regression software allows for observation weights.

heteroscedasticity

weighted least squares

4. Outliers

An *outlier* is a point for which y_i is far from the value predicted by the outlier

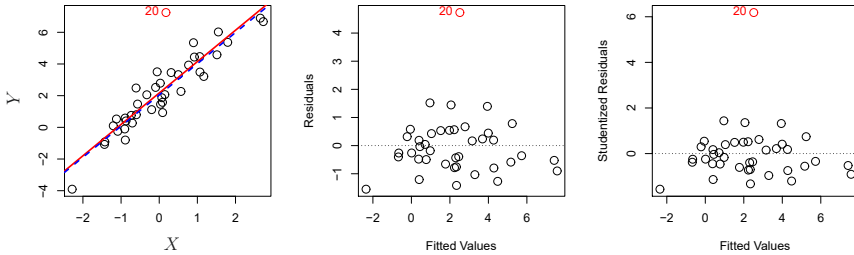


FIGURE 3.12. Left: The least squares regression line is shown in red, and the regression line after removing the outlier is shown in blue. Center: The residual plot clearly identifies the outlier. Right: The outlier has a studentized residual of 6; typically we expect values between -3 and 3 .

model. Outliers can arise for a variety of reasons, such as incorrect recording of an observation during data collection.

The red point (observation 20) in the left-hand panel of Figure 3.12 illustrates a typical outlier. The red solid line is the least squares regression fit, while the blue dashed line is the least squares fit after removal of the outlier. In this case, removing the outlier has little effect on the least squares line: it leads to almost no change in the slope, and a minuscule reduction in the intercept. It is typical for an outlier that does not have an unusual predictor value to have little effect on the least squares fit. However, even if an outlier does not have much effect on the least squares fit, it can cause other problems. For instance, in this example, the RSE is 1.09 when the outlier is included in the regression, but it is only 0.77 when the outlier is removed. Since the RSE is used to compute all confidence intervals and p -values, such a dramatic increase caused by a single data point can have implications for the interpretation of the fit. Similarly, inclusion of the outlier causes the R^2 to decline from 0.892 to 0.805.

Residual plots can be used to identify outliers. In this example, the outlier is clearly visible in the residual plot illustrated in the center panel of Figure 3.12. But in practice, it can be difficult to decide how large a residual needs to be before we consider the point to be an outlier. To address this problem, instead of plotting the residuals, we can plot the *studentized residuals*, computed by dividing each residual e_i by its estimated standard error. Observations whose studentized residuals are greater than 3 in absolute value are possible outliers. In the right-hand panel of Figure 3.12, the outlier's studentized residual exceeds 6, while all other observations have studentized residuals between -2 and 2 .

studentized residual

If we believe that an outlier has occurred due to an error in data collection or recording, then one solution is to simply remove the observation. However, care should be taken, since an outlier may instead indicate a deficiency with the model, such as a missing predictor.

5. High Leverage Points

We just saw that outliers are observations for which the response y_i is unusual given the predictor x_i . In contrast, observations with *high leverage* have an unusual value for x_i . For example, observation 41 in the left-hand

high leverage

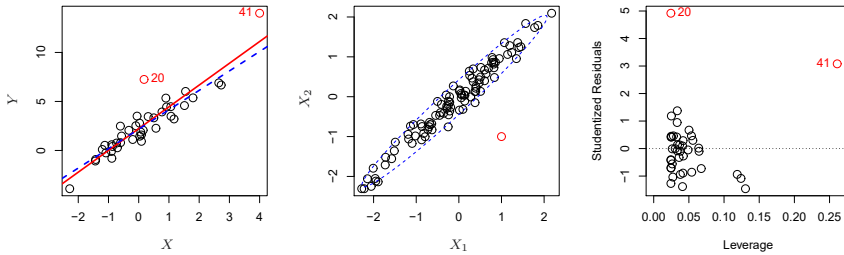


FIGURE 3.13. Left: Observation 41 is a high leverage point, while 20 is not. The red line is the fit to all the data, and the blue line is the fit with observation 41 removed. Center: The red observation is not unusual in terms of its X_1 value or its X_2 value, but still falls outside the bulk of the data, and hence has high leverage. Right: Observation 41 has a high leverage and a high residual.

panel of Figure 3.13 has high leverage, in that the predictor value for this observation is large relative to the other observations. (Note that the data displayed in Figure 3.13 are the same as the data displayed in Figure 3.12, but with the addition of a single high leverage observation.) The red solid line is the least squares fit to the data, while the blue dashed line is the fit produced when observation 41 is removed. Comparing the left-hand panels of Figures 3.12 and 3.13, we observe that removing the high leverage observation has a much more substantial impact on the least squares line than removing the outlier. In fact, high leverage observations tend to have a sizable impact on the estimated regression line. It is cause for concern if the least squares line is heavily affected by just a couple of observations, because any problems with these points may invalidate the entire fit. For this reason, it is important to identify high leverage observations.

In a simple linear regression, high leverage observations are fairly easy to identify, since we can simply look for observations for which the predictor value is outside of the normal range of the observations. But in a multiple linear regression with many predictors, it is possible to have an observation that is well within the range of each individual predictor's values, but that is unusual in terms of the full set of predictors. An example is shown in the center panel of Figure 3.13, for a data set with two predictors, X_1 and X_2 . Most of the observations' predictor values fall within the blue dashed ellipse, but the red observation is well outside of this range. But neither its value for X_1 nor its value for X_2 is unusual. So if we examine just X_1 or just X_2 , we will fail to notice this high leverage point. This problem is more pronounced in multiple regression settings with more than two predictors, because then there is no simple way to plot all dimensions of the data simultaneously.

In order to quantify an observation's leverage, we compute the *leverage statistic*. A large value of this statistic indicates an observation with high leverage. For a simple linear regression,

leverage
statistic

$$h_i = \frac{1}{n} + \frac{(x_i - \bar{x})^2}{\sum_{i'=1}^n (x_{i'} - \bar{x})^2}. \quad (3.37)$$

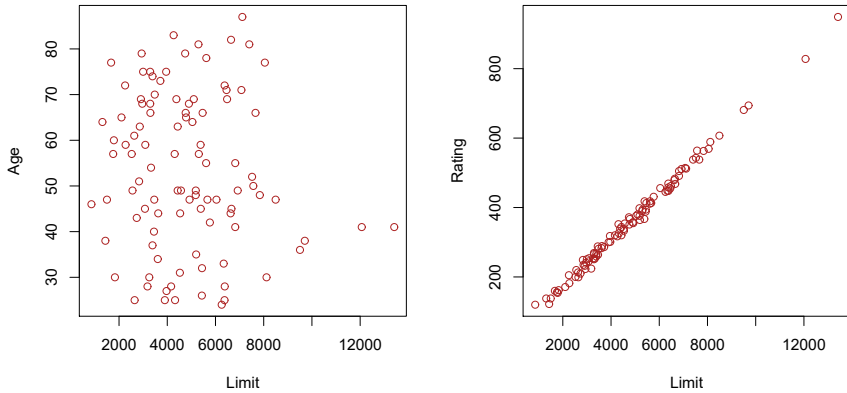


FIGURE 3.14. Scatterplots of the observations from the `Credit` data set. Left: A plot of `age` versus `limit`. These two variables are not collinear. Right: A plot of `rating` versus `limit`. There is high collinearity.

It is clear from this equation that h_i increases with the distance of x_i from \bar{x} . There is a simple extension of h_i to the case of multiple predictors, though we do not provide the formula here. The leverage statistic h_i is always between $1/n$ and 1, and the average leverage for all the observations is always equal to $(p+1)/n$. So if a given observation has a leverage statistic that greatly exceeds $(p+1)/n$, then we may suspect that the corresponding point has high leverage.

The right-hand panel of Figure 3.13 provides a plot of the studentized residuals versus h_i for the data in the left-hand panel of Figure 3.13. Observation 41 stands out as having a very high leverage statistic as well as a high studentized residual. In other words, it is an outlier as well as a high leverage observation. This is a particularly dangerous combination! This plot also reveals the reason that observation 20 had relatively little effect on the least squares fit in Figure 3.12: it has low leverage.

6. Collinearity

Collinearity refers to the situation in which two or more predictor variables are closely related to one another. The concept of collinearity is illustrated in Figure 3.14 using the `Credit` data set. In the left-hand panel of Figure 3.14, the two predictors `limit` and `age` appear to have no obvious relationship. In contrast, in the right-hand panel of Figure 3.14, the predictors `limit` and `rating` are very highly correlated with each other, and we say that they are *collinear*. The presence of collinearity can pose problems in the regression context, since it can be difficult to separate out the individual effects of collinear variables on the response. In other words, since `limit` and `rating` tend to increase or decrease together, it can be difficult to determine how each one separately is associated with the response, `balance`.

collinearity

Figure 3.15 illustrates some of the difficulties that can result from collinearity. The left-hand panel of Figure 3.15 is a contour plot of the RSS (3.22) associated with different possible coefficient estimates for the regression of `balance` on `limit` and `age`. Each ellipse represents a set of coefficients

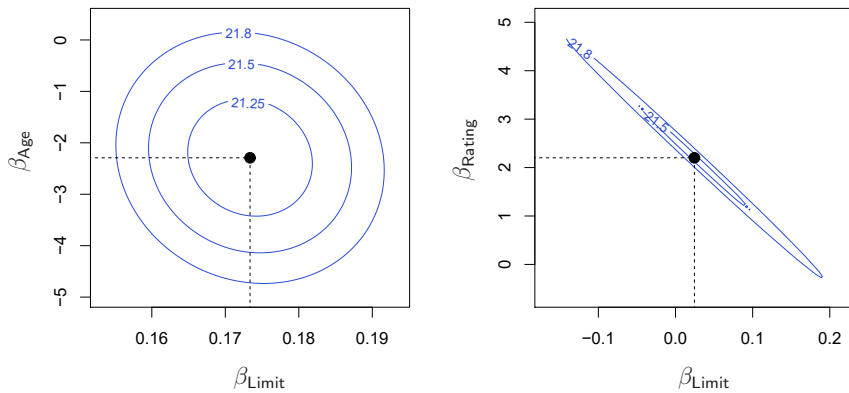


FIGURE 3.15. Contour plots for the RSS values as a function of the parameters β for various regressions involving the `Credit` data set. In each plot, the black dots represent the coefficient values corresponding to the minimum RSS. Left: A contour plot of RSS for the regression of `balance` onto `age` and `limit`. The minimum value is well defined. Right: A contour plot of RSS for the regression of `balance` onto `rating` and `limit`. Because of the collinearity, there are many pairs $(\beta_{\text{Limit}}, \beta_{\text{Rating}})$ with a similar value for RSS.

that correspond to the same RSS, with ellipses nearest to the center taking on the lowest values of RSS. The black dots and associated dashed lines represent the coefficient estimates that result in the smallest possible RSS—in other words, these are the least squares estimates. The axes for `limit` and `age` have been scaled so that the plot includes possible coefficient estimates that are up to four standard errors on either side of the least squares estimates. Thus the plot includes all plausible values for the coefficients. For example, we see that the true `limit` coefficient is almost certainly somewhere between 0.15 and 0.20.

In contrast, the right-hand panel of Figure 3.15 displays contour plots of the RSS associated with possible coefficient estimates for the regression of `balance` onto `limit` and `rating`, which we know to be highly collinear. Now the contours run along a narrow valley; there is a broad range of values for the coefficient estimates that result in equal values for RSS. Hence a small change in the data could cause the pair of coefficient values that yield the smallest RSS—that is, the least squares estimates—to move anywhere along this valley. This results in a great deal of uncertainty in the coefficient estimates. Notice that the scale for the `limit` coefficient now runs from roughly -0.2 to 0.2 ; this is an eight-fold increase over the plausible range of the `limit` coefficient in the regression with `age`. Interestingly, even though the `limit` and `rating` coefficients now have much more individual uncertainty, they will almost certainly lie somewhere in this contour valley. For example, we would not expect the true value of the `limit` and `rating` coefficients to be -0.1 and 1 respectively, even though such a value is plausible for each coefficient individually.

Since collinearity reduces the accuracy of the estimates of the regression coefficients, it causes the standard error for $\hat{\beta}_j$ to grow. Recall that the t -statistic for each predictor is calculated by dividing $\hat{\beta}_j$ by its standard

		Coefficient	Std. error	t-statistic	p-value
Model 1	Intercept	-173.411	43.828	-3.957	< 0.0001
	age	-2.292	0.672	-3.407	0.0007
	limit	0.173	0.005	34.496	< 0.0001
Model 2	Intercept	-377.537	45.254	-8.343	< 0.0001
	rating	2.202	0.952	2.312	0.0213
	limit	0.025	0.064	0.384	0.7012

TABLE 3.11. The results for two multiple regression models involving the `Credit` data set are shown. Model 1 is a regression of `balance` on `age` and `limit`, and Model 2 a regression of `balance` on `rating` and `limit`. The standard error of $\hat{\beta}_{\text{limit}}$ increases 12-fold in the second regression, due to collinearity.

error. Consequently, collinearity results in a decline in the t -statistic. As a result, in the presence of collinearity, we may fail to reject $H_0 : \beta_j = 0$. This means that the *power* of the hypothesis test—the probability of correctly detecting a *non-zero* coefficient—is reduced by collinearity.

Table 3.11 compares the coefficient estimates obtained from two separate multiple regression models. The first is a regression of `balance` on `age` and `limit`, and the second is a regression of `balance` on `rating` and `limit`. In the first regression, both `age` and `limit` are highly significant with very small p -values. In the second, the collinearity between `limit` and `rating` has caused the standard error for the `limit` coefficient estimate to increase by a factor of 12 and the p -value to increase to 0.701. In other words, the importance of the `limit` variable has been masked due to the presence of collinearity. To avoid such a situation, it is desirable to identify and address potential collinearity problems while fitting the model.

A simple way to detect collinearity is to look at the correlation matrix of the predictors. An element of this matrix that is large in absolute value indicates a pair of highly correlated variables, and therefore a collinearity problem in the data. Unfortunately, not all collinearity problems can be detected by inspection of the correlation matrix: it is possible for collinearity to exist between three or more variables even if no pair of variables has a particularly high correlation. We call this situation *multicollinearity*. Instead of inspecting the correlation matrix, a better way to assess multicollinearity is to compute the *variance inflation factor* (VIF). The VIF is the ratio of the variance of $\hat{\beta}_j$ when fitting the full model divided by the variance of $\hat{\beta}_j$ if fit on its own. The smallest possible value for VIF is 1, which indicates the complete absence of collinearity. Typically in practice there is a small amount of collinearity among the predictors. As a rule of thumb, a VIF value that exceeds 5 or 10 indicates a problematic amount of collinearity. The VIF for each variable can be computed using the formula

$$\text{VIF}(\hat{\beta}_j) = \frac{1}{1 - R_{X_j|X_{-j}}^2},$$

where $R_{X_j|X_{-j}}^2$ is the R^2 from a regression of X_j onto all of the other predictors. If $R_{X_j|X_{-j}}^2$ is close to one, then collinearity is present, and so the VIF will be large.

power

multi-collinearity
variance inflation factor

In the `Credit` data, a regression of `balance` on `age`, `rating`, and `limit` indicates that the predictors have VIF values of 1.01, 160.67, and 160.59. As we suspected, there is considerable collinearity in the data!

When faced with the problem of collinearity, there are two simple solutions. The first is to drop one of the problematic variables from the regression. This can usually be done without much compromise to the regression fit, since the presence of collinearity implies that the information that this variable provides about the response is redundant in the presence of the other variables. For instance, if we regress `balance` onto `age` and `limit`, without the `rating` predictor, then the resulting VIF values are close to the minimum possible value of 1, and the R^2 drops from 0.754 to 0.75. So dropping `rating` from the set of predictors has effectively solved the collinearity problem without compromising the fit. The second solution is to combine the collinear variables together into a single predictor. For instance, we might take the average of standardized versions of `limit` and `rating` in order to create a new variable that measures *credit worthiness*.

3.4 The Marketing Plan

We now briefly return to the seven questions about the `Advertising` data that we set out to answer at the beginning of this chapter.

1. Is there a relationship between sales and advertising budget?

This question can be answered by fitting a multiple regression model of `sales` onto `TV`, `radio`, and `newspaper`, as in (3.20), and testing the hypothesis $H_0 : \beta_{\text{TV}} = \beta_{\text{radio}} = \beta_{\text{newspaper}} = 0$. In Section 3.2.2, we showed that the F -statistic can be used to determine whether or not we should reject this null hypothesis. In this case the p -value corresponding to the F -statistic in Table 3.6 is very low, indicating clear evidence of a relationship between advertising and sales.

2. How strong is the relationship?

We discussed two measures of model accuracy in Section 3.1.3. First, the RSE estimates the standard deviation of the response from the population regression line. For the `Advertising` data, the RSE is 1.69 units while the mean value for the response is 14.022, indicating a percentage error of roughly 12 %. Second, the R^2 statistic records the percentage of variability in the response that is explained by the predictors. The predictors explain almost 90 % of the variance in `sales`. The RSE and R^2 statistics are displayed in Table 3.6.

3. Which media are associated with sales?

To answer this question, we can examine the p -values associated with each predictor's t -statistic (Section 3.1.2). In the multiple linear regression displayed in Table 3.4, the p -values for `TV` and `radio` are low, but the p -value for `newspaper` is not. This suggests that only `TV` and `radio` are related to `sales`. In Chapter 6 we explore this question in greater detail.

4. *How large is the association between each medium and sales?*

We saw in Section 3.1.2 that the standard error of $\hat{\beta}_j$ can be used to construct confidence intervals for β_j . For the **Advertising** data, we can use the results in Table 3.4 to compute the 95 % confidence intervals for the coefficients in a multiple regression model using all three media budgets as predictors. The confidence intervals are as follows: (0.043, 0.049) for **TV**, (0.172, 0.206) for **radio**, and (-0.013, 0.011) for **newspaper**. The confidence intervals for **TV** and **radio** are narrow and far from zero, providing evidence that these media are related to **sales**. But the interval for **newspaper** includes zero, indicating that the variable is not statistically significant given the values of **TV** and **radio**.

We saw in Section 3.3.3 that collinearity can result in very wide standard errors. Could collinearity be the reason that the confidence interval associated with **newspaper** is so wide? The VIF scores are 1.005, 1.145, and 1.145 for **TV**, **radio**, and **newspaper**, suggesting no evidence of collinearity.

In order to assess the association of each medium individually on sales, we can perform three separate simple linear regressions. Results are shown in Tables 3.1 and 3.3. There is evidence of an extremely strong association between **TV** and **sales** and between **radio** and **sales**. There is evidence of a mild association between **newspaper** and **sales**, when the values of **TV** and **radio** are ignored.

5. *How accurately can we predict future sales?*

The response can be predicted using (3.21). The accuracy associated with this estimate depends on whether we wish to predict an individual response, $Y = f(X) + \epsilon$, or the average response, $f(X)$ (Section 3.2.2). If the former, we use a prediction interval, and if the latter, we use a confidence interval. Prediction intervals will always be wider than confidence intervals because they account for the uncertainty associated with ϵ , the irreducible error.

6. *Is the relationship linear?*

In Section 3.3.3, we saw that residual plots can be used in order to identify non-linearity. If the relationships are linear, then the residual plots should display no pattern. In the case of the **Advertising** data, we observe a non-linear effect in Figure 3.5, though this effect could also be observed in a residual plot. In Section 3.3.2, we discussed the inclusion of transformations of the predictors in the linear regression model in order to accommodate non-linear relationships.

7. *Is there synergy among the advertising media?*

The standard linear regression model assumes an additive relationship between the predictors and the response. An additive model is easy to interpret because the association between each predictor and the response is unrelated to the values of the other predictors. However, the additive assumption may be unrealistic for certain data sets. In Section 3.3.2, we showed how to include an interaction term

in the regression model in order to accommodate non-additive relationships. A small p -value associated with the interaction term indicates the presence of such relationships. Figure 3.5 suggested that the **Advertising** data may not be additive. Including an interaction term in the model results in a substantial increase in R^2 , from around 90 % to almost 97 %.

3.5 Comparison of Linear Regression with K -Nearest Neighbors

As discussed in Chapter 2, linear regression is an example of a *parametric* approach because it assumes a linear functional form for $f(X)$. Parametric methods have several advantages. They are often easy to fit, because one need estimate only a small number of coefficients. In the case of linear regression, the coefficients have simple interpretations, and tests of statistical significance can be easily performed. But parametric methods do have a disadvantage: by construction, they make strong assumptions about the form of $f(X)$. If the specified functional form is far from the truth, and prediction accuracy is our goal, then the parametric method will perform poorly. For instance, if we assume a linear relationship between X and Y but the true relationship is far from linear, then the resulting model will provide a poor fit to the data, and any conclusions drawn from it will be suspect.

In contrast, *non-parametric* methods do not explicitly assume a parametric form for $f(X)$, and thereby provide an alternative and more flexible approach for performing regression. We discuss various non-parametric methods in this book. Here we consider one of the simplest and best-known non-parametric methods, *K -nearest neighbors regression* (KNN regression). The KNN regression method is closely related to the KNN classifier discussed in Chapter 2. Given a value for K and a prediction point x_0 , KNN regression first identifies the K training observations that are closest to x_0 , represented by \mathcal{N}_0 . It then estimates $f(x_0)$ using the average of all the training responses in \mathcal{N}_0 . In other words,

$$\hat{f}(x_0) = \frac{1}{K} \sum_{x_i \in \mathcal{N}_0} y_i.$$

*K -nearest
neighbors
regression*

Figure 3.16 illustrates two KNN fits on a data set with $p = 2$ predictors. The fit with $K = 1$ is shown in the left-hand panel, while the right-hand panel corresponds to $K = 9$. We see that when $K = 1$, the KNN fit perfectly interpolates the training observations, and consequently takes the form of a step function. When $K = 9$, the KNN fit still is a step function, but averaging over nine observations results in much smaller regions of constant prediction, and consequently a smoother fit. In general, the optimal value for K will depend on the *bias-variance tradeoff*, which we introduced in Chapter 2. A small value for K provides the most flexible fit, which will have low bias but high variance. This variance is due to the fact that the prediction in a given region is entirely dependent on just one observation.

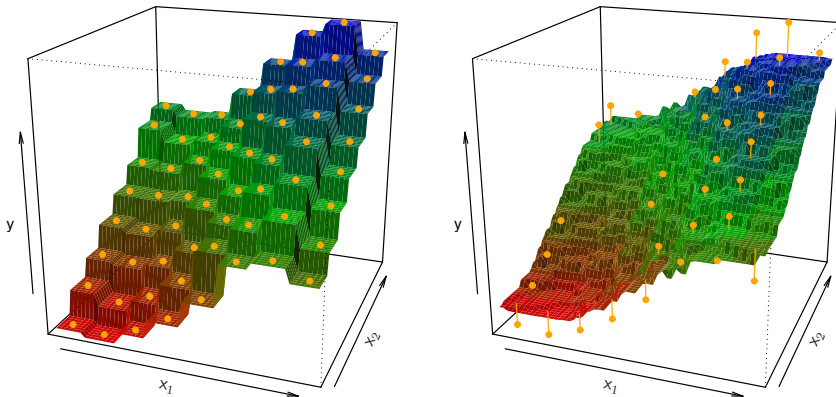


FIGURE 3.16. Plots of $\hat{f}(X)$ using KNN regression on a two-dimensional data set with 64 observations (orange dots). Left: $K = 1$ results in a rough step function fit. Right: $K = 9$ produces a much smoother fit.

In contrast, larger values of K provide a smoother and less variable fit; the prediction in a region is an average of several points, and so changing one observation has a smaller effect. However, the smoothing may cause bias by masking some of the structure in $f(X)$. In Chapter 5, we introduce several approaches for estimating test error rates. These methods can be used to identify the optimal value of K in KNN regression.

In what setting will a parametric approach such as least squares linear regression outperform a non-parametric approach such as KNN regression? The answer is simple: *the parametric approach will outperform the non-parametric approach if the parametric form that has been selected is close to the true form of f .* Figure 3.17 provides an example with data generated from a one-dimensional linear regression model. The black solid lines represent $f(X)$, while the blue curves correspond to the KNN fits using $K = 1$ and $K = 9$. In this case, the $K = 1$ predictions are far too variable, while the smoother $K = 9$ fit is much closer to $f(X)$. However, since the true relationship is linear, it is hard for a non-parametric approach to compete with linear regression: a non-parametric approach incurs a cost in variance that is not offset by a reduction in bias. The blue dashed line in the left-hand panel of Figure 3.18 represents the linear regression fit to the same data. It is almost perfect. The right-hand panel of Figure 3.18 reveals that linear regression outperforms KNN for this data. The green solid line, plotted as a function of $1/K$, represents the test set mean squared error (MSE) for KNN. The KNN errors are well above the black dashed line, which is the test MSE for linear regression. When the value of K is large, then KNN performs only a little worse than least squares regression in terms of MSE. It performs far worse when K is small.

In practice, the true relationship between X and Y is rarely exactly linear. Figure 3.19 examines the relative performances of least squares regression and KNN under increasing levels of non-linearity in the relationship between X and Y . In the top row, the true relationship is nearly linear. In this case we see that the test MSE for linear regression is still superior

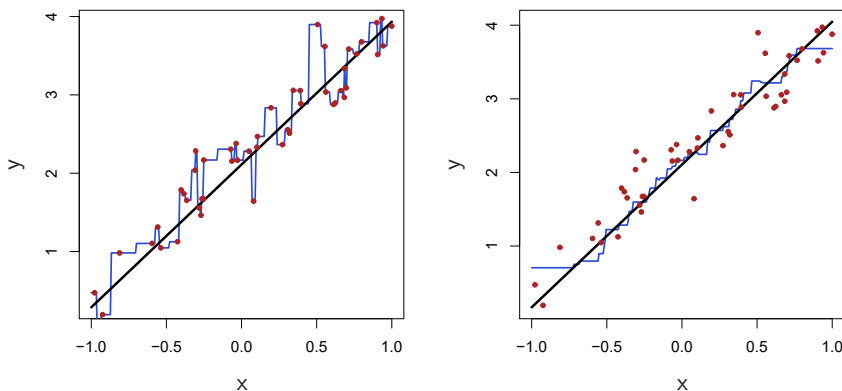


FIGURE 3.17. Plots of $\hat{f}(X)$ using KNN regression on a one-dimensional data set with 50 observations. The true relationship is given by the black solid line. Left: The blue curve corresponds to $K = 1$ and interpolates (i.e. passes directly through) the training data. Right: The blue curve corresponds to $K = 9$, and represents a smoother fit.

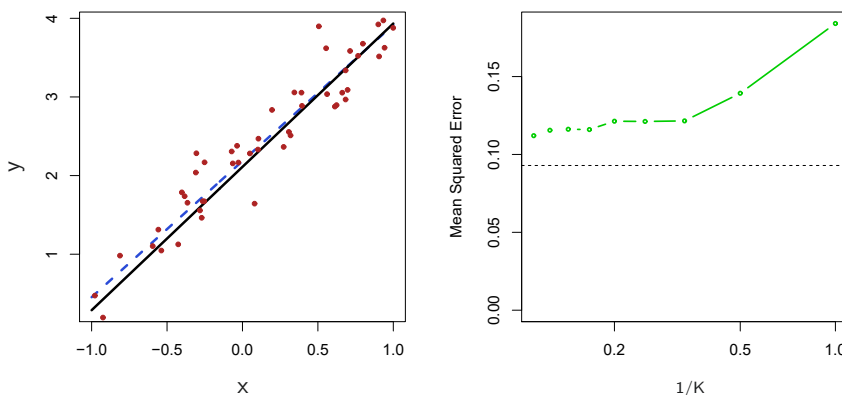


FIGURE 3.18. The same data set shown in Figure 3.17 is investigated further. Left: The blue dashed line is the least squares fit to the data. Since $f(X)$ is in fact linear (displayed as the black line), the least squares regression line provides a very good estimate of $f(X)$. Right: The dashed horizontal line represents the least squares test set MSE, while the green solid line corresponds to the MSE for KNN as a function of $1/K$ (on the log scale). Linear regression achieves a lower test MSE than does KNN regression, since $f(X)$ is in fact linear. For KNN regression, the best results occur with a very large value of K , corresponding to a small value of $1/K$.

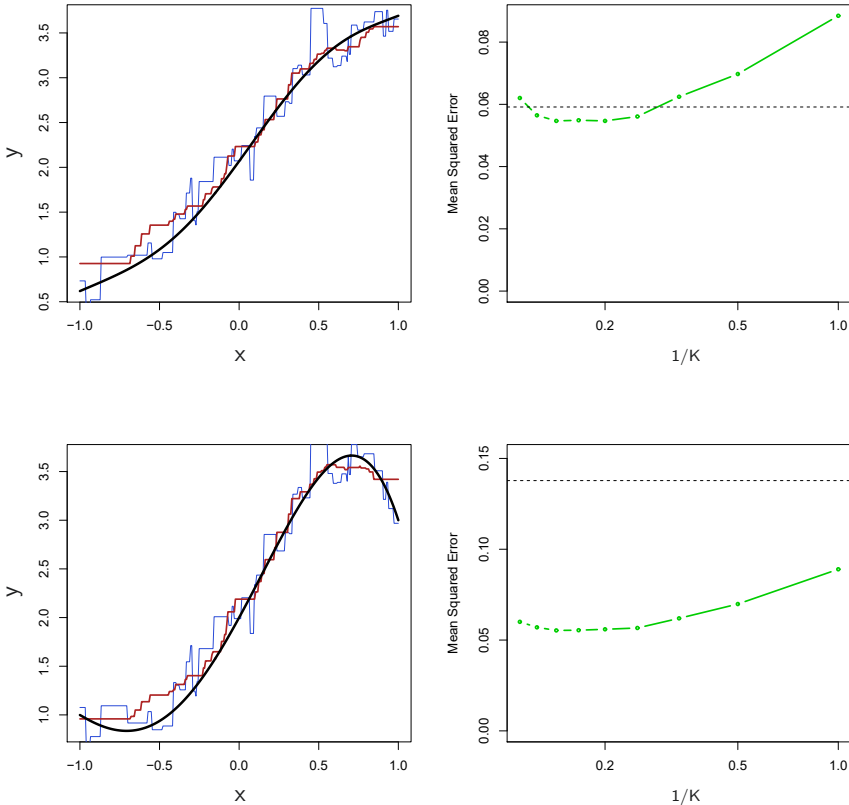


FIGURE 3.19. Top Left: In a setting with a slightly non-linear relationship between X and Y (solid black line), the KNN fits with $K = 1$ (blue) and $K = 9$ (red) are displayed. Top Right: For the slightly non-linear data, the test set MSE for least squares regression (horizontal black) and KNN with various values of $1/K$ (green) are displayed. Bottom Left and Bottom Right: As in the top panel, but with a strongly non-linear relationship between X and Y .

to that of KNN for low values of K . However, for $K \geq 4$, KNN outperforms linear regression. The second row illustrates a more substantial deviation from linearity. In this situation, KNN substantially outperforms linear regression for all values of K . Note that as the extent of non-linearity increases, there is little change in the test set MSE for the non-parametric KNN method, but there is a large increase in the test set MSE of linear regression.

Figures 3.18 and 3.19 display situations in which KNN performs slightly worse than linear regression when the relationship is linear, but much better than linear regression for nonlinear situations. In a real life situation in which the true relationship is unknown, one might suspect that KNN should be favored over linear regression because it will at worst be slightly inferior to linear regression if the true relationship is linear, and may give substantially better results if the true relationship is non-linear. But in reality, even when the true relationship is highly non-linear, KNN may still provide inferior results to linear regression. In particular, both Figures 3.18

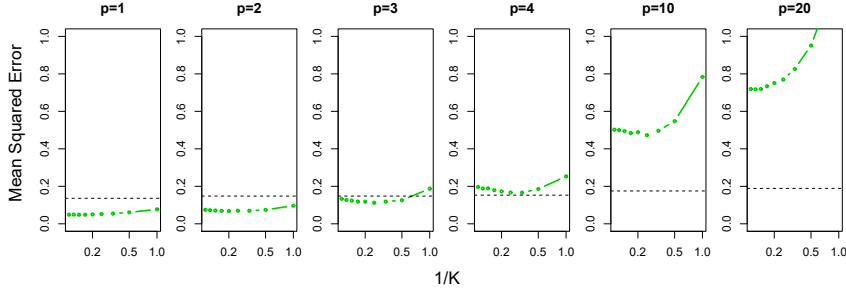


FIGURE 3.20. Test MSE for linear regression (black dashed lines) and KNN (green curves) as the number of variables p increases. The true function is non-linear in the first variable, as in the lower panel in Figure 3.19, and does not depend on the additional variables. The performance of linear regression deteriorates slowly in the presence of these additional noise variables, whereas KNN's performance degrades much more quickly as p increases.

and 3.19 illustrate settings with $p = 1$ predictor. But in higher dimensions, KNN often performs worse than linear regression.

Figure 3.20 considers the same strongly non-linear situation as in the second row of Figure 3.19, except that we have added additional *noise* predictors that are not associated with the response. When $p = 1$ or $p = 2$, KNN outperforms linear regression. But for $p = 3$ the results are mixed, and for $p \geq 4$ linear regression is superior to KNN. In fact, the increase in dimension has only caused a small deterioration in the linear regression test set MSE, but it has caused more than a ten-fold increase in the MSE for KNN. This decrease in performance as the dimension increases is a common problem for KNN, and results from the fact that in higher dimensions there is effectively a reduction in sample size. In this data set there are 50 training observations; when $p = 1$, this provides enough information to accurately estimate $f(X)$. However, spreading 50 observations over $p = 20$ dimensions results in a phenomenon in which a given observation has no *nearby neighbors*—this is the so-called *curse of dimensionality*. That is, the K observations that are nearest to a given test observation x_0 may be very far away from x_0 in p -dimensional space when p is large, leading to a very poor prediction of $f(x_0)$ and hence a poor KNN fit. As a general rule, parametric methods will tend to outperform non-parametric approaches when there is a small number of observations per predictor.

curse of dimensionality

Even when the dimension is small, we might prefer linear regression to KNN from an interpretability standpoint. If the test MSE of KNN is only slightly lower than that of linear regression, we might be willing to forego a little bit of prediction accuracy for the sake of a simple model that can be described in terms of just a few coefficients, and for which p -values are available.

CompPrice	0.0929	0.004	22.567	0.000
Income	0.0109	0.003	4.183	0.000
Advertising	0.0702	0.023	3.107	0.002
Population	0.0002	0.000	0.433	0.665
Price	-0.1008	0.007	-13.549	0.000
ShelveLoc[Good]	4.8487	0.153	31.724	0.000
ShelveLoc[Medium]	1.9533	0.126	15.531	0.000
Age	-0.0579	0.016	-3.633	0.000
Education	-0.0209	0.020	-1.063	0.288
Urban[Yes]	0.1402	0.112	1.247	0.213
US[Yes]	-0.1576	0.149	-1.058	0.291
Income:Advertising	0.0008	0.000	2.698	0.007
Price:Age	0.0001	0.000	0.801	0.424

In the first line above, we made `allvars` a list, so that we could add the interaction terms two lines down. Our model-matrix builder has created a `ShelveLoc[Good]` dummy variable that takes on a value of 1 if the shelving location is good, and 0 otherwise. It has also created a `ShelveLoc[Medium]` dummy variable that equals 1 if the shelving location is medium, and 0 otherwise. A bad shelving location corresponds to a zero for each of the two dummy variables. The fact that the coefficient for `ShelveLoc[Good]` in the regression output is positive indicates that a good shelving location is associated with high sales (relative to a bad location). And `ShelveLoc[Medium]` has a smaller positive coefficient, indicating that a medium shelving location leads to higher sales than a bad shelving location, but lower sales than a good shelving location.

3.7 Exercises

Conceptual

1. Describe the null hypotheses to which the p -values given in Table 3.4 correspond. Explain what conclusions you can draw based on these p -values. Your explanation should be phrased in terms of `sales`, `TV`, `radio`, and `newspaper`, rather than in terms of the coefficients of the linear model.
2. Carefully explain the differences between the KNN classifier and KNN regression methods.
3. Suppose we have a data set with five predictors, $X_1 = \text{GPA}$, $X_2 = \text{IQ}$, $X_3 = \text{Level}$ (1 for College and 0 for High School), $X_4 = \text{Interaction between GPA and IQ}$, and $X_5 = \text{Interaction between GPA and Level}$. The response is starting salary after graduation (in thousands of dollars). Suppose we use least squares to fit the model, and get $\hat{\beta}_0 = 50$, $\hat{\beta}_1 = 20$, $\hat{\beta}_2 = 0.07$, $\hat{\beta}_3 = 35$, $\hat{\beta}_4 = 0.01$, $\hat{\beta}_5 = -10$.
 - (a) Which answer is correct, and why?
 - i. For a fixed value of IQ and GPA, high school graduates earn more, on average, than college graduates.
 - ii. For a fixed value of IQ and GPA, college graduates earn more, on average, than high school graduates.

- iii. For a fixed value of IQ and GPA, high school graduates earn more, on average, than college graduates provided that the GPA is high enough.
 - iv. For a fixed value of IQ and GPA, college graduates earn more, on average, than high school graduates provided that the GPA is high enough.
- (b) Predict the salary of a college graduate with IQ of 110 and a GPA of 4.0.
- (c) True or false: Since the coefficient for the GPA/IQ interaction term is very small, there is very little evidence of an interaction effect. Justify your answer.
4. I collect a set of data ($n = 100$ observations) containing a single predictor and a quantitative response. I then fit a linear regression model to the data, as well as a separate cubic regression, i.e. $Y = \beta_0 + \beta_1 X + \beta_2 X^2 + \beta_3 X^3 + \epsilon$.
- (a) Suppose that the true relationship between X and Y is linear, i.e. $Y = \beta_0 + \beta_1 X + \epsilon$. Consider the training residual sum of squares (RSS) for the linear regression, and also the training RSS for the cubic regression. Would we expect one to be lower than the other, would we expect them to be the same, or is there not enough information to tell? Justify your answer.
- (b) Answer (a) using test rather than training RSS.
- (c) Suppose that the true relationship between X and Y is not linear, but we don't know how far it is from linear. Consider the training RSS for the linear regression, and also the training RSS for the cubic regression. Would we expect one to be lower than the other, would we expect them to be the same, or is there not enough information to tell? Justify your answer.
- (d) Answer (c) using test rather than training RSS.
5. Consider the fitted values that result from performing linear regression without an intercept. In this setting, the i th fitted value takes the form

$$\hat{y}_i = x_i \hat{\beta},$$

where

$$\hat{\beta} = \left(\sum_{i=1}^n x_i y_i \right) / \left(\sum_{i'=1}^n x_{i'}^2 \right). \quad (3.38)$$

Show that we can write

$$\hat{y}_i = \sum_{i'=1}^n a_{i'} y_{i'}.$$

What is $a_{i'}$?

Note: We interpret this result by saying that the fitted values from linear regression are linear combinations of the response values.

6. Using (3.4), argue that in the case of simple linear regression, the least squares line always passes through the point (\bar{x}, \bar{y}) .
7. It is claimed in the text that in the case of simple linear regression of Y onto X , the R^2 statistic (3.17) is equal to the square of the correlation between X and Y (3.18). Prove that this is the case. For simplicity, you may assume that $\bar{x} = \bar{y} = 0$. 

Applied

8. This question involves the use of simple linear regression on the `Auto` data set.
 - (a) Use the `sm.OLS()` function to perform a simple linear regression with `mpg` as the response and `horsepower` as the predictor. Use the `summarize()` function to print the results. Comment on the output. For example:
 - i. Is there a relationship between the predictor and the response?
 - ii. How strong is the relationship between the predictor and the response?
 - iii. Is the relationship between the predictor and the response positive or negative?
 - iv. What is the predicted `mpg` associated with a `horsepower` of 98? What are the associated 95 % confidence and prediction intervals?
 - (b) Plot the response and the predictor in a new set of axes `ax`. Use the `ax.axline()` method or the `abline()` function defined in the lab to display the least squares regression line.
 - (c) Produce some of diagnostic plots of the least squares regression fit as described in the lab. Comment on any problems you see with the fit.
9. This question involves the use of multiple linear regression on the `Auto` data set.
 - (a) Produce a scatterplot matrix which includes all of the variables in the data set.
 - (b) Compute the matrix of correlations between the variables using the `DataFrame.corr()` method.
 - (c) Use the `sm.OLS()` function to perform a multiple linear regression with `mpg` as the response and all other variables except `name` as the predictors. Use the `summarize()` function to print the results. Comment on the output. For instance:
 - i. Is there a relationship between the predictors and the response? Use the `anova_lm()` function from `statsmodels` to answer this question.

- ii. Which predictors appear to have a statistically significant relationship to the response?
 - iii. What does the coefficient for the `year` variable suggest?
- (d) Produce some of diagnostic plots of the linear regression fit as described in the lab. Comment on any problems you see with the fit. Do the residual plots suggest any unusually large outliers? Does the leverage plot identify any observations with unusually high leverage?
- (e) Fit some models with interactions as described in the lab. Do any interactions appear to be statistically significant?
- (f) Try a few different transformations of the variables, such as $\log(X)$, \sqrt{X} , X^2 . Comment on your findings.
10. This question should be answered using the `Carseats` data set.
- (a) Fit a multiple regression model to predict `Sales` using `Price`, `Urban`, and `US`.
 - (b) Provide an interpretation of each coefficient in the model. Be careful—some of the variables in the model are qualitative!
 - (c) Write out the model in equation form, being careful to handle the qualitative variables properly.
 - (d) For which of the predictors can you reject the null hypothesis $H_0 : \beta_j = 0$?
 - (e) On the basis of your response to the previous question, fit a smaller model that only uses the predictors for which there is evidence of association with the outcome.
 - (f) How well do the models in (a) and (e) fit the data?
 - (g) Using the model from (e), obtain 95 % confidence intervals for the coefficient(s).
 - (h) Is there evidence of outliers or high leverage observations in the model from (e)?
11. In this problem we will investigate the t -statistic for the null hypothesis $H_0 : \beta = 0$ in simple linear regression without an intercept. To begin, we generate a predictor `x` and a response `y` as follows.

```
rng = np.random.default_rng(1)
x = rng.normal(size=100)
y = 2 * x + rng.normal(size=100)
```

- (a) Perform a simple linear regression of `y` onto `x`, *without* an intercept. Report the coefficient estimate $\hat{\beta}$, the standard error of this coefficient estimate, and the t -statistic and p -value associated with the null hypothesis $H_0 : \beta = 0$. Comment on these results. (You can perform regression without an intercept using the keyword argument `intercept=False` to `ModelSpec()`.)

- (b) Now perform a simple linear regression of \mathbf{x} onto \mathbf{y} without an intercept, and report the coefficient estimate, its standard error, and the corresponding t -statistic and p -values associated with the null hypothesis $H_0 : \beta = 0$. Comment on these results.
- (c) What is the relationship between the results obtained in (a) and (b)?
- (d) For the regression of Y onto X without an intercept, the t -statistic for $H_0 : \beta = 0$ takes the form $\hat{\beta}/\text{SE}(\hat{\beta})$, where $\hat{\beta}$ is given by (3.38), and where

$$\text{SE}(\hat{\beta}) = \sqrt{\frac{\sum_{i=1}^n (y_i - x_i \hat{\beta})^2}{(n-1) \sum_{i'=1}^n x_{i'}^2}}.$$

(These formulas are slightly different from those given in Sections 3.1.1 and 3.1.2, since here we are performing regression without an intercept.) Show algebraically, and confirm numerically in R, that the t -statistic can be written as

$$\frac{(\sqrt{n-1}) \sum_{i=1}^n x_i y_i}{\sqrt{(\sum_{i=1}^n x_i^2)(\sum_{i'=1}^n y_{i'}^2) - (\sum_{i'=1}^n x_{i'} y_{i'})^2}}.$$

- (e) Using the results from (d), argue that the t -statistic for the regression of \mathbf{y} onto \mathbf{x} is the same as the t -statistic for the regression of \mathbf{x} onto \mathbf{y} .
- (f) In R, show that when regression is performed *with* an intercept, the t -statistic for $H_0 : \beta_1 = 0$ is the same for the regression of \mathbf{y} onto \mathbf{x} as it is for the regression of \mathbf{x} onto \mathbf{y} .
12. This problem involves simple linear regression without an intercept.
- (a) Recall that the coefficient estimate $\hat{\beta}$ for the linear regression of Y onto X without an intercept is given by (3.38). Under what circumstance is the coefficient estimate for the regression of X onto Y the same as the coefficient estimate for the regression of Y onto X ?
- (b) Generate an example in Python with $n = 100$ observations in which the coefficient estimate for the regression of X onto Y is *different from* the coefficient estimate for the regression of Y onto X .
- (c) Generate an example in Python with $n = 100$ observations in which the coefficient estimate for the regression of X onto Y is *the same as* the coefficient estimate for the regression of Y onto X .
13. In this exercise you will create some simulated data and will fit simple linear regression models to it. Make sure to use the default random number generator with seed set to 1 prior to starting part (a) to ensure consistent results.



- (a) Using the `normal()` method of your random number generator, create a vector, `x`, containing 100 observations drawn from a $N(0, 1)$ distribution. This represents a feature, X .
- (b) Using the `normal()` method, create a vector, `eps`, containing 100 observations drawn from a $N(0, 0.25)$ distribution—a normal distribution with mean zero and variance 0.25.
- (c) Using `x` and `eps`, generate a vector `y` according to the model

$$Y = -1 + 0.5X + \epsilon. \quad (3.39)$$

What is the length of the vector `y`? What are the values of β_0 and β_1 in this linear model?

- (d) Create a scatterplot displaying the relationship between `x` and `y`. Comment on what you observe.
- (e) Fit a least squares linear model to predict `y` using `x`. Comment on the model obtained. How do $\hat{\beta}_0$ and $\hat{\beta}_1$ compare to β_0 and β_1 ?
- (f) Display the least squares line on the scatterplot obtained in (d). Draw the population regression line on the plot, in a different color. Use the `legend()` method of the axes to create an appropriate legend.
- (g) Now fit a polynomial regression model that predicts `y` using `x` and `x2`. Is there evidence that the quadratic term improves the model fit? Explain your answer.
- (h) Repeat (a)–(f) after modifying the data generation process in such a way that there is *less* noise in the data. The model (3.39) should remain the same. You can do this by decreasing the variance of the normal distribution used to generate the error term ϵ in (b). Describe your results.
- (i) Repeat (a)–(f) after modifying the data generation process in such a way that there is *more* noise in the data. The model (3.39) should remain the same. You can do this by increasing the variance of the normal distribution used to generate the error term ϵ in (b). Describe your results.
- (j) What are the confidence intervals for β_0 and β_1 based on the original data set, the noisier data set, and the less noisy data set? Comment on your results.

14. This problem focuses on the *collinearity* problem.

- (a) Perform the following commands in **Python**:

```
rng = np.random.default_rng(10)
x1 = rng.uniform(0, 1, size=100)
x2 = 0.5 * x1 + rng.normal(size=100) / 10
y = 2 + 2 * x1 + 0.3 * x2 + rng.normal(size=100)
```

The last line corresponds to creating a linear model in which `y` is a function of `x1` and `x2`. Write out the form of the linear model. What are the regression coefficients?

- (b) What is the correlation between x_1 and x_2 ? Create a scatterplot displaying the relationship between the variables.
- (c) Using this data, fit a least squares regression to predict y using x_1 and x_2 . Describe the results obtained. What are $\hat{\beta}_0$, $\hat{\beta}_1$, and $\hat{\beta}_2$? How do these relate to the true β_0 , β_1 , and β_2 ? Can you reject the null hypothesis $H_0 : \beta_1 = 0$? How about the null hypothesis $H_0 : \beta_2 = 0$?
- (d) Now fit a least squares regression to predict y using only x_1 . Comment on your results. Can you reject the null hypothesis $H_0 : \beta_1 = 0$?
- (e) Now fit a least squares regression to predict y using only x_2 . Comment on your results. Can you reject the null hypothesis $H_0 : \beta_1 = 0$?
- (f) Do the results obtained in (c)–(e) contradict each other? Explain your answer.
- (g) Suppose we obtain one additional observation, which was unfortunately mismeasured. We use the function `np.concatenate()` to add this additional observation to each of x_1 , x_2 and y .

```
x1 = np.concatenate([x1, [0.1]])
x2 = np.concatenate([x2, [0.8]])
y = np.concatenate([y, [6]])
```

`np.concatenate()`

Re-fit the linear models from (c) to (e) using this new data. What effect does this new observation have on the each of the models? In each model, is this observation an outlier? A high-leverage point? Both? Explain your answers.

15. This problem involves the `Boston` data set, which we saw in the lab for this chapter. We will now try to predict per capita crime rate using the other variables in this data set. In other words, per capita crime rate is the response, and the other variables are the predictors.
- (a) For each predictor, fit a simple linear regression model to predict the response. Describe your results. In which of the models is there a statistically significant association between the predictor and the response? Create some plots to back up your assertions.
- (b) Fit a multiple regression model to predict the response using all of the predictors. Describe your results. For which predictors can we reject the null hypothesis $H_0 : \beta_j = 0$?
- (c) How do your results from (a) compare to your results from (b)? Create a plot displaying the univariate regression coefficients from (a) on the x -axis, and the multiple regression coefficients from (b) on the y -axis. That is, each predictor is displayed as a single point in the plot. Its coefficient in a simple linear regression model is shown on the x -axis, and its coefficient estimate in the multiple linear regression model is shown on the y -axis.

- (d) Is there evidence of non-linear association between any of the predictors and the response? To answer this question, for each predictor X , fit a model of the form

$$Y = \beta_0 + \beta_1 X + \beta_2 X^2 + \beta_3 X^3 + \epsilon.$$



The linear regression model discussed in Chapter 3 assumes that the response variable Y is quantitative. But in many situations, the response variable is instead *qualitative*. For example, eye color is qualitative. Often qualitative variables are referred to as *categorical*; we will use these terms interchangeably. In this chapter, we study approaches for predicting qualitative responses, a process that is known as *classification*. Predicting a qualitative response for an observation can be referred to as *classifying* that observation, since it involves assigning the observation to a category, or class. On the other hand, often the methods used for classification first predict the probability that the observation belongs to each of the categories of a qualitative variable, as the basis for making the classification. In this sense they also behave like regression methods.

There are many possible classification techniques, or *classifiers*, that one might use to predict a qualitative response. We touched on some of these in Sections 2.1.5 and 2.2.3. In this chapter we discuss some widely-used classifiers: *logistic regression*, *linear discriminant analysis*, *quadratic discriminant analysis*, *naive Bayes*, and *K-nearest neighbors*. The discussion of logistic regression is used as a jumping-off point for a discussion of *generalized linear models*, and in particular, *Poisson regression*. We discuss more computer-intensive classification methods in later chapters: these include generalized additive models (Chapter 7); trees, random forests, and boosting (Chapter 8); and support vector machines (Chapter 9).

qualitative
classification
classifier
logistic regression
linear discriminant analysis
quadratic discriminant analysis
naive Bayes
K-nearest neighbors
generalized linear models
Poisson regression

4.1 An Overview of Classification

Classification problems occur often, perhaps even more so than regression problems. Some examples include:

1. A person arrives at the emergency room with a set of symptoms that could possibly be attributed to one of three medical conditions. Which of the three conditions does the individual have?
2. An online banking service must be able to determine whether or not a transaction being performed on the site is fraudulent, on the basis of the user's IP address, past transaction history, and so forth.
3. On the basis of DNA sequence data for a number of patients with and without a given disease, a biologist would like to figure out which DNA mutations are deleterious (disease-causing) and which are not.

Just as in the regression setting, in the classification setting we have a set of training observations $(x_1, y_1), \dots, (x_n, y_n)$ that we can use to build a classifier. We want our classifier to perform well not only on the training data, but also on test observations that were not used to train the classifier.

In this chapter, we will illustrate the concept of classification using the simulated `Default` data set. We are interested in predicting whether an individual will default on his or her credit card payment, on the basis of annual income and monthly credit card balance. The data set is displayed in Figure 4.1. In the left-hand panel of Figure 4.1, we have plotted annual `income` and monthly credit card `balance` for a subset of 10,000 individuals. The individuals who defaulted in a given month are shown in orange, and those who did not in blue. (The overall default rate is about 3%, so we have plotted only a fraction of the individuals who did not default.) It appears that individuals who defaulted tended to have higher credit card balances than those who did not. In the center and right-hand panels of Figure 4.1, two pairs of boxplots are shown. The first shows the distribution of `balance` split by the binary `default` variable; the second is a similar plot for `income`. In this chapter, we learn how to build a model to predict `default` (Y) for any given value of `balance` (X_1) and `income` (X_2). Since Y is not quantitative, the simple linear regression model of Chapter 3 is not a good choice: we will elaborate on this further in Section 4.2.

It is worth noting that Figure 4.1 displays a very pronounced relationship between the predictor `balance` and the response `default`. In most real applications, the relationship between the predictor and the response will not be nearly so strong. However, for the sake of illustrating the classification procedures discussed in this chapter, we use an example in which the relationship between the predictor and the response is somewhat exaggerated.

4.2 Why Not Linear Regression?

We have stated that linear regression is not appropriate in the case of a qualitative response. Why not?

Suppose that we are trying to predict the medical condition of a patient in the emergency room on the basis of her symptoms. In this simplified example, there are three possible diagnoses: `stroke`, `drug overdose`, and

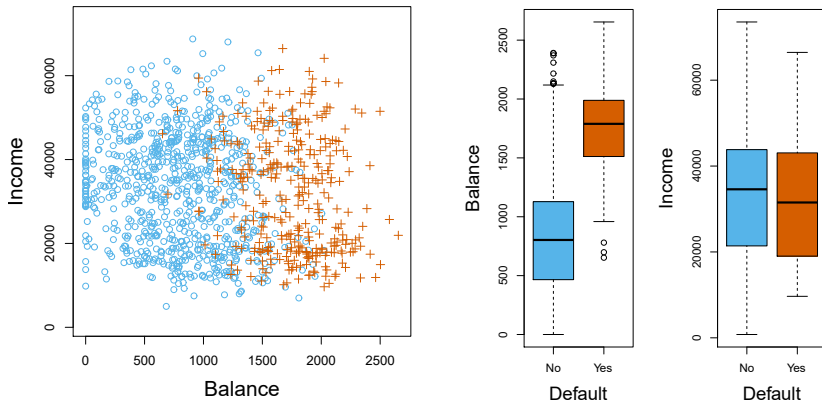


FIGURE 4.1. The `Default` data set. Left: The annual incomes and monthly credit card balances of a number of individuals. The individuals who defaulted on their credit card payments are shown in orange, and those who did not are shown in blue. Center: Boxplots of `balance` as a function of `default` status. Right: Boxplots of `income` as a function of `default` status.

epileptic seizure. We could consider encoding these values as a quantitative response variable, Y , as follows:

$$Y = \begin{cases} 1 & \text{if } \text{stroke}; \\ 2 & \text{if } \text{drug overdose}; \\ 3 & \text{if } \text{epileptic seizure}. \end{cases}$$

Using this coding, least squares could be used to fit a linear regression model to predict Y on the basis of a set of predictors X_1, \dots, X_p . Unfortunately, this coding implies an ordering on the outcomes, putting `drug overdose` in between `stroke` and `epileptic seizure`, and insisting that the difference between `stroke` and `drug overdose` is the same as the difference between `drug overdose` and `epileptic seizure`. In practice there is no particular reason that this needs to be the case. For instance, one could choose an equally reasonable coding,

$$Y = \begin{cases} 1 & \text{if } \text{epileptic seizure}; \\ 2 & \text{if } \text{stroke}; \\ 3 & \text{if } \text{drug overdose}, \end{cases}$$

which would imply a totally different relationship among the three conditions. Each of these codings would produce fundamentally different linear models that would ultimately lead to different sets of predictions on test observations.

If the response variable's values did take on a natural ordering, such as *mild*, *moderate*, and *severe*, and we felt the gap between *mild* and *moderate* was similar to the gap between *moderate* and *severe*, then a 1, 2, 3 coding would be reasonable. Unfortunately, in general there is no natural way to

convert a qualitative response variable with more than two levels into a quantitative response that is ready for linear regression.

For a *binary* (two level) qualitative response, the situation is better. For instance, perhaps there are only two possibilities for the patient's medical condition: `stroke` and `drug overdose`. We could then potentially use the *dummy variable* approach from Section 3.3.1 to code the response as follows:

$$Y = \begin{cases} 0 & \text{if } \text{stroke}; \\ 1 & \text{if } \text{drug overdose}. \end{cases}$$

We could then fit a linear regression to this binary response, and predict `drug overdose` if $\hat{Y} > 0.5$ and `stroke` otherwise. In the binary case it is not hard to show that even if we flip the above coding, linear regression will produce the same final predictions.

For a binary response with a 0/1 coding as above, regression by least squares is not completely unreasonable: it can be shown that the $X\hat{\beta}$ obtained using linear regression is in fact an estimate of $\Pr(\text{drug overdose}|X)$ in this special case. However, if we use linear regression, some of our estimates might be outside the [0, 1] interval (see Figure 4.2), making them hard to interpret as probabilities! Nevertheless, the predictions provide an ordering and can be interpreted as crude probability estimates. Curiously, it turns out that the classifications that we get if we use linear regression to predict a binary response will be the same as for the linear discriminant analysis (LDA) procedure we discuss in Section 4.4.

To summarize, there are at least two reasons not to perform classification using a regression method: (a) a regression method cannot accommodate a qualitative response with more than two classes; (b) a regression method will not provide meaningful estimates of $\Pr(Y|X)$, even with just two classes. Thus, it is preferable to use a classification method that is truly suited for qualitative response values. In the next section, we present logistic regression, which is well-suited for the case of a binary qualitative response; in later sections we will cover classification methods that are appropriate when the qualitative response has two or more classes.

4.3 Logistic Regression

Consider again the `Default` data set, where the response `default` falls into one of two categories, `Yes` or `No`. Rather than modeling this response Y directly, logistic regression models the *probability* that Y belongs to a particular category.

For the `Default` data, logistic regression models the probability of default. For example, the probability of default given `balance` can be written as

$$\Pr(\text{default} = \text{Yes}|\text{balance}).$$

The values of $\Pr(\text{default} = \text{Yes}|\text{balance})$, which we abbreviate $p(\text{balance})$, will range between 0 and 1. Then for any given value of `balance`, a prediction can be made for `default`. For example, one might predict `default = Yes`

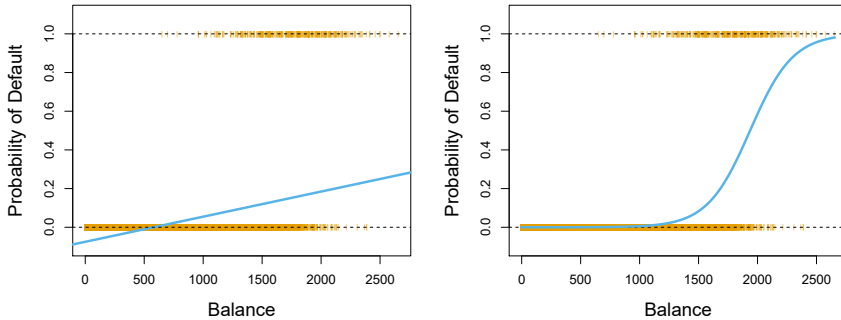


FIGURE 4.2. Classification using the `Default` data. Left: Estimated probability of `default` using linear regression. Some estimated probabilities are negative! The orange ticks indicate the 0/1 values coded for `default`(No or Yes). Right: Predicted probabilities of `default` using logistic regression. All probabilities lie between 0 and 1.

for any individual for whom $p(\text{balance}) > 0.5$. Alternatively, if a company wishes to be conservative in predicting individuals who are at risk for default, then they may choose to use a lower threshold, such as $p(\text{balance}) > 0.1$.

4.3.1 The Logistic Model

How should we model the relationship between $p(X) = \Pr(Y = 1|X)$ and X ? (For convenience we are using the generic 0/1 coding for the response.) In Section 4.2 we considered using a linear regression model to represent these probabilities:

$$p(X) = \beta_0 + \beta_1 X. \quad (4.1)$$

If we use this approach to predict `default=Yes` using `balance`, then we obtain the model shown in the left-hand panel of Figure 4.2. Here we see the problem with this approach: for balances close to zero we predict a negative probability of default; if we were to predict for very large balances, we would get values bigger than 1. These predictions are not sensible, since of course the true probability of default, regardless of credit card balance, must fall between 0 and 1. This problem is not unique to the credit default data. Any time a straight line is fit to a binary response that is coded as 0 or 1, in principle we can always predict $p(X) < 0$ for some values of X and $p(X) > 1$ for others (unless the range of X is limited).

To avoid this problem, we must model $p(X)$ using a function that gives outputs between 0 and 1 for all values of X . Many functions meet this description. In logistic regression, we use the *logistic function*,

$$p(X) = \frac{e^{\beta_0 + \beta_1 X}}{1 + e^{\beta_0 + \beta_1 X}}. \quad (4.2)$$

To fit the model (4.2), we use a method called *maximum likelihood*, which we discuss in the next section. The right-hand panel of Figure 4.2 illustrates the fit of the logistic regression model to the `Default` data. Notice that for

logistic
function

maximum
likelihood

low balances we now predict the probability of default as close to, but never below, zero. Likewise, for high balances we predict a default probability close to, but never above, one. The logistic function will always produce an *S-shaped* curve of this form, and so regardless of the value of X , we will obtain a sensible prediction. We also see that the logistic model is better able to capture the range of probabilities than is the linear regression model in the left-hand plot. The average fitted probability in both cases is 0.0333 (averaged over the training data), which is the same as the overall proportion of defaulters in the data set.

After a bit of manipulation of (4.2), we find that

$$\frac{p(X)}{1 - p(X)} = e^{\beta_0 + \beta_1 X}. \quad (4.3)$$

The quantity $p(X)/[1 - p(X)]$ is called the *odds*, and can take on any value between 0 and ∞ . Values of the odds close to 0 and ∞ indicate very low and very high probabilities of default, respectively. For example, on average 1 in 5 people with an odds of 1/4 will default, since $p(X) = 0.2$ implies an odds of $\frac{0.2}{1-0.2} = 1/4$. Likewise, on average nine out of every ten people with an odds of 9 will default, since $p(X) = 0.9$ implies an odds of $\frac{0.9}{1-0.9} = 9$. Odds are traditionally used instead of probabilities in horse-racing, since they relate more naturally to the correct betting strategy.

odds

By taking the logarithm of both sides of (4.3), we arrive at

$$\log\left(\frac{p(X)}{1 - p(X)}\right) = \beta_0 + \beta_1 X. \quad (4.4)$$

The left-hand side is called the *log odds* or *logit*. We see that the logistic regression model (4.2) has a logit that is linear in X .

log odds
logit

Recall from Chapter 3 that in a linear regression model, β_1 gives the average change in Y associated with a one-unit increase in X . By contrast, in a logistic regression model, increasing X by one unit changes the log odds by β_1 (4.4). Equivalently, it multiplies the odds by e^{β_1} (4.3). However, because the relationship between $p(X)$ and X in (4.2) is not a straight line, β_1 does *not* correspond to the change in $p(X)$ associated with a one-unit increase in X . The amount that $p(X)$ changes due to a one-unit change in X depends on the current value of X . But regardless of the value of X , if β_1 is positive then increasing X will be associated with increasing $p(X)$, and if β_1 is negative then increasing X will be associated with decreasing $p(X)$. The fact that there is not a straight-line relationship between $p(X)$ and X , and the fact that the rate of change in $p(X)$ per unit change in X depends on the current value of X , can also be seen by inspection of the right-hand panel of Figure 4.2.

4.3.2 Estimating the Regression Coefficients

The coefficients β_0 and β_1 in (4.2) are unknown, and must be estimated based on the available training data. In Chapter 3, we used the least squares approach to estimate the unknown linear regression coefficients. Although we could use (non-linear) least squares to fit the model (4.4), the more general method of *maximum likelihood* is preferred, since it has better statistical properties. The basic intuition behind using maximum likelihood

to fit a logistic regression model is as follows: we seek estimates for β_0 and β_1 such that the predicted probability $\hat{p}(x_i)$ of default for each individual, using (4.2), corresponds as closely as possible to the individual's observed default status. In other words, we try to find $\hat{\beta}_0$ and $\hat{\beta}_1$ such that plugging these estimates into the model for $p(X)$, given in (4.2), yields a number close to one for all individuals who defaulted, and a number close to zero for all individuals who did not. This intuition can be formalized using a mathematical equation called a *likelihood function*:

$$\ell(\beta_0, \beta_1) = \prod_{i:y_i=1} p(x_i) \prod_{i':y_{i'}=0} (1 - p(x_{i'})). \quad (4.5)$$

likelihood
function

The estimates $\hat{\beta}_0$ and $\hat{\beta}_1$ are chosen to *maximize* this likelihood function.

Maximum likelihood is a very general approach that is used to fit many of the non-linear models that we examine throughout this book. In the linear regression setting, the least squares approach is in fact a special case of maximum likelihood. The mathematical details of maximum likelihood are beyond the scope of this book. However, in general, logistic regression and other models can be easily fit using statistical software such as R, and so we do not need to concern ourselves with the details of the maximum likelihood fitting procedure.

Table 4.1 shows the coefficient estimates and related information that result from fitting a logistic regression model on the **Default** data in order to predict the probability of **default=Yes** using **balance**. We see that $\hat{\beta}_1 = 0.0055$; this indicates that an increase in **balance** is associated with an increase in the probability of **default**. To be precise, a one-unit increase in **balance** is associated with an increase in the log odds of **default** by 0.0055 units.

Many aspects of the logistic regression output shown in Table 4.1 are similar to the linear regression output of Chapter 3. For example, we can measure the accuracy of the coefficient estimates by computing their standard errors. The z -statistic in Table 4.1 plays the same role as the t -statistic in the linear regression output, for example in Table 3.1 on page 77. For instance, the z -statistic associated with β_1 is equal to $\hat{\beta}_1/\text{SE}(\hat{\beta}_1)$, and so a large (absolute) value of the z -statistic indicates evidence against the null hypothesis $H_0 : \beta_1 = 0$. This null hypothesis implies that $p(X) = \frac{e^{\beta_0}}{1+e^{\beta_0}}$: in other words, that the probability of **default** does not depend on **balance**. Since the p -value associated with **balance** in Table 4.1 is tiny, we can reject H_0 . In other words, we conclude that there is indeed an association between **balance** and probability of **default**. The estimated intercept in Table 4.1 is typically not of interest; its main purpose is to adjust the average fitted probabilities to the proportion of ones in the data (in this case, the overall default rate).

4.3.3 Making Predictions

Once the coefficients have been estimated, we can compute the probability of **default** for any given credit card balance. For example, using the coefficient estimates given in Table 4.1, we predict that the default probability

	Coefficient	Std. error	<i>z</i> -statistic	<i>p</i> -value
Intercept	-10.6513	0.3612	-29.5	<0.0001
balance	0.0055	0.0002	24.9	<0.0001

TABLE 4.1. For the `Default` data, estimated coefficients of the logistic regression model that predicts the probability of `default` using `balance`. A one-unit increase in `balance` is associated with an increase in the log odds of `default` by 0.0055 units.

	Coefficient	Std. error	<i>z</i> -statistic	<i>p</i> -value
Intercept	-3.5041	0.0707	-49.55	<0.0001
student[Yes]	0.4049	0.1150	3.52	0.0004

TABLE 4.2. For the `Default` data, estimated coefficients of the logistic regression model that predicts the probability of `default` using student status. Student status is encoded as a dummy variable, with a value of 1 for a student and a value of 0 for a non-student, and represented by the variable `student[Yes]` in the table.

for an individual with a `balance` of \$1,000 is

$$\hat{p}(X) = \frac{e^{\hat{\beta}_0 + \hat{\beta}_1 X}}{1 + e^{\hat{\beta}_0 + \hat{\beta}_1 X}} = \frac{e^{-10.6513 + 0.0055 \times 1,000}}{1 + e^{-10.6513 + 0.0055 \times 1,000}} = 0.00576,$$

which is below 1%. In contrast, the predicted probability of default for an individual with a balance of \$2,000 is much higher, and equals 0.586 or 58.6%.

One can use qualitative predictors with the logistic regression model using the dummy variable approach from Section 3.3.1. As an example, the `Default` data set contains the qualitative variable `student`. To fit a model that uses student status as a predictor variable, we simply create a dummy variable that takes on a value of 1 for students and 0 for non-students. The logistic regression model that results from predicting probability of default from student status can be seen in Table 4.2. The coefficient associated with the dummy variable is positive, and the associated *p*-value is statistically significant. This indicates that students tend to have higher default probabilities than non-students:

$$\widehat{\Pr}(\text{default=Yes} | \text{student=Yes}) = \frac{e^{-3.5041 + 0.4049 \times 1}}{1 + e^{-3.5041 + 0.4049 \times 1}} = 0.0431,$$

$$\widehat{\Pr}(\text{default=Yes} | \text{student=No}) = \frac{e^{-3.5041 + 0.4049 \times 0}}{1 + e^{-3.5041 + 0.4049 \times 0}} = 0.0292.$$

4.3.4 Multiple Logistic Regression

We now consider the problem of predicting a binary response using multiple predictors. By analogy with the extension from simple to multiple linear regression in Chapter 3, we can generalize (4.4) as follows:

$$\log \left(\frac{p(X)}{1 - p(X)} \right) = \beta_0 + \beta_1 X_1 + \cdots + \beta_p X_p, \quad (4.6)$$

where $X = (X_1, \dots, X_p)$ are p predictors. Equation 4.6 can be rewritten as

$$p(X) = \frac{e^{\beta_0 + \beta_1 X_1 + \cdots + \beta_p X_p}}{1 + e^{\beta_0 + \beta_1 X_1 + \cdots + \beta_p X_p}}. \quad (4.7)$$

	Coefficient	Std. error	<i>z</i> -statistic	<i>p</i> -value
Intercept	−10.8690	0.4923	−22.08	<0.0001
balance	0.0057	0.0002	24.74	<0.0001
income	0.0030	0.0082	0.37	0.7115
student [Yes]	−0.6468	0.2362	−2.74	0.0062

TABLE 4.3. For the `Default` data, estimated coefficients of the logistic regression model that predicts the probability of `default` using `balance`, `income`, and student status. Student status is encoded as a dummy variable `student[Yes]`, with a value of 1 for a student and a value of 0 for a non-student. In fitting this model, `income` was measured in thousands of dollars.

Just as in Section 4.3.2, we use the maximum likelihood method to estimate $\beta_0, \beta_1, \dots, \beta_p$.

Table 4.3 shows the coefficient estimates for a logistic regression model that uses `balance`, `income` (in thousands of dollars), and `student` status to predict probability of `default`. There is a surprising result here. The *p*-values associated with `balance` and the dummy variable for `student` status are very small, indicating that each of these variables is associated with the probability of `default`. However, the coefficient for the dummy variable is negative, indicating that students are less likely to default than non-students. In contrast, the coefficient for the dummy variable is positive in Table 4.2. How is it possible for student status to be associated with an *increase* in probability of default in Table 4.2 and a *decrease* in probability of default in Table 4.3? The left-hand panel of Figure 4.3 provides a graphical illustration of this apparent paradox. The orange and blue solid lines show the average default rates for students and non-students, respectively, as a function of credit card balance. The negative coefficient for `student` in the multiple logistic regression indicates that *for a fixed value of balance and income*, a student is less likely to default than a non-student. Indeed, we observe from the left-hand panel of Figure 4.3 that the student default rate is at or below that of the non-student default rate for every value of `balance`. But the horizontal broken lines near the base of the plot, which show the default rates for students and non-students averaged over all values of `balance` and `income`, suggest the opposite effect: the overall student default rate is higher than the non-student default rate. Consequently, there is a positive coefficient for `student` in the single variable logistic regression output shown in Table 4.2.

The right-hand panel of Figure 4.3 provides an explanation for this discrepancy. The variables `student` and `balance` are correlated. Students tend to hold higher levels of debt, which is in turn associated with higher probability of default. In other words, students are more likely to have large credit card balances, which, as we know from the left-hand panel of Figure 4.3, tend to be associated with high default rates. Thus, even though an individual student with a given credit card balance will tend to have a lower probability of default than a non-student with the same credit card balance, the fact that students on the whole tend to have higher credit card balances means that overall, students tend to default at a higher rate than non-students. This is an important distinction for a credit card company that is trying to determine to whom they should offer credit. A student is riskier than a non-student if no information about the student's credit card

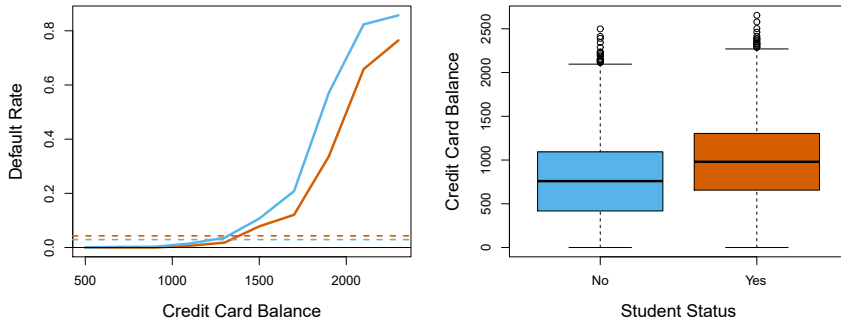


FIGURE 4.3. Confounding in the `Default` data. Left: Default rates are shown for students (orange) and non-students (blue). The solid lines display default rate as a function of `balance`, while the horizontal broken lines display the overall default rates. Right: Boxplots of `balance` for students (orange) and non-students (blue) are shown.

balance is available. However, that student is less risky than a non-student with the same credit card balance!

This simple example illustrates the dangers and subtleties associated with performing regressions involving only a single predictor when other predictors may also be relevant. As in the linear regression setting, the results obtained using one predictor may be quite different from those obtained using multiple predictors, especially when there is correlation among the predictors. In general, the phenomenon seen in Figure 4.3 is known as *confounding*.

By substituting estimates for the regression coefficients from Table 4.3 into (4.7), we can make predictions. For example, a student with a credit card balance of \$1,500 and an income of \$40,000 has an estimated probability of default of

$$\hat{p}(X) = \frac{e^{-10.869 + 0.00574 \times 1,500 + 0.003 \times 40 - 0.6468 \times 1}}{1 + e^{-10.869 + 0.00574 \times 1,500 + 0.003 \times 40 - 0.6468 \times 1}} = 0.058. \quad (4.8)$$

A non-student with the same balance and income has an estimated probability of default of

$$\hat{p}(X) = \frac{e^{-10.869 + 0.00574 \times 1,500 + 0.003 \times 40 - 0.6468 \times 0}}{1 + e^{-10.869 + 0.00574 \times 1,500 + 0.003 \times 40 - 0.6468 \times 0}} = 0.105. \quad (4.9)$$

(Here we multiply the `income` coefficient estimate from Table 4.3 by 40, rather than by 40,000, because in that table the model was fit with `income` measured in units of \$1,000.)

4.3.5 Multinomial Logistic Regression

We sometimes wish to classify a response variable that has more than two classes. For example, in Section 4.2 we had three categories of medical condition in the emergency room: `stroke`, `drug overdose`, `epileptic seizure`. However, the logistic regression approach that we have seen in this section only allows for $K = 2$ classes for the response variable.

confounding

It turns out that it is possible to extend the two-class logistic regression approach to the setting of $K > 2$ classes. This extension is sometimes known as *multinomial logistic regression*. To do this, we first select a single class to serve as the *baseline*; without loss of generality, we select the K th class for this role. Then we replace the model (4.7) with the model

$$\Pr(Y = k|X = x) = \frac{e^{\beta_{k0} + \beta_{k1}x_1 + \dots + \beta_{kp}x_p}}{1 + \sum_{l=1}^{K-1} e^{\beta_{l0} + \beta_{l1}x_1 + \dots + \beta_{lp}x_p}} \quad (4.10)$$

for $k = 1, \dots, K-1$, and

$$\Pr(Y = K|X = x) = \frac{1}{1 + \sum_{l=1}^{K-1} e^{\beta_{l0} + \beta_{l1}x_1 + \dots + \beta_{lp}x_p}}. \quad (4.11)$$

It is not hard to show that for $k = 1, \dots, K-1$,

$$\log \left(\frac{\Pr(Y = k|X = x)}{\Pr(Y = K|X = x)} \right) = \beta_{k0} + \beta_{k1}x_1 + \dots + \beta_{kp}x_p. \quad (4.12)$$

Notice that (4.12) is quite similar to (4.6). Equation 4.12 indicates that once again, the log odds between any pair of classes is linear in the features.

It turns out that in (4.10)–(4.12), the decision to treat the K th class as the baseline is unimportant. For example, when classifying emergency room visits into **stroke**, **drug overdose**, and **epileptic seizure**, suppose that we fit two multinomial logistic regression models: one treating **stroke** as the baseline, another treating **drug overdose** as the baseline. The coefficient estimates will differ between the two fitted models due to the differing choice of baseline, but the fitted values (predictions), the log odds between any pair of classes, and the other key model outputs will remain the same.

Nonetheless, interpretation of the coefficients in a multinomial logistic regression model must be done with care, since it is tied to the choice of baseline. For example, if we set **epileptic seizure** to be the baseline, then we can interpret $\beta_{\text{stroke}0}$ as the log odds of **stroke** versus **epileptic seizure**, given that $x_1 = \dots = x_p = 0$. Furthermore, a one-unit increase in X_j is associated with a $\beta_{\text{stroke}j}$ increase in the log odds of **stroke** over **epileptic seizure**. Stated another way, if X_j increases by one unit, then

$$\frac{\Pr(Y = \text{stroke}|X = x)}{\Pr(Y = \text{epileptic seizure}|X = x)}$$

increases by $e^{\beta_{\text{stroke}j}}$.

We now briefly present an alternative coding for multinomial logistic regression, known as the *softmax* coding. The softmax coding is equivalent to the coding just described in the sense that the fitted values, log odds between any pair of classes, and other key model outputs will remain the same, regardless of coding. But the softmax coding is used extensively in some areas of the machine learning literature (and will appear again in Chapter 10), so it is worth being aware of it. In the softmax coding, rather than selecting a baseline class, we treat all K classes symmetrically, and assume that for $k = 1, \dots, K$,

$$\Pr(Y = k|X = x) = \frac{e^{\beta_{k0} + \beta_{k1}x_1 + \dots + \beta_{kp}x_p}}{\sum_{l=1}^K e^{\beta_{l0} + \beta_{l1}x_1 + \dots + \beta_{lp}x_p}}. \quad (4.13)$$

multinomial logistic regression

softmax

Thus, rather than estimating coefficients for $K - 1$ classes, we actually estimate coefficients for all K classes. It is not hard to see that as a result of (4.13), the log odds ratio between the k th and k' th classes equals

$$\log \left(\frac{\Pr(Y = k|X = x)}{\Pr(Y = k'|X = x)} \right) = (\beta_{k0} - \beta_{k'0}) + (\beta_{k1} - \beta_{k'1})x_1 + \cdots + (\beta_{kp} - \beta_{k'p})x_p. \quad (4.14)$$

4.4 Generative Models for Classification

Logistic regression involves directly modeling $\Pr(Y = k|X = x)$ using the logistic function, given by (4.7) for the case of two response classes. In statistical jargon, we model the conditional distribution of the response Y , given the predictor(s) X . We now consider an alternative and less direct approach to estimating these probabilities. In this new approach, we model the distribution of the predictors X separately in each of the response classes (i.e. for each value of Y). We then use Bayes' theorem to flip these around into estimates for $\Pr(Y = k|X = x)$. When the distribution of X within each class is assumed to be normal, it turns out that the model is very similar in form to logistic regression.

Why do we need another method, when we have logistic regression? There are several reasons:

- When there is substantial separation between the two classes, the parameter estimates for the logistic regression model are surprisingly unstable. The methods that we consider in this section do not suffer from this problem.
- If the distribution of the predictors X is approximately normal in each of the classes and the sample size is small, then the approaches in this section may be more accurate than logistic regression.
- The methods in this section can be naturally extended to the case of more than two response classes. (In the case of more than two response classes, we can also use multinomial logistic regression from Section 4.3.5.)

Suppose that we wish to classify an observation into one of K classes, where $K \geq 2$. In other words, the qualitative response variable Y can take on K possible distinct and unordered values. Let π_k represent the overall or *prior* probability that a randomly chosen observation comes from the k th class. Let $f_k(X) \equiv \Pr(X|Y = k)$ ¹ denote the *density function* of X for an observation that comes from the k th class. In other words, $f_k(x)$ is relatively large if there is a high probability that an observation in the k th class has $X \approx x$, and $f_k(x)$ is small if it is very unlikely that an observation in the k th class has $X \approx x$. Then *Bayes' theorem* states that

prior
density
function

Bayes'
theorem

¹Technically, this definition is only correct if X is a qualitative random variable. If X is quantitative, then $f_k(x)dx$ corresponds to the probability of X falling in a small region dx around x .

$$\Pr(Y = k|X = x) = \frac{\pi_k f_k(x)}{\sum_{l=1}^K \pi_l f_l(x)}. \quad (4.15)$$

In accordance with our earlier notation, we will use the abbreviation $p_k(x) = \Pr(Y = k|X = x)$; this is the *posterior* probability that an observation $X = x$ belongs to the k th class. That is, it is the probability that the observation belongs to the k th class, *given* the predictor value for that observation.

posterior

Equation 4.15 suggests that instead of directly computing the posterior probability $p_k(x)$ as in Section 4.3.1, we can simply plug in estimates of π_k and $f_k(x)$ into (4.15). In general, estimating π_k is easy if we have a random sample from the population: we simply compute the fraction of the training observations that belong to the k th class. However, estimating the density function $f_k(x)$ is much more challenging. As we will see, to estimate $f_k(x)$, we will typically have to make some simplifying assumptions.

We know from Chapter 2 that the Bayes classifier, which classifies an observation x to the class for which $p_k(x)$ is largest, has the lowest possible error rate out of all classifiers. (Of course, this is only true if all of the terms in (4.15) are correctly specified.) Therefore, if we can find a way to estimate $f_k(x)$, then we can plug it into (4.15) in order to approximate the Bayes classifier.

In the following sections, we discuss three classifiers that use different estimates of $f_k(x)$ in (4.15) to approximate the Bayes classifier: *linear discriminant analysis*, *quadratic discriminant analysis*, and *naive Bayes*.

4.4.1 Linear Discriminant Analysis for $p = 1$

For now, assume that $p = 1$ —that is, we have only one predictor. We would like to obtain an estimate for $f_k(x)$ that we can plug into (4.15) in order to estimate $p_k(x)$. We will then classify an observation to the class for which $p_k(x)$ is greatest. To estimate $f_k(x)$, we will first make some assumptions about its form.

In particular, we assume that $f_k(x)$ is *normal* or *Gaussian*. In the one-dimensional setting, the normal density takes the form

$$f_k(x) = \frac{1}{\sqrt{2\pi}\sigma_k} \exp\left(-\frac{1}{2\sigma_k^2}(x - \mu_k)^2\right), \quad (4.16)$$

normal
Gaussian

where μ_k and σ_k^2 are the mean and variance parameters for the k th class. For now, let us further assume that $\sigma_1^2 = \dots = \sigma_K^2$: that is, there is a shared variance term across all K classes, which for simplicity we can denote by σ^2 . Plugging (4.16) into (4.15), we find that

$$p_k(x) = \frac{\pi_k \frac{1}{\sqrt{2\pi}\sigma} \exp\left(-\frac{1}{2\sigma^2}(x - \mu_k)^2\right)}{\sum_{l=1}^K \pi_l \frac{1}{\sqrt{2\pi}\sigma} \exp\left(-\frac{1}{2\sigma^2}(x - \mu_l)^2\right)}. \quad (4.17)$$

(Note that in (4.17), π_k denotes the prior probability that an observation belongs to the k th class, not to be confused with $\pi \approx 3.14159$, the mathematical constant.) The Bayes classifier² involves assigning an observation

²Recall that the *Bayes classifier* assigns an observation to the class for which $p_k(x)$ is largest. This is different from *Bayes' theorem* in (4.15), which allows us to manipulate conditional distributions.

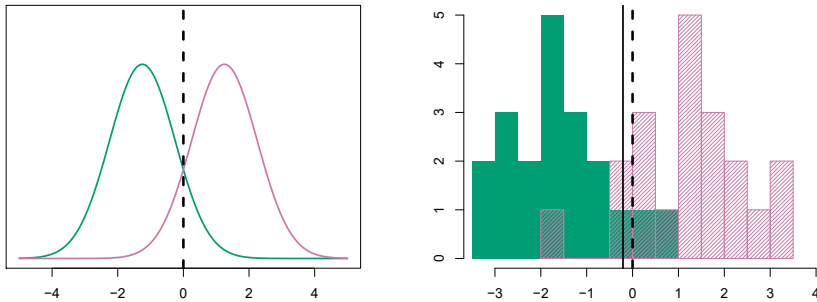


FIGURE 4.4. Left: Two one-dimensional normal density functions are shown. The dashed vertical line represents the Bayes decision boundary. Right: 20 observations were drawn from each of the two classes, and are shown as histograms. The Bayes decision boundary is again shown as a dashed vertical line. The solid vertical line represents the LDA decision boundary estimated from the training data.

$X = x$ to the class for which (4.17) is largest. Taking the log of (4.17) and rearranging the terms, it is not hard to show³ that this is equivalent to assigning the observation to the class for which

$$\delta_k(x) = x \cdot \frac{\mu_k}{\sigma^2} - \frac{\mu_k^2}{2\sigma^2} + \log(\pi_k) \quad (4.18)$$

is largest. For instance, if $K = 2$ and $\pi_1 = \pi_2$, then the Bayes classifier assigns an observation to class 1 if $2x(\mu_1 - \mu_2) > \mu_1^2 - \mu_2^2$, and to class 2 otherwise. The Bayes decision boundary is the point for which $\delta_1(x) = \delta_2(x)$; one can show that this amounts to

$$x = \frac{\mu_1^2 - \mu_2^2}{2(\mu_1 - \mu_2)} = \frac{\mu_1 + \mu_2}{2}. \quad (4.19)$$

An example is shown in the left-hand panel of Figure 4.4. The two normal density functions that are displayed, $f_1(x)$ and $f_2(x)$, represent two distinct classes. The mean and variance parameters for the two density functions are $\mu_1 = -1.25$, $\mu_2 = 1.25$, and $\sigma_1^2 = \sigma_2^2 = 1$. The two densities overlap, and so given that $X = x$, there is some uncertainty about the class to which the observation belongs. If we assume that an observation is equally likely to come from either class—that is, $\pi_1 = \pi_2 = 0.5$ —then by inspection of (4.19), we see that the Bayes classifier assigns the observation to class 1 if $x < 0$ and class 2 otherwise. Note that in this case, we can compute the Bayes classifier because we know that X is drawn from a Gaussian distribution within each class, and we know all of the parameters involved. In a real-life situation, we are not able to calculate the Bayes classifier.

In practice, even if we are quite certain of our assumption that X is drawn from a Gaussian distribution within each class, to apply the Bayes classifier we still have to estimate the parameters μ_1, \dots, μ_K , π_1, \dots, π_K , and σ^2 . The *linear discriminant analysis* (LDA) method approximates the Bayes classifier by plugging estimates for π_k , μ_k , and σ^2 into (4.18). In

linear
discriminant
analysis

³See Exercise 2 at the end of this chapter.

particular, the following estimates are used:

$$\begin{aligned}\hat{\mu}_k &= \frac{1}{n_k} \sum_{i:y_i=k} x_i \\ \hat{\sigma}^2 &= \frac{1}{n-K} \sum_{k=1}^K \sum_{i:y_i=k} (x_i - \hat{\mu}_k)^2\end{aligned}\quad (4.20)$$

where n is the total number of training observations, and n_k is the number of training observations in the k th class. The estimate for μ_k is simply the average of all the training observations from the k th class, while $\hat{\sigma}^2$ can be seen as a weighted average of the sample variances for each of the K classes. Sometimes we have knowledge of the class membership probabilities π_1, \dots, π_K , which can be used directly. In the absence of any additional information, LDA estimates π_k using the proportion of the training observations that belong to the k th class. In other words,

$$\hat{\pi}_k = n_k/n. \quad (4.21)$$

The LDA classifier plugs the estimates given in (4.20) and (4.21) into (4.18), and assigns an observation $X = x$ to the class for which

$$\hat{\delta}_k(x) = x \cdot \frac{\hat{\mu}_k}{\hat{\sigma}^2} - \frac{\hat{\mu}_k^2}{2\hat{\sigma}^2} + \log(\hat{\pi}_k) \quad (4.22)$$

is largest. The word *linear* in the classifier's name stems from the fact that the *discriminant functions* $\hat{\delta}_k(x)$ in (4.22) are linear functions of x (as opposed to a more complex function of x).

discriminant function

The right-hand panel of Figure 4.4 displays a histogram of a random sample of 20 observations from each class. To implement LDA, we began by estimating π_k , μ_k , and σ^2 using (4.20) and (4.21). We then computed the decision boundary, shown as a black solid line, that results from assigning an observation to the class for which (4.22) is largest. All points to the left of this line will be assigned to the green class, while points to the right of this line are assigned to the purple class. In this case, since $n_1 = n_2 = 20$, we have $\hat{\pi}_1 = \hat{\pi}_2$. As a result, the decision boundary corresponds to the midpoint between the sample means for the two classes, $(\hat{\mu}_1 + \hat{\mu}_2)/2$. The figure indicates that the LDA decision boundary is slightly to the left of the optimal Bayes decision boundary, which instead equals $(\mu_1 + \mu_2)/2 = 0$. How well does the LDA classifier perform on this data? Since this is simulated data, we can generate a large number of test observations in order to compute the Bayes error rate and the LDA test error rate. These are 10.6% and 11.1%, respectively. In other words, the LDA classifier's error rate is only 0.5% above the smallest possible error rate! This indicates that LDA is performing pretty well on this data set.

To reiterate, the LDA classifier results from assuming that the observations within each class come from a normal distribution with a class-specific mean and a common variance σ^2 , and plugging estimates for these parameters into the Bayes classifier. In Section 4.4.3, we will consider a less stringent set of assumptions, by allowing the observations in the k th class to have a class-specific variance, σ_k^2 .

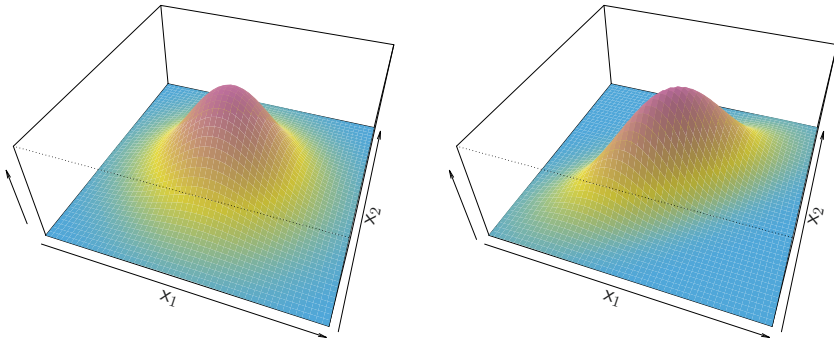


FIGURE 4.5. Two multivariate Gaussian density functions are shown, with $p = 2$. Left: The two predictors are uncorrelated. Right: The two variables have a correlation of 0.7.

4.4.2 Linear Discriminant Analysis for $p > 1$

We now extend the LDA classifier to the case of multiple predictors. To do this, we will assume that $X = (X_1, X_2, \dots, X_p)$ is drawn from a *multivariate Gaussian* (or multivariate normal) distribution, with a class-specific mean vector and a common covariance matrix. We begin with a brief review of this distribution.

multivariate Gaussian

The multivariate Gaussian distribution assumes that each individual predictor follows a one-dimensional normal distribution, as in (4.16), with some correlation between each pair of predictors. Two examples of multivariate Gaussian distributions with $p = 2$ are shown in Figure 4.5. The height of the surface at any particular point represents the probability that both X_1 and X_2 fall in a small region around that point. In either panel, if the surface is cut along the X_1 axis or along the X_2 axis, the resulting cross-section will have the shape of a one-dimensional normal distribution. The left-hand panel of Figure 4.5 illustrates an example in which $\text{Var}(X_1) = \text{Var}(X_2)$ and $\text{Cor}(X_1, X_2) = 0$; this surface has a characteristic *bell shape*. However, the bell shape will be distorted if the predictors are correlated or have unequal variances, as is illustrated in the right-hand panel of Figure 4.5. In this situation, the base of the bell will have an elliptical, rather than circular, shape. To indicate that a p -dimensional random variable X has a multivariate Gaussian distribution, we write $X \sim N(\mu, \Sigma)$. Here $E(X) = \mu$ is the mean of X (a vector with p components), and $\text{Cov}(X) = \Sigma$ is the $p \times p$ covariance matrix of X . Formally, the multivariate Gaussian density is defined as

$$f(x) = \frac{1}{(2\pi)^{p/2} |\Sigma|^{1/2}} \exp\left(-\frac{1}{2}(x - \mu)^T \Sigma^{-1} (x - \mu)\right). \quad (4.23)$$

In the case of $p > 1$ predictors, the LDA classifier assumes that the observations in the k th class are drawn from a multivariate Gaussian distribution $N(\mu_k, \Sigma)$, where μ_k is a class-specific mean vector, and Σ is a covariance matrix that is common to all K classes. Plugging the density function for the k th class, $f_k(X = x)$, into (4.15) and performing a little bit of algebra reveals that the Bayes classifier assigns an observation $X = x$

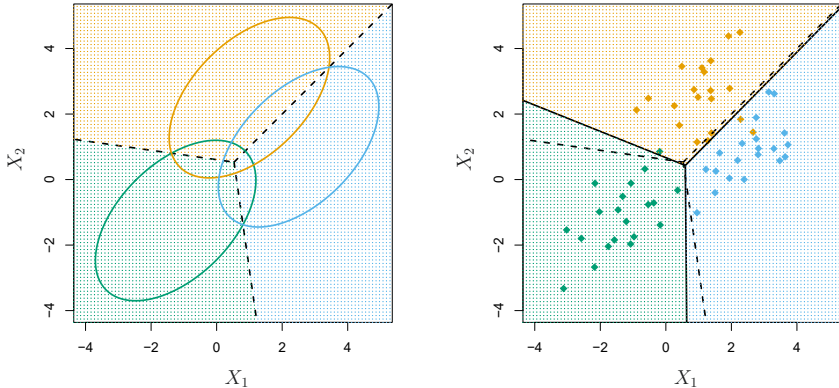


FIGURE 4.6. An example with three classes. The observations from each class are drawn from a multivariate Gaussian distribution with $p = 2$, with a class-specific mean vector and a common covariance matrix. Left: Ellipses that contain 95 % of the probability for each of the three classes are shown. The dashed lines are the Bayes decision boundaries. Right: 20 observations were generated from each class, and the corresponding LDA decision boundaries are indicated using solid black lines. The Bayes decision boundaries are once again shown as dashed lines.

to the class for which

$$\delta_k(x) = x^T \Sigma^{-1} \mu_k - \frac{1}{2} \mu_k^T \Sigma^{-1} \mu_k + \log \pi_k \quad (4.24)$$

is largest. This is the vector/matrix version of (4.18).

An example is shown in the left-hand panel of Figure 4.6. Three equally-sized Gaussian classes are shown with class-specific mean vectors and a common covariance matrix. The three ellipses represent regions that contain 95 % of the probability for each of the three classes. The dashed lines are the Bayes decision boundaries. In other words, they represent the set of values x for which $\delta_k(x) = \delta_\ell(x)$; i.e.

$$x^T \Sigma^{-1} \mu_k - \frac{1}{2} \mu_k^T \Sigma^{-1} \mu_k = x^T \Sigma^{-1} \mu_l - \frac{1}{2} \mu_l^T \Sigma^{-1} \mu_l \quad (4.25)$$

for $k \neq l$. (The $\log \pi_k$ term from (4.24) has disappeared because each of the three classes has the same number of training observations; i.e. π_k is the same for each class.) Note that there are three lines representing the Bayes decision boundaries because there are three *pairs of classes* among the three classes. That is, one Bayes decision boundary separates class 1 from class 2, one separates class 1 from class 3, and one separates class 2 from class 3. These three Bayes decision boundaries divide the predictor space into three regions. The Bayes classifier will classify an observation according to the region in which it is located.

Once again, we need to estimate the unknown parameters μ_1, \dots, μ_K , π_1, \dots, π_K , and Σ ; the formulas are similar to those used in the one-dimensional case, given in (4.20). To assign a new observation $X = x$, LDA plugs these estimates into (4.24) to obtain quantities $\hat{\delta}_k(x)$, and classifies to the class for which $\hat{\delta}_k(x)$ is largest. Note that in (4.24) $\delta_k(x)$ is a linear function of x ; that is, the LDA decision rule depends on x only

		True default status		
		No	Yes	Total
Predicted default status	No	9644	252	9896
	Yes	23	81	104
Total	9667	333	10000	

TABLE 4.4. A confusion matrix compares the LDA predictions to the true default statuses for the 10,000 training observations in the `Default` data set. Elements on the diagonal of the matrix represent individuals whose default statuses were correctly predicted, while off-diagonal elements represent individuals that were misclassified. LDA made incorrect predictions for 23 individuals who did not default and for 252 individuals who did default.

through a linear combination of its elements. As previously discussed, this is the reason for the word *linear* in LDA.

In the right-hand panel of Figure 4.6, 20 observations drawn from each of the three classes are displayed, and the resulting LDA decision boundaries are shown as solid black lines. Overall, the LDA decision boundaries are pretty close to the Bayes decision boundaries, shown again as dashed lines. The test error rates for the Bayes and LDA classifiers are 0.0746 and 0.0770, respectively. This indicates that LDA is performing well on this data.

We can perform LDA on the `Default` data in order to predict whether or not an individual will default on the basis of credit card balance and student status.⁴ The LDA model fit to the 10,000 training samples results in a *training* error rate of 2.75 %. This sounds like a low error rate, but two caveats must be noted.

- First of all, training error rates will usually be lower than test error rates, which are the real quantity of interest. In other words, we might expect this classifier to perform worse if we use it to predict whether or not a new set of individuals will default. The reason is that we specifically adjust the parameters of our model to do well on the training data. The higher the ratio of parameters p to number of samples n , the more we expect this *overfitting* to play a role. For these data we don't expect this to be a problem, since $p = 2$ and $n = 10,000$.
- Second, since only 3.33 % of the individuals in the training sample defaulted, a simple but useless classifier that always predicts that an individual will not default, regardless of his or her credit card balance and student status, will result in an error rate of 3.33 %. In other words, the trivial *null* classifier will achieve an error rate that is only a bit higher than the LDA training set error rate.

overfitting

null

In practice, a binary classifier such as this one can make two types of errors: it can incorrectly assign an individual who defaults to the *no default* category, or it can incorrectly assign an individual who does not default to

⁴The careful reader will notice that student status is qualitative — thus, the normality assumption made by LDA is clearly violated in this example! However, LDA is often remarkably robust to model violations, as this example shows. Naive Bayes, discussed in Section 4.4.4, provides an alternative to LDA that does not assume normally distributed predictors.

the *default* category. It is often of interest to determine which of these two types of errors are being made. A *confusion matrix*, shown for the **Default** data in Table 4.4, is a convenient way to display this information. The table reveals that LDA predicted that a total of 104 people would default. Of these people, 81 actually defaulted and 23 did not. Hence only 23 out of 9,667 of the individuals who did not default were incorrectly labeled. This looks like a pretty low error rate! However, of the 333 individuals who defaulted, 252 (or 75.7%) were missed by LDA. So while the overall error rate is low, the error rate among individuals who defaulted is very high. From the perspective of a credit card company that is trying to identify high-risk individuals, an error rate of $252/333 = 75.7\%$ among individuals who default may well be unacceptable.

Class-specific performance is also important in medicine and biology, where the terms *sensitivity* and *specificity* characterize the performance of a classifier or screening test. In this case the sensitivity is the percentage of true defaulters that are identified; it equals 24.3%. The specificity is the percentage of non-defaulters that are correctly identified; it equals $(1 - 23/9667) = 99.8\%$.

Why does LDA do such a poor job of classifying the customers who default? In other words, why does it have such low sensitivity? As we have seen, LDA is trying to approximate the Bayes classifier, which has the lowest *total* error rate out of all classifiers. That is, the Bayes classifier will yield the smallest possible total number of misclassified observations, regardless of the class from which the errors stem. Some misclassifications will result from incorrectly assigning a customer who does not default to the default class, and others will result from incorrectly assigning a customer who defaults to the non-default class. In contrast, a credit card company might particularly wish to avoid incorrectly classifying an individual who will default, whereas incorrectly classifying an individual who will not default, though still to be avoided, is less problematic. We will now see that it is possible to modify LDA in order to develop a classifier that better meets the credit card company's needs.

The Bayes classifier works by assigning an observation to the class for which the posterior probability $p_k(X)$ is greatest. In the two-class case, this amounts to assigning an observation to the *default* class if

$$\Pr(\text{default} = \text{Yes} | X = x) > 0.5. \quad (4.26)$$

Thus, the Bayes classifier, and by extension LDA, uses a threshold of 50% for the posterior probability of default in order to assign an observation to the *default* class. However, if we are concerned about incorrectly predicting the default status for individuals who default, then we can consider lowering this threshold. For instance, we might label any customer with a posterior probability of default above 20% to the *default* class. In other words, instead of assigning an observation to the *default* class if (4.26) holds, we could instead assign an observation to this class if

$$\Pr(\text{default} = \text{Yes} | X = x) > 0.2. \quad (4.27)$$

The error rates that result from taking this approach are shown in Table 4.5. Now LDA predicts that 430 individuals will default. Of the 333 individuals who default, LDA correctly predicts all but 138, or 41.4%. This is a vast

confusion
matrix

sensitivity
specificity

		<i>True default status</i>		Total
		No	Yes	
<i>Predicted default status</i>	No	9432	138	9570
	Yes	235	195	430
	Total	9667	333	10000

TABLE 4.5. A confusion matrix compares the LDA predictions to the true default statuses for the 10,000 training observations in the **Default** data set, using a modified threshold value that predicts default for any individuals whose posterior default probability exceeds 20 %.

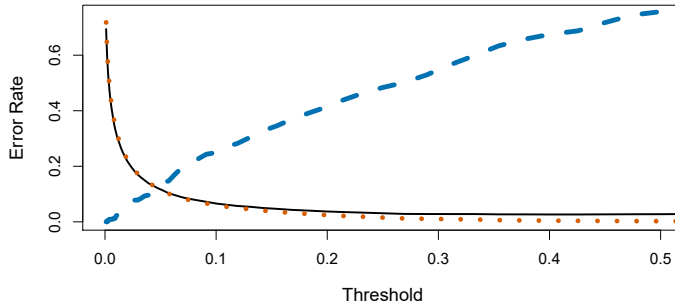


FIGURE 4.7. For the **Default** data set, error rates are shown as a function of the threshold value for the posterior probability that is used to perform the assignment. The black solid line displays the overall error rate. The blue dashed line represents the fraction of defaulting customers that are incorrectly classified, and the orange dotted line indicates the fraction of errors among the non-defaulting customers.

improvement over the error rate of 75.7 % that resulted from using the threshold of 50 %. However, this improvement comes at a cost: now 235 individuals who do not default are incorrectly classified. As a result, the overall error rate has increased slightly to 3.73 %. But a credit card company may consider this slight increase in the total error rate to be a small price to pay for more accurate identification of individuals who do indeed default.

Figure 4.7 illustrates the trade-off that results from modifying the threshold old value for the posterior probability of default. Various error rates are shown as a function of the threshold value. Using a threshold of 0.5, as in (4.26), minimizes the overall error rate, shown as a black solid line. This is to be expected, since the Bayes classifier uses a threshold of 0.5 and is known to have the lowest overall error rate. But when a threshold of 0.5 is used, the error rate among the individuals who default is quite high (blue dashed line). As the threshold is reduced, the error rate among individuals who default decreases steadily, but the error rate among the individuals who do not default increases. How can we decide which threshold value is best? Such a decision must be based on *domain knowledge*, such as detailed information about the costs associated with default.

The *ROC curve* is a popular graphic for simultaneously displaying the two types of errors for all possible thresholds. The name “ROC” is historic, and comes from communications theory. It is an acronym for *receiver operating characteristics*. Figure 4.8 displays the ROC curve for the LDA classifier on the training data. The overall performance of a classifier, sum-

ROC curve

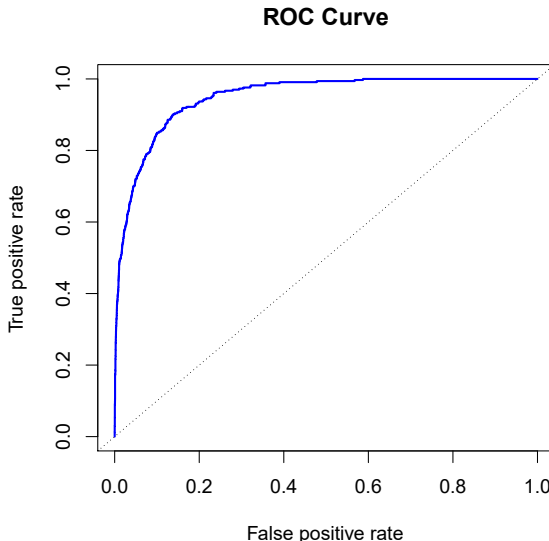


FIGURE 4.8. A ROC curve for the LDA classifier on the `Default` data. It traces out two types of error as we vary the threshold value for the posterior probability of default. The actual thresholds are not shown. The true positive rate is the sensitivity: the fraction of defaulters that are correctly identified, using a given threshold value. The false positive rate is 1-specificity: the fraction of non-defaulters that we classify incorrectly as defaulters, using that same threshold value. The ideal ROC curve hugs the top left corner, indicating a high true positive rate and a low false positive rate. The dotted line represents the “no information” classifier; this is what we would expect if student status and credit card balance are not associated with probability of default.

marized over all possible thresholds, is given by the *area under the (ROC) curve* (AUC). An ideal ROC curve will hug the top left corner, so the larger the AUC the better the classifier. For this data the AUC is 0.95, which is close to the maximum of 1.0, so would be considered very good. We expect a classifier that performs no better than chance to have an AUC of 0.5 (when evaluated on an independent test set not used in model training). ROC curves are useful for comparing different classifiers, since they take into account all possible thresholds. It turns out that the ROC curve for the logistic regression model of Section 4.3.4 fit to these data is virtually indistinguishable from this one for the LDA model, so we do not display it here.

area under
the (ROC)
curve

As we have seen above, varying the classifier threshold changes its true positive and false positive rate. These are also called the *sensitivity* and one minus the *specificity* of our classifier. Since there is an almost bewildering array of terms used in this context, we now give a summary. Table 4.6 shows the possible results when applying a classifier (or diagnostic test) to a population. To make the connection with the epidemiology literature, we think of “+” as the “disease” that we are trying to detect, and “−” as the “non-disease” state. To make the connection to the classical hypothesis testing literature, we think of “−” as the null hypothesis and “+” as the

sensitivity
specificity

		<i>True class</i>		
		– or Null	+ or Non-null	Total
<i>Predicted class</i>	– or Null	True Neg. (TN)	False Neg. (FN)	N*
	+ or Non-null	False Pos. (FP)	True Pos. (TP)	P*
Total		N	P	

TABLE 4.6. Possible results when applying a classifier or diagnostic test to a population.

Name	Definition	Synonyms
False Pos. rate	FP/N	Type I error, 1–Specificity
True Pos. rate	TP/P	1–Type II error, power, sensitivity, recall
Pos. Pred. value	TP/P*	Precision, 1–false discovery proportion
Neg. Pred. value	TN/N*	

TABLE 4.7. Important measures for classification and diagnostic testing, derived from quantities in Table 4.6.

alternative (non-null) hypothesis. In the context of the **Default** data, “+” indicates an individual who defaults, and “–” indicates one who does not.

Table 4.7 lists many of the popular performance measures that are used in this context. The denominators for the false positive and true positive rates are the actual population counts in each class. In contrast, the denominators for the positive predictive value and the negative predictive value are the total predicted counts for each class.

4.4.3 Quadratic Discriminant Analysis

As we have discussed, LDA assumes that the observations within each class are drawn from a multivariate Gaussian distribution with a class-specific mean vector and a covariance matrix that is common to all K classes. *Quadratic discriminant analysis* (QDA) provides an alternative approach. Like LDA, the QDA classifier results from assuming that the observations from each class are drawn from a Gaussian distribution, and plugging estimates for the parameters into Bayes’ theorem in order to perform prediction. However, unlike LDA, QDA assumes that each class has its own covariance matrix. That is, it assumes that an observation from the k th class is of the form $X \sim N(\mu_k, \Sigma_k)$, where Σ_k is a covariance matrix for the k th class. Under this assumption, the Bayes classifier assigns an observation $X = x$ to the class for which

$$\begin{aligned} \delta_k(x) &= -\frac{1}{2}(x - \mu_k)^T \Sigma_k^{-1} (x - \mu_k) - \frac{1}{2} \log |\Sigma_k| + \log \pi_k \\ &= -\frac{1}{2}x^T \Sigma_k^{-1} x + x^T \Sigma_k^{-1} \mu_k - \frac{1}{2}\mu_k^T \Sigma_k^{-1} \mu_k - \frac{1}{2} \log |\Sigma_k| + \log \pi_k \end{aligned} \tag{4.28}$$

quadratic
discriminant
analysis

is largest. So the QDA classifier involves plugging estimates for Σ_k , μ_k , and π_k into (4.28), and then assigning an observation $X = x$ to the class for which this quantity is largest. Unlike in (4.24), the quantity x appears as a *quadratic* function in (4.28). This is where QDA gets its name.

Why does it matter whether or not we assume that the K classes share a common covariance matrix? In other words, why would one prefer LDA to

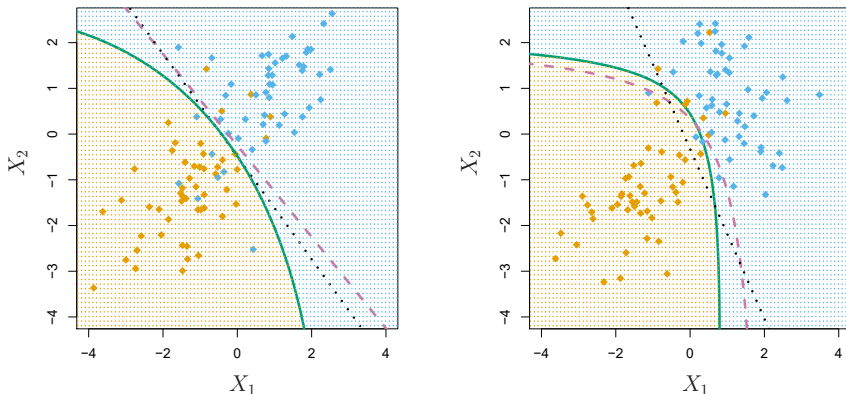


FIGURE 4.9. Left: The Bayes (purple dashed), LDA (black dotted), and QDA (green solid) decision boundaries for a two-class problem with $\Sigma_1 = \Sigma_2$. The shading indicates the QDA decision rule. Since the Bayes decision boundary is linear, it is more accurately approximated by LDA than by QDA. Right: Details are as given in the left-hand panel, except that $\Sigma_1 \neq \Sigma_2$. Since the Bayes decision boundary is non-linear, it is more accurately approximated by QDA than by LDA.

QDA, or vice-versa? The answer lies in the bias-variance trade-off. When there are p predictors, then estimating a covariance matrix requires estimating $p(p+1)/2$ parameters. QDA estimates a separate covariance matrix for each class, for a total of $Kp(p+1)/2$ parameters. With 50 predictors this is some multiple of 1,275, which is a lot of parameters. By instead assuming that the K classes share a common covariance matrix, the LDA model becomes linear in x , which means there are Kp linear coefficients to estimate. Consequently, LDA is a much less flexible classifier than QDA, and so has substantially lower variance. This can potentially lead to improved prediction performance. But there is a trade-off: if LDA's assumption that the K classes share a common covariance matrix is badly off, then LDA can suffer from high bias. Roughly speaking, LDA tends to be a better bet than QDA if there are relatively few training observations and so reducing variance is crucial. In contrast, QDA is recommended if the training set is very large, so that the variance of the classifier is not a major concern, or if the assumption of a common covariance matrix for the K classes is clearly untenable.

Figure 4.9 illustrates the performances of LDA and QDA in two scenarios. In the left-hand panel, the two Gaussian classes have a common correlation of 0.7 between X_1 and X_2 . As a result, the Bayes decision boundary is linear and is accurately approximated by the LDA decision boundary. The QDA decision boundary is inferior, because it suffers from higher variance without a corresponding decrease in bias. In contrast, the right-hand panel displays a situation in which the orange class has a correlation of 0.7 between the variables and the blue class has a correlation of -0.7. Now the Bayes decision boundary is quadratic, and so QDA more accurately approximates this boundary than does LDA.

4.4.4 Naive Bayes

In previous sections, we used Bayes' theorem (4.15) to develop the LDA and QDA classifiers. Here, we use Bayes' theorem to motivate the popular *naive Bayes* classifier.

Recall that Bayes' theorem (4.15) provides an expression for the posterior probability $p_k(x) = \Pr(Y = k|X = x)$ in terms of π_1, \dots, π_K and $f_1(x), \dots, f_K(x)$. To use (4.15) in practice, we need estimates for π_1, \dots, π_K and $f_1(x), \dots, f_K(x)$. As we saw in previous sections, estimating the prior probabilities π_1, \dots, π_K is typically straightforward: for instance, we can estimate $\hat{\pi}_k$ as the proportion of training observations belonging to the k th class, for $k = 1, \dots, K$.

naive Bayes

However, estimating $f_1(x), \dots, f_K(x)$ is more subtle. Recall that $f_k(x)$ is the p -dimensional density function for an observation in the k th class, for $k = 1, \dots, K$. In general, estimating a p -dimensional density function is challenging. In LDA, we make a very strong assumption that greatly simplifies the task: we assume that f_k is the density function for a multivariate normal random variable with class-specific mean μ_k , and shared covariance matrix Σ . By contrast, in QDA, we assume that f_k is the density function for a multivariate normal random variable with class-specific mean μ_k , and class-specific covariance matrix Σ_k . By making these very strong assumptions, we are able to replace the very challenging problem of estimating K p -dimensional density functions with the much simpler problem of estimating K p -dimensional mean vectors and one (in the case of LDA) or K (in the case of QDA) $(p \times p)$ -dimensional covariance matrices.

The naive Bayes classifier takes a different tack for estimating $f_1(x), \dots, f_K(x)$. Instead of assuming that these functions belong to a particular family of distributions (e.g. multivariate normal), we instead make a single assumption:

Within the k th class, the p predictors are independent.

Stated mathematically, this assumption means that for $k = 1, \dots, K$,

$$f_k(x) = f_{k1}(x_1) \times f_{k2}(x_2) \times \cdots \times f_{kp}(x_p), \quad (4.29)$$

where f_{kj} is the density function of the j th predictor among observations in the k th class.

Why is this assumption so powerful? Essentially, estimating a p -dimensional density function is challenging because we must consider not only the *marginal distribution* of each predictor — that is, the distribution of each predictor on its own — but also the *joint distribution* of the predictors — that is, the association between the different predictors. In the case of a multivariate normal distribution, the association between the different predictors is summarized by the off-diagonal elements of the covariance matrix. However, in general, this association can be very hard to characterize, and exceedingly challenging to estimate. But by assuming that the p covariates are independent within each class, we completely eliminate the need to worry about the association between the p predictors, because we have simply assumed that there is *no* association between the predictors!

marginal
distribution
joint
distribution

Do we really believe the naive Bayes assumption that the p covariates are independent within each class? In most settings, we do not. But even though this modeling assumption is made for convenience, it often leads to

pretty decent results, especially in settings where n is not large enough relative to p for us to effectively estimate the joint distribution of the predictors within each class. In fact, since estimating a joint distribution requires such a huge amount of data, naive Bayes is a good choice in a wide range of settings. Essentially, the naive Bayes assumption introduces some bias, but reduces variance, leading to a classifier that works quite well in practice as a result of the bias-variance trade-off.

Once we have made the naive Bayes assumption, we can plug (4.29) into (4.15) to obtain an expression for the posterior probability,

$$\Pr(Y = k|X = x) = \frac{\pi_k \times f_{k1}(x_1) \times f_{k2}(x_2) \times \cdots \times f_{kp}(x_p)}{\sum_{l=1}^K \pi_l \times f_{l1}(x_1) \times f_{l2}(x_2) \times \cdots \times f_{lp}(x_p)} \quad (4.30)$$

for $k = 1, \dots, K$.

To estimate the one-dimensional density function f_{kj} using training data x_{1j}, \dots, x_{nj} , we have a few options.

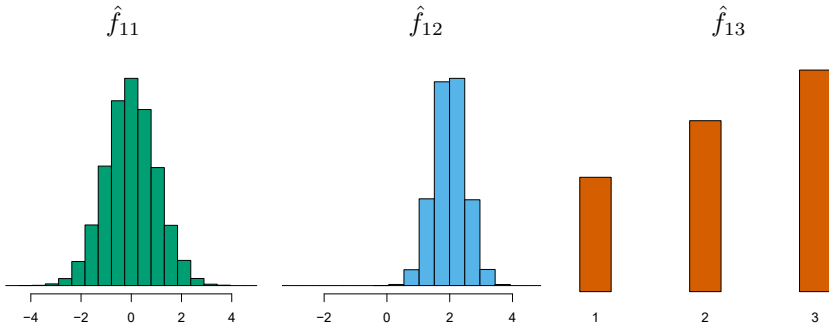
- If X_j is quantitative, then we can assume that $X_j|Y = k \sim N(\mu_{jk}, \sigma_{jk}^2)$. In other words, we assume that within each class, the j th predictor is drawn from a (univariate) normal distribution. While this may sound a bit like QDA, there is one key difference, in that here we are assuming that the predictors are independent; this amounts to QDA with an additional assumption that the class-specific covariance matrix is diagonal.
- If X_j is quantitative, then another option is to use a non-parametric estimate for f_{kj} . A very simple way to do this is by making a histogram for the observations of the j th predictor within each class. Then we can estimate $f_{kj}(x_j)$ as the fraction of the training observations in the k th class that belong to the same histogram bin as x_j . Alternatively, we can use a *kernel density estimator*, which is essentially a smoothed version of a histogram.
- If X_j is qualitative, then we can simply count the proportion of training observations for the j th predictor corresponding to each class. For instance, suppose that $X_j \in \{1, 2, 3\}$, and we have 100 observations in the k th class. Suppose that the j th predictor takes on values of 1, 2, and 3 in 32, 55, and 13 of those observations, respectively. Then we can estimate f_{kj} as

$$\hat{f}_{kj}(x_j) = \begin{cases} 0.32 & \text{if } x_j = 1 \\ 0.55 & \text{if } x_j = 2 \\ 0.13 & \text{if } x_j = 3. \end{cases}$$

kernel
density
estimator

We now consider the naive Bayes classifier in a toy example with $p = 3$ predictors and $K = 2$ classes. The first two predictors are quantitative, and the third predictor is qualitative with three levels. Suppose further that $\hat{\pi}_1 = \hat{\pi}_2 = 0.5$. The estimated density functions \hat{f}_{kj} for $k = 1, 2$ and $j = 1, 2, 3$ are displayed in Figure 4.10. Now suppose that we wish to classify a new observation, $x^* = (0.4, 1.5, 1)^T$. It turns out that in this

Density estimates for class k=1



Density estimates for class k=2

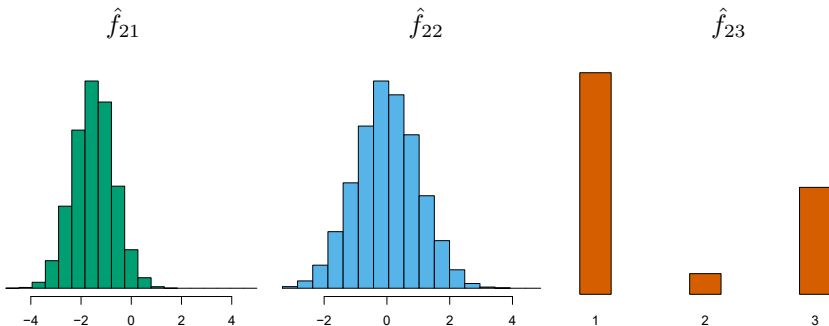


FIGURE 4.10. In the toy example in Section 4.4.4, we generate data with $p = 3$ predictors and $K = 2$ classes. The first two predictors are quantitative, and the third predictor is qualitative with three levels. In each class, the estimated density for each of the three predictors is displayed. If the prior probabilities for the two classes are equal, then the observation $x^* = (0.4, 1.5, 1)^T$ has a 94.4% posterior probability of belonging to the first class.

		True default status		Total
		No	Yes	
Predicted default status	No	9621	244	9865
	Yes	46	89	135
	Total	9667	333	10000

TABLE 4.8. Comparison of the naive Bayes predictions to the true default status for the 10,000 training observations in the `Default` data set, when we predict default for any observation for which $P(Y = \text{default}|X = x) > 0.5$.

example, $\hat{f}_{11}(0.4) = 0.368$, $\hat{f}_{12}(1.5) = 0.484$, $\hat{f}_{13}(1) = 0.226$, and $\hat{f}_{21}(0.4) = 0.030$, $\hat{f}_{22}(1.5) = 0.130$, $\hat{f}_{23}(1) = 0.616$. Plugging these estimates into (4.30) results in posterior probability estimates of $\Pr(Y = 1|X = x^*) = 0.944$ and $\Pr(Y = 2|X = x^*) = 0.056$.

Table 4.8 provides the confusion matrix resulting from applying the naive Bayes classifier to the `Default` data set, where we predict a default if the posterior probability of a default — that is, $P(Y = \text{default}|X = x)$ — exceeds 0.5. Comparing this to the results for LDA in Table 4.4, our findings are mixed. While LDA has a slightly lower overall error rate, naive Bayes

		True default status		
		No	Yes	Total
Predicted default status	No	9339	130	9469
	Yes	328	203	531
Total	9667	333	10000	

TABLE 4.9. Comparison of the naive Bayes predictions to the true default status for the 10,000 training observations in the `Default` data set, when we predict default for any observation for which $P(Y = \text{default}|X = x) > 0.2$.

correctly predicts a higher fraction of the true defaulters. In this implementation of naive Bayes, we have assumed that each quantitative predictor is drawn from a Gaussian distribution (and, of course, that within each class, each predictor is independent).

Just as with LDA, we can easily adjust the probability threshold for predicting a default. For example, Table 4.9 provides the confusion matrix resulting from predicting a default if $P(Y = \text{default}|X = x) > 0.2$. Again, the results are mixed relative to LDA with the same threshold (Table 4.5). Naive Bayes has a higher error rate, but correctly predicts almost two-thirds of the true defaults.

In this example, it should not be too surprising that naive Bayes does not convincingly outperform LDA: this data set has $n = 10,000$ and $p = 2$, and so the reduction in variance resulting from the naive Bayes assumption is not necessarily worthwhile. We expect to see a greater pay-off to using naive Bayes relative to LDA or QDA in instances where p is larger or n is smaller, so that reducing the variance is very important.

4.5 A Comparison of Classification Methods

4.5.1 An Analytical Comparison

We now perform an *analytical* (or mathematical) comparison of LDA, QDA, naive Bayes, and logistic regression. We consider these approaches in a setting with K classes, so that we assign an observation to the class that maximizes $\Pr(Y = k|X = x)$. Equivalently, we can set K as the *baseline* class and assign an observation to the class that maximizes

$$\log \left(\frac{\Pr(Y = k|X = x)}{\Pr(Y = K|X = x)} \right) \quad (4.31)$$

for $k = 1, \dots, K$. Examining the specific form of (4.31) for each method provides a clear understanding of their similarities and differences.

First, for LDA, we can make use of Bayes' theorem (4.15) as well as the assumption that the predictors within each class are drawn from a multivariate normal density (4.23) with class-specific mean and shared co-

variance matrix in order to show that

$$\begin{aligned}
\log \left(\frac{\Pr(Y = k|X = x)}{\Pr(Y = K|X = x)} \right) &= \log \left(\frac{\pi_k f_k(x)}{\pi_K f_K(x)} \right) \\
&= \log \left(\frac{\pi_k \exp \left(-\frac{1}{2}(x - \mu_k)^T \Sigma^{-1} (x - \mu_k) \right)}{\pi_K \exp \left(-\frac{1}{2}(x - \mu_K)^T \Sigma^{-1} (x - \mu_K) \right)} \right) \\
&= \log \left(\frac{\pi_k}{\pi_K} \right) - \frac{1}{2}(x - \mu_k)^T \Sigma^{-1} (x - \mu_k) \\
&\quad + \frac{1}{2}(x - \mu_K)^T \Sigma^{-1} (x - \mu_K) \\
&= \log \left(\frac{\pi_k}{\pi_K} \right) - \frac{1}{2}(\mu_k + \mu_K)^T \Sigma^{-1} (\mu_k - \mu_K) \\
&\quad + x^T \Sigma^{-1} (\mu_k - \mu_K) \\
&= a_k + \sum_{j=1}^p b_{kj} x_j,
\end{aligned} \tag{4.32}$$

where $a_k = \log \left(\frac{\pi_k}{\pi_K} \right) - \frac{1}{2}(\mu_k + \mu_K)^T \Sigma^{-1} (\mu_k - \mu_K)$ and b_{kj} is the j th component of $\Sigma^{-1} (\mu_k - \mu_K)$. Hence LDA, like logistic regression, assumes that the log odds of the posterior probabilities is linear in x .

Using similar calculations, in the QDA setting (4.31) becomes

$$\log \left(\frac{\Pr(Y = k|X = x)}{\Pr(Y = K|X = x)} \right) = a_k + \sum_{j=1}^p b_{kj} x_j + \sum_{j=1}^p \sum_{l=1}^p c_{kjl} x_j x_l, \tag{4.33}$$

where a_k, b_{kj} , and c_{kjl} are functions of $\pi_k, \pi_K, \mu_k, \mu_K, \Sigma_k$ and Σ_K . Again, as the name suggests, QDA assumes that the log odds of the posterior probabilities is quadratic in x .

Finally, we examine (4.31) in the naive Bayes setting. Recall that in this setting, $f_k(x)$ is modeled as a product of p one-dimensional functions $f_{kj}(x_j)$ for $j = 1, \dots, p$. Hence,

$$\begin{aligned}
\log \left(\frac{\Pr(Y = k|X = x)}{\Pr(Y = K|X = x)} \right) &= \log \left(\frac{\pi_k f_k(x)}{\pi_K f_K(x)} \right) \\
&= \log \left(\frac{\pi_k \prod_{j=1}^p f_{kj}(x_j)}{\pi_K \prod_{j=1}^p f_{Kj}(x_j)} \right) \\
&= \log \left(\frac{\pi_k}{\pi_K} \right) + \sum_{j=1}^p \log \left(\frac{f_{kj}(x_j)}{f_{Kj}(x_j)} \right) \\
&= a_k + \sum_{j=1}^p g_{kj}(x_j),
\end{aligned} \tag{4.34}$$

where $a_k = \log \left(\frac{\pi_k}{\pi_K} \right)$ and $g_{kj}(x_j) = \log \left(\frac{f_{kj}(x_j)}{f_{Kj}(x_j)} \right)$. Hence, the right-hand side of (4.34) takes the form of a *generalized additive model*, a topic that is discussed further in Chapter 7.

Inspection of (4.32), (4.33), and (4.34) yields the following observations about LDA, QDA, and naive Bayes:

- LDA is a special case of QDA with $c_{kjl} = 0$ for all $j = 1, \dots, p$, $l = 1, \dots, p$, and $k = 1, \dots, K$. (Of course, this is not surprising, since LDA is simply a restricted version of QDA with $\Sigma_1 = \dots = \Sigma_K = \Sigma$.)
- Any classifier with a linear decision boundary is a special case of naive Bayes with $g_{kj}(x_j) = b_{kj}x_j$. In particular, this means that LDA is a special case of naive Bayes! This is not at all obvious from the descriptions of LDA and naive Bayes earlier in this chapter, since each method makes very different assumptions: LDA assumes that the features are normally distributed with a common within-class covariance matrix, and naive Bayes instead assumes independence of the features.
- If we model $f_{kj}(x_j)$ in the naive Bayes classifier using a one-dimensional Gaussian distribution $N(\mu_{kj}, \sigma_j^2)$, then we end up with $g_{kj}(x_j) = b_{kj}x_j$ where $b_{kj} = (\mu_{kj} - \mu_{Kj})/\sigma_j^2$. In this case, naive Bayes is actually a special case of LDA with Σ restricted to be a diagonal matrix with j th diagonal element equal to σ_j^2 .
- Neither QDA nor naive Bayes is a special case of the other. Naive Bayes can produce a more flexible fit, since any choice can be made for $g_{kj}(x_j)$. However, it is restricted to a purely *additive* fit, in the sense that in (4.34), a function of x_j is *added* to a function of x_l , for $j \neq l$; however, these terms are never multiplied. By contrast, QDA includes multiplicative terms of the form $c_{kjl}x_jx_l$. Therefore, QDA has the potential to be more accurate in settings where interactions among the predictors are important in discriminating between classes.

None of these methods uniformly dominates the others: in any setting, the choice of method will depend on the true distribution of the predictors in each of the K classes, as well as other considerations, such as the values of n and p . The latter ties into the bias-variance trade-off.

How does logistic regression tie into this story? Recall from (4.12) that multinomial logistic regression takes the form

$$\log \left(\frac{\Pr(Y = k|X = x)}{\Pr(Y = K|X = x)} \right) = \beta_{k0} + \sum_{j=1}^p \beta_{kj}x_j.$$

This is identical to the linear form of LDA (4.32): in both cases, $\log \left(\frac{\Pr(Y = k|X = x)}{\Pr(Y = K|X = x)} \right)$ is a linear function of the predictors. In LDA, the coefficients in this linear function are functions of estimates for π_k , π_K , μ_k , μ_K , and Σ obtained by assuming that X_1, \dots, X_p follow a normal distribution within each class. By contrast, in logistic regression, the coefficients are chosen to maximize the likelihood function (4.5). Thus, we expect LDA to outperform logistic regression when the normality assumption (approximately) holds, and we expect logistic regression to perform better when it does not.

We close with a brief discussion of *K-nearest neighbors* (KNN), introduced in Chapter 2. Recall that KNN takes a completely different approach from the classifiers seen in this chapter. In order to make a prediction for an observation $X = x$, the training observations that are closest to x are identified. Then X is assigned to the class to which the plurality of these observations belong. Hence KNN is a completely non-parametric approach: no assumptions are made about the shape of the decision boundary. We make the following observations about KNN:

- Because KNN is completely non-parametric, we can expect this approach to dominate LDA and logistic regression when the decision boundary is highly non-linear, provided that n is very large and p is small.
- In order to provide accurate classification, KNN requires *a lot* of observations relative to the number of predictors—that is, n much larger than p . This has to do with the fact that KNN is non-parametric, and thus tends to reduce the bias while incurring a lot of variance.
- In settings where the decision boundary is non-linear but n is only modest, or p is not very small, then QDA may be preferred to KNN. This is because QDA can provide a non-linear decision boundary while taking advantage of a parametric form, which means that it requires a smaller sample size for accurate classification, relative to KNN.
- Unlike logistic regression, KNN does not tell us which predictors are important: we don't get a table of coefficients as in Table 4.3.

4.5.2 An Empirical Comparison

We now compare the *empirical* (practical) performance of logistic regression, LDA, QDA, naive Bayes, and KNN. We generated data from six different scenarios, each of which involves a binary (two-class) classification problem. In three of the scenarios, the Bayes decision boundary is linear, and in the remaining scenarios it is non-linear. For each scenario, we produced 100 random training data sets. On each of these training sets, we fit each method to the data and computed the resulting test error rate on a large test set. Results for the linear scenarios are shown in Figure 4.11, and the results for the non-linear scenarios are in Figure 4.12. The KNN method requires selection of K , the number of neighbors (not to be confused with the number of classes in earlier sections of this chapter). We performed KNN with two values of K : $K = 1$, and a value of K that was chosen automatically using an approach called *cross-validation*, which we discuss further in Chapter 5. We applied naive Bayes assuming univariate Gaussian densities for the features within each class (and, of course — since this is the key characteristic of naive Bayes — assuming independence of the features).

In each of the six scenarios, there were $p = 2$ quantitative predictors. The scenarios were as follows:

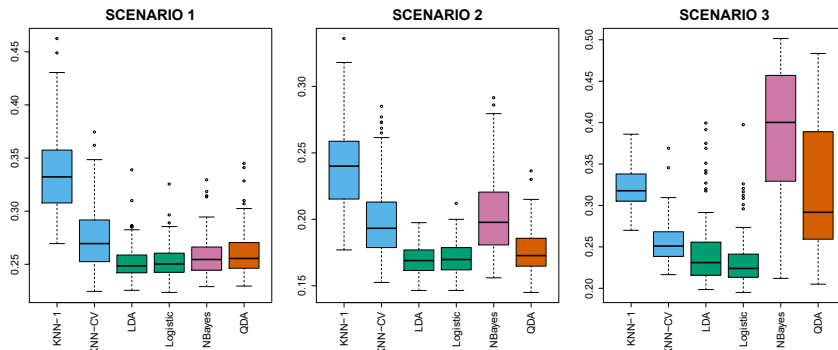


FIGURE 4.11. Boxplots of the test error rates for each of the linear scenarios described in the main text.

Scenario 1: There were 20 training observations in each of two classes. The observations within each class were uncorrelated random normal variables with a different mean in each class. The left-hand panel of Figure 4.11 shows that LDA performed well in this setting, as one would expect since this is the model assumed by LDA. Logistic regression also performed quite well, since it assumes a linear decision boundary. KNN performed poorly because it paid a price in terms of variance that was not offset by a reduction in bias. QDA also performed worse than LDA, since it fit a more flexible classifier than necessary. The performance of naive Bayes was slightly better than QDA, because the naive Bayes assumption of independent predictors is correct.

Scenario 2: Details are as in Scenario 1, except that within each class, the two predictors had a correlation of -0.5 . The center panel of Figure 4.11 indicates that the performance of most methods is similar to the previous scenario. The notable exception is naive Bayes, which performs very poorly here, since the naive Bayes assumption of independent predictors is violated.

Scenario 3: As in the previous scenario, there is substantial negative correlation between the predictors within each class. However, this time we generated X_1 and X_2 from the t -distribution, with 50 observations per class. The t -distribution has a similar shape to the normal distribution, but it has a tendency to yield more extreme points—that is, more points that are far from the mean. In this setting, the decision boundary was still linear, and so fit into the logistic regression framework. The set-up violated the assumptions of LDA, since the observations were not drawn from a normal distribution. The right-hand panel of Figure 4.11 shows that logistic regression outperformed LDA, though both methods were superior to the other approaches. In particular, the QDA results deteriorated considerably as a consequence of non-normality. Naive Bayes performed very poorly because the independence assumption is violated.

t -distribution

Scenario 4: The data were generated from a normal distribution, with a correlation of 0.5 between the predictors in the first class, and correlation of -0.5 between the predictors in the second class. This setup corresponded to the QDA assumption, and resulted in quadratic decision boundaries. The left-hand panel of Figure 4.12 shows that QDA outperformed all of the

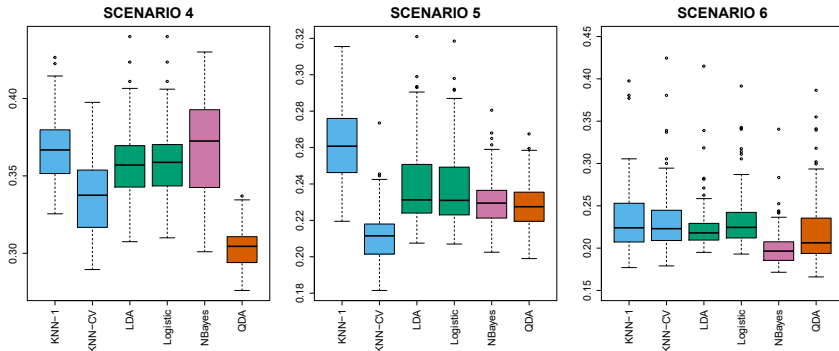


FIGURE 4.12. Boxplots of the test error rates for each of the non-linear scenarios described in the main text.

other approaches. The naive Bayes assumption of independent predictors is violated, so naive Bayes performs poorly.

Scenario 5: The data were generated from a normal distribution with uncorrelated predictors. Then the responses were sampled from the logistic function applied to a complicated non-linear function of the predictors. The center panel of Figure 4.12 shows that both QDA and naive Bayes gave slightly better results than the linear methods, while the much more flexible KNN-CV method gave the best results. But KNN with $K = 1$ gave the worst results out of all methods. This highlights the fact that even when the data exhibits a complex non-linear relationship, a non-parametric method such as KNN can still give poor results if the level of smoothness is not chosen correctly.

Scenario 6: The observations were generated from a normal distribution with a different diagonal covariance matrix for each class. However, the sample size was *very* small: just $n = 6$ in each class. Naive Bayes performed very well, because its assumptions are met. LDA and logistic regression performed poorly because the true decision boundary is non-linear, due to the unequal covariance matrices. QDA performed a bit worse than naive Bayes, because given the very small sample size, the former incurred too much variance in estimating the correlation between the predictors within each class. KNN's performance also suffered due to the very small sample size.

These six examples illustrate that no one method will dominate the others in every situation. When the true decision boundaries are linear, then the LDA and logistic regression approaches will tend to perform well. When the boundaries are moderately non-linear, QDA or naive Bayes may give better results. Finally, for much more complicated decision boundaries, a non-parametric approach such as KNN can be superior. But the level of smoothness for a non-parametric approach must be chosen carefully. In the next chapter we examine a number of approaches for choosing the correct level of smoothness and, in general, for selecting the best overall method.

Finally, recall from Chapter 3 that in the regression setting we can accommodate a non-linear relationship between the predictors and the response by performing regression using transformations of the predictors. A similar approach could be taken in the classification setting. For instance, we could

	Coefficient	Std. error	t-statistic	p-value
Intercept	73.60	5.13	14.34	0.00
workingday	1.27	1.78	0.71	0.48
temp	157.21	10.26	15.32	0.00
weathersit [cloudy/misty]	-12.89	1.96	-6.56	0.00
weathersit [light rain/snow]	-66.49	2.97	-22.43	0.00
weathersit [heavy rain/snow]	-109.75	76.67	-1.43	0.15

TABLE 4.10. Results for a least squares linear model fit to predict `bikers` in the `Bikeshare` data. The predictors `mnth` and `hr` are omitted from this table due to space constraints, and can be seen in Figure 4.13. For the qualitative variable `weathersit`, the baseline level corresponds to clear skies.

create a more flexible version of logistic regression by including X^2 , X^3 , and even X^4 as predictors. This may or may not improve logistic regression's performance, depending on whether the increase in variance due to the added flexibility is offset by a sufficiently large reduction in bias. We could do the same for LDA. If we added all possible quadratic terms and cross-products to LDA, the form of the model would be the same as the QDA model, although the parameter estimates would be different. This device allows us to move somewhere between an LDA and a QDA model.

4.6 Generalized Linear Models

In Chapter 3, we assumed that the response Y is quantitative, and explored the use of least squares linear regression to predict Y . Thus far in this chapter, we have instead assumed that Y is qualitative. However, we may sometimes be faced with situations in which Y is neither qualitative nor quantitative, and so neither linear regression from Chapter 3 nor the classification approaches covered in this chapter is applicable.

As a concrete example, we consider the `Bikeshare` data set. The response is `bikers`, the number of hourly users of a bike sharing program in Washington, DC. This response value is neither qualitative nor quantitative: instead, it takes on non-negative integer values, or *counts*. We will consider predicting `bikers` using the covariates `mnth` (month of the year), `hr` (hour of the day, from 0 to 23), `workingday` (an indicator variable that equals 1 if it is neither a weekend nor a holiday), `temp` (the normalized temperature, in Celsius), and `weathersit` (a qualitative variable that takes on one of four possible values: clear; misty or cloudy; light rain or light snow; or heavy rain or heavy snow.)

counts

In the analyses that follow, we will treat `mnth`, `hr`, and `weathersit` as qualitative variables.

4.6.1 Linear Regression on the Bikeshare Data

To begin, we consider predicting `bikers` using linear regression. The results are shown in Table 4.10.

We see, for example, that a progression of weather from clear to cloudy results in, on average, 12.89 fewer bikers per hour; however, if the weather progresses further to rain or snow, then this further results in 53.60 fewer bikers per hour. Figure 4.13 displays the coefficients associated with `mnth`

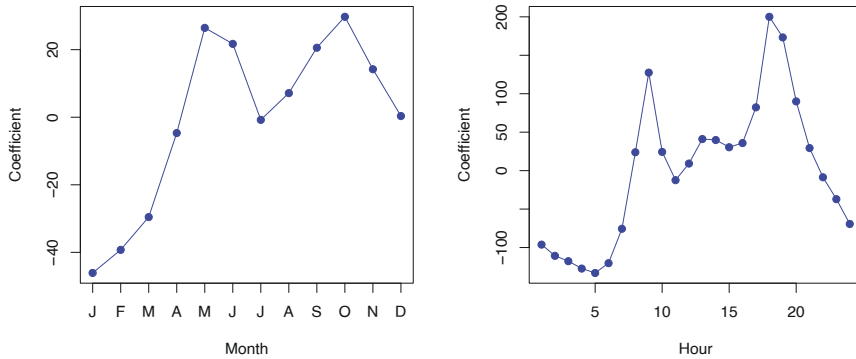


FIGURE 4.13. A least squares linear regression model was fit to predict `bikers` in the `Bikeshare` data set. Left: The coefficients associated with the month of the year. Bike usage is highest in the spring and fall, and lowest in the winter. Right: The coefficients associated with the hour of the day. Bike usage is highest during peak commute times, and lowest overnight.

and the coefficients associated with `hr`. We see that bike usage is highest in the spring and fall, and lowest during the winter months. Furthermore, bike usage is greatest around rush hour (9 AM and 6 PM), and lowest overnight. Thus, at first glance, fitting a linear regression model to the `Bikeshare` data set seems to provide reasonable and intuitive results.

But upon more careful inspection, some issues become apparent. For example, 9.6% of the fitted values in the `Bikeshare` data set are negative: that is, the linear regression model predicts a *negative* number of users during 9.6% of the hours in the data set. This calls into question our ability to perform meaningful predictions on the data, and it also raises concerns about the accuracy of the coefficient estimates, confidence intervals, and other outputs of the regression model.

Furthermore, it is reasonable to suspect that when the expected value of `bikers` is small, the variance of `bikers` should be small as well. For instance, at 2 AM during a heavy December snow storm, we expect that extremely few people will use a bike, and moreover that there should be little variance associated with the number of users during those conditions. This is borne out in the data: between 1 AM and 4 AM, in December, January, and February, when it is raining, there are 5.05 users, on average, with a standard deviation of 3.73. By contrast, between 7 AM and 10 AM, in April, May, and June, when skies are clear, there are 243.59 users, on average, with a standard deviation of 131.7. The mean-variance relationship is displayed in the left-hand panel of Figure 4.14. This is a major violation of the assumptions of a linear model, which state that $Y = \sum_{j=1}^p X_j \beta_j + \epsilon$, where ϵ is a mean-zero error term with variance σ^2 that is *constant*, and not a function of the covariates. Therefore, the heteroscedasticity of the data calls into question the suitability of a linear regression model.

Finally, the response `bikers` is integer-valued. But under a linear model, $Y = \beta_0 + \sum_{j=1}^p X_j \beta_j + \epsilon$, where ϵ is a continuous-valued error term. This means that in a linear model, the response Y is necessarily continuous-valued (quantitative). Thus, the integer nature of the response `bikers` suggests that a linear regression model is not entirely satisfactory for this data set.

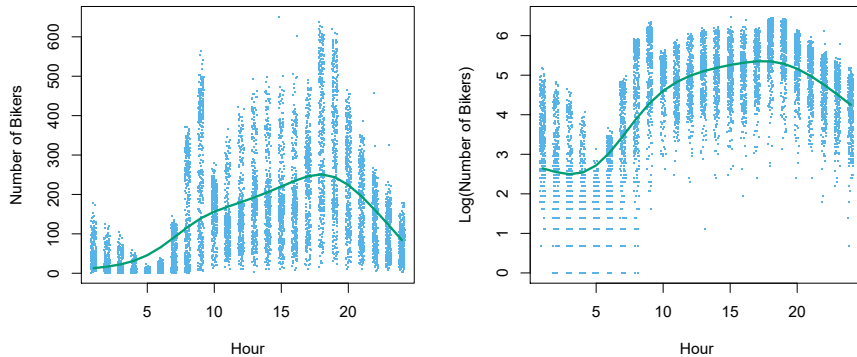


FIGURE 4.14. Left: On the `Bikeshare` dataset, the number of bikers is displayed on the y -axis, and the hour of the day is displayed on the x -axis. Jitter was applied for ease of visualization. For the most part, as the mean number of bikers increases, so does the variance in the number of bikers. A smoothing spline fit is shown in green. Right: The log of the number of bikers is now displayed on the y -axis.

Some of the problems that arise when fitting a linear regression model to the `Bikeshare` data can be overcome by transforming the response; for instance, we can fit the model

$$\log(Y) = \sum_{j=1}^p X_j \beta_j + \epsilon.$$

Transforming the response avoids the possibility of negative predictions, and it overcomes much of the heteroscedasticity in the untransformed data, as is shown in the right-hand panel of Figure 4.14. However, it is not quite a satisfactory solution, since predictions and inference are made in terms of the log of the response, rather than the response. This leads to challenges in interpretation, e.g. “*a one-unit increase in X_j is associated with an increase in the mean of the log of Y by an amount β_j* ”. Furthermore, a log transformation of the response cannot be applied in settings where the response can take on a value of 0. Thus, while fitting a linear model to a transformation of the response may be an adequate approach for some count-valued data sets, it often leaves something to be desired. We will see in the next section that a Poisson regression model provides a much more natural and elegant approach for this task.

4.6.2 Poisson Regression on the Bikeshare Data

To overcome the inadequacies of linear regression for analyzing the `Bikeshare` data set, we will make use of an alternative approach, called *Poisson regression*. Before we can talk about Poisson regression, we must first introduce the *Poisson distribution*.

Suppose that a random variable Y takes on nonnegative integer values, i.e. $Y \in \{0, 1, 2, \dots\}$. If Y follows the Poisson distribution, then

$$\Pr(Y = k) = \frac{e^{-\lambda} \lambda^k}{k!} \quad \text{for } k = 0, 1, 2, \dots \quad (4.35)$$



Poisson regression
Poisson distribution

Here, $\lambda > 0$ is the expected value of Y , i.e. $E(Y)$. It turns out that λ also equals the variance of Y , i.e. $\lambda = E(Y) = \text{Var}(Y)$. This means that if Y follows the Poisson distribution, then the larger the mean of Y , the larger its variance. (In (4.35), the notation $k!$, pronounced “ k factorial”, is defined as $k! = k \times (k - 1) \times (k - 2) \times \dots \times 3 \times 2 \times 1$.)

The Poisson distribution is typically used to model *counts*; this is a natural choice for a number of reasons, including the fact that counts, like the Poisson distribution, take on nonnegative integer values. To see how we might use the Poisson distribution in practice, let Y denote the number of users of the bike sharing program during a particular hour of the day, under a particular set of weather conditions, and during a particular month of the year. We might model Y as a Poisson distribution with mean $E(Y) = \lambda = 5$. This means that the probability of no users during this particular hour is $\Pr(Y = 0) = \frac{e^{-5}5^0}{0!} = e^{-5} = 0.0067$ (where $0! = 1$ by convention). The probability that there is exactly one user is $\Pr(Y = 1) = \frac{e^{-5}5^1}{1!} = 5e^{-5} = 0.034$, the probability of two users is $\Pr(Y = 2) = \frac{e^{-5}5^2}{2!} = 0.084$, and so on.

Of course, in reality, we expect the mean number of users of the bike sharing program, $\lambda = E(Y)$, to vary as a function of the hour of the day, the month of the year, the weather conditions, and so forth. So rather than modeling the number of bikers, Y , as a Poisson distribution with a fixed mean value like $\lambda = 5$, we would like to allow the mean to vary as a function of the covariates. In particular, we consider the following model for the mean $\lambda = E(Y)$, which we now write as $\lambda(X_1, \dots, X_p)$ to emphasize that it is a function of the covariates X_1, \dots, X_p :

$$\log(\lambda(X_1, \dots, X_p)) = \beta_0 + \beta_1 X_1 + \dots + \beta_p X_p \quad (4.36)$$

or equivalently

$$\lambda(X_1, \dots, X_p) = e^{\beta_0 + \beta_1 X_1 + \dots + \beta_p X_p}. \quad (4.37)$$

Here, $\beta_0, \beta_1, \dots, \beta_p$ are parameters to be estimated. Together, (4.35) and (4.36) define the Poisson regression model. Notice that in (4.36), we take the *log* of $\lambda(X_1, \dots, X_p)$ to be linear in X_1, \dots, X_p , rather than having $\lambda(X_1, \dots, X_p)$ itself be linear in X_1, \dots, X_p ; this ensures that $\lambda(X_1, \dots, X_p)$ takes on nonnegative values for all values of the covariates.

To estimate the coefficients $\beta_0, \beta_1, \dots, \beta_p$, we use the same maximum likelihood approach that we adopted for logistic regression in Section 4.3.2. Specifically, given n independent observations from the Poisson regression model, the likelihood takes the form

$$\ell(\beta_0, \beta_1, \dots, \beta_p) = \prod_{i=1}^n \frac{e^{-\lambda(x_i)} \lambda(x_i)^{y_i}}{y_i!}, \quad (4.38)$$

where $\lambda(x_i) = e^{\beta_0 + \beta_1 x_{i1} + \dots + \beta_p x_{ip}}$, due to (4.37). We estimate the coefficients that maximize the likelihood $\ell(\beta_0, \beta_1, \dots, \beta_p)$, i.e. that make the observed data as likely as possible.

We now fit a Poisson regression model to the **Bikeshare** data set. The results are shown in Table 4.11 and Figure 4.15. Qualitatively, the results are similar to those from linear regression in Section 4.6.1. We again see that bike usage is highest in the spring and fall and during rush hour,

	Coefficient	Std. error	z-statistic	p-value
Intercept	4.12	0.01	683.96	0.00
workingday	0.01	0.00	7.5	0.00
temp	0.79	0.01	68.43	0.00
weathersit[cloudy/misty]	-0.08	0.00	-34.53	0.00
weathersit[light rain/snow]	-0.58	0.00	-141.91	0.00
weathersit[heavy rain/snow]	-0.93	0.17	-5.55	0.00

TABLE 4.11. Results for a Poisson regression model fit to predict `bikers` in the `Bikeshare` data. The predictors `mnth` and `hr` are omitted from this table due to space constraints, and can be seen in Figure 4.15. For the qualitative variable `weathersit`, the baseline corresponds to clear skies.

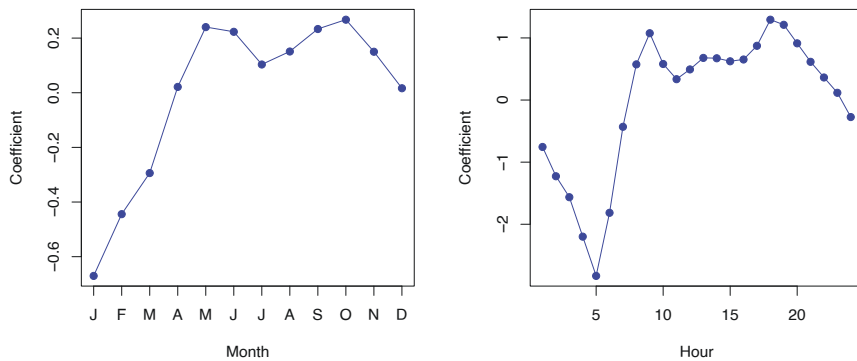


FIGURE 4.15. A Poisson regression model was fit to predict `bikers` in the `Bikeshare` data set. Left: The coefficients associated with the month of the year. Bike usage is highest in the spring and fall, and lowest in the winter. Right: The coefficients associated with the hour of the day. Bike usage is highest during peak commute times, and lowest overnight.

and lowest during the winter and in the early morning hours. Moreover, bike usage increases as the temperature increases, and decreases as the weather worsens. Interestingly, the coefficient associated with `workingday` is statistically significant under the Poisson regression model, but not under the linear regression model.

Some important distinctions between the Poisson regression model and the linear regression model are as follows:

- *Interpretation:* To interpret the coefficients in the Poisson regression model, we must pay close attention to (4.37), which states that an increase in X_j by one unit is associated with a change in $E(Y) = \lambda$ by a factor of $\exp(\beta_j)$. For example, a change in weather from clear to cloudy skies is associated with a change in mean bike usage by a factor of $\exp(-0.08) = 0.923$, i.e. on average, only 92.3% as many people will use bikes when it is cloudy relative to when it is clear. If the weather worsens further and it begins to rain, then the mean bike usage will further change by a factor of $\exp(-0.5) = 0.607$, i.e. on average only 60.7% as many people will use bikes when it is rainy relative to when it is cloudy.

- *Mean-variance relationship:* As mentioned earlier, under the Poisson model, $\lambda = E(Y) = \text{Var}(Y)$. Thus, by modeling bike usage with a Poisson regression, we implicitly assume that mean bike usage in a given hour equals the variance of bike usage during that hour. By contrast, under a linear regression model, the variance of bike usage always takes on a constant value. Recall from Figure 4.14 that in the **Bikeshare** data, when biking conditions are favorable, both the mean and the variance in bike usage are much higher than when conditions are unfavorable. Thus, the Poisson regression model is able to handle the mean-variance relationship seen in the **Bikeshare** data in a way that the linear regression model is not.⁵

overdispersion

- *nonnegative fitted values:* There are no negative predictions using the Poisson regression model. This is because the Poisson model itself only allows for nonnegative values; see (4.35). By contrast, when we fit a linear regression model to the **Bikeshare** data set, almost 10% of the predictions were negative.

4.6.3 Generalized Linear Models in Greater Generality

We have now discussed three types of regression models: linear, logistic and Poisson. These approaches share some common characteristics:



1. Each approach uses predictors X_1, \dots, X_p to predict a response Y . We assume that, conditional on X_1, \dots, X_p , Y belongs to a certain family of distributions. For linear regression, we typically assume that Y follows a Gaussian or normal distribution. For logistic regression, we assume that Y follows a Bernoulli distribution. Finally, for Poisson regression, we assume that Y follows a Poisson distribution.
2. Each approach models the mean of Y as a function of the predictors. In linear regression, the mean of Y takes the form

$$E(Y|X_1, \dots, X_p) = \beta_0 + \beta_1 X_1 + \dots + \beta_p X_p, \quad (4.39)$$

i.e. it is a linear function of the predictors. For logistic regression, the mean instead takes the form

$$\begin{aligned} E(Y|X_1, \dots, X_p) &= \Pr(Y = 1|X_1, \dots, X_p) \\ &= \frac{e^{\beta_0 + \beta_1 X_1 + \dots + \beta_p X_p}}{1 + e^{\beta_0 + \beta_1 X_1 + \dots + \beta_p X_p}}, \end{aligned} \quad (4.40)$$

while for Poisson regression it takes the form

$$E(Y|X_1, \dots, X_p) = \lambda(X_1, \dots, X_p) = e^{\beta_0 + \beta_1 X_1 + \dots + \beta_p X_p}. \quad (4.41)$$

Equations (4.39)–(4.41) can be expressed using a *link function*, η , which

link function

⁵In fact, the variance in the **Bikeshare** data appears to be much higher than the mean, a situation referred to as *overdispersion*. This causes the Z-values to be inflated in Table 4.11. A more careful analysis should account for this overdispersion to obtain more accurate Z-values, and there are a variety of methods for doing this. But they are beyond the scope of this book.

applies a transformation to $E(Y|X_1, \dots, X_p)$ so that the transformed mean is a linear function of the predictors. That is,

$$\eta(E(Y|X_1, \dots, X_p)) = \beta_0 + \beta_1 X_1 + \dots + \beta_p X_p. \quad (4.42)$$

The link functions for linear, logistic and Poisson regression are $\eta(\mu) = \mu$, $\eta(\mu) = \log(\mu/(1 - \mu))$, and $\eta(\mu) = \log(\mu)$, respectively.

The Gaussian, Bernoulli and Poisson distributions are all members of a wider class of distributions, known as the *exponential family*. Other well-known members of this family are the *exponential* distribution, the *Gamma* distribution, and the *negative binomial* distribution. In general, we can perform a regression by modeling the response Y as coming from a particular member of the exponential family, and then transforming the mean of the response so that the transformed mean is a linear function of the predictors via (4.42). Any regression approach that follows this very general recipe is known as a *generalized linear model* (GLM). Thus, linear regression, logistic regression, and Poisson regression are three examples of GLMs. Other examples not covered here include *Gamma regression* and *negative binomial regression*.

exponential family
exponential
Gamma
negative binomial
generalized linear model

4.7 Lab: Logistic Regression, LDA, QDA, and KNN

4.7.1 The Stock Market Data

In this lab we will examine the `Smarket` data, which is part of the `ISLP` library. This data set consists of percentage returns for the S&P 500 stock index over 1,250 days, from the beginning of 2001 until the end of 2005. For each date, we have recorded the percentage returns for each of the five previous trading days, `Lag1` through `Lag5`. We have also recorded `Volume` (the number of shares traded on the previous day, in billions), `Today` (the percentage return on the date in question) and `Direction` (whether the market was `Up` or `Down` on this date).

We start by importing our libraries at this top level; these are all imports we have seen in previous labs.

```
In [1]: import numpy as np
import pandas as pd
from matplotlib.pyplot import subplots
import statsmodels.api as sm
from ISLP import load_data
from ISLP.models import (ModelSpec as MS,
                         summarize)
```

We also collect together the new imports needed for this lab.

```
In [2]: from ISLP import confusion_table
from ISLP.models import contrast
from sklearn.discriminant_analysis import \
    (LinearDiscriminantAnalysis as LDA,
     QuadraticDiscriminantAnalysis as QDA)
from sklearn.naive_bayes import GaussianNB
from sklearn.neighbors import KNeighborsClassifier
from sklearn.preprocessing import StandardScaler
```

```
ax.set_ylabel('Poisson Regression Fit', fontsize=20)
ax.axline([0,0], c='black', linewidth=3,
          linestyle='--', slope=1);
```

The predictions from the Poisson regression model are correlated with those from the linear model; however, the former are non-negative. As a result the Poisson regression predictions tend to be larger than those from the linear model for either very low or very high levels of ridership.

In this section, we fit Poisson regression models using the `sm.GLM()` function with the argument `family=sm.families.Poisson()`. Earlier in this lab we used the `sm.GLM()` function with `family=sm.families.Binomial()` to perform logistic regression. Other choices for the `family` argument can be used to fit other types of GLMs. For instance, `family=sm.families.Gamma()` fits a Gamma regression model.

4.8 Exercises

Conceptual

1. Using a little bit of algebra, prove that (4.2) is equivalent to (4.3). In other words, the logistic function representation and logit representation for the logistic regression model are equivalent.
2. It was stated in the text that classifying an observation to the class for which (4.17) is largest is equivalent to classifying an observation to the class for which (4.18) is largest. Prove that this is the case. In other words, under the assumption that the observations in the k th class are drawn from a $N(\mu_k, \sigma^2)$ distribution, the Bayes classifier assigns an observation to the class for which the discriminant function is maximized.
3. This problem relates to the QDA model, in which the observations within each class are drawn from a normal distribution with a class-specific mean vector and a class specific covariance matrix. We consider the simple case where $p = 1$; i.e. there is only one feature.

Suppose that we have K classes, and that if an observation belongs to the k th class then X comes from a one-dimensional normal distribution, $X \sim N(\mu_k, \sigma_k^2)$. Recall that the density function for the one-dimensional normal distribution is given in (4.16). Prove that in this case, the Bayes classifier is *not* linear. Argue that it is in fact quadratic.

Hint: For this problem, you should follow the arguments laid out in Section 4.4.1, but without making the assumption that $\sigma_1^2 = \dots = \sigma_K^2$.

4. When the number of features p is large, there tends to be a deterioration in the performance of KNN and other *local* approaches that perform prediction using only observations that are *near* the test observation for which a prediction must be made. This phenomenon is known as the *curse of dimensionality*, and it ties into the fact that non-parametric approaches often perform poorly when p is large. We will now investigate this curse.



curse of dimensionality

- (a) Suppose that we have a set of observations, each with measurements on $p = 1$ feature, X . We assume that X is uniformly (evenly) distributed on $[0, 1]$. Associated with each observation is a response value. Suppose that we wish to predict a test observation's response using only observations that are within 10 % of the range of X closest to that test observation. For instance, in order to predict the response for a test observation with $X = 0.6$, we will use observations in the range $[0.55, 0.65]$. On average, what fraction of the available observations will we use to make the prediction?
- (b) Now suppose that we have a set of observations, each with measurements on $p = 2$ features, X_1 and X_2 . We assume that (X_1, X_2) are uniformly distributed on $[0, 1] \times [0, 1]$. We wish to predict a test observation's response using only observations that are within 10 % of the range of X_1 and within 10 % of the range of X_2 closest to that test observation. For instance, in order to predict the response for a test observation with $X_1 = 0.6$ and $X_2 = 0.35$, we will use observations in the range $[0.55, 0.65]$ for X_1 and in the range $[0.3, 0.4]$ for X_2 . On average, what fraction of the available observations will we use to make the prediction?
- (c) Now suppose that we have a set of observations on $p = 100$ features. Again the observations are uniformly distributed on each feature, and again each feature ranges in value from 0 to 1. We wish to predict a test observation's response using observations within the 10 % of each feature's range that is closest to that test observation. What fraction of the available observations will we use to make the prediction?
- (d) Using your answers to parts (a)–(c), argue that a drawback of KNN when p is large is that there are very few training observations “near” any given test observation.
- (e) Now suppose that we wish to make a prediction for a test observation by creating a p -dimensional hypercube centered around the test observation that contains, on average, 10 % of the training observations. For $p = 1, 2$, and 100, what is the length of each side of the hypercube? Comment on your answer.

Note: A hypercube is a generalization of a cube to an arbitrary number of dimensions. When $p = 1$, a hypercube is simply a line segment, when $p = 2$ it is a square, and when $p = 100$ it is a 100-dimensional cube.

5. We now examine the differences between LDA and QDA.

- (a) If the Bayes decision boundary is linear, do we expect LDA or QDA to perform better on the training set? On the test set?
- (b) If the Bayes decision boundary is non-linear, do we expect LDA or QDA to perform better on the training set? On the test set?

- (c) In general, as the sample size n increases, do we expect the test prediction accuracy of QDA relative to LDA to improve, decline, or be unchanged? Why?
- (d) True or False: Even if the Bayes decision boundary for a given problem is linear, we will probably achieve a superior test error rate using QDA rather than LDA because QDA is flexible enough to model a linear decision boundary. Justify your answer.
6. Suppose we collect data for a group of students in a statistics class with variables $X_1 = \text{hours studied}$, $X_2 = \text{undergrad GPA}$, and $Y = \text{receive an A}$. We fit a logistic regression and produce estimated coefficient, $\hat{\beta}_0 = -6$, $\hat{\beta}_1 = 0.05$, $\hat{\beta}_2 = 1$.
- Estimate the probability that a student who studies for 40 h and has an undergrad GPA of 3.5 gets an A in the class.
 - How many hours would the student in part (a) need to study to have a 50% chance of getting an A in the class?
7. Suppose that we wish to predict whether a given stock will issue a dividend this year (“Yes” or “No”) based on X , last year’s percent profit. We examine a large number of companies and discover that the mean value of X for companies that issued a dividend was $\bar{X} = 10$, while the mean for those that didn’t was $\bar{X} = 0$. In addition, the variance of X for these two sets of companies was $\hat{\sigma}^2 = 36$. Finally, 80% of companies issued dividends. Assuming that X follows a normal distribution, predict the probability that a company will issue a dividend this year given that its percentage profit was $X = 4$ last year.

Hint: Recall that the density function for a normal random variable is $f(x) = \frac{1}{\sqrt{2\pi\sigma^2}}e^{-(x-\mu)^2/2\sigma^2}$. You will need to use Bayes’ theorem.

8. Suppose that we take a data set, divide it into equally-sized training and test sets, and then try out two different classification procedures. First we use logistic regression and get an error rate of 20% on the training data and 30% on the test data. Next we use 1-nearest neighbors (i.e. $K = 1$) and get an average error rate (averaged over both test and training data sets) of 18%. Based on these results, which method should we prefer to use for classification of new observations? Why?
9. This problem has to do with *odds*.
- On average, what fraction of people with an odds of 0.37 of defaulting on their credit card payment will in fact default?
 - Suppose that an individual has a 16% chance of defaulting on her credit card payment. What are the odds that she will default?

10. Equation 4.32 derived an expression for $\log\left(\frac{\Pr(Y=k|X=x)}{\Pr(Y=K|X=x)}\right)$ in the setting where $p > 1$, so that the mean for the k th class, μ_k , is a p -dimensional vector, and the shared covariance Σ is a $p \times p$ matrix. However, in the setting with $p = 1$, (4.32) takes a simpler form, since the means μ_1, \dots, μ_K and the variance σ^2 are scalars. In this simpler setting, repeat the calculation in (4.32), and provide expressions for a_k and b_{kj} in terms of π_k , π_K , μ_k , μ_K , and σ^2 . 
11. Work out the detailed forms of a_k , b_{kj} , and b_{kj1} in (4.33). Your answer should involve π_k , π_K , μ_k , μ_K , Σ_k , and Σ_K . 
12. Suppose that you wish to classify an observation $X \in \mathbb{R}$ into **apples** and **oranges**. You fit a logistic regression model and find that

$$\widehat{\Pr}(Y = \text{orange}|X = x) = \frac{\exp(\hat{\beta}_0 + \hat{\beta}_1 x)}{1 + \exp(\hat{\beta}_0 + \hat{\beta}_1 x)}.$$

Your friend fits a logistic regression model to the same data using the *softmax* formulation in (4.13), and finds that

$$\widehat{\Pr}(Y = \text{orange}|X = x) = \frac{\exp(\hat{\alpha}_{\text{orange}0} + \hat{\alpha}_{\text{orange}1}x)}{\exp(\hat{\alpha}_{\text{orange}0} + \hat{\alpha}_{\text{orange}1}x) + \exp(\hat{\alpha}_{\text{apple}0} + \hat{\alpha}_{\text{apple}1}x)}.$$

- (a) What is the log odds of **orange** versus **apple** in your model?
- (b) What is the log odds of **orange** versus **apple** in your friend's model?
- (c) Suppose that in your model, $\hat{\beta}_0 = 2$ and $\hat{\beta}_1 = -1$. What are the coefficient estimates in your friend's model? Be as specific as possible.
- (d) Now suppose that you and your friend fit the same two models on a different data set. This time, your friend gets the coefficient estimates $\hat{\alpha}_{\text{orange}0} = 1.2$, $\hat{\alpha}_{\text{orange}1} = -2$, $\hat{\alpha}_{\text{orange}0} = 3$, $\hat{\alpha}_{\text{orange}1} = 0.6$. What are the coefficient estimates in your model?
- (e) Finally, suppose you apply both models from (d) to a data set with 2,000 test observations. What fraction of the time do you expect the predicted class labels from your model to agree with those from your friend's model? Explain your answer.

Applied

13. This question should be answered using the **Weekly** data set, which is part of the **ISLP** package. This data is similar in nature to the **Smarket** data from this chapter's lab, except that it contains 1,089 weekly returns for 21 years, from the beginning of 1990 to the end of 2010.
- (a) Produce some numerical and graphical summaries of the **Weekly** data. Do there appear to be any patterns?

- (b) Use the full data set to perform a logistic regression with `Direction` as the response and the five lag variables plus `Volume` as predictors. Use the `summary` function to print the results. Do any of the predictors appear to be statistically significant? If so, which ones?
- (c) Compute the confusion matrix and overall fraction of correct predictions. Explain what the confusion matrix is telling you about the types of mistakes made by logistic regression.
- (d) Now fit the logistic regression model using a training data period from 1990 to 2008, with `Lag2` as the only predictor. Compute the confusion matrix and the overall fraction of correct predictions for the held out data (that is, the data from 2009 and 2010).
- (e) Repeat (d) using LDA.
- (f) Repeat (d) using QDA.
- (g) Repeat (d) using KNN with $K = 1$.
- (h) Repeat (d) using naive Bayes.
- (i) Which of these methods appears to provide the best results on this data?
- (j) Experiment with different combinations of predictors, including possible transformations and interactions, for each of the methods. Report the variables, method, and associated confusion matrix that appears to provide the best results on the held out data. Note that you should also experiment with values for K in the KNN classifier.
14. In this problem, you will develop a model to predict whether a given car gets high or low gas mileage based on the `Auto` data set.
- (a) Create a binary variable, `mpg01`, that contains a 1 if `mpg` contains a value above its median, and a 0 if `mpg` contains a value below its median. You can compute the median using the `median()` method of the data frame. Note you may find it helpful to add a column `mpg01` to the data frame by assignment. Assuming you have stored the data frame as `Auto`, this can be done as follows:
- ```
Auto['mpg01'] = mpg01
```
- (b) Explore the data graphically in order to investigate the association between `mpg01` and the other features. Which of the other features seem most likely to be useful in predicting `mpg01`? Scatterplots and boxplots may be useful tools to answer this question. Describe your findings.
- (c) Split the data into a training set and a test set.
- (d) Perform LDA on the training data in order to predict `mpg01` using the variables that seemed most associated with `mpg01` in (b). What is the test error of the model obtained?

- (e) Perform QDA on the training data in order to predict `mpg01` using the variables that seemed most associated with `mpg01` in (b). What is the test error of the model obtained?
- (f) Perform logistic regression on the training data in order to predict `mpg01` using the variables that seemed most associated with `mpg01` in (b). What is the test error of the model obtained?
- (g) Perform naive Bayes on the training data in order to predict `mpg01` using the variables that seemed most associated with `mpg01` in (b). What is the test error of the model obtained?
- (h) Perform KNN on the training data, with several values of  $K$ , in order to predict `mpg01`. Use only the variables that seemed most associated with `mpg01` in (b). What test errors do you obtain? Which value of  $K$  seems to perform the best on this data set?

15. This problem involves writing functions.

- (a) Write a function, `Power()`, that prints out the result of raising 2 to the 3rd power. In other words, your function should compute  $2^3$  and print out the results.  
*Hint: Recall that `x**a` raises `x` to the power `a`. Use the `print()` function to display the result.*
- (b) Create a new function, `Power2()`, that allows you to pass *any* two numbers, `x` and `a`, and prints out the value of `x**a`. You can do this by beginning your function with the line

```
def Power2(x, a):
```

You should be able to call your function by entering, for instance,

```
Power2(3, 8)
```

on the command line. This should output the value of  $3^8$ , namely, 6,561.

- (c) Using the `Power2()` function that you just wrote, compute  $10^3$ ,  $8^{17}$ , and  $131^3$ .
- (d) Now create a new function, `Power3()`, that actually *returns* the result `x**a` as a `Python` object, rather than simply printing it to the screen. That is, if you store the value `x**a` in an object called `result` within your function, then you can simply `return` `result` this result, using the following line:

```
 return result
```

Note that the line above should be the last line in your function, and it should be indented 4 spaces.

- (e) Now using the `Power3()` function, create a plot of  $f(x) = x^2$ . The  $x$ -axis should display a range of integers from 1 to 10, and the  $y$ -axis should display  $x^2$ . Label the axes appropriately, and use an appropriate title for the figure. Consider displaying either the  $x$ -axis, the  $y$ -axis, or both on the log-scale. You can do this by using the `ax.set_xscale()` and `ax.set_yscale()` methods of the axes you are plotting to.

```
.set_xscale()
.set_yscale()
```

- (f) Create a function, `PlotPower()`, that allows you to create a plot of `x` against `x**a` for a fixed `a` and a sequence of values of `x`. For instance, if you call

```
PlotPower(np.arange(1, 11), 3)
```

then a plot should be created with an *x*-axis taking on values 1, 2, ..., 10, and a *y*-axis taking on values  $1^3, 2^3, \dots, 10^3$ .

16. Using the `Boston` data set, fit classification models in order to predict whether a given suburb has a crime rate above or below the median. Explore logistic regression, LDA, naive Bayes, and KNN models using various subsets of the predictors. Describe your findings.

*Hint: You will have to create the response variable yourself, using the variables that are contained in the `Boston` data set.*

# 5



## Resampling Methods

*Resampling methods* are an indispensable tool in modern statistics. They involve repeatedly drawing samples from a training set and refitting a model of interest on each sample in order to obtain additional information about the fitted model. For example, in order to estimate the variability of a linear regression fit, we can repeatedly draw different samples from the training data, fit a linear regression to each new sample, and then examine the extent to which the resulting fits differ. Such an approach may allow us to obtain information that would not be available from fitting the model only once using the original training sample.

Resampling approaches can be computationally expensive, because they involve fitting the same statistical method multiple times using different subsets of the training data. However, due to recent advances in computing power, the computational requirements of resampling methods generally are not prohibitive. In this chapter, we discuss two of the most commonly used resampling methods, *cross-validation* and the *bootstrap*. Both methods are important tools in the practical application of many statistical learning procedures. For example, cross-validation can be used to estimate the test error associated with a given statistical learning method in order to evaluate its performance, or to select the appropriate level of flexibility. The process of evaluating a model's performance is known as *model assessment*, whereas the process of selecting the proper level of flexibility for a model is known as *model selection*. The bootstrap is used in several contexts, most commonly to provide a measure of accuracy of a parameter estimate or of a given statistical learning method.

model  
assessment  
model  
selection

## 5.1 Cross-Validation

In Chapter 2 we discuss the distinction between the *test error rate* and the *training error rate*. The test error is the average error that results from using a statistical learning method to predict the response on a new observation—that is, a measurement that was not used in training the method. Given a data set, the use of a particular statistical learning method is warranted if it results in a low test error. The test error can be easily calculated if a designated test set is available. Unfortunately, this is usually not the case. In contrast, the training error can be easily calculated by applying the statistical learning method to the observations used in its training. But as we saw in Chapter 2, the training error rate often is quite different from the test error rate, and in particular the former can dramatically underestimate the latter.

In the absence of a very large designated test set that can be used to directly estimate the test error rate, a number of techniques can be used to estimate this quantity using the available training data. Some methods make a mathematical adjustment to the training error rate in order to estimate the test error rate. Such approaches are discussed in Chapter 6. In this section, we instead consider a class of methods that estimate the test error rate by *holding out* a subset of the training observations from the fitting process, and then applying the statistical learning method to those held out observations.

In Sections 5.1.1–5.1.4, for simplicity we assume that we are interested in performing regression with a quantitative response. In Section 5.1.5 we consider the case of classification with a qualitative response. As we will see, the key concepts remain the same regardless of whether the response is quantitative or qualitative.

### 5.1.1 The Validation Set Approach

Suppose that we would like to estimate the test error associated with fitting a particular statistical learning method on a set of observations. The *validation set approach*, displayed in Figure 5.1, is a very simple strategy for this task. It involves randomly dividing the available set of observations into two parts, a *training set* and a *validation set* or *hold-out set*. The model is fit on the training set, and the fitted model is used to predict the responses for the observations in the validation set. The resulting validation set error rate—typically assessed using MSE in the case of a quantitative response—provides an estimate of the test error rate.

validation  
set approach  
validation  
set  
hold-out set

We illustrate the validation set approach on the `Auto` data set. Recall from Chapter 3 that there appears to be a non-linear relationship between `mpg` and `horsepower`, and that a model that predicts `mpg` using `horsepower` and `horsepower2` gives better results than a model that uses only a linear term. It is natural to wonder whether a cubic or higher-order fit might provide even better results. We answer this question in Chapter 3 by looking at the p-values associated with a cubic term and higher-order polynomial terms in a linear regression. But we could also answer this question using the validation method. We randomly split the 392 observations into two



**FIGURE 5.1.** A schematic display of the validation set approach. A set of  $n$  observations are randomly split into a training set (shown in blue, containing observations 7, 22, and 13, among others) and a validation set (shown in beige, and containing observation 91, among others). The statistical learning method is fit on the training set, and its performance is evaluated on the validation set.

sets, a training set containing 196 of the data points, and a validation set containing the remaining 196 observations. The validation set error rates that result from fitting various regression models on the training sample and evaluating their performance on the validation sample, using MSE as a measure of validation set error, are shown in the left-hand panel of Figure 5.2. The validation set MSE for the quadratic fit is considerably smaller than for the linear fit. However, the validation set MSE for the cubic fit is actually slightly larger than for the quadratic fit. This implies that including a cubic term in the regression does not lead to better prediction than simply using a quadratic term.

Recall that in order to create the left-hand panel of Figure 5.2, we randomly divided the data set into two parts, a training set and a validation set. If we repeat the process of randomly splitting the sample set into two parts, we will get a somewhat different estimate for the test MSE. As an illustration, the right-hand panel of Figure 5.2 displays ten different validation set MSE curves from the `Auto` data set, produced using ten different random splits of the observations into training and validation sets. All ten curves indicate that the model with a quadratic term has a dramatically smaller validation set MSE than the model with only a linear term. Furthermore, all ten curves indicate that there is not much benefit in including cubic or higher-order polynomial terms in the model. But it is worth noting that each of the ten curves results in a different test MSE estimate for each of the ten regression models considered. And there is no consensus among the curves as to which model results in the smallest validation set MSE. Based on the variability among these curves, all that we can conclude with any confidence is that the linear fit is not adequate for this data.

The validation set approach is conceptually simple and is easy to implement. But it has two potential drawbacks:

1. As is shown in the right-hand panel of Figure 5.2, the validation estimate of the test error rate can be highly variable, depending on precisely which observations are included in the training set and which observations are included in the validation set.
2. In the validation approach, only a subset of the observations—those that are included in the training set rather than in the validation set—are used to fit the model. Since statistical methods tend to perform worse when trained on fewer observations, this suggests that the

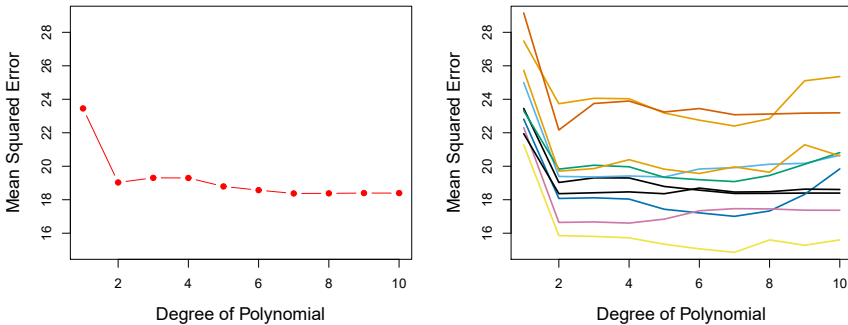


**FIGURE 5.2.** The validation set approach was used on the `Auto` data set in order to estimate the test error that results from predicting `mpg` using polynomial functions of `horsepower`. Left: Validation error estimates for a single split into training and validation data sets. Right: The validation method was repeated ten times, each time using a different random split of the observations into a training set and a validation set. This illustrates the variability in the estimated test MSE that results from this approach.

validation set error rate may tend to *overestimate* the test error rate for the model fit on the entire data set.

In the coming subsections, we will present *cross-validation*, a refinement of the validation set approach that addresses these two issues.

### 5.1.2 Leave-One-Out Cross-Validation

Leave-one-out cross-validation (LOOCV) is closely related to the validation set approach of Section 5.1.1, but it attempts to address that method's drawbacks.

Like the validation set approach, LOOCV involves splitting the set of observations into two parts. However, instead of creating two subsets of comparable size, a single observation  $(x_1, y_1)$  is used for the validation set, and the remaining observations  $\{(x_2, y_2), \dots, (x_n, y_n)\}$  make up the training set. The statistical learning method is fit on the  $n - 1$  training observations, and a prediction  $\hat{y}_1$  is made for the excluded observation, using its value  $x_1$ . Since  $(x_1, y_1)$  was not used in the fitting process,  $MSE_1 = (y_1 - \hat{y}_1)^2$  provides an approximately unbiased estimate for the test error. But even though  $MSE_1$  is unbiased for the test error, it is a poor estimate because it is highly variable, since it is based upon a single observation  $(x_1, y_1)$ .

We can repeat the procedure by selecting  $(x_2, y_2)$  for the validation data, training the statistical learning procedure on the  $n - 1$  observations  $\{(x_1, y_1), (x_3, y_3), \dots, (x_n, y_n)\}$ , and computing  $MSE_2 = (y_2 - \hat{y}_2)^2$ . Repeating this approach  $n$  times produces  $n$  squared errors,  $MSE_1, \dots, MSE_n$ . The LOOCV estimate for the test MSE is the average of these  $n$  test error estimates:

$$CV_{(n)} = \frac{1}{n} \sum_{i=1}^n MSE_i. \quad (5.1)$$

leave-one-out cross-validation



**FIGURE 5.3.** A schematic display of LOOCV. A set of  $n$  data points is repeatedly split into a training set (shown in blue) containing all but one observation, and a validation set that contains only that observation (shown in beige). The test error is then estimated by averaging the  $n$  resulting MSEs. The first training set contains all but observation 1, the second training set contains all but observation 2, and so forth.

A schematic of the LOOCV approach is illustrated in Figure 5.3.

LOOCV has a couple of major advantages over the validation set approach. First, it has far less bias. In LOOCV, we repeatedly fit the statistical learning method using training sets that contain  $n - 1$  observations, almost as many as are in the entire data set. This is in contrast to the validation set approach, in which the training set is typically around half the size of the original data set. Consequently, the LOOCV approach tends not to overestimate the test error rate as much as the validation set approach does. Second, in contrast to the validation approach which will yield different results when applied repeatedly due to randomness in the training/validation set splits, performing LOOCV multiple times will always yield the same results: there is no randomness in the training/validation set splits.

We used LOOCV on the `Auto` data set in order to obtain an estimate of the test set MSE that results from fitting a linear regression model to predict `mpg` using polynomial functions of `horsepower`. The results are shown in the left-hand panel of Figure 5.4.

LOOCV has the potential to be expensive to implement, since the model has to be fit  $n$  times. This can be very time consuming if  $n$  is large, and if each individual model is slow to fit. With least squares linear or polynomial regression, an amazing shortcut makes the cost of LOOCV the same as that of a single model fit! The following formula holds:

$$\text{CV}_{(n)} = \frac{1}{n} \sum_{i=1}^n \left( \frac{y_i - \hat{y}_i}{1 - h_i} \right)^2, \quad (5.2)$$

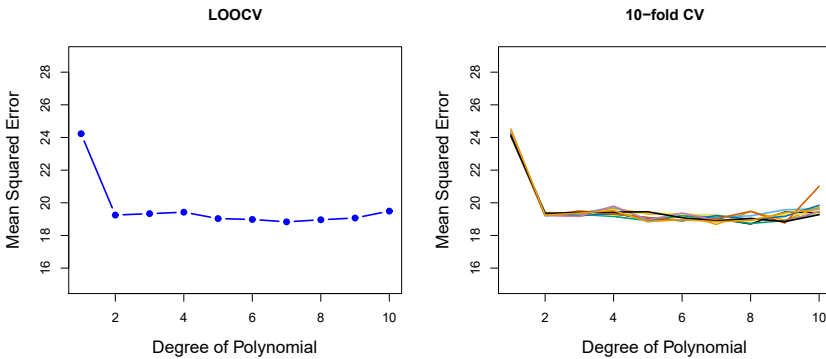


**FIGURE 5.4.** Cross-validation was used on the `Auto` data set in order to estimate the test error that results from predicting `mpg` using polynomial functions of `horsepower`. Left: The LOOCV error curve. Right: 10-fold CV was run nine separate times, each with a different random split of the data into ten parts. The figure shows the nine slightly different CV error curves.

where  $\hat{y}_i$  is the  $i$ th fitted value from the original least squares fit, and  $h_i$  is the leverage defined in (3.37) on page 105.<sup>1</sup> This is like the ordinary MSE, except the  $i$ th residual is divided by  $1 - h_i$ . The leverage lies between  $1/n$  and 1, and reflects the amount that an observation influences its own fit. Hence the residuals for high-leverage points are inflated in this formula by exactly the right amount for this equality to hold.

LOOCV is a very general method, and can be used with any kind of predictive modeling. For example we could use it with logistic regression or linear discriminant analysis, or any of the methods discussed in later chapters. The magic formula (5.2) does not hold in general, in which case the model has to be refit  $n$  times.

### 5.1.3 *k*-Fold Cross-Validation

An alternative to LOOCV is *k*-fold CV. This approach involves randomly dividing the set of observations into  $k$  groups, or *folds*, of approximately equal size. The first fold is treated as a validation set, and the method is fit on the remaining  $k - 1$  folds. The mean squared error,  $MSE_1$ , is then computed on the observations in the held-out fold. This procedure is repeated  $k$  times; each time, a different group of observations is treated as a validation set. This process results in  $k$  estimates of the test error,  $MSE_1, MSE_2, \dots, MSE_k$ . The *k*-fold CV estimate is computed by averaging these values,

$$CV_{(k)} = \frac{1}{k} \sum_{i=1}^k MSE_i. \quad (5.3)$$

Figure 5.5 illustrates the *k*-fold CV approach.

<sup>1</sup>In the case of multiple linear regression, the leverage takes a slightly more complicated form than (3.37), but (5.2) still holds.

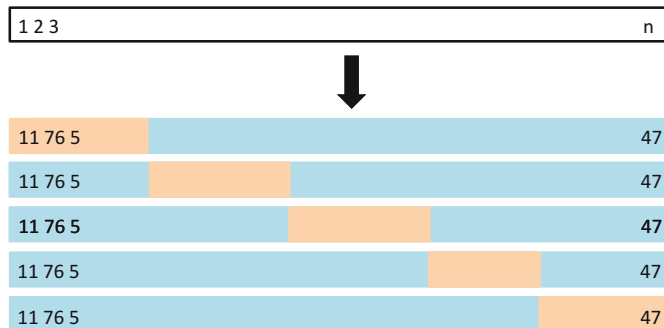


**FIGURE 5.5.** A schematic display of 5-fold CV. A set of  $n$  observations is randomly split into five non-overlapping groups. Each of these fifths acts as a validation set (shown in beige), and the remainder as a training set (shown in blue). The test error is estimated by averaging the five resulting MSE estimates.

It is not hard to see that LOOCV is a special case of  $k$ -fold CV in which  $k$  is set to equal  $n$ . In practice, one typically performs  $k$ -fold CV using  $k = 5$  or  $k = 10$ . What is the advantage of using  $k = 5$  or  $k = 10$  rather than  $k = n$ ? The most obvious advantage is computational. LOOCV requires fitting the statistical learning method  $n$  times. This has the potential to be computationally expensive (except for linear models fit by least squares, in which case formula (5.2) can be used). But cross-validation is a very general approach that can be applied to almost any statistical learning method. Some statistical learning methods have computationally intensive fitting procedures, and so performing LOOCV may pose computational problems, especially if  $n$  is extremely large. In contrast, performing 10-fold CV requires fitting the learning procedure only ten times, which may be much more feasible. As we see in Section 5.1.4, there also can be other non-computational advantages to performing 5-fold or 10-fold CV, which involve the bias-variance trade-off.

The right-hand panel of Figure 5.4 displays nine different 10-fold CV estimates for the **Auto** data set, each resulting from a different random split of the observations into ten folds. As we can see from the figure, there is some variability in the CV estimates as a result of the variability in how the observations are divided into ten folds. But this variability is typically much lower than the variability in the test error estimates that results from the validation set approach (right-hand panel of Figure 5.2).

When we examine real data, we do not know the *true* test MSE, and so it is difficult to determine the accuracy of the cross-validation estimate. However, if we examine simulated data, then we can compute the true test MSE, and can thereby evaluate the accuracy of our cross-validation results. In Figure 5.6, we plot the cross-validation estimates and true test error rates that result from applying smoothing splines to the simulated data sets illustrated in Figures 2.9–2.11 of Chapter 2. The true test MSE is displayed in blue. The black dashed and orange solid lines respectively show the estimated LOOCV and 10-fold CV estimates. In all three plots, the two cross-validation estimates are very similar. In the right-hand panel

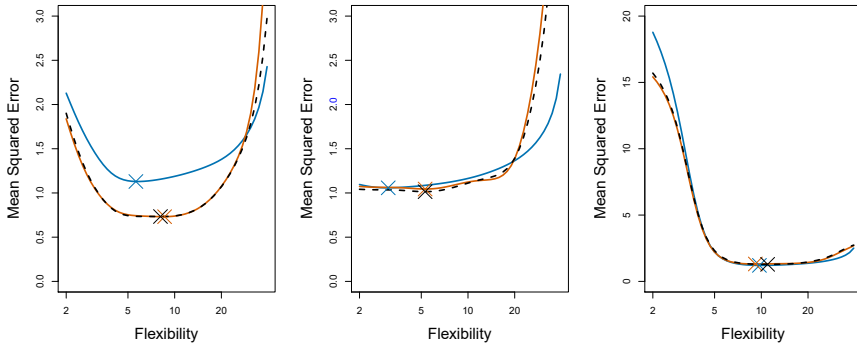


**FIGURE 5.6.** True and estimated test MSE for the simulated data sets in Figures 2.9 (left), 2.10 (center), and 2.11 (right). The true test MSE is shown in blue, the LOOCV estimate is shown as a black dashed line, and the 10-fold CV estimate is shown in orange. The crosses indicate the minimum of each of the MSE curves.

of Figure 5.6, the true test MSE and the cross-validation curves are almost identical. In the center panel of Figure 5.6, the two sets of curves are similar at the lower degrees of flexibility, while the CV curves overestimate the test set MSE for higher degrees of flexibility. In the left-hand panel of Figure 5.6, the CV curves have the correct general shape, but they underestimate the true test MSE.

When we perform cross-validation, our goal might be to determine how well a given statistical learning procedure can be expected to perform on independent data; in this case, the actual estimate of the test MSE is of interest. But at other times we are interested only in the location of the *minimum point in the estimated test MSE curve*. This is because we might be performing cross-validation on a number of statistical learning methods, or on a single method using different levels of flexibility, in order to identify the method that results in the lowest test error. For this purpose, the location of the minimum point in the estimated test MSE curve is important, but the actual value of the estimated test MSE is not. We find in Figure 5.6 that despite the fact that they sometimes underestimate the true test MSE, all of the CV curves come close to identifying the correct level of flexibility—that is, the flexibility level corresponding to the smallest test MSE.

#### 5.1.4 Bias-Variance Trade-Off for $k$ -Fold Cross-Validation

We mentioned in Section 5.1.3 that  $k$ -fold CV with  $k < n$  has a computational advantage to LOOCV. But putting computational issues aside, a less obvious but potentially more important advantage of  $k$ -fold CV is that it often gives more accurate estimates of the test error rate than does LOOCV. This has to do with a bias-variance trade-off.

It was mentioned in Section 5.1.1 that the validation set approach can lead to overestimates of the test error rate, since in this approach the training set used to fit the statistical learning method contains only half the observations of the entire data set. Using this logic, it is not hard to see

that LOOCV will give approximately unbiased estimates of the test error, since each training set contains  $n - 1$  observations, which is almost as many as the number of observations in the full data set. And performing  $k$ -fold CV for, say,  $k = 5$  or  $k = 10$  will lead to an intermediate level of bias, since each training set contains approximately  $(k - 1)n/k$  observations—fewer than in the LOOCV approach, but substantially more than in the validation set approach. Therefore, from the perspective of bias reduction, it is clear that LOOCV is to be preferred to  $k$ -fold CV.

However, we know that bias is not the only source for concern in an estimating procedure; we must also consider the procedure's variance. It turns out that LOOCV has higher variance than does  $k$ -fold CV with  $k < n$ . Why is this the case? When we perform LOOCV, we are in effect averaging the outputs of  $n$  fitted models, each of which is trained on an almost identical set of observations; therefore, these outputs are highly (positively) correlated with each other. In contrast, when we perform  $k$ -fold CV with  $k < n$ , we are averaging the outputs of  $k$  fitted models that are somewhat less correlated with each other, since the overlap between the training sets in each model is smaller. Since the mean of many highly correlated quantities has higher variance than does the mean of many quantities that are not as highly correlated, the test error estimate resulting from LOOCV tends to have higher variance than does the test error estimate resulting from  $k$ -fold CV.

To summarize, there is a bias-variance trade-off associated with the choice of  $k$  in  $k$ -fold cross-validation. Typically, given these considerations, one performs  $k$ -fold cross-validation using  $k = 5$  or  $k = 10$ , as these values have been shown empirically to yield test error rate estimates that suffer neither from excessively high bias nor from very high variance.

### 5.1.5 Cross-Validation on Classification Problems

In this chapter so far, we have illustrated the use of cross-validation in the regression setting where the outcome  $Y$  is quantitative, and so have used MSE to quantify test error. But cross-validation can also be a very useful approach in the classification setting when  $Y$  is qualitative. In this setting, cross-validation works just as described earlier in this chapter, except that rather than using MSE to quantify test error, we instead use the number of misclassified observations. For instance, in the classification setting, the LOOCV error rate takes the form

$$\text{CV}_{(n)} = \frac{1}{n} \sum_{i=1}^n \text{Err}_i, \quad (5.4)$$

where  $\text{Err}_i = I(y_i \neq \hat{y}_i)$ . The  $k$ -fold CV error rate and validation set error rates are defined analogously.

As an example, we fit various logistic regression models on the two-dimensional classification data displayed in Figure 2.13. In the top-left panel of Figure 5.7, the black solid line shows the estimated decision boundary resulting from fitting a standard logistic regression model to this data set. Since this is simulated data, we can compute the *true* test error rate, which takes a value of 0.201 and so is substantially larger than the Bayes

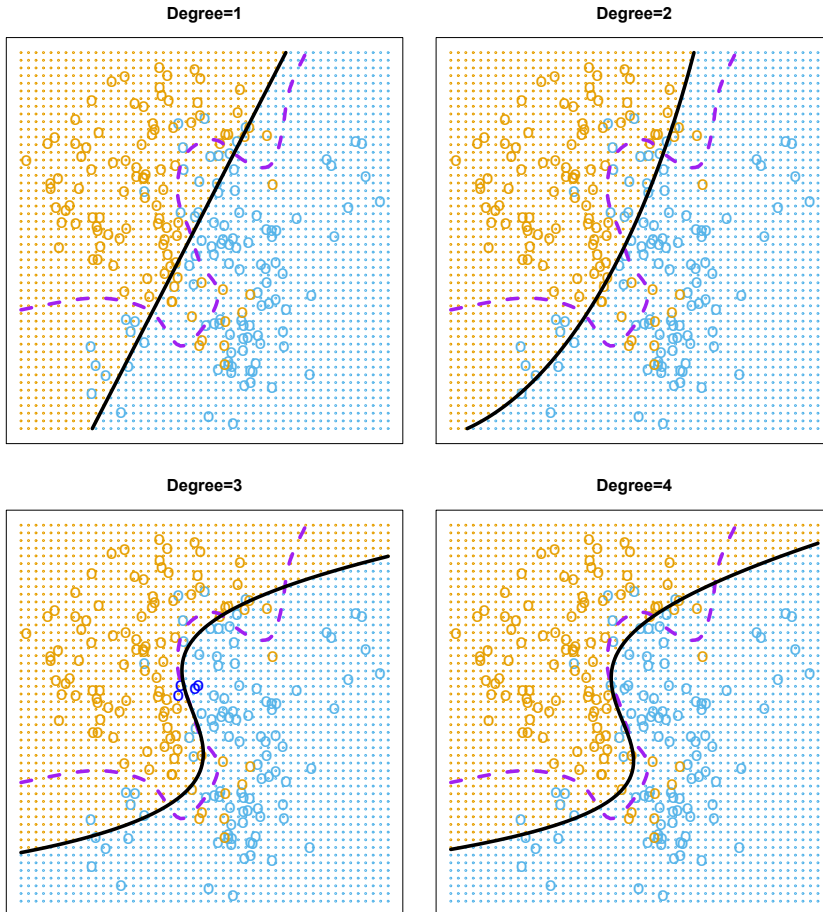


**FIGURE 5.7.** Logistic regression fits on the two-dimensional classification data displayed in Figure 2.13. The Bayes decision boundary is represented using a purple dashed line. Estimated decision boundaries from linear, quadratic, cubic and quartic (degrees 1–4) logistic regressions are displayed in black. The test error rates for the four logistic regression fits are respectively 0.201, 0.197, 0.160, and 0.162, while the Bayes error rate is 0.133.

error rate of 0.133. Clearly logistic regression does not have enough flexibility to model the Bayes decision boundary in this setting. We can easily extend logistic regression to obtain a non-linear decision boundary by using polynomial functions of the predictors, as we did in the regression setting in Section 3.3.2. For example, we can fit a *quadratic* logistic regression model, given by

$$\log \left( \frac{p}{1-p} \right) = \beta_0 + \beta_1 X_1 + \beta_2 X_1^2 + \beta_3 X_2 + \beta_4 X_2^2. \quad (5.5)$$

The top-right panel of Figure 5.7 displays the resulting decision boundary, which is now curved. However, the test error rate has improved only slightly, to 0.197. A much larger improvement is apparent in the bottom-left panel

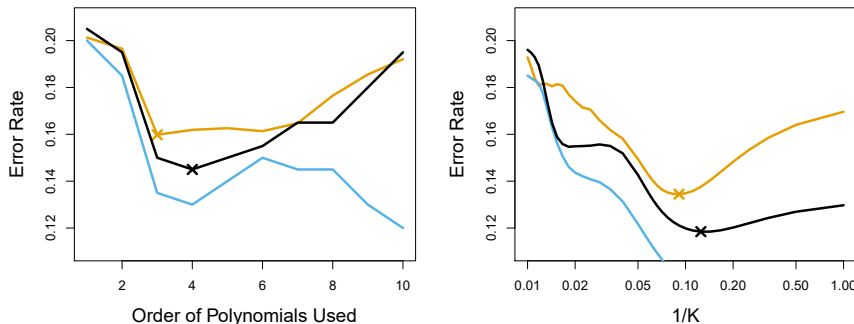


**FIGURE 5.8.** Test error (brown), training error (blue), and 10-fold CV error (black) on the two-dimensional classification data displayed in Figure 5.7. Left: Logistic regression using polynomial functions of the predictors. The order of the polynomials used is displayed on the x-axis. Right: The KNN classifier with different values of  $K$ , the number of neighbors used in the KNN classifier.

of Figure 5.7, in which we have fit a logistic regression model involving cubic polynomials of the predictors. Now the test error rate has decreased to 0.160. Going to a quartic polynomial (bottom-right) slightly increases the test error.

In practice, for real data, the Bayes decision boundary and the test error rates are unknown. So how might we decide between the four logistic regression models displayed in Figure 5.7? We can use cross-validation in order to make this decision. The left-hand panel of Figure 5.8 displays in black the 10-fold CV error rates that result from fitting ten logistic regression models to the data, using polynomial functions of the predictors up to tenth order. The true test errors are shown in brown, and the training errors are shown in blue. As we have seen previously, the training error tends to decrease as the flexibility of the fit increases. (The figure indicates that though the training error rate doesn't quite decrease monotonically, it tends to decrease on the whole as the model complexity increases.) In contrast, the test error displays a characteristic U-shape. The 10-fold CV error rate provides a pretty good approximation to the test error rate. While it somewhat underestimates the error rate, it reaches a minimum when fourth-order polynomials are used, which is very close to the minimum of the test curve, which occurs when third-order polynomials are used. In fact, using fourth-order polynomials would likely lead to good test set performance, as the true test error rate is approximately the same for third, fourth, fifth, and sixth-order polynomials.

The right-hand panel of Figure 5.8 displays the same three curves using the KNN approach for classification, as a function of the value of  $K$  (which in this context indicates the number of neighbors used in the KNN classifier, rather than the number of CV folds used). Again the training error rate declines as the method becomes more flexible, and so we see that the training error rate cannot be used to select the optimal value for  $K$ . Though the cross-validation error curve slightly underestimates the test error rate, it takes on a minimum very close to the best value for  $K$ .

## 5.2 The Bootstrap

The *bootstrap* is a widely applicable and extremely powerful statistical tool that can be used to quantify the uncertainty associated with a given estimator or statistical learning method. As a simple example, the bootstrap can be used to estimate the standard errors of the coefficients from a linear regression fit. In the specific case of linear regression, this is not particularly useful, since we saw in Chapter 3 that standard statistical software such as **R** outputs such standard errors automatically. However, the power of the bootstrap lies in the fact that it can be easily applied to a wide range of statistical learning methods, including some for which a measure of variability is otherwise difficult to obtain and is not automatically output by statistical software.

bootstrap

In this section we illustrate the bootstrap on a toy example in which we wish to determine the best investment allocation under a simple model. In Section 5.3 we explore the use of the bootstrap to assess the variability associated with the regression coefficients in a linear model fit.

Suppose that we wish to invest a fixed sum of money in two financial assets that yield returns of  $X$  and  $Y$ , respectively, where  $X$  and  $Y$  are random quantities. We will invest a fraction  $\alpha$  of our money in  $X$ , and will invest the remaining  $1 - \alpha$  in  $Y$ . Since there is variability associated with the returns on these two assets, we wish to choose  $\alpha$  to minimize the total risk, or variance, of our investment. In other words, we want to minimize  $\text{Var}(\alpha X + (1 - \alpha)Y)$ . One can show that the value that minimizes the risk is given by

$$\alpha = \frac{\sigma_Y^2 - \sigma_{XY}}{\sigma_X^2 + \sigma_Y^2 - 2\sigma_{XY}}, \quad (5.6)$$

where  $\sigma_X^2 = \text{Var}(X)$ ,  $\sigma_Y^2 = \text{Var}(Y)$ , and  $\sigma_{XY} = \text{Cov}(X, Y)$ .

In reality, the quantities  $\sigma_X^2$ ,  $\sigma_Y^2$ , and  $\sigma_{XY}$  are unknown. We can compute estimates for these quantities,  $\hat{\sigma}_X^2$ ,  $\hat{\sigma}_Y^2$ , and  $\hat{\sigma}_{XY}$ , using a data set that contains past measurements for  $X$  and  $Y$ . We can then estimate the value of  $\alpha$  that minimizes the variance of our investment using

$$\hat{\alpha} = \frac{\hat{\sigma}_Y^2 - \hat{\sigma}_{XY}}{\hat{\sigma}_X^2 + \hat{\sigma}_Y^2 - 2\hat{\sigma}_{XY}}. \quad (5.7)$$

Figure 5.9 illustrates this approach for estimating  $\alpha$  on a simulated data set. In each panel, we simulated 100 pairs of returns for the investments  $X$  and  $Y$ . We used these returns to estimate  $\sigma_X^2$ ,  $\sigma_Y^2$ , and  $\sigma_{XY}$ , which we then substituted into (5.7) in order to obtain estimates for  $\alpha$ . The value of  $\hat{\alpha}$  resulting from each simulated data set ranges from 0.532 to 0.657.

It is natural to wish to quantify the accuracy of our estimate of  $\alpha$ . To estimate the standard deviation of  $\hat{\alpha}$ , we repeated the process of simulating 100 paired observations of  $X$  and  $Y$ , and estimating  $\alpha$  using (5.7), 1,000 times. We thereby obtained 1,000 estimates for  $\alpha$ , which we can call  $\hat{\alpha}_1, \hat{\alpha}_2, \dots, \hat{\alpha}_{1,000}$ . The left-hand panel of Figure 5.10 displays a histogram of the resulting estimates. For these simulations the parameters were set to  $\sigma_X^2 = 1$ ,  $\sigma_Y^2 = 1.25$ , and  $\sigma_{XY} = 0.5$ , and so we know that the true value of  $\alpha$  is 0.6. We indicated this value using a solid vertical line on the histogram.

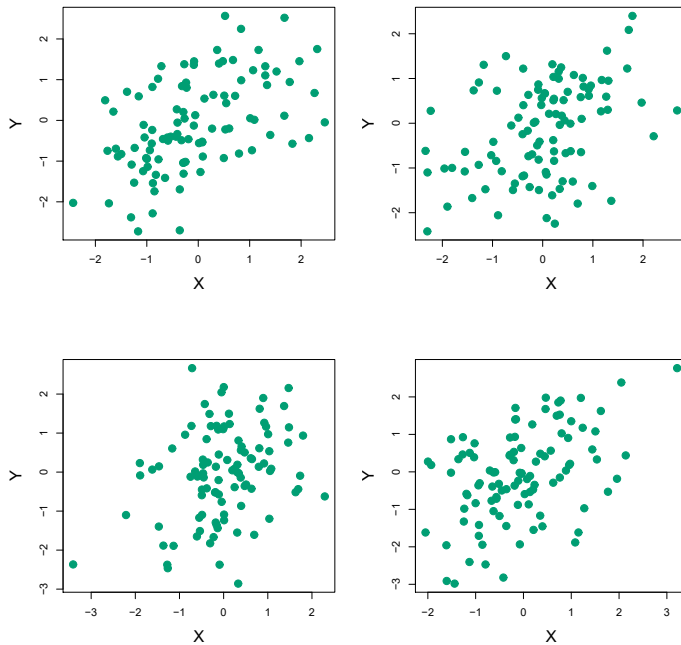


**FIGURE 5.9.** Each panel displays 100 simulated returns for investments  $X$  and  $Y$ . From left to right and top to bottom, the resulting estimates for  $\alpha$  are 0.576, 0.532, 0.657, and 0.651.

The mean over all 1,000 estimates for  $\alpha$  is

$$\bar{\alpha} = \frac{1}{1000} \sum_{r=1}^{1000} \hat{\alpha}_r = 0.5996,$$

very close to  $\alpha = 0.6$ , and the standard deviation of the estimates is

$$\sqrt{\frac{1}{1000 - 1} \sum_{r=1}^{1000} (\hat{\alpha}_r - \bar{\alpha})^2} = 0.083.$$

This gives us a very good idea of the accuracy of  $\hat{\alpha}$ :  $SE(\hat{\alpha}) \approx 0.083$ . So roughly speaking, for a random sample from the population, we would expect  $\hat{\alpha}$  to differ from  $\alpha$  by approximately 0.08, on average.

In practice, however, the procedure for estimating  $SE(\hat{\alpha})$  outlined above cannot be applied, because for real data we cannot generate new samples from the original population. However, the bootstrap approach allows us to use a computer to emulate the process of obtaining new sample sets, so that we can estimate the variability of  $\hat{\alpha}$  without generating additional samples. Rather than repeatedly obtaining independent data sets from the population, we instead obtain distinct data sets by repeatedly sampling observations *from the original data set*.

This approach is illustrated in Figure 5.11 on a simple data set, which we call  $Z$ , that contains only  $n = 3$  observations. We randomly select  $n$  observations from the data set in order to produce a bootstrap data set,

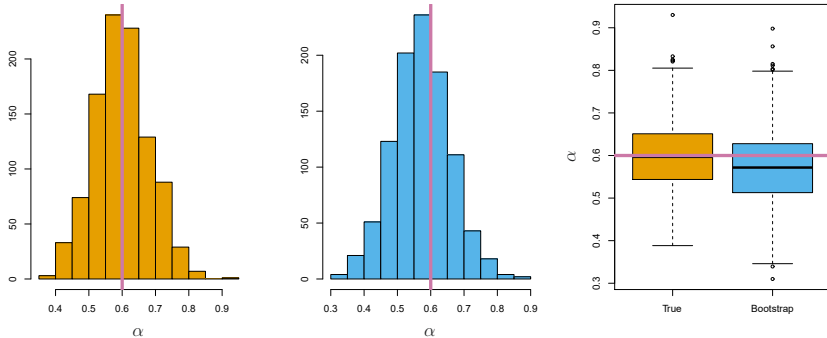


**FIGURE 5.10.** Left: A histogram of the estimates of  $\alpha$  obtained by generating 1,000 simulated data sets from the true population. Center: A histogram of the estimates of  $\alpha$  obtained from 1,000 bootstrap samples from a single data set. Right: The estimates of  $\alpha$  displayed in the left and center panels are shown as boxplots. In each panel, the pink line indicates the true value of  $\alpha$ .

$Z^{*1}$ . The sampling is performed *with replacement*, which means that the same observation can occur more than once in the bootstrap data set. In this example,  $Z^{*1}$  contains the third observation twice, the first observation once, and no instances of the second observation. Note that if an observation is contained in  $Z^{*1}$ , then both its  $X$  and  $Y$  values are included. We can use  $Z^{*1}$  to produce a new bootstrap estimate for  $\alpha$ , which we call  $\hat{\alpha}^{*1}$ . This procedure is repeated  $B$  times for some large value of  $B$ , in order to produce  $B$  different bootstrap data sets,  $Z^{*1}, Z^{*2}, \dots, Z^{*B}$ , and  $B$  corresponding  $\alpha$  estimates,  $\hat{\alpha}^{*1}, \hat{\alpha}^{*2}, \dots, \hat{\alpha}^{*B}$ . We can compute the standard error of these bootstrap estimates using the formula

$$\text{SE}_B(\hat{\alpha}) = \sqrt{\frac{1}{B-1} \sum_{r=1}^B \left( \hat{\alpha}^{*r} - \frac{1}{B} \sum_{r'=1}^B \hat{\alpha}^{*r'} \right)^2}. \quad (5.8)$$

This serves as an estimate of the standard error of  $\hat{\alpha}$  estimated from the original data set.

The bootstrap approach is illustrated in the center panel of Figure 5.10, which displays a histogram of 1,000 bootstrap estimates of  $\alpha$ , each computed using a distinct bootstrap data set. This panel was constructed on the basis of a single data set, and hence could be created using real data. Note that the histogram looks very similar to the left-hand panel, which displays the idealized histogram of the estimates of  $\alpha$  obtained by generating 1,000 simulated data sets from the true population. In particular the bootstrap estimate  $\text{SE}(\hat{\alpha})$  from (5.8) is 0.087, very close to the estimate of 0.083 obtained using 1,000 simulated data sets. The right-hand panel displays the information in the center and left panels in a different way, via boxplots of the estimates for  $\alpha$  obtained by generating 1,000 simulated data sets from the true population and using the bootstrap approach. Again, the boxplots have similar spreads, indicating that the bootstrap approach can be used to effectively estimate the variability associated with  $\hat{\alpha}$ .

with  
replacement

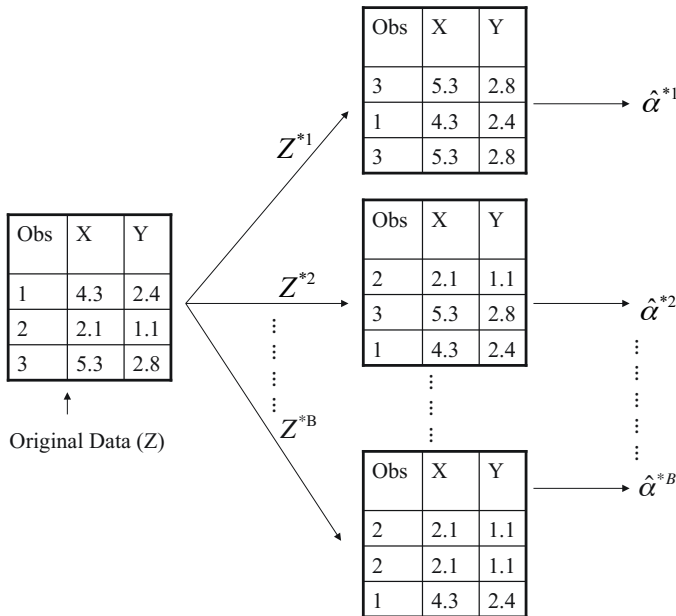


**FIGURE 5.11.** A graphical illustration of the bootstrap approach on a small sample containing  $n = 3$  observations. Each bootstrap data set contains  $n$  observations, sampled with replacement from the original data set. Each bootstrap data set is used to obtain an estimate of  $\alpha$ .

## 5.3 Lab: Cross-Validation and the Bootstrap

In this lab, we explore the resampling techniques covered in this chapter. Some of the commands in this lab may take a while to run on your computer.

We again begin by placing most of our imports at this top level.

```
In [1]: import numpy as np
import statsmodels.api as sm
from ISLP import load_data
from ISLP.models import (ModelSpec as MS,
 summarize,
 poly)
from sklearn.model_selection import train_test_split
```

There are several new imports needed for this lab.

```
In [2]: from functools import partial
from sklearn.model_selection import \
 (cross_validate,
 KFold,
 ShuffleSplit)
from sklearn.base import clone
from ISLP.models import sklearn_sm
```

```
Out[25]: intercept 2.067840
poly(horsepower, 2, raw=True)[0] 0.033019
poly(horsepower, 2, raw=True)[1] 0.000120
dtype: float64
```

We compare the results to the standard errors computed using `sm.OLS()`.

```
In [26]: M = sm.OLS(Auto['mpg'],
 quad_model.fit_transform(Auto))
summarize(M.fit())['std err']
```

```
Out[26]: intercept 1.800
poly(horsepower, 2, raw=True)[0] 0.031
poly(horsepower, 2, raw=True)[1] 0.000
Name: std err, dtype: float64
```

## 5.4 Exercises

### Conceptual

1. Using basic statistical properties of the variance, as well as single-variable calculus, derive (5.6). In other words, prove that  $\alpha$  given by (5.6) does indeed minimize  $\text{Var}(\alpha X + (1 - \alpha)Y)$ .
2. We will now derive the probability that a given observation is part of a bootstrap sample. Suppose that we obtain a bootstrap sample from a set of  $n$  observations.
  - (a) What is the probability that the first bootstrap observation is *not* the  $j$ th observation from the original sample? Justify your answer.
  - (b) What is the probability that the second bootstrap observation is *not* the  $j$ th observation from the original sample?
  - (c) Argue that the probability that the  $j$ th observation is *not* in the bootstrap sample is  $(1 - 1/n)^n$ .
  - (d) When  $n = 5$ , what is the probability that the  $j$ th observation is in the bootstrap sample?
  - (e) When  $n = 100$ , what is the probability that the  $j$ th observation is in the bootstrap sample?
  - (f) When  $n = 10,000$ , what is the probability that the  $j$ th observation is in the bootstrap sample?
  - (g) Create a plot that displays, for each integer value of  $n$  from 1 to 100,000, the probability that the  $j$ th observation is in the bootstrap sample. Comment on what you observe.
  - (h) We will now investigate numerically the probability that a bootstrap sample of size  $n = 100$  contains the  $j$ th observation. Here  $j = 4$ . We first create an array `store` with values that will subsequently be overwritten using the function `np.empty()`. We then

`np.empty()`

repeatedly create bootstrap samples, and each time we record whether or not the fifth observation is contained in the bootstrap sample.

```
rng = np.random.default_rng(10)
store = np.empty(10000)
for i in range(10000):
 store[i] = np.sum(rng.choice(100, replace=True) == 4
 > 0
np.mean(store)
```

Comment on the results obtained.

3. We now review  $k$ -fold cross-validation.
  - (a) Explain how  $k$ -fold cross-validation is implemented.
  - (b) What are the advantages and disadvantages of  $k$ -fold cross-validation relative to:
    - i. The validation set approach?
    - ii. LOOCV?
4. Suppose that we use some statistical learning method to make a prediction for the response  $Y$  for a particular value of the predictor  $X$ . Carefully describe how we might estimate the standard deviation of our prediction.

### Applied

5. In Chapter 4, we used logistic regression to predict the probability of `default` using `income` and `balance` on the `Default` data set. We will now estimate the test error of this logistic regression model using the validation set approach. Do not forget to set a random seed before beginning your analysis.
  - (a) Fit a logistic regression model that uses `income` and `balance` to predict `default`.
  - (b) Using the validation set approach, estimate the test error of this model. In order to do this, you must perform the following steps:
    - i. Split the sample set into a training set and a validation set.
    - ii. Fit a multiple logistic regression model using only the training observations.
    - iii. Obtain a prediction of default status for each individual in the validation set by computing the posterior probability of default for that individual, and classifying the individual to the `default` category if the posterior probability is greater than 0.5.
    - iv. Compute the validation set error, which is the fraction of the observations in the validation set that are misclassified.
  - (c) Repeat the process in (b) three times, using three different splits of the observations into a training set and a validation set. Comment on the results obtained.

- (d) Now consider a logistic regression model that predicts the probability of `default` using `income`, `balance`, and a dummy variable for `student`. Estimate the test error for this model using the validation set approach. Comment on whether or not including a dummy variable for `student` leads to a reduction in the test error rate.
6. We continue to consider the use of a logistic regression model to predict the probability of `default` using `income` and `balance` on the `Default` data set. In particular, we will now compute estimates for the standard errors of the `income` and `balance` logistic regression coefficients in two different ways: (1) using the bootstrap, and (2) using the standard formula for computing the standard errors in the `sm.GLM()` function. Do not forget to set a random seed before beginning your analysis.
- (a) Using the `summarize()` and `sm.GLM()` functions, determine the estimated standard errors for the coefficients associated with `income` and `balance` in a multiple logistic regression model that uses both predictors.
  - (b) Write a function, `boot_fn()`, that takes as input the `Default` data set as well as an index of the observations, and that outputs the coefficient estimates for `income` and `balance` in the multiple logistic regression model.
  - (c) Following the bootstrap example in the lab, use your `boot_fn()` function to estimate the standard errors of the logistic regression coefficients for `income` and `balance`.
  - (d) Comment on the estimated standard errors obtained using the `sm.GLM()` function and using the bootstrap.
7. In Sections 5.1.2 and 5.1.3, we saw that the `cross_validate()` function can be used in order to compute the LOOCV test error estimate. Alternatively, one could compute those quantities using just `sm.GLM()` and the `predict()` method of the fitted model within a for loop. You will now take this approach in order to compute the LOOCV error for a simple logistic regression model on the `Weekly` data set. Recall that in the context of classification problems, the LOOCV error is given in (5.4).
- (a) Fit a logistic regression model that predicts `Direction` using `Lag1` and `Lag2`.
  - (b) Fit a logistic regression model that predicts `Direction` using `Lag1` and `Lag2` *using all but the first observation*.
  - (c) Use the model from (b) to predict the direction of the first observation. You can do this by predicting that the first observation will go up if  $P(\text{Direction} = \text{"Up"} | \text{Lag1}, \text{Lag2}) > 0.5$ . Was this observation correctly classified?
  - (d) Write a for loop from  $i = 1$  to  $i = n$ , where  $n$  is the number of observations in the data set, that performs each of the following steps:

- i. Fit a logistic regression model using all but the  $i$ th observation to predict `Direction` using `Lag1` and `Lag2`.
  - ii. Compute the posterior probability of the market moving up for the  $i$ th observation.
  - iii. Use the posterior probability for the  $i$ th observation in order to predict whether or not the market moves up.
  - iv. Determine whether or not an error was made in predicting the direction for the  $i$ th observation. If an error was made, then indicate this as a 1, and otherwise indicate it as a 0.
  - (e) Take the average of the  $n$  numbers obtained in (d)iv in order to obtain the LOOCV estimate for the test error. Comment on the results.
8. We will now perform cross-validation on a simulated data set.
- (a) Generate a simulated data set as follows:
- ```
rng = np.random.default_rng(1)
x = rng.normal(size=100)
y = x - 2 * x**2 + rng.normal(size=100)
```
- In this data set, what is n and what is p ? Write out the model used to generate the data in equation form.
- (b) Create a scatterplot of X against Y . Comment on what you find.
 - (c) Set a random seed, and then compute the LOOCV errors that result from fitting the following four models using least squares:
 - i. $Y = \beta_0 + \beta_1 X + \epsilon$
 - ii. $Y = \beta_0 + \beta_1 X + \beta_2 X^2 + \epsilon$
 - iii. $Y = \beta_0 + \beta_1 X + \beta_2 X^2 + \beta_3 X^3 + \epsilon$
 - iv. $Y = \beta_0 + \beta_1 X + \beta_2 X^2 + \beta_3 X^3 + \beta_4 X^4 + \epsilon$.
- Note you may find it helpful to use the `data.frame()` function to create a single data set containing both X and Y .
- (d) Repeat (c) using another random seed, and report your results. Are your results the same as what you got in (c)? Why?
 - (e) Which of the models in (c) had the smallest LOOCV error? Is this what you expected? Explain your answer.
 - (f) Comment on the statistical significance of the coefficient estimates that results from fitting each of the models in (c) using least squares. Do these results agree with the conclusions drawn based on the cross-validation results?
9. We will now consider the `Boston` housing data set, from the `ISLP` library.
- (a) Based on this data set, provide an estimate for the population mean of `medv`. Call this estimate $\hat{\mu}$.

- (b) Provide an estimate of the standard error of $\hat{\mu}$. Interpret this result.

Hint: We can compute the standard error of the sample mean by dividing the sample standard deviation by the square root of the number of observations.

- (c) Now estimate the standard error of $\hat{\mu}$ using the bootstrap. How does this compare to your answer from (b)?
- (d) Based on your bootstrap estimate from (c), provide a 95 % confidence interval for the mean of `medv`. Compare it to the results obtained by using `Boston['medv'].std()` and the two standard error rule (3.9).

Hint: You can approximate a 95 % confidence interval using the formula $[\hat{\mu} - 2\text{SE}(\hat{\mu}), \hat{\mu} + 2\text{SE}(\hat{\mu})]$.

- (e) Based on this data set, provide an estimate, $\hat{\mu}_{med}$, for the median value of `medv` in the population.
- (f) We now would like to estimate the standard error of $\hat{\mu}_{med}$. Unfortunately, there is no simple formula for computing the standard error of the median. Instead, estimate the standard error of the median using the bootstrap. Comment on your findings.
- (g) Based on this data set, provide an estimate for the tenth percentile of `medv` in Boston census tracts. Call this quantity $\hat{\mu}_{0.1}$. (You can use the `np.percentile()` function.)
- (h) Use the bootstrap to estimate the standard error of $\hat{\mu}_{0.1}$. Comment on your findings.

`np.`

`percentile()`

6



Linear Model Selection and Regularization

In the regression setting, the standard linear model

$$Y = \beta_0 + \beta_1 X_1 + \cdots + \beta_p X_p + \epsilon \quad (6.1)$$

is commonly used to describe the relationship between a response Y and a set of variables X_1, X_2, \dots, X_p . We have seen in Chapter 3 that one typically fits this model using least squares.

In the chapters that follow, we consider some approaches for extending the linear model framework. In Chapter 7 we generalize (6.1) in order to accommodate non-linear, but still additive, relationships, while in Chapters 8 and 10 we consider even more general non-linear models. However, the linear model has distinct advantages in terms of inference and, on real-world problems, is often surprisingly competitive in relation to non-linear methods. Hence, before moving to the non-linear world, we discuss in this chapter some ways in which the simple linear model can be improved, by replacing plain least squares fitting with some alternative fitting procedures.

Why might we want to use another fitting procedure instead of least squares? As we will see, alternative fitting procedures can yield better *prediction accuracy* and *model interpretability*.

- *Prediction Accuracy:* Provided that the true relationship between the response and the predictors is approximately linear, the least squares estimates will have low bias. If $n \gg p$ —that is, if n , the number of observations, is much larger than p , the number of variables—then the least squares estimates tend to also have low variance, and hence will perform well on test observations. However, if n is not much larger than p , then there can be a lot of variability in the least squares fit, resulting in overfitting and consequently poor predictions on future observations not used in model training. And if $p > n$, then there is no longer a unique least squares coefficient estimate: there are infinitely

many solutions. Each of these least squares solutions gives zero error on the training data, but typically very poor test set performance due to extremely high variance.¹ By *constraining* or *shrinking* the estimated coefficients, we can often substantially reduce the variance at the cost of a negligible increase in bias. This can lead to substantial improvements in the accuracy with which we can predict the response for observations not used in model training.

- *Model Interpretability:* It is often the case that some or many of the variables used in a multiple regression model are in fact not associated with the response. Including such *irrelevant* variables leads to unnecessary complexity in the resulting model. By removing these variables—that is, by setting the corresponding coefficient estimates to zero—we can obtain a model that is more easily interpreted. Now least squares is extremely unlikely to yield any coefficient estimates that are exactly zero. In this chapter, we see some approaches for automatically performing *feature selection* or *variable selection*—that is, for excluding irrelevant variables from a multiple regression model.

feature
selection
variable
selection

There are many alternatives, both classical and modern, to using least squares to fit (6.1). In this chapter, we discuss three important classes of methods.

- *Subset Selection.* This approach involves identifying a subset of the p predictors that we believe to be related to the response. We then fit a model using least squares on the reduced set of variables.
- *Shrinkage.* This approach involves fitting a model involving all p predictors. However, the estimated coefficients are shrunk towards zero relative to the least squares estimates. This shrinkage (also known as *regularization*) has the effect of reducing variance. Depending on what type of shrinkage is performed, some of the coefficients may be estimated to be exactly zero. Hence, shrinkage methods can also perform variable selection.
- *Dimension Reduction.* This approach involves *projecting* the p predictors into an M -dimensional subspace, where $M < p$. This is achieved by computing M different *linear combinations*, or *projections*, of the variables. Then these M projections are used as predictors to fit a linear regression model by least squares.

In the following sections we describe each of these approaches in greater detail, along with their advantages and disadvantages. Although this chapter describes extensions and modifications to the linear model for regression seen in Chapter 3, the same concepts apply to other methods, such as the classification models seen in Chapter 4.

¹When $p \gg n$, the least squares solution that has the smallest sum of squared coefficients can sometimes perform quite well. See Section 10.8 for a more detailed discussion.

6.1 Subset Selection

In this section we consider some methods for selecting subsets of predictors. These include best subset and stepwise model selection procedures.

6.1.1 Best Subset Selection

To perform *best subset selection*, we fit a separate least squares regression for each possible combination of the p predictors. That is, we fit all p models that contain exactly one predictor, all $\binom{p}{2} = p(p-1)/2$ models that contain exactly two predictors, and so forth. We then look at all of the resulting models, with the goal of identifying the one that is *best*.

best subset selection

The problem of selecting the *best model* from among the 2^p possibilities considered by best subset selection is not trivial. This is usually broken up into two stages, as described in Algorithm 6.1.

Algorithm 6.1 Best subset selection

1. Let \mathcal{M}_0 denote the *null model*, which contains no predictors. This model simply predicts the sample mean for each observation.
 2. For $k = 1, 2, \dots, p$:
 - (a) Fit all $\binom{p}{k}$ models that contain exactly k predictors.
 - (b) Pick the best among these $\binom{p}{k}$ models, and call it \mathcal{M}_k . Here *best* is defined as having the smallest RSS, or equivalently largest R^2 .
 3. Select a single best model from among $\mathcal{M}_0, \dots, \mathcal{M}_p$ using the prediction error on a validation set, C_p (AIC), BIC, or adjusted R^2 . Or use the cross-validation method.
-

In Algorithm 6.1, Step 2 identifies the best model (on the training data) for each subset size, in order to reduce the problem from one of 2^p possible models to one of $p + 1$ possible models. In Figure 6.1, these models form the lower frontier depicted in red.

Now in order to select a single best model, we must simply choose among these $p + 1$ options. This task must be performed with care, because the RSS of these $p + 1$ models decreases monotonically, and the R^2 increases monotonically, as the number of features included in the models increases. Therefore, if we use these statistics to select the best model, then we will always end up with a model involving all of the variables. The problem is that a low RSS or a high R^2 indicates a model with a low *training* error, whereas we wish to choose a model that has a low *test* error. (As shown in Chapter 2 in Figures 2.9–2.11, training error tends to be quite a bit smaller than test error, and a low training error by no means guarantees a low test error.) Therefore, in Step 3, we use the error on a validation set, C_p , BIC, or adjusted R^2 in order to select among $\mathcal{M}_0, \mathcal{M}_1, \dots, \mathcal{M}_p$. If cross-validation is used to select the best model, then Step 2 is repeated on each training fold, and the validation errors are averaged to select the best value of k .

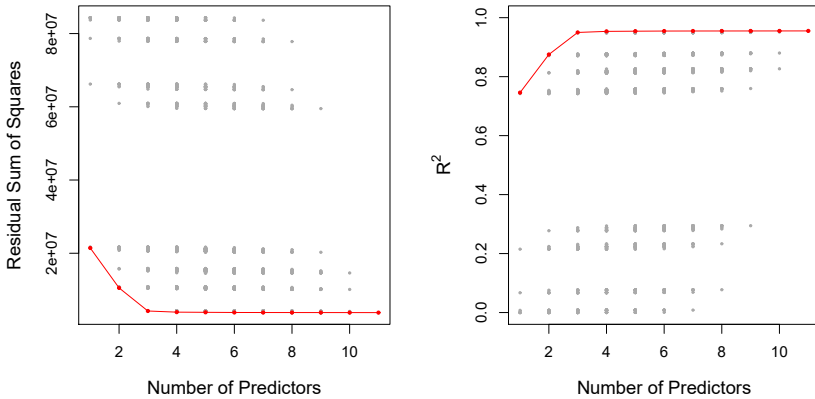


FIGURE 6.1. For each possible model containing a subset of the ten predictors in the `Credit` data set, the RSS and R^2 are displayed. The red frontier tracks the best model for a given number of predictors, according to RSS and R^2 . Though the data set contains only ten predictors, the x-axis ranges from 1 to 11, since one of the variables is categorical and takes on three values, leading to the creation of two dummy variables.

Then the model \mathcal{M}_k fit on the full training set is delivered for the chosen k . These approaches are discussed in Section 6.1.3.

An application of best subset selection is shown in Figure 6.1. Each plotted point corresponds to a least squares regression model fit using a different subset of the 10 predictors in the `Credit` data set, discussed in Chapter 3. Here the variable `region` is a three-level qualitative variable, and so is represented by two dummy variables, which are selected separately in this case. Hence, there are a total of 11 possible variables which can be included in the model. We have plotted the RSS and R^2 statistics for each model, as a function of the number of variables. The red curves connect the best models for each model size, according to RSS or R^2 . The figure shows that, as expected, these quantities improve as the number of variables increases; however, from the three-variable model on, there is little improvement in RSS and R^2 as a result of including additional predictors.

Although we have presented best subset selection here for least squares regression, the same ideas apply to other types of models, such as logistic regression. In the case of logistic regression, instead of ordering models by RSS in Step 2 of Algorithm 6.1, we instead use the *deviance*, a measure that plays the role of RSS for a broader class of models. The deviance is negative two times the maximized log-likelihood; the smaller the deviance, the better the fit.

While best subset selection is a simple and conceptually appealing approach, it suffers from computational limitations. The number of possible models that must be considered grows rapidly as p increases. In general, there are 2^p models that involve subsets of p predictors. So if $p = 10$, then there are approximately 1,000 possible models to be considered, and if $p = 20$, then there are over one million possibilities! Consequently, best subset selection becomes computationally infeasible for values of p greater than

deviance

Algorithm 6.2 *Forward stepwise selection*

1. Let \mathcal{M}_0 denote the *null* model, which contains no predictors.
 2. For $k = 0, \dots, p - 1$:
 - (a) Consider all $p - k$ models that augment the predictors in \mathcal{M}_k with one additional predictor.
 - (b) Choose the *best* among these $p - k$ models, and call it \mathcal{M}_{k+1} . Here *best* is defined as having smallest RSS or highest R^2 .
 3. Select a single best model from among $\mathcal{M}_0, \dots, \mathcal{M}_p$ using the prediction error on a validation set, C_p (AIC), BIC, or adjusted R^2 . Or use the cross-validation method.
-

around 40, even with extremely fast modern computers. There are computational shortcuts—so called branch-and-bound techniques—for eliminating some choices, but these have their limitations as p gets large. They also only work for least squares linear regression. We present computationally efficient alternatives to best subset selection next.

6.1.2 Stepwise Selection

For computational reasons, best subset selection cannot be applied with very large p . Best subset selection may also suffer from statistical problems when p is large. The larger the search space, the higher the chance of finding models that look good on the training data, even though they might not have any predictive power on future data. Thus an enormous search space can lead to overfitting and high variance of the coefficient estimates.

For both of these reasons, *stepwise* methods, which explore a far more restricted set of models, are attractive alternatives to best subset selection.

Forward Stepwise Selection

Forward stepwise selection is a computationally efficient alternative to best subset selection. While the best subset selection procedure considers all 2^p possible models containing subsets of the p predictors, forward stepwise considers a much smaller set of models. Forward stepwise selection begins with a model containing no predictors, and then adds predictors to the model, one-at-a-time, until all of the predictors are in the model. In particular, at each step the variable that gives the greatest *additional* improvement to the fit is added to the model. More formally, the forward stepwise selection procedure is given in Algorithm 6.2.

forward
stepwise
selection

Unlike best subset selection, which involved fitting 2^p models, forward stepwise selection involves fitting one null model, along with $p - k$ models in the k th iteration, for $k = 0, \dots, p - 1$. This amounts to a total of $1 + \sum_{k=0}^{p-1} (p - k) = 1 + p(p + 1)/2$ models. This is a substantial difference: when

# Variables	Best subset	Forward stepwise
One	<code>rating</code>	<code>rating</code>
Two	<code>rating, income</code>	<code>rating, income</code>
Three	<code>rating, income, student</code>	<code>rating, income, student</code>
Four	<code>cards, income</code> <code>student, limit</code>	<code>rating, income,</code> <code>student, limit</code>

TABLE 6.1. The first four selected models for best subset selection and forward stepwise selection on the `Credit` data set. The first three models are identical but the fourth models differ.

$p = 20$, best subset selection requires fitting 1,048,576 models, whereas forward stepwise selection requires fitting only 211 models.²

In Step 2(b) of Algorithm 6.2, we must identify the *best* model from among those $p - k$ that augment \mathcal{M}_k with one additional predictor. We can do this by simply choosing the model with the lowest RSS or the highest R^2 . However, in Step 3, we must identify the best model among a set of models with different numbers of variables. This is more challenging, and is discussed in Section 6.1.3.

Forward stepwise selection's computational advantage over best subset selection is clear. Though forward stepwise tends to do well in practice, it is not guaranteed to find the best possible model out of all 2^p models containing subsets of the p predictors. For instance, suppose that in a given data set with $p = 3$ predictors, the best possible one-variable model contains X_1 , and the best possible two-variable model instead contains X_2 and X_3 . Then forward stepwise selection will fail to select the best possible two-variable model, because \mathcal{M}_1 will contain X_1 , so \mathcal{M}_2 must also contain X_1 together with one additional variable.

Table 6.1, which shows the first four selected models for best subset and forward stepwise selection on the `Credit` data set, illustrates this phenomenon. Both best subset selection and forward stepwise selection choose `rating` for the best one-variable model and then include `income` and `student` for the two- and three-variable models. However, best subset selection replaces `rating` by `cards` in the four-variable model, while forward stepwise selection must maintain `rating` in its four-variable model. In this example, Figure 6.1 indicates that there is not much difference between the three- and four-variable models in terms of RSS, so either of the four-variable models will likely be adequate.

Forward stepwise selection can be applied even in the high-dimensional setting where $n < p$; however, in this case, it is possible to construct submodels $\mathcal{M}_0, \dots, \mathcal{M}_{n-1}$ only, since each submodel is fit using least squares, which will not yield a unique solution if $p \geq n$.

Backward Stepwise Selection

Like forward stepwise selection, *backward stepwise selection* provides an

backward
stepwise
selection

²Though forward stepwise selection considers $p(p + 1)/2 + 1$ models, it performs a *guided* search over model space, and so the *effective* model space considered contains substantially more than $p(p + 1)/2 + 1$ models.

efficient alternative to best subset selection. However, unlike forward stepwise selection, it begins with the full least squares model containing all p predictors, and then iteratively removes the least useful predictor, one-at-a-time. Details are given in Algorithm 6.3.

Algorithm 6.3 Backward stepwise selection

1. Let \mathcal{M}_p denote the *full* model, which contains all p predictors.
 2. For $k = p, p - 1, \dots, 1$:
 - (a) Consider all k models that contain all but one of the predictors in \mathcal{M}_k , for a total of $k - 1$ predictors.
 - (b) Choose the *best* among these k models, and call it \mathcal{M}_{k-1} . Here *best* is defined as having smallest RSS or highest R^2 .
 3. Select a single best model from among $\mathcal{M}_0, \dots, \mathcal{M}_p$ using the prediction error on a validation set, C_p (AIC), BIC, or adjusted R^2 . Or use the cross-validation method.
-

Like forward stepwise selection, the backward selection approach searches through only $1 + p(p+1)/2$ models, and so can be applied in settings where p is too large to apply best subset selection.³ Also like forward stepwise selection, backward stepwise selection is not guaranteed to yield the *best* model containing a subset of the p predictors.

Backward selection requires that the number of samples n is larger than the number of variables p (so that the full model can be fit). In contrast, forward stepwise can be used even when $n < p$, and so is the only viable subset method when p is very large.

Hybrid Approaches

The best subset, forward stepwise, and backward stepwise selection approaches generally give similar but not identical models. As another alternative, hybrid versions of forward and backward stepwise selection are available, in which variables are added to the model sequentially, in analogy to forward selection. However, after adding each new variable, the method may also remove any variables that no longer provide an improvement in the model fit. Such an approach attempts to more closely mimic best subset selection while retaining the computational advantages of forward and backward stepwise selection.

6.1.3 Choosing the Optimal Model

Best subset selection, forward selection, and backward selection result in the creation of a set of models, each of which contains a subset of the p

³Like forward stepwise selection, backward stepwise selection performs a *guided* search over model space, and so effectively considers substantially more than $1 + p(p+1)/2$ models.

predictors. To apply these methods, we need a way to determine which of these models is *best*. As we discussed in Section 6.1.1, the model containing all of the predictors will always have the smallest RSS and the largest R^2 , since these quantities are related to the training error. Instead, we wish to choose a model with a low test error. As is evident here, and as we show in Chapter 2, the training error can be a poor estimate of the test error. Therefore, RSS and R^2 are not suitable for selecting the best model among a collection of models with different numbers of predictors.

In order to select the best model with respect to test error, we need to estimate this test error. There are two common approaches:

1. We can indirectly estimate test error by making an *adjustment* to the training error to account for the bias due to overfitting.
2. We can *directly* estimate the test error, using either a validation set approach or a cross-validation approach, as discussed in Chapter 5.

We consider both of these approaches below.

C_p , AIC, BIC, and Adjusted R^2

We show in Chapter 2 that the training set MSE is generally an underestimate of the test MSE. (Recall that $\text{MSE} = \text{RSS}/n$.) This is because when we fit a model to the training data using least squares, we specifically estimate the regression coefficients such that the training RSS (but not the test RSS) is as small as possible. In particular, the training error will decrease as more variables are included in the model, but the test error may not. Therefore, training set RSS and training set R^2 cannot be used to select from among a set of models with different numbers of variables.

However, a number of techniques for *adjusting* the training error for the model size are available. These approaches can be used to select among a set of models with different numbers of variables. We now consider four such approaches: C_p , Akaike information criterion (AIC), Bayesian information criterion (BIC), and adjusted R^2 . Figure 6.2 displays C_p , BIC, and adjusted R^2 for the best model of each size produced by best subset selection on the **Credit** data set.

For a fitted least squares model containing d predictors, the C_p estimate of test MSE is computed using the equation

$$C_p = \frac{1}{n} (\text{RSS} + 2d\hat{\sigma}^2), \quad (6.2)$$

C_p	Akaike information criterion
BIC	Bayesian information criterion
adjusted R^2	

where $\hat{\sigma}^2$ is an estimate of the variance of the error ϵ associated with each response measurement in (6.1).⁴ Typically $\hat{\sigma}^2$ is estimated using the full model containing all predictors. Essentially, the C_p statistic adds a penalty of $2d\hat{\sigma}^2$ to the training RSS in order to adjust for the fact that the training error tends to underestimate the test error. Clearly, the penalty increases as the number of predictors in the model increases; this is intended to adjust

⁴Mallow's C_p is sometimes defined as $C'_p = \text{RSS}/\hat{\sigma}^2 + 2d - n$. This is equivalent to the definition given above in the sense that $C_p = \frac{1}{n}\hat{\sigma}^2(C'_p + n)$, and so the model with smallest C_p also has smallest C'_p .

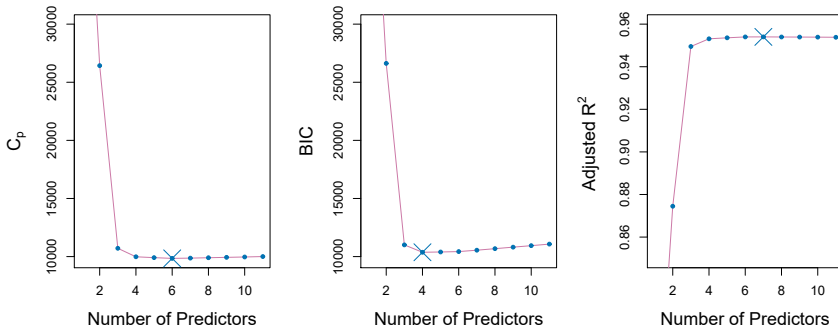


FIGURE 6.2. C_p , BIC, and adjusted R^2 are shown for the best models of each size for the **Credit** data set (the lower frontier in Figure 6.1). C_p and BIC are estimates of test MSE. In the middle plot we see that the BIC estimate of test error shows an increase after four variables are selected. The other two plots are rather flat after four variables are included.

for the corresponding decrease in training RSS. Though it is beyond the scope of this book, one can show that if $\hat{\sigma}^2$ is an unbiased estimate of σ^2 in (6.2), then C_p is an unbiased estimate of test MSE. As a consequence, the C_p statistic tends to take on a small value for models with a low test error, so when determining which of a set of models is best, we choose the model with the lowest C_p value. In Figure 6.2, C_p selects the six-variable model containing the predictors `income`, `limit`, `rating`, `cards`, `age` and `student`.

The AIC criterion is defined for a large class of models fit by maximum likelihood. In the case of the model (6.1) with Gaussian errors, maximum likelihood and least squares are the same thing. In this case AIC is given by

$$\text{AIC} = \frac{1}{n} (\text{RSS} + 2d\hat{\sigma}^2),$$

where, for simplicity, we have omitted irrelevant constants.⁵ Hence for least squares models, C_p and AIC are proportional to each other, and so only C_p is displayed in Figure 6.2.

BIC is derived from a Bayesian point of view, but ends up looking similar to C_p (and AIC) as well. For the least squares model with d predictors, the BIC is, up to irrelevant constants, given by

$$\text{BIC} = \frac{1}{n} (\text{RSS} + \log(n)d\hat{\sigma}^2). \quad (6.3)$$

Like C_p , the BIC will tend to take on a small value for a model with a low test error, and so generally we select the model that has the lowest BIC value. Notice that BIC replaces the $2d\hat{\sigma}^2$ used by C_p with a $\log(n)d\hat{\sigma}^2$ term, where n is the number of observations. Since $\log n > 2$ for any $n > 7$,

⁵There are two formulas for AIC for least squares regression. The formula that we provide here requires an expression for σ^2 , which we obtain using the full model containing all predictors. The second formula is appropriate when σ^2 is unknown and we do not want to explicitly estimate it; that formula has a $\log(\text{RSS})$ term instead of an RSS term. Detailed derivations of these two formulas are outside of the scope of this book.

the BIC statistic generally places a heavier penalty on models with many variables, and hence results in the selection of smaller models than C_p . In Figure 6.2, we see that this is indeed the case for the `Credit` data set; BIC chooses a model that contains only the four predictors `income`, `limit`, `cards`, and `student`. In this case the curves are very flat and so there does not appear to be much difference in accuracy between the four-variable and six-variable models.

The adjusted R^2 statistic is another popular approach for selecting among a set of models that contain different numbers of variables. Recall from Chapter 3 that the usual R^2 is defined as $1 - \text{RSS}/\text{TSS}$, where $\text{TSS} = \sum(y_i - \bar{y})^2$ is the *total sum of squares* for the response. Since RSS always decreases as more variables are added to the model, the R^2 always increases as more variables are added. For a least squares model with d variables, the adjusted R^2 statistic is calculated as

$$\text{Adjusted } R^2 = 1 - \frac{\text{RSS}/(n - d - 1)}{\text{TSS}/(n - 1)}. \quad (6.4)$$

Unlike C_p , AIC, and BIC, for which a *small* value indicates a model with a low test error, a *large* value of adjusted R^2 indicates a model with a small test error. Maximizing the adjusted R^2 is equivalent to minimizing $\frac{\text{RSS}}{n-d-1}$. While RSS always decreases as the number of variables in the model increases, $\frac{\text{RSS}}{n-d-1}$ may increase or decrease, due to the presence of d in the denominator.

The intuition behind the adjusted R^2 is that once all of the correct variables have been included in the model, adding additional *noise* variables will lead to only a very small decrease in RSS. Since adding noise variables leads to an increase in d , such variables will lead to an increase in $\frac{\text{RSS}}{n-d-1}$, and consequently a decrease in the adjusted R^2 . Therefore, in theory, the model with the largest adjusted R^2 will have only correct variables and no noise variables. Unlike the R^2 statistic, the adjusted R^2 statistic *pays a price* for the inclusion of unnecessary variables in the model. Figure 6.2 displays the adjusted R^2 for the `Credit` data set. Using this statistic results in the selection of a model that contains seven variables, adding `own` to the model selected by C_p and AIC.

C_p , AIC, and BIC all have rigorous theoretical justifications that are beyond the scope of this book. These justifications rely on asymptotic arguments (scenarios where the sample size n is very large). Despite its popularity, and even though it is quite intuitive, the adjusted R^2 is not as well motivated in statistical theory as AIC, BIC, and C_p . All of these measures are simple to use and compute. Here we have presented their formulas in the case of a linear model fit using least squares; however, AIC and BIC can also be defined for more general types of models.

Validation and Cross-Validation

As an alternative to the approaches just discussed, we can directly estimate the test error using the validation set and cross-validation methods discussed in Chapter 5. We can compute the validation set error or the cross-validation error for each model under consideration, and then select

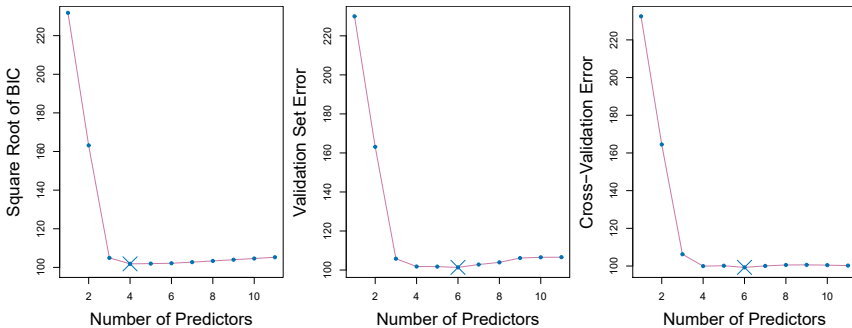


FIGURE 6.3. For the `Credit` data set, three quantities are displayed for the best model containing d predictors, for d ranging from 1 to 11. The overall best model, based on each of these quantities, is shown as a blue cross. Left: Square root of BIC. Center: Validation set errors. Right: Cross-validation errors.

the model for which the resulting estimated test error is smallest. This procedure has an advantage relative to AIC, BIC, C_p , and adjusted R^2 , in that it provides a direct estimate of the test error, and makes fewer assumptions about the true underlying model. It can also be used in a wider range of model selection tasks, even in cases where it is hard to pinpoint the model degrees of freedom (e.g. the number of predictors in the model) or hard to estimate the error variance σ^2 . Note that when cross-validation is used, the sequence of models \mathcal{M}_k in Algorithms 6.1–6.3 is determined separately for each training fold, and the validation errors are averaged over all folds for each model size k . This means, for example with best-subset regression, that \mathcal{M}_k , the best subset of size k , can differ across the folds. Once the best size k is chosen, we find the best model of that size on the full data set.

In the past, performing cross-validation was computationally prohibitive for many problems with large p and/or large n , and so AIC, BIC, C_p , and adjusted R^2 were more attractive approaches for choosing among a set of models. However, nowadays with fast computers, the computations required to perform cross-validation are hardly ever an issue. Thus, cross-validation is a very attractive approach for selecting from among a number of models under consideration.

Figure 6.3 displays, as a function of d , the BIC, validation set errors, and cross-validation errors on the `Credit` data, for the best d -variable model. The validation errors were calculated by randomly selecting three-quarters of the observations as the training set, and the remainder as the validation set. The cross-validation errors were computed using $k = 10$ folds. In this case, the validation and cross-validation methods both result in a six-variable model. However, all three approaches suggest that the four-, five-, and six-variable models are roughly equivalent in terms of their test errors.

In fact, the estimated test error curves displayed in the center and right-hand panels of Figure 6.3 are quite flat. While a three-variable model clearly has lower estimated test error than a two-variable model, the estimated test errors of the 3- to 11-variable models are quite similar. Furthermore, if we

repeated the validation set approach using a different split of the data into a training set and a validation set, or if we repeated cross-validation using a different set of cross-validation folds, then the precise model with the lowest estimated test error would surely change. In this setting, we can select a model using the *one-standard-error rule*. We first calculate the standard error of the estimated test MSE for each model size, and then select the smallest model for which the estimated test error is within one standard error of the lowest point on the curve. The rationale here is that if a set of models appear to be more or less equally good, then we might as well choose the simplest model—that is, the model with the smallest number of predictors. In this case, applying the one-standard-error rule to the validation set or cross-validation approach leads to selection of the three-variable model.

one-
standard-
error
rule

6.2 Shrinkage Methods

The subset selection methods described in Section 6.1 involve using least squares to fit a linear model that contains a subset of the predictors. As an alternative, we can fit a model containing all p predictors using a technique that *constrains* or *regularizes* the coefficient estimates, or equivalently, that *shrinks* the coefficient estimates towards zero. It may not be immediately obvious why such a constraint should improve the fit, but it turns out that shrinking the coefficient estimates can significantly reduce their variance. The two best-known techniques for shrinking the regression coefficients towards zero are *ridge regression* and the *lasso*.

6.2.1 Ridge Regression

Recall from Chapter 3 that the least squares fitting procedure estimates $\beta_0, \beta_1, \dots, \beta_p$ using the values that minimize

$$\text{RSS} = \sum_{i=1}^n \left(y_i - \beta_0 - \sum_{j=1}^p \beta_j x_{ij} \right)^2.$$

Ridge regression is very similar to least squares, except that the coefficients are estimated by minimizing a slightly different quantity. In particular, the ridge regression coefficient estimates $\hat{\beta}^R$ are the values that minimize

$$\sum_{i=1}^n \left(y_i - \beta_0 - \sum_{j=1}^p \beta_j x_{ij} \right)^2 + \lambda \sum_{j=1}^p \beta_j^2 = \text{RSS} + \lambda \sum_{j=1}^p \beta_j^2, \quad (6.5)$$

where $\lambda \geq 0$ is a *tuning parameter*, to be determined separately. Equation 6.5 trades off two different criteria. As with least squares, ridge regression seeks coefficient estimates that fit the data well, by making the RSS small. However, the second term, $\lambda \sum_j \beta_j^2$, called a *shrinkage penalty*, is small when β_1, \dots, β_p are close to zero, and so it has the effect of *shrinking* the estimates of β_j towards zero. The tuning parameter λ serves to control

ridge
regression

tuning
parameter

shrinkage
penalty

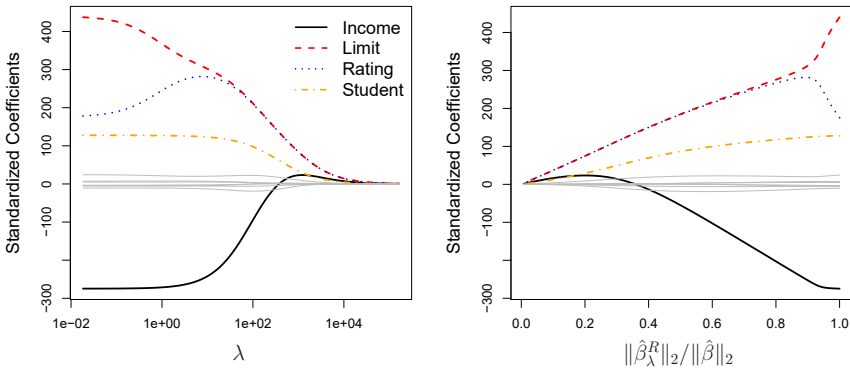


FIGURE 6.4. The standardized ridge regression coefficients are displayed for the `Credit` data set, as a function of λ and $\|\hat{\beta}_\lambda^R\|_2/\|\hat{\beta}\|_2$.

the relative impact of these two terms on the regression coefficient estimates. When $\lambda = 0$, the penalty term has no effect, and ridge regression will produce the least squares estimates. However, as $\lambda \rightarrow \infty$, the impact of the shrinkage penalty grows, and the ridge regression coefficient estimates will approach zero. Unlike least squares, which generates only one set of coefficient estimates, ridge regression will produce a different set of coefficient estimates, $\hat{\beta}_\lambda^R$, for each value of λ . Selecting a good value for λ is critical; we defer this discussion to Section 6.2.3, where we use cross-validation.

Note that in (6.5), the shrinkage penalty is applied to β_1, \dots, β_p , but not to the intercept β_0 . We want to shrink the estimated association of each variable with the response; however, we do not want to shrink the intercept, which is simply a measure of the mean value of the response when $x_{i1} = x_{i2} = \dots = x_{ip} = 0$. If we assume that the variables—that is, the columns of the data matrix \mathbf{X} —have been centered to have mean zero before ridge regression is performed, then the estimated intercept will take the form $\hat{\beta}_0 = \bar{y} = \sum_{i=1}^n y_i/n$.

An Application to the Credit Data

In Figure 6.4, the ridge regression coefficient estimates for the `Credit` data set are displayed. In the left-hand panel, each curve corresponds to the ridge regression coefficient estimate for one of the ten variables, plotted as a function of λ . For example, the black solid line represents the ridge regression estimate for the `income` coefficient, as λ is varied. At the extreme left-hand side of the plot, λ is essentially zero, and so the corresponding ridge coefficient estimates are the same as the usual least squares estimates. But as λ increases, the ridge coefficient estimates shrink towards zero. When λ is extremely large, then all of the ridge coefficient estimates are basically zero; this corresponds to the *null model* that contains no predictors. In this plot, the `income`, `limit`, `rating`, and `student` variables are displayed in distinct colors, since these variables tend to have by far the largest coefficient estimates. While the ridge coefficient estimates tend to decrease in aggregate as λ increases, individual coefficients, such as `rating` and `income`, may occasionally increase as λ increases.

The right-hand panel of Figure 6.4 displays the same ridge coefficient estimates as the left-hand panel, but instead of displaying λ on the x -axis, we now display $\|\hat{\beta}_\lambda^R\|_2/\|\hat{\beta}\|_2$, where $\hat{\beta}$ denotes the vector of least squares coefficient estimates. The notation $\|\beta\|_2$ denotes the ℓ_2 norm (pronounced “ell 2”) of a vector, and is defined as $\|\beta\|_2 = \sqrt{\sum_{j=1}^p \beta_j^2}$. It measures the distance of β from zero. As λ increases, the ℓ_2 norm of $\hat{\beta}_\lambda^R$ will *always* decrease, and so will $\|\hat{\beta}_\lambda^R\|_2/\|\hat{\beta}\|_2$. The latter quantity ranges from 1 (when $\lambda = 0$, in which case the ridge regression coefficient estimate is the same as the least squares estimate, and so their ℓ_2 norms are the same) to 0 (when $\lambda = \infty$, in which case the ridge regression coefficient estimate is a vector of zeros, with ℓ_2 norm equal to zero). Therefore, we can think of the x -axis in the right-hand panel of Figure 6.4 as the amount that the ridge regression coefficient estimates have been shrunk towards zero; a small value indicates that they have been shrunk very close to zero.

The standard least squares coefficient estimates discussed in Chapter 3 are *scale equivariant*: multiplying X_j by a constant c simply leads to a scaling of the least squares coefficient estimates by a factor of $1/c$. In other words, regardless of how the j th predictor is scaled, $X_j \hat{\beta}_j$ will remain the same. In contrast, the ridge regression coefficient estimates can change *substantially* when multiplying a given predictor by a constant. For instance, consider the `income` variable, which is measured in dollars. One could reasonably have measured income in thousands of dollars, which would result in a reduction in the observed values of `income` by a factor of 1,000. Now due to the sum of squared coefficients term in the ridge regression formulation (6.5), such a change in scale will not simply cause the ridge regression coefficient estimate for `income` to change by a factor of 1,000. In other words, $X_j \hat{\beta}_{j,\lambda}^R$ will depend not only on the value of λ , but also on the scaling of the j th predictor. In fact, the value of $X_j \hat{\beta}_{j,\lambda}^R$ may even depend on the scaling of the *other* predictors! Therefore, it is best to apply ridge regression after *standardizing the predictors*, using the formula

$$\tilde{x}_{ij} = \frac{x_{ij}}{\sqrt{\frac{1}{n} \sum_{i=1}^n (x_{ij} - \bar{x}_j)^2}}, \quad (6.6)$$

so that they are all on the same scale. In (6.6), the denominator is the estimated standard deviation of the j th predictor. Consequently, all of the standardized predictors will have a standard deviation of one. As a result the final fit will not depend on the scale on which the predictors are measured. In Figure 6.4, the y -axis displays the standardized ridge regression coefficient estimates—that is, the coefficient estimates that result from performing ridge regression using standardized predictors.

Why Does Ridge Regression Improve Over Least Squares?

Ridge regression’s advantage over least squares is rooted in the *bias-variance trade-off*. As λ increases, the flexibility of the ridge regression fit decreases, leading to decreased variance but increased bias. This is illustrated in the left-hand panel of Figure 6.5, using a simulated data set containing $p = 45$ predictors and $n = 50$ observations. The green curve in the left-hand panel

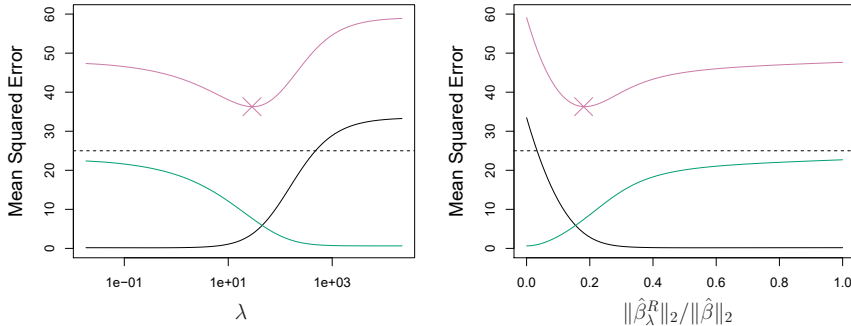


FIGURE 6.5. Squared bias (black), variance (green), and test mean squared error (purple) for the ridge regression predictions on a simulated data set, as a function of λ and $\|\hat{\beta}_\lambda^R\|_2 / \|\hat{\beta}\|_2$. The horizontal dashed lines indicate the minimum possible MSE. The purple crosses indicate the ridge regression models for which the MSE is smallest.

of Figure 6.5 displays the variance of the ridge regression predictions as a function of λ . At the least squares coefficient estimates, which correspond to ridge regression with $\lambda = 0$, the variance is high but there is no bias. But as λ increases, the shrinkage of the ridge coefficient estimates leads to a substantial reduction in the variance of the predictions, at the expense of a slight increase in bias. Recall that the test mean squared error (MSE), plotted in purple, is closely related to the variance plus the squared bias. For values of λ up to about 10, the variance decreases rapidly, with very little increase in bias, plotted in black. Consequently, the MSE drops considerably as λ increases from 0 to 10. Beyond this point, the decrease in variance due to increasing λ slows, and the shrinkage on the coefficients causes them to be significantly underestimated, resulting in a large increase in the bias. The minimum MSE is achieved at approximately $\lambda = 30$. Interestingly, because of its high variance, the MSE associated with the least squares fit, when $\lambda = 0$, is almost as high as that of the null model for which all coefficient estimates are zero, when $\lambda = \infty$. However, for an intermediate value of λ , the MSE is considerably lower.

The right-hand panel of Figure 6.5 displays the same curves as the left-hand panel, this time plotted against the ℓ_2 norm of the ridge regression coefficient estimates divided by the ℓ_2 norm of the least squares estimates. Now as we move from left to right, the fits become more flexible, and so the bias decreases and the variance increases.

In general, in situations where the relationship between the response and the predictors is close to linear, the least squares estimates will have low bias but may have high variance. This means that a small change in the training data can cause a large change in the least squares coefficient estimates. In particular, when the number of variables p is almost as large as the number of observations n , as in the example in Figure 6.5, the least squares estimates will be extremely variable. And if $p > n$, then the least squares estimates do not even have a unique solution, whereas ridge regression can still perform well by trading off a small increase in bias for a

large decrease in variance. Hence, ridge regression works best in situations where the least squares estimates have high variance.

Ridge regression also has substantial computational advantages over best subset selection, which requires searching through 2^p models. As we discussed previously, even for moderate values of p , such a search can be computationally infeasible. In contrast, for any fixed value of λ , ridge regression only fits a single model, and the model-fitting procedure can be performed quite quickly. In fact, one can show that the computations required to solve (6.5), *simultaneously for all values of λ* , are almost identical to those for fitting a model using least squares.

6.2.2 The Lasso

Ridge regression does have one obvious disadvantage. Unlike best subset, forward stepwise, and backward stepwise selection, which will generally select models that involve just a subset of the variables, ridge regression will include all p predictors in the final model. The penalty $\lambda \sum \beta_j^2$ in (6.5) will shrink all of the coefficients towards zero, but it will not set any of them exactly to zero (unless $\lambda = \infty$). This may not be a problem for prediction accuracy, but it can create a challenge in model interpretation in settings in which the number of variables p is quite large. For example, in the `Credit` data set, it appears that the most important variables are `income`, `limit`, `rating`, and `student`. So we might wish to build a model including just these predictors. However, ridge regression will always generate a model involving all ten predictors. Increasing the value of λ will tend to reduce the magnitudes of the coefficients, but will not result in exclusion of any of the variables.

The *lasso* is a relatively recent alternative to ridge regression that overcomes this disadvantage. The lasso coefficients, $\hat{\beta}_\lambda^L$, minimize the quantity

$$\sum_{i=1}^n \left(y_i - \beta_0 - \sum_{j=1}^p \beta_j x_{ij} \right)^2 + \lambda \sum_{j=1}^p |\beta_j| = \text{RSS} + \lambda \sum_{j=1}^p |\beta_j|. \quad (6.7)$$

Comparing (6.7) to (6.5), we see that the lasso and ridge regression have similar formulations. The only difference is that the β_j^2 term in the ridge regression penalty (6.5) has been replaced by $|\beta_j|$ in the lasso penalty (6.7). In statistical parlance, the lasso uses an ℓ_1 (pronounced “ell 1”) penalty instead of an ℓ_2 penalty. The ℓ_1 norm of a coefficient vector β is given by $\|\beta\|_1 = \sum |\beta_j|$.

As with ridge regression, the lasso shrinks the coefficient estimates towards zero. However, in the case of the lasso, the ℓ_1 penalty has the effect of forcing some of the coefficient estimates to be exactly equal to zero when the tuning parameter λ is sufficiently large. Hence, much like best subset selection, the lasso performs *variable selection*. As a result, models generated from the lasso are generally much easier to interpret than those produced by ridge regression. We say that the lasso yields *sparse* models—that is, models that involve only a subset of the variables. As in ridge regression, selecting a good value of λ for the lasso is critical; we defer this discussion to Section 6.2.3, where we use cross-validation.

lasso

sparse

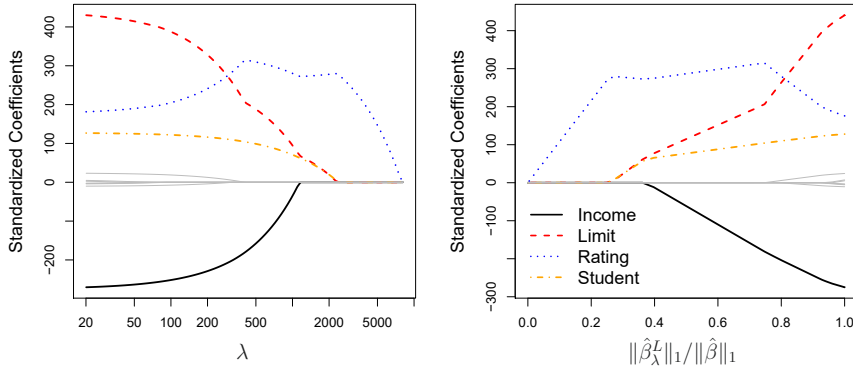


FIGURE 6.6. The standardized lasso coefficients on the `Credit` data set are shown as a function of λ and $\|\hat{\beta}_\lambda^L\|_1 / \|\hat{\beta}\|_1$.

As an example, consider the coefficient plots in Figure 6.6, which are generated from applying the lasso to the `Credit` data set. When $\lambda = 0$, then the lasso simply gives the least squares fit, and when λ becomes sufficiently large, the lasso gives the null model in which all coefficient estimates equal zero. However, in between these two extremes, the ridge regression and lasso models are quite different from each other. Moving from left to right in the right-hand panel of Figure 6.6, we observe that at first the lasso results in a model that contains only the `rating` predictor. Then `student` and `limit` enter the model almost simultaneously, shortly followed by `income`. Eventually, the remaining variables enter the model. Hence, depending on the value of λ , the lasso can produce a model involving any number of variables. In contrast, ridge regression will always include all of the variables in the model, although the magnitude of the coefficient estimates will depend on λ .

Another Formulation for Ridge Regression and the Lasso

One can show that the lasso and ridge regression coefficient estimates solve the problems

$$\underset{\beta}{\text{minimize}} \left\{ \sum_{i=1}^n \left(y_i - \beta_0 - \sum_{j=1}^p \beta_j x_{ij} \right)^2 \right\} \quad \text{subject to} \quad \sum_{j=1}^p |\beta_j| \leq s \quad (6.8)$$

and

$$\underset{\beta}{\text{minimize}} \left\{ \sum_{i=1}^n \left(y_i - \beta_0 - \sum_{j=1}^p \beta_j x_{ij} \right)^2 \right\} \quad \text{subject to} \quad \sum_{j=1}^p \beta_j^2 \leq s, \quad (6.9)$$

respectively. In other words, for every value of λ , there is some s such that the Equations (6.7) and (6.8) will give the same lasso coefficient estimates. Similarly, for every value of λ there is a corresponding s such that Equations (6.5) and (6.9) will give the same ridge regression coefficient estimates.

When $p = 2$, then (6.8) indicates that the lasso coefficient estimates have the smallest RSS out of all points that lie within the diamond defined by $|\beta_1| + |\beta_2| \leq s$. Similarly, the ridge regression estimates have the smallest RSS out of all points that lie within the circle defined by $\beta_1^2 + \beta_2^2 \leq s$.

We can think of (6.8) as follows. When we perform the lasso we are trying to find the set of coefficient estimates that lead to the smallest RSS, subject to the constraint that there is a *budget* s for how large $\sum_{j=1}^p |\beta_j|$ can be. When s is extremely large, then this budget is not very restrictive, and so the coefficient estimates can be large. In fact, if s is large enough that the least squares solution falls within the budget, then (6.8) will simply yield the least squares solution. In contrast, if s is small, then $\sum_{j=1}^p |\beta_j|$ must be small in order to avoid violating the budget. Similarly, (6.9) indicates that when we perform ridge regression, we seek a set of coefficient estimates such that the RSS is as small as possible, subject to the requirement that $\sum_{j=1}^p \beta_j^2$ not exceed the budget s .

The formulations (6.8) and (6.9) reveal a close connection between the lasso, ridge regression, and best subset selection. Consider the problem

$$\underset{\beta}{\text{minimize}} \left\{ \sum_{i=1}^n \left(y_i - \beta_0 - \sum_{j=1}^p \beta_j x_{ij} \right)^2 \right\} \quad \text{subject to} \quad \sum_{j=1}^p I(\beta_j \neq 0) \leq s. \quad (6.10)$$

Here $I(\beta_j \neq 0)$ is an indicator variable: it takes on a value of 1 if $\beta_j \neq 0$, and equals zero otherwise. Then (6.10) amounts to finding a set of coefficient estimates such that RSS is as small as possible, subject to the constraint that no more than s coefficients can be nonzero. The problem (6.10) is equivalent to best subset selection. Unfortunately, solving (6.10) is computationally infeasible when p is large, since it requires considering all $\binom{p}{s}$ models containing s predictors. Therefore, we can interpret ridge regression and the lasso as computationally feasible alternatives to best subset selection that replace the intractable form of the budget in (6.10) with forms that are much easier to solve. Of course, the lasso is much more closely related to best subset selection, since the lasso performs feature selection for s sufficiently small in (6.8), while ridge regression does not.

The Variable Selection Property of the Lasso

Why is it that the lasso, unlike ridge regression, results in coefficient estimates that are exactly equal to zero? The formulations (6.8) and (6.9) can be used to shed light on the issue. Figure 6.7 illustrates the situation. The least squares solution is marked as $\hat{\beta}$, while the blue diamond and circle represent the lasso and ridge regression constraints in (6.8) and (6.9), respectively. If s is sufficiently large, then the constraint regions will contain $\hat{\beta}$, and so the ridge regression and lasso estimates will be the same as the least squares estimates. (Such a large value of s corresponds to $\lambda = 0$ in (6.5) and (6.7).) However, in Figure 6.7 the least squares estimates lie outside of the diamond and the circle, and so the least squares estimates are not the same as the lasso and ridge regression estimates.

Each of the ellipses centered around $\hat{\beta}$ represents a *contour*: this means that all of the points on a particular ellipse have the same RSS value. As

contour

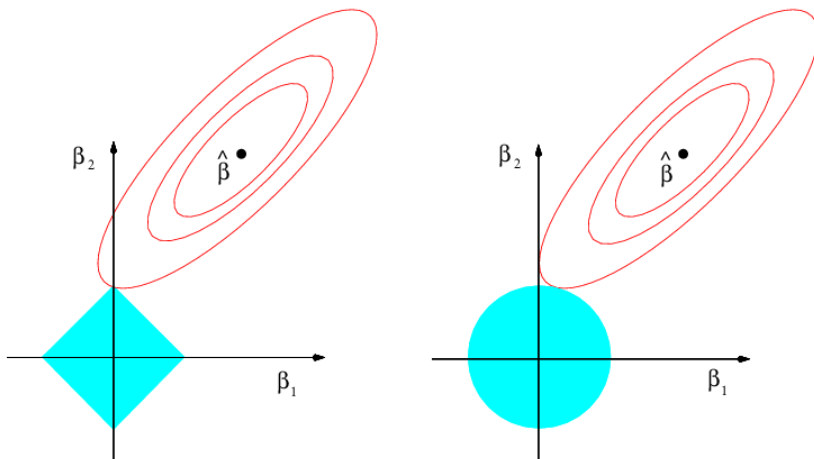


FIGURE 6.7. Contours of the error and constraint functions for the lasso (left) and ridge regression (right). The solid blue areas are the constraint regions, $|\beta_1| + |\beta_2| \leq s$ and $\beta_1^2 + \beta_2^2 \leq s$, while the red ellipses are the contours of the RSS.

the ellipses expand away from the least squares coefficient estimates, the RSS increases. Equations (6.8) and (6.9) indicate that the lasso and ridge regression coefficient estimates are given by the first point at which an ellipse contacts the constraint region. Since ridge regression has a circular constraint with no sharp points, this intersection will not generally occur on an axis, and so the ridge regression coefficient estimates will be exclusively non-zero. However, the lasso constraint has *corners* at each of the axes, and so the ellipse will often intersect the constraint region at an axis. When this occurs, one of the coefficients will equal zero. In higher dimensions, many of the coefficient estimates may equal zero simultaneously. In Figure 6.7, the intersection occurs at $\beta_1 = 0$, and so the resulting model will only include β_2 .

In Figure 6.7, we considered the simple case of $p = 2$. When $p = 3$, then the constraint region for ridge regression becomes a sphere, and the constraint region for the lasso becomes a polyhedron. When $p > 3$, the constraint for ridge regression becomes a hypersphere, and the constraint for the lasso becomes a polytope. However, the key ideas depicted in Figure 6.7 still hold. In particular, the lasso leads to feature selection when $p > 2$ due to the sharp corners of the polyhedron or polytope.

Comparing the Lasso and Ridge Regression

It is clear that the lasso has a major advantage over ridge regression, in that it produces simpler and more interpretable models that involve only a subset of the predictors. However, which method leads to better prediction accuracy? Figure 6.8 displays the variance, squared bias, and test MSE of the lasso applied to the same simulated data as in Figure 6.5. Clearly the lasso leads to qualitatively similar behavior to ridge regression, in that as λ increases, the variance decreases and the bias increases. In the right-hand

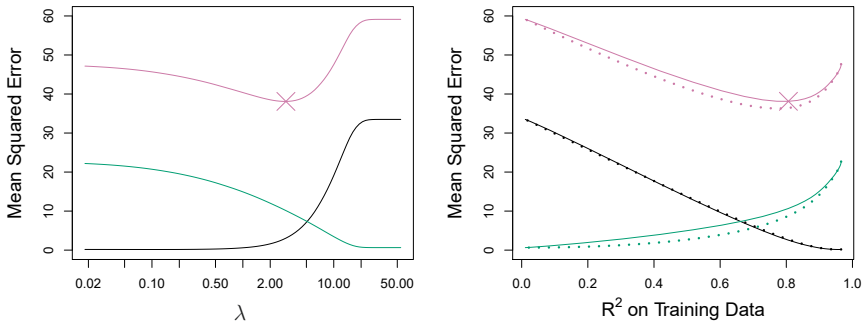


FIGURE 6.8. Left: Plots of squared bias (black), variance (green), and test MSE (purple) for the lasso on a simulated data set. Right: Comparison of squared bias, variance, and test MSE between lasso (solid) and ridge (dotted). Both are plotted against their R^2 on the training data, as a common form of indexing. The crosses in both plots indicate the lasso model for which the MSE is smallest.

panel of Figure 6.8, the dotted lines represent the ridge regression fits. Here we plot both against their R^2 on the training data. This is another useful way to index models, and can be used to compare models with different types of regularization, as is the case here. In this example, the lasso and ridge regression result in almost identical biases. However, the variance of ridge regression is slightly lower than the variance of the lasso. Consequently, the minimum MSE of ridge regression is slightly smaller than that of the lasso.

However, the data in Figure 6.8 were generated in such a way that all 45 predictors were related to the response—that is, none of the true coefficients $\beta_1, \dots, \beta_{45}$ equaled zero. The lasso implicitly assumes that a number of the coefficients truly equal zero. Consequently, it is not surprising that ridge regression outperforms the lasso in terms of prediction error in this setting. Figure 6.9 illustrates a similar situation, except that now the response is a function of only 2 out of 45 predictors. Now the lasso tends to outperform ridge regression in terms of bias, variance, and MSE.

These two examples illustrate that neither ridge regression nor the lasso will universally dominate the other. In general, one might expect the lasso to perform better in a setting where a relatively small number of predictors have substantial coefficients, and the remaining predictors have coefficients that are very small or that equal zero. Ridge regression will perform better when the response is a function of many predictors, all with coefficients of roughly equal size. However, the number of predictors that is related to the response is never known *a priori* for real data sets. A technique such as cross-validation can be used in order to determine which approach is better on a particular data set.

As with ridge regression, when the least squares estimates have excessively high variance, the lasso solution can yield a reduction in variance at the expense of a small increase in bias, and consequently can generate more accurate predictions. Unlike ridge regression, the lasso performs variable selection, and hence results in models that are easier to interpret.

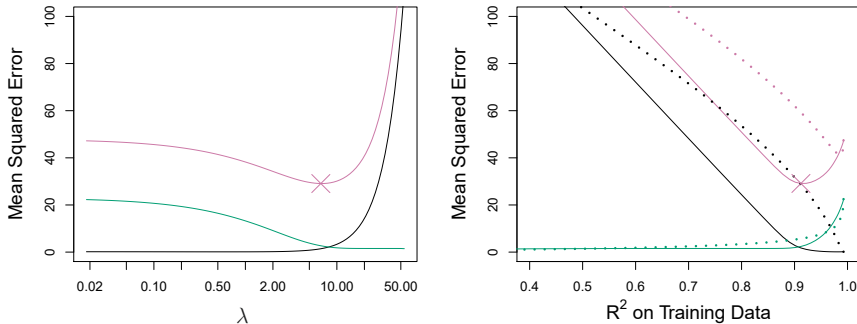


FIGURE 6.9. Left: Plots of squared bias (black), variance (green), and test MSE (purple) for the lasso. The simulated data is similar to that in Figure 6.8, except that now only two predictors are related to the response. Right: Comparison of squared bias, variance, and test MSE between lasso (solid) and ridge (dotted). Both are plotted against their R^2 on the training data, as a common form of indexing. The crosses in both plots indicate the lasso model for which the MSE is smallest.

There are very efficient algorithms for fitting both ridge and lasso models; in both cases the entire coefficient paths can be computed with about the same amount of work as a single least squares fit. We will explore this further in the lab at the end of this chapter.

A Simple Special Case for Ridge Regression and the Lasso

In order to obtain a better intuition about the behavior of ridge regression and the lasso, consider a simple special case with $n = p$, and \mathbf{X} a diagonal matrix with 1's on the diagonal and 0's in all off-diagonal elements. To simplify the problem further, assume also that we are performing regression without an intercept. With these assumptions, the usual least squares problem simplifies to finding β_1, \dots, β_p that minimize

$$\sum_{j=1}^p (y_j - \beta_j)^2. \quad (6.11)$$

In this case, the least squares solution is given by

$$\hat{\beta}_j = y_j.$$

And in this setting, ridge regression amounts to finding β_1, \dots, β_p such that

$$\sum_{j=1}^p (y_j - \beta_j)^2 + \lambda \sum_{j=1}^p \beta_j^2 \quad (6.12)$$

is minimized, and the lasso amounts to finding the coefficients such that

$$\sum_{j=1}^p (y_j - \beta_j)^2 + \lambda \sum_{j=1}^p |\beta_j| \quad (6.13)$$

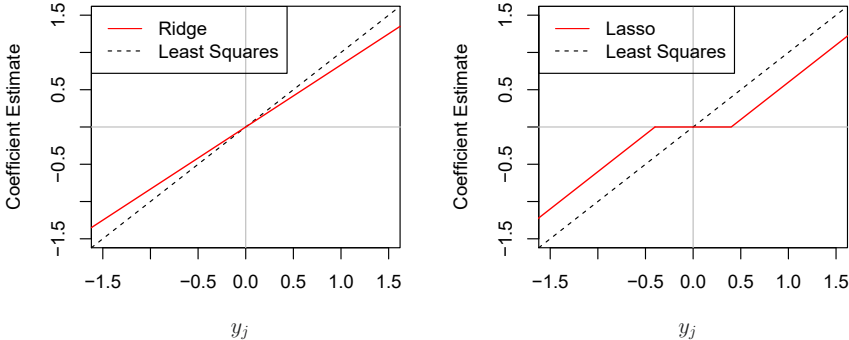


FIGURE 6.10. The ridge regression and lasso coefficient estimates for a simple setting with $n = p$ and \mathbf{X} a diagonal matrix with 1's on the diagonal. Left: The ridge regression coefficient estimates are shrunken proportionally towards zero, relative to the least squares estimates. Right: The lasso coefficient estimates are soft-thresholded towards zero.

is minimized. One can show that in this setting, the ridge regression estimates take the form

$$\hat{\beta}_j^R = y_j / (1 + \lambda), \quad (6.14)$$

and the lasso estimates take the form

$$\hat{\beta}_j^L = \begin{cases} y_j - \lambda/2 & \text{if } y_j > \lambda/2; \\ y_j + \lambda/2 & \text{if } y_j < -\lambda/2; \\ 0 & \text{if } |y_j| \leq \lambda/2. \end{cases} \quad (6.15)$$

Figure 6.10 displays the situation. We can see that ridge regression and the lasso perform two very different types of shrinkage. In ridge regression, each least squares coefficient estimate is shrunken by the same proportion. In contrast, the lasso shrinks each least squares coefficient towards zero by a constant amount, $\lambda/2$; the least squares coefficients that are less than $\lambda/2$ in absolute value are shrunk entirely to zero. The type of shrinkage performed by the lasso in this simple setting (6.15) is known as *soft-thresholding*. The fact that some lasso coefficients are shrunk entirely to zero explains why the lasso performs feature selection.

soft-thresholding

In the case of a more general data matrix \mathbf{X} , the story is a little more complicated than what is depicted in Figure 6.10, but the main ideas still hold approximately: ridge regression more or less shrinks every dimension of the data by the same proportion, whereas the lasso more or less shrinks all coefficients toward zero by a similar amount, and sufficiently small coefficients are shrunk all the way to zero.

Bayesian Interpretation of Ridge Regression and the Lasso



We now show that one can view ridge regression and the lasso through a Bayesian lens. A Bayesian viewpoint for regression assumes that the coefficient vector β has some *prior* distribution, say $p(\beta)$, where $\beta = (\beta_0, \beta_1, \dots, \beta_p)^T$. The likelihood of the data can be written as $f(Y|X, \beta)$,

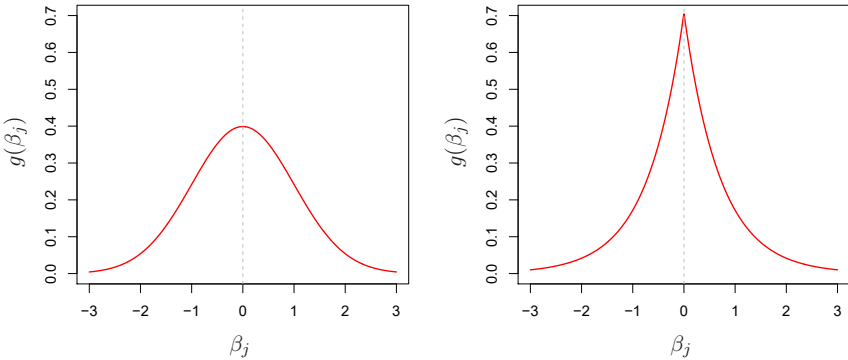


FIGURE 6.11. Left: Ridge regression is the posterior mode for β under a Gaussian prior. Right: The lasso is the posterior mode for β under a double-exponential prior.

where $X = (X_1, \dots, X_p)$. Multiplying the prior distribution by the likelihood gives us (up to a proportionality constant) the *posterior distribution*, which takes the form

$$p(\beta|X, Y) \propto f(Y|X, \beta)p(\beta|X) = f(Y|X, \beta)p(\beta),$$

where the proportionality above follows from Bayes' theorem, and the equality above follows from the assumption that X is fixed.

We assume the usual linear model,

$$Y = \beta_0 + X_1\beta_1 + \dots + X_p\beta_p + \epsilon,$$

and suppose that the errors are independent and drawn from a normal distribution. Furthermore, assume that $p(\beta) = \prod_{j=1}^p g(\beta_j)$, for some density function g . It turns out that ridge regression and the lasso follow naturally from two special cases of g :

- If g is a Gaussian distribution with mean zero and standard deviation a function of λ , then it follows that the *posterior mode* for β —that is, the most likely value for β , given the data—is given by the ridge regression solution. (In fact, the ridge regression solution is also the posterior mean.)
- If g is a double-exponential (Laplace) distribution with mean zero and scale parameter a function of λ , then it follows that the posterior mode for β is the lasso solution. (However, the lasso solution is *not* the posterior mean, and in fact, the posterior mean does not yield a sparse coefficient vector.)

posterior distribution

posterior mode

The Gaussian and double-exponential priors are displayed in Figure 6.11. Therefore, from a Bayesian viewpoint, ridge regression and the lasso follow directly from assuming the usual linear model with normal errors, together with a simple prior distribution for β . Notice that the lasso prior is steeply peaked at zero, while the Gaussian is flatter and fatter at zero. Hence, the lasso expects a priori that many of the coefficients are (exactly) zero, while ridge assumes the coefficients are randomly distributed about zero.

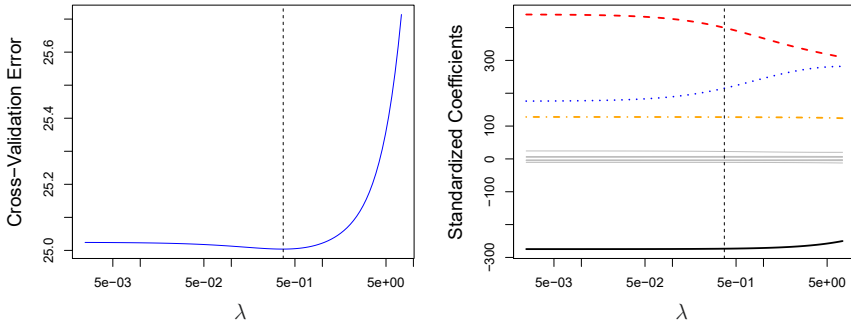


FIGURE 6.12. Left: Cross-validation errors that result from applying ridge regression to the `Credit` data set with various values of λ . Right: The coefficient estimates as a function of λ . The vertical dashed lines indicate the value of λ selected by cross-validation.

6.2.3 Selecting the Tuning Parameter

Just as the subset selection approaches considered in Section 6.1 require a method to determine which of the models under consideration is best, implementing ridge regression and the lasso requires a method for selecting a value for the tuning parameter λ in (6.5) and (6.7), or equivalently, the value of the constraint s in (6.9) and (6.8). Cross-validation provides a simple way to tackle this problem. We choose a grid of λ values, and compute the cross-validation error for each value of λ , as described in Chapter 5. We then select the tuning parameter value for which the cross-validation error is smallest. Finally, the model is re-fit using all of the available observations and the selected value of the tuning parameter.

Figure 6.12 displays the choice of λ that results from performing leave-one-out cross-validation on the ridge regression fits from the `Credit` data set. The dashed vertical lines indicate the selected value of λ . In this case the value is relatively small, indicating that the optimal fit only involves a small amount of shrinkage relative to the least squares solution. In addition, the dip is not very pronounced, so there is rather a wide range of values that would give a very similar error. In a case like this we might simply use the least squares solution.

Figure 6.13 provides an illustration of ten-fold cross-validation applied to the lasso fits on the sparse simulated data from Figure 6.9. The left-hand panel of Figure 6.13 displays the cross-validation error, while the right-hand panel displays the coefficient estimates. The vertical dashed lines indicate the point at which the cross-validation error is smallest. The two colored lines in the right-hand panel of Figure 6.13 represent the two predictors that are related to the response, while the grey lines represent the unrelated predictors; these are often referred to as *signal* and *noise* variables, respectively. Not only has the lasso correctly given much larger coefficient estimates to the two signal predictors, but also the minimum cross-validation error corresponds to a set of coefficient estimates for which only the signal variables are non-zero. Hence cross-validation together with the lasso has correctly identified the two signal variables in the model, even though this is a challenging setting, with $p = 45$ variables and only $n = 50$

signal

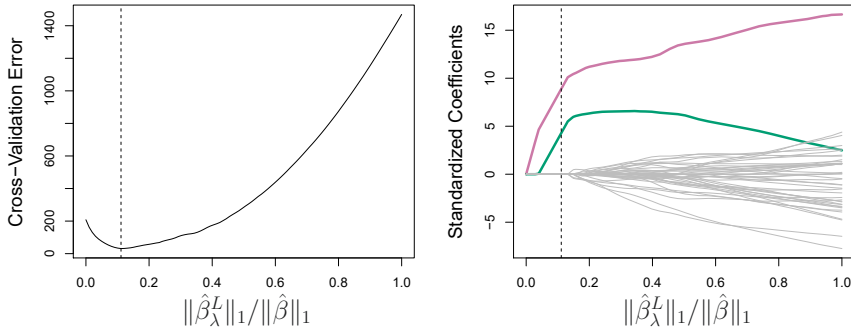


FIGURE 6.13. Left: Ten-fold cross-validation MSE for the lasso, applied to the sparse simulated data set from Figure 6.9. Right: The corresponding lasso coefficient estimates are displayed. The two signal variables are shown in color, and the noise variables are in gray. The vertical dashed lines indicate the lasso fit for which the cross-validation error is smallest.

observations. In contrast, the least squares solution—displayed on the far right of the right-hand panel of Figure 6.13—assigns a large coefficient estimate to only one of the two signal variables.

6.3 Dimension Reduction Methods

The methods that we have discussed so far in this chapter have controlled variance in two different ways, either by using a subset of the original variables, or by shrinking their coefficients toward zero. All of these methods are defined using the original predictors, X_1, X_2, \dots, X_p . We now explore a class of approaches that *transform* the predictors and then fit a least squares model using the transformed variables. We will refer to these techniques as *dimension reduction* methods.

Let Z_1, Z_2, \dots, Z_M represent $M < p$ linear combinations of our original p predictors. That is,

$$Z_m = \sum_{j=1}^p \phi_{jm} X_j \quad (6.16)$$

dimension
reduction
linear
combination

for some constants $\phi_{1m}, \phi_{2m}, \dots, \phi_{pm}$, $m = 1, \dots, M$. We can then fit the linear regression model

$$y_i = \theta_0 + \sum_{m=1}^M \theta_m z_{im} + \epsilon_i, \quad i = 1, \dots, n, \quad (6.17)$$

using least squares. Note that in (6.17), the regression coefficients are given by $\theta_0, \theta_1, \dots, \theta_M$. If the constants $\phi_{1m}, \phi_{2m}, \dots, \phi_{pm}$ are chosen wisely, then such dimension reduction approaches can often outperform least squares regression. In other words, fitting (6.17) using least squares can lead to better results than fitting (6.1) using least squares.

The term *dimension reduction* comes from the fact that this approach reduces the problem of estimating the $p+1$ coefficients $\beta_0, \beta_1, \dots, \beta_p$ to the

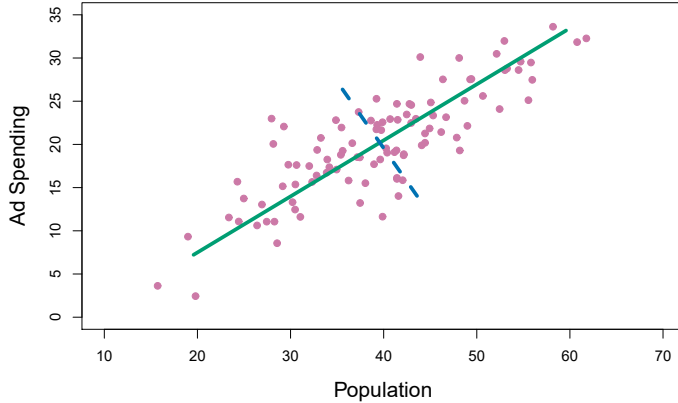


FIGURE 6.14. The population size (pop) and ad spending (ad) for 100 different cities are shown as purple circles. The green solid line indicates the first principal component, and the blue dashed line indicates the second principal component.

simpler problem of estimating the $M + 1$ coefficients $\theta_0, \theta_1, \dots, \theta_M$, where $M < p$. In other words, the dimension of the problem has been reduced from $p + 1$ to $M + 1$.

Notice that from (6.16),

$$\sum_{m=1}^M \theta_m z_{im} = \sum_{m=1}^M \theta_m \sum_{j=1}^p \phi_{jm} x_{ij} = \sum_{j=1}^p \sum_{m=1}^M \theta_m \phi_{jm} x_{ij} = \sum_{j=1}^p \beta_j x_{ij},$$

where

$$\beta_j = \sum_{m=1}^M \theta_m \phi_{jm}. \quad (6.18)$$

Hence (6.17) can be thought of as a special case of the original linear regression model given by (6.1). Dimension reduction serves to constrain the estimated β_j coefficients, since now they must take the form (6.18). This constraint on the form of the coefficients has the potential to bias the coefficient estimates. However, in situations where p is large relative to n , selecting a value of $M \ll p$ can significantly reduce the variance of the fitted coefficients. If $M = p$, and all the Z_m are linearly independent, then (6.18) poses no constraints. In this case, no dimension reduction occurs, and so fitting (6.17) is equivalent to performing least squares on the original p predictors.

All dimension reduction methods work in two steps. First, the transformed predictors Z_1, Z_2, \dots, Z_M are obtained. Second, the model is fit using these M predictors. However, the choice of Z_1, Z_2, \dots, Z_M , or equivalently, the selection of the ϕ_{jm} 's, can be achieved in different ways. In this chapter, we will consider two approaches for this task: *principal components* and *partial least squares*.

6.3.1 Principal Components Regression

Principal components analysis (PCA) is a popular approach for deriving

principal
components
analysis

a low-dimensional set of features from a large set of variables. PCA is discussed in greater detail as a tool for *unsupervised learning* in Chapter 12. Here we describe its use as a dimension reduction technique for regression.

An Overview of Principal Components Analysis

PCA is a technique for reducing the dimension of an $n \times p$ data matrix \mathbf{X} . The *first principal component* direction of the data is that along which the observations *vary the most*. For instance, consider Figure 6.14, which shows population size (`pop`) in tens of thousands of people, and ad spending for a particular company (`ad`) in thousands of dollars, for 100 cities.⁶ The green solid line represents the first principal component direction of the data. We can see by eye that this is the direction along which there is the greatest variability in the data. That is, if we *projected* the 100 observations onto this line (as shown in the left-hand panel of Figure 6.15), then the resulting projected observations would have the largest possible variance; projecting the observations onto any other line would yield projected observations with lower variance. Projecting a point onto a line simply involves finding the location on the line which is closest to the point.

The first principal component is displayed graphically in Figure 6.14, but how can it be summarized mathematically? It is given by the formula

$$Z_1 = 0.839 \times (\text{pop} - \overline{\text{pop}}) + 0.544 \times (\text{ad} - \overline{\text{ad}}). \quad (6.19)$$

Here $\phi_{11} = 0.839$ and $\phi_{21} = 0.544$ are the principal component loadings, which define the direction referred to above. In (6.19), $\overline{\text{pop}}$ indicates the mean of all `pop` values in this data set, and $\overline{\text{ad}}$ indicates the mean of all advertising spending. The idea is that out of every possible *linear combination* of `pop` and `ad` such that $\phi_{11}^2 + \phi_{21}^2 = 1$, this particular linear combination yields the highest variance: i.e. this is the linear combination for which $\text{Var}(\phi_{11} \times (\text{pop} - \overline{\text{pop}}) + \phi_{21} \times (\text{ad} - \overline{\text{ad}}))$ is maximized. It is necessary to consider only linear combinations of the form $\phi_{11}^2 + \phi_{21}^2 = 1$, since otherwise we could increase ϕ_{11} and ϕ_{21} arbitrarily in order to blow up the variance. In (6.19), the two loadings are both positive and have similar size, and so Z_1 is almost an *average* of the two variables.

Since $n = 100$, `pop` and `ad` are vectors of length 100, and so is Z_1 in (6.19). For instance,

$$z_{i1} = 0.839 \times (\text{pop}_i - \overline{\text{pop}}) + 0.544 \times (\text{ad}_i - \overline{\text{ad}}). \quad (6.20)$$

The values of z_{11}, \dots, z_{n1} are known as the *principal component scores*, and can be seen in the right-hand panel of Figure 6.15.

There is also another interpretation of PCA: the first principal component vector defines the line that is *as close as possible* to the data. For instance, in Figure 6.14, the first principal component line minimizes the sum of the squared perpendicular distances between each point and the line. These distances are plotted as dashed line segments in the left-hand

⁶This dataset is distinct from the `Advertising` data discussed in Chapter 3.

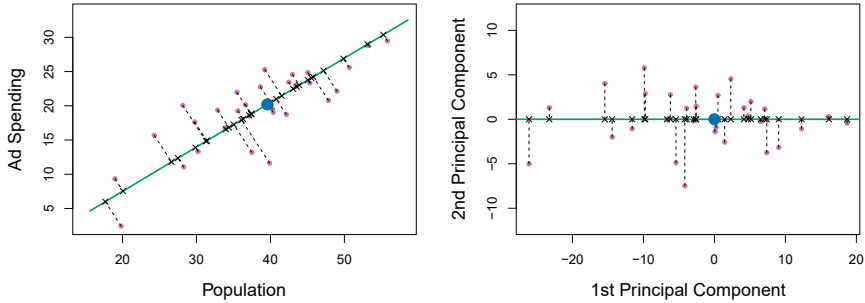


FIGURE 6.15. A subset of the advertising data. The mean `pop` and `ad` budgets are indicated with a blue circle. Left: The first principal component direction is shown in green. It is the dimension along which the data vary the most, and it also defines the line that is closest to all n of the observations. The distances from each observation to the principal component are represented using the black dashed line segments. The blue dot represents $(\bar{\text{pop}}, \bar{\text{ad}})$. Right: The left-hand panel has been rotated so that the first principal component direction coincides with the x -axis.

panel of Figure 6.15, in which the crosses represent the *projection* of each point onto the first principal component line. The first principal component has been chosen so that the projected observations are *as close as possible* to the original observations.

In the right-hand panel of Figure 6.15, the left-hand panel has been rotated so that the first principal component direction coincides with the x -axis. It is possible to show that the *first principal component score* for the i th observation, given in (6.20), is the distance in the x -direction of the i th cross from zero. So for example, the point in the bottom-left corner of the left-hand panel of Figure 6.15 has a large negative principal component score, $z_{i1} = -26.1$, while the point in the top-right corner has a large positive score, $z_{i1} = 18.7$. These scores can be computed directly using (6.20).

We can think of the values of the principal component Z_1 as single-number summaries of the joint `pop` and `ad` budgets for each location. In this example, if $z_{i1} = 0.839 \times (\text{pop}_i - \bar{\text{pop}}) + 0.544 \times (\text{ad}_i - \bar{\text{ad}}) < 0$, then this indicates a city with below-average population size and below-average ad spending. A positive score suggests the opposite. How well can a single number represent both `pop` and `ad`? In this case, Figure 6.14 indicates that `pop` and `ad` have approximately a linear relationship, and so we might expect that a single-number summary will work well. Figure 6.16 displays z_{i1} versus both `pop` and `ad`.⁷ The plots show a strong relationship between the first principal component and the two features. In other words, the first principal component appears to capture most of the information contained in the `pop` and `ad` predictors.

So far we have concentrated on the first principal component. In general, one can construct up to p distinct principal components. The second

⁷The principal components were calculated after first standardizing both `pop` and `ad`, a common approach. Hence, the x -axes on Figures 6.15 and 6.16 are not on the same scale.

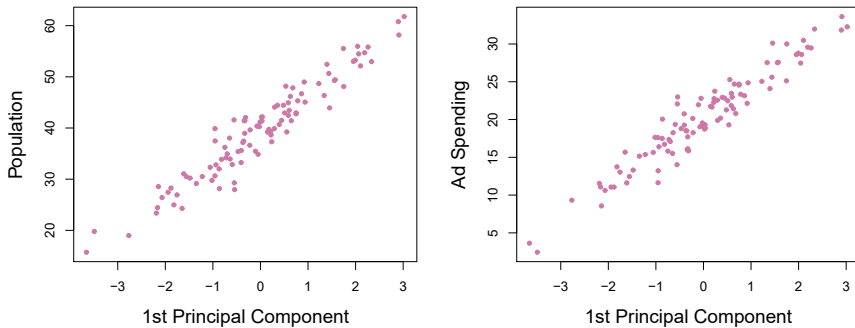


FIGURE 6.16. Plots of the first principal component scores z_{i1} versus `pop` and `ad`. The relationships are strong.

principal component Z_2 is a linear combination of the variables that is uncorrelated with Z_1 , and has largest variance subject to this constraint. The second principal component direction is illustrated as a dashed blue line in Figure 6.14. It turns out that the zero correlation condition of Z_1 with Z_2 is equivalent to the condition that the direction must be *perpendicular*, or *orthogonal*, to the first principal component direction. The second principal component is given by the formula

$$Z_2 = 0.544 \times (\text{pop} - \overline{\text{pop}}) - 0.839 \times (\text{ad} - \overline{\text{ad}}).$$

perpendicular
orthogonal

Since the advertising data has two predictors, the first two principal components contain all of the information that is in `pop` and `ad`. However, by construction, the first component will contain the most information. Consider, for example, the much larger variability of z_{i1} (the x -axis) versus z_{i2} (the y -axis) in the right-hand panel of Figure 6.15. The fact that the second principal component scores are much closer to zero indicates that this component captures far less information. As another illustration, Figure 6.17 displays z_{i2} versus `pop` and `ad`. There is little relationship between the second principal component and these two predictors, again suggesting that in this case, one only needs the first principal component in order to accurately represent the `pop` and `ad` budgets.

With two-dimensional data, such as in our advertising example, we can construct at most two principal components. However, if we had other predictors, such as population age, income level, education, and so forth, then additional components could be constructed. They would successively maximize variance, subject to the constraint of being uncorrelated with the preceding components.

The Principal Components Regression Approach

The *principal components regression* (PCR) approach involves constructing the first M principal components, Z_1, \dots, Z_M , and then using these components as the predictors in a linear regression model that is fit using least squares. The key idea is that often a small number of principal components suffice to explain most of the variability in the data, as well as the relationship with the response. In other words, we assume that *the*

principal
components
regression

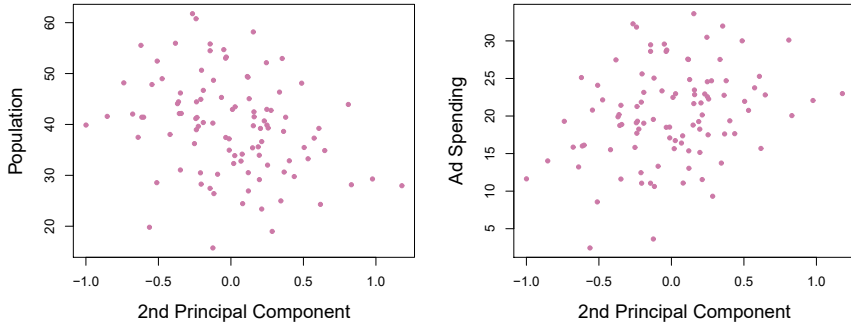


FIGURE 6.17. Plots of the second principal component scores z_{i2} versus `pop` and `ad`. The relationships are weak.

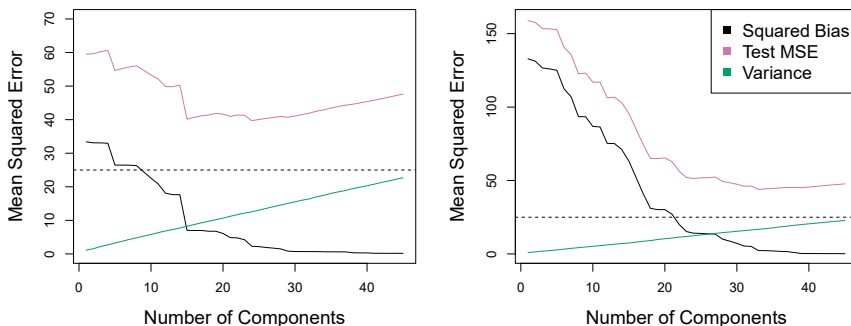


FIGURE 6.18. PCR was applied to two simulated data sets. In each panel, the horizontal dashed line represents the irreducible error. Left: Simulated data from Figure 6.8. Right: Simulated data from Figure 6.9.

directions in which X_1, \dots, X_p show the most variation are the directions that are associated with Y . While this assumption is not guaranteed to be true, it often turns out to be a reasonable enough approximation to give good results.

If the assumption underlying PCR holds, then fitting a least squares model to Z_1, \dots, Z_M will lead to better results than fitting a least squares model to X_1, \dots, X_p , since most or all of the information in the data that relates to the response is contained in Z_1, \dots, Z_M , and by estimating only $M \ll p$ coefficients we can mitigate overfitting. In the advertising data, the first principal component explains most of the variance in both `pop` and `ad`, so a principal component regression that uses this single variable to predict some response of interest, such as `sales`, will likely perform quite well.

Figure 6.18 displays the PCR fits on the simulated data sets from Figures 6.8 and 6.9. Recall that both data sets were generated using $n = 50$ observations and $p = 45$ predictors. However, while the response in the first data set was a function of all the predictors, the response in the second data set was generated using only two of the predictors. The curves are plotted as a function of M , the number of principal components used as predictors in the regression model. As more principal components are used

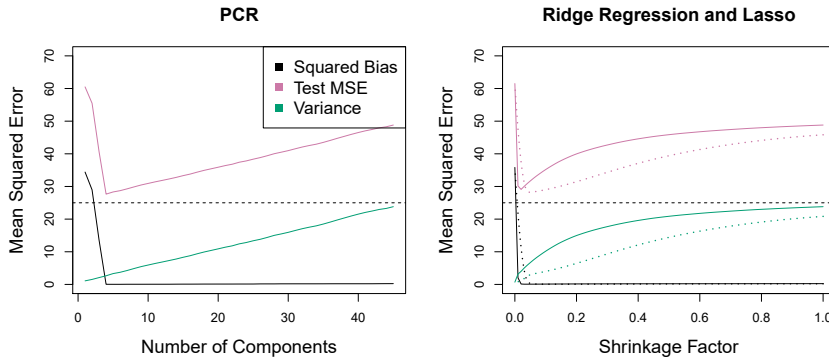


FIGURE 6.19. PCR, ridge regression, and the lasso were applied to a simulated data set in which the first five principal components of X contain all the information about the response Y . In each panel, the irreducible error $\text{Var}(\epsilon)$ is shown as a horizontal dashed line. Left: Results for PCR. Right: Results for lasso (solid) and ridge regression (dotted). The x -axis displays the shrinkage factor of the coefficient estimates, defined as the ℓ_2 norm of the shrunken coefficient estimates divided by the ℓ_2 norm of the least squares estimate.

in the regression model, the bias decreases, but the variance increases. This results in a typical U-shape for the mean squared error. When $M = p = 45$, then PCR amounts simply to a least squares fit using all of the original predictors. The figure indicates that performing PCR with an appropriate choice of M can result in a substantial improvement over least squares, especially in the left-hand panel. However, by examining the ridge regression and lasso results in Figures 6.5, 6.8, and 6.9, we see that PCR does not perform as well as the two shrinkage methods in this example.

The relatively worse performance of PCR in Figure 6.18 is a consequence of the fact that the data were generated in such a way that many principal components are required in order to adequately model the response. In contrast, PCR will tend to do well in cases when the first few principal components are sufficient to capture most of the variation in the predictors as well as the relationship with the response. The left-hand panel of Figure 6.19 illustrates the results from another simulated data set designed to be more favorable to PCR. Here the response was generated in such a way that it depends exclusively on the first five principal components. Now the bias drops to zero rapidly as M , the number of principal components used in PCR, increases. The mean squared error displays a clear minimum at $M = 5$. The right-hand panel of Figure 6.19 displays the results on these data using ridge regression and the lasso. All three methods offer a significant improvement over least squares. However, PCR and ridge regression slightly outperform the lasso.

We note that even though PCR provides a simple way to perform regression using $M < p$ predictors, it is *not* a feature selection method. This is because each of the M principal components used in the regression is a linear combination of all p of the *original* features. For instance, in (6.19), Z_1 was a linear combination of both **pop** and **ad**. Therefore, while PCR often performs quite well in many practical settings, it does not result in the

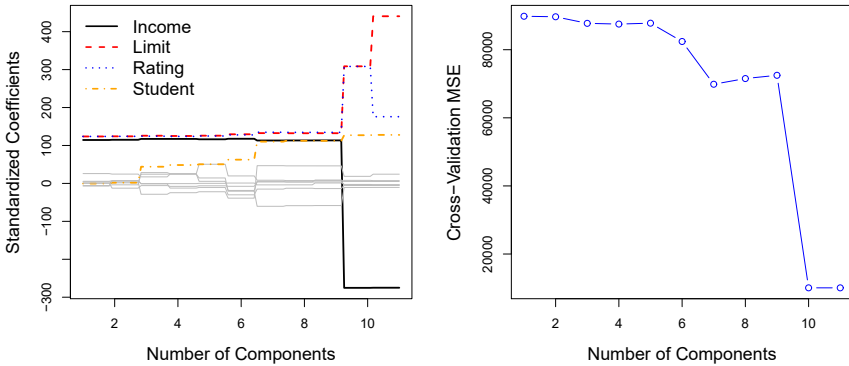


FIGURE 6.20. Left: PCR standardized coefficient estimates on the `Credit` data set for different values of M . Right: The ten-fold cross-validation MSE obtained using PCR, as a function of M .

development of a model that relies upon a small set of the original features. In this sense, PCR is more closely related to ridge regression than to the lasso. In fact, one can show that PCR and ridge regression are very closely related. One can even think of ridge regression as a continuous version of PCR!⁸

In PCR, the number of principal components, M , is typically chosen by cross-validation. The results of applying PCR to the `Credit` data set are shown in Figure 6.20; the right-hand panel displays the cross-validation errors obtained, as a function of M . On these data, the lowest cross-validation error occurs when there are $M = 10$ components; this corresponds to almost no dimension reduction at all, since PCR with $M = 11$ is equivalent to simply performing least squares.

When performing PCR, we generally recommend *standardizing* each predictor, using (6.6), prior to generating the principal components. This standardization ensures that all variables are on the same scale. In the absence of standardization, the high-variance variables will tend to play a larger role in the principal components obtained, and the scale on which the variables are measured will ultimately have an effect on the final PCR model. However, if the variables are all measured in the same units (say, kilograms, or inches), then one might choose not to standardize them.

6.3.2 Partial Least Squares

The PCR approach that we just described involves identifying linear combinations, or *directions*, that best represent the predictors X_1, \dots, X_p . These directions are identified in an *unsupervised* way, since the response Y is not used to help determine the principal component directions. That is, the response does not *supervise* the identification of the principal components. Consequently, PCR suffers from a drawback: there is no guarantee

⁸More details can be found in Section 3.5 of *The Elements of Statistical Learning* by Hastie, Tibshirani, and Friedman.

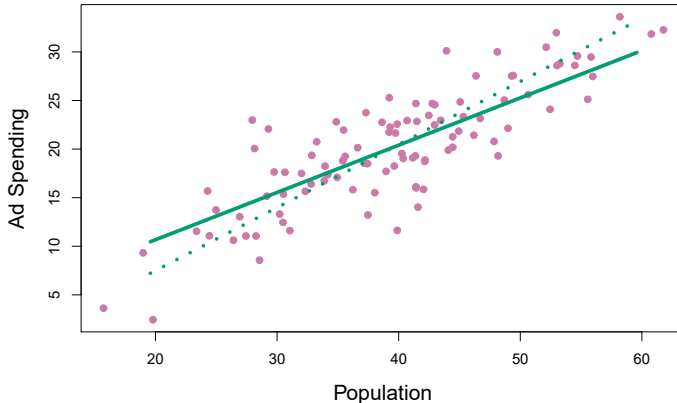


FIGURE 6.21. For the advertising data, the first PLS direction (solid line) and first PCR direction (dotted line) are shown.

that the directions that best explain the predictors will also be the best directions to use for predicting the response. Unsupervised methods are discussed further in Chapter 12.

We now present *partial least squares* (PLS), a *supervised* alternative to PCR. Like PCR, PLS is a dimension reduction method, which first identifies a new set of features Z_1, \dots, Z_M that are linear combinations of the original features, and then fits a linear model via least squares using these M new features. But unlike PCR, PLS identifies these new features in a supervised way—that is, it makes use of the response Y in order to identify new features that not only approximate the old features well, but also that *are related to the response*. Roughly speaking, the PLS approach attempts to find directions that help explain both the response and the predictors.

partial least squares

We now describe how the first PLS direction is computed. After standardizing the p predictors, PLS computes the first direction Z_1 by setting each ϕ_{j1} in (6.16) equal to the coefficient from the simple linear regression of Y onto X_j . One can show that this coefficient is proportional to the correlation between Y and X_j . Hence, in computing $Z_1 = \sum_{j=1}^p \phi_{j1} X_j$, PLS places the highest weight on the variables that are most strongly related to the response.

Figure 6.21 displays an example of PLS on a synthetic dataset with Sales in each of 100 regions as the response, and two predictors; Population Size and Advertising Spending. The solid green line indicates the first PLS direction, while the dotted line shows the first principal component direction. PLS has chosen a direction that has less change in the `ad` dimension per unit change in the `pop` dimension, relative to PCA. This suggests that `pop` is more highly correlated with the response than is `ad`. The PLS direction does not fit the predictors as closely as does PCA, but it does a better job explaining the response.

To identify the second PLS direction we first *adjust* each of the variables for Z_1 , by regressing each variable on Z_1 and taking *residuals*. These residuals can be interpreted as the remaining information that has not been explained by the first PLS direction. We then compute Z_2 using this *or-*

thogonalized data in exactly the same fashion as Z_1 was computed based on the original data. This iterative approach can be repeated M times to identify multiple PLS components Z_1, \dots, Z_M . Finally, at the end of this procedure, we use least squares to fit a linear model to predict Y using Z_1, \dots, Z_M in exactly the same fashion as for PCR.

As with PCR, the number M of partial least squares directions used in PLS is a tuning parameter that is typically chosen by cross-validation. We generally standardize the predictors and response before performing PLS.

PLS is popular in the field of chemometrics, where many variables arise from digitized spectrometry signals. In practice it often performs no better than ridge regression or PCR. While the supervised dimension reduction of PLS can reduce bias, it also has the potential to increase variance, so that the overall benefit of PLS relative to PCR is a wash.

6.4 Considerations in High Dimensions

6.4.1 High-Dimensional Data

Most traditional statistical techniques for regression and classification are intended for the *low-dimensional* setting in which n , the number of observations, is much greater than p , the number of features. This is due in part to the fact that throughout most of the field's history, the bulk of scientific problems requiring the use of statistics have been low-dimensional. For instance, consider the task of developing a model to predict a patient's blood pressure on the basis of his or her age, sex, and body mass index (BMI). There are three predictors, or four if an intercept is included in the model, and perhaps several thousand patients for whom blood pressure and age, sex, and BMI are available. Hence $n \gg p$, and so the problem is low-dimensional. (By dimension here we are referring to the size of p .)

low-dimensional

In the past 20 years, new technologies have changed the way that data are collected in fields as diverse as finance, marketing, and medicine. It is now commonplace to collect an almost unlimited number of feature measurements (p very large). While p can be extremely large, the number of observations n is often limited due to cost, sample availability, or other considerations. Two examples are as follows:

1. Rather than predicting blood pressure on the basis of just age, sex, and BMI, one might also collect measurements for half a million *single nucleotide polymorphisms* (SNPs; these are individual DNA mutations that are relatively common in the population) for inclusion in the predictive model. Then $n \approx 200$ and $p \approx 500,000$.
2. A marketing analyst interested in understanding people's online shopping patterns could treat as features all of the search terms entered by users of a search engine. This is sometimes known as the "bag-of-words" model. The same researcher might have access to the search histories of only a few hundred or a few thousand search engine users who have consented to share their information with the researcher. For a given user, each of the p search terms is scored present (0) or

absent (1), creating a large binary feature vector. Then $n \approx 1,000$ and p is much larger.

Data sets containing more features than observations are often referred to as *high-dimensional*. Classical approaches such as least squares linear regression are not appropriate in this setting. Many of the issues that arise in the analysis of high-dimensional data were discussed earlier in this book, since they apply also when $n > p$: these include the role of the bias-variance trade-off and the danger of overfitting. Though these issues are always relevant, they can become particularly important when the number of features is very large relative to the number of observations.

high-dimensional

We have defined the *high-dimensional setting* as the case where the number of features p is larger than the number of observations n . But the considerations that we will now discuss certainly also apply if p is slightly smaller than n , and are best always kept in mind when performing supervised learning.

6.4.2 What Goes Wrong in High Dimensions?

In order to illustrate the need for extra care and specialized techniques for regression and classification when $p > n$, we begin by examining what can go wrong if we apply a statistical technique not intended for the high-dimensional setting. For this purpose, we examine least squares regression. But the same concepts apply to logistic regression, linear discriminant analysis, and other classical statistical approaches.

When the number of features p is as large as, or larger than, the number of observations n , least squares as described in Chapter 3 cannot (or rather, *should not*) be performed. The reason is simple: regardless of whether or not there truly is a relationship between the features and the response, least squares will yield a set of coefficient estimates that result in a perfect fit to the data, such that the residuals are zero.

An example is shown in Figure 6.22 with $p = 1$ feature (plus an intercept) in two cases: when there are 20 observations, and when there are only two observations. When there are 20 observations, $n > p$ and the least squares regression line does not perfectly fit the data; instead, the regression line seeks to approximate the 20 observations as well as possible. On the other hand, when there are only two observations, then regardless of the values of those observations, the regression line will fit the data exactly. This is problematic because this perfect fit will almost certainly lead to overfitting of the data. In other words, though it is possible to perfectly fit the training data in the high-dimensional setting, the resulting linear model will perform extremely poorly on an independent test set, and therefore does not constitute a useful model. In fact, we can see that this happened in Figure 6.22: the least squares line obtained in the right-hand panel will perform very poorly on a test set comprised of the observations in the left-hand panel. The problem is simple: when $p > n$ or $p \approx n$, a simple least squares regression line is too *flexible* and hence overfits the data.

Figure 6.23 further illustrates the risk of carelessly applying least squares when the number of features p is large. Data were simulated with $n = 20$ observations, and regression was performed with between 1 and 20 features,

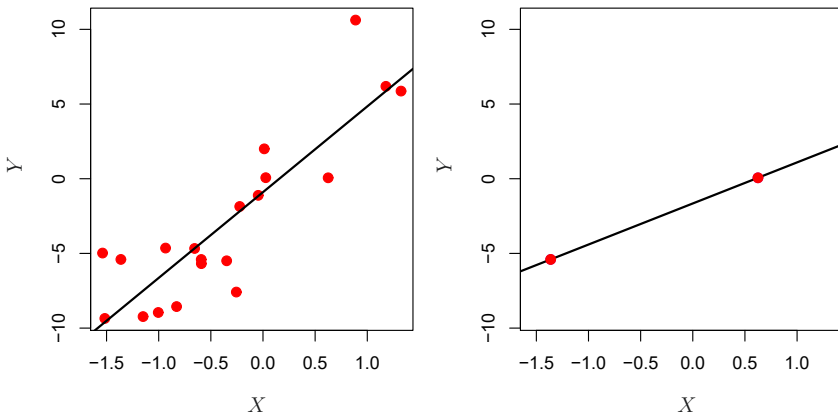


FIGURE 6.22. Left: Least squares regression in the low-dimensional setting. Right: Least squares regression with $n = 2$ observations and two parameters to be estimated (an intercept and a coefficient).

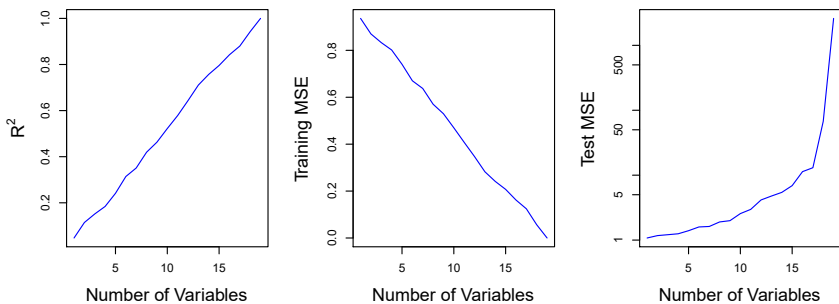


FIGURE 6.23. On a simulated example with $n = 20$ training observations, features that are completely unrelated to the outcome are added to the model. Left: The R^2 increases to 1 as more features are included. Center: The training set MSE decreases to 0 as more features are included. Right: The test set MSE increases as more features are included.

each of which was completely unrelated to the response. As shown in the figure, the model R^2 increases to 1 as the number of features included in the model increases, and correspondingly the training set MSE decreases to 0 as the number of features increases, *even though the features are completely unrelated to the response*. On the other hand, the MSE on an *independent test set* becomes extremely large as the number of features included in the model increases, because including the additional predictors leads to a vast increase in the variance of the coefficient estimates. Looking at the test set MSE, it is clear that the best model contains at most a few variables. However, someone who carelessly examines only the R^2 or the training set MSE might erroneously conclude that the model with the greatest number of variables is best. This indicates the importance of applying extra care when analyzing data sets with a large number of variables, and of always evaluating model performance on an independent test set.

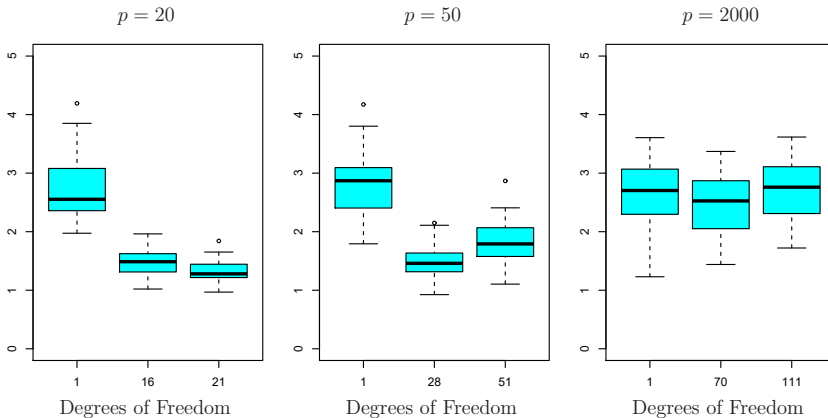


FIGURE 6.24. The lasso was performed with $n = 100$ observations and three values of p , the number of features. Of the p features, 20 were associated with the response. The boxplots show the test MSEs that result using three different values of the tuning parameter λ in (6.7). For ease of interpretation, rather than reporting λ , the degrees of freedom are reported; for the lasso this turns out to be simply the number of estimated non-zero coefficients. When $p = 20$, the lowest test MSE was obtained with the smallest amount of regularization. When $p = 50$, the lowest test MSE was achieved when there is a substantial amount of regularization. When $p = 2,000$ the lasso performed poorly regardless of the amount of regularization, due to the fact that only 20 of the 2,000 features truly are associated with the outcome.

In Section 6.1.3, we saw a number of approaches for adjusting the training set RSS or R^2 in order to account for the number of variables used to fit a least squares model. Unfortunately, the C_p , AIC, and BIC approaches are not appropriate in the high-dimensional setting, because estimating $\hat{\sigma}^2$ is problematic. (For instance, the formula for $\hat{\sigma}^2$ from Chapter 3 yields an estimate $\hat{\sigma}^2 = 0$ in this setting.) Similarly, problems arise in the application of adjusted R^2 in the high-dimensional setting, since one can easily obtain a model with an adjusted R^2 value of 1. Clearly, alternative approaches that are better-suited to the high-dimensional setting are required.

6.4.3 Regression in High Dimensions

It turns out that many of the methods seen in this chapter for fitting less flexible least squares models, such as forward stepwise selection, ridge regression, the lasso, and principal components regression, are particularly useful for performing regression in the high-dimensional setting. Essentially, these approaches avoid overfitting by using a less flexible fitting approach than least squares.

Figure 6.24 illustrates the performance of the lasso in a simple simulated example. There are $p = 20, 50$, or 2,000 features, of which 20 are truly associated with the outcome. The lasso was performed on $n = 100$ training observations, and the mean squared error was evaluated on an independent test set. As the number of features increases, the test set error increases. When $p = 20$, the lowest validation set error was achieved when λ in

(6.7) was small; however, when p was larger then the lowest validation set error was achieved using a larger value of λ . In each boxplot, rather than reporting the values of λ used, the *degrees of freedom* of the resulting lasso solution is displayed; this is simply the number of non-zero coefficient estimates in the lasso solution, and is a measure of the flexibility of the lasso fit. Figure 6.24 highlights three important points: (1) regularization or shrinkage plays a key role in high-dimensional problems, (2) appropriate tuning parameter selection is crucial for good predictive performance, and (3) the test error tends to increase as the dimensionality of the problem (i.e. the number of features or predictors) increases, unless the additional features are truly associated with the response.

The third point above is in fact a key principle in the analysis of high-dimensional data, which is known as the *curse of dimensionality*. One might think that as the number of features used to fit a model increases, the quality of the fitted model will increase as well. However, comparing the left-hand and right-hand panels in Figure 6.24, we see that this is not necessarily the case: in this example, the test set MSE almost doubles as p increases from 20 to 2,000. In general, *adding additional signal features that are truly associated with the response will improve the fitted model*, in the sense of leading to a reduction in test set error. However, adding noise features that are not truly associated with the response will lead to a deterioration in the fitted model, and consequently an increased test set error. This is because noise features increase the dimensionality of the problem, exacerbating the risk of overfitting (since noise features may be assigned nonzero coefficients due to chance associations with the response on the training set) without any potential upside in terms of improved test set error. Thus, we see that new technologies that allow for the collection of measurements for thousands or millions of features are a double-edged sword: they can lead to improved predictive models if these features are in fact relevant to the problem at hand, but will lead to worse results if the features are not relevant. Even if they are relevant, the variance incurred in fitting their coefficients may outweigh the reduction in bias that they bring.

curse of dimensionality

6.4.4 Interpreting Results in High Dimensions

When we perform the lasso, ridge regression, or other regression procedures in the high-dimensional setting, we must be quite cautious in the way that we report the results obtained. In Chapter 3, we learned about *multicollinearity*, the concept that the variables in a regression might be correlated with each other. In the high-dimensional setting, the multicollinearity problem is extreme: any variable in the model can be written as a linear combination of all of the other variables in the model. Essentially, this means that we can never know exactly which variables (if any) truly are predictive of the outcome, and we can never identify the *best* coefficients for use in the regression. At most, we can hope to assign large regression coefficients to variables that are correlated with the variables that truly are predictive of the outcome.

For instance, suppose that we are trying to predict blood pressure on the basis of half a million SNPs, and that forward stepwise selection indicates that 17 of those SNPs lead to a good predictive model on the training data. It would be incorrect to conclude that these 17 SNPs predict blood pressure more effectively than the other SNPs not included in the model. There are likely to be many sets of 17 SNPs that would predict blood pressure just as well as the selected model. If we were to obtain an independent data set and perform forward stepwise selection on that data set, we would likely obtain a model containing a different, and perhaps even non-overlapping, set of SNPs. This does not detract from the value of the model obtained—for instance, the model might turn out to be very effective in predicting blood pressure on an independent set of patients, and might be clinically useful for physicians. But we must be careful not to overstate the results obtained, and to make it clear that what we have identified is simply *one of many possible models* for predicting blood pressure, and that it must be further validated on independent data sets.

It is also important to be particularly careful in reporting errors and measures of model fit in the high-dimensional setting. We have seen that when $p > n$, it is easy to obtain a useless model that has zero residuals. Therefore, one should *never* use sum of squared errors, p-values, R^2 statistics, or other traditional measures of model fit on the training data as evidence of a good model fit in the high-dimensional setting. For instance, as we saw in Figure 6.23, one can easily obtain a model with $R^2 = 1$ when $p > n$. Reporting this fact might mislead others into thinking that a statistically valid and useful model has been obtained, whereas in fact this provides absolutely no evidence of a compelling model. It is important to instead report results on an independent test set, or cross-validation errors. For instance, the MSE or R^2 on an independent test set is a valid measure of model fit, but the MSE on the training set certainly is not.

6.5 Lab: Linear Models and Regularization Methods

In this lab we implement many of the techniques discussed in this chapter. We import some of our libraries at this top level.

```
In [1]: import numpy as np
import pandas as pd
from matplotlib.pyplot import subplots
from statsmodels.api import OLS
import sklearn.model_selection as skm
import sklearn.linear_model as skl
from sklearn.preprocessing import StandardScaler
from ISLP import load_data
from ISLP.models import ModelSpec as MS
from functools import partial
```

We again collect the new imports needed for this lab.

```
In [2]: from sklearn.pipeline import Pipeline
from sklearn.decomposition import PCA
```

6.6 Exercises

Conceptual

1. We perform best subset, forward stepwise, and backward stepwise selection on a single data set. For each approach, we obtain $p + 1$ models, containing $0, 1, 2, \dots, p$ predictors. Explain your answers:
 - (a) Which of the three models with k predictors has the smallest *training* RSS?
 - (b) Which of the three models with k predictors has the smallest *test* RSS?
 - (c) True or False:
 - i. The predictors in the k -variable model identified by forward stepwise are a subset of the predictors in the $(k+1)$ -variable model identified by forward stepwise selection.
 - ii. The predictors in the k -variable model identified by backward stepwise are a subset of the predictors in the $(k+1)$ -variable model identified by backward stepwise selection.
 - iii. The predictors in the k -variable model identified by backward stepwise are a subset of the predictors in the $(k+1)$ -variable model identified by forward stepwise selection.
 - iv. The predictors in the k -variable model identified by forward stepwise are a subset of the predictors in the $(k+1)$ -variable model identified by backward stepwise selection.
 - v. The predictors in the k -variable model identified by best subset are a subset of the predictors in the $(k+1)$ -variable model identified by best subset selection.
2. For parts (a) through (c), indicate which of i. through iv. is correct. Justify your answer.
 - (a) The lasso, relative to least squares, is:
 - i. More flexible and hence will give improved prediction accuracy when its increase in bias is less than its decrease in variance.
 - ii. More flexible and hence will give improved prediction accuracy when its increase in variance is less than its decrease in bias.
 - iii. Less flexible and hence will give improved prediction accuracy when its increase in bias is less than its decrease in variance.
 - iv. Less flexible and hence will give improved prediction accuracy when its increase in variance is less than its decrease in bias.
 - (b) Repeat (a) for ridge regression relative to least squares.
 - (c) Repeat (a) for non-linear methods relative to least squares.

3. Suppose we estimate the regression coefficients in a linear regression model by minimizing

$$\sum_{i=1}^n \left(y_i - \beta_0 - \sum_{j=1}^p \beta_j x_{ij} \right)^2 \text{ subject to } \sum_{j=1}^p |\beta_j| \leq s$$

for a particular value of s . For parts (a) through (e), indicate which of i. through v. is correct. Justify your answer.

- (a) As we increase s from 0, the training RSS will:
 - i. Increase initially, and then eventually start decreasing in an inverted U shape.
 - ii. Decrease initially, and then eventually start increasing in a U shape.
 - iii. Steadily increase.
 - iv. Steadily decrease.
 - v. Remain constant.
 - (b) Repeat (a) for test RSS.
 - (c) Repeat (a) for variance.
 - (d) Repeat (a) for (squared) bias.
 - (e) Repeat (a) for the irreducible error.
4. Suppose we estimate the regression coefficients in a linear regression model by minimizing

$$\sum_{i=1}^n \left(y_i - \beta_0 - \sum_{j=1}^p \beta_j x_{ij} \right)^2 + \lambda \sum_{j=1}^p \beta_j^2$$

for a particular value of λ . For parts (a) through (e), indicate which of i. through v. is correct. Justify your answer.

- (a) As we increase λ from 0, the training RSS will:
 - i. Increase initially, and then eventually start decreasing in an inverted U shape.
 - ii. Decrease initially, and then eventually start increasing in a U shape.
 - iii. Steadily increase.
 - iv. Steadily decrease.
 - v. Remain constant.
- (b) Repeat (a) for test RSS.
- (c) Repeat (a) for variance.
- (d) Repeat (a) for (squared) bias.
- (e) Repeat (a) for the irreducible error.

5. It is well-known that ridge regression tends to give similar coefficient values to correlated variables, whereas the lasso may give quite different coefficient values to correlated variables. We will now explore this property in a very simple setting.



Suppose that $n = 2$, $p = 2$, $x_{11} = x_{12}$, $x_{21} = x_{22}$. Furthermore, suppose that $y_1 + y_2 = 0$ and $x_{11} + x_{21} = 0$ and $x_{12} + x_{22} = 0$, so that the estimate for the intercept in a least squares, ridge regression, or lasso model is zero: $\hat{\beta}_0 = 0$.

- (a) Write out the ridge regression optimization problem in this setting.
- (b) Argue that in this setting, the ridge coefficient estimates satisfy $\hat{\beta}_1 = \hat{\beta}_2$.
- (c) Write out the lasso optimization problem in this setting.
- (d) Argue that in this setting, the lasso coefficients $\hat{\beta}_1$ and $\hat{\beta}_2$ are not unique—in other words, there are many possible solutions to the optimization problem in (c). Describe these solutions.

6. We will now explore (6.12) and (6.13) further.

- (a) Consider (6.12) with $p = 1$. For some choice of y_1 and $\lambda > 0$, plot (6.12) as a function of β_1 . Your plot should confirm that (6.12) is solved by (6.14).
- (b) Consider (6.13) with $p = 1$. For some choice of y_1 and $\lambda > 0$, plot (6.13) as a function of β_1 . Your plot should confirm that (6.13) is solved by (6.15).

7. We will now derive the Bayesian connection to the lasso and ridge regression discussed in Section 6.2.2.



- (a) Suppose that $y_i = \beta_0 + \sum_{j=1}^p x_{ij}\beta_j + \epsilon_i$ where $\epsilon_1, \dots, \epsilon_n$ are independent and identically distributed from a $N(0, \sigma^2)$ distribution. Write out the likelihood for the data.
- (b) Assume the following prior for β : β_1, \dots, β_p are independent and identically distributed according to a double-exponential distribution with mean 0 and common scale parameter b : i.e. $p(\beta) = \frac{1}{2b} \exp(-|\beta|/b)$. Write out the posterior for β in this setting.
- (c) Argue that the lasso estimate is the *mode* for β under this posterior distribution.
- (d) Now assume the following prior for β : β_1, \dots, β_p are independent and identically distributed according to a normal distribution with mean zero and variance c . Write out the posterior for β in this setting.
- (e) Argue that the ridge regression estimate is both the *mode* and the *mean* for β under this posterior distribution.

Applied

8. In this exercise, we will generate simulated data, and will then use this data to perform forward and backward stepwise selection.
- Create a random number generator and use its `normal()` method to generate a predictor X of length $n = 100$, as well as a noise vector ϵ of length $n = 100$.
 - Generate a response vector Y of length $n = 100$ according to the model

$$Y = \beta_0 + \beta_1 X + \beta_2 X^2 + \beta_3 X^3 + \epsilon,$$

where β_0 , β_1 , β_2 , and β_3 are constants of your choice.

- Use forward stepwise selection in order to select a model containing the predictors X, X^2, \dots, X^{10} . What is the model obtained according to C_p ? Report the coefficients of the model obtained.
- Repeat (c), using backwards stepwise selection. How does your answer compare to the results in (c)?
- Now fit a lasso model to the simulated data, again using X, X^2, \dots, X^{10} as predictors. Use cross-validation to select the optimal value of λ . Create plots of the cross-validation error as a function of λ . Report the resulting coefficient estimates, and discuss the results obtained.
- Now generate a response vector Y according to the model

$$Y = \beta_0 + \beta_7 X^7 + \epsilon,$$

and perform forward stepwise selection and the lasso. Discuss the results obtained.

9. In this exercise, we will predict the number of applications received using the other variables in the `College` data set.
- Split the data set into a training set and a test set.
 - Fit a linear model using least squares on the training set, and report the test error obtained.
 - Fit a ridge regression model on the training set, with λ chosen by cross-validation. Report the test error obtained.
 - Fit a lasso model on the training set, with λ chosen by cross-validation. Report the test error obtained, along with the number of non-zero coefficient estimates.
 - Fit a PCR model on the training set, with M chosen by cross-validation. Report the test error obtained, along with the value of M selected by cross-validation.
 - Fit a PLS model on the training set, with M chosen by cross-validation. Report the test error obtained, along with the value of M selected by cross-validation.

- (g) Comment on the results obtained. How accurately can we predict the number of college applications received? Is there much difference among the test errors resulting from these five approaches?
10. We have seen that as the number of features used in a model increases, the training error will necessarily decrease, but the test error may not. We will now explore this in a simulated data set.
- (a) Generate a data set with $p = 20$ features, $n = 1,000$ observations, and an associated quantitative response vector generated according to the model
- $$Y = X\beta + \epsilon,$$
- where β has some elements that are exactly equal to zero.
- (b) Split your data set into a training set containing 100 observations and a test set containing 900 observations.
- (c) Perform best subset selection on the training set, and plot the training set MSE associated with the best model of each size.
- (d) Plot the test set MSE associated with the best model of each size.
- (e) For which model size does the test set MSE take on its minimum value? Comment on your results. If it takes on its minimum value for a model containing only an intercept or a model containing all of the features, then play around with the way that you are generating the data in (a) until you come up with a scenario in which the test set MSE is minimized for an intermediate model size.
- (f) How does the model at which the test set MSE is minimized compare to the true model used to generate the data? Comment on the coefficient values.
- (g) Create a plot displaying $\sqrt{\sum_{j=1}^p (\beta_j - \hat{\beta}_j^r)^2}$ for a range of values of r , where $\hat{\beta}_j^r$ is the j th coefficient estimate for the best model containing r coefficients. Comment on what you observe. How does this compare to the test MSE plot from (d)?
11. We will now try to predict per capita crime rate in the **Boston** data set.
- (a) Try out some of the regression methods explored in this chapter, such as best subset selection, the lasso, ridge regression, and PCR. Present and discuss results for the approaches that you consider.
- (b) Propose a model (or set of models) that seem to perform well on this data set, and justify your answer. Make sure that you are evaluating model performance using validation set error, cross-validation, or some other reasonable alternative, as opposed to using training error.

- (c) Does your chosen model involve all of the features in the data set? Why or why not?



Moving Beyond Linearity

So far in this book, we have mostly focused on linear models. Linear models are relatively simple to describe and implement, and have advantages over other approaches in terms of interpretation and inference. However, standard linear regression can have significant limitations in terms of predictive power. This is because the linearity assumption is almost always an approximation, and sometimes a poor one. In Chapter 6 we see that we can improve upon least squares using ridge regression, the lasso, principal components regression, and other techniques. In that setting, the improvement is obtained by reducing the complexity of the linear model, and hence the variance of the estimates. But we are still using a linear model, which can only be improved so far! In this chapter we relax the linearity assumption while still attempting to maintain as much interpretability as possible. We do this by examining very simple extensions of linear models like polynomial regression and step functions, as well as more sophisticated approaches such as splines, local regression, and generalized additive models.

- *Polynomial regression* extends the linear model by adding extra predictors, obtained by raising each of the original predictors to a power. For example, a *cubic* regression uses three variables, X , X^2 , and X^3 , as predictors. This approach provides a simple way to provide a non-linear fit to data.
- *Step functions* cut the range of a variable into K distinct regions in order to produce a qualitative variable. This has the effect of fitting a piecewise constant function.
- *Regression splines* are more flexible than polynomials and step functions, and in fact are an extension of the two. They involve dividing the range of X into K distinct regions. Within each region, a polynomial function is fit to the data. However, these polynomials are

constrained so that they join smoothly at the region boundaries, or *knots*. Provided that the interval is divided into enough regions, this can produce an extremely flexible fit.

- *Smoothing splines* are similar to regression splines, but arise in a slightly different situation. Smoothing splines result from minimizing a residual sum of squares criterion subject to a smoothness penalty.
- *Local regression* is similar to splines, but differs in an important way. The regions are allowed to overlap, and indeed they do so in a very smooth way.
- *Generalized additive models* allow us to extend the methods above to deal with multiple predictors.

In Sections 7.1–7.6, we present a number of approaches for modeling the relationship between a response Y and a single predictor X in a flexible way. In Section 7.7, we show that these approaches can be seamlessly integrated in order to model a response Y as a function of several predictors X_1, \dots, X_p .

7.1 Polynomial Regression

Historically, the standard way to extend linear regression to settings in which the relationship between the predictors and the response is non-linear has been to replace the standard linear model

$$y_i = \beta_0 + \beta_1 x_i + \epsilon_i$$

with a polynomial function

$$y_i = \beta_0 + \beta_1 x_i + \beta_2 x_i^2 + \beta_3 x_i^3 + \dots + \beta_d x_i^d + \epsilon_i, \quad (7.1)$$

where ϵ_i is the error term. This approach is known as *polynomial regression*, and in fact we saw an example of this method in Section 3.3.2. For large enough degree d , a polynomial regression allows us to produce an extremely non-linear curve. Notice that the coefficients in (7.1) can be easily estimated using least squares linear regression because this is just a standard linear model with predictors $x_i, x_i^2, x_i^3, \dots, x_i^d$. Generally speaking, it is unusual to use d greater than 3 or 4 because for large values of d , the polynomial curve can become overly flexible and can take on some very strange shapes. This is especially true near the boundary of the X variable.

polynomial regression

The left-hand panel in Figure 7.1 is a plot of `wage` against `age` for the `Wage` data set, which contains income and demographic information for males who reside in the central Atlantic region of the United States. We see the results of fitting a degree-4 polynomial using least squares (solid blue curve). Even though this is a linear regression model like any other, the individual coefficients are not of particular interest. Instead, we look at the entire fitted function across a grid of 63 values for `age` from 18 to 80 in order to understand the relationship between `age` and `wage`.

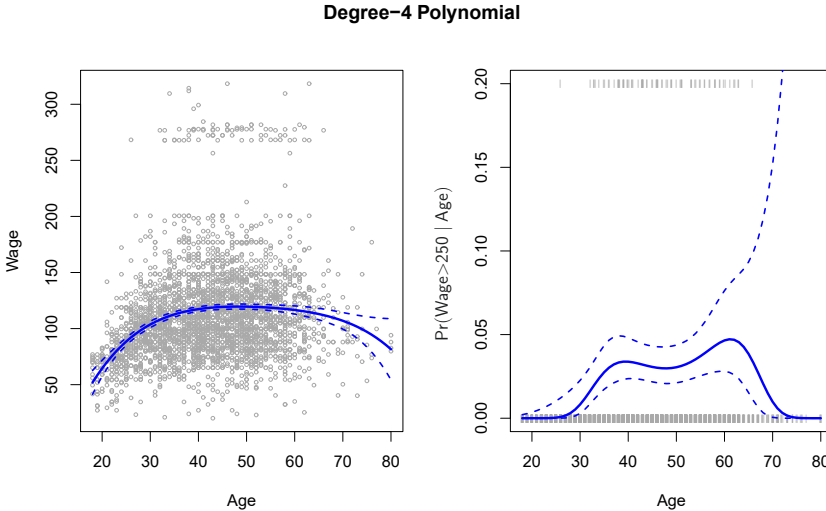


FIGURE 7.1. The `Wage` data. Left: The solid blue curve is a degree-4 polynomial of `wage` (in thousands of dollars) as a function of `age`, fit by least squares. The dashed curves indicate an estimated 95 % confidence interval. Right: We model the binary event `wage>250` using logistic regression, again with a degree-4 polynomial. The fitted posterior probability of `wage` exceeding \$250,000 is shown in blue, along with an estimated 95 % confidence interval.

In Figure 7.1, a pair of dashed curves accompanies the fit; these are $(2 \times)$ standard error curves. Let's see how these arise. Suppose we have computed the fit at a particular value of `age`, x_0 :

$$\hat{f}(x_0) = \hat{\beta}_0 + \hat{\beta}_1 x_0 + \hat{\beta}_2 x_0^2 + \hat{\beta}_3 x_0^3 + \hat{\beta}_4 x_0^4. \quad (7.2)$$

What is the variance of the fit, i.e. $\text{Var}[\hat{f}(x_0)]$? Least squares returns variance estimates for each of the fitted coefficients $\hat{\beta}_j$, as well as the covariances between pairs of coefficient estimates. We can use these to compute the estimated variance of $\hat{f}(x_0)$.¹ The estimated pointwise standard error of $\hat{f}(x_0)$ is the square-root of this variance. This computation is repeated at each reference point x_0 , and we plot the fitted curve, as well as twice the standard error on either side of the fitted curve. We plot twice the standard error because, for normally distributed error terms, this quantity corresponds to an approximate 95 % confidence interval.

It seems like the wages in Figure 7.1 are from two distinct populations: there appears to be a *high earners* group earning more than \$250,000 per annum, as well as a *low earners* group. We can treat `wage` as a binary variable by splitting it into these two groups. Logistic regression can then be used to predict this binary response, using polynomial functions of `age`

¹If $\hat{\mathbf{C}}$ is the 5×5 covariance matrix of the $\hat{\beta}_j$, and if $\ell_0^T = (1, x_0, x_0^2, x_0^3, x_0^4)$, then $\text{Var}[\hat{f}(x_0)] = \ell_0^T \hat{\mathbf{C}} \ell_0$.

as predictors. In other words, we fit the model

$$\Pr(y_i > 250|x_i) = \frac{\exp(\beta_0 + \beta_1 x_i + \beta_2 x_i^2 + \cdots + \beta_d x_i^d)}{1 + \exp(\beta_0 + \beta_1 x_i + \beta_2 x_i^2 + \cdots + \beta_d x_i^d)}. \quad (7.3)$$

The result is shown in the right-hand panel of Figure 7.1. The gray marks on the top and bottom of the panel indicate the ages of the high earners and the low earners. The solid blue curve indicates the fitted probabilities of being a high earner, as a function of `age`. The estimated 95 % confidence interval is shown as well. We see that here the confidence intervals are fairly wide, especially on the right-hand side. Although the sample size for this data set is substantial ($n = 3,000$), there are only 79 high earners, which results in a high variance in the estimated coefficients and consequently wide confidence intervals.

7.2 Step Functions

Using polynomial functions of the features as predictors in a linear model imposes a *global* structure on the non-linear function of X . We can instead use *step functions* in order to avoid imposing such a global structure. Here we break the range of X into *bins*, and fit a different constant in each bin. This amounts to converting a continuous variable into an *ordered categorical variable*.

In greater detail, we create cutpoints c_1, c_2, \dots, c_K in the range of X , and then construct $K + 1$ new variables

$$\begin{aligned} C_0(X) &= I(X < c_1), \\ C_1(X) &= I(c_1 \leq X < c_2), \\ C_2(X) &= I(c_2 \leq X < c_3), \\ &\vdots \\ C_{K-1}(X) &= I(c_{K-1} \leq X < c_K), \\ C_K(X) &= I(c_K \leq X), \end{aligned} \quad (7.4)$$

where $I(\cdot)$ is an *indicator function* that returns a 1 if the condition is true, and returns a 0 otherwise. For example, $I(c_K \leq X)$ equals 1 if $c_K \leq X$, and equals 0 otherwise. These are sometimes called *dummy* variables. Notice that for any value of X , $C_0(X) + C_1(X) + \cdots + C_K(X) = 1$, since X must be in exactly one of the $K + 1$ intervals. We then use least squares to fit a linear model using $C_1(X), C_2(X), \dots, C_K(X)$ as predictors²:

$$y_i = \beta_0 + \beta_1 C_1(x_i) + \beta_2 C_2(x_i) + \cdots + \beta_K C_K(x_i) + \epsilon_i. \quad (7.5)$$

For a given value of X , at most one of C_1, C_2, \dots, C_K can be non-zero. Note that when $X < c_1$, all of the predictors in (7.5) are zero, so β_0 can

²We exclude $C_0(X)$ as a predictor in (7.5) because it is redundant with the intercept. This is similar to the fact that we need only two dummy variables to code a qualitative variable with three levels, provided that the model will contain an intercept. The decision to exclude $C_0(X)$ instead of some other $C_k(X)$ in (7.5) is arbitrary. Alternatively, we could include $C_0(X), C_1(X), \dots, C_K(X)$, and exclude the intercept.

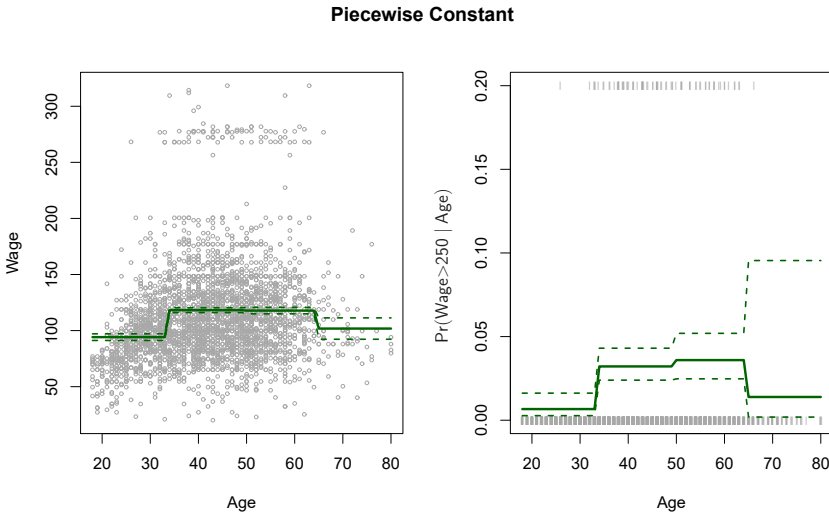


FIGURE 7.2. The `Wage` data. Left: The solid curve displays the fitted value from a least squares regression of `wage` (in thousands of dollars) using step functions of `age`. The dashed curves indicate an estimated 95 % confidence interval. Right: We model the binary event `wage>250` using logistic regression, again using step functions of `age`. The fitted posterior probability of `wage` exceeding \$250,000 is shown, along with an estimated 95 % confidence interval.

be interpreted as the mean value of Y for $X < c_1$. By comparison, (7.5) predicts a response of $\beta_0 + \beta_j$ for $c_j \leq X < c_{j+1}$, so β_j represents the average increase in the response for X in $c_j \leq X < c_{j+1}$ relative to $X < c_1$.

An example of fitting step functions to the `Wage` data from Figure 7.1 is shown in the left-hand panel of Figure 7.2. We also fit the logistic regression model

$$\Pr(y_i > 250|x_i) = \frac{\exp(\beta_0 + \beta_1 C_1(x_i) + \cdots + \beta_K C_K(x_i))}{1 + \exp(\beta_0 + \beta_1 C_1(x_i) + \cdots + \beta_K C_K(x_i))} \quad (7.6)$$

in order to predict the probability that an individual is a high earner on the basis of `age`. The right-hand panel of Figure 7.2 displays the fitted posterior probabilities obtained using this approach.

Unfortunately, unless there are natural breakpoints in the predictors, piecewise-constant functions can miss the action. For example, in the left-hand panel of Figure 7.2, the first bin clearly misses the increasing trend of `wage` with `age`. Nevertheless, step function approaches are very popular in biostatistics and epidemiology, among other disciplines. For example, 5-year age groups are often used to define the bins.

7.3 Basis Functions

Polynomial and piecewise-constant regression models are in fact special cases of a *basis function* approach. The idea is to have at hand a fam-

basis
function

ily of functions or transformations that can be applied to a variable X : $b_1(X), b_2(X), \dots, b_K(X)$. Instead of fitting a linear model in X , we fit the model

$$y_i = \beta_0 + \beta_1 b_1(x_i) + \beta_2 b_2(x_i) + \beta_3 b_3(x_i) + \cdots + \beta_K b_K(x_i) + \epsilon_i. \quad (7.7)$$

Note that the basis functions $b_1(\cdot), b_2(\cdot), \dots, b_K(\cdot)$ are fixed and known. (In other words, we choose the functions ahead of time.) For polynomial regression, the basis functions are $b_j(x_i) = x_i^j$, and for piecewise constant functions they are $b_j(x_i) = I(c_j \leq x_i < c_{j+1})$. We can think of (7.7) as a standard linear model with predictors $b_1(x_i), b_2(x_i), \dots, b_K(x_i)$. Hence, we can use least squares to estimate the unknown regression coefficients in (7.7). Importantly, this means that all of the inference tools for linear models that are discussed in Chapter 3, such as standard errors for the coefficient estimates and F-statistics for the model's overall significance, are available in this setting.

Thus far we have considered the use of polynomial functions and piecewise constant functions for our basis functions; however, many alternatives are possible. For instance, we can use wavelets or Fourier series to construct basis functions. In the next section, we investigate a very common choice for a basis function: *regression splines*.

regression
spline

7.4 Regression Splines

Now we discuss a flexible class of basis functions that extends upon the polynomial regression and piecewise constant regression approaches that we have just seen.

7.4.1 Piecewise Polynomials

Instead of fitting a high-degree polynomial over the entire range of X , *piecewise polynomial regression* involves fitting separate low-degree polynomials over different regions of X . For example, a piecewise cubic polynomial works by fitting a cubic regression model of the form

$$y_i = \beta_0 + \beta_1 x_i + \beta_2 x_i^2 + \beta_3 x_i^3 + \epsilon_i, \quad (7.8)$$

where the coefficients $\beta_0, \beta_1, \beta_2$, and β_3 differ in different parts of the range of X . The points where the coefficients change are called *knots*.

For example, a piecewise cubic with no knots is just a standard cubic polynomial, as in (7.1) with $d = 3$. A piecewise cubic polynomial with a single knot at a point c takes the form

$$y_i = \begin{cases} \beta_{01} + \beta_{11}x_i + \beta_{21}x_i^2 + \beta_{31}x_i^3 + \epsilon_i & \text{if } x_i < c \\ \beta_{02} + \beta_{12}x_i + \beta_{22}x_i^2 + \beta_{32}x_i^3 + \epsilon_i & \text{if } x_i \geq c. \end{cases}$$

In other words, we fit two different polynomial functions to the data, one on the subset of the observations with $x_i < c$, and one on the subset of the observations with $x_i \geq c$. The first polynomial function has coefficients

piecewise
polynomial
regression

knot

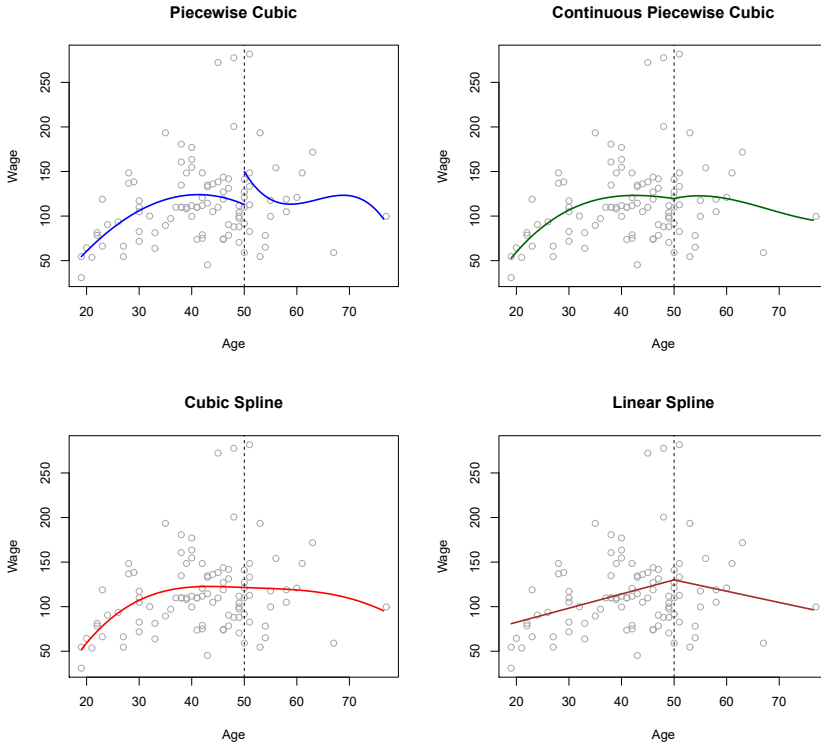


FIGURE 7.3. Various piecewise polynomials are fit to a subset of the `Wage` data, with a knot at `age=50`. Top Left: The cubic polynomials are unconstrained. Top Right: The cubic polynomials are constrained to be continuous at `age=50`. Bottom Left: The cubic polynomials are constrained to be continuous, and to have continuous first and second derivatives. Bottom Right: A linear spline is shown, which is constrained to be continuous.

$\beta_{01}, \beta_{11}, \beta_{21}$, and β_{31} , and the second has coefficients $\beta_{02}, \beta_{12}, \beta_{22}$, and β_{32} . Each of these polynomial functions can be fit using least squares applied to simple functions of the original predictor.

Using more knots leads to a more flexible piecewise polynomial. In general, if we place K different knots throughout the range of X , then we will end up fitting $K + 1$ different cubic polynomials. Note that we do not need to use a cubic polynomial. For example, we can instead fit piecewise linear functions. In fact, our piecewise constant functions of Section 7.2 are piecewise polynomials of degree 0!

The top left panel of Figure 7.3 shows a piecewise cubic polynomial fit to a subset of the `Wage` data, with a single knot at `age=50`. We immediately see a problem: the function is discontinuous and looks ridiculous! Since each polynomial has four parameters, we are using a total of eight *degrees of freedom* in fitting this piecewise polynomial model.

degrees of freedom

7.4.2 Constraints and Splines

The top left panel of Figure 7.3 looks wrong because the fitted curve is just too flexible. To remedy this problem, we can fit a piecewise polynomial under the *constraint* that the fitted curve must be continuous. In other words, there cannot be a jump when `age=50`. The top right plot in Figure 7.3 shows the resulting fit. This looks better than the top left plot, but the V-shaped join looks unnatural.

In the lower left plot, we have added two additional constraints: now both the first and second *derivatives* of the piecewise polynomials are continuous at `age=50`. In other words, we are requiring that the piecewise polynomial be not only continuous when `age=50`, but also very *smooth*. Each constraint that we impose on the piecewise cubic polynomials effectively frees up one degree of freedom, by reducing the complexity of the resulting piecewise polynomial fit. So in the top left plot, we are using eight degrees of freedom, but in the bottom left plot we imposed three constraints (continuity, continuity of the first derivative, and continuity of the second derivative) and so are left with five degrees of freedom. The curve in the bottom left plot is called a *cubic spline*.³ In general, a cubic spline with K knots uses a total of $4 + K$ degrees of freedom.

derivative

cubic spline

linear spline

In Figure 7.3, the lower right plot is a *linear spline*, which is continuous at `age=50`. The general definition of a degree- d spline is that it is a piecewise degree- d polynomial, with continuity in derivatives up to degree $d - 1$ at each knot. Therefore, a linear spline is obtained by fitting a line in each region of the predictor space defined by the knots, requiring continuity at each knot.

In Figure 7.3, there is a single knot at `age=50`. Of course, we could add more knots, and impose continuity at each.

7.4.3 The Spline Basis Representation

The regression splines that we just saw in the previous section may have seemed somewhat complex: how can we fit a piecewise degree- d polynomial under the constraint that it (and possibly its first $d - 1$ derivatives) be continuous? It turns out that we can use the basis model (7.7) to represent a regression spline. A cubic spline with K knots can be modeled as

$$y_i = \beta_0 + \beta_1 b_1(x_i) + \beta_2 b_2(x_i) + \cdots + \beta_{K+3} b_{K+3}(x_i) + \epsilon_i, \quad (7.9)$$

for an appropriate choice of basis functions b_1, b_2, \dots, b_{K+3} . The model (7.9) can then be fit using least squares.

Just as there were several ways to represent polynomials, there are also many equivalent ways to represent cubic splines using different choices of basis functions in (7.9). The most direct way to represent a cubic spline using (7.9) is to start off with a basis for a cubic polynomial—namely, x, x^2 , and x^3 —and then add one *truncated power basis* function per knot.

truncated power basis

³Cubic splines are popular because most human eyes cannot detect the discontinuity at the knots.

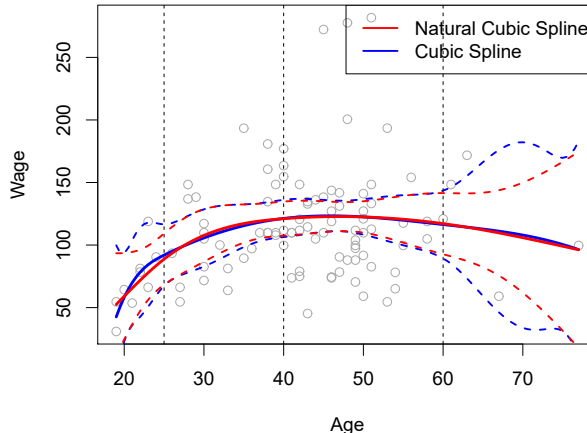


FIGURE 7.4. A cubic spline and a natural cubic spline, with three knots, fit to a subset of the `Wage` data. The dashed lines denote the knot locations.

A truncated power basis function is defined as

$$h(x, \xi) = (x - \xi)_+^3 = \begin{cases} (x - \xi)^3 & \text{if } x > \xi \\ 0 & \text{otherwise,} \end{cases} \quad (7.10)$$

where ξ is the knot. One can show that adding a term of the form $\beta_4 h(x, \xi)$ to the model (7.8) for a cubic polynomial will lead to a discontinuity in only the third derivative at ξ ; the function will remain continuous, with continuous first and second derivatives, at each of the knots.

In other words, in order to fit a cubic spline to a data set with K knots, we perform least squares regression with an intercept and $3 + K$ predictors, of the form $X, X^2, X^3, h(X, \xi_1), h(X, \xi_2), \dots, h(X, \xi_K)$, where ξ_1, \dots, ξ_K are the knots. This amounts to estimating a total of $K + 4$ regression coefficients; for this reason, fitting a cubic spline with K knots uses $K + 4$ degrees of freedom.

Unfortunately, splines can have high variance at the outer range of the predictors—that is, when X takes on either a very small or very large value. Figure 7.4 shows a fit to the `Wage` data with three knots. We see that the confidence bands in the boundary region appear fairly wild. A *natural spline* is a regression spline with additional *boundary constraints*: the function is required to be linear at the boundary (in the region where X is smaller than the smallest knot, or larger than the largest knot). This additional constraint means that natural splines generally produce more stable estimates at the boundaries. In Figure 7.4, a natural cubic spline is also displayed as a red line. Note that the corresponding confidence intervals are narrower.

natural
spline

7.4.4 Choosing the Number and Locations of the Knots

When we fit a spline, where should we place the knots? The regression spline is most flexible in regions that contain a lot of knots, because in those regions the polynomial coefficients can change rapidly. Hence, one

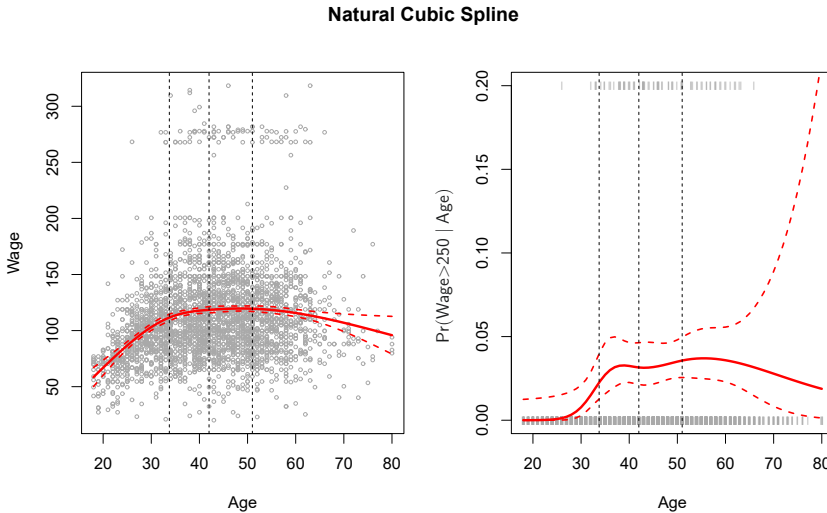


FIGURE 7.5. A natural cubic spline function with four degrees of freedom is fit to the `Wage` data. Left: A spline is fit to `wage` (in thousands of dollars) as a function of `age`. Right: Logistic regression is used to model the binary event `wage>250` as a function of `age`. The fitted posterior probability of `wage` exceeding \$250,000 is shown. The dashed lines denote the knot locations.

option is to place more knots in places where we feel the function might vary most rapidly, and to place fewer knots where it seems more stable. While this option can work well, in practice it is common to place knots in a uniform fashion. One way to do this is to specify the desired degrees of freedom, and then have the software automatically place the corresponding number of knots at uniform quantiles of the data.

Figure 7.5 shows an example on the `Wage` data. As in Figure 7.4, we have fit a natural cubic spline with three knots, except this time the knot locations were chosen automatically as the 25th, 50th, and 75th percentiles of `age`. This was specified by requesting four degrees of freedom. The argument by which four degrees of freedom leads to three interior knots is somewhat technical.⁴

How many knots should we use, or equivalently how many degrees of freedom should our spline contain? One option is to try out different numbers of knots and see which produces the best looking curve. A somewhat more objective approach is to use cross-validation, as discussed in Chapters 5 and 6. With this method, we remove a portion of the data (say 10%), fit a spline with a certain number of knots to the remaining data, and then use the spline to make predictions for the held-out portion. We repeat this process multiple times until each observation has been left out once, and

⁴There are actually five knots, including the two boundary knots. A cubic spline with five knots has nine degrees of freedom. But natural cubic splines have two additional *natural* constraints at each boundary to enforce linearity, resulting in $9 - 4 = 5$ degrees of freedom. Since this includes a constant, which is absorbed in the intercept, we count it as four degrees of freedom.

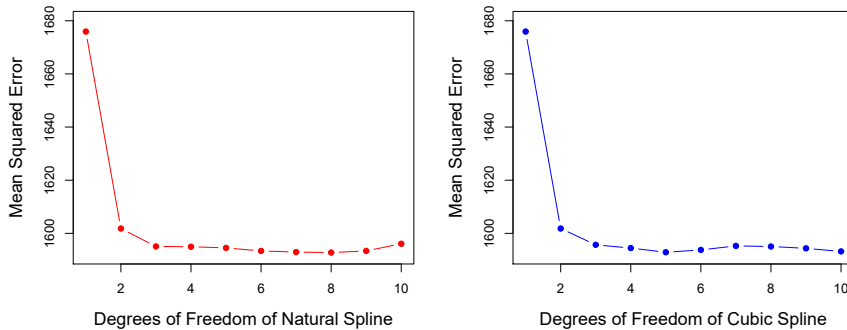


FIGURE 7.6. Ten-fold cross-validated mean squared errors for selecting the degrees of freedom when fitting splines to the `Wage` data. The response is `wage` and the predictor `age`. Left: A natural cubic spline. Right: A cubic spline.

then compute the overall cross-validated RSS. This procedure can be repeated for different numbers of knots K . Then the value of K giving the smallest RSS is chosen.

Figure 7.6 shows ten-fold cross-validated mean squared errors for splines with various degrees of freedom fit to the `Wage` data. The left-hand panel corresponds to a natural cubic spline and the right-hand panel to a cubic spline. The two methods produce almost identical results, with clear evidence that a one-degree fit (a linear regression) is not adequate. Both curves flatten out quickly, and it seems that three degrees of freedom for the natural spline and four degrees of freedom for the cubic spline are quite adequate.

In Section 7.7 we fit additive spline models simultaneously on several variables at a time. This could potentially require the selection of degrees of freedom for each variable. In cases like this we typically adopt a more pragmatic approach and set the degrees of freedom to a fixed number, say four, for all terms.

7.4.5 Comparison to Polynomial Regression

Figure 7.7 compares a natural cubic spline with 15 degrees of freedom to a degree-15 polynomial on the `Wage` data set. The extra flexibility in the polynomial produces undesirable results at the boundaries, while the natural cubic spline still provides a reasonable fit to the data. Regression splines often give superior results to polynomial regression. This is because unlike polynomials, which must use a high degree (exponent in the highest monomial term, e.g. X^{15}) to produce flexible fits, splines introduce flexibility by increasing the number of knots but keeping the degree fixed. Generally, this approach produces more stable estimates. Splines also allow us to place more knots, and hence flexibility, over regions where the function f seems to be changing rapidly, and fewer knots where f appears more stable.

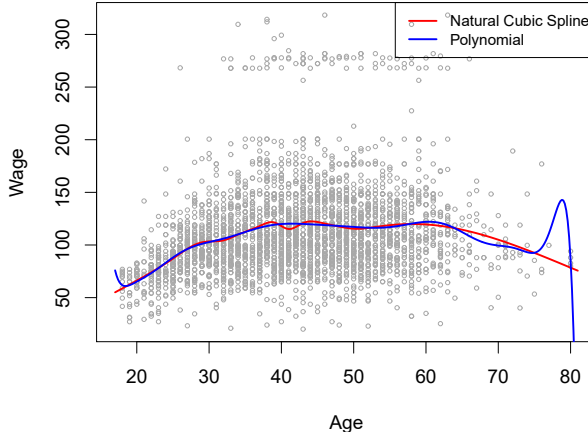


FIGURE 7.7. On the `Wage` data set, a natural cubic spline with 15 degrees of freedom is compared to a degree-15 polynomial. Polynomials can show wild behavior, especially near the tails.

7.5 Smoothing Splines

In the last section we discussed regression splines, which we create by specifying a set of knots, producing a sequence of basis functions, and then using least squares to estimate the spline coefficients. We now introduce a somewhat different approach that also produces a spline.

7.5.1 An Overview of Smoothing Splines

In fitting a smooth curve to a set of data, what we really want to do is find some function, say $g(x)$, that fits the observed data well: that is, we want $\text{RSS} = \sum_{i=1}^n (y_i - g(x_i))^2$ to be small. However, there is a problem with this approach. If we don't put any constraints on $g(x_i)$, then we can always make RSS zero simply by choosing g such that it *interpolates* all of the y_i . Such a function would woefully overfit the data—it would be far too flexible. What we really want is a function g that makes RSS small, but that is also *smooth*.

How might we ensure that g is smooth? There are a number of ways to do this. A natural approach is to find the function g that minimizes

$$\sum_{i=1}^n (y_i - g(x_i))^2 + \lambda \int g''(t)^2 dt \quad (7.11)$$

where λ is a nonnegative *tuning parameter*. The function g that minimizes (7.11) is known as a *smoothing spline*.

What does (7.11) mean? Equation 7.11 takes the “Loss+Penalty” formulation that we encounter in the context of ridge regression and the lasso in Chapter 6. The term $\sum_{i=1}^n (y_i - g(x_i))^2$ is a *loss function* that encourages g to fit the data well, and the term $\lambda \int g''(t)^2 dt$ is a *penalty term* that penalizes the variability in g . The notation $g''(t)$ indicates the second derivative of the function g . The first derivative $g'(t)$ measures the slope

smoothing
spline

loss function

of a function at t , and the second derivative corresponds to the amount by which the slope is changing. Hence, broadly speaking, the second derivative of a function is a measure of its *roughness*: it is large in absolute value if $g(t)$ is very wiggly near t , and it is close to zero otherwise. (The second derivative of a straight line is zero; note that a line is perfectly smooth.) The \int notation is an *integral*, which we can think of as a summation over the range of t . In other words, $\int g''(t)^2 dt$ is simply a measure of the total change in the function $g'(t)$, over its entire range. If g is very smooth, then $g'(t)$ will be close to constant and $\int g''(t)^2 dt$ will take on a small value. Conversely, if g is jumpy and variable then $g'(t)$ will vary significantly and $\int g''(t)^2 dt$ will take on a large value. Therefore, in (7.11), $\lambda \int g''(t)^2 dt$ encourages g to be smooth. The larger the value of λ , the smoother g will be.

When $\lambda = 0$, then the penalty term in (7.11) has no effect, and so the function g will be very jumpy and will exactly interpolate the training observations. When $\lambda \rightarrow \infty$, g will be perfectly smooth—it will just be a straight line that passes as closely as possible to the training points. In fact, in this case, g will be the linear least squares line, since the loss function in (7.11) amounts to minimizing the residual sum of squares. For an intermediate value of λ , g will approximate the training observations but will be somewhat smooth. We see that λ controls the bias-variance trade-off of the smoothing spline.

The function $g(x)$ that minimizes (7.11) can be shown to have some special properties: it is a piecewise cubic polynomial with knots at the unique values of x_1, \dots, x_n , and continuous first and second derivatives at each knot. Furthermore, it is linear in the region outside of the extreme knots. In other words, *the function $g(x)$ that minimizes (7.11) is a natural cubic spline with knots at x_1, \dots, x_n !* However, it is not the same natural cubic spline that one would get if one applied the basis function approach described in Section 7.4.3 with knots at x_1, \dots, x_n —rather, it is a *shrunken* version of such a natural cubic spline, where the value of the tuning parameter λ in (7.11) controls the level of shrinkage.

7.5.2 Choosing the Smoothing Parameter λ

We have seen that a smoothing spline is simply a natural cubic spline with knots at every unique value of x_i . It might seem that a smoothing spline will have far too many degrees of freedom, since a knot at each data point allows a great deal of flexibility. But the tuning parameter λ controls the roughness of the smoothing spline, and hence the *effective degrees of freedom*. It is possible to show that as λ increases from 0 to ∞ , the effective degrees of freedom, which we write df_λ , decrease from n to 2.

In the context of smoothing splines, why do we discuss *effective degrees of freedom* instead of *degrees of freedom*? Usually degrees of freedom refer to the number of free parameters, such as the number of coefficients fit in a polynomial or cubic spline. Although a smoothing spline has n parameters and hence n nominal degrees of freedom, these n parameters are heavily constrained or shrunk down. Hence df_λ is a measure of the flexibility of the smoothing spline—the higher it is, the more flexible (and the lower-bias but higher-variance) the smoothing spline. The definition of effective degrees of

effective
degrees of
freedom

freedom is somewhat technical. We can write

$$\hat{\mathbf{g}}_\lambda = \mathbf{S}_\lambda \mathbf{y}, \quad (7.12)$$

where $\hat{\mathbf{g}}_\lambda$ is the solution to (7.11) for a particular choice of λ —that is, it is an n -vector containing the fitted values of the smoothing spline at the training points x_1, \dots, x_n . Equation 7.12 indicates that the vector of fitted values when applying a smoothing spline to the data can be written as a $n \times n$ matrix \mathbf{S}_λ (for which there is a formula) times the response vector \mathbf{y} . Then the effective degrees of freedom is defined to be

$$df_\lambda = \sum_{i=1}^n \{\mathbf{S}_\lambda\}_{ii}, \quad (7.13)$$

the sum of the diagonal elements of the matrix \mathbf{S}_λ .

In fitting a smoothing spline, we do not need to select the number or location of the knots—there will be a knot at each training observation, x_1, \dots, x_n . Instead, we have another problem: we need to choose the value of λ . It should come as no surprise that one possible solution to this problem is cross-validation. In other words, we can find the value of λ that makes the cross-validated RSS as small as possible. It turns out that the *leave-one-out* cross-validation error (LOOCV) can be computed very efficiently for smoothing splines, with essentially the same cost as computing a single fit, using the following formula:

$$\text{RSS}_{cv}(\lambda) = \sum_{i=1}^n (y_i - \hat{g}_\lambda^{(-i)}(x_i))^2 = \sum_{i=1}^n \left[\frac{y_i - \hat{g}_\lambda(x_i)}{1 - \{\mathbf{S}_\lambda\}_{ii}} \right]^2.$$

The notation $\hat{g}_\lambda^{(-i)}(x_i)$ indicates the fitted value for this smoothing spline evaluated at x_i , where the fit uses all of the training observations except for the i th observation (x_i, y_i) . In contrast, $\hat{g}_\lambda(x_i)$ indicates the smoothing spline function fit to all of the training observations and evaluated at x_i . This remarkable formula says that we can compute each of these *leave-one-out* fits using only \hat{g}_λ , the original fit to *all* of the data!⁵ We have a very similar formula (5.2) on page 205 in Chapter 5 for least squares linear regression. Using (5.2), we can very quickly perform LOOCV for the regression splines discussed earlier in this chapter, as well as for least squares regression using arbitrary basis functions.

Figure 7.8 shows the results from fitting a smoothing spline to the `Wage` data. The red curve indicates the fit obtained from pre-specifying that we would like a smoothing spline with 16 effective degrees of freedom. The blue curve is the smoothing spline obtained when λ is chosen using LOOCV; in this case, the value of λ chosen results in 6.8 effective degrees of freedom (computed using (7.13)). For this data, there is little discernible difference between the two smoothing splines, beyond the fact that the one with 16 degrees of freedom seems slightly wigglier. Since there is little difference between the two fits, the smoothing spline fit with 6.8 degrees of freedom

⁵The exact formulas for computing $\hat{g}(x_i)$ and \mathbf{S}_λ are very technical; however, efficient algorithms are available for computing these quantities.

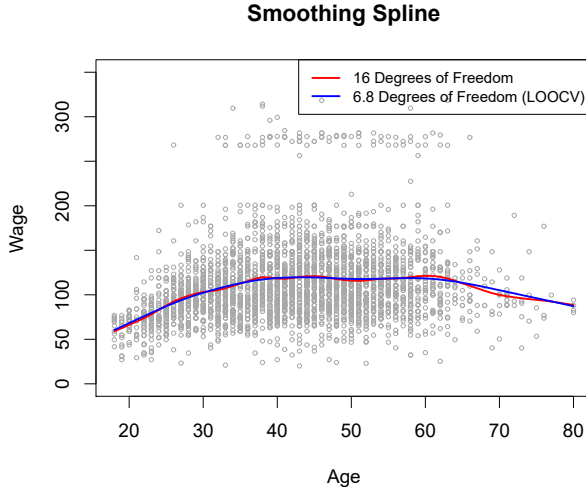


FIGURE 7.8. Smoothing spline fits to the `Wage` data. The red curve results from specifying 16 effective degrees of freedom. For the blue curve, λ was found automatically by leave-one-out cross-validation, which resulted in 6.8 effective degrees of freedom.

is preferable, since in general simpler models are better unless the data provides evidence in support of a more complex model.

7.6 Local Regression

Local regression is a different approach for fitting flexible non-linear functions, which involves computing the fit at a target point x_0 using only the nearby training observations. Figure 7.9 illustrates the idea on some simulated data, with one target point near 0.4, and another near the boundary at 0.05. In this figure the blue line represents the function $f(x)$ from which the data were generated, and the light orange line corresponds to the local regression estimate $\hat{f}(x)$. Local regression is described in Algorithm 7.1.

local
regression

Note that in Step 3 of Algorithm 7.1, the weights K_{i0} will differ for each value of x_0 . In other words, in order to obtain the local regression fit at a new point, we need to fit a new weighted least squares regression model by minimizing (7.14) for a new set of weights. Local regression is sometimes referred to as a *memory-based* procedure, because like nearest-neighbors, we need all the training data each time we wish to compute a prediction. We will avoid getting into the technical details of local regression here—there are books written on the topic.

In order to perform local regression, there are a number of choices to be made, such as how to define the weighting function K , and whether to fit a linear, constant, or quadratic regression in Step 3. (Equation 7.14 corresponds to a linear regression.) While all of these choices make some difference, the most important choice is the *span* s , which is the proportion of points used to compute the local regression at x_0 , as defined in Step 1 above. The span plays a role like that of the tuning parameter λ in smooth-

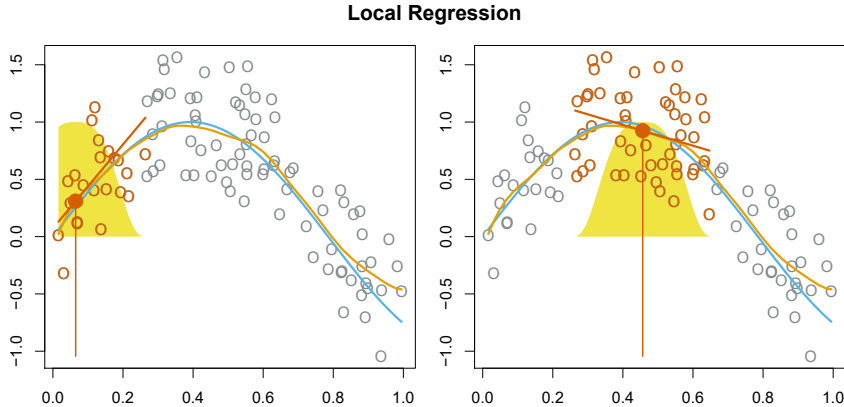


FIGURE 7.9. Local regression illustrated on some simulated data, where the blue curve represents $f(x)$ from which the data were generated, and the light orange curve corresponds to the local regression estimate $\hat{f}(x)$. The orange colored points are local to the target point x_0 , represented by the orange vertical line. The yellow bell-shape superimposed on the plot indicates weights assigned to each point, decreasing to zero with distance from the target point. The fit $\hat{f}(x_0)$ at x_0 is obtained by fitting a weighted linear regression (orange line segment), and using the fitted value at x_0 (orange solid dot) as the estimate $\hat{f}(x_0)$.

ing splines: it controls the flexibility of the non-linear fit. The smaller the value of s , the more *local* and wiggly will be our fit; alternatively, a very large value of s will lead to a global fit to the data using all of the training observations. We can again use cross-validation to choose s , or we can specify it directly. Figure 7.10 displays local linear regression fits on the **Wage** data, using two values of s : 0.7 and 0.2. As expected, the fit obtained using $s = 0.7$ is smoother than that obtained using $s = 0.2$.

The idea of local regression can be generalized in many different ways. In a setting with multiple features X_1, X_2, \dots, X_p , one very useful generalization involves fitting a multiple linear regression model that is global in some variables, but local in another, such as time. Such *varying coefficient models* are a useful way of adapting a model to the most recently gathered data. Local regression also generalizes very naturally when we want to fit models that are local in a pair of variables X_1 and X_2 , rather than one. We can simply use two-dimensional neighborhoods, and fit bivariate linear regression models using the observations that are near each target point in two-dimensional space. Theoretically the same approach can be implemented in higher dimensions, using linear regressions fit to p -dimensional neighborhoods. However, local regression can perform poorly if p is much larger than about 3 or 4 because there will generally be very few training observations close to x_0 . Nearest-neighbors regression, discussed in Chapter 3, suffers from a similar problem in high dimensions.

varying
coefficient
model

Algorithm 7.1 Local Regression At $X = x_0$

1. Gather the fraction $s = k/n$ of training points whose x_i are closest to x_0 .
2. Assign a weight $K_{i0} = K(x_i, x_0)$ to each point in this neighborhood, so that the point furthest from x_0 has weight zero, and the closest has the highest weight. All but these k nearest neighbors get weight zero.
3. Fit a *weighted least squares regression* of the y_i on the x_i using the aforementioned weights, by finding $\hat{\beta}_0$ and $\hat{\beta}_1$ that minimize

$$\sum_{i=1}^n K_{i0}(y_i - \beta_0 - \beta_1 x_i)^2. \quad (7.14)$$

4. The fitted value at x_0 is given by $\hat{f}(x_0) = \hat{\beta}_0 + \hat{\beta}_1 x_0$.

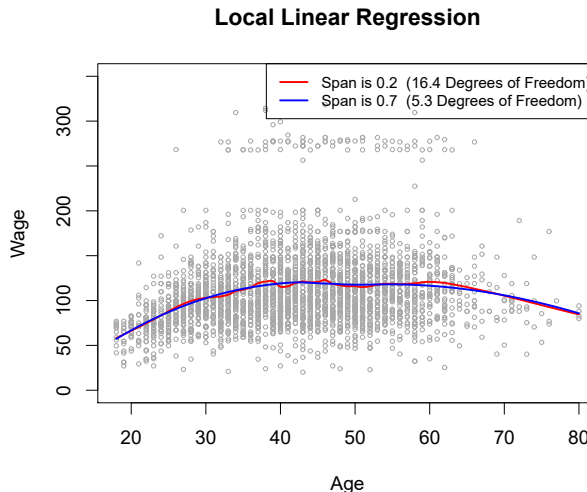


FIGURE 7.10. Local linear fits to the `Wage` data. The span specifies the fraction of the data used to compute the fit at each target point.

7.7 Generalized Additive Models

In Sections 7.1–7.6, we present a number of approaches for flexibly predicting a response Y on the basis of a single predictor X . These approaches can be seen as extensions of simple linear regression. Here we explore the problem of flexibly predicting Y on the basis of several predictors, X_1, \dots, X_p . This amounts to an extension of multiple linear regression.

Generalized additive models (GAMs) provide a general framework for extending a standard linear model by allowing non-linear functions of each of the variables, while maintaining *additivity*. Just like linear models, GAMs can be applied with both quantitative and qualitative responses. We first

generalized
additive
model
additivity

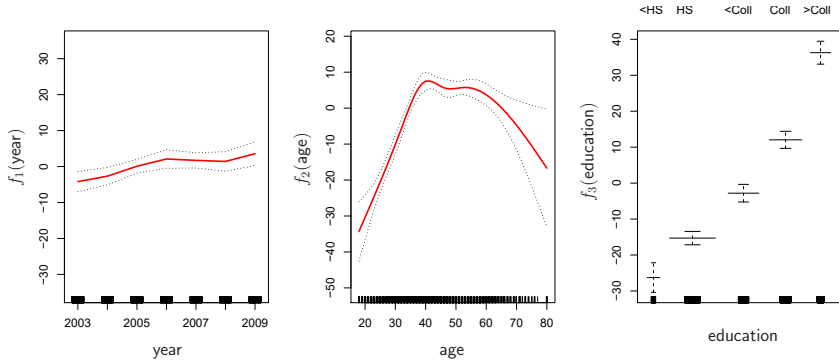


FIGURE 7.11. For the `Wage` data, plots of the relationship between each feature and the response, `wage`, in the fitted model (7.16). Each plot displays the fitted function and pointwise standard errors. The first two functions are natural splines in `year` and `age`, with four and five degrees of freedom, respectively. The third function is a step function, fit to the qualitative variable `education`.

examine GAMs for a quantitative response in Section 7.7.1, and then for a qualitative response in Section 7.7.2.

7.7.1 GAMs for Regression Problems

A natural way to extend the multiple linear regression model

$$y_i = \beta_0 + \beta_1 x_{i1} + \beta_2 x_{i2} + \cdots + \beta_p x_{ip} + \epsilon_i$$

in order to allow for non-linear relationships between each feature and the response is to replace each linear component $\beta_j x_{ij}$ with a (smooth) non-linear function $f_j(x_{ij})$. We would then write the model as

$$\begin{aligned} y_i &= \beta_0 + \sum_{j=1}^p f_j(x_{ij}) + \epsilon_i \\ &= \beta_0 + f_1(x_{i1}) + f_2(x_{i2}) + \cdots + f_p(x_{ip}) + \epsilon_i. \end{aligned} \quad (7.15)$$

This is an example of a GAM. It is called an *additive* model because we calculate a separate f_j for each X_j , and then add together all of their contributions.

In Sections 7.1–7.6, we discuss many methods for fitting functions to a single variable. The beauty of GAMs is that we can use these methods as building blocks for fitting an additive model. In fact, for most of the methods that we have seen so far in this chapter, this can be done fairly trivially. Take, for example, natural splines, and consider the task of fitting the model

$$\text{wage} = \beta_0 + f_1(\text{year}) + f_2(\text{age}) + f_3(\text{education}) + \epsilon \quad (7.16)$$

on the `Wage` data. Here `year` and `age` are quantitative variables, while the variable `education` is qualitative with five levels: `<HS`, `HS`, `<Coll`, `Coll`, `>Coll`, referring to the amount of high school or college education that an individual has completed. We fit the first two functions using natural splines. We

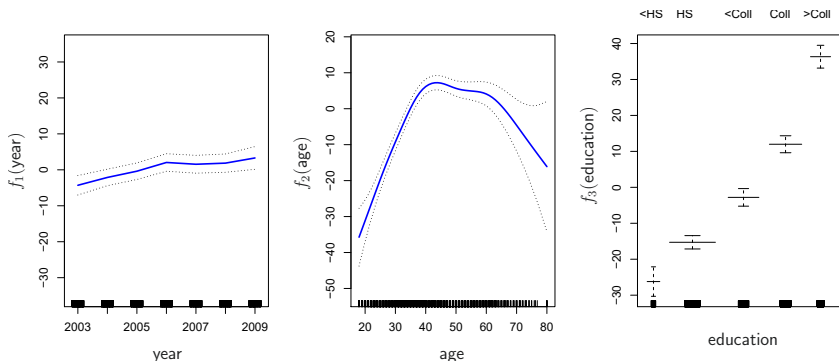


FIGURE 7.12. Details are as in Figure 7.11, but now f_1 and f_2 are smoothing splines with four and five degrees of freedom, respectively.

fit the third function using a separate constant for each level, via the usual dummy variable approach of Section 3.3.1.

Figure 7.11 shows the results of fitting the model (7.16) using least squares. This is easy to do, since as discussed in Section 7.4, natural splines can be constructed using an appropriately chosen set of basis functions. Hence the entire model is just a big regression onto spline basis variables and dummy variables, all packed into one big regression matrix.

Figure 7.11 can be easily interpreted. The left-hand panel indicates that holding `age` and `education` fixed, `wage` tends to increase slightly with `year`; this may be due to inflation. The center panel indicates that holding `education` and `year` fixed, `wage` tends to be highest for intermediate values of `age`, and lowest for the very young and very old. The right-hand panel indicates that holding `year` and `age` fixed, `wage` tends to increase with `education`: the more educated a person is, the higher their salary, on average. All of these findings are intuitive.

Figure 7.12 shows a similar triple of plots, but this time f_1 and f_2 are smoothing splines with four and five degrees of freedom, respectively. Fitting a GAM with a smoothing spline is not quite as simple as fitting a GAM with a natural spline, since in the case of smoothing splines, least squares cannot be used. However, standard software such as the `Python` package `pygam` can be used to fit GAMs using smoothing splines, via an approach known as *backfitting*. This method fits a model involving multiple predictors by repeatedly updating the fit for each predictor in turn, holding the others fixed. The beauty of this approach is that each time we update a function, we simply apply the fitting method for that variable to a *partial residual*.⁶

`pygam`
backfitting

The fitted functions in Figures 7.11 and 7.12 look rather similar. In most situations, the differences in the GAMs obtained using smoothing splines versus natural splines are small.

⁶A partial residual for X_3 , for example, has the form $r_i = y_i - f_1(x_{i1}) - f_2(x_{i2})$. If we know f_1 and f_2 , then we can fit f_3 by treating this residual as a response in a non-linear regression on X_3 .

We do not have to use splines as the building blocks for GAMs: we can just as well use local regression, polynomial regression, or any combination of the approaches seen earlier in this chapter in order to create a GAM. GAMs are investigated in further detail in the lab at the end of this chapter.

Pros and Cons of GAMs

Before we move on, let us summarize the advantages and limitations of a GAM.

- ▲ GAMs allow us to fit a non-linear f_j to each X_j , so that we can automatically model non-linear relationships that standard linear regression will miss. This means that we do not need to manually try out many different transformations on each variable individually.
- ▲ The non-linear fits can potentially make more accurate predictions for the response Y .
- ▲ Because the model is additive, we can examine the effect of each X_j on Y individually while holding all of the other variables fixed.
- ▲ The smoothness of the function f_j for the variable X_j can be summarized via degrees of freedom.
- ◆ The main limitation of GAMs is that the model is restricted to be additive. With many variables, important interactions can be missed. However, as with linear regression, we can manually add interaction terms to the GAM model by including additional predictors of the form $X_j \times X_k$. In addition we can add low-dimensional interaction functions of the form $f_{jk}(X_j, X_k)$ into the model; such terms can be fit using two-dimensional smoothers such as local regression, or two-dimensional splines (not covered here).

For fully general models, we have to look for even more flexible approaches such as random forests and boosting, described in Chapter 8. GAMs provide a useful compromise between linear and fully nonparametric models.

7.7.2 GAMs for Classification Problems

GAMs can also be used in situations where Y is qualitative. For simplicity, here we assume Y takes on values 0 or 1, and let $p(X) = \Pr(Y = 1|X)$ be the conditional probability (given the predictors) that the response equals one. Recall the logistic regression model (4.6):

$$\log \left(\frac{p(X)}{1 - p(X)} \right) = \beta_0 + \beta_1 X_1 + \beta_2 X_2 + \cdots + \beta_p X_p. \quad (7.17)$$

The left-hand side is the log of the odds of $P(Y = 1|X)$ versus $P(Y = 0|X)$, which (7.17) represents as a linear function of the predictors. A natural way to extend (7.17) to allow for non-linear relationships is to use the model

$$\log \left(\frac{p(X)}{1 - p(X)} \right) = \beta_0 + f_1(X_1) + f_2(X_2) + \cdots + f_p(X_p). \quad (7.18)$$

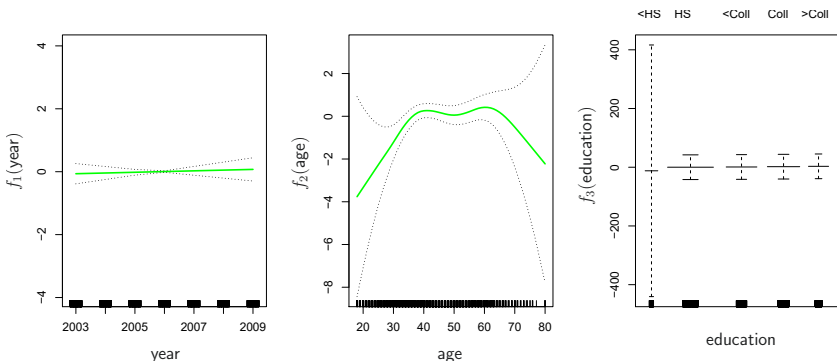


FIGURE 7.13. For the `Wage` data, the logistic regression GAM given in (7.19) is fit to the binary response `I(wage > 250)`. Each plot displays the fitted function and pointwise standard errors. The first function is linear in `year`, the second function a smoothing spline with five degrees of freedom in `age`, and the third a step function for `education`. There are very wide standard errors for the first level `<HS` of `education`.

Equation 7.18 is a logistic regression GAM. It has all the same pros and cons as discussed in the previous section for quantitative responses.

We fit a GAM to the `Wage` data in order to predict the probability that an individual's income exceeds \$250,000 per year. The GAM that we fit takes the form

$$\log \left(\frac{p(X)}{1 - p(X)} \right) = \beta_0 + \beta_1 \times \text{year} + f_2(\text{age}) + f_3(\text{education}), \quad (7.19)$$

where

$$p(X) = \Pr(\text{wage} > 250 | \text{year}, \text{age}, \text{education}).$$

Once again f_2 is fit using a smoothing spline with five degrees of freedom, and f_3 is fit as a step function, by creating dummy variables for each of the levels of education. The resulting fit is shown in Figure 7.13. The last panel looks suspicious, with very wide confidence intervals for level `<HS`. In fact, no response values equal one for that category: no individuals with less than a high school education make more than \$250,000 per year. Hence we refit the GAM, excluding the individuals with less than a high school education. The resulting model is shown in Figure 7.14. As in Figures 7.11 and 7.12, all three panels have similar vertical scales. This allows us to visually assess the relative contributions of each of the variables. We observe that `age` and `education` have a much larger effect than `year` on the probability of being a high earner.

7.8 Lab: Non-Linear Modeling

In this lab, we demonstrate some of the nonlinear models discussed in this chapter. We use the `Wage` data as a running example, and show that many of the complex non-linear fitting procedures discussed can easily be implemented in `Python`.

```

    age,
    frac=span,
    xvals=age_grid)
ax.plot(age_grid,
        fitted,
        label='{:1f}'.format(span),
        linewidth=4)
ax.set_xlabel('Age', fontsize=20)
ax.set_ylabel('Wage', fontsize=20);
ax.legend(title='span', fontsize=15);

```

7.9 Exercises

Conceptual

1. It was mentioned in this chapter that a cubic regression spline with one knot at ξ can be obtained using a basis of the form $x, x^2, x^3, (x - \xi)_+^3$, where $(x - \xi)_+^3 = (x - \xi)^3$ if $x > \xi$ and equals 0 otherwise. We will now show that a function of the form

$$f(x) = \beta_0 + \beta_1 x + \beta_2 x^2 + \beta_3 x^3 + \beta_4 (x - \xi)_+^3$$

is indeed a cubic regression spline, regardless of the values of $\beta_0, \beta_1, \beta_2, \beta_3, \beta_4$.

- (a) Find a cubic polynomial

$$f_1(x) = a_1 + b_1 x + c_1 x^2 + d_1 x^3$$

such that $f(x) = f_1(x)$ for all $x \leq \xi$. Express a_1, b_1, c_1, d_1 in terms of $\beta_0, \beta_1, \beta_2, \beta_3, \beta_4$.

- (b) Find a cubic polynomial

$$f_2(x) = a_2 + b_2 x + c_2 x^2 + d_2 x^3$$

such that $f(x) = f_2(x)$ for all $x > \xi$. Express a_2, b_2, c_2, d_2 in terms of $\beta_0, \beta_1, \beta_2, \beta_3, \beta_4$. We have now established that $f(x)$ is a piecewise polynomial.

- (c) Show that $f_1(\xi) = f_2(\xi)$. That is, $f(x)$ is continuous at ξ .
 (d) Show that $f'_1(\xi) = f'_2(\xi)$. That is, $f'(x)$ is continuous at ξ .
 (e) Show that $f''_1(\xi) = f''_2(\xi)$. That is, $f''(x)$ is continuous at ξ .

Therefore, $f(x)$ is indeed a cubic spline.

Hint: Parts (d) and (e) of this problem require knowledge of single-variable calculus. As a reminder, given a cubic polynomial

$$f_1(x) = a_1 + b_1 x + c_1 x^2 + d_1 x^3,$$

the first derivative takes the form

$$f'_1(x) = b_1 + 2c_1 x + 3d_1 x^2$$



and the second derivative takes the form

$$f_1''(x) = 2c_1 + 6d_1x.$$

2. Suppose that a curve \hat{g} is computed to smoothly fit a set of n points using the following formula:

$$\hat{g} = \arg \min_g \left(\sum_{i=1}^n (y_i - g(x_i))^2 + \lambda \int [g^{(m)}(x)]^2 dx \right),$$

where $g^{(m)}$ represents the m th derivative of g (and $g^{(0)} = g$). Provide example sketches of \hat{g} in each of the following scenarios.

- (a) $\lambda = \infty, m = 0$.
 - (b) $\lambda = \infty, m = 1$.
 - (c) $\lambda = \infty, m = 2$.
 - (d) $\lambda = \infty, m = 3$.
 - (e) $\lambda = 0, m = 3$.
3. Suppose we fit a curve with basis functions $b_1(X) = X$, $b_2(X) = (X - 1)^2 I(X \geq 1)$. (Note that $I(X \geq 1)$ equals 1 for $X \geq 1$ and 0 otherwise.) We fit the linear regression model

$$Y = \beta_0 + \beta_1 b_1(X) + \beta_2 b_2(X) + \epsilon,$$

and obtain coefficient estimates $\hat{\beta}_0 = 1, \hat{\beta}_1 = 1, \hat{\beta}_2 = -2$. Sketch the estimated curve between $X = -2$ and $X = 2$. Note the intercepts, slopes, and other relevant information.

4. Suppose we fit a curve with basis functions $b_1(X) = I(0 \leq X \leq 2) - (X - 1)I(1 \leq X \leq 2)$, $b_2(X) = (X - 3)I(3 \leq X \leq 4) + I(4 < X \leq 5)$. We fit the linear regression model

$$Y = \beta_0 + \beta_1 b_1(X) + \beta_2 b_2(X) + \epsilon,$$

and obtain coefficient estimates $\hat{\beta}_0 = 1, \hat{\beta}_1 = 1, \hat{\beta}_2 = 3$. Sketch the estimated curve between $X = -2$ and $X = 6$. Note the intercepts, slopes, and other relevant information.

5. Consider two curves, \hat{g}_1 and \hat{g}_2 , defined by

$$\hat{g}_1 = \arg \min_g \left(\sum_{i=1}^n (y_i - g(x_i))^2 + \lambda \int [g^{(3)}(x)]^2 dx \right),$$

$$\hat{g}_2 = \arg \min_g \left(\sum_{i=1}^n (y_i - g(x_i))^2 + \lambda \int [g^{(4)}(x)]^2 dx \right),$$

where $g^{(m)}$ represents the m th derivative of g .

- (a) As $\lambda \rightarrow \infty$, will \hat{g}_1 or \hat{g}_2 have the smaller training RSS?
- (b) As $\lambda \rightarrow \infty$, will \hat{g}_1 or \hat{g}_2 have the smaller test RSS?
- (c) For $\lambda = 0$, will \hat{g}_1 or \hat{g}_2 have the smaller training and test RSS?

Applied

6. In this exercise, you will further analyze the `Wage` data set considered throughout this chapter.
 - (a) Perform polynomial regression to predict `wage` using `age`. Use cross-validation to select the optimal degree d for the polynomial. What degree was chosen, and how does this compare to the results of hypothesis testing using ANOVA? Make a plot of the resulting polynomial fit to the data.
 - (b) Fit a step function to predict `wage` using `age`, and perform cross-validation to choose the optimal number of cuts. Make a plot of the fit obtained.
7. The `Wage` data set contains a number of other features not explored in this chapter, such as marital status (`maritl`), job class (`jobclass`), and others. Explore the relationships between some of these other predictors and `wage`, and use non-linear fitting techniques in order to fit flexible models to the data. Create plots of the results obtained, and write a summary of your findings.
8. Fit some of the non-linear models investigated in this chapter to the `Auto` data set. Is there evidence for non-linear relationships in this data set? Create some informative plots to justify your answer.
9. This question uses the variables `dis` (the weighted mean of distances to five Boston employment centers) and `nox` (nitrogen oxides concentration in parts per 10 million) from the `Boston` data. We will treat `dis` as the predictor and `nox` as the response.
 - (a) Use the `poly()` function from the `ISLP.models` module to fit a cubic polynomial regression to predict `nox` using `dis`. Report the regression output, and plot the resulting data and polynomial fits.
 - (b) Plot the polynomial fits for a range of different polynomial degrees (say, from 1 to 10), and report the associated residual sum of squares.
 - (c) Perform cross-validation or another approach to select the optimal degree for the polynomial, and explain your results.
 - (d) Use the `bs()` function from the `ISLP.models` module to fit a regression spline to predict `nox` using `dis`. Report the output for the fit using four degrees of freedom. How did you choose the knots? Plot the resulting fit.
 - (e) Now fit a regression spline for a range of degrees of freedom, and plot the resulting fits and report the resulting RSS. Describe the results obtained.
 - (f) Perform cross-validation or another approach in order to select the best degrees of freedom for a regression spline on this data. Describe your results.

10. This question relates to the `College` data set.
- Split the data into a training set and a test set. Using out-of-state tuition as the response and the other variables as the predictors, perform forward stepwise selection on the training set in order to identify a satisfactory model that uses just a subset of the predictors.
 - Fit a GAM on the training data, using out-of-state tuition as the response and the features selected in the previous step as the predictors. Plot the results, and explain your findings.
 - Evaluate the model obtained on the test set, and explain the results obtained.
 - For which variables, if any, is there evidence of a non-linear relationship with the response?

11. In Section 7.7, it was mentioned that GAMs are generally fit using a *backfitting* approach. The idea behind backfitting is actually quite simple. We will now explore backfitting in the context of multiple linear regression.

Suppose that we would like to perform multiple linear regression, but we do not have software to do so. Instead, we only have software to perform simple linear regression. Therefore, we take the following iterative approach: we repeatedly hold all but one coefficient estimate fixed at its current value, and update only that coefficient estimate using a simple linear regression. The process is continued until *convergence*—that is, until the coefficient estimates stop changing.

We now try this out on a toy example.

- Generate a response Y and two predictors X_1 and X_2 , with $n = 100$.
- Write a function `simple_reg()` that takes two arguments `outcome` and `feature`, fits a simple linear regression model with this outcome and feature, and returns the estimated intercept and slope.
- Initialize `beta1` to take on a value of your choice. It does not matter what value you choose.
- Keeping `beta1` fixed, use your function `simple_reg()` to fit the model:

$$Y - \text{beta1} \cdot X_1 = \beta_0 + \beta_2 X_2 + \epsilon.$$

Store the resulting values as `beta0` and `beta2`.

- Keeping `beta2` fixed, fit the model

$$Y - \text{beta2} \cdot X_2 = \beta_0 + \beta_1 X_1 + \epsilon.$$

Store the result as `beta0` and `beta1` (overwriting their previous values).

- Write a for loop to repeat (c) and (d) 1,000 times. Report the estimates of `beta0`, `beta1`, and `beta2` at each iteration of the for loop. Create a plot in which each of these values is displayed, with `beta0`, `beta1`, and `beta2`.

- (g) Compare your answer in (e) to the results of simply performing multiple linear regression to predict Y using X_1 and X_2 . Use `axline()` method to overlay those multiple linear regression coefficient estimates on the plot obtained in (e).
- (h) On this data set, how many backfitting iterations were required in order to obtain a “good” approximation to the multiple regression coefficient estimates?
12. This problem is a continuation of the previous exercise. In a toy example with $p = 100$, show that one can approximate the multiple linear regression coefficient estimates by repeatedly performing simple linear regression in a backfitting procedure. How many backfitting iterations are required in order to obtain a “good” approximation to the multiple regression coefficient estimates? Create a plot to justify your answer.



Tree-Based Methods

In this chapter, we describe *tree-based* methods for regression and classification. These involve *stratifying* or *segmenting* the predictor space into a number of simple regions. In order to make a prediction for a given observation, we typically use the mean or the mode response value for the training observations in the region to which it belongs. Since the set of splitting rules used to segment the predictor space can be summarized in a tree, these types of approaches are known as *decision tree* methods.

Tree-based methods are simple and useful for interpretation. However, they typically are not competitive with the best supervised learning approaches, such as those seen in Chapters 6 and 7, in terms of prediction accuracy. Hence in this chapter we also introduce *bagging*, *random forests*, *boosting*, and *Bayesian additive regression trees*. Each of these approaches involves producing multiple trees which are then combined to yield a single consensus prediction. We will see that combining a large number of trees can often result in dramatic improvements in prediction accuracy, at the expense of some loss in interpretation.

decision tree

8.1 The Basics of Decision Trees

Decision trees can be applied to both regression and classification problems. We first consider regression problems, and then move on to classification.

8.1.1 Regression Trees

In order to motivate *regression trees*, we begin with a simple example.

regression tree

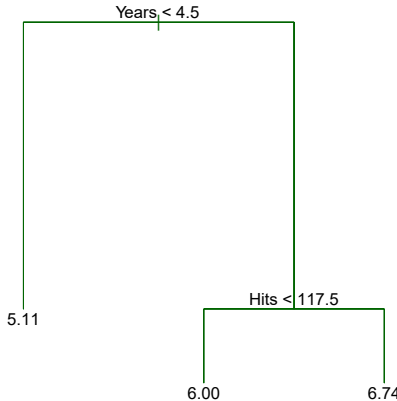


FIGURE 8.1. For the **Hitters** data, a regression tree for predicting the log salary of a baseball player, based on the number of years that he has played in the major leagues and the number of hits that he made in the previous year. At a given internal node, the label (of the form $X_j < t_k$) indicates the left-hand branch emanating from that split, and the right-hand branch corresponds to $X_j \geq t_k$. For instance, the split at the top of the tree results in two large branches. The left-hand branch corresponds to **Years**<4.5, and the right-hand branch corresponds to **Years**>=4.5. The tree has two internal nodes and three terminal nodes, or leaves. The number in each leaf is the mean of the response for the observations that fall there.

Predicting Baseball Players' Salaries Using Regression Trees

We use the **Hitters** data set to predict a baseball player's **Salary** based on **Years** (the number of years that he has played in the major leagues) and **Hits** (the number of hits that he made in the previous year). We first remove observations that are missing **Salary** values, and log-transform **Salary** so that its distribution has more of a typical bell-shape. (Recall that **Salary** is measured in thousands of dollars.)

Figure 8.1 shows a regression tree fit to this data. It consists of a series of splitting rules, starting at the top of the tree. The top split assigns observations having **Years**<4.5 to the left branch.¹ The predicted salary for these players is given by the mean response value for the players in the data set with **Years**<4.5. For such players, the mean log salary is 5.107, and so we make a prediction of $e^{5.107}$ thousands of dollars, i.e. \$165,174, for these players. Players with **Years**>=4.5 are assigned to the right branch, and then that group is further subdivided by **Hits**. Overall, the tree stratifies or segments the players into three regions of predictor space: players who have played for four or fewer years, players who have played for five or more years and who made fewer than 118 hits last year, and players who have played for five or more years and who made at least 118 hits last year. These three regions can be written as $R_1 = \{X \mid \text{Years} < 4.5\}$, $R_2 = \{X \mid \text{Years} \geq 4.5, \text{Hits} < 117.5\}$, and $R_3 = \{X \mid \text{Years} \geq 4.5, \text{Hits} \geq 117.5\}$. Figure 8.2 illustrates

¹Both **Years** and **Hits** are integers in these data; the function used to fit this tree labels the splits at the midpoint between two adjacent values.

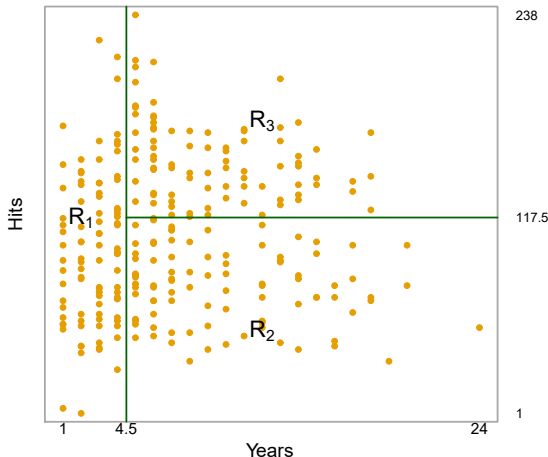


FIGURE 8.2. The three-region partition for the `Hitters` data set from the regression tree illustrated in Figure 8.1.

the regions as a function of `Years` and `Hits`. The predicted salaries for these three groups are $\$1,000 \times e^{5.107} = \$165,174$, $\$1,000 \times e^{5.999} = \$402,834$, and $\$1,000 \times e^{6.740} = \$845,346$ respectively.

In keeping with the *tree* analogy, the regions R_1 , R_2 , and R_3 are known as *terminal nodes* or *leaves* of the tree. As is the case for Figure 8.1, decision trees are typically drawn *upside down*, in the sense that the leaves are at the bottom of the tree. The points along the tree where the predictor space is split are referred to as *internal nodes*. In Figure 8.1, the two internal nodes are indicated by the text `Years<4.5` and `Hits<117.5`. We refer to the segments of the trees that connect the nodes as *branches*.

We might interpret the regression tree displayed in Figure 8.1 as follows: `Years` is the most important factor in determining `Salary`, and players with less experience earn lower salaries than more experienced players. Given that a player is less experienced, the number of hits that he made in the previous year seems to play little role in his salary. But among players who have been in the major leagues for five or more years, the number of hits made in the previous year does affect salary, and players who made more hits last year tend to have higher salaries. The regression tree shown in Figure 8.1 is likely an over-simplification of the true relationship between `Hits`, `Years`, and `Salary`. However, it has advantages over other types of regression models (such as those seen in Chapters 3 and 6): it is easier to interpret, and has a nice graphical representation.

terminal node
leaf
internal node
branch

Prediction via Stratification of the Feature Space

We now discuss the process of building a regression tree. Roughly speaking, there are two steps.

1. We divide the predictor space — that is, the set of possible values for X_1, X_2, \dots, X_p — into J distinct and non-overlapping regions, R_1, R_2, \dots, R_J .

2. For every observation that falls into the region R_j , we make the same prediction, which is simply the mean of the response values for the training observations in R_j .

For instance, suppose that in Step 1 we obtain two regions, R_1 and R_2 , and that the response mean of the training observations in the first region is 10, while the response mean of the training observations in the second region is 20. Then for a given observation $X = x$, if $x \in R_1$ we will predict a value of 10, and if $x \in R_2$ we will predict a value of 20.

We now elaborate on Step 1 above. How do we construct the regions R_1, \dots, R_J ? In theory, the regions could have any shape. However, we choose to divide the predictor space into high-dimensional rectangles, or *boxes*, for simplicity and for ease of interpretation of the resulting predictive model. The goal is to find boxes R_1, \dots, R_J that minimize the RSS, given by

$$\sum_{j=1}^J \sum_{i \in R_j} (y_i - \hat{y}_{R_j})^2, \quad (8.1)$$

where \hat{y}_{R_j} is the mean response for the training observations within the j th box. Unfortunately, it is computationally infeasible to consider every possible partition of the feature space into J boxes. For this reason, we take a *top-down, greedy* approach that is known as *recursive binary splitting*. The approach is *top-down* because it begins at the top of the tree (at which point all observations belong to a single region) and then successively splits the predictor space; each split is indicated via two new branches further down on the tree. It is *greedy* because at each step of the tree-building process, the *best* split is made at that particular step, rather than looking ahead and picking a split that will lead to a better tree in some future step.

recursive
binary
splitting

In order to perform recursive binary splitting, we first select the predictor X_j and the cutpoint s such that splitting the predictor space into the regions $\{X|X_j < s\}$ and $\{X|X_j \geq s\}$ leads to the greatest possible reduction in RSS. (The notation $\{X|X_j < s\}$ means *the region of predictor space in which X_j takes on a value less than s* .) That is, we consider all predictors X_1, \dots, X_p , and all possible values of the cutpoint s for each of the predictors, and then choose the predictor and cutpoint such that the resulting tree has the lowest RSS. In greater detail, for any j and s , we define the pair of half-planes

$$R_1(j, s) = \{X|X_j < s\} \text{ and } R_2(j, s) = \{X|X_j \geq s\}, \quad (8.2)$$

and we seek the value of j and s that minimize the equation

$$\sum_{i: x_i \in R_1(j,s)} (y_i - \hat{y}_{R_1})^2 + \sum_{i: x_i \in R_2(j,s)} (y_i - \hat{y}_{R_2})^2, \quad (8.3)$$

where \hat{y}_{R_1} is the mean response for the training observations in $R_1(j, s)$, and \hat{y}_{R_2} is the mean response for the training observations in $R_2(j, s)$. Finding the values of j and s that minimize (8.3) can be done quite quickly, especially when the number of features p is not too large.

Next, we repeat the process, looking for the best predictor and best cutpoint in order to split the data further so as to minimize the RSS within

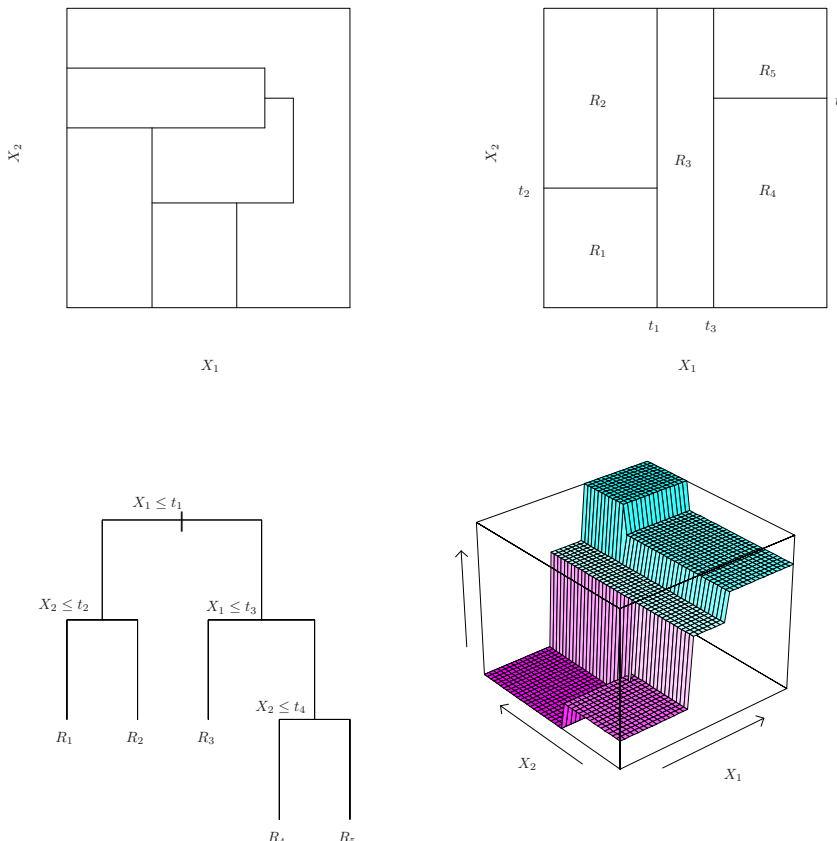


FIGURE 8.3. Top Left: *A partition of two-dimensional feature space that could not result from recursive binary splitting.* Top Right: *The output of recursive binary splitting on a two-dimensional example.* Bottom Left: *A tree corresponding to the partition in the top right panel.* Bottom Right: *A perspective plot of the prediction surface corresponding to that tree.*

each of the resulting regions. However, this time, instead of splitting the entire predictor space, we split one of the two previously identified regions. We now have three regions. Again, we look to split one of these three regions further, so as to minimize the RSS. The process continues until a stopping criterion is reached; for instance, we may continue until no region contains more than five observations.

Once the regions R_1, \dots, R_J have been created, we predict the response for a given test observation using the mean of the training observations in the region to which that test observation belongs.

A five-region example of this approach is shown in Figure 8.3.

Tree Pruning

The process described above may produce good predictions on the training set, but is likely to overfit the data, leading to poor test set performance. This is because the resulting tree might be too complex. A smaller tree

with fewer splits (that is, fewer regions R_1, \dots, R_J) might lead to lower variance and better interpretation at the cost of a little bias. One possible alternative to the process described above is to build the tree only so long as the decrease in the RSS due to each split exceeds some (high) threshold. This strategy will result in smaller trees, but is too short-sighted since a seemingly worthless split early on in the tree might be followed by a very good split—that is, a split that leads to a large reduction in RSS later on.

Therefore, a better strategy is to grow a very large tree T_0 , and then *prune* it back in order to obtain a *subtree*. How do we determine the best way to prune the tree? Intuitively, our goal is to select a subtree that leads to the lowest test error rate. Given a subtree, we can estimate its test error using cross-validation or the validation set approach. However, estimating the cross-validation error for every possible subtree would be too cumbersome, since there is an extremely large number of possible subtrees. Instead, we need a way to select a small set of subtrees for consideration.

Cost complexity pruning—also known as *weakest link pruning*—gives us a way to do just this. Rather than considering every possible subtree, we consider a sequence of trees indexed by a nonnegative tuning parameter α . For each value of α there corresponds a subtree $T \subset T_0$ such that

$$\sum_{m=1}^{|T|} \sum_{i: x_i \in R_m} (y_i - \hat{y}_{R_m})^2 + \alpha|T| \quad (8.4)$$

prune
subtree

cost
complexity
pruning
weakest link
pruning

is as small as possible. Here $|T|$ indicates the number of terminal nodes of the tree T , R_m is the rectangle (i.e. the subset of predictor space) corresponding to the m th terminal node, and \hat{y}_{R_m} is the predicted response associated with R_m —that is, the mean of the training observations in R_m . The tuning parameter α controls a trade-off between the subtree's complexity and its fit to the training data. When $\alpha = 0$, then the subtree T will simply equal T_0 , because then (8.4) just measures the training error. However, as α increases, there is a price to pay for having a tree with many terminal nodes, and so the quantity (8.4) will tend to be minimized for a smaller subtree. Equation 8.4 is reminiscent of the lasso (6.7) from Chapter 6, in which a similar formulation was used in order to control the complexity of a linear model.

It turns out that as we increase α from zero in (8.4), branches get pruned from the tree in a nested and predictable fashion, so obtaining the whole sequence of subtrees as a function of α is easy. We can select a value of α using a validation set or using cross-validation. We then return to the full data set and obtain the subtree corresponding to α . This process is summarized in Algorithm 8.1.

Figures 8.4 and 8.5 display the results of fitting and pruning a regression tree on the **Hitters** data, using nine of the features. First, we randomly divided the data set in half, yielding 132 observations in the training set and 131 observations in the test set. We then built a large regression tree on the training data and varied α in (8.4) in order to create subtrees with different numbers of terminal nodes. Finally, we performed six-fold cross-validation in order to estimate the cross-validated MSE of the trees as

Algorithm 8.1 Building a Regression Tree

-
1. Use recursive binary splitting to grow a large tree on the training data, stopping only when each terminal node has fewer than some minimum number of observations.
 2. Apply cost complexity pruning to the large tree in order to obtain a sequence of best subtrees, as a function of α .
 3. Use K-fold cross-validation to choose α . That is, divide the training observations into K folds. For each $k = 1, \dots, K$:
 - (a) Repeat Steps 1 and 2 on all but the k th fold of the training data.
 - (b) Evaluate the mean squared prediction error on the data in the left-out k th fold, as a function of α .
 Average the results for each value of α , and pick α to minimize the average error.
 4. Return the subtree from Step 2 that corresponds to the chosen value of α .
-

a function of α . (We chose to perform six-fold cross-validation because 132 is an exact multiple of six.) The unpruned regression tree is shown in Figure 8.4. The green curve in Figure 8.5 shows the CV error as a function of the number of leaves,² while the orange curve indicates the test error. Also shown are standard error bars around the estimated errors. For reference, the training error curve is shown in black. The CV error is a reasonable approximation of the test error: the CV error takes on its minimum for a three-node tree, while the test error also dips down at the three-node tree (though it takes on its lowest value at the ten-node tree). The pruned tree containing three terminal nodes is shown in Figure 8.1.

8.1.2 Classification Trees

A *classification tree* is very similar to a regression tree, except that it is used to predict a qualitative response rather than a quantitative one. Recall that for a regression tree, the predicted response for an observation is given by the mean response of the training observations that belong to the same terminal node. In contrast, for a classification tree, we predict that each observation belongs to the *most commonly occurring class* of training observations in the region to which it belongs. In interpreting the results of a classification tree, we are often interested not only in the class prediction corresponding to a particular terminal node region, but also in the *class proportions* among the training observations that fall into that region.

classification
tree

The task of growing a classification tree is quite similar to the task of growing a regression tree. Just as in the regression setting, we use recursive

²Although CV error is computed as a function of α , it is convenient to display the result as a function of $|T|$, the number of leaves; this is based on the relationship between α and $|T|$ in the original tree grown to all the training data.

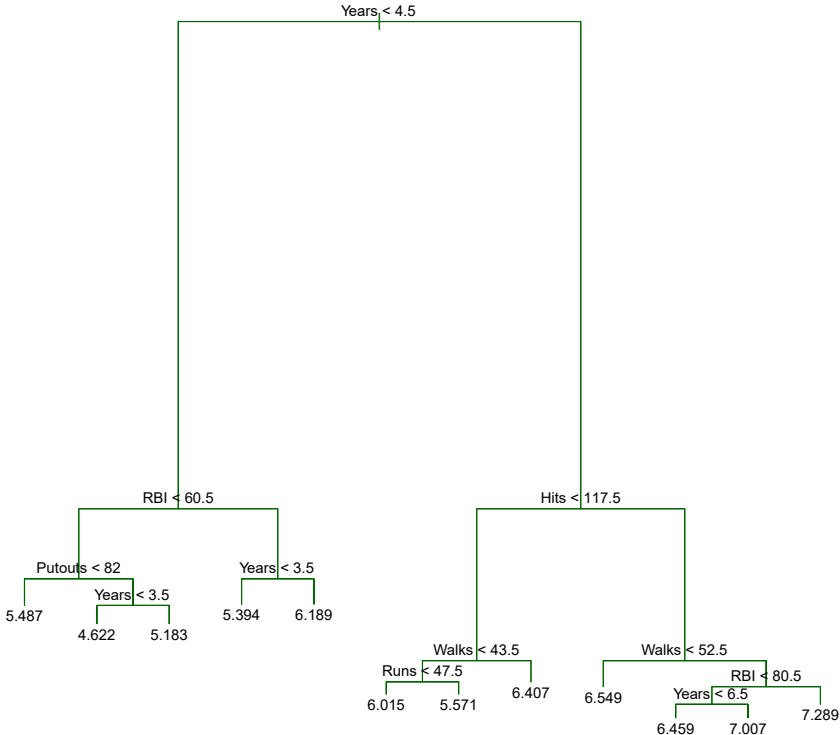


FIGURE 8.4. Regression tree analysis for the `Hitters` data. The unpruned tree that results from top-down greedy splitting on the training data is shown.

binary splitting to grow a classification tree. However, in the classification setting, RSS cannot be used as a criterion for making the binary splits. A natural alternative to RSS is the *classification error rate*. Since we plan to assign an observation in a given region to the *most commonly occurring class* of training observations in that region, the classification error rate is simply the fraction of the training observations in that region that do not belong to the most common class:

$$E = 1 - \max_k(\hat{p}_{mk}). \quad (8.5)$$

Here \hat{p}_{mk} represents the proportion of training observations in the m th region that are from the k th class. However, it turns out that classification error is not sufficiently sensitive for tree-growing, and in practice two other measures are preferable.

The *Gini index* is defined by

classification
error rate

Gini index

$$G = \sum_{k=1}^K \hat{p}_{mk}(1 - \hat{p}_{mk}), \quad (8.6)$$

a measure of total variance across the K classes. It is not hard to see that the Gini index takes on a small value if all of the \hat{p}_{mk} 's are close to zero or one. For this reason the Gini index is referred to as a measure of

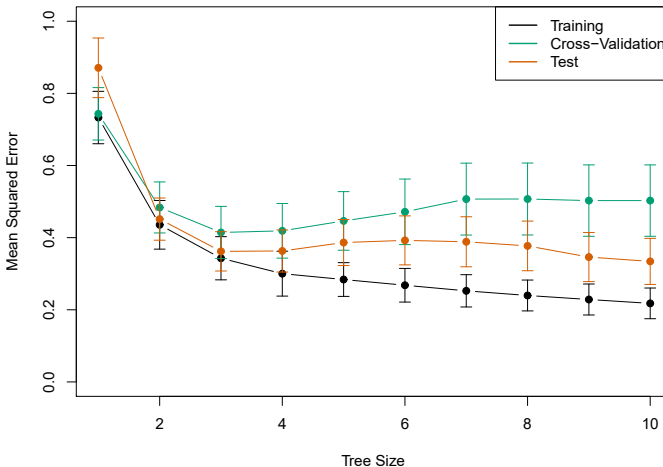


FIGURE 8.5. Regression tree analysis for the `Hitters` data. The training, cross-validation, and test MSE are shown as a function of the number of terminal nodes in the pruned tree. Standard error bands are displayed. The minimum cross-validation error occurs at a tree size of three.

node *purity*—a small value indicates that a node contains predominantly observations from a single class.

An alternative to the Gini index is *entropy*, given by

entropy

$$D = - \sum_{k=1}^K \hat{p}_{mk} \log \hat{p}_{mk}. \quad (8.7)$$

Since $0 \leq \hat{p}_{mk} \leq 1$, it follows that $0 \leq -\hat{p}_{mk} \log \hat{p}_{mk}$. One can show that the entropy will take on a value near zero if the \hat{p}_{mk} 's are all near zero or near one. Therefore, like the Gini index, the entropy will take on a small value if the m th node is pure. In fact, it turns out that the Gini index and the entropy are quite similar numerically.

When building a classification tree, either the Gini index or the entropy are typically used to evaluate the quality of a particular split, since these two approaches are more sensitive to node purity than is the classification error rate. Any of these three approaches might be used when *pruning* the tree, but the classification error rate is preferable if prediction accuracy of the final pruned tree is the goal.

Figure 8.6 shows an example on the `Heart` data set. These data contain a binary outcome `HD` for 303 patients who presented with chest pain. An outcome value of `Yes` indicates the presence of heart disease based on an angiographic test, while `No` means no heart disease. There are 13 predictors including `Age`, `Sex`, `Chol` (a cholesterol measurement), and other heart and lung function measurements. Cross-validation results in a tree with six terminal nodes.

In our discussion thus far, we have assumed that the predictor variables take on continuous values. However, decision trees can be constructed even in the presence of qualitative predictor variables. For instance, in the `Heart` data, some of the predictors, such as `Sex`, `Thal` (Thallium stress test),

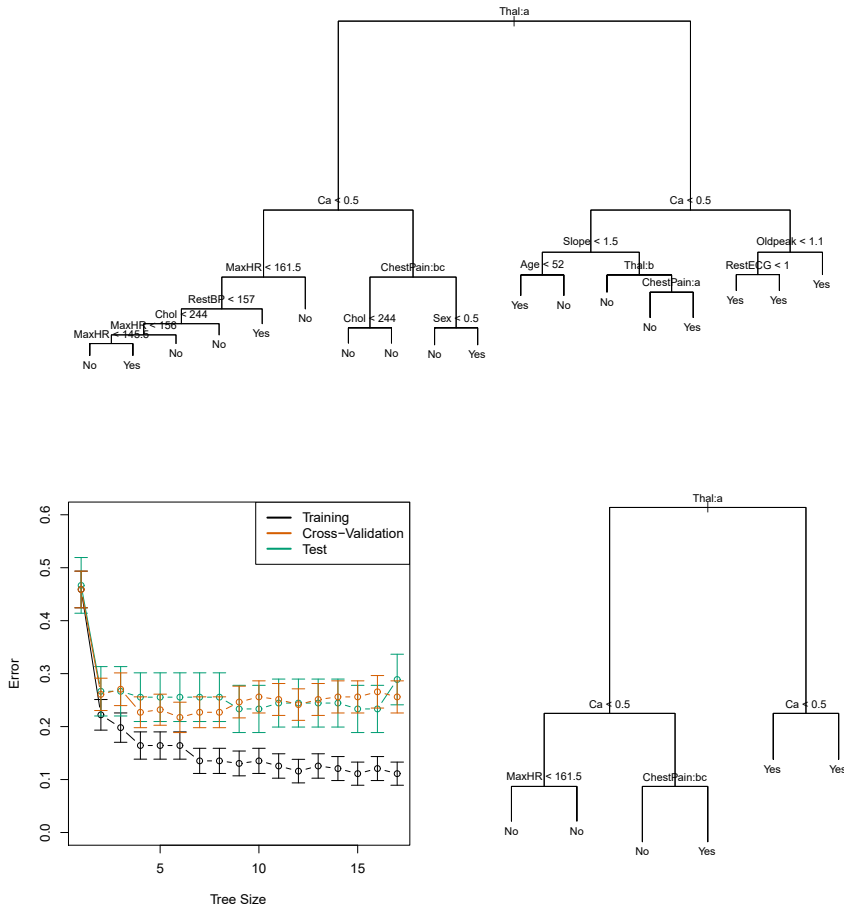


FIGURE 8.6. Heart data. Top: The unpruned tree. Bottom Left: Cross-validation error, training, and test error, for different sizes of the pruned tree. Bottom Right: The pruned tree corresponding to the minimal cross-validation error.

and **ChestPain**, are qualitative. Therefore, a split on one of these variables amounts to assigning some of the qualitative values to one branch and assigning the remaining to the other branch. In Figure 8.6, some of the internal nodes correspond to splitting qualitative variables. For instance, the top internal node corresponds to splitting **Thal**. The text **Thal:a** indicates that the left-hand branch coming out of that node consists of observations with the first value of the **Thal** variable (normal), and the right-hand node consists of the remaining observations (fixed or reversible defects). The text **ChestPain:bc** two splits down the tree on the left indicates that the left-hand branch coming out of that node consists of observations with the second and third values of the **ChestPain** variable, where the possible values are typical angina, atypical angina, non-anginal pain, and asymptomatic.

Figure 8.6 has a surprising characteristic: some of the splits yield two terminal nodes that have the *same predicted value*. For instance, consider the split **RestECG<1** near the bottom right of the unpruned tree. Regardless of the value of **RestECG**, a response value of **Yes** is predicted for those ob-

servations. Why, then, is the split performed at all? The split is performed because it leads to increased *node purity*. That is, all 9 of the observations corresponding to the right-hand leaf have a response value of **Yes**, whereas 7/11 of those corresponding to the left-hand leaf have a response value of **Yes**. Why is node purity important? Suppose that we have a test observation that belongs to the region given by that right-hand leaf. Then we can be pretty certain that its response value is **Yes**. In contrast, if a test observation belongs to the region given by the left-hand leaf, then its response value is probably **Yes**, but we are much less certain. Even though the split `RestECG<1` does not reduce the classification error, it improves the Gini index and the entropy, which are more sensitive to node purity.

8.1.3 Trees Versus Linear Models

Regression and classification trees have a very different flavor from the more classical approaches for regression and classification presented in Chapters 3 and 4. In particular, linear regression assumes a model of the form

$$f(X) = \beta_0 + \sum_{j=1}^p X_j \beta_j, \quad (8.8)$$

whereas regression trees assume a model of the form

$$f(X) = \sum_{m=1}^M c_m \cdot 1_{(X \in R_m)} \quad (8.9)$$

where R_1, \dots, R_M represent a partition of feature space, as in Figure 8.3.

Which model is better? It depends on the problem at hand. If the relationship between the features and the response is well approximated by a linear model as in (8.8), then an approach such as linear regression will likely work well, and will outperform a method such as a regression tree that does not exploit this linear structure. If instead there is a highly non-linear and complex relationship between the features and the response as indicated by model (8.9), then decision trees may outperform classical approaches. An illustrative example is displayed in Figure 8.7. The relative performances of tree-based and classical approaches can be assessed by estimating the test error, using either cross-validation or the validation set approach (Chapter 5).

Of course, other considerations beyond simply test error may come into play in selecting a statistical learning method; for instance, in certain settings, prediction using a tree may be preferred for the sake of interpretability and visualization.

8.1.4 Advantages and Disadvantages of Trees

Decision trees for regression and classification have a number of advantages over the more classical approaches seen in Chapters 3 and 4:

- ▲ Trees are very easy to explain to people. In fact, they are even easier to explain than linear regression!

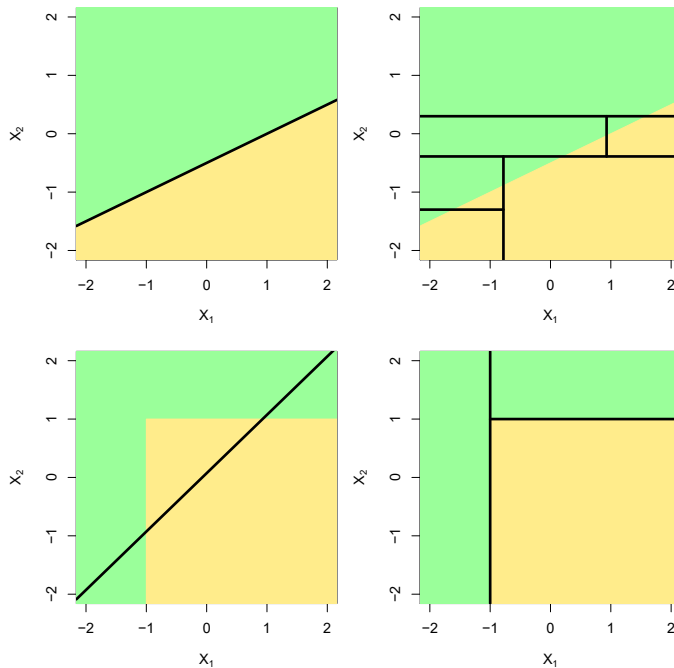


FIGURE 8.7. Top Row: A two-dimensional classification example in which the true decision boundary is linear, and is indicated by the shaded regions. A classical approach that assumes a linear boundary (left) will outperform a decision tree that performs splits parallel to the axes (right). Bottom Row: Here the true decision boundary is non-linear. Here a linear model is unable to capture the true decision boundary (left), whereas a decision tree is successful (right).

- ▲ Some people believe that decision trees more closely mirror human decision-making than do the regression and classification approaches seen in previous chapters.
- ▲ Trees can be displayed graphically, and are easily interpreted even by a non-expert (especially if they are small).
- ▲ Trees can easily handle qualitative predictors without the need to create dummy variables.
- ▼ Unfortunately, trees generally do not have the same level of predictive accuracy as some of the other regression and classification approaches seen in this book.
- ▼ Additionally, trees can be very non-robust. In other words, a small change in the data can cause a large change in the final estimated tree.

However, by aggregating many decision trees, using methods like *bagging*, *random forests*, and *boosting*, the predictive performance of trees can be substantially improved. We introduce these concepts in the next section.

8.2 Bagging, Random Forests, Boosting, and Bayesian Additive Regression Trees

An *ensemble* method is an approach that combines many simple “building block” models in order to obtain a single and potentially very powerful model. These simple building block models are sometimes known as *weak learners*, since they may lead to mediocre predictions on their own.

We will now discuss bagging, random forests, boosting, and Bayesian additive regression trees. These are ensemble methods for which the simple building block is a regression or a classification tree.

8.2.1 Bagging

The bootstrap, introduced in Chapter 5, is an extremely powerful idea. It is used in many situations in which it is hard or even impossible to directly compute the standard deviation of a quantity of interest. We see here that the bootstrap can be used in a completely different context, in order to improve statistical learning methods such as decision trees.

The decision trees discussed in Section 8.1 suffer from *high variance*. This means that if we split the training data into two parts at random, and fit a decision tree to both halves, the results that we get could be quite different. In contrast, a procedure with *low variance* will yield similar results if applied repeatedly to distinct data sets; linear regression tends to have low variance, if the ratio of n to p is moderately large. *Bootstrap aggregation*, or *bagging*, is a general-purpose procedure for reducing the variance of a statistical learning method; we introduce it here because it is particularly useful and frequently used in the context of decision trees.

Recall that given a set of n independent observations Z_1, \dots, Z_n , each with variance σ^2 , the variance of the mean \bar{Z} of the observations is given by σ^2/n . In other words, *averaging a set of observations reduces variance*. Hence a natural way to reduce the variance and increase the test set accuracy of a statistical learning method is to take many training sets from the population, build a separate prediction model using each training set, and average the resulting predictions. In other words, we could calculate $\hat{f}^1(x), \hat{f}^2(x), \dots, \hat{f}^B(x)$ using B separate training sets, and average them in order to obtain a single low-variance statistical learning model, given by

$$\hat{f}_{\text{avg}}(x) = \frac{1}{B} \sum_{b=1}^B \hat{f}^b(x).$$

Of course, this is not practical because we generally do not have access to multiple training sets. Instead, we can bootstrap, by taking repeated samples from the (single) training data set. In this approach we generate B different bootstrapped training data sets. We then train our method on the b th bootstrapped training set in order to get $\hat{f}^{*b}(x)$, and finally average all the predictions, to obtain

$$\hat{f}_{\text{bag}}(x) = \frac{1}{B} \sum_{b=1}^B \hat{f}^{*b}(x).$$

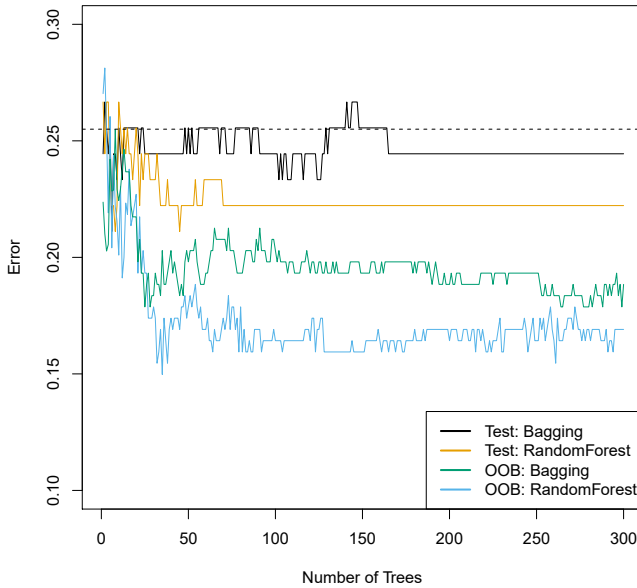


FIGURE 8.8. Bagging and random forest results for the `Heart` data. The test error (black and orange) is shown as a function of B , the number of bootstrapped training sets used. Random forests were applied with $m = \sqrt{p}$. The dashed line indicates the test error resulting from a single classification tree. The green and blue traces show the OOB error, which in this case is — by chance — considerably lower.

This is called bagging.

While bagging can improve predictions for many regression methods, it is particularly useful for decision trees. To apply bagging to regression trees, we simply construct B regression trees using B bootstrapped training sets, and average the resulting predictions. These trees are grown deep, and are not pruned. Hence each individual tree has high variance, but low bias. Averaging these B trees reduces the variance. Bagging has been demonstrated to give impressive improvements in accuracy by combining together hundreds or even thousands of trees into a single procedure.

Thus far, we have described the bagging procedure in the regression context, to predict a quantitative outcome Y . How can bagging be extended to a classification problem where Y is qualitative? In that situation, there are a few possible approaches, but the simplest is as follows. For a given test observation, we can record the class predicted by each of the B trees, and take a *majority vote*: the overall prediction is the most commonly occurring class among the B predictions.

Figure 8.8 shows the results from bagging trees on the `Heart` data. The test error rate is shown as a function of B , the number of trees constructed using bootstrapped training data sets. We see that the bagging test error rate is slightly lower in this case than the test error rate obtained from a single tree. The number of trees B is not a critical parameter with bagging; using a very large value of B will not lead to overfitting. In practice we

majority
vote

use a value of B sufficiently large that the error has settled down. Using $B = 100$ is sufficient to achieve good performance in this example.

Out-of-Bag Error Estimation

It turns out that there is a very straightforward way to estimate the test error of a bagged model, without the need to perform cross-validation or the validation set approach. Recall that the key to bagging is that trees are repeatedly fit to bootstrapped subsets of the observations. One can show that on average, each bagged tree makes use of around two-thirds of the observations.³ The remaining one-third of the observations not used to fit a given bagged tree are referred to as the *out-of-bag* (OOB) observations. We can predict the response for the i th observation using each of the trees in which that observation was OOB. This will yield around $B/3$ predictions for the i th observation. In order to obtain a single prediction for the i th observation, we can average these predicted responses (if regression is the goal) or can take a majority vote (if classification is the goal). This leads to a single OOB prediction for the i th observation. An OOB prediction can be obtained in this way for each of the n observations, from which the overall OOB MSE (for a regression problem) or classification error (for a classification problem) can be computed. The resulting OOB error is a valid estimate of the test error for the bagged model, since the response for each observation is predicted using only the trees that were not fit using that observation. Figure 8.8 displays the OOB error on the **Heart** data. It can be shown that with B sufficiently large, OOB error is virtually equivalent to leave-one-out cross-validation error. The OOB approach for estimating the test error is particularly convenient when performing bagging on large data sets for which cross-validation would be computationally onerous.

out-of-bag

Variable Importance Measures

As we have discussed, bagging typically results in improved accuracy over prediction using a single tree. Unfortunately, however, it can be difficult to interpret the resulting model. Recall that one of the advantages of decision trees is the attractive and easily interpreted diagram that results, such as the one displayed in Figure 8.1. However, when we bag a large number of trees, it is no longer possible to represent the resulting statistical learning procedure using a single tree, and it is no longer clear which variables are most important to the procedure. Thus, bagging improves prediction accuracy at the expense of interpretability.

Although the collection of bagged trees is much more difficult to interpret than a single tree, one can obtain an overall summary of the importance of each predictor using the RSS (for bagging regression trees) or the Gini index (for bagging classification trees). In the case of bagging regression trees, we can record the total amount that the RSS (8.1) is decreased due to splits over a given predictor, averaged over all B trees. A large value indicates an important predictor. Similarly, in the context of bagging classification

³This relates to Exercise 2 of Chapter 5.

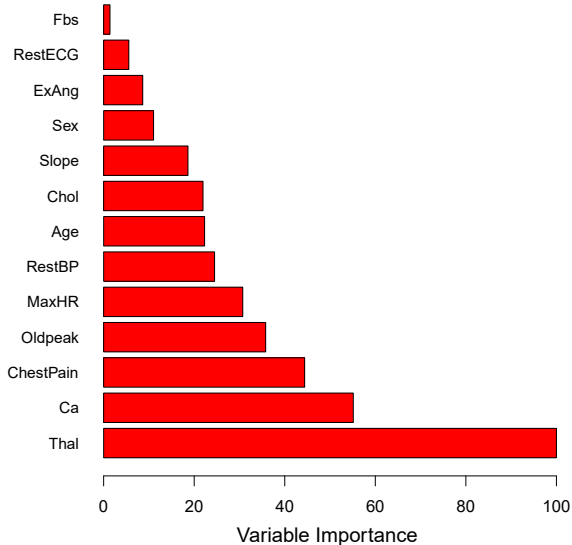


FIGURE 8.9. A variable importance plot for the `Heart` data. Variable importance is computed using the mean decrease in Gini index, and expressed relative to the maximum.

trees, we can add up the total amount that the Gini index (8.6) is decreased by splits over a given predictor, averaged over all B trees.

A graphical representation of the *variable importances* in the `Heart` data is shown in Figure 8.9. We see the mean decrease in Gini index for each variable, relative to the largest. The variables with the largest mean decrease in Gini index are `Thal`, `Ca`, and `ChestPain`.

variable
importance

8.2.2 Random Forests

Random forests provide an improvement over bagged trees by way of a small tweak that *decorrelates* the trees. As in bagging, we build a number of decision trees on bootstrapped training samples. But when building these decision trees, each time a split in a tree is considered, *a random sample of m predictors* is chosen as split candidates from the full set of p predictors. The split is allowed to use only one of those m predictors. A fresh sample of m predictors is taken at each split, and typically we choose $m \approx \sqrt{p}$ —that is, the number of predictors considered at each split is approximately equal to the square root of the total number of predictors (4 out of the 13 for the `Heart` data).

random
forest

In other words, in building a random forest, at each split in the tree, the algorithm is *not even allowed to consider* a majority of the available predictors. This may sound crazy, but it has a clever rationale. Suppose that there is one very strong predictor in the data set, along with a number of other moderately strong predictors. Then in the collection of bagged trees, most or all of the trees will use this strong predictor in the top split. Consequently, all of the bagged trees will look quite similar to each other.

Hence the predictions from the bagged trees will be highly correlated. Unfortunately, averaging many highly correlated quantities does not lead to as large of a reduction in variance as averaging many uncorrelated quantities. In particular, this means that bagging will not lead to a substantial reduction in variance over a single tree in this setting.

Random forests overcome this problem by forcing each split to consider only a subset of the predictors. Therefore, on average $(p - m)/p$ of the splits will not even consider the strong predictor, and so other predictors will have more of a chance. We can think of this process as *decorrelating* the trees, thereby making the average of the resulting trees less variable and hence more reliable.

The main difference between bagging and random forests is the choice of predictor subset size m . For instance, if a random forest is built using $m = p$, then this amounts simply to bagging. On the `Heart` data, random forests using $m = \sqrt{p}$ leads to a reduction in both test error and OOB error over bagging (Figure 8.8).

Using a small value of m in building a random forest will typically be helpful when we have a large number of correlated predictors. We applied random forests to a high-dimensional biological data set consisting of expression measurements of 4,718 genes measured on tissue samples from 349 patients. There are around 20,000 genes in humans, and individual genes have different levels of activity, or expression, in particular cells, tissues, and biological conditions. In this data set, each of the patient samples has a qualitative label with 15 different levels: either normal or 1 of 14 different types of cancer. Our goal was to use random forests to predict cancer type based on the 500 genes that have the largest variance in the training set. We randomly divided the observations into a training and a test set, and applied random forests to the training set for three different values of the number of splitting variables m . The results are shown in Figure 8.10. The error rate of a single tree is 45.7 %, and the null rate is 75.4 %.⁴ We see that using 400 trees is sufficient to give good performance, and that the choice $m = \sqrt{p}$ gave a small improvement in test error over bagging ($m = p$) in this example. As with bagging, random forests will not overfit if we increase B , so in practice we use a value of B sufficiently large for the error rate to have settled down.

8.2.3 Boosting

We now discuss *boosting*, yet another approach for improving the predictions resulting from a decision tree. Like bagging, boosting is a general approach that can be applied to many statistical learning methods for regression or classification. Here we restrict our discussion of boosting to the context of decision trees.

boosting

Recall that bagging involves creating multiple copies of the original training data set using the bootstrap, fitting a separate decision tree to each copy, and then combining all of the trees in order to create a single predic-

⁴The null rate results from simply classifying each observation to the dominant class overall, which is in this case the normal class.

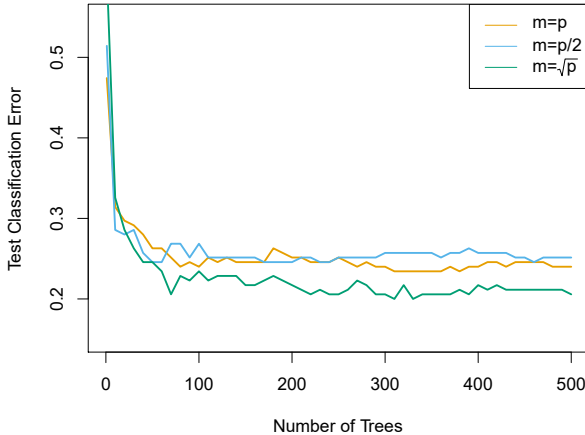


FIGURE 8.10. Results from random forests for the 15-class gene expression data set with $p = 500$ predictors. The test error is displayed as a function of the number of trees. Each colored line corresponds to a different value of m , the number of predictors available for splitting at each interior tree node. Random forests ($m < p$) lead to a slight improvement over bagging ($m = p$). A single classification tree has an error rate of 45.7%.

tive model. Notably, each tree is built on a bootstrap data set, independent of the other trees. Boosting works in a similar way, except that the trees are grown *sequentially*: each tree is grown using information from previously grown trees. Boosting does not involve bootstrap sampling; instead each tree is fit on a modified version of the original data set.

Consider first the regression setting. Like bagging, boosting involves combining a large number of decision trees, $\hat{f}^1, \dots, \hat{f}^B$. Boosting is described in Algorithm 8.2.

What is the idea behind this procedure? Unlike fitting a single large decision tree to the data, which amounts to *fitting the data hard* and potentially overfitting, the boosting approach instead *learns slowly*. Given the current model, we fit a decision tree to the residuals from the model. That is, we fit a tree using the current residuals, rather than the outcome Y , as the response. We then add this new decision tree into the fitted function in order to update the residuals. Each of these trees can be rather small, with just a few terminal nodes, determined by the parameter d in the algorithm. By fitting small trees to the residuals, we slowly improve \hat{f} in areas where it does not perform well. The shrinkage parameter λ slows the process down even further, allowing more and different shaped trees to attack the residuals. In general, statistical learning approaches that *learn slowly* tend to perform well. Note that in boosting, unlike in bagging, the construction of each tree depends strongly on the trees that have already been grown.

We have just described the process of boosting regression trees. Boosting classification trees proceeds in a similar but slightly more complex way, and the details are omitted here.

Algorithm 8.2 *Boosting for Regression Trees*

-
1. Set $\hat{f}(x) = 0$ and $r_i = y_i$ for all i in the training set.
 2. For $b = 1, 2, \dots, B$, repeat:
 - (a) Fit a tree \hat{f}^b with d splits ($d + 1$ terminal nodes) to the training data (X, r) .
 - (b) Update \hat{f} by adding in a shrunken version of the new tree:

$$\hat{f}(x) \leftarrow \hat{f}(x) + \lambda \hat{f}^b(x). \quad (8.10)$$

- (c) Update the residuals,

$$r_i \leftarrow r_i - \lambda \hat{f}^b(x_i). \quad (8.11)$$

3. Output the boosted model,

$$\hat{f}(x) = \sum_{b=1}^B \lambda \hat{f}^b(x). \quad (8.12)$$

Boosting has three tuning parameters:

1. The number of trees B . Unlike bagging and random forests, boosting can overfit if B is too large, although this overfitting tends to occur slowly if at all. We use cross-validation to select B .
2. The shrinkage parameter λ , a small positive number. This controls the rate at which boosting learns. Typical values are 0.01 or 0.001, and the right choice can depend on the problem. Very small λ can require using a very large value of B in order to achieve good performance.
3. The number d of splits in each tree, which controls the complexity of the boosted ensemble. Often $d = 1$ works well, in which case each tree is a *stump*, consisting of a single split. In this case, the boosted ensemble is fitting an additive model, since each term involves only a single variable. More generally d is the *interaction depth*, and controls the interaction order of the boosted model, since d splits can involve at most d variables.

stump

interaction
depth

In Figure 8.11, we applied boosting to the 15-class cancer gene expression data set, in order to develop a classifier that can distinguish the normal class from the 14 cancer classes. We display the test error as a function of the total number of trees and the interaction depth d . We see that simple stumps with an interaction depth of one perform well if enough of them are included. This model outperforms the depth-two model, and both outperform a random forest. This highlights one difference between boosting and random forests: in boosting, because the growth of a particular tree takes into account the other trees that have already been grown, smaller

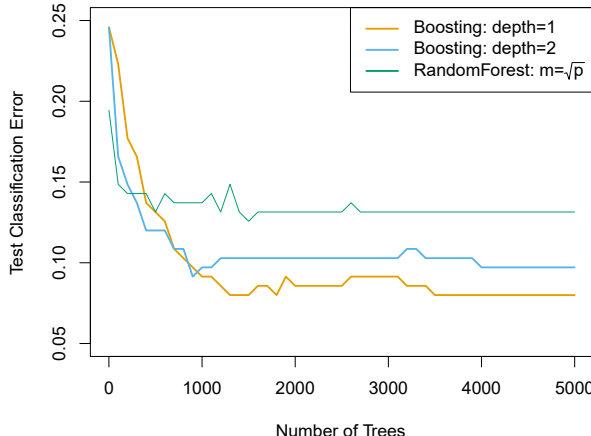


FIGURE 8.11. Results from performing boosting and random forests on the 15-class gene expression data set in order to predict cancer versus normal. The test error is displayed as a function of the number of trees. For the two boosted models, $\lambda = 0.01$. Depth-1 trees slightly outperform depth-2 trees, and both outperform the random forest, although the standard errors are around 0.02, making none of these differences significant. The test error rate for a single tree is 24 %.

trees are typically sufficient. Using smaller trees can aid in interpretability as well; for instance, using stumps leads to an additive model.

8.2.4 Bayesian Additive Regression Trees

Finally, we discuss *Bayesian additive regression trees* (BART), another ensemble method that uses decision trees as its building blocks. For simplicity, we present BART for regression (as opposed to classification).

Recall that bagging and random forests make predictions from an average of regression trees, each of which is built using a random sample of data and/or predictors. Each tree is built separately from the others. By contrast, boosting uses a weighted sum of trees, each of which is constructed by fitting a tree to the residual of the current fit. Thus, each new tree attempts to capture signal that is not yet accounted for by the current set of trees. BART is related to both approaches: each tree is constructed in a random manner as in bagging and random forests, and each tree tries to capture signal not yet accounted for by the current model, as in boosting. The main novelty in BART is the way in which new trees are generated.

Bayesian additive regression trees

Before we introduce the BART algorithm, we define some notation. We let K denote the number of regression trees, and B the number of iterations for which the BART algorithm will be run. The notation $\hat{f}_k^b(x)$ represents the prediction at x for the k th regression tree used in the b th iteration. At the end of each iteration, the K trees from that iteration will be summed, i.e. $\hat{f}^b(x) = \sum_{k=1}^K \hat{f}_k^b(x)$ for $b = 1, \dots, B$.

In the first iteration of the BART algorithm, all trees are initialized to have a single root node, with $\hat{f}_k^1(x) = \frac{1}{nK} \sum_{i=1}^n y_i$, the mean of the response

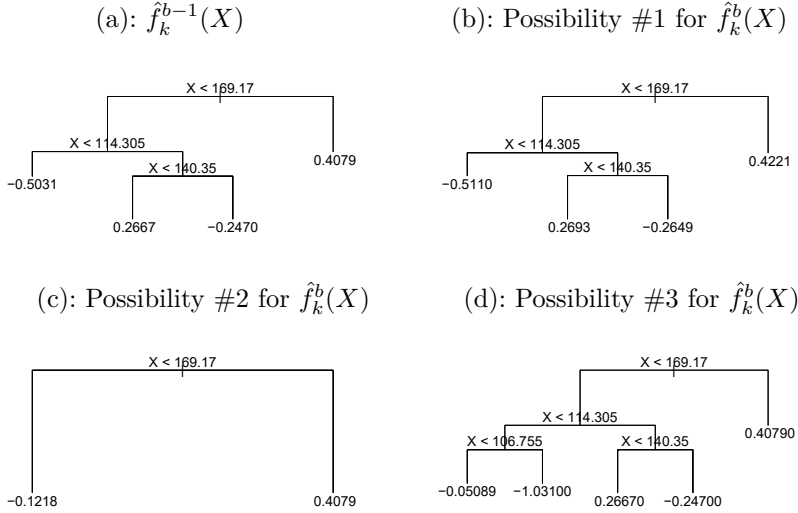


FIGURE 8.12. A schematic of perturbed trees from the BART algorithm. (a): The k th tree at the $(b-1)$ st iteration, $\hat{f}_k^{b-1}(X)$, is displayed. Panels (b)–(d) display three of many possibilities for $\hat{f}_k^b(X)$, given the form of $\hat{f}_k^{b-1}(X)$. (b): One possibility is that $\hat{f}_k^b(X)$ has the same structure as $\hat{f}_k^{b-1}(X)$, but with different predictions at the terminal nodes. (c): Another possibility is that $\hat{f}_k^b(X)$ results from pruning $\hat{f}_k^{b-1}(X)$. (d): Alternatively, $\hat{f}_k^b(X)$ may have more terminal nodes than $\hat{f}_k^{b-1}(X)$.

values divided by the total number of trees. Thus, $\hat{f}^1(x) = \sum_{k=1}^K \hat{f}_k^1(x) = \frac{1}{n} \sum_{i=1}^n y_i$.

In subsequent iterations, BART updates each of the K trees, one at a time. In the b th iteration, to update the k th tree, we subtract from each response value the predictions from all but the k th tree, in order to obtain a *partial residual*

$$r_i = y_i - \sum_{k' < k} \hat{f}_{k'}^b(x_i) - \sum_{k' > k} \hat{f}_{k'}^{b-1}(x_i)$$

for the i th observation, $i = 1, \dots, n$. Rather than fitting a fresh tree to this partial residual, BART randomly chooses a perturbation to the tree from the previous iteration (\hat{f}_k^{b-1}) from a set of possible perturbations, favoring ones that improve the fit to the partial residual. There are two components to this perturbation:

1. We may change the structure of the tree by adding or pruning branches.
2. We may change the prediction in each terminal node of the tree.

Figure 8.12 illustrates examples of possible perturbations to a tree.

The output of BART is a collection of prediction models,

$$\hat{f}^b(x) = \sum_{k=1}^K \hat{f}_k^b(x), \text{ for } b = 1, 2, \dots, B.$$

Algorithm 8.3 Bayesian Additive Regression Trees

1. Let $\hat{f}_1^1(x) = \hat{f}_2^1(x) = \dots = \hat{f}_K^1(x) = \frac{1}{nK} \sum_{i=1}^n y_i$.

2. Compute $\hat{f}^1(x) = \sum_{k=1}^K \hat{f}_k^1(x) = \frac{1}{n} \sum_{i=1}^n y_i$.

3. For $b = 2, \dots, B$:

(a) For $k = 1, 2, \dots, K$:

i. For $i = 1, \dots, n$, compute the current partial residual

$$r_i = y_i - \sum_{k' < k} \hat{f}_{k'}^b(x_i) - \sum_{k' > k} \hat{f}_{k'}^{b-1}(x_i).$$

ii. Fit a new tree, $\hat{f}_k^b(x)$, to r_i , by randomly perturbing the k th tree from the previous iteration, $\hat{f}_k^{b-1}(x)$. Perturbations that improve the fit are favored.

(b) Compute $\hat{f}^b(x) = \sum_{k=1}^K \hat{f}_k^b(x)$.

4. Compute the mean after L burn-in samples,

$$\hat{f}(x) = \frac{1}{B-L} \sum_{b=L+1}^B \hat{f}^b(x).$$

We typically throw away the first few of these prediction models, since models obtained in the earlier iterations — known as the *burn-in* period — tend not to provide very good results. We can let L denote the number of burn-in iterations; for instance, we might take $L = 200$. Then, to obtain a single prediction, we simply take the average after the burn-in iterations, $\hat{f}(x) = \frac{1}{B-L} \sum_{b=L+1}^B \hat{f}^b(x)$. However, it is also possible to compute quantities other than the average: for instance, the percentiles of $\hat{f}^{L+1}(x), \dots, \hat{f}^B(x)$ provide a measure of uncertainty in the final prediction. The overall BART procedure is summarized in Algorithm 8.3.

burn-in

A key element of the BART approach is that in Step 3(a)ii., we do *not* fit a fresh tree to the current partial residual: instead, we try to improve the fit to the current partial residual by slightly modifying the tree obtained in the previous iteration (see Figure 8.12). Roughly speaking, this guards against overfitting since it limits how “hard” we fit the data in each iteration. Furthermore, the individual trees are typically quite small. We limit the tree size in order to avoid overfitting the data, which would be more likely to occur if we grew very large trees.

Figure 8.13 shows the result of applying BART to the **Heart** data, using $K = 200$ trees, as the number of iterations is increased to 10,000. During the initial iterations, the test and training errors jump around a bit. After this initial burn-in period, the error rates settle down. We note that there is only a small difference between the training error and the test error, indicating that the tree perturbation process largely avoids overfitting.

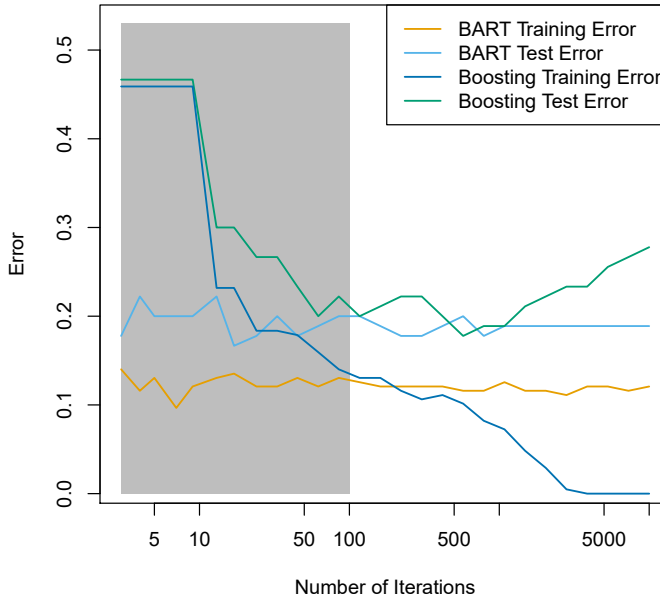


FIGURE 8.13. BART and boosting results for the [Heart](#) data. Both training and test errors are displayed. After a burn-in period of 100 iterations (shown in gray), the error rates for BART settle down. Boosting begins to overfit after a few hundred iterations.

The training and test errors for boosting are also displayed in Figure 8.13. We see that the test error for boosting approaches that of BART, but then begins to increase as the number of iterations increases. Furthermore, the training error for boosting decreases as the number of iterations increases, indicating that boosting has overfit the data.

Though the details are outside of the scope of this book, it turns out that the BART method can be viewed as a *Bayesian* approach to fitting an ensemble of trees: each time we randomly perturb a tree in order to fit the residuals, we are in fact drawing a new tree from a *posterior* distribution. (Of course, this Bayesian connection is the motivation for BART’s name.) Furthermore, Algorithm 8.3 can be viewed as a *Markov chain Monte Carlo* algorithm for fitting the BART model.

When we apply BART, we must select the number of trees K , the number of iterations B , and the number of burn-in iterations L . We typically choose large values for B and K , and a moderate value for L : for instance, $K = 200$, $B = 1,000$, and $L = 100$ is a reasonable choice. BART has been shown to have very impressive out-of-box performance — that is, it performs well with minimal tuning.

Markov
chain Monte
Carlo

8.2.5 Summary of Tree Ensemble Methods

Trees are an attractive choice of weak learner for an ensemble method for a number of reasons, including their flexibility and ability to handle

predictors of mixed types (i.e. qualitative as well as quantitative). We have now seen four approaches for fitting an ensemble of trees: bagging, random forests, boosting, and BART.

- In *bagging*, the trees are grown independently on random samples of the observations. Consequently, the trees tend to be quite similar to each other. Thus, bagging can get caught in local optima and can fail to thoroughly explore the model space.
- In *random forests*, the trees are once again grown independently on random samples of the observations. However, each split on each tree is performed using a random subset of the features, thereby decorrelating the trees, and leading to a more thorough exploration of model space relative to bagging.
- In *boosting*, we only use the original data, and do not draw any random samples. The trees are grown successively, using a “slow” learning approach: each new tree is fit to the signal that is left over from the earlier trees, and shrunken down before it is used.
- In *BART*, we once again only make use of the original data, and we grow the trees successively. However, each tree is perturbed in order to avoid local minima and achieve a more thorough exploration of the model space.

8.3 Lab: Tree-Based Methods

We import some of our usual libraries at this top level.

```
In [1]: import numpy as np
import pandas as pd
from matplotlib.pyplot import subplots
from statsmodels.datasets import get_rdataset
import sklearn.model_selection as skm
from ISLP import load_data, confusion_table
from ISLP.models import ModelSpec as MS
```

We also collect the new imports needed for this lab.

```
In [2]: from sklearn.tree import (DecisionTreeClassifier as DTC,
                               DecisionTreeRegressor as DTR,
                               plot_tree,
                               export_text)
from sklearn.metrics import (accuracy_score,
                             log_loss)
from sklearn.ensemble import \
    (RandomForestRegressor as RF,
     GradientBoostingRegressor as GBR)
from ISLP.bart import BART
```

```
In [35]: var_inclusion = pd.Series(bart_boston.variable_inclusion_.mean(0),
                                 index=D.columns)
var_inclusion
```

```
Out[35]:    crim      25.333333
              zn       27.000000
            indus     21.266667
            chas      20.466667
            nox       25.400000
            rm        32.400000
            age       26.133333
            dis       25.666667
            rad       24.666667
            tax       23.933333
          ptratio     25.000000
           lstat     31.866667
dtype: float64
```

8.4 Exercises

Conceptual

1. Draw an example (of your own invention) of a partition of two-dimensional feature space that could result from recursive binary splitting. Your example should contain at least six regions. Draw a decision tree corresponding to this partition. Be sure to label all aspects of your figures, including the regions R_1, R_2, \dots , the cutpoints t_1, t_2, \dots , and so forth.

Hint: Your result should look something like Figures 8.1 and 8.2.

2. It is mentioned in Section 8.2.3 that boosting using depth-one trees (or *stumps*) leads to an *additive* model: that is, a model of the form

$$f(X) = \sum_{j=1}^p f_j(X_j).$$

Explain why this is the case. You can begin with (8.12) in Algorithm 8.2.

3. Consider the Gini index, classification error, and entropy in a simple classification setting with two classes. Create a single plot that displays each of these quantities as a function of \hat{p}_{m1} . The x -axis should display \hat{p}_{m1} , ranging from 0 to 1, and the y -axis should display the value of the Gini index, classification error, and entropy.

Hint: In a setting with two classes, $\hat{p}_{m1} = 1 - \hat{p}_{m2}$. You could make this plot by hand, but it will be much easier to make in R.

4. This question relates to the plots in Figure 8.14.

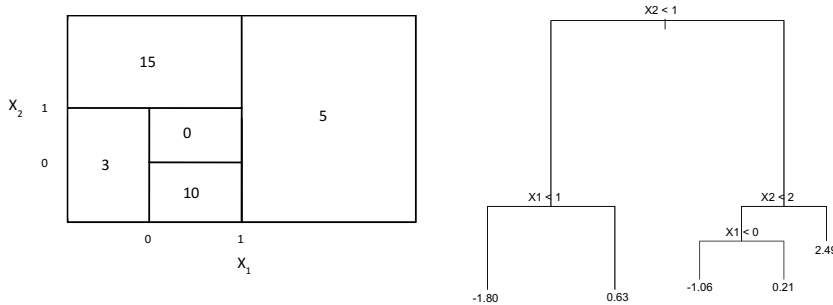


FIGURE 8.14. Left: A partition of the predictor space corresponding to Exercise 4a. Right: A tree corresponding to Exercise 4b.

- (a) Sketch the tree corresponding to the partition of the predictor space illustrated in the left-hand panel of Figure 8.14. The numbers inside the boxes indicate the mean of Y within each region.
 - (b) Create a diagram similar to the left-hand panel of Figure 8.14, using the tree illustrated in the right-hand panel of the same figure. You should divide up the predictor space into the correct regions, and indicate the mean for each region.
5. Suppose we produce ten bootstrapped samples from a data set containing red and green classes. We then apply a classification tree to each bootstrapped sample and, for a specific value of X , produce 10 estimates of $P(\text{Class is Red}|X)$:
- $$0.1, 0.15, 0.2, 0.2, 0.55, 0.6, 0.6, 0.65, 0.7, \text{ and } 0.75.$$
- There are two common ways to combine these results together into a single class prediction. One is the majority vote approach discussed in this chapter. The second approach is to classify based on the average probability. In this example, what is the final classification under each of these two approaches?
6. Provide a detailed explanation of the algorithm that is used to fit a regression tree.

Applied

- 7. In Section 8.3.3, we applied random forests to the `Boston` data using `max_features = 6` and using `n_estimators = 100` and `n_estimators = 500`. Create a plot displaying the test error resulting from random forests on this data set for a more comprehensive range of values for `max_features` and `n_estimators`. You can model your plot after Figure 8.10. Describe the results obtained.
- 8. In the lab, a classification tree was applied to the `Carseats` data set after converting `Sales` into a qualitative response variable. Now we will seek to predict `Sales` using regression trees and related approaches, treating the response as a quantitative variable.

- (a) Split the data set into a training set and a test set.
 - (b) Fit a regression tree to the training set. Plot the tree, and interpret the results. What test MSE do you obtain?
 - (c) Use cross-validation in order to determine the optimal level of tree complexity. Does pruning the tree improve the test MSE?
 - (d) Use the bagging approach in order to analyze this data. What test MSE do you obtain? Use the `feature_importance_` values to determine which variables are most important.
 - (e) Use random forests to analyze this data. What test MSE do you obtain? Use the `feature_importance_` values to determine which variables are most important. Describe the effect of m , the number of variables considered at each split, on the error rate obtained.
 - (f) Now analyze the data using BART, and report your results.
9. This problem involves the `OJ` data set which is part of the `ISLR` package.
- (a) Create a training set containing a random sample of 800 observations, and a test set containing the remaining observations.
 - (b) Fit a tree to the training data, with `Purchase` as the response and the other variables as predictors. What is the training error rate?
 - (c) Create a plot of the tree, and interpret the results. How many terminal nodes does the tree have?
 - (d) Use the `export_tree()` function to produce a text summary of the fitted tree. Pick one of the terminal nodes, and interpret the information displayed.
 - (e) Predict the response on the test data, and produce a confusion matrix comparing the test labels to the predicted test labels. What is the test error rate?
 - (f) Use cross-validation on the training set in order to determine the optimal tree size.
 - (g) Produce a plot with tree size on the x -axis and cross-validated classification error rate on the y -axis.
 - (h) Which tree size corresponds to the lowest cross-validated classification error rate?
 - (i) Produce a pruned tree corresponding to the optimal tree size obtained using cross-validation. If cross-validation does not lead to selection of a pruned tree, then create a pruned tree with five terminal nodes.
 - (j) Compare the training error rates between the pruned and unpruned trees. Which is higher?
 - (k) Compare the test error rates between the pruned and unpruned trees. Which is higher?

10. We now use boosting to predict **Salary** in the **Hitters** data set.
 - (a) Remove the observations for whom the salary information is unknown, and then log-transform the salaries.
 - (b) Create a training set consisting of the first 200 observations, and a test set consisting of the remaining observations.
 - (c) Perform boosting on the training set with 1,000 trees for a range of values of the shrinkage parameter λ . Produce a plot with different shrinkage values on the x -axis and the corresponding training set MSE on the y -axis.
 - (d) Produce a plot with different shrinkage values on the x -axis and the corresponding test set MSE on the y -axis.
 - (e) Compare the test MSE of boosting to the test MSE that results from applying two of the regression approaches seen in Chapters 3 and 6.
 - (f) Which variables appear to be the most important predictors in the boosted model?
 - (g) Now apply bagging to the training set. What is the test set MSE for this approach?
11. This question uses the **Caravan** data set.
 - (a) Create a training set consisting of the first 1,000 observations, and a test set consisting of the remaining observations.
 - (b) Fit a boosting model to the training set with **Purchase** as the response and the other variables as predictors. Use 1,000 trees, and a shrinkage value of 0.01. Which predictors appear to be the most important?
 - (c) Use the boosting model to predict the response on the test data. Predict that a person will make a purchase if the estimated probability of purchase is greater than 20 %. Form a confusion matrix. What fraction of the people predicted to make a purchase do in fact make one? How does this compare with the results obtained from applying KNN or logistic regression to this data set?
12. Apply boosting, bagging, random forests, and BART to a data set of your choice. Be sure to fit the models on a training set and to evaluate their performance on a test set. How accurate are the results compared to simple methods like linear or logistic regression? Which of these approaches yields the best performance?



Support Vector Machines

In this chapter, we discuss the *support vector machine* (SVM), an approach for classification that was developed in the computer science community in the 1990s and that has grown in popularity since then. SVMs have been shown to perform well in a variety of settings, and are often considered one of the best “out of the box” classifiers.

The support vector machine is a generalization of a simple and intuitive classifier called the *maximal margin classifier*, which we introduce in Section 9.1. Though it is elegant and simple, we will see that this classifier unfortunately cannot be applied to most data sets, since it requires that the classes be separable by a linear boundary. In Section 9.2, we introduce the *support vector classifier*, an extension of the maximal margin classifier that can be applied in a broader range of cases. Section 9.3 introduces the *support vector machine*, which is a further extension of the support vector classifier in order to accommodate non-linear class boundaries. Support vector machines are intended for the binary classification setting in which there are two classes; in Section 9.4 we discuss extensions of support vector machines to the case of more than two classes. In Section 9.5 we discuss the close connections between support vector machines and other statistical methods such as logistic regression.

People often loosely refer to the maximal margin classifier, the support vector classifier, and the support vector machine as “support vector machines”. To avoid confusion, we will carefully distinguish between these three notions in this chapter.

9.1 Maximal Margin Classifier

In this section, we define a hyperplane and introduce the concept of an optimal separating hyperplane.

9.1.1 What Is a Hyperplane?

In a p -dimensional space, a *hyperplane* is a flat affine subspace of dimension $p - 1$.¹ For instance, in two dimensions, a hyperplane is a flat one-dimensional subspace—in other words, a line. In three dimensions, a hyperplane is a flat two-dimensional subspace—that is, a plane. In $p > 3$ dimensions, it can be hard to visualize a hyperplane, but the notion of a $(p - 1)$ -dimensional flat subspace still applies.

The mathematical definition of a hyperplane is quite simple. In two dimensions, a hyperplane is defined by the equation

$$\beta_0 + \beta_1 X_1 + \beta_2 X_2 = 0 \quad (9.1)$$

for parameters β_0, β_1 , and β_2 . When we say that (9.1) “defines” the hyperplane, we mean that any $X = (X_1, X_2)^T$ for which (9.1) holds is a point on the hyperplane. Note that (9.1) is simply the equation of a line, since indeed in two dimensions a hyperplane is a line.

Equation 9.1 can be easily extended to the p -dimensional setting:

$$\beta_0 + \beta_1 X_1 + \beta_2 X_2 + \cdots + \beta_p X_p = 0 \quad (9.2)$$

defines a p -dimensional hyperplane, again in the sense that if a point $X = (X_1, X_2, \dots, X_p)^T$ in p -dimensional space (i.e. a vector of length p) satisfies (9.2), then X lies on the hyperplane.

Now, suppose that X does not satisfy (9.2); rather,

$$\beta_0 + \beta_1 X_1 + \beta_2 X_2 + \cdots + \beta_p X_p > 0. \quad (9.3)$$

Then this tells us that X lies to one side of the hyperplane. On the other hand, if

$$\beta_0 + \beta_1 X_1 + \beta_2 X_2 + \cdots + \beta_p X_p < 0, \quad (9.4)$$

then X lies on the other side of the hyperplane. So we can think of the hyperplane as dividing p -dimensional space into two halves. One can easily determine on which side of the hyperplane a point lies by simply calculating the sign of the left-hand side of (9.2). A hyperplane in two-dimensional space is shown in Figure 9.1.

9.1.2 Classification Using a Separating Hyperplane

Now suppose that we have an $n \times p$ data matrix \mathbf{X} that consists of n training observations in p -dimensional space,

$$x_1 = \begin{pmatrix} x_{11} \\ \vdots \\ x_{1p} \end{pmatrix}, \dots, x_n = \begin{pmatrix} x_{n1} \\ \vdots \\ x_{np} \end{pmatrix}, \quad (9.5)$$

and that these observations fall into two classes—that is, $y_1, \dots, y_n \in \{-1, 1\}$ where -1 represents one class and 1 the other class. We also have a

¹The word *affine* indicates that the subspace need not pass through the origin.

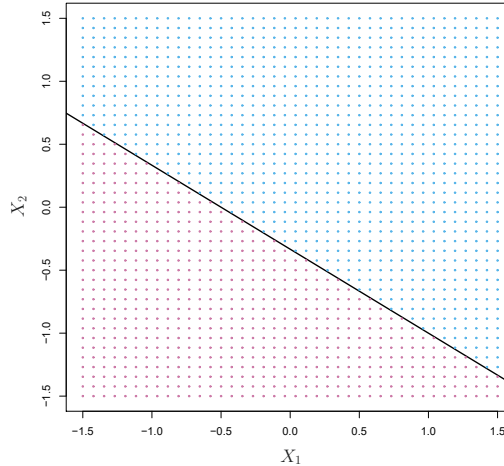


FIGURE 9.1. The hyperplane $1 + 2X_1 + 3X_2 = 0$ is shown. The blue region is the set of points for which $1 + 2X_1 + 3X_2 > 0$, and the purple region is the set of points for which $1 + 2X_1 + 3X_2 < 0$.

test observation, a p -vector of observed features $x^* = (x_1^* \dots x_p^*)^T$. Our goal is to develop a classifier based on the training data that will correctly classify the test observation using its feature measurements. We have seen a number of approaches for this task, such as linear discriminant analysis and logistic regression in Chapter 4, and classification trees, bagging, and boosting in Chapter 8. We will now see a new approach that is based upon the concept of a *separating hyperplane*.

Suppose that it is possible to construct a hyperplane that separates the training observations perfectly according to their class labels. Examples of three such *separating hyperplanes* are shown in the left-hand panel of Figure 9.2. We can label the observations from the blue class as $y_i = 1$ and those from the purple class as $y_i = -1$. Then a separating hyperplane has the property that

$$\beta_0 + \beta_1 x_{i1} + \beta_2 x_{i2} + \dots + \beta_p x_{ip} > 0 \text{ if } y_i = 1, \quad (9.6)$$

and

$$\beta_0 + \beta_1 x_{i1} + \beta_2 x_{i2} + \dots + \beta_p x_{ip} < 0 \text{ if } y_i = -1. \quad (9.7)$$

Equivalently, a separating hyperplane has the property that

$$y_i(\beta_0 + \beta_1 x_{i1} + \beta_2 x_{i2} + \dots + \beta_p x_{ip}) > 0 \quad (9.8)$$

for all $i = 1, \dots, n$.

If a separating hyperplane exists, we can use it to construct a very natural classifier: a test observation is assigned a class depending on which side of the hyperplane it is located. The right-hand panel of Figure 9.2 shows an example of such a classifier. That is, we classify the test observation x^* based on the sign of $f(x^*) = \beta_0 + \beta_1 x_1^* + \beta_2 x_2^* + \dots + \beta_p x_p^*$. If $f(x^*)$ is positive, then we assign the test observation to class 1, and if $f(x^*)$ is negative, then we assign it to class -1 . We can also make use of the *magnitude* of $f(x^*)$. If

separating hyperplane

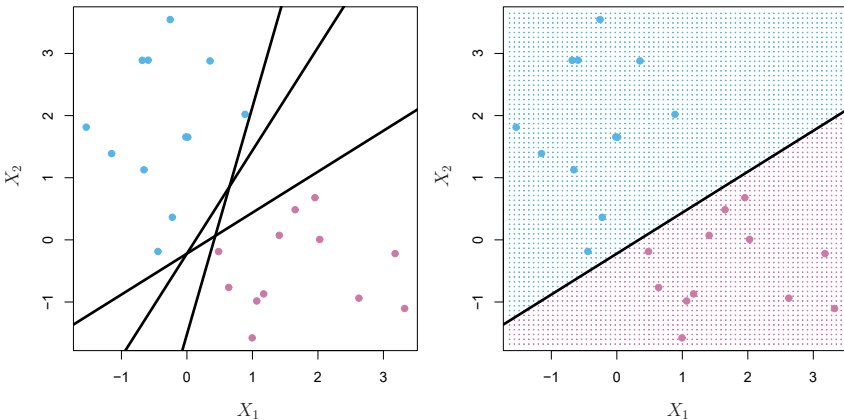


FIGURE 9.2. Left: There are two classes of observations, shown in blue and in purple, each of which has measurements on two variables. Three separating hyperplanes, out of many possible, are shown in black. Right: A separating hyperplane is shown in black. The blue and purple grid indicates the decision rule made by a classifier based on this separating hyperplane: a test observation that falls in the blue portion of the grid will be assigned to the blue class, and a test observation that falls into the purple portion of the grid will be assigned to the purple class.

$f(x^*)$ is far from zero, then this means that x^* lies far from the hyperplane, and so we can be confident about our class assignment for x^* . On the other hand, if $f(x^*)$ is close to zero, then x^* is located near the hyperplane, and so we are less certain about the class assignment for x^* . Not surprisingly, and as we see in Figure 9.2, a classifier that is based on a separating hyperplane leads to a linear decision boundary.

9.1.3 The Maximal Margin Classifier

In general, if our data can be perfectly separated using a hyperplane, then there will in fact exist an infinite number of such hyperplanes. This is because a given separating hyperplane can usually be shifted a tiny bit up or down, or rotated, without coming into contact with any of the observations. Three possible separating hyperplanes are shown in the left-hand panel of Figure 9.2. In order to construct a classifier based upon a separating hyperplane, we must have a reasonable way to decide which of the infinite possible separating hyperplanes to use.

A natural choice is the *maximal margin hyperplane* (also known as the *optimal separating hyperplane*), which is the separating hyperplane that is farthest from the training observations. That is, we can compute the (perpendicular) distance from each training observation to a given separating hyperplane; the smallest such distance is the minimal distance from the observations to the hyperplane, and is known as the *margin*. The maximal margin hyperplane is the separating hyperplane for which the margin is largest—that is, it is the hyperplane that has the farthest minimum distance to the training observations. We can then classify a test observation based on which side of the maximal margin hyperplane it lies. This is known

maximal
margin
hyperplane
optimal
separating
hyperplane
margin

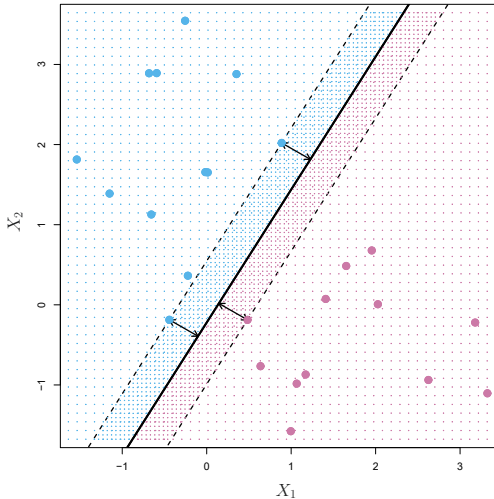


FIGURE 9.3. There are two classes of observations, shown in blue and in purple. The maximal margin hyperplane is shown as a solid line. The margin is the distance from the solid line to either of the dashed lines. The two blue points and the purple point that lie on the dashed lines are the support vectors, and the distance from those points to the hyperplane is indicated by arrows. The purple and blue grid indicates the decision rule made by a classifier based on this separating hyperplane.

as the *maximal margin classifier*. We hope that a classifier that has a large margin on the training data will also have a large margin on the test data, and hence will classify the test observations correctly. Although the maximal margin classifier is often successful, it can also lead to overfitting when p is large.

If $\beta_0, \beta_1, \dots, \beta_p$ are the coefficients of the maximal margin hyperplane, then the maximal margin classifier classifies the test observation x^* based on the sign of $f(x^*) = \beta_0 + \beta_1 x_1^* + \beta_2 x_2^* + \dots + \beta_p x_p^*$.

Figure 9.3 shows the maximal margin hyperplane on the data set of Figure 9.2. Comparing the right-hand panel of Figure 9.2 to Figure 9.3, we see that the maximal margin hyperplane shown in Figure 9.3 does indeed result in a greater minimal distance between the observations and the separating hyperplane—that is, a larger margin. In a sense, the maximal margin hyperplane represents the mid-line of the widest “slab” that we can insert between the two classes.

Examining Figure 9.3, we see that three training observations are equidistant from the maximal margin hyperplane and lie along the dashed lines indicating the width of the margin. These three observations are known as *support vectors*, since they are vectors in p -dimensional space (in Figure 9.3, $p = 2$) and they “support” the maximal margin hyperplane in the sense that if these points were moved slightly then the maximal margin hyperplane would move as well. Interestingly, the maximal margin hyperplane depends directly on the support vectors, but not on the other observations: a movement to any of the other observations would not affect the separating hyperplane, provided that the observation’s movement does not cause it to

maximal
margin
classifier

support
vector

cross the boundary set by the margin. The fact that the maximal margin hyperplane depends directly on only a small subset of the observations is an important property that will arise later in this chapter when we discuss the support vector classifier and support vector machines.

9.1.4 Construction of the Maximal Margin Classifier

We now consider the task of constructing the maximal margin hyperplane based on a set of n training observations $x_1, \dots, x_n \in \mathbb{R}^p$ and associated class labels $y_1, \dots, y_n \in \{-1, 1\}$. Briefly, the maximal margin hyperplane is the solution to the optimization problem

$$\underset{\beta_0, \beta_1, \dots, \beta_p, M}{\text{maximize}} \quad M \quad (9.9)$$

$$\text{subject to } \sum_{j=1}^p \beta_j^2 = 1, \quad (9.10)$$

$$y_i(\beta_0 + \beta_1 x_{i1} + \beta_2 x_{i2} + \dots + \beta_p x_{ip}) \geq M \quad \forall i = 1, \dots, n. \quad (9.11)$$

This optimization problem (9.9)–(9.11) is actually simpler than it looks. First of all, the constraint in (9.11) that

$$y_i(\beta_0 + \beta_1 x_{i1} + \beta_2 x_{i2} + \dots + \beta_p x_{ip}) \geq M \quad \forall i = 1, \dots, n$$

guarantees that each observation will be on the correct side of the hyperplane, provided that M is positive. (Actually, for each observation to be on the correct side of the hyperplane we would simply need $y_i(\beta_0 + \beta_1 x_{i1} + \beta_2 x_{i2} + \dots + \beta_p x_{ip}) > 0$, so the constraint in (9.11) in fact requires that each observation be on the correct side of the hyperplane, with some cushion, provided that M is positive.)

Second, note that (9.10) is not really a constraint on the hyperplane, since if $\beta_0 + \beta_1 x_{i1} + \beta_2 x_{i2} + \dots + \beta_p x_{ip} = 0$ defines a hyperplane, then so does $k(\beta_0 + \beta_1 x_{i1} + \beta_2 x_{i2} + \dots + \beta_p x_{ip}) = 0$ for any $k \neq 0$. However, (9.10) adds meaning to (9.11); one can show that with this constraint the perpendicular distance from the i th observation to the hyperplane is given by

$$y_i(\beta_0 + \beta_1 x_{i1} + \beta_2 x_{i2} + \dots + \beta_p x_{ip}).$$

Therefore, the constraints (9.10) and (9.11) ensure that each observation is on the correct side of the hyperplane and at least a distance M from the hyperplane. Hence, M represents the margin of our hyperplane, and the optimization problem chooses $\beta_0, \beta_1, \dots, \beta_p$ to maximize M . This is exactly the definition of the maximal margin hyperplane! The problem (9.9)–(9.11) can be solved efficiently, but details of this optimization are outside of the scope of this book.

9.1.5 The Non-separable Case

The maximal margin classifier is a very natural way to perform classification, *if a separating hyperplane exists*. However, as we have hinted, in many cases no separating hyperplane exists, and so there is no maximal

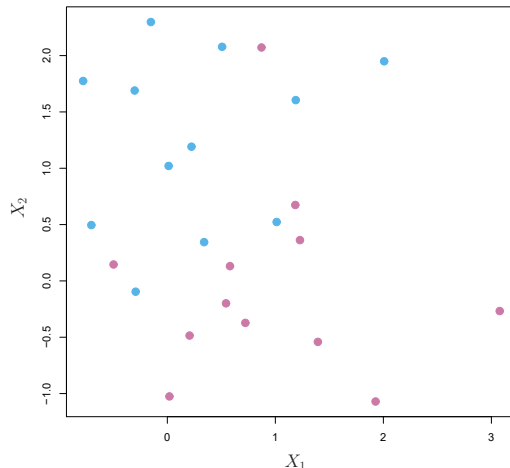


FIGURE 9.4. There are two classes of observations, shown in blue and in purple. In this case, the two classes are not separable by a hyperplane, and so the maximal margin classifier cannot be used.

margin classifier. In this case, the optimization problem (9.9)–(9.11) has no solution with $M > 0$. An example is shown in Figure 9.4. In this case, we cannot *exactly* separate the two classes. However, as we will see in the next section, we can extend the concept of a separating hyperplane in order to develop a hyperplane that *almost* separates the classes, using a so-called *soft margin*. The generalization of the maximal margin classifier to the non-separable case is known as the *support vector classifier*.

9.2 Support Vector Classifiers

9.2.1 Overview of the Support Vector Classifier

In Figure 9.4, we see that observations that belong to two classes are not necessarily separable by a hyperplane. In fact, even if a separating hyperplane does exist, then there are instances in which a classifier based on a separating hyperplane might not be desirable. A classifier based on a separating hyperplane will necessarily perfectly classify all of the training observations; this can lead to sensitivity to individual observations. An example is shown in Figure 9.5. The addition of a single observation in the right-hand panel of Figure 9.5 leads to a dramatic change in the maximal margin hyperplane. The resulting maximal margin hyperplane is not satisfactory—for one thing, it has only a tiny margin. This is problematic because as discussed previously, the distance of an observation from the hyperplane can be seen as a measure of our confidence that the observation was correctly classified. Moreover, the fact that the maximal margin hyperplane is extremely sensitive to a change in a single observation suggests that it may have overfit the training data.

In this case, we might be willing to consider a classifier based on a hyperplane that does *not* perfectly separate the two classes, in the interest of

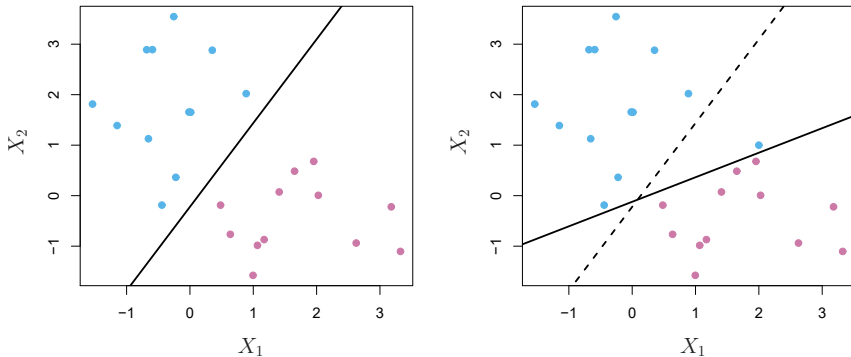


FIGURE 9.5. Left: Two classes of observations are shown in blue and in purple, along with the maximal margin hyperplane. Right: An additional blue observation has been added, leading to a dramatic shift in the maximal margin hyperplane shown as a solid line. The dashed line indicates the maximal margin hyperplane that was obtained in the absence of this additional point.

- Greater robustness to individual observations, and
- Better classification of *most* of the training observations.

That is, it could be worthwhile to misclassify a few training observations in order to do a better job in classifying the remaining observations.

The *support vector classifier*, sometimes called a *soft margin classifier*, does exactly this. Rather than seeking the largest possible margin so that every observation is not only on the correct side of the hyperplane but also on the correct side of the margin, we instead allow some observations to be on the incorrect side of the margin, or even the incorrect side of the hyperplane. (The margin is *soft* because it can be violated by some of the training observations.) An example is shown in the left-hand panel of Figure 9.6. Most of the observations are on the correct side of the margin. However, a small subset of the observations are on the wrong side of the margin.

support
vector
classifier
soft margin
classifier

An observation can be not only on the wrong side of the margin, but also on the wrong side of the hyperplane. In fact, when there is no separating hyperplane, such a situation is inevitable. Observations on the wrong side of the hyperplane correspond to training observations that are misclassified by the support vector classifier. The right-hand panel of Figure 9.6 illustrates such a scenario.

9.2.2 Details of the Support Vector Classifier

The support vector classifier classifies a test observation depending on which side of a hyperplane it lies. The hyperplane is chosen to correctly separate most of the training observations into the two classes, but may

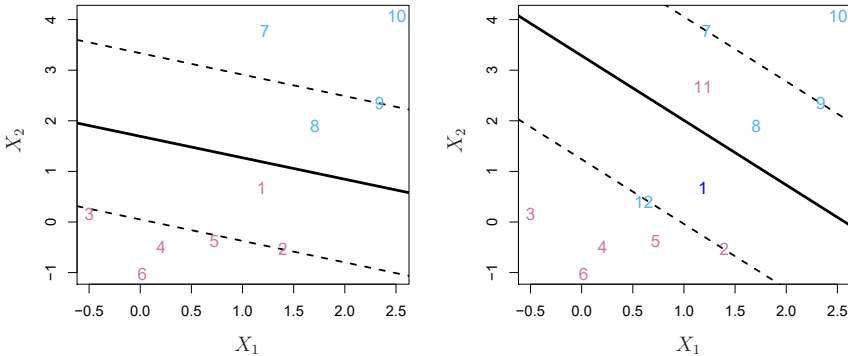


FIGURE 9.6. Left: A support vector classifier was fit to a small data set. The hyperplane is shown as a solid line and the margins are shown as dashed lines. Purple observations: Observations 3, 4, 5, and 6 are on the correct side of the margin, observation 2 is on the margin, and observation 1 is on the wrong side of the margin. Blue observations: Observations 7 and 10 are on the correct side of the margin, observation 9 is on the margin, and observation 8 is on the wrong side of the margin. No observations are on the wrong side of the hyperplane. Right: Same as left panel with two additional points, 11 and 12. These two observations are on the wrong side of the hyperplane and the wrong side of the margin.

misclassify a few observations. It is the solution to the optimization problem

$$\underset{\beta_0, \beta_1, \dots, \beta_p, \epsilon_1, \dots, \epsilon_n, M}{\text{maximize}} \quad M \quad (9.12)$$

$$\text{subject to } \sum_{j=1}^p \beta_j^2 = 1, \quad (9.13)$$

$$y_i(\beta_0 + \beta_1 x_{i1} + \beta_2 x_{i2} + \dots + \beta_p x_{ip}) \geq M(1 - \epsilon_i), \quad (9.14)$$

$$\epsilon_i \geq 0, \quad \sum_{i=1}^n \epsilon_i \leq C, \quad (9.15)$$

where C is a nonnegative tuning parameter. As in (9.11), M is the width of the margin; we seek to make this quantity as large as possible. In (9.14), $\epsilon_1, \dots, \epsilon_n$ are *slack variables* that allow individual observations to be on the wrong side of the margin or the hyperplane; we will explain them in greater detail momentarily. Once we have solved (9.12)–(9.15), we classify a test observation x^* as before, by simply determining on which side of the hyperplane it lies. That is, we classify the test observation based on the sign of $f(x^*) = \beta_0 + \beta_1 x_1^* + \dots + \beta_p x_p^*$.

slack
variable

The problem (9.12)–(9.15) seems complex, but insight into its behavior can be made through a series of simple observations presented below. First of all, the slack variable ϵ_i tells us where the i th observation is located, relative to the hyperplane and relative to the margin. If $\epsilon_i = 0$ then the i th observation is on the correct side of the margin, as we saw in Section 9.1.4. If $\epsilon_i > 0$ then the i th observation is on the wrong side of the margin, and we say that the i th observation has *violated* the margin. If $\epsilon_i > 1$ then it is on the wrong side of the hyperplane.

We now consider the role of the tuning parameter C . In (9.15), C bounds the sum of the ϵ_i 's, and so it determines the number and severity of the violations to the margin (and to the hyperplane) that we will tolerate. We can think of C as a *budget* for the amount that the margin can be violated by the n observations. If $C = 0$ then there is no budget for violations to the margin, and it must be the case that $\epsilon_1 = \dots = \epsilon_n = 0$, in which case (9.12)–(9.15) simply amounts to the maximal margin hyperplane optimization problem (9.9)–(9.11). (Of course, a maximal margin hyperplane exists only if the two classes are separable.) For $C > 0$ no more than C observations can be on the wrong side of the hyperplane, because if an observation is on the wrong side of the hyperplane then $\epsilon_i > 1$, and (9.15) requires that $\sum_{i=1}^n \epsilon_i \leq C$. As the budget C increases, we become more tolerant of violations to the margin, and so the margin will widen. Conversely, as C decreases, we become less tolerant of violations to the margin and so the margin narrows. An example is shown in Figure 9.7.

In practice, C is treated as a tuning parameter that is generally chosen via cross-validation. As with the tuning parameters that we have seen throughout this book, C controls the bias-variance trade-off of the statistical learning technique. When C is small, we seek narrow margins that are rarely violated; this amounts to a classifier that is highly fit to the data, which may have low bias but high variance. On the other hand, when C is larger, the margin is wider and we allow more violations to it; this amounts to fitting the data less hard and obtaining a classifier that is potentially more biased but may have lower variance.

The optimization problem (9.12)–(9.15) has a very interesting property: it turns out that only observations that either lie on the margin or that violate the margin will affect the hyperplane, and hence the classifier obtained. In other words, an observation that lies strictly on the correct side of the margin does not affect the support vector classifier! Changing the position of that observation would not change the classifier at all, provided that its position remains on the correct side of the margin. Observations that lie directly on the margin, or on the wrong side of the margin for their class, are known as *support vectors*. These observations do affect the support vector classifier.

The fact that only support vectors affect the classifier is in line with our previous assertion that C controls the bias-variance trade-off of the support vector classifier. When the tuning parameter C is large, then the margin is wide, many observations violate the margin, and so there are many support vectors. In this case, many observations are involved in determining the hyperplane. The top left panel in Figure 9.7 illustrates this setting: this classifier has low variance (since many observations are support vectors) but potentially high bias. In contrast, if C is small, then there will be fewer support vectors and hence the resulting classifier will have low bias but high variance. The bottom right panel in Figure 9.7 illustrates this setting, with only eight support vectors.

The fact that the support vector classifier's decision rule is based only on a potentially small subset of the training observations (the support vectors) means that it is quite robust to the behavior of observations that are far away from the hyperplane. This property is distinct from some of

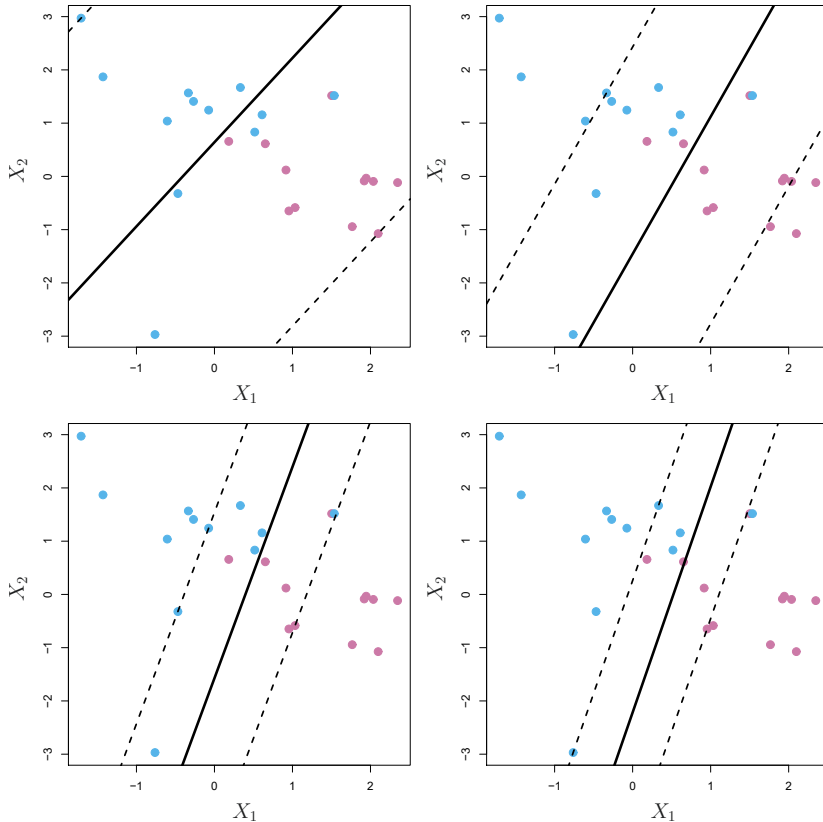


FIGURE 9.7. A support vector classifier was fit using four different values of the tuning parameter C in (9.12)–(9.15). The largest value of C was used in the top left panel, and smaller values were used in the top right, bottom left, and bottom right panels. When C is large, then there is a high tolerance for observations being on the wrong side of the margin, and so the margin will be large. As C decreases, the tolerance for observations being on the wrong side of the margin decreases, and the margin narrows.

the other classification methods that we have seen in preceding chapters, such as linear discriminant analysis. Recall that the LDA classification rule depends on the mean of *all* of the observations within each class, as well as the within-class covariance matrix computed using *all* of the observations. In contrast, logistic regression, unlike LDA, has very low sensitivity to observations far from the decision boundary. In fact we will see in Section 9.5 that the support vector classifier and logistic regression are closely related.

9.3 Support Vector Machines

We first discuss a general mechanism for converting a linear classifier into one that produces non-linear decision boundaries. We then introduce the support vector machine, which does this in an automatic way.

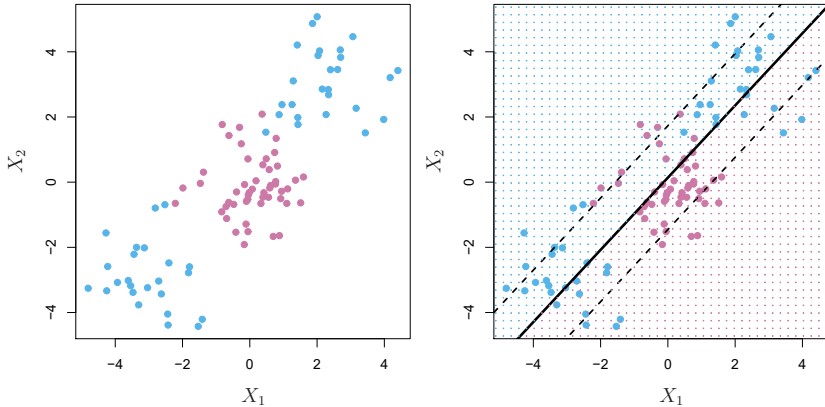


FIGURE 9.8. Left: The observations fall into two classes, with a non-linear boundary between them. Right: The support vector classifier seeks a linear boundary, and consequently performs very poorly.

9.3.1 Classification with Non-Linear Decision Boundaries

The support vector classifier is a natural approach for classification in the two-class setting, if the boundary between the two classes is linear. However, in practice we are sometimes faced with non-linear class boundaries. For instance, consider the data in the left-hand panel of Figure 9.8. It is clear that a support vector classifier or any linear classifier will perform poorly here. Indeed, the support vector classifier shown in the right-hand panel of Figure 9.8 is useless here.

In Chapter 7, we are faced with an analogous situation. We see there that the performance of linear regression can suffer when there is a non-linear relationship between the predictors and the outcome. In that case, we consider enlarging the feature space using functions of the predictors, such as quadratic and cubic terms, in order to address this non-linearity. In the case of the support vector classifier, we could address the problem of possibly non-linear boundaries between classes in a similar way, by enlarging the feature space using quadratic, cubic, and even higher-order polynomial functions of the predictors. For instance, rather than fitting a support vector classifier using p features

$$X_1, X_2, \dots, X_p,$$

we could instead fit a support vector classifier using $2p$ features

$$X_1, X_1^2, X_2, X_2^2, \dots, X_p, X_p^2.$$

Then (9.12)–(9.15) would become

$$\begin{aligned} & \underset{\beta_0, \beta_{11}, \beta_{12}, \dots, \beta_{p1}, \beta_{p2}, \epsilon_1, \dots, \epsilon_n, M}{\text{maximize}} \quad M \\ & \text{subject to } y_i \left(\beta_0 + \sum_{j=1}^p \beta_{j1} x_{ij} + \sum_{j=1}^p \beta_{j2} x_{ij}^2 \right) \geq M(1 - \epsilon_i), \\ & \sum_{i=1}^n \epsilon_i \leq C, \quad \epsilon_i \geq 0, \quad \sum_{j=1}^p \sum_{k=1}^2 \beta_{jk}^2 = 1. \end{aligned} \tag{9.16}$$

Why does this lead to a non-linear decision boundary? In the enlarged feature space, the decision boundary that results from (9.16) is in fact linear. But in the original feature space, the decision boundary is of the form $q(x) = 0$, where q is a quadratic polynomial, and its solutions are generally non-linear. One might additionally want to enlarge the feature space with higher-order polynomial terms, or with interaction terms of the form $X_j X_{j'}$ for $j \neq j'$. Alternatively, other functions of the predictors could be considered rather than polynomials. It is not hard to see that there are many possible ways to enlarge the feature space, and that unless we are careful, we could end up with a huge number of features. Then computations would become unmanageable. The support vector machine, which we present next, allows us to enlarge the feature space used by the support vector classifier in a way that leads to efficient computations.

9.3.2 The Support Vector Machine

The *support vector machine* (SVM) is an extension of the support vector classifier that results from enlarging the feature space in a specific way, using *kernels*. We will now discuss this extension, the details of which are somewhat complex and beyond the scope of this book. However, the main idea is described in Section 9.3.1: we may want to enlarge our feature space in order to accommodate a non-linear boundary between the classes. The kernel approach that we describe here is simply an efficient computational approach for enacting this idea.

support
vector
machine
kernel

We have not discussed exactly how the support vector classifier is computed because the details become somewhat technical. However, it turns out that the solution to the support vector classifier problem (9.12)–(9.15) involves only the *inner products* of the observations (as opposed to the observations themselves). The inner product of two r -vectors a and b is defined as $\langle a, b \rangle = \sum_{i=1}^r a_i b_i$. Thus the inner product of two observations $x_i, x_{i'}$ is given by

$$\langle x_i, x_{i'} \rangle = \sum_{j=1}^p x_{ij} x_{i'j}. \tag{9.17}$$

It can be shown that

- The linear support vector classifier can be represented as

$$f(x) = \beta_0 + \sum_{i=1}^n \alpha_i \langle x, x_i \rangle, \tag{9.18}$$

where there are n parameters α_i , $i = 1, \dots, n$, one per training observation.

- To estimate the parameters $\alpha_1, \dots, \alpha_n$ and β_0 , all we need are the $\binom{n}{2}$ inner products $\langle x_i, x_{i'} \rangle$ between all pairs of training observations. (The notation $\binom{n}{2}$ means $n(n - 1)/2$, and gives the number of pairs among a set of n items.)

Notice that in (9.18), in order to evaluate the function $f(x)$, we need to compute the inner product between the new point x and each of the training points x_i . However, it turns out that α_i is nonzero only for the support vectors in the solution—that is, if a training observation is not a support vector, then its α_i equals zero. So if \mathcal{S} is the collection of indices of these support points, we can rewrite any solution function of the form (9.18) as

$$f(x) = \beta_0 + \sum_{i \in \mathcal{S}} \alpha_i \langle x, x_i \rangle, \quad (9.19)$$

which typically involves far fewer terms than in (9.18).²

To summarize, in representing the linear classifier $f(x)$, and in computing its coefficients, all we need are inner products.

Now suppose that every time the inner product (9.17) appears in the representation (9.18), or in a calculation of the solution for the support vector classifier, we replace it with a *generalization* of the inner product of the form

$$K(x_i, x_{i'}), \quad (9.20)$$

where K is some function that we will refer to as a *kernel*. A kernel is a function that quantifies the similarity of two observations. For instance, we could simply take

$$K(x_i, x_{i'}) = \sum_{j=1}^p x_{ij} x_{i'j}, \quad (9.21)$$

which would just give us back the support vector classifier. Equation 9.21 is known as a *linear kernel* because the support vector classifier is linear in the features; the linear kernel essentially quantifies the similarity of a pair of observations using Pearson (standard) correlation. But one could instead choose another form for (9.20). For instance, one could replace every instance of $\sum_{j=1}^p x_{ij} x_{i'j}$ with the quantity

$$K(x_i, x_{i'}) = (1 + \sum_{j=1}^p x_{ij} x_{i'j})^d. \quad (9.22)$$

This is known as a *polynomial kernel* of degree d , where d is a positive integer. Using such a kernel with $d > 1$, instead of the standard linear kernel (9.21), in the support vector classifier algorithm leads to a much more flexible decision boundary. It essentially amounts to fitting a support vector

polynomial kernel

²By expanding each of the inner products in (9.19), it is easy to see that $f(x)$ is a linear function of the coordinates of x . Doing so also establishes the correspondence between the α_i and the original parameters β_j .

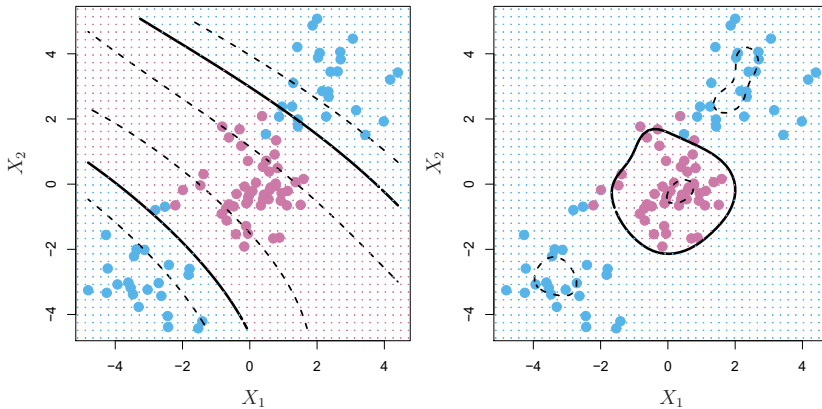


FIGURE 9.9. Left: An SVM with a polynomial kernel of degree 3 is applied to the non-linear data from Figure 9.8, resulting in a far more appropriate decision rule. Right: An SVM with a radial kernel is applied. In this example, either kernel is capable of capturing the decision boundary.

classifier in a higher-dimensional space involving polynomials of degree d , rather than in the original feature space. When the support vector classifier is combined with a non-linear kernel such as (9.22), the resulting classifier is known as a support vector machine. Note that in this case the (non-linear) function has the form

$$f(x) = \beta_0 + \sum_{i \in S} \alpha_i K(x, x_i). \quad (9.23)$$

The left-hand panel of Figure 9.9 shows an example of an SVM with a polynomial kernel applied to the non-linear data from Figure 9.8. The fit is a substantial improvement over the linear support vector classifier. When $d = 1$, then the SVM reduces to the support vector classifier seen earlier in this chapter.

The polynomial kernel shown in (9.22) is one example of a possible non-linear kernel, but alternatives abound. Another popular choice is the *radial kernel*, which takes the form

$$K(x_i, x_{i'}) = \exp(-\gamma \sum_{j=1}^p (x_{ij} - x_{i'j})^2). \quad (9.24)$$

radial kernel

In (9.24), γ is a positive constant. The right-hand panel of Figure 9.9 shows an example of an SVM with a radial kernel on this non-linear data; it also does a good job in separating the two classes.

How does the radial kernel (9.24) actually work? If a given test observation $x^* = (x_1^*, \dots, x_p^*)^T$ is far from a training observation x_i in terms of Euclidean distance, then $\sum_{j=1}^p (x_j^* - x_{ij})^2$ will be large, and so $K(x^*, x_i) = \exp(-\gamma \sum_{j=1}^p (x_j^* - x_{ij})^2)$ will be tiny. This means that in (9.23), x_i will play virtually no role in $f(x^*)$. Recall that the predicted class label for the test observation x^* is based on the sign of $f(x^*)$. In other words, training observations that are far from x^* will play essentially no role in the predicted class label for x^* . This means that the radial kernel has very *local*

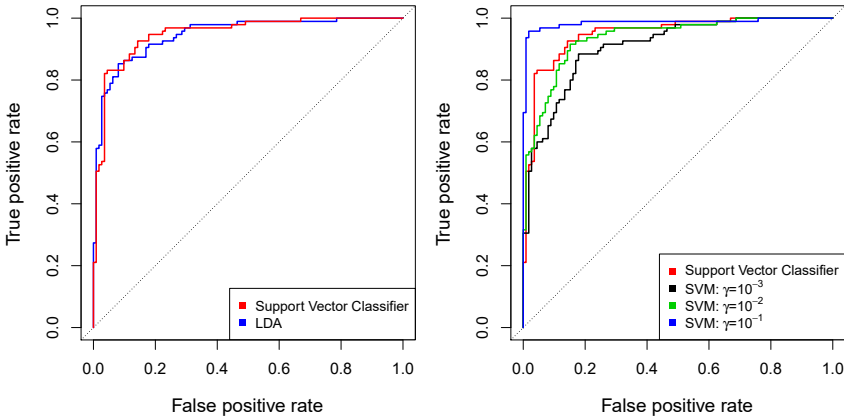


FIGURE 9.10. ROC curves for the [Heart](#) data training set. Left: The support vector classifier and LDA are compared. Right: The support vector classifier is compared to an SVM using a radial basis kernel with $\gamma = 10^{-3}$, 10^{-2} , and 10^{-1} .

behavior, in the sense that only nearby training observations have an effect on the class label of a test observation.

What is the advantage of using a kernel rather than simply enlarging the feature space using functions of the original features, as in (9.16)? One advantage is computational, and it amounts to the fact that using kernels, one need only compute $K(x_i, x'_i)$ for all $\binom{n}{2}$ distinct pairs i, i' . This can be done without explicitly working in the enlarged feature space. This is important because in many applications of SVMs, the enlarged feature space is so large that computations are intractable. For some kernels, such as the radial kernel (9.24), the feature space is *implicit* and infinite-dimensional, so we could never do the computations there anyway!

9.3.3 An Application to the Heart Disease Data

In Chapter 8 we apply decision trees and related methods to the [Heart](#) data. The aim is to use 13 predictors such as [Age](#), [Sex](#), and [Chol](#) in order to predict whether an individual has heart disease. We now investigate how an SVM compares to LDA on this data. After removing 6 missing observations, the data consist of 297 subjects, which we randomly split into 207 training and 90 test observations.

We first fit LDA and the support vector classifier to the training data. Note that the support vector classifier is equivalent to an SVM using a polynomial kernel of degree $d = 1$. The left-hand panel of Figure 9.10 displays ROC curves (described in Section 4.4.2) for the training set predictions for both LDA and the support vector classifier. Both classifiers compute scores of the form $\hat{f}(X) = \hat{\beta}_0 + \hat{\beta}_1 X_1 + \hat{\beta}_2 X_2 + \cdots + \hat{\beta}_p X_p$ for each observation. For any given cutoff t , we classify observations into the *heart disease* or *no heart disease* categories depending on whether $\hat{f}(X) < t$ or $\hat{f}(X) \geq t$. The ROC curve is obtained by forming these predictions and computing the false positive and true positive rates for a range of values of t . An optimal classifier will hug the top left corner of the ROC plot. In this instance

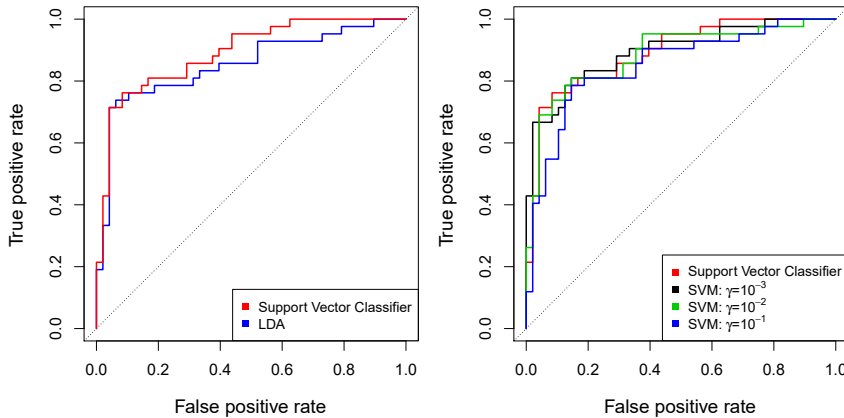


FIGURE 9.11. ROC curves for the test set of the Heart data. Left: The support vector classifier and LDA are compared. Right: The support vector classifier is compared to an SVM using a radial basis kernel with $\gamma = 10^{-3}$, 10^{-2} , and 10^{-1} .

LDA and the support vector classifier both perform well, though there is a suggestion that the support vector classifier may be slightly superior.

The right-hand panel of Figure 9.10 displays ROC curves for SVMs using a radial kernel, with various values of γ . As γ increases and the fit becomes more non-linear, the ROC curves improve. Using $\gamma = 10^{-1}$ appears to give an almost perfect ROC curve. However, these curves represent training error rates, which can be misleading in terms of performance on new test data. Figure 9.11 displays ROC curves computed on the 90 test observations. We observe some differences from the training ROC curves. In the left-hand panel of Figure 9.11, the support vector classifier appears to have a small advantage over LDA (although these differences are not statistically significant). In the right-hand panel, the SVM using $\gamma = 10^{-1}$, which showed the best results on the training data, produces the worst estimates on the test data. This is once again evidence that while a more flexible method will often produce lower training error rates, this does not necessarily lead to improved performance on test data. The SVMs with $\gamma = 10^{-2}$ and $\gamma = 10^{-3}$ perform comparably to the support vector classifier, and all three outperform the SVM with $\gamma = 10^{-1}$.

9.4 SVMs with More than Two Classes

So far, our discussion has been limited to the case of binary classification: that is, classification in the two-class setting. How can we extend SVMs to the more general case where we have some arbitrary number of classes? It turns out that the concept of separating hyperplanes upon which SVMs are based does not lend itself naturally to more than two classes. Though a number of proposals for extending SVMs to the K -class case have been made, the two most popular are the *one-versus-one* and *one-versus-all* approaches. We briefly discuss those two approaches here.

9.4.1 One-Versus-One Classification

Suppose that we would like to perform classification using SVMs, and there are $K > 2$ classes. A *one-versus-one* or *all-pairs* approach constructs $\binom{K}{2}$ SVMs, each of which compares a pair of classes. For example, one such SVM might compare the k th class, coded as +1, to the k' th class, coded as -1. We classify a test observation using each of the $\binom{K}{2}$ classifiers, and we tally the number of times that the test observation is assigned to each of the K classes. The final classification is performed by assigning the test observation to the class to which it was most frequently assigned in these $\binom{K}{2}$ pairwise classifications.

one-versus-one

9.4.2 One-Versus-All Classification

The *one-versus-all* approach (also referred to as *one-versus-rest*) is an alternative procedure for applying SVMs in the case of $K > 2$ classes. We fit K SVMs, each time comparing one of the K classes to the remaining $K - 1$ classes. Let $\beta_{0k}, \beta_{1k}, \dots, \beta_{pk}$ denote the parameters that result from fitting an SVM comparing the k th class (coded as +1) to the others (coded as -1). Let x^* denote a test observation. We assign the observation to the class for which $\beta_{0k} + \beta_{1k}x_1^* + \beta_{2k}x_2^* + \dots + \beta_{pk}x_p^*$ is largest, as this amounts to a high level of confidence that the test observation belongs to the k th class rather than to any of the other classes.

one-versus-all
one-versus-rest

9.5 Relationship to Logistic Regression



When SVMs were first introduced in the mid-1990s, they made quite a splash in the statistical and machine learning communities. This was due in part to their good performance, good marketing, and also to the fact that the underlying approach seemed both novel and mysterious. The idea of finding a hyperplane that separates the data as well as possible, while allowing some violations to this separation, seemed distinctly different from classical approaches for classification, such as logistic regression and linear discriminant analysis. Moreover, the idea of using a kernel to expand the feature space in order to accommodate non-linear class boundaries appeared to be a unique and valuable characteristic.

However, since that time, deep connections between SVMs and other more classical statistical methods have emerged. It turns out that one can rewrite the criterion (9.12)–(9.15) for fitting the support vector classifier $f(X) = \beta_0 + \beta_1 X_1 + \dots + \beta_p X_p$ as

$$\underset{\beta_0, \beta_1, \dots, \beta_p}{\text{minimize}} \left\{ \sum_{i=1}^n \max [0, 1 - y_i f(x_i)] + \lambda \sum_{j=1}^p \beta_j^2 \right\}, \quad (9.25)$$

where λ is a nonnegative tuning parameter. When λ is large then β_1, \dots, β_p are small, more violations to the margin are tolerated, and a low-variance but high-bias classifier will result. When λ is small then few violations to the margin will occur; this amounts to a high-variance but low-bias

classifier. Thus, a small value of λ in (9.25) amounts to a small value of C in (9.15). Note that the $\lambda \sum_{j=1}^p \beta_j^2$ term in (9.25) is the ridge penalty term from Section 6.2.1, and plays a similar role in controlling the bias-variance trade-off for the support vector classifier.

Now (9.25) takes the “Loss + Penalty” form that we have seen repeatedly throughout this book:

$$\underset{\beta_0, \beta_1, \dots, \beta_p}{\text{minimize}} \{L(\mathbf{X}, \mathbf{y}, \beta) + \lambda P(\beta)\}. \quad (9.26)$$

In (9.26), $L(\mathbf{X}, \mathbf{y}, \beta)$ is some loss function quantifying the extent to which the model, parametrized by β , fits the data (\mathbf{X}, \mathbf{y}) , and $P(\beta)$ is a penalty function on the parameter vector β whose effect is controlled by a nonnegative tuning parameter λ . For instance, ridge regression and the lasso both take this form with

$$L(\mathbf{X}, \mathbf{y}, \beta) = \sum_{i=1}^n \left(y_i - \beta_0 - \sum_{j=1}^p x_{ij} \beta_j \right)^2$$

and with $P(\beta) = \sum_{j=1}^p \beta_j^2$ for ridge regression and $P(\beta) = \sum_{j=1}^p |\beta_j|$ for the lasso. In the case of (9.25) the loss function instead takes the form

$$L(\mathbf{X}, \mathbf{y}, \beta) = \sum_{i=1}^n \max [0, 1 - y_i(\beta_0 + \beta_1 x_{i1} + \dots + \beta_p x_{ip})].$$

This is known as *hinge loss*, and is depicted in Figure 9.12. However, it turns out that the hinge loss function is closely related to the loss function used in logistic regression, also shown in Figure 9.12.

hinge loss

An interesting characteristic of the support vector classifier is that only support vectors play a role in the classifier obtained; observations on the correct side of the margin do not affect it. This is due to the fact that the loss function shown in Figure 9.12 is exactly zero for observations for which $y_i(\beta_0 + \beta_1 x_{i1} + \dots + \beta_p x_{ip}) \geq 1$; these correspond to observations that are on the correct side of the margin.³ In contrast, the loss function for logistic regression shown in Figure 9.12 is not exactly zero anywhere. But it is very small for observations that are far from the decision boundary. Due to the similarities between their loss functions, logistic regression and the support vector classifier often give very similar results. When the classes are well separated, SVMs tend to behave better than logistic regression; in more overlapping regimes, logistic regression is often preferred.

When the support vector classifier and SVM were first introduced, it was thought that the tuning parameter C in (9.15) was an unimportant “nuisance” parameter that could be set to some default value, like 1. However, the “Loss + Penalty” formulation (9.25) for the support vector classifier indicates that this is not the case. The choice of tuning parameter is very important and determines the extent to which the model underfits or overfits the data, as illustrated, for example, in Figure 9.7.

³With this hinge-loss + penalty representation, the margin corresponds to the value one, and the width of the margin is determined by $\sum \beta_j^2$.

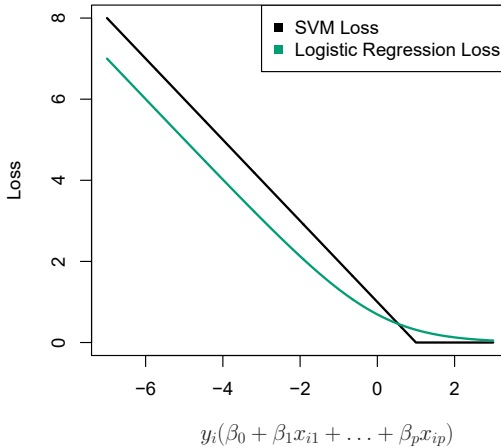


FIGURE 9.12. The SVM and logistic regression loss functions are compared, as a function of $y_i(\beta_0 + \beta_1x_{i1} + \dots + \beta_px_{ip})$. When $y_i(\beta_0 + \beta_1x_{i1} + \dots + \beta_px_{ip})$ is greater than 1, then the SVM loss is zero, since this corresponds to an observation that is on the correct side of the margin. Overall, the two loss functions have quite similar behavior.

We have established that the support vector classifier is closely related to logistic regression and other preexisting statistical methods. Is the SVM unique in its use of kernels to enlarge the feature space to accommodate non-linear class boundaries? The answer to this question is “no”. We could just as well perform logistic regression or many of the other classification methods seen in this book using non-linear kernels; this is closely related to some of the non-linear approaches seen in Chapter 7. However, for historical reasons, the use of non-linear kernels is much more widespread in the context of SVMs than in the context of logistic regression or other methods.

Though we have not addressed it here, there is in fact an extension of the SVM for regression (i.e. for a quantitative rather than a qualitative response), called *support vector regression*. In Chapter 3, we saw that least squares regression seeks coefficients $\beta_0, \beta_1, \dots, \beta_p$ such that the sum of squared residuals is as small as possible. (Recall from Chapter 3 that residuals are defined as $y_i - \beta_0 - \beta_1x_{i1} - \dots - \beta_px_{ip}$.) Support vector regression instead seeks coefficients that minimize a different type of loss, where only residuals larger in absolute value than some positive constant contribute to the loss function. This is an extension of the margin used in support vector classifiers to the regression setting.

support
vector
regression

We are more interested in the support vector classifier's performance on the test observations.

```
In [34]: confusion_table(khan_linear.predict(Khan['xtest']),
                      Khan['ytest'])
```

```
Out[34]:   Truth      1   2   3   4
Predicted
    1      3   0   0   0
    2      0   6   2   0
    3      0   0   4   0
    4      0   0   0   5
```

We see that using $C=10$ yields two test set errors on these data.

9.7 Exercises

Conceptual

1. This problem involves hyperplanes in two dimensions.
 - (a) Sketch the hyperplane $1 + 3X_1 - X_2 = 0$. Indicate the set of points for which $1 + 3X_1 - X_2 > 0$, as well as the set of points for which $1 + 3X_1 - X_2 < 0$.
 - (b) On the same plot, sketch the hyperplane $-2 + X_1 + 2X_2 = 0$. Indicate the set of points for which $-2 + X_1 + 2X_2 > 0$, as well as the set of points for which $-2 + X_1 + 2X_2 < 0$.
2. We have seen that in $p = 2$ dimensions, a linear decision boundary takes the form $\beta_0 + \beta_1 X_1 + \beta_2 X_2 = 0$. We now investigate a non-linear decision boundary.
 - (a) Sketch the curve

$$(1 + X_1)^2 + (2 - X_2)^2 = 4.$$
 - (b) On your sketch, indicate the set of points for which

$$(1 + X_1)^2 + (2 - X_2)^2 > 4,$$
 as well as the set of points for which

$$(1 + X_1)^2 + (2 - X_2)^2 \leq 4.$$
 - (c) Suppose that a classifier assigns an observation to the blue class if

$$(1 + X_1)^2 + (2 - X_2)^2 > 4,$$
 and to the red class otherwise. To what class is the observation $(0, 0)$ classified? $(-1, 1)$? $(2, 2)$? $(3, 8)$?
 - (d) Argue that while the decision boundary in (c) is not linear in terms of X_1 and X_2 , it is linear in terms of X_1 , X_1^2 , X_2 , and X_2^2 .

3. Here we explore the maximal margin classifier on a toy data set.

- (a) We are given $n = 7$ observations in $p = 2$ dimensions. For each observation, there is an associated class label.

Obs.	X_1	X_2	Y
1	3	4	Red
2	2	2	Red
3	4	4	Red
4	1	4	Red
5	2	1	Blue
6	4	3	Blue
7	4	1	Blue

Sketch the observations.

- (b) Sketch the optimal separating hyperplane, and provide the equation for this hyperplane (of the form (9.1)).
- (c) Describe the classification rule for the maximal margin classifier. It should be something along the lines of “Classify to Red if $\beta_0 + \beta_1 X_1 + \beta_2 X_2 > 0$, and classify to Blue otherwise.” Provide the values for β_0 , β_1 , and β_2 .
- (d) On your sketch, indicate the margin for the maximal margin hyperplane.
- (e) Indicate the support vectors for the maximal margin classifier.
- (f) Argue that a slight movement of the seventh observation would not affect the maximal margin hyperplane.
- (g) Sketch a hyperplane that is *not* the optimal separating hyperplane, and provide the equation for this hyperplane.
- (h) Draw an additional observation on the plot so that the two classes are no longer separable by a hyperplane.

Applied

- 4. Generate a simulated two-class data set with 100 observations and two features in which there is a visible but non-linear separation between the two classes. Show that in this setting, a support vector machine with a polynomial kernel (with degree greater than 1) or a radial kernel will outperform a support vector classifier on the training data. Which technique performs best on the test data? Make plots and report training and test error rates in order to back up your assertions.
- 5. We have seen that we can fit an SVM with a non-linear kernel in order to perform classification using a non-linear decision boundary. We will now see that we can also obtain a non-linear decision boundary by performing logistic regression using non-linear transformations of the features.

- (a) Generate a data set with $n = 500$ and $p = 2$, such that the observations belong to two classes with a quadratic decision boundary between them. For instance, you can do this as follows:

```
rng = np.random.default_rng(5)
x1 = rng.uniform(size=500) - 0.5
x2 = rng.uniform(size=500) - 0.5
y = x1**2 - x2**2 > 0
```

- (b) Plot the observations, colored according to their class labels. Your plot should display X_1 on the x -axis, and X_2 on the y -axis.
- (c) Fit a logistic regression model to the data, using X_1 and X_2 as predictors.
- (d) Apply this model to the *training data* in order to obtain a predicted class label for each training observation. Plot the observations, colored according to the *predicted* class labels. The decision boundary should be linear.
- (e) Now fit a logistic regression model to the data using non-linear functions of X_1 and X_2 as predictors (e.g. X_1^2 , $X_1 \times X_2$, $\log(X_2)$, and so forth).
- (f) Apply this model to the *training data* in order to obtain a predicted class label for each training observation. Plot the observations, colored according to the *predicted* class labels. The decision boundary should be obviously non-linear. If it is not, then repeat (a)–(e) until you come up with an example in which the predicted class labels are obviously non-linear.
- (g) Fit a support vector classifier to the data with X_1 and X_2 as predictors. Obtain a class prediction for each training observation. Plot the observations, colored according to the *predicted class labels*.
- (h) Fit a SVM using a non-linear kernel to the data. Obtain a class prediction for each training observation. Plot the observations, colored according to the *predicted class labels*.
- (i) Comment on your results.
6. At the end of Section 9.6.1, it is claimed that in the case of data that is just barely linearly separable, a support vector classifier with a small value of C that misclassifies a couple of training observations may perform better on test data than one with a huge value of C that does not misclassify any training observations. You will now investigate this claim.
- (a) Generate two-class data with $p = 2$ in such a way that the classes are just barely linearly separable.
- (b) Compute the cross-validation error rates for support vector classifiers with a range of C values. How many training observations are misclassified for each value of C considered, and how does this relate to the cross-validation errors obtained?

- (c) Generate an appropriate test data set, and compute the test errors corresponding to each of the values of `C` considered. Which value of `C` leads to the fewest test errors, and how does this compare to the values of `C` that yield the fewest training errors and the fewest cross-validation errors?
- (d) Discuss your results.
7. In this problem, you will use support vector approaches in order to predict whether a given car gets high or low gas mileage based on the `Auto` data set.
- Create a binary variable that takes on a 1 for cars with gas mileage above the median, and a 0 for cars with gas mileage below the median.
 - Fit a support vector classifier to the data with various values of `C`, in order to predict whether a car gets high or low gas mileage. Report the cross-validation errors associated with different values of this parameter. Comment on your results. Note you will need to fit the classifier without the gas mileage variable to produce sensible results.
 - Now repeat (b), this time using SVMs with radial and polynomial basis kernels, with different values of `gamma` and `degree` and `C`. Comment on your results.
 - Make some plots to back up your assertions in (b) and (c).

Hint: In the lab, we used the `plot_svm()` function for fitted SVMs. When $p > 2$, you can use the keyword argument `features` to create plots displaying pairs of variables at a time.

8. This problem involves the `OJ` data set which is part of the `ISLR` package.
- Create a training set containing a random sample of 800 observations, and a test set containing the remaining observations.
 - Fit a support vector classifier to the training data using `C = 0.01`, with `Purchase` as the response and the other variables as predictors. How many support points are there?
 - What are the training and test error rates?
 - Use cross-validation to select an optimal `C`. Consider values in the range 0.01 to 10.
 - Compute the training and test error rates using this new value for `C`.
 - Repeat parts (b) through (e) using a support vector machine with a radial kernel. Use the default value for `gamma`.
 - Repeat parts (b) through (e) using a support vector machine with a polynomial kernel. Set `degree = 2`.
 - Overall, which approach seems to give the best results on this data?

10

Deep Learning



This chapter covers the important topic of *deep learning*. At the time of writing (2020), deep learning is a very active area of research in the machine learning and artificial intelligence communities. The cornerstone of deep learning is the *neural network*.

deep
learning

neural
network

Neural networks rose to fame in the late 1980s. There was a lot of excitement and a certain amount of hype associated with this approach, and they were the impetus for the popular *Neural Information Processing Systems* meetings (NeurIPS, formerly NIPS) held every year, typically in exotic places like ski resorts. This was followed by a synthesis stage, where the properties of neural networks were analyzed by machine learners, mathematicians and statisticians; algorithms were improved, and the methodology stabilized. Then along came SVMs, boosting, and random forests, and neural networks fell somewhat from favor. Part of the reason was that neural networks required a lot of tinkering, while the new methods were more automatic. Also, on many problems the new methods outperformed poorly-trained neural networks. This was the *status quo* for the first decade in the new millennium.

All the while, though, a core group of neural-network enthusiasts were pushing their technology harder on ever-larger computing architectures and data sets. Neural networks resurfaced after 2010 with the new name *deep learning*, with new architectures, additional bells and whistles, and a string of success stories on some niche problems such as image and video classification, speech and text modeling. Many in the field believe that the major reason for these successes is the availability of ever-larger training datasets, made possible by the wide-scale use of digitization in science and industry.

In this chapter we discuss the basics of neural networks and deep learning, and then go into some of the specializations for specific problems, such as convolutional neural networks (CNNs) for image classification, and recurrent neural networks (RNNs) for time series and other sequences. We

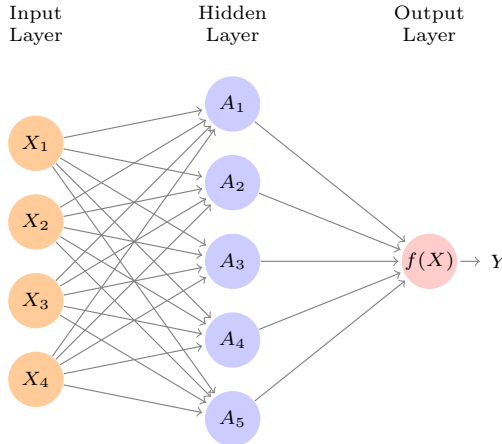


FIGURE 10.1. Neural network with a single hidden layer. The hidden layer computes activations $A_k = h_k(X)$ that are nonlinear transformations of linear combinations of the inputs X_1, X_2, \dots, X_p . Hence these A_k are not directly observed. The functions $h_k(\cdot)$ are not fixed in advance, but are learned during the training of the network. The output layer is a linear model that uses these activations A_k as inputs, resulting in a function $f(X)$.

will also demonstrate these models using the **Python torch** package, along with a number of helper packages.

The material in this chapter is slightly more challenging than elsewhere in this book.

10.1 Single Layer Neural Networks

A neural network takes an input vector of p variables $X = (X_1, X_2, \dots, X_p)$ and builds a nonlinear function $f(X)$ to predict the response Y . We have built nonlinear prediction models in earlier chapters, using trees, boosting and generalized additive models. What distinguishes neural networks from these methods is the particular *structure* of the model. Figure 10.1 shows a simple *feed-forward neural network* for modeling a quantitative response using $p = 4$ predictors. In the terminology of neural networks, the four features X_1, \dots, X_4 make up the units in the *input layer*. The arrows indicate that each of the inputs from the input layer feeds into each of the K *hidden units* (we get to pick K ; here we chose 5). The neural network model has the form

$$\begin{aligned} f(X) &= \beta_0 + \sum_{k=1}^K \beta_k h_k(X) \\ &= \beta_0 + \sum_{k=1}^K \beta_k g(w_{k0} + \sum_{j=1}^p w_{kj} X_j). \end{aligned} \tag{10.1}$$

It is built up here in two steps. First the K *activations* A_k , $k = 1, \dots, K$, in the hidden layer are computed as functions of the input features X_1, \dots, X_p ,

$$A_k = h_k(X) = g(w_{k0} + \sum_{j=1}^p w_{kj} X_j), \tag{10.2}$$

feed-forward
neural
network
input layer
hidden units

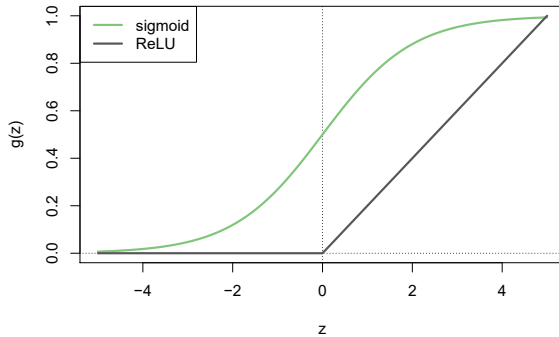


FIGURE 10.2. Activation functions. The piecewise-linear ReLU function is popular for its efficiency and computability. We have scaled it down by a factor of five for ease of comparison.

where $g(z)$ is a nonlinear *activation function* that is specified in advance. We can think of each A_k as a different transformation $h_k(X)$ of the original features, much like the basis functions of Chapter 7. These K activations from the hidden layer then feed into the output layer, resulting in

$$f(X) = \beta_0 + \sum_{k=1}^K \beta_k A_k, \quad (10.3)$$

a linear regression model in the $K = 5$ activations. All the parameters β_0, \dots, β_K and w_{10}, \dots, w_{Kp} need to be estimated from data. In the early instances of neural networks, the *sigmoid* activation function was favored,

$$g(z) = \frac{e^z}{1 + e^z} = \frac{1}{1 + e^{-z}}, \quad (10.4)$$

which is the same function used in logistic regression to convert a linear function into probabilities between zero and one (see Figure 10.2). The preferred choice in modern neural networks is the *ReLU* (*rectified linear unit*) activation function, which takes the form

$$g(z) = (z)_+ = \begin{cases} 0 & \text{if } z < 0 \\ z & \text{otherwise.} \end{cases} \quad (10.5)$$

A ReLU activation can be computed and stored more efficiently than a sigmoid activation. Although it thresholds at zero, because we apply it to a linear function (10.2) the constant term w_{k0} will shift this inflection point.

So in words, the model depicted in Figure 10.1 derives five new features by computing five different linear combinations of X , and then squashes each through an activation function $g(\cdot)$ to transform it. The final model is linear in these derived variables.

The name *neural network* originally derived from thinking of these hidden units as analogous to neurons in the brain — values of the activations $A_k = h_k(X)$ close to one are *firing*, while those close to zero are *silent* (using the sigmoid activation function).

The nonlinearity in the activation function $g(\cdot)$ is essential, since without it the model $f(X)$ in (10.1) would collapse into a simple linear model in

activation
function

sigmoid

ReLU
rectified
linear unit

X_1, \dots, X_p . Moreover, having a nonlinear activation function allows the model to capture complex nonlinearities and interaction effects. Consider a very simple example with $p = 2$ input variables $X = (X_1, X_2)$, and $K = 2$ hidden units $h_1(X)$ and $h_2(X)$ with $g(z) = z^2$. We specify the other parameters as

$$\begin{aligned}\beta_0 &= 0, & \beta_1 &= \frac{1}{4}, & \beta_2 &= -\frac{1}{4}, \\ w_{10} &= 0, & w_{11} &= 1, & w_{12} &= 1, \\ w_{20} &= 0, & w_{21} &= 1, & w_{22} &= -1.\end{aligned}\tag{10.6}$$

From (10.2), this means that

$$\begin{aligned}h_1(X) &= (0 + X_1 + X_2)^2, \\ h_2(X) &= (0 + X_1 - X_2)^2.\end{aligned}\tag{10.7}$$

Then plugging (10.7) into (10.1), we get

$$\begin{aligned}f(X) &= 0 + \frac{1}{4} \cdot (0 + X_1 + X_2)^2 - \frac{1}{4} \cdot (0 + X_1 - X_2)^2 \\ &= \frac{1}{4} [(X_1 + X_2)^2 - (X_1 - X_2)^2] \\ &= X_1 X_2.\end{aligned}\tag{10.8}$$

So the sum of two nonlinear transformations of linear functions can give us an interaction! In practice we would not use a quadratic function for $g(z)$, since we would always get a second-degree polynomial in the original coordinates X_1, \dots, X_p . The sigmoid or ReLU activations do not have such a limitation.

Fitting a neural network requires estimating the unknown parameters in (10.1). For a quantitative response, typically squared-error loss is used, so that the parameters are chosen to minimize

$$\sum_{i=1}^n (y_i - f(x_i))^2.\tag{10.9}$$

Details about how to perform this minimization are provided in Section 10.7.

10.2 Multilayer Neural Networks

Modern neural networks typically have more than one hidden layer, and often many units per layer. In theory a single hidden layer with a large number of units has the ability to approximate most functions. However, the learning task of discovering a good solution is made much easier with multiple layers each of modest size.

We will illustrate a large dense network on the famous and publicly available **MNIST** handwritten digit dataset.¹ Figure 10.3 shows examples of these digits. The idea is to build a model to classify the images into their correct digit class 0–9. Every image has $p = 28 \times 28 = 784$ pixels, each of which is an eight-bit grayscale value between 0 and 255 representing

¹See LeCun, Cortes, and Burges (2010) “The MNIST database of handwritten digits”, available at <http://yann.lecun.com/exdb/mnist>.

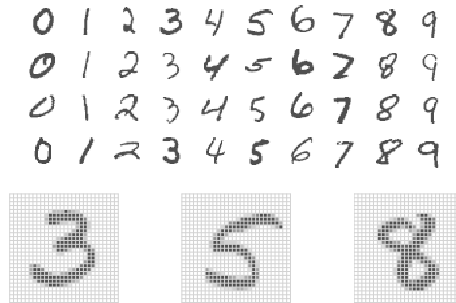


FIGURE 10.3. Examples of handwritten digits from the **MNIST** corpus. Each grayscale image has 28×28 pixels, each of which is an eight-bit number (0–255) which represents how dark that pixel is. The first 3, 5, and 8 are enlarged to show their 784 individual pixel values.

the relative amount of the written digit in that tiny square.² These pixels are stored in the input vector X (in, say, column order). The output is the class label, represented by a vector $Y = (Y_0, Y_1, \dots, Y_9)$ of 10 dummy variables, with a one in the position corresponding to the label, and zeros elsewhere. In the machine learning community, this is known as *one-hot encoding*. There are 60,000 training images, and 10,000 test images.

On a historical note, digit recognition problems were the catalyst that accelerated the development of neural network technology in the late 1980s at AT&T Bell Laboratories and elsewhere. Pattern recognition tasks of this kind are relatively simple for humans. Our visual system occupies a large fraction of our brains, and good recognition is an evolutionary force for survival. These tasks are not so simple for machines, and it has taken more than 30 years to refine the neural-network architectures to match human performance.

Figure 10.4 shows a multilayer network architecture that works well for solving the digit-classification task. It differs from Figure 10.1 in several ways:

- It has two hidden layers L_1 (256 units) and L_2 (128 units) rather than one. Later we will see a network with seven hidden layers.
- It has ten output variables, rather than one. In this case the ten variables really represent a single qualitative variable and so are quite dependent. (We have indexed them by the digit class 0–9 rather than 1–10, for clarity.) More generally, in *multi-task learning* one can predict different responses simultaneously with a single network; they all have a say in the formation of the hidden layers.
- The loss function used for training the network is tailored for the multiclass classification task.

one-hot
encoding

multi-task
learning

²In the analog-to-digital conversion process, only part of the written numeral may fall in the square representing a particular pixel.

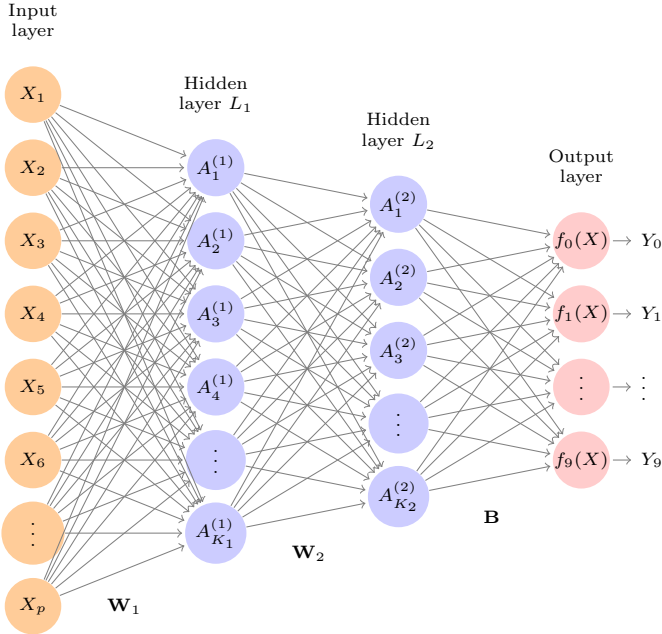


FIGURE 10.4. Neural network diagram with two hidden layers and multiple outputs, suitable for the MNIST handwritten-digit problem. The input layer has $p = 784$ units, the two hidden layers $K_1 = 256$ and $K_2 = 128$ units respectively, and the output layer 10 units. Along with intercepts (referred to as biases in the deep-learning community) this network has 235,146 parameters (referred to as weights).

The first hidden layer is as in (10.2), with

$$\begin{aligned} A_k^{(1)} &= h_k^{(1)}(X) \\ &= g(w_{k0}^{(1)} + \sum_{j=1}^p w_{kj}^{(1)} X_j) \end{aligned} \quad (10.10)$$

for $k = 1, \dots, K_1$. The second hidden layer treats the activations $A_k^{(1)}$ of the first hidden layer as inputs and computes new activations

$$\begin{aligned} A_\ell^{(2)} &= h_\ell^{(2)}(X) \\ &= g(w_{\ell 0}^{(2)} + \sum_{k=1}^{K_1} w_{\ell k}^{(2)} A_k^{(1)}) \end{aligned} \quad (10.11)$$

for $\ell = 1, \dots, K_2$. Notice that each of the activations in the second layer $A_\ell^{(2)} = h_\ell^{(2)}(X)$ is a function of the input vector X . This is the case because while they are explicitly a function of the activations $A_k^{(1)}$ from layer L_1 , these in turn are functions of X . This would also be the case with more hidden layers. Thus, through a chain of transformations, the network is able to build up fairly complex transformations of X that ultimately feed into the output layer as features.

We have introduced additional superscript notation such as $h_\ell^{(2)}(X)$ and $w_{\ell j}^{(2)}$ in (10.10) and (10.11) to indicate to which layer the activations and weights (coefficients) belong, in this case layer 2. The notation \mathbf{W}_1 in Fig-

weights

ure 10.4 represents the entire matrix of weights that feed from the input layer to the first hidden layer L_1 . This matrix will have $785 \times 256 = 200,960$ elements; there are 785 rather than 784 because we must account for the intercept or *bias* term.³

Each element $A_k^{(1)}$ feeds to the second hidden layer L_2 via the matrix of weights \mathbf{W}_2 of dimension $257 \times 128 = 32,896$.

We now get to the output layer, where we now have ten responses rather than one. The first step is to compute ten different linear models similar to our single model (10.1),

$$\begin{aligned} Z_m &= \beta_{m0} + \sum_{\ell=1}^{K_2} \beta_{m\ell} h_{\ell}^{(2)}(X) \\ &= \beta_{m0} + \sum_{\ell=1}^{K_2} \beta_{m\ell} A_{\ell}^{(2)}, \end{aligned} \tag{10.12}$$

for $m = 0, 1, \dots, 9$. The matrix \mathbf{B} stores all $129 \times 10 = 1,290$ of these weights.

If these were all separate quantitative responses, we would simply set each $f_m(X) = Z_m$ and be done. However, we would like our estimates to represent class probabilities $f_m(X) = \Pr(Y = m|X)$, just like in multinomial logistic regression in Section 4.3.5. So we use the special *softmax* activation function (see (4.13) on page 145),

$$f_m(X) = \Pr(Y = m|X) = \frac{e^{Z_m}}{\sum_{\ell=0}^9 e^{Z_{\ell}}}, \tag{10.13}$$

for $m = 0, 1, \dots, 9$. This ensures that the 10 numbers behave like probabilities (non-negative and sum to one). Even though the goal is to build a classifier, our model actually estimates a probability for each of the 10 classes. The classifier then assigns the image to the class with the highest probability.

To train this network, since the response is qualitative, we look for coefficient estimates that minimize the negative multinomial log-likelihood

$$-\sum_{i=1}^n \sum_{m=0}^9 y_{im} \log(f_m(x_i)), \tag{10.14}$$

also known as the *cross-entropy*. This is a generalization of the criterion (4.5) for two-class logistic regression. Details on how to minimize this objective are given in Section 10.7. If the response were quantitative, we would instead minimize squared-error loss as in (10.9).

cross-
entropy

Table 10.1 compares the test performance of the neural network with two simple models presented in Chapter 4 that make use of linear decision boundaries: multinomial logistic regression and linear discriminant analysis. The improvement of neural networks over both of these linear methods is dramatic: the network with dropout regularization achieves a test error rate below 2% on the 10,000 test images. (We describe dropout regularization in Section 10.7.3.) In Section 10.9.2 of the lab, we present the code for fitting this model, which runs in just over two minutes on a laptop computer.

³The use of “weights” for coefficients and “bias” for the intercepts w_{k0} in (10.2) is popular in the machine learning community; this use of bias is not to be confused with the “bias-variance” usage elsewhere in this book.

Method	Test Error
Neural Network + Ridge Regularization	2.3%
Neural Network + Dropout Regularization	1.8%
Multinomial Logistic Regression	7.2%
Linear Discriminant Analysis	12.7%

TABLE 10.1. Test error rate on the MNIST data, for neural networks with two forms of regularization, as well as multinomial logistic regression and linear discriminant analysis. In this example, the extra complexity of the neural network leads to a marked improvement in test error.

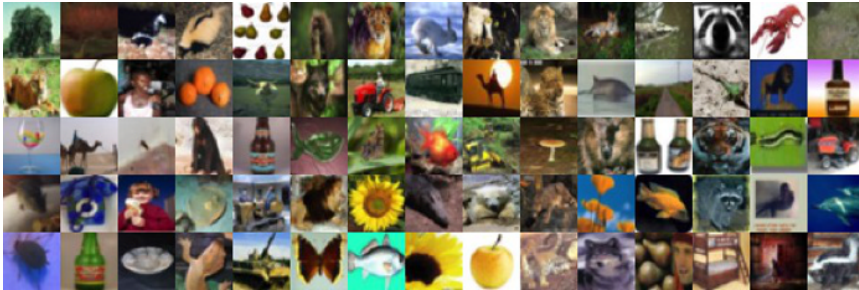


FIGURE 10.5. A sample of images from the CIFAR100 database: a collection of natural images from everyday life, with 100 different classes represented.

Adding the number of coefficients in \mathbf{W}_1 , \mathbf{W}_2 and \mathbf{B} , we get 235,146 in all, more than 33 times the number $785 \times 9 = 7,065$ needed for multinomial logistic regression. Recall that there are 60,000 images in the training set. While this might seem like a large training set, there are almost four times as many coefficients in the neural network model as there are observations in the training set! To avoid overfitting, some regularization is needed. In this example, we used two forms of regularization: ridge regularization, which is similar to ridge regression from Chapter 6, and dropout regularization. We discuss both forms of regularization in Section 10.7.

dropout

10.3 Convolutional Neural Networks

Neural networks rebounded around 2010 with big successes in image classification. Around that time, massive databases of labeled images were being accumulated, with ever-increasing numbers of classes. Figure 10.5 shows 75 images drawn from the CIFAR100 database.⁴ This database consists of 60,000 images labeled according to 20 superclasses (e.g. aquatic mammals), with five classes per superclass (beaver, dolphin, otter, seal, whale). Each image has a resolution of 32×32 pixels, with three eight-bit numbers per pixel representing red, green and blue. The numbers for each image are organized in a three-dimensional array called a *feature map*. The first two

feature map

⁴See Chapter 3 of Krizhevsky (2009) “Learning multiple layers of features from tiny images”, available at <https://www.cs.toronto.edu/~kriz/learning-features-2009-TR.pdf>.

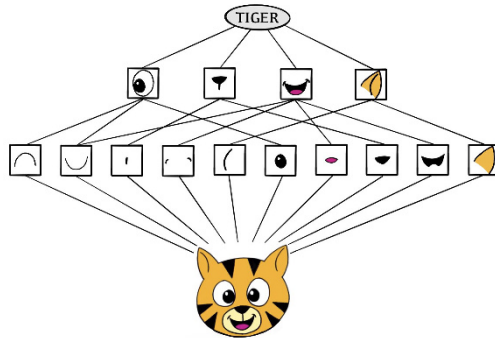


FIGURE 10.6. Schematic showing how a convolutional neural network classifies an image of a tiger. The network takes in the image and identifies local features. It then combines the local features in order to create compound features, which in this example include eyes and ears. These compound features are used to output the label “tiger”.

axes are spatial (both are 32-dimensional), and the third is the *channel* axis,⁵ representing the three colors. There is a designated training set of 50,000 images, and a test set of 10,000.

A special family of *convolutional neural networks* (CNNs) has evolved for classifying images such as these, and has shown spectacular success on a wide range of problems. CNNs mimic to some degree how humans classify images, by recognizing specific features or patterns anywhere in the image that distinguish each particular object class. In this section we give a brief overview of how they work.

Figure 10.6 illustrates the idea behind a convolutional neural network on a cartoon image of a tiger.⁶

The network first identifies low-level features in the input image, such as small edges, patches of color, and the like. These low-level features are then combined to form higher-level features, such as parts of ears, eyes, and so on. Eventually, the presence or absence of these higher-level features contributes to the probability of any given output class.

How does a convolutional neural network build up this hierarchy? It combines two specialized types of hidden layers, called *convolution* layers and *pooling* layers. Convolution layers search for instances of small patterns in the image, whereas pooling layers downsample these to select a prominent subset. In order to achieve state-of-the-art results, contemporary neural-network architectures make use of many convolution and pooling layers. We describe convolution and pooling layers next.

10.3.1 Convolution Layers

A *convolution layer* is made up of a large number of *convolution filters*, each

channel
convolutional
neural
networks

convolution
layer
convolution
filter

⁵The term *channel* is taken from the signal-processing literature. Each channel is a distinct source of information.

⁶Thanks to Elena Tuzhilina for producing the diagram and <https://www.cartooning4kids.com/> for permission to use the cartoon tiger.

of which is a template that determines whether a particular local feature is present in an image. A convolution filter relies on a very simple operation, called a *convolution*, which basically amounts to repeatedly multiplying matrix elements and then adding the results.

To understand how a convolution filter works, consider a very simple example of a 4×3 image:

$$\text{Original Image} = \begin{bmatrix} a & b & c \\ d & e & f \\ g & h & i \\ j & k & l \end{bmatrix}.$$

Now consider a 2×2 filter of the form

$$\text{Convolution Filter} = \begin{bmatrix} \alpha & \beta \\ \gamma & \delta \end{bmatrix}.$$

When we *convolve* the image with the filter, we get the result⁷

$$\text{Convolved Image} = \begin{bmatrix} a\alpha + b\beta + d\gamma + e\delta & b\alpha + c\beta + e\gamma + f\delta \\ d\alpha + e\beta + g\gamma + h\delta & e\alpha + f\beta + h\gamma + i\delta \\ g\alpha + h\beta + j\gamma + k\delta & h\alpha + i\beta + k\gamma + l\delta \end{bmatrix}.$$

For instance, the top-left element comes from multiplying each element in the 2×2 filter by the corresponding element in the top left 2×2 portion of the image, and adding the results. The other elements are obtained in a similar way: the convolution filter is applied to every 2×2 submatrix of the original image in order to obtain the convolved image. If a 2×2 submatrix of the original image resembles the convolution filter, then it will have a *large* value in the convolved image; otherwise, it will have a *small* value. Thus, *the convolved image highlights regions of the original image that resemble the convolution filter*. We have used 2×2 as an example; in general convolution filters are small $\ell_1 \times \ell_2$ arrays, with ℓ_1 and ℓ_2 small positive integers that are not necessarily equal.

Figure 10.7 illustrates the application of two convolution filters to a 192×179 image of a tiger, shown on the left-hand side.⁸ Each convolution filter is a 15×15 image containing mostly zeros (black), with a narrow strip of ones (white) oriented either vertically or horizontally within the image. When each filter is convolved with the image of the tiger, areas of the tiger that resemble the filter (i.e. that have either horizontal or vertical stripes or edges) are given large values, and areas of the tiger that do not resemble the feature are given small values. The convolved images are displayed on the right-hand side. We see that the horizontal stripe filter picks out horizontal stripes and edges in the original image, whereas the vertical stripe filter picks out vertical stripes and edges in the original image.

⁷The convolved image is smaller than the original image because its dimension is given by the number of 2×2 submatrices in the original image. Note that 2×2 is the dimension of the convolution filter. If we want the convolved image to have the same dimension as the original image, then padding can be applied.

⁸The tiger image used in Figures 10.7–10.9 was obtained from the public domain image resource <https://www.needpix.com/>.

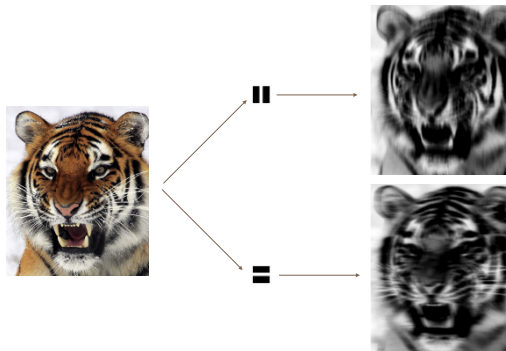


FIGURE 10.7. Convolution filters find local features in an image, such as edges and small shapes. We begin with the image of the tiger shown on the left, and apply the two small convolution filters in the middle. The convolved images highlight areas in the original image where details similar to the filters are found. Specifically, the top convolved image highlights the tiger’s vertical stripes, whereas the bottom convolved image highlights the tiger’s horizontal stripes. We can think of the original image as the input layer in a convolutional neural network, and the convolved images as the units in the first hidden layer.

We have used a large image and two large filters in Figure 10.7 for illustration. For the **CIFAR100** database there are 32×32 color pixels per image, and we use 3×3 convolution filters.

In a convolution layer, we use a whole bank of filters to pick out a variety of differently-oriented edges and shapes in the image. Using predefined filters in this way is standard practice in image processing. By contrast, with CNNs the filters are *learned* for the specific classification task. We can think of the filter weights as the parameters going from an input layer to a hidden layer, with one hidden unit for each pixel in the convolved image. This is in fact the case, though the parameters are highly structured and constrained (see Exercise 4 for more details). They operate on localized patches in the input image (so there are many structural zeros), and the same weights in a given filter are reused for all possible patches in the image (so the weights are constrained).⁹

We now give some additional details.

- Since the input image is in color, it has three channels represented by a three-dimensional feature map (array). Each channel is a two-dimensional (32×32) feature map — one for red, one for green, and one for blue. A single convolution filter will also have three channels, one per color, each of dimension 3×3 , with potentially different filter weights. The results of the three convolutions are summed to form a two-dimensional output feature map. Note that at this point the color information has been used, and is not passed on to subsequent layers except through its role in the convolution.

⁹This used to be called *weight sharing* in the early years of neural networks.

- If we use K different convolution filters at this first hidden layer, we get K two-dimensional output feature maps, which together are treated as a single three-dimensional feature map. We view each of the K output feature maps as a separate channel of information, so now we have K channels in contrast to the three color channels of the original input feature map. The three-dimensional feature map is just like the activations in a hidden layer of a simple neural network, except organized and produced in a spatially structured way.
- We typically apply the ReLU activation function (10.5) to the convolved image. This step is sometimes viewed as a separate layer in the convolutional neural network, in which case it is referred to as a *detector layer*.

detector
layer

10.3.2 Pooling Layers

A *pooling* layer provides a way to condense a large image into a smaller summary image. While there are a number of possible ways to perform pooling, the *max pooling* operation summarizes each non-overlapping 2×2 block of pixels in an image using the maximum value in the block. This reduces the size of the image by a factor of two in each direction, and it also provides some *location invariance*: i.e. as long as there is a large value in one of the four pixels in the block, the whole block registers as a large value in the reduced image.

pooling

Here is a simple example of max pooling:

$$\text{Max pool} \begin{bmatrix} 1 & 2 & 5 & 3 \\ 3 & 0 & 1 & 2 \\ 2 & 1 & 3 & 4 \\ 1 & 1 & 2 & 0 \end{bmatrix} \rightarrow \begin{bmatrix} 3 & 5 \\ 2 & 4 \end{bmatrix}.$$

10.3.3 Architecture of a Convolutional Neural Network

So far we have defined a single convolution layer — each filter produces a new two-dimensional feature map. The number of convolution filters in a convolution layer is akin to the number of units at a particular hidden layer in a fully-connected neural network of the type we saw in Section 10.2. This number also defines the number of channels in the resulting three-dimensional feature map. We have also described a pooling layer, which reduces the first two dimensions of each three-dimensional feature map. Deep CNNs have many such layers. Figure 10.8 shows a typical architecture for a CNN for the **CIFAR100** image classification task.

At the input layer, we see the three-dimensional feature map of a color image, where the channel axis represents each color by a 32×32 two-dimensional feature map of pixels. Each convolution filter produces a new channel at the first hidden layer, each of which is a 32×32 feature map (after some padding at the edges). After this first round of convolutions, we now have a new “image”; a feature map with considerably more channels than the three color input channels (six in the figure, since we used six convolution filters).

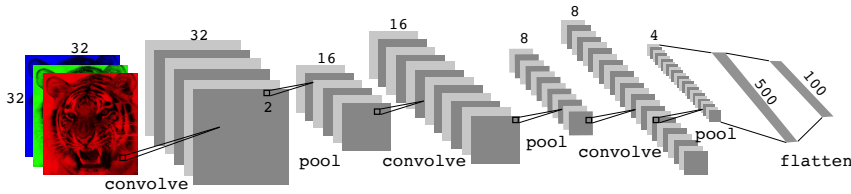


FIGURE 10.8. Architecture of a deep CNN for the **CIFAR100** classification task. Convolution layers are interspersed with 2×2 max-pool layers, which reduce the size by a factor of 2 in both dimensions.

This is followed by a max-pool layer, which reduces the size of the feature map in each channel by a factor of four: two in each dimension.

This convolve-then-pool sequence is now repeated for the next two layers. Some details are as follows:

- Each subsequent convolve layer is similar to the first. It takes as input the three-dimensional feature map from the previous layer and treats it like a single multi-channel image. Each convolution filter learned has as many channels as this feature map.
- Since the channel feature maps are reduced in size after each pool layer, we usually increase the number of filters in the next convolve layer to compensate.
- Sometimes we repeat several convolve layers before a pool layer. This effectively increases the dimension of the filter.

These operations are repeated until the pooling has reduced each channel feature map down to just a few pixels in each dimension. At this point the three-dimensional feature maps are *flattened* — the pixels are treated as separate units — and fed into one or more fully-connected layers before reaching the output layer, which is a *softmax activation* for the 100 classes (as in (10.13)).

There are many tuning parameters to be selected in constructing such a network, apart from the number, nature, and sizes of each layer. Dropout learning can be used at each layer, as well as lasso or ridge regularization (see Section 10.7). The details of constructing a convolutional neural network can seem daunting. Fortunately, terrific software is available, with extensive examples and vignettes that provide guidance on sensible choices for the parameters. For the **CIFAR100** official test set, the best accuracy as of this writing is just above 75%, but undoubtedly this performance will continue to improve.

10.3.4 Data Augmentation

An additional important trick used with image modeling is *data augmentation*. Essentially, each training image is replicated many times, with each replicate randomly distorted in a natural way such that human recognition is unaffected. Figure 10.9 shows some examples. Typical distortions are

data augmentation



FIGURE 10.9. *Data augmentation. The original image (leftmost) is distorted in natural ways to produce different images with the same class label. These distortions do not fool humans, and act as a form of regularization when fitting the CNN.*

zoom, horizontal and vertical shift, shear, small rotations, and in this case horizontal flips. At face value this is a way of increasing the training set considerably with somewhat different examples, and thus protects against overfitting. In fact we can see this as a form of regularization: we build a cloud of images around each original image, all with the same label. This kind of fattening of the data is similar in spirit to ridge regularization.

We will see in Section 10.7.2 that the stochastic gradient descent algorithms for fitting deep learning models repeatedly process randomly-selected batches of, say, 128 training images at a time. This works hand-in-glove with augmentation, because we can distort each image in the batch on the fly, and hence do not have to store all the new images.

10.3.5 Results Using a Pretrained Classifier

Here we use an industry-level pretrained classifier to predict the class of some new images. The `resnet50` classifier is a convolutional neural network that was trained using the `imagenet` data set, which consists of millions of images that belong to an ever-growing number of categories.¹⁰ Figure 10.10 demonstrates the performance of `resnet50` on six photographs (private collection of one of the authors).¹¹ The CNN does a reasonable job classifying the hawk in the second image. If we zoom out as in the third image, it gets confused and chooses the fountain rather than the hawk. In the final image a “jacamar” is a tropical bird from South and Central America with similar coloring to the South African Cape Weaver. We give more details on this example in Section 10.9.4.

Much of the work in fitting a CNN is in learning the convolution filters at the hidden layers; these are the coefficients of a CNN. For models fit to massive corpora such as `imagenet` with many classes, the output of these filters can serve as features for general natural-image classification problems. One can use these pretrained hidden layers for new problems with much smaller training sets (a process referred to as *weight freezing*), and just train the last few layers of the network, which requires much less data.

weight
freezing

¹⁰For more information about `resnet50`, see He, Zhang, Ren, and Sun (2015) “Deep residual learning for image recognition”, <https://arxiv.org/abs/1512.03385>. For details about `imagenet`, see Russakovsky, Deng, et al. (2015) “ImageNet Large Scale Visual Recognition Challenge”, in *International Journal of Computer Vision*.

¹¹These `resnet` results can change with time, since the publicly-trained model gets updated periodically.

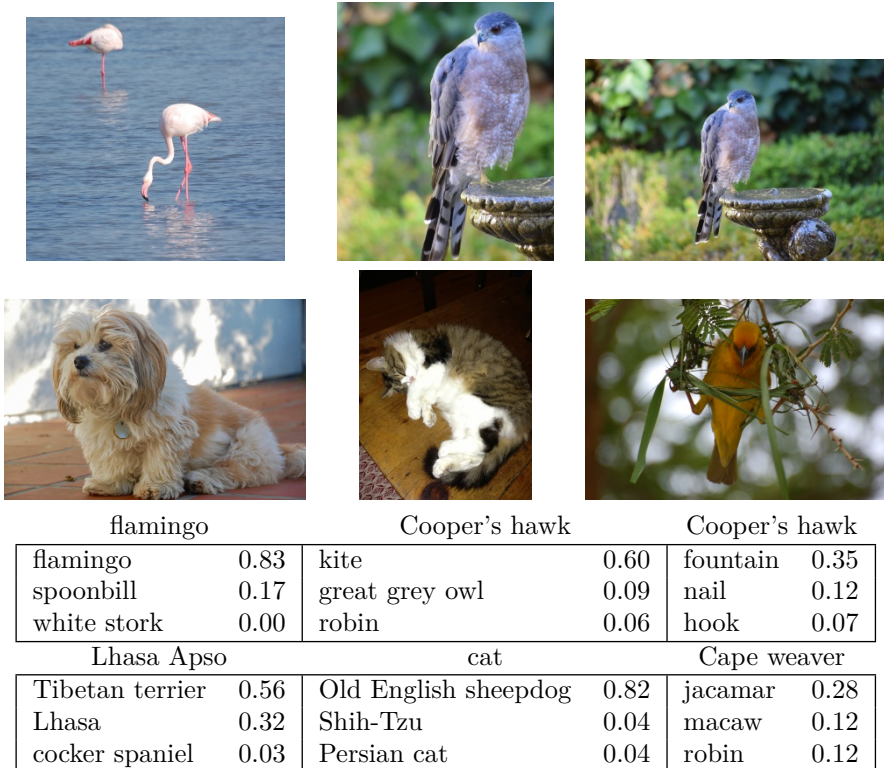


FIGURE 10.10. Classification of six photographs using the `resnet50` CNN trained on the `imagenet` corpus. The table below the images displays the true (intended) label at the top of each panel, and the top three choices of the classifier (out of 100). The numbers are the estimated probabilities for each choice. (A kite is a raptor, but not a hawk.)

The vignettes and book¹² that accompany the `keras` package give more details on such applications.

10.4 Document Classification

In this section we introduce a new type of example that has important applications in industry and science: predicting attributes of documents. Examples of documents include articles in medical journals, Reuters news feeds, emails, tweets, and so on. Our example will be `IMDb` (Internet Movie Database) ratings — short documents where viewers have written critiques of movies.¹³ The response in this case is the `sentiment` of the review, which will be *positive* or *negative*.

¹²Deep Learning with R by F. Chollet and J.J. Allaire, 2018, Manning Publications.

¹³For details, see Maas et al. (2011) “Learning word vectors for sentiment analysis”, in *Proceedings of the 49th Annual Meeting of the Association for Computational Linguistics: Human Language Technologies*, pages 142–150.

Here is the beginning of a rather amusing negative review:

This has to be one of the worst films of the 1990s. When my friends & I were watching this film (being the target audience it was aimed at) we just sat & watched the first half an hour with our jaws touching the floor at how bad it really was. The rest of the time, everyone else in the theater just started talking to each other, leaving or generally crying into their popcorn . . .

Each review can be a different length, include slang or non-words, have spelling errors, etc. We need to find a way to *featurize* such a document. This is modern parlance for defining a set of predictors.

featurize

The simplest and most common featurization is the *bag-of-words* model. We score each document for the presence or absence of each of the words in a language dictionary — in this case an English dictionary. If the dictionary contains M words, that means for each document we create a binary feature vector of length M , and score a 1 for every word present, and 0 otherwise. That can be a very wide feature vector, so we limit the dictionary — in this case to the 10,000 most frequently occurring words in the training corpus of 25,000 reviews. Fortunately there are nice tools for doing this automatically. Here is the beginning of a positive review that has been redacted in this way:

bag-of-words

<START> this film was just brilliant casting location scenery story direction everyone's really suited the part they played and you could just imagine being there robert <UNK> is an amazing actor and now the same being director <UNK> father came from the same scottish island as myself so i loved . . .

Here we can see many words have been omitted, and some unknown words (UNK) have been marked as such. With this reduction the binary feature vector has length 10,000, and consists mostly of 0's and a smattering of 1's in the positions corresponding to words that are present in the document. We have a training set and test set, each with 25,000 examples, and each balanced with regard to *sentiment*. The resulting training feature matrix \mathbf{X} has dimension $25,000 \times 10,000$, but only 1.3% of the binary entries are non-zero. We call such a matrix sparse, because most of the values are the same (zero in this case); it can be stored efficiently in *sparse matrix format*.¹⁴ There are a variety of ways to account for the document length; here we only score a word as in or out of the document, but for example one could instead record the relative frequency of words. We split off a validation set of size 2,000 from the 25,000 training observations (for model tuning), and fit two model sequences:

sparse matrix format

- A lasso logistic regression using the `glmnet` package;
- A two-class neural network with two hidden layers, each with 16 ReLU units.

¹⁴Rather than store the whole matrix, we can store instead the location and values for the nonzero entries. In this case, since the nonzero entries are all 1, just the locations are stored.

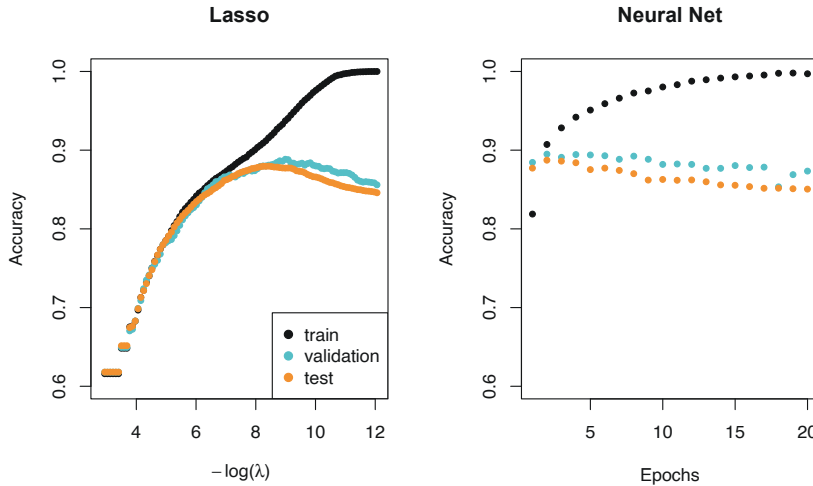


FIGURE 10.11. Accuracy of the lasso and a two-hidden-layer neural network on the **IMDb** data. For the lasso, the x -axis displays $-\log(\lambda)$, while for the neural network it displays epochs (number of times the fitting algorithm passes through the training set). Both show a tendency to overfit, and achieve approximately the same test accuracy.

Both methods produce a sequence of solutions. The lasso sequence is indexed by the regularization parameter λ . The neural-net sequence is indexed by the number of gradient-descent iterations used in the fitting, as measured by training epochs or passes through the training set (Section 10.7). Notice that the training accuracy in Figure 10.11 (black points) increases monotonically in both cases. We can use the validation error to pick a good solution from each sequence (blue points in the plots), which would then be used to make predictions on the test data set.

Note that a two-class neural network amounts to a nonlinear logistic regression model. From (10.12) and (10.13) we can see that

$$\begin{aligned} \log \left(\frac{\Pr(Y=1|X)}{\Pr(Y=0|X)} \right) &= Z_1 - Z_0 \\ &= (\beta_{10} - \beta_{00}) + \sum_{\ell=1}^{K_2} (\beta_{1\ell} - \beta_{0\ell}) A_\ell^{(2)}. \end{aligned} \quad (10.15)$$

(This shows the redundancy in the softmax function; for K classes we really only need to estimate $K-1$ sets of coefficients. See Section 4.3.5.) In Figure 10.11 we show *accuracy* (fraction correct) rather than classification error (fraction incorrect), the former being more popular in the machine learning community. Both models achieve a test-set accuracy of about 88%.

accuracy

The bag-of-words model summarizes a document by the words present, and ignores their context. There are at least two popular ways to take the context into account:

- The *bag-of-n-grams* model. For example, a bag of 2-grams records

bag-of-n-
grams

the consecutive co-occurrence of every distinct pair of words. “Blissfully long” can be seen as a positive phrase in a movie review, while “blissfully short” a negative.

- Treat the document as a sequence, taking account of all the words in the context of those that preceded and those that follow.

In the next section we explore models for sequences of data, which have applications in weather forecasting, speech recognition, language translation, and time-series prediction, to name a few. We continue with this [IMDb](#) example there.

10.5 Recurrent Neural Networks

Many data sources are sequential in nature, and call for special treatment when building predictive models. Examples include:

- Documents such as book and movie reviews, newspaper articles, and tweets. The sequence and relative positions of words in a document capture the narrative, theme and tone, and can be exploited in tasks such as topic classification, sentiment analysis, and language translation.
- Time series of temperature, rainfall, wind speed, air quality, and so on. We may want to forecast the weather several days ahead, or climate several decades ahead.
- Financial time series, where we track market indices, trading volumes, stock and bond prices, and exchange rates. Here prediction is often difficult, but as we will see, certain indices can be predicted with reasonable accuracy.
- Recorded speech, musical recordings, and other sound recordings. We may want to give a text transcription of a speech, or perhaps a language translation. We may want to assess the quality of a piece of music, or assign certain attributes.
- Handwriting, such as doctor’s notes, and handwritten digits such as zip codes. Here we want to turn the handwriting into digital text, or read the digits (optical character recognition).

In a *recurrent neural network* (RNN), the input object X is a *sequence*. Consider a corpus of documents, such as the collection of [IMDb](#) movie reviews. Each document can be represented as a sequence of L words, so $X = \{X_1, X_2, \dots, X_L\}$, where each X_ℓ represents a word. The order of the words, and closeness of certain words in a sentence, convey semantic meaning. RNNs are designed to accommodate and take advantage of the sequential nature of such input objects, much like convolutional neural networks accommodate the spatial structure of image inputs. The output Y can also be a sequence (such as in language translation), but often is a scalar, like the binary sentiment label of a movie review document.

recurrent
neural
network

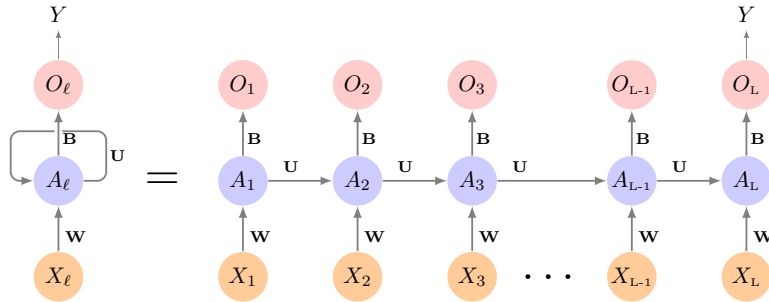


FIGURE 10.12. Schematic of a simple recurrent neural network. The input is a sequence of vectors $\{X_\ell\}_1^L$, and here the target is a single response. The network processes the input sequence X sequentially; each X_ℓ feeds into the hidden layer, which also has as input the activation vector $A_{\ell-1}$ from the previous element in the sequence, and produces the current activation vector A_ℓ . The same collections of weights \mathbf{W} , \mathbf{U} and \mathbf{B} are used as each element of the sequence is processed. The output layer produces a sequence of predictions O_ℓ from the current activation A_ℓ , but typically only the last of these, O_L , is of relevance. To the left of the equal sign is a concise representation of the network, which is unrolled into a more explicit version on the right.

Figure 10.12 illustrates the structure of a very basic RNN with a sequence $X = \{X_1, X_2, \dots, X_L\}$ as input, a simple output Y , and a hidden-layer sequence $\{A_\ell\}_1^L = \{A_1, A_2, \dots, A_L\}$. Each X_ℓ is a vector; in the document example X_ℓ could represent a one-hot encoding for the ℓ th word based on the language dictionary for the corpus (see the top panel in Figure 10.13 for a simple example). As the sequence is processed one vector X_ℓ at a time, the network updates the activations A_ℓ in the hidden layer, taking as input the vector X_ℓ and the activation vector $A_{\ell-1}$ from the previous step in the sequence. Each A_ℓ feeds into the output layer and produces a prediction O_ℓ for Y . O_L , the last of these, is the most relevant.

In detail, suppose each vector X_ℓ of the input sequence has p components $X_\ell^T = (X_{\ell 1}, X_{\ell 2}, \dots, X_{\ell p})$, and the hidden layer consists of K units $A_\ell^T = (A_{\ell 1}, A_{\ell 2}, \dots, A_{\ell K})$. As in Figure 10.4, we represent the collection of $K \times (p+1)$ shared weights w_{kj} for the input layer by a matrix \mathbf{W} , and similarly \mathbf{U} is a $K \times K$ matrix of the weights u_{ks} for the hidden-to-hidden layers, and \mathbf{B} is a $K + 1$ vector of weights β_k for the output layer. Then

$$A_{\ell k} = g\left(w_{k0} + \sum_{j=1}^p w_{kj} X_{\ell j} + \sum_{s=1}^K u_{ks} A_{\ell-1,s}\right), \quad (10.16)$$

and the output O_ℓ is computed as

$$O_\ell = \beta_0 + \sum_{k=1}^K \beta_k A_{\ell k} \quad (10.17)$$

for a quantitative response, or with an additional sigmoid activation function for a binary response, for example. Here $g(\cdot)$ is an activation function such as ReLU. Notice that the same weights \mathbf{W} , \mathbf{U} and \mathbf{B} are used as we

process each element in the sequence, i.e. they are not functions of ℓ . This is a form of *weight sharing* used by RNNs, and similar to the use of filters in convolutional neural networks (Section 10.3.1.) As we proceed from beginning to end, the activations A_ℓ accumulate a history of what has been seen before, so that the learned context can be used for prediction.

weight sharing

For regression problems the loss function for an observation (X, Y) is

$$(Y - O_L)^2, \quad (10.18)$$

which only references the final output $O_L = \beta_0 + \sum_{k=1}^K \beta_k A_{Lk}$. Thus O_1, O_2, \dots, O_{L-1} are not used. When we fit the model, each element X_ℓ of the input sequence X contributes to O_L via the chain (10.16), and hence contributes indirectly to learning the shared parameters \mathbf{W} , \mathbf{U} and \mathbf{B} via the loss (10.18). With n input sequence/response pairs (x_i, y_i) , the parameters are found by minimizing the sum of squares

$$\sum_{i=1}^n (y_i - o_{iL})^2 = \sum_{i=1}^n \left(y_i - \left(\beta_0 + \sum_{k=1}^K \beta_k g\left(w_{k0} + \sum_{j=1}^p w_{kj} x_{iLj} + \sum_{s=1}^K u_{ks} a_{i,L-1,s} \right) \right) \right)^2. \quad (10.19)$$

Here we use lowercase letters for the observed y_i and vector sequences $x_i = \{x_{i1}, x_{i2}, \dots, x_{iL}\}$,¹⁵ as well as the derived activations.

Since the intermediate outputs O_ℓ are not used, one may well ask why they are there at all. First of all, they come for free, since they use the same output weights \mathbf{B} needed to produce O_L , and provide an evolving prediction for the output. Furthermore, for some learning tasks the response is also a sequence, and so the output sequence $\{O_1, O_2, \dots, O_L\}$ is explicitly needed.

When used at full strength, recurrent neural networks can be quite complex. We illustrate their use in two simple applications. In the first, we continue with the [IMDb](#) sentiment analysis of the previous section, where we process the words in the reviews sequentially. In the second application, we illustrate their use in a financial time series forecasting problem.

10.5.1 Sequential Models for Document Classification

Here we return to our classification task with the [IMDb](#) reviews. Our approach in Section 10.4 was to use the bag-of-words model. Here the plan is to use instead the sequence of words occurring in a document to make predictions about the label for the entire document.

We have, however, a dimensionality problem: each word in our document is represented by a one-hot-encoded vector (dummy variable) with 10,000 elements (one per word in the dictionary)! An approach that has become popular is to represent each word in a much lower-dimensional *embedding* space. This means that rather than representing each word by a binary vector with 9,999 zeros and a single one in some position, we will represent it instead by a set of m real numbers, none of which are typically zero. Here m is the embedding dimension, and can be in the low 100s, or even less. This means (in our case) that we need a matrix \mathbf{E} of dimension $m \times 10,000$,

embedding

¹⁵This is a sequence of vectors; each element $x_{i\ell}$ is a p -vector.

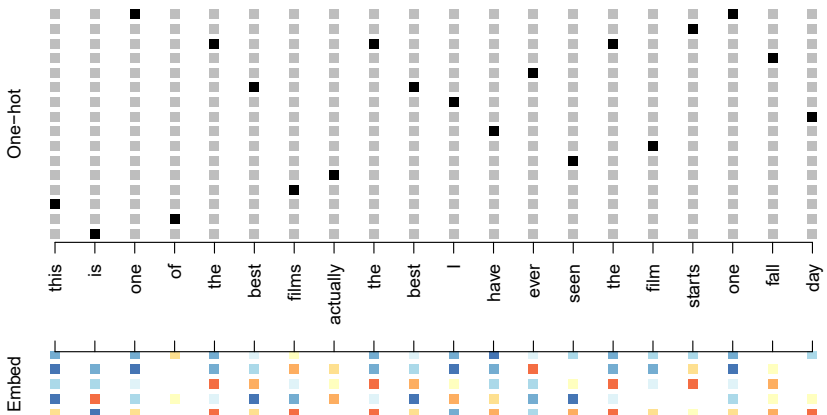


FIGURE 10.13. Depiction of a sequence of 20 words representing a single document: one-hot encoded using a dictionary of 16 words (top panel) and embedded in an m -dimensional space with $m = 5$ (bottom panel).

where each column is indexed by one of the 10,000 words in our dictionary, and the values in that column give the m coordinates for that word in the embedding space.

Figure 10.13 illustrates the idea (with a dictionary of 16 rather than 10,000, and $m = 5$). Where does \mathbf{E} come from? If we have a large corpus of labeled documents, we can have the neural network learn \mathbf{E} as part of the optimization. In this case \mathbf{E} is referred to as an *embedding layer*, and a specialized \mathbf{E} is learned for the task at hand. Otherwise we can insert a precomputed matrix \mathbf{E} in the embedding layer, a process known as *weight freezing*. Two pretrained embeddings, `word2vec` and `GloVe`, are widely used.¹⁶ These are built from a very large corpus of documents by a variant of principal components analysis (Section 12.2). The idea is that the positions of words in the embedding space preserve semantic meaning; e.g. synonyms should appear near each other.

So far, so good. Each document is now represented as a sequence of m -vectors that represents the sequence of words. The next step is to limit each document to the last L words. Documents that are shorter than L get padded with zeros upfront. So now each document is represented by a series consisting of L vectors $X = \{X_1, X_2, \dots, X_L\}$, and each X_ℓ in the sequence has m components.

We now use the RNN structure in Figure 10.12. The training corpus consists of n separate series (documents) of length L , each of which gets processed sequentially from left to right. In the process, a parallel series of hidden activation vectors A_ℓ , $\ell = 1, \dots, L$ is created as in (10.16) for each document. A_ℓ feeds into the output layer to produce the evolving prediction O_ℓ . We use the final value O_L to predict the response: the sentiment of the review.

embedding layer
weight freezing
`word2vec`
`GloVe`

¹⁶ `word2vec` is described in Mikolov, Chen, Corrado, and Dean (2013), available at <https://code.google.com/archive/p/word2vec>. `GloVe` is described in Pennington, Socher, and Manning (2014), available at <https://nlp.stanford.edu/projects/glove>.

This is a simple RNN, and has relatively few parameters. If there are K hidden units, the common weight matrix \mathbf{W} has $K \times (m + 1)$ parameters, the matrix \mathbf{U} has $K \times K$ parameters, and \mathbf{B} has $2(K + 1)$ for the two-class logistic regression as in (10.15). These are used repeatedly as we process the sequence $X = \{X_\ell\}_1^L$ from left to right, much like we use a single convolution filter to process each patch in an image (Section 10.3.1). If the embedding layer \mathbf{E} is learned, that adds an additional $m \times D$ parameters ($D = 10,000$ here), and is by far the biggest cost.

We fit the RNN as described in Figure 10.12 and the accompanying text to the **IMDb** data. The model had an embedding matrix \mathbf{E} with $m = 32$ (which was learned in training as opposed to precomputed), followed by a single recurrent layer with $K = 32$ hidden units. The model was trained with dropout regularization on the 25,000 reviews in the designated training set, and achieved a disappointing 76% accuracy on the **IMDb** test data. A network using the **GloVe** pretrained embedding matrix \mathbf{E} performed slightly worse.

For ease of exposition we have presented a very simple RNN. More elaborate versions use *long term* and *short term* memory (LSTM). Two tracks of hidden-layer activations are maintained, so that when the activation A_ℓ is computed, it gets input from hidden units both further back in time, and closer in time — a so-called *LSTM RNN*. With long sequences, this overcomes the problem of early signals being washed out by the time they get propagated through the chain to the final activation vector A_L .

LSTM RNN

When we refit our model using the LSTM architecture for the hidden layer, the performance improved to 87% on the **IMDb** test data. This is comparable with the 88% achieved by the bag-of-words model in Section 10.4. We give details on fitting these models in Section 10.9.6.

Despite this added LSTM complexity, our RNN is still somewhat “entry level”. We could probably achieve slightly better results by changing the size of the model, changing the regularization, and including additional hidden layers. However, LSTM models take a long time to train, which makes exploring many architectures and parameter optimization tedious.

RNNs provide a rich framework for modeling data sequences, and they continue to evolve. There have been many advances in the development of RNNs — in architecture, data augmentation, and in the learning algorithms. At the time of this writing (early 2020) the leading RNN configurations report accuracy above 95% on the **IMDb** data. The details are beyond the scope of this book.¹⁷

10.5.2 Time Series Forecasting

Figure 10.14 shows historical trading statistics from the New York Stock Exchange. Shown are three daily time series covering the period December 3, 1962 to December 31, 1986.¹⁸

¹⁷An **IMDb** leaderboard can be found at <https://paperswithcode.com/sota/sentiment-analysis-on-imdb>.

¹⁸These data were assembled by LeBaron and Weigend (1998) *IEEE Transactions on Neural Networks*, 9(1): 213–220.

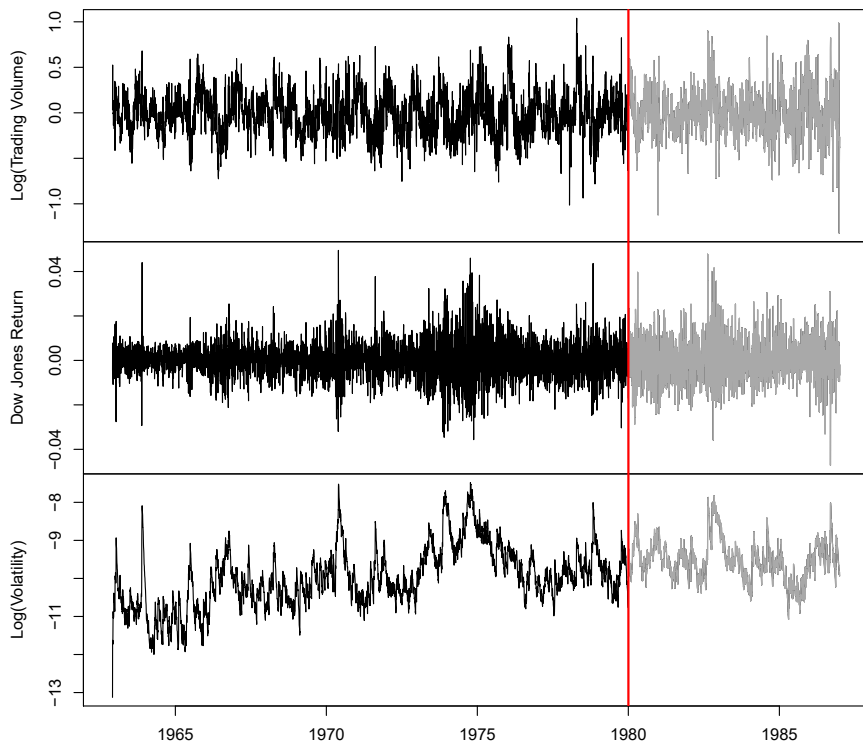


FIGURE 10.14. Historical trading statistics from the New York Stock Exchange. Daily values of the normalized log trading volume, DJIA return, and log volatility are shown for a 24-year period from 1962–1986. We wish to predict trading volume on any day, given the history on all earlier days. To the left of the red bar (January 2, 1980) is training data, and to the right test data.

- **Log trading volume.** This is the fraction of all outstanding shares that are traded on that day, relative to a 100-day moving average of past turnover, on the log scale.
- **Dow Jones return.** This is the difference between the log of the Dow Jones Industrial Index on consecutive trading days.
- **Log volatility.** This is based on the absolute values of daily price movements.

Predicting stock prices is a notoriously hard problem, but it turns out that predicting trading volume based on recent past history is more manageable (and is useful for planning trading strategies).

An observation here consists of the measurements (v_t, r_t, z_t) on day t , in this case the values for `log_volume`, `DJ_return` and `log_volatility`. There are a total of $T = 6,051$ such triples, each of which is plotted as a time series in Figure 10.14. One feature that strikes us immediately is that the day-to-day observations are not independent of each other. The series exhibit *auto-correlation* — in this case values nearby in time tend to be similar to each other. This distinguishes time series from other data sets we have encountered, in which observations can be assumed to be independent of

auto-correlation

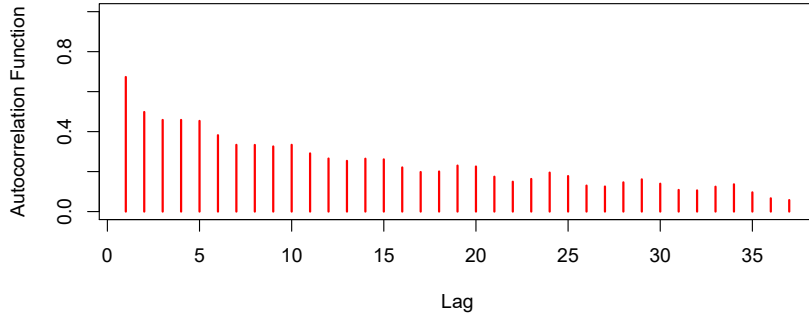


FIGURE 10.15. The autocorrelation function for `log_volume`. We see that nearby values are fairly strongly correlated, with correlations above 0.2 as far as 20 days apart.

each other. To be clear, consider pairs of observations $(v_t, v_{t-\ell})$, a *lag* of ℓ days apart. If we take all such pairs in the v_t series and compute their correlation coefficient, this gives the autocorrelation at lag ℓ . Figure 10.15 shows the autocorrelation function for all lags up to 37, and we see considerable correlation.

Another interesting characteristic of this forecasting problem is that the response variable v_t — `log_volume` — is also a predictor! In particular, we will use the past values of `log_volume` to predict values in the future.

RNN forecaster

We wish to predict a value v_t from past values v_{t-1}, v_{t-2}, \dots , and also to make use of past values of the other series r_{t-1}, r_{t-2}, \dots and z_{t-1}, z_{t-2}, \dots . Although our combined data is quite a long series with 6,051 trading days, the structure of the problem is different from the previous document-classification example.

- We only have one series of data, not 25,000.
- We have an entire *series* of targets v_t , and the inputs include past values of this series.

How do we represent this problem in terms of the structure displayed in Figure 10.12? The idea is to extract many short mini-series of input sequences $X = \{X_1, X_2, \dots, X_L\}$ with a predefined length L (called the *lag* in this context), and a corresponding target Y . They have the form

$$X_1 = \begin{pmatrix} v_{t-L} \\ r_{t-L} \\ z_{t-L} \end{pmatrix}, \quad X_2 = \begin{pmatrix} v_{t-L+1} \\ r_{t-L+1} \\ z_{t-L+1} \end{pmatrix}, \dots, \quad X_L = \begin{pmatrix} v_{t-1} \\ r_{t-1} \\ z_{t-1} \end{pmatrix}, \quad \text{and } Y = v_t. \quad (10.20)$$

So here the target Y is the value of `log_volume` v_t at a single timepoint t , and the input sequence X is the series of 3-vectors $\{X_\ell\}_1^L$ each consisting of the three measurements `log_volume`, `DJ_return` and `log_volatility` from day $t - L$, $t - L + 1$, up to $t - 1$. Each value of t makes a separate (X, Y) pair, for t running from $L + 1$ to T . For the `NYSE` data we will use the past

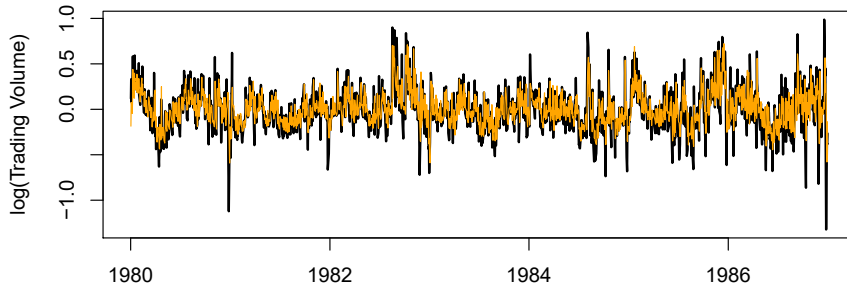


FIGURE 10.16. RNN forecast of `log_volume` on the NYSE test data. The black lines are the true volumes, and the superimposed orange the forecasts. The forecasted series accounts for 42% of the variance of `log_volume`.

five trading days to predict the next day's trading volume. Hence, we use $L = 5$. Since $T = 6,051$, we can create 6,046 such (X, Y) pairs. Clearly L is a parameter that should be chosen with care, perhaps using validation data.

We fit this model with $K = 12$ hidden units using the 4,281 training sequences derived from the data before January 2, 1980 (see Figure 10.14), and then used it to forecast the 1,770 values of `log_volume` after this date. We achieve an $R^2 = 0.42$ on the test data. Details are given in Section 10.9.6. As a *straw man*,¹⁹ using yesterday's value for `log_volume` as the prediction for today has $R^2 = 0.18$. Figure 10.16 shows the forecast results. We have plotted the observed values of the daily `log_volume` for the test period 1980–1986 in black, and superimposed the predicted series in orange. The correspondence seems rather good.

In forecasting the value of `log_volume` in the test period, we have to use the test data itself in forming the input sequences X . This may feel like cheating, but in fact it is not; we are always using past data to predict the future.

Autoregression

The RNN we just fit has much in common with a traditional *autoregression* (AR) linear model, which we present now for comparison. We first consider the response sequence v_t alone, and construct a response vector \mathbf{y} and a matrix \mathbf{M} of predictors for least squares regression as follows:

$$\mathbf{y} = \begin{bmatrix} v_{L+1} \\ v_{L+2} \\ v_{L+3} \\ \vdots \\ v_T \end{bmatrix} \quad \mathbf{M} = \begin{bmatrix} 1 & v_L & v_{L-1} & \cdots & v_1 \\ 1 & v_{L+1} & v_L & \cdots & v_2 \\ 1 & v_{L+2} & v_{L+1} & \cdots & v_3 \\ \vdots & \vdots & \vdots & \ddots & \vdots \\ 1 & v_{T-1} & v_{T-2} & \cdots & v_{T-L} \end{bmatrix}. \quad (10.21)$$

\mathbf{M} and \mathbf{y} each have $T - L$ rows, one per observation. We see that the predictors for any given response v_t on day t are the previous L values

auto-regression

¹⁹A straw man here refers to a simple and sensible prediction that can be used as a baseline for comparison.

of the same series. Fitting a regression of \mathbf{y} on \mathbf{M} amounts to fitting the model

$$\hat{v}_t = \hat{\beta}_0 + \hat{\beta}_1 v_{t-1} + \hat{\beta}_2 v_{t-2} + \cdots + \hat{\beta}_L v_{t-L}, \quad (10.22)$$

and is called an order- L autoregressive model, or simply AR(L). For the **NYSE** data we can include lagged versions of **DJ_return** and **log_volatility**, r_t and z_t , in the predictor matrix \mathbf{M} , resulting in $3L + 1$ columns. An AR model with $L = 5$ achieves a test R^2 of 0.41, slightly inferior to the 0.42 achieved by the RNN.

Of course the RNN and AR models are very similar. They both use the same response Y and input sequences X of length $L = 5$ and dimension $p = 3$ in this case. The RNN processes this sequence from left to right with the same weights \mathbf{W} (for the input layer), while the AR model simply treats all L elements of the sequence equally as a vector of $L \times p$ predictors — a process called *flattening* in the neural network literature. Of course the RNN also includes the hidden layer activations A_ℓ which transfer information along the sequence, and introduces additional nonlinearity. From (10.19) with $K = 12$ hidden units, we see that the RNN has $13 + 12 \times (1 + 3 + 12) = 205$ parameters, compared to the 16 for the AR(5) model.

flattening

An obvious extension of the AR model is to use the set of lagged predictors as the input vector to an ordinary feedforward neural network (10.1), and hence add more flexibility. This achieved a test $R^2 = 0.42$, slightly better than the linear AR, and the same as the RNN.

All the models can be improved by including the variable **day_of_week** corresponding to the day t of the target v_t (which can be learned from the calendar dates supplied with the data); trading volume is often higher on Mondays and Fridays. Since there are five trading days, this one-hot encodes to five binary variables. The performance of the AR model improved to $R^2 = 0.46$ as did the RNN, and the nonlinear AR model improved to $R^2 = 0.47$.

We used the most simple version of the RNN in our examples here. Additional experiments with the LSTM extension of the RNN yielded small improvements, typically of up to 1% in R^2 in these examples.

We give details of how we fit all three models in Section 10.9.6.

10.5.3 Summary of RNNs

We have illustrated RNNs through two simple use cases, and have only scratched the surface.

There are many variations and enhancements of the simple RNN we used for sequence modeling. One approach we did not discuss uses a one-dimensional convolutional neural network, treating the sequence of vectors (say words, as represented in the embedding space) as an image. The convolution filter slides along the sequence in a one-dimensional fashion, with the potential to learn particular phrases or short subsequences relevant to the learning task.

One can also have additional hidden layers in an RNN. For example, with two hidden layers, the sequence A_ℓ is treated as an input sequence to the next hidden layer in an obvious fashion.

The RNN we used scanned the document from beginning to end; alternative *bidirectional* RNNs scan the sequences in both directions.

In language translation the target is also a sequence of words, in a language different from that of the input sequence. Both the input sequence and the target sequence are represented by a structure similar to Figure 10.12, and they share the hidden units. In this so-called *Seq2Seq* learning, the hidden units are thought to capture the semantic meaning of the sentences. Some of the big breakthroughs in language modeling and translation resulted from the relatively recent improvements in such RNNs.

Algorithms used to fit RNNs can be complex and computationally costly. Fortunately, good software protects users somewhat from these complexities, and makes specifying and fitting these models relatively painless. Many of the models that we enjoy in daily life (like *Google Translate*) use state-of-the-art architectures developed by teams of highly skilled engineers, and have been trained using massive computational and data resources.

bidirectional
Seq2Seq

10.6 When to Use Deep Learning

The performance of deep learning in this chapter has been rather impressive. It nailed the digit classification problem, and deep CNNs have really revolutionized image classification. We see daily reports of new success stories for deep learning. Many of these are related to image classification tasks, such as machine diagnosis of mammograms or digital X-ray images, ophthalmology eye scans, annotations of MRI scans, and so on. Likewise there are numerous successes of RNNs in speech and language translation, forecasting, and document modeling. The question that then begs an answer is: *should we discard all our older tools, and use deep learning on every problem with data?* To address this question, we revisit our **Hitters** dataset from Chapter 6.

This is a regression problem, where the goal is to predict the **Salary** of a baseball player in 1987 using his performance statistics from 1986. After removing players with missing responses, we are left with 263 players and 19 variables. We randomly split the data into a training set of 176 players (two thirds), and a test set of 87 players (one third). We used three methods for fitting a regression model to these data.

- A linear model was used to fit the training data, and make predictions on the test data. The model has 20 parameters.
- The same linear model was fit with lasso regularization. The tuning parameter was selected by 10-fold cross-validation on the training data. It selected a model with 12 variables having nonzero coefficients.
- A neural network with one hidden layer consisting of 64 **ReLU** units was fit to the data. This model has 1,345 parameters.²⁰

²⁰The model was fit by stochastic gradient descent with a batch size of 32 for 1,000 epochs, and 10% dropout regularization. The test error performance flattened out and started to slowly increase after 1,000 epochs. These fitting details are discussed in Section 10.7.

Model	# Parameters	Mean Abs. Error	Test Set R^2
Linear Regression	20	254.7	0.56
Lasso	12	252.3	0.51
Neural Network	1345	257.4	0.54

TABLE 10.2. Prediction results on the `Hitters` test data for linear models fit by ordinary least squares and lasso, compared to a neural network fit by stochastic gradient descent with dropout regularization.

	Coefficient	Std. error	t-statistic	p-value
<code>Intercept</code>	-226.67	86.26	-2.63	0.0103
<code>Hits</code>	3.06	1.02	3.00	0.0036
<code>Walks</code>	0.181	2.04	0.09	0.9294
<code>CRuns</code>	0.859	0.12	7.09	< 0.0001
<code>PutOuts</code>	0.465	0.13	3.60	0.0005

TABLE 10.3. Least squares coefficient estimates associated with the regression of `Salary` on four variables chosen by lasso on the `Hitters` data set. This model achieved the best performance on the test data, with a mean absolute error of 224.8. The results reported here were obtained from a regression on the test data, which was not used in fitting the lasso model.

Table 10.2 compares the results. We see similar performance for all three models. We report the mean absolute error on the test data, as well as the test R^2 for each method, which are all respectable (see Exercise 5). We spent a fair bit of time fiddling with the configuration parameters of the neural network to achieve these results. It is possible that if we were to spend more time, and got the form and amount of regularization just right, that we might be able to match or even outperform linear regression and the lasso. But with great ease we obtained linear models that work well. Linear models are much easier to present and understand than the neural network, which is essentially a black box. The lasso selected 12 of the 19 variables in making its prediction. So in cases like this we are much better off following the *Occam's razor* principle: when faced with several methods that give roughly equivalent performance, pick the simplest.

After a bit more exploration with the lasso model, we identified an even simpler model with four variables. We then refit the linear model with these four variables to the training data (the so-called *relaxed lasso*), and achieved a test mean absolute error of 224.8, the overall winner! It is tempting to present the summary table from this fit, so we can see coefficients and p-values; however, since the model was selected on the training data, there would be *selection bias*. Instead, we refit the model on the test data, which was not used in the selection. Table 10.3 shows the results.

We have a number of very powerful tools at our disposal, including neural networks, random forests and boosting, support vector machines and generalized additive models, to name a few. And then we have linear models, and simple variants of these. When faced with new data modeling and prediction problems, it's tempting to always go for the trendy new methods. Often they give extremely impressive results, especially when the datasets are very large and can support the fitting of high-dimensional nonlinear models. However, if we can produce models with the simpler tools that

Occam's
razor

perform as well, they are likely to be easier to fit and understand, and potentially less fragile than the more complex approaches. Wherever possible, it makes sense to try the simpler models as well, and then make a choice based on the performance/complexity tradeoff.

Typically we expect deep learning to be an attractive choice when the sample size of the training set is extremely large, and when interpretability of the model is not a high priority.

10.7 Fitting a Neural Network



Fitting neural networks is somewhat complex, and we give a brief overview here. The ideas generalize to much more complex networks. Readers who find this material challenging can safely skip it. Fortunately, as we see in the lab at the end of this chapter, good software is available to fit neural network models in a relatively automated way, without worrying about the technical details of the model-fitting procedure.

We start with the simple network depicted in Figure 10.1 in Section 10.1. In model (10.1) the parameters are $\beta = (\beta_0, \beta_1, \dots, \beta_K)$, as well as each of the $w_k = (w_{k0}, w_{k1}, \dots, w_{kp})$, $k = 1, \dots, K$. Given observations (x_i, y_i) , $i = 1, \dots, n$, we could fit the model by solving a nonlinear least squares problem

$$\underset{\{w_k\}_1^K, \beta}{\text{minimize}} \frac{1}{2} \sum_{i=1}^n (y_i - f(x_i))^2, \quad (10.23)$$

where

$$f(x_i) = \beta_0 + \sum_{k=1}^K \beta_k g\left(w_{k0} + \sum_{j=1}^p w_{kj} x_{ij}\right). \quad (10.24)$$

The objective in (10.23) looks simple enough, but because of the nested arrangement of the parameters and the symmetry of the hidden units, it is not straightforward to minimize. The problem is nonconvex in the parameters, and hence there are multiple solutions. As an example, Figure 10.17 shows a simple nonconvex function of a single variable θ ; there are two solutions: one is a *local minimum* and the other is a *global minimum*. Furthermore, (10.1) is the very simplest of neural networks; in this chapter we have presented much more complex ones where these problems are compounded. To overcome some of these issues and to protect from overfitting, two general strategies are employed when fitting neural networks.

local
minimum
global
minimum

gradient
descent

- *Slow Learning:* the model is fit in a somewhat slow iterative fashion, using *gradient descent*. The fitting process is then stopped when overfitting is detected.
- *Regularization:* penalties are imposed on the parameters, usually lasso or ridge as discussed in Section 6.2.

Suppose we represent all the parameters in one long vector θ . Then we can rewrite the objective in (10.23) as

$$R(\theta) = \frac{1}{2} \sum_{i=1}^n (y_i - f_\theta(x_i))^2, \quad (10.25)$$

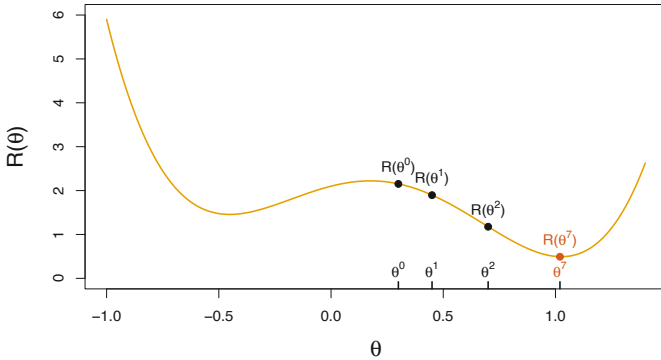


FIGURE 10.17. Illustration of gradient descent for one-dimensional θ . The objective function $R(\theta)$ is not convex, and has two minima, one at $\theta = -0.46$ (local), the other at $\theta = 1.02$ (global). Starting at some value θ^0 (typically randomly chosen), each step in θ moves downhill — against the gradient — until it cannot go down any further. Here gradient descent reached the global minimum in 7 steps.

where we make explicit the dependence of f on the parameters. The idea of gradient descent is very simple.

1. Start with a guess θ^0 for all the parameters in θ , and set $t = 0$.
2. Iterate until the objective (10.25) fails to decrease:
 - (a) Find a vector δ that reflects a small change in θ , such that $\theta^{t+1} = \theta^t + \delta$ reduces the objective; i.e. such that $R(\theta^{t+1}) < R(\theta^t)$.
 - (b) Set $t \leftarrow t + 1$.

One can visualize (Figure 10.17) standing in a mountainous terrain, and the goal is to get to the bottom through a series of steps. As long as each step goes downhill, we must eventually get to the bottom. In this case we were lucky, because with our starting guess θ^0 we end up at the global minimum. In general we can hope to end up at a (good) local minimum.

10.7.1 Backpropagation

How do we find the directions to move θ so as to decrease the objective $R(\theta)$ in (10.25)? The *gradient* of $R(\theta)$, evaluated at some current value $\theta = \theta^m$, is the vector of partial derivatives at that point:

$$\nabla R(\theta^m) = \frac{\partial R(\theta)}{\partial \theta} \Big|_{\theta=\theta^m}. \quad (10.26)$$

The subscript $\theta = \theta^m$ means that after computing the vector of derivatives, we evaluate it at the current guess, θ^m . This gives the direction in θ -space in which $R(\theta)$ increases most rapidly. The idea of gradient descent is to move θ a little in the *opposite* direction (since we wish to go downhill):

$$\theta^{m+1} \leftarrow \theta^m - \rho \nabla R(\theta^m). \quad (10.27)$$

For a small enough value of the *learning rate* ρ , this step will decrease the objective $R(\theta)$; i.e. $R(\theta^{m+1}) \leq R(\theta^m)$. If the gradient vector is zero, then we may have arrived at a minimum of the objective.

How complicated is the calculation (10.26)? It turns out that it is quite simple here, and remains simple even for much more complex networks, because of the *chain rule* of differentiation.

Since $R(\theta) = \sum_{i=1}^n R_i(\theta) = \frac{1}{2} \sum_{i=1}^n (y_i - f_\theta(x_i))^2$ is a sum, its gradient is also a sum over the n observations, so we will just examine one of these terms,

$$R_i(\theta) = \frac{1}{2} \left(y_i - \beta_0 - \sum_{k=1}^K \beta_k g\left(w_{k0} + \sum_{j=1}^p w_{kj} x_{ij}\right) \right)^2. \quad (10.28)$$

To simplify the expressions to follow, we write $z_{ik} = w_{k0} + \sum_{j=1}^p w_{kj} x_{ij}$. First we take the derivative with respect to β_k :

$$\begin{aligned} \frac{\partial R_i(\theta)}{\partial \beta_k} &= \frac{\partial R_i(\theta)}{\partial f_\theta(x_i)} \cdot \frac{\partial f_\theta(x_i)}{\partial \beta_k} \\ &= -(y_i - f_\theta(x_i)) \cdot g(z_{ik}). \end{aligned} \quad (10.29)$$

And now we take the derivative with respect to w_{kj} :

$$\begin{aligned} \frac{\partial R_i(\theta)}{\partial w_{kj}} &= \frac{\partial R_i(\theta)}{\partial f_\theta(x_i)} \cdot \frac{\partial f_\theta(x_i)}{\partial g(z_{ik})} \cdot \frac{\partial g(z_{ik})}{\partial z_{ik}} \cdot \frac{\partial z_{ik}}{\partial w_{kj}} \\ &= -(y_i - f_\theta(x_i)) \cdot \beta_k \cdot g'(z_{ik}) \cdot x_{ij}. \end{aligned} \quad (10.30)$$

Notice that both these expressions contain the residual $y_i - f_\theta(x_i)$. In (10.29) we see that a fraction of that residual gets attributed to each of the hidden units according to the value of $g(z_{ik})$. Then in (10.30) we see a similar attribution to input j via hidden unit k . So the act of differentiation assigns a fraction of the residual to each of the parameters via the chain rule — a process known as *backpropagation* in the neural network literature. Although these calculations are straightforward, it takes careful bookkeeping to keep track of all the pieces.

learning rate

chain rule

backpropagation

minibatch

stochastic gradient descent

10.7.2 Regularization and Stochastic Gradient Descent

Gradient descent usually takes many steps to reach a local minimum. In practice, there are a number of approaches for accelerating the process. Also, when n is large, instead of summing (10.29)–(10.30) over all n observations, we can sample a small fraction or *minibatch* of them each time we compute a gradient step. This process is known as *stochastic gradient descent* (SGD) and is the state of the art for learning deep neural networks. Fortunately, there is very good software for setting up deep learning models, and for fitting them to data, so most of the technicalities are hidden from the user.

We now turn to the multilayer network (Figure 10.4) used in the digit recognition problem. The network has over 235,000 weights, which is around four times the number of training examples. Regularization is essential here

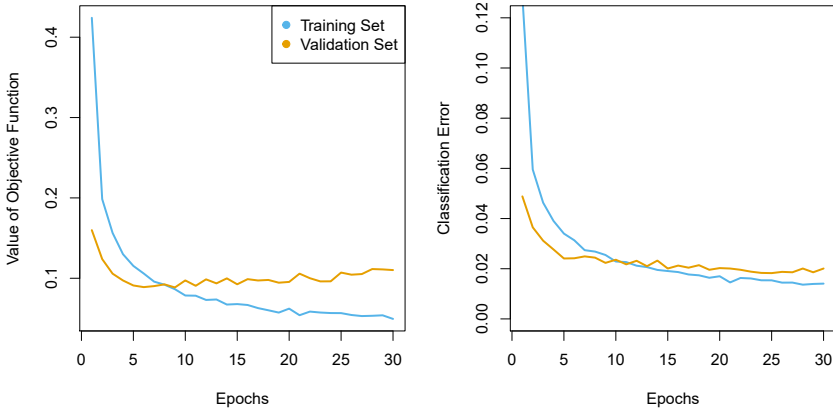


FIGURE 10.18. Evolution of training and validation errors for the **MNIST** neural network depicted in Figure 10.4, as a function of training epochs. The objective refers to the log-likelihood (10.14).

to avoid overfitting. The first row in Table 10.1 uses ridge regularization on the weights. This is achieved by augmenting the objective function (10.14) with a penalty term:

$$R(\theta; \lambda) = -\sum_{i=1}^n \sum_{m=0}^9 y_{im} \log(f_m(x_i)) + \lambda \sum_j \theta_j^2. \quad (10.31)$$

The parameter λ is often preset at a small value, or else it is found using the validation-set approach of Section 5.3.1. We can also use different values of λ for the groups of weights from different layers; in this case \mathbf{W}_1 and \mathbf{W}_2 were penalized, while the relatively few weights \mathbf{B} of the output layer were not penalized at all. Lasso regularization is also popular as an additional form of regularization, or as an alternative to ridge.

Figure 10.18 shows some metrics that evolve during the training of the network on the **MNIST** data. It turns out that SGD naturally enforces its own form of approximately quadratic regularization.²¹ Here the minibatch size was 128 observations per gradient update. The term *epochs* labeling the horizontal axis in Figure 10.18 counts the number of times an equivalent of the full training set has been processed. For this network, 20% of the 60,000 training observations were used as a validation set in order to determine when training should stop. So in fact 48,000 observations were used for training, and hence there are $48,000/128 \approx 375$ minibatch gradient updates per epoch. We see that the value of the validation objective actually starts to increase by 30 epochs, so *early stopping* can also be used as an additional form of regularization.

epochs
early
stopping

²¹This and other properties of SGD for deep learning are the subject of much research in the machine learning literature at the time of writing.

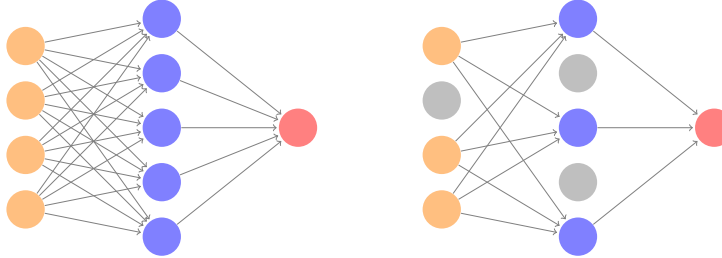


FIGURE 10.19. Dropout Learning. Left: a fully connected network. Right: network with dropout in the input and hidden layer. The nodes in grey are selected at random, and ignored in an instance of training.

10.7.3 Dropout Learning

The second row in Table 10.1 is labeled *dropout*. This is a relatively new and efficient form of regularization, similar in some respects to ridge regularization. Inspired by random forests (Section 8.2), the idea is to randomly remove a fraction ϕ of the units in a layer when fitting the model. Figure 10.19 illustrates this. This is done separately each time a training observation is processed. The surviving units stand in for those missing, and their weights are scaled up by a factor of $1/(1 - \phi)$ to compensate. This prevents nodes from becoming over-specialized, and can be seen as a form of regularization. In practice dropout is achieved by randomly setting the activations for the “dropped out” units to zero, while keeping the architecture intact.

dropout

10.7.4 Network Tuning

The network in Figure 10.4 is considered to be relatively straightforward; it nevertheless requires a number of choices that all have an effect on the performance:

- *The number of hidden layers, and the number of units per layer.* Modern thinking is that the number of units per hidden layer can be large, and overfitting can be controlled via the various forms of regularization.
- *Regularization tuning parameters.* These include the dropout rate ϕ and the strength λ of lasso and ridge regularization, and are typically set separately at each layer.
- *Details of stochastic gradient descent.* These include the batch size, the number of epochs, and if used, details of data augmentation (Section 10.3.4.)

Choices such as these can make a difference. In preparing this MNIST example, we achieved a respectable 1.8% misclassification error after some trial and error. Finer tuning and training of a similar network can get under 1% error on these data, but the tinkering process can be tedious, and can result in overfitting if done carelessly.

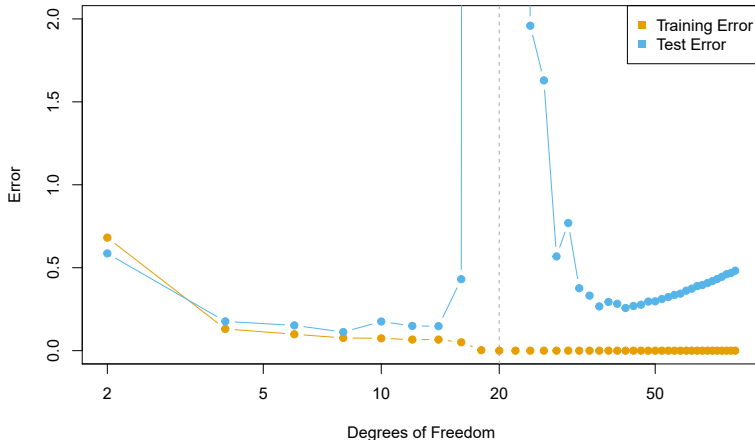


FIGURE 10.20. Double descent phenomenon, illustrated using error plots for a one-dimensional natural spline example. The horizontal axis refers to the number of spline basis functions on the log scale. The training error hits zero when the degrees of freedom coincides with the sample size $n = 20$, the “interpolation threshold”, and remains zero thereafter. The test error increases dramatically at this threshold, but then descends again to a reasonable value before finally increasing again.

10.8 Interpolation and Double Descent

Throughout this book, we have repeatedly discussed the bias-variance trade-off, first presented in Section 2.2.2. This trade-off indicates that statistical learning methods tend to perform the best, in terms of test-set error, for an intermediate level of model complexity. In particular, if we plot “flexibility” on the x -axis and error on the y -axis, then we generally expect to see that test error has a U-shape, whereas training error decreases monotonically. Two “typical” examples of this behavior can be seen in the right-hand panel of Figure 2.9 on page 29, and in Figure 2.17 on page 39. One implication of the bias-variance trade-off is that it is generally not a good idea to *interpolate* the training data — that is, to get zero training error — since that will often result in very high test error.

However, it turns out that in certain specific settings it can be possible for a statistical learning method that interpolates the training data to perform well — or at least, better than a slightly less complex model that does not quite interpolate the data. This phenomenon is known as *double descent*, and is displayed in Figure 10.20. “Double descent” gets its name from the fact that the test error has a U-shape before the interpolation threshold is reached, and then it descends again (for a while, at least) as an increasingly flexible model is fit.

We now describe the set-up that resulted in Figure 10.20. We simulated $n = 20$ observations from the model

$$Y = \sin(X) + \epsilon,$$

where $X \sim U[-5, 5]$ (uniform distribution), and $\epsilon \sim N(0, \sigma^2)$ with $\sigma = 0.3$. We then fit a natural spline to the data, as described in Section 7.4, with d

interpolate

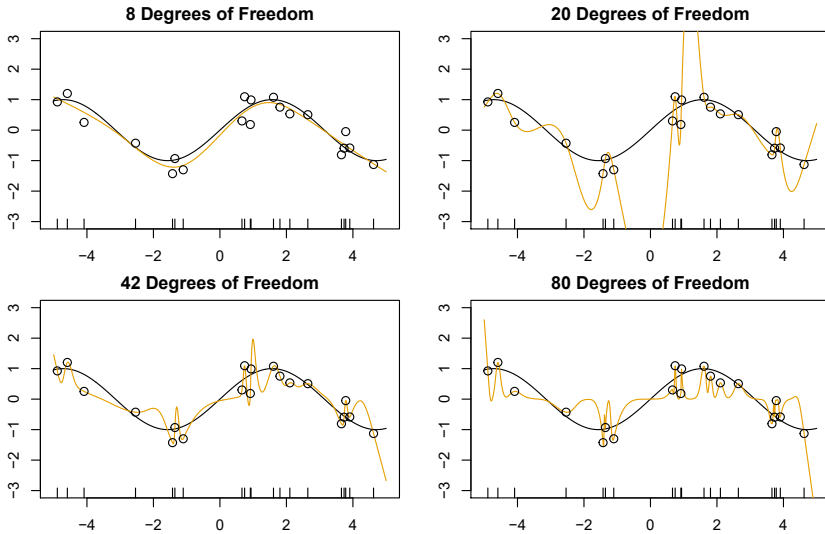


FIGURE 10.21. Fitted functions $\hat{f}_d(X)$ (orange), true function $f(X)$ (black) and the observed 20 training data points. A different value of d (degrees of freedom) is used in each panel. For $d \geq 20$ the orange curves all interpolate the training points, and hence the training error is zero.

degrees of freedom.²² Recall from Section 7.4 that fitting a natural spline with d degrees of freedom amounts to fitting a least-squares regression of the response onto a set of d basis functions. The upper-left panel of Figure 10.21 shows the data, the true function $f(X)$, and $\hat{f}_8(X)$, the fitted natural spline with $d = 8$ degrees of freedom.

Next, we fit a natural spline with $d = 20$ degrees of freedom. Since $n = 20$, this means that $n = d$, and we have zero training error; in other words, we have interpolated the training data! We can see from the top-right panel of Figure 10.21 that $\hat{f}_{20}(X)$ makes wild excursions, and hence the test error will be large.

We now continue to fit natural splines to the data, with increasing values of d . For $d > 20$, the least squares regression of Y onto d basis functions is not unique: there are an infinite number of least squares coefficient estimates that achieve zero error. To select among them, we choose the one with the smallest sum of squared coefficients, $\sum_{j=1}^d \hat{\beta}_j^2$. This is known as the *minimum-norm* solution.

The two lower panels of Figure 10.21 show the minimum-norm natural spline fits with $d = 42$ and $d = 80$ degrees of freedom. Incredibly, $\hat{f}_{42}(X)$ is quite a bit less wild than $\hat{f}_{20}(X)$, even though it makes use of more degrees of freedom. And $\hat{f}_{80}(X)$ is not much different. How can this be? Essentially, $\hat{f}_{20}(X)$ is very wild because there is just a single way to interpolate $n = 20$ observations using $d = 20$ basis functions, and that single way results in a somewhat extreme fitted function. By contrast, there are an

²²This implies the choice of d knots, here chosen at d equi-probability quantiles of the training data. When $d > n$, the quantiles are found by interpolation.

infinite number of ways to interpolate $n = 20$ observations using $d = 42$ or $d = 80$ basis functions, and the smoothest of them — that is, the minimum norm solution — is much less wild than $\hat{f}_{20}(X)$!

In Figure 10.20, we display the training error and test error associated with $\hat{f}_d(X)$, for a range of values of the degrees of freedom d . We see that the training error drops to zero once $d = 20$ and beyond; i.e. once the interpolation threshold is reached. By contrast, the test error shows a U -shape for $d \leq 20$, grows extremely large around $d = 20$, and then shows a second region of descent for $d > 20$. For this example the signal-to-noise ratio — $\text{Var}(f(X))/\sigma^2$ — is 5.9, which is quite high (the data points are close to the true curve). So an estimate that interpolates the data and does not wander too far inbetween the observed data points will likely do well.

In Figures 10.20 and 10.21, we have illustrated the double descent phenomenon in a simple one-dimensional setting using natural splines. However, it turns out that the same phenomenon can arise for deep learning. Basically, when we fit neural networks with a huge number of parameters, we are sometimes able to get good results with zero training error. This is particularly true in problems with high signal-to-noise ratio, such as natural image recognition and language translation, for example. This is because the techniques used to fit neural networks, including stochastic gradient descent, naturally lend themselves to selecting a “smooth” interpolating model that has good test-set performance on these kinds of problems.

Some points are worth emphasizing:

- *The double-descent phenomenon does not contradict the bias-variance trade-off, as presented in Section 2.2.2.* Rather, the double-descent curve seen in the right-hand side of Figure 10.20 is a consequence of the fact that the x -axis displays the number of spline basis functions used, which does not properly capture the true “flexibility” of models that interpolate the training data. Stated another way, in this example, the minimum-norm natural spline with $d = 42$ has lower variance than the natural spline with $d = 20$.
- *Most of the statistical learning methods seen in this book do not exhibit double descent.* For instance, regularization approaches typically do not interpolate the training data, and thus double descent does not occur. This is not a drawback of regularized methods: they can give great results *without interpolating the data!*

In particular, in the examples here, if we had fit the natural splines using ridge regression with an appropriately-chosen penalty rather than least squares, then we would not have seen double descent, and in fact would have obtained better test error results.

- *In Chapter 9, we saw that maximal margin classifiers and SVMs that have zero training error nonetheless often achieve very good test error.* This is in part because those methods seek smooth minimum norm solutions. This is similar to the fact that the minimum-norm natural spline can give good results with zero training error.
- *The double-descent phenomenon has been used by the machine learning community to explain the successful practice of using an over-*

parametrized neural network (many layers, and many hidden units), and then fitting all the way to zero training error. However, fitting to zero error is not always optimal, and whether it is advisable depends on the signal-to-noise ratio. For instance, we may use ridge regularization to avoid overfitting a neural network, as in (10.31). In this case, provided that we use an appropriate choice for the tuning parameter λ , we will never interpolate the training data, and thus will not see the double descent phenomenon. Nonetheless we can get very good test-set performance, likely much better than we would have achieved had we interpolated the training data. Early stopping during stochastic gradient descent can also serve as a form of regularization that prevents us from interpolating the training data, while still getting very good results on test data.

To summarize: though double descent can sometimes occur in neural networks, we typically do not want to rely on this behavior. Moreover, it is important to remember that the bias-variance trade-off always holds (though it is possible that test error as a function of flexibility may not exhibit a U-shape, depending on how we have parametrized the notion of “flexibility” on the x -axis).

10.9 Lab: Deep Learning

In this section we demonstrate how to fit the examples discussed in the text. We use the `Python torch` package, along with the `pytorch_lightning` package which provides utilities to simplify fitting and evaluating models. This code can be impressively fast with certain special processors, such as Apple’s new M1 chip. The package is well-structured, flexible, and will feel comfortable to `Python` users. A good companion is the site pytorch.org/tutorials. Much of our code is adapted from there, as well as the `pytorch_lightning` documentation.²³

`torch`
`pytorch_`
`lightning`

We start with several standard imports that we have seen before.

```
In [1]: import numpy as np, pandas as pd
from matplotlib.pyplot import subplots
from sklearn.linear_model import \
    (LinearRegression,
     LogisticRegression,
     Lasso)
from sklearn.preprocessing import StandardScaler
from sklearn.model_selection import KFold
from sklearn.pipeline import Pipeline
from ISLP import load_data
from ISLP.models import ModelSpec as MS
from sklearn.model_selection import \
    (train_test_split,
     GridSearchCV)
```

²³The precise URLs at the time of writing are <https://pytorch.org/tutorials/beginner/basics/intro.html> and <https://pytorch-lightning.readthedocs.io/en/latest/>.

We continue with the usual training steps, fit the model, and evaluate the test error. We see the test R^2 is a slight improvement over the linear AR model that also includes `day_of_week`.

```
In [112]: nl_trainer = Trainer(deterministic=True,
                           max_epochs=20,
                           callbacks=[ErrorTracker()])
nl_trainer.fit(nl_module, datamodule=day_dm)
nl_trainer.test(nl_module, datamodule=day_dm)
```

```
Out[112]: {'test_loss': 0.5625, 'test_r2': 0.4662}]
```

10.10 Exercises

Conceptual

1. Consider a neural network with two hidden layers: $p = 4$ input units, 2 units in the first hidden layer, 3 units in the second hidden layer, and a single output.
 - (a) Draw a picture of the network, similar to Figures 10.1 or 10.4.
 - (b) Write out an expression for $f(X)$, assuming ReLU activation functions. Be as explicit as you can!
 - (c) Now plug in some values for the coefficients and write out the value of $f(X)$.
 - (d) How many parameters are there?
2. Consider the *softmax* function in (10.13) (see also (4.13) on page 145) for modeling multinomial probabilities.
 - (a) In (10.13), show that if we add a constant c to each of the z_ℓ , then the probability is unchanged.
 - (b) In (4.13), show that if we add constants c_j , $j = 0, 1, \dots, p$, to each of the corresponding coefficients for each of the classes, then the predictions at any new point x are unchanged.

This shows that the softmax function is *over-parametrized*. However, regularization and SGD typically constrain the solutions so that this over-parametrized

3. Show that the negative multinomial log-likelihood (10.14) is equivalent to the negative log of the likelihood expression (4.5) when there are $M = 2$ classes.
4. Consider a CNN that takes in 32×32 grayscale images and has a single convolution layer with three 5×5 convolution filters (without boundary padding).
 - (a) Draw a sketch of the input and first hidden layer similar to Figure 10.8.

- (b) How many parameters are in this model?
 - (c) Explain how this model can be thought of as an ordinary feed-forward neural network with the individual pixels as inputs, and with constraints on the weights in the hidden units. What are the constraints?
 - (d) If there were no constraints, then how many weights would there be in the ordinary feed-forward neural network in (c)?
5. In Table 10.2 on page 426, we see that the ordering of the three methods with respect to mean absolute error is different from the ordering with respect to test set R^2 . How can this be?

Applied

6. Consider the simple function $R(\beta) = \sin(\beta) + \beta/10$.
 - (a) Draw a graph of this function over the range $\beta \in [-6, 6]$.
 - (b) What is the derivative of this function?
 - (c) Given $\beta^0 = 2.3$, run gradient descent to find a local minimum of $R(\beta)$ using a learning rate of $\rho = 0.1$. Show each of β^0, β^1, \dots in your plot, as well as the final answer.
 - (d) Repeat with $\beta^0 = 1.4$.
7. Fit a neural network to the **Default** data. Use a single hidden layer with 10 units, and dropout regularization. Have a look at Labs 10.9.1–10.9.2 for guidance. Compare the classification performance of your model with that of linear logistic regression.
8. From your collection of personal photographs, pick 10 images of animals (such as dogs, cats, birds, farm animals, etc.). If the subject does not occupy a reasonable part of the image, then crop the image. Now use a pretrained image classification CNN as in Lab 10.9.4 to predict the class of each of your images, and report the probabilities for the top five predicted classes for each image.
9. Fit a lag-5 autoregressive model to the **NYSE** data, as described in the text and Lab 10.9.6. Refit the model with a 12-level factor representing the month. Does this factor improve the performance of the model?
10. In Section 10.9.6, we showed how to fit a linear AR model to the **NYSE** data using the `LinearRegression()` function. However, we also mentioned that we can “flatten” the short sequences produced for the RNN model in order to fit a linear AR model. Use this latter approach to fit a linear AR model to the **NYSE** data. Compare the test R^2 of this linear AR model to that of the linear AR model that we fit in the lab. What are the advantages/disadvantages of each approach?
11. Repeat the previous exercise, but now fit a nonlinear AR model by “flattening” the short sequences produced for the RNN model.

12. Consider the RNN fit to the **NYSE** data in Section 10.9.6. Modify the code to allow inclusion of the variable **day_of_week**, and fit the RNN. Compute the test R^2 .
13. Repeat the analysis of Lab 10.9.5 on the **IMDb** data using a similarly structured neural network. We used 16 hidden units at each of two hidden layers. Explore the effect of increasing this to 32 and 64 units per layer, with and without 30% dropout regularization.



Unsupervised Learning

Most of this book concerns *supervised learning* methods such as regression and classification. In the supervised learning setting, we typically have access to a set of p features X_1, X_2, \dots, X_p , measured on n observations, and a response Y also measured on those same n observations. The goal is then to predict Y using X_1, X_2, \dots, X_p .

This chapter will instead focus on *unsupervised learning*, a set of statistical tools intended for the setting in which we have only a set of features X_1, X_2, \dots, X_p measured on n observations. We are not interested in prediction, because we do not have an associated response variable Y . Rather, the goal is to discover interesting things about the measurements on X_1, X_2, \dots, X_p . Is there an informative way to visualize the data? Can we discover subgroups among the variables or among the observations? Unsupervised learning refers to a diverse set of techniques for answering questions such as these. In this chapter, we will focus on two particular types of unsupervised learning: *principal components analysis*, a tool used for data visualization or data pre-processing before supervised techniques are applied, and *clustering*, a broad class of methods for discovering unknown subgroups in data.

12.1 The Challenge of Unsupervised Learning

Supervised learning is a well-understood area. In fact, if you have read the preceding chapters in this book, then you should by now have a good grasp of supervised learning. For instance, if you are asked to predict a binary outcome from a data set, you have a very well developed set of tools at your disposal (such as logistic regression, linear discriminant analysis, classification trees, support vector machines, and more) as well as a clear

understanding of how to assess the quality of the results obtained (using cross-validation, validation on an independent test set, and so forth).

In contrast, unsupervised learning is often much more challenging. The exercise tends to be more subjective, and there is no simple goal for the analysis, such as prediction of a response. Unsupervised learning is often performed as part of an *exploratory data analysis*. Furthermore, it can be hard to assess the results obtained from unsupervised learning methods, since there is no universally accepted mechanism for performing cross-validation or validating results on an independent data set. The reason for this difference is simple. If we fit a predictive model using a supervised learning technique, then it is possible to *check our work* by seeing how well our model predicts the response Y on observations not used in fitting the model. However, in unsupervised learning, there is no way to check our work because we don't know the true answer—the problem is unsupervised.

exploratory
data
analysis

Techniques for unsupervised learning are of growing importance in a number of fields. A cancer researcher might assay gene expression levels in 100 patients with breast cancer. He or she might then look for subgroups among the breast cancer samples, or among the genes, in order to obtain a better understanding of the disease. An online shopping site might try to identify groups of shoppers with similar browsing and purchase histories, as well as items that are of particular interest to the shoppers within each group. Then an individual shopper can be preferentially shown the items in which he or she is particularly likely to be interested, based on the purchase histories of similar shoppers. A search engine might choose which search results to display to a particular individual based on the click histories of other individuals with similar search patterns. These statistical learning tasks, and many more, can be performed via unsupervised learning techniques.

12.2 Principal Components Analysis

Principal components are discussed in Section 6.3.1 in the context of principal components regression. When faced with a large set of correlated variables, principal components allow us to summarize this set with a smaller number of representative variables that collectively explain most of the variability in the original set. The principal component directions are presented in Section 6.3.1 as directions in feature space along which the original data are *highly variable*. These directions also define lines and subspaces that are *as close as possible* to the data cloud. To perform principal components regression, we simply use principal components as predictors in a regression model in place of the original larger set of variables.

principal
components
analysis

Principal components analysis (PCA) refers to the process by which principal components are computed, and the subsequent use of these components in understanding the data. PCA is an unsupervised approach, since it involves only a set of features X_1, X_2, \dots, X_p , and no associated response Y . Apart from producing derived variables for use in supervised learning problems, PCA also serves as a tool for data visualization (visualization of

the observations or visualization of the variables). It can also be used as a tool for data imputation — that is, for filling in missing values in a data matrix.

We now discuss PCA in greater detail, focusing on the use of PCA as a tool for unsupervised data exploration, in keeping with the topic of this chapter.

12.2.1 What Are Principal Components?

Suppose that we wish to visualize n observations with measurements on a set of p features, X_1, X_2, \dots, X_p , as part of an exploratory data analysis. We could do this by examining two-dimensional scatterplots of the data, each of which contains the n observations' measurements on two of the features. However, there are $\binom{p}{2} = p(p-1)/2$ such scatterplots; for example, with $p = 10$ there are 45 plots! If p is large, then it will certainly not be possible to look at all of them; moreover, most likely none of them will be informative since they each contain just a small fraction of the total information present in the data set. Clearly, a better method is required to visualize the n observations when p is large. In particular, we would like to find a low-dimensional representation of the data that captures as much of the information as possible. For instance, if we can obtain a two-dimensional representation of the data that captures most of the information, then we can plot the observations in this low-dimensional space.

PCA provides a tool to do just this. It finds a low-dimensional representation of a data set that contains as much as possible of the variation. The idea is that each of the n observations lives in p -dimensional space, but not all of these dimensions are equally interesting. PCA seeks a small number of dimensions that are as interesting as possible, where the concept of *interesting* is measured by the amount that the observations vary along each dimension. Each of the dimensions found by PCA is a linear combination of the p features. We now explain the manner in which these dimensions, or *principal components*, are found.

The *first principal component* of a set of features X_1, X_2, \dots, X_p is the normalized linear combination of the features

$$Z_1 = \phi_{11}X_1 + \phi_{21}X_2 + \cdots + \phi_{p1}X_p \quad (12.1)$$

that has the largest variance. By *normalized*, we mean that $\sum_{j=1}^p \phi_{j1}^2 = 1$. We refer to the elements $\phi_{11}, \dots, \phi_{p1}$ as the *loadings* of the first principal component; together, the loadings make up the principal component loading vector, $\phi_1 = (\phi_{11} \ \phi_{21} \ \dots \ \phi_{p1})^T$. We constrain the loadings so that their sum of squares is equal to one, since otherwise setting these elements to be arbitrarily large in absolute value could result in an arbitrarily large variance.

loading

Given an $n \times p$ data set \mathbf{X} , how do we compute the first principal component? Since we are only interested in variance, we assume that each of the variables in \mathbf{X} has been centered to have mean zero (that is, the column means of \mathbf{X} are zero). We then look for the linear combination of the sample feature values of the form

$$z_{i1} = \phi_{11}x_{i1} + \phi_{21}x_{i2} + \cdots + \phi_{p1}x_{ip} \quad (12.2)$$

that has largest sample variance, subject to the constraint that $\sum_{j=1}^p \phi_{j1}^2 = 1$. In other words, the first principal component loading vector solves the optimization problem

$$\underset{\phi_{11}, \dots, \phi_{p1}}{\text{maximize}} \left\{ \frac{1}{n} \sum_{i=1}^n \left(\sum_{j=1}^p \phi_{j1} x_{ij} \right)^2 \right\} \text{ subject to } \sum_{j=1}^p \phi_{j1}^2 = 1. \quad (12.3)$$

From (12.2) we can write the objective in (12.3) as $\frac{1}{n} \sum_{i=1}^n z_{i1}^2$. Since $\frac{1}{n} \sum_{i=1}^n x_{ij} = 0$, the average of the z_{11}, \dots, z_{n1} will be zero as well. Hence the objective that we are maximizing in (12.3) is just the sample variance of the n values of z_{i1} . We refer to z_{11}, \dots, z_{n1} as the *scores* of the first principal component. Problem (12.3) can be solved via an *eigen decomposition*, a standard technique in linear algebra, but the details are outside of the scope of this book.¹

score
eigen decom-
position

There is a nice geometric interpretation of the first principal component. The loading vector ϕ_1 with elements $\phi_{11}, \phi_{21}, \dots, \phi_{p1}$ defines a direction in feature space along which the data vary the most. If we project the n data points x_1, \dots, x_n onto this direction, the projected values are the principal component scores z_{11}, \dots, z_{n1} themselves. For instance, Figure 6.14 on page 254 displays the first principal component loading vector (green solid line) on an advertising data set. In these data, there are only two features, and so the observations as well as the first principal component loading vector can be easily displayed. As can be seen from (6.19), in that data set $\phi_{11} = 0.839$ and $\phi_{21} = 0.544$.

After the first principal component Z_1 of the features has been determined, we can find the second principal component Z_2 . The second principal component is the linear combination of X_1, \dots, X_p that has maximal variance out of all linear combinations that are *uncorrelated* with Z_1 . The second principal component scores $z_{12}, z_{22}, \dots, z_{n2}$ take the form

$$z_{i2} = \phi_{12} x_{i1} + \phi_{22} x_{i2} + \dots + \phi_{p2} x_{ip}, \quad (12.4)$$

where ϕ_2 is the second principal component loading vector, with elements $\phi_{12}, \phi_{22}, \dots, \phi_{p2}$. It turns out that constraining Z_2 to be uncorrelated with Z_1 is equivalent to constraining the direction ϕ_2 to be orthogonal (perpendicular) to the direction ϕ_1 . In the example in Figure 6.14, the observations lie in two-dimensional space (since $p = 2$), and so once we have found ϕ_1 , there is only one possibility for ϕ_2 , which is shown as a blue dashed line. (From Section 6.3.1, we know that $\phi_{12} = 0.544$ and $\phi_{22} = -0.839$.) But in a larger data set with $p > 2$ variables, there are multiple distinct principal components, and they are defined in a similar manner. To find ϕ_2 , we solve a problem similar to (12.3) with ϕ_2 replacing ϕ_1 , and with the additional constraint that ϕ_2 is orthogonal to ϕ_1 .²

¹As an alternative to the eigen decomposition, a related technique called the singular value decomposition can be used. This will be explored in the lab at the end of this chapter.

²On a technical note, the principal component directions $\phi_1, \phi_2, \phi_3, \dots$ are given by the ordered sequence of eigenvectors of the matrix $\mathbf{X}^T \mathbf{X}$, and the variances of the components are the eigenvalues. There are at most $\min(n-1, p)$ principal components.

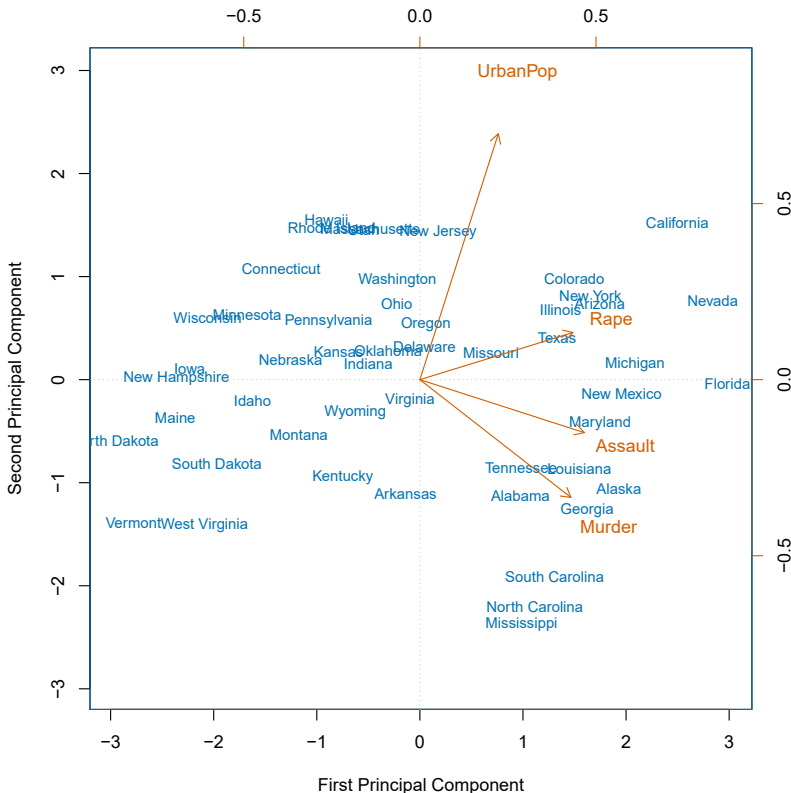


FIGURE 12.1. The first two principal components for the **USArrests** data. The blue state names represent the scores for the first two principal components. The orange arrows indicate the first two principal component loading vectors (with axes on the top and right). For example, the loading for **Rape** on the first component is 0.54, and its loading on the second principal component 0.17 (the word **Rape** is centered at the point (0.54, 0.17)). This figure is known as a biplot, because it displays both the principal component scores and the principal component loadings.

Once we have computed the principal components, we can plot them against each other in order to produce low-dimensional views of the data. For instance, we can plot the score vector Z_1 against Z_2 , Z_1 against Z_3 , Z_2 against Z_3 , and so forth. Geometrically, this amounts to projecting the original data down onto the subspace spanned by ϕ_1 , ϕ_2 , and ϕ_3 , and plotting the projected points.

We illustrate the use of PCA on the **USArrests** data set. For each of the 50 states in the United States, the data set contains the number of arrests per 100,000 residents for each of three crimes: **Assault**, **Murder**, and **Rape**. We also record **UrbanPop** (the percent of the population in each state living in urban areas). The principal component score vectors have length $n = 50$, and the principal component loading vectors have length $p = 4$. PCA was performed after standardizing each variable to have mean zero and standard

	PC1	PC2
Murder	0.5358995	-0.4181809
Assault	0.5831836	-0.1879856
UrbanPop	0.2781909	0.8728062
Rape	0.5434321	0.1673186

TABLE 12.1. The principal component loading vectors, ϕ_1 and ϕ_2 , for the **USArrests** data. These are also displayed in Figure 12.1.

deviation one. Figure 12.1 plots the first two principal components of these data. The figure represents both the principal component scores and the loading vectors in a single *biplot* display. The loadings are also given in Table 12.2.1.

In Figure 12.1, we see that the first loading vector places approximately equal weight on **Assault**, **Murder**, and **Rape**, but with much less weight on **UrbanPop**. Hence this component roughly corresponds to a measure of overall rates of serious crimes. The second loading vector places most of its weight on **UrbanPop** and much less weight on the other three features. Hence, this component roughly corresponds to the level of urbanization of the state. Overall, we see that the crime-related variables (**Murder**, **Assault**, and **Rape**) are located close to each other, and that the **UrbanPop** variable is far from the other three. This indicates that the crime-related variables are correlated with each other—states with high murder rates tend to have high assault and rape rates—and that the **UrbanPop** variable is less correlated with the other three.

We can examine differences between the states via the two principal component score vectors shown in Figure 12.1. Our discussion of the loading vectors suggests that states with large positive scores on the first component, such as California, Nevada and Florida, have high crime rates, while states like North Dakota, with negative scores on the first component, have low crime rates. California also has a high score on the second component, indicating a high level of urbanization, while the opposite is true for states like Mississippi. States close to zero on both components, such as Indiana, have approximately average levels of both crime and urbanization.

12.2.2 Another Interpretation of Principal Components

The first two principal component loading vectors in a simulated three-dimensional data set are shown in the left-hand panel of Figure 12.2; these two loading vectors span a plane along which the observations have the highest variance.

In the previous section, we describe the principal component loading vectors as the directions in feature space along which the data vary the most, and the principal component scores as projections along these directions. However, an alternative interpretation of principal components can also be

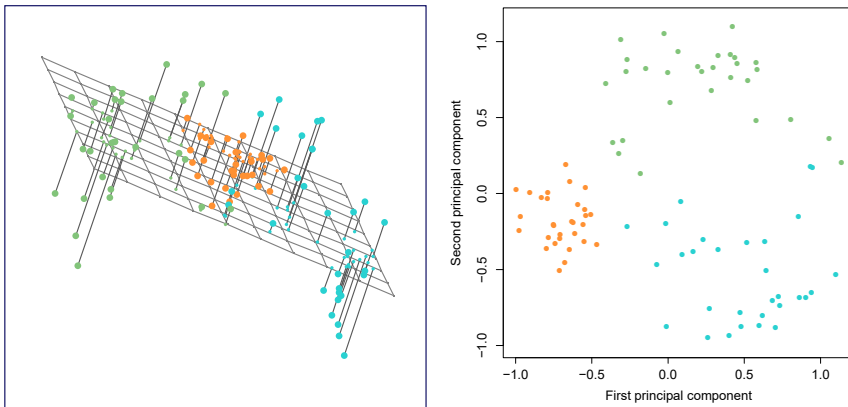


FIGURE 12.2. Ninety observations simulated in three dimensions. The observations are displayed in color for ease of visualization. Left: the first two principal component directions span the plane that best fits the data. The plane is positioned to minimize the sum of squared distances to each point. Right: the first two principal component score vectors give the coordinates of the projection of the 90 observations onto the plane.

useful: principal components provide low-dimensional linear surfaces that are *closest* to the observations. We expand upon that interpretation here.³

The first principal component loading vector has a very special property: it is the line in p -dimensional space that is *closest* to the n observations (using average squared Euclidean distance as a measure of closeness). This interpretation can be seen in the left-hand panel of Figure 6.15; the dashed lines indicate the distance between each observation and the line defined by the first principal component loading vector. The appeal of this interpretation is clear: we seek a single dimension of the data that lies as close as possible to all of the data points, since such a line will likely provide a good summary of the data.

The notion of principal components as the dimensions that are closest to the n observations extends beyond just the first principal component. For instance, the first two principal components of a data set span the plane that is closest to the n observations, in terms of average squared Euclidean distance. An example is shown in the left-hand panel of Figure 12.2. The first three principal components of a data set span the three-dimensional hyperplane that is closest to the n observations, and so forth.

Using this interpretation, together the first M principal component score vectors and the first M principal component loading vectors provide the best M -dimensional approximation (in terms of Euclidean distance) to

³In this section, we continue to assume that each column of the data matrix \mathbf{X} has been centered to have mean zero—that is, the column mean has been subtracted from each column.

the i th observation x_{ij} . This representation can be written as

$$x_{ij} \approx \sum_{m=1}^M z_{im} \phi_{jm}. \quad (12.5)$$

We can state this more formally by writing down an optimization problem. Suppose the data matrix \mathbf{X} is column-centered. Out of all approximations of the form $x_{ij} \approx \sum_{m=1}^M a_{im} b_{jm}$, we could ask for the one with the smallest residual sum of squares:

$$\underset{\mathbf{A} \in \mathbb{R}^{n \times M}, \mathbf{B} \in \mathbb{R}^{p \times M}}{\text{minimize}} \left\{ \sum_{j=1}^p \sum_{i=1}^n \left(x_{ij} - \sum_{m=1}^M a_{im} b_{jm} \right)^2 \right\}. \quad (12.6)$$

Here, \mathbf{A} is an $n \times M$ matrix whose (i, m) element is a_{im} , and \mathbf{B} is a $p \times M$ element whose (j, m) element is b_{jm} .

It can be shown that for any value of M , the columns of the matrices $\hat{\mathbf{A}}$ and $\hat{\mathbf{B}}$ that solve (12.6) are in fact the first M principal components score and loading vectors. In other words, if $\hat{\mathbf{A}}$ and $\hat{\mathbf{B}}$ solve (12.6), then $\hat{a}_{im} = z_{im}$ and $\hat{b}_{jm} = \phi_{jm}$.⁴ This means that the smallest possible value of the objective in (12.6) is

$$\sum_{j=1}^p \sum_{i=1}^n \left(x_{ij} - \sum_{m=1}^M z_{im} \phi_{jm} \right)^2. \quad (12.7)$$

In summary, together the M principal component score vectors and M principal component loading vectors can give a good approximation to the data when M is sufficiently large. When $M = \min(n - 1, p)$, then the representation is exact: $x_{ij} = \sum_{m=1}^M z_{im} \phi_{jm}$.

12.2.3 The Proportion of Variance Explained

In Figure 12.2, we performed PCA on a three-dimensional data set (left-hand panel) and projected the data onto the first two principal component loading vectors in order to obtain a two-dimensional view of the data (i.e. the principal component score vectors; right-hand panel). We see that this two-dimensional representation of the three-dimensional data does successfully capture the major pattern in the data: the orange, green, and cyan observations that are near each other in three-dimensional space remain nearby in the two-dimensional representation. Similarly, we have seen on the **USArrests** data set that we can summarize the 50 observations and 4 variables using just the first two principal component score vectors and the first two principal component loading vectors.

We can now ask a natural question: how much of the information in a given data set is lost by projecting the observations onto the first few principal components? That is, how much of the variance in the data is *not* contained in the first few principal components? More generally, we are interested in knowing the *proportion of variance explained* (PVE) by each

proportion
of variance
explained

⁴Technically, the solution to (12.6) is not unique. Thus, it is more precise to state that any solution to (12.6) can be easily transformed to yield the principal components.

principal component. The *total variance* present in a data set (assuming that the variables have been centered to have mean zero) is defined as

$$\sum_{j=1}^p \text{Var}(X_j) = \sum_{j=1}^p \frac{1}{n} \sum_{i=1}^n x_{ij}^2, \quad (12.8)$$

and the variance explained by the m th principal component is

$$\frac{1}{n} \sum_{i=1}^n z_{im}^2 = \frac{1}{n} \sum_{i=1}^n \left(\sum_{j=1}^p \phi_{jm} x_{ij} \right)^2. \quad (12.9)$$

Therefore, the PVE of the m th principal component is given by

$$\frac{\sum_{i=1}^n z_{im}^2}{\sum_{j=1}^p \sum_{i=1}^n x_{ij}^2} = \frac{\sum_{i=1}^n \left(\sum_{j=1}^p \phi_{jm} x_{ij} \right)^2}{\sum_{j=1}^p \sum_{i=1}^n x_{ij}^2}. \quad (12.10)$$

The PVE of each principal component is a positive quantity. In order to compute the cumulative PVE of the first M principal components, we can simply sum (12.10) over each of the first M PVEs. In total, there are $\min(n - 1, p)$ principal components, and their PVEs sum to one.

In Section 12.2.2, we showed that the first M principal component loading and score vectors can be interpreted as the best M -dimensional approximation to the data, in terms of residual sum of squares. It turns out that the variance of the data can be decomposed into the variance of the first M principal components plus the mean squared error of this M -dimensional approximation, as follows:

$$\underbrace{\sum_{j=1}^p \frac{1}{n} \sum_{i=1}^n x_{ij}^2}_{\text{Var. of data}} = \underbrace{\sum_{m=1}^M \frac{1}{n} \sum_{i=1}^n z_{im}^2}_{\text{Var. of first } M \text{ PCs}} + \underbrace{\frac{1}{n} \sum_{j=1}^p \sum_{i=1}^n \left(x_{ij} - \sum_{m=1}^M z_{im} \phi_{jm} \right)^2}_{\text{MSE of } M\text{-dimensional approximation}} \quad (12.11)$$

The three terms in this decomposition are discussed in (12.8), (12.9), and (12.7), respectively. Since the first term is fixed, we see that by maximizing the variance of the first M principal components, we minimize the mean squared error of the M -dimensional approximation, and vice versa. This explains why principal components can be equivalently viewed as minimizing the approximation error (as in Section 12.2.2) or maximizing the variance (as in Section 12.2.1).

Moreover, we can use (12.11) to see that the PVE defined in (12.10) equals

$$1 - \frac{\sum_{j=1}^p \sum_{i=1}^n \left(x_{ij} - \sum_{m=1}^M z_{im} \phi_{jm} \right)^2}{\sum_{j=1}^p \sum_{i=1}^n x_{ij}^2} = 1 - \frac{\text{RSS}}{\text{TSS}},$$

where TSS represents the total sum of squared elements of \mathbf{X} , and RSS represents the residual sum of squares of the M -dimensional approximation given by the principal components. Recalling the definition of R^2 from (3.17), this means that we can interpret the PVE as the R^2 of the approximation for \mathbf{X} given by the first M principal components.

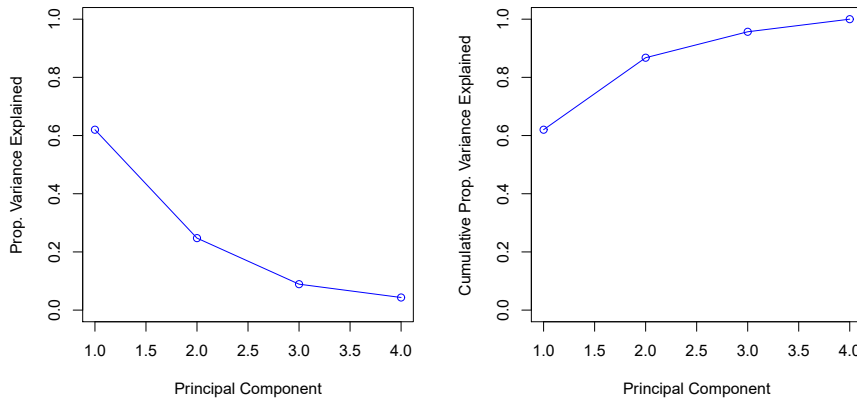


FIGURE 12.3. Left: a scree plot depicting the proportion of variance explained by each of the four principal components in the **USArrests** data. Right: the cumulative proportion of variance explained by the four principal components in the **USArrests** data.

In the **USArrests** data, the first principal component explains 62.0 % of the variance in the data, and the next principal component explains 24.7 % of the variance. Together, the first two principal components explain almost 87 % of the variance in the data, and the last two principal components explain only 13 % of the variance. This means that Figure 12.1 provides a pretty accurate summary of the data using just two dimensions. The PVE of each principal component, as well as the cumulative PVE, is shown in Figure 12.3. The left-hand panel is known as a *scree plot*, and will be discussed later in this chapter.

scree plot

12.2.4 More on PCA

Scaling the Variables

We have already mentioned that before PCA is performed, the variables should be centered to have mean zero. Furthermore, *the results obtained when we perform PCA will also depend on whether the variables have been individually scaled* (each multiplied by a different constant). This is in contrast to some other supervised and unsupervised learning techniques, such as linear regression, in which scaling the variables has no effect. (In linear regression, multiplying a variable by a factor of c will simply lead to multiplication of the corresponding coefficient estimate by a factor of $1/c$, and thus will have no substantive effect on the model obtained.)

For instance, Figure 12.1 was obtained after scaling each of the variables to have standard deviation one. This is reproduced in the left-hand plot in Figure 12.4. Why does it matter that we scaled the variables? In these data, the variables are measured in different units; **Murder**, **Rape**, and **Assault** are reported as the number of occurrences per 100,000 people, and **UrbanPop** is the percentage of the state's population that lives in an urban area. These four variables have variances of 18.97, 87.73, 6945.16, and 209.5, respectively. Consequently, if we perform PCA on the unscaled variables, then

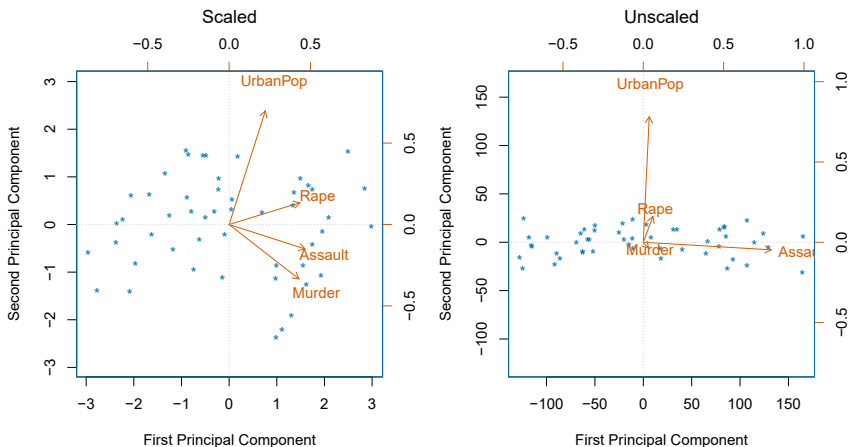


FIGURE 12.4. Two principal component biplots for the **USArrests** data. Left: the same as Figure 12.1, with the variables scaled to have unit standard deviations. Right: principal components using unscaled data. **Assault** has by far the largest loading on the first principal component because it has the highest variance among the four variables. In general, scaling the variables to have standard deviation one is recommended.

the first principal component loading vector will have a very large loading for **Assault**, since that variable has by far the highest variance. The right-hand plot in Figure 12.4 displays the first two principal components for the **USArrests** data set, without scaling the variables to have standard deviation one. As predicted, the first principal component loading vector places almost all of its weight on **Assault**, while the second principal component loading vector places almost all of its weight on **UrbanPop**. Comparing this to the left-hand plot, we see that scaling does indeed have a substantial effect on the results obtained.

However, this result is simply a consequence of the scales on which the variables were measured. For instance, if **Assault** were measured in units of the number of occurrences per 100 people (rather than number of occurrences per 100,000 people), then this would amount to dividing all of the elements of that variable by 1,000. Then the variance of the variable would be tiny, and so the first principal component loading vector would have a very small value for that variable. Because it is undesirable for the principal components obtained to depend on an arbitrary choice of scaling, we typically scale each variable to have standard deviation one before we perform PCA.

In certain settings, however, the variables may be measured in the same units. In this case, we might not wish to scale the variables to have standard deviation one before performing PCA. For instance, suppose that the variables in a given data set correspond to expression levels for p genes. Then since expression is measured in the same “units” for each gene, we might choose not to scale the genes to each have standard deviation one.

Uniqueness of the Principal Components

While in theory the principal components need not be unique, in almost all practical settings they are (up to sign flips). This means that two different software packages will yield the same principal component loading vectors, although the signs of those loading vectors may differ. The signs may differ because each principal component loading vector specifies a direction in p -dimensional space: flipping the sign has no effect as the direction does not change. (Consider Figure 6.14—the principal component loading vector is a line that extends in either direction, and flipping its sign would have no effect.) Similarly, the score vectors are unique up to a sign flip, since the variance of Z is the same as the variance of $-Z$. It is worth noting that when we use (12.5) to approximate x_{ij} we multiply z_{im} by ϕ_{jm} . Hence, if the sign is flipped on both the loading and score vectors, the final product of the two quantities is unchanged.

Deciding How Many Principal Components to Use

In general, an $n \times p$ data matrix \mathbf{X} has $\min(n - 1, p)$ distinct principal components. However, we usually are not interested in all of them; rather, we would like to use just the first few principal components in order to visualize or interpret the data. In fact, we would like to use the smallest number of principal components required to get a *good* understanding of the data. How many principal components are needed? Unfortunately, there is no single (or simple!) answer to this question.

We typically decide on the number of principal components required to visualize the data by examining a *scree plot*, such as the one shown in the left-hand panel of Figure 12.3. We choose the smallest number of principal components that are required in order to explain a sizable amount of the variation in the data. This is done by eyeballing the scree plot, and looking for a point at which the proportion of variance explained by each subsequent principal component drops off. This drop is often referred to as an *elbow* in the scree plot. For instance, by inspection of Figure 12.3, one might conclude that a fair amount of variance is explained by the first two principal components, and that there is an elbow after the second component. After all, the third principal component explains less than ten percent of the variance in the data, and the fourth principal component explains less than half that and so is essentially worthless.

However, this type of visual analysis is inherently *ad hoc*. Unfortunately, there is no well-accepted objective way to decide how many principal components are *enough*. In fact, the question of how many principal components are enough is inherently ill-defined, and will depend on the specific area of application and the specific data set. In practice, we tend to look at the first few principal components in order to find interesting patterns in the data. If no interesting patterns are found in the first few principal components, then further principal components are unlikely to be of interest. Conversely, if the first few principal components are interesting, then we typically continue to look at subsequent principal components until no further interesting patterns are found. This is admittedly a subjective ap-

proach, and is reflective of the fact that PCA is generally used as a tool for exploratory data analysis.

On the other hand, if we compute principal components for use in a supervised analysis, such as the principal components regression presented in Section 6.3.1, then there is a simple and objective way to determine how many principal components to use: we can treat the number of principal component score vectors to be used in the regression as a tuning parameter to be selected via cross-validation or a related approach. The comparative simplicity of selecting the number of principal components for a supervised analysis is one manifestation of the fact that supervised analyses tend to be more clearly defined and more objectively evaluated than unsupervised analyses.

12.2.5 Other Uses for Principal Components

We saw in Section 6.3.1 that we can perform regression using the principal component score vectors as features. In fact, many statistical techniques, such as regression, classification, and clustering, can be easily adapted to use the $n \times M$ matrix whose columns are the first $M \ll p$ principal component score vectors, rather than using the full $n \times p$ data matrix. This can lead to *less noisy* results, since it is often the case that the signal (as opposed to the noise) in a data set is concentrated in its first few principal components.

12.3 Missing Values and Matrix Completion

Often datasets have missing values, which can be a nuisance. For example, suppose that we wish to analyze the `USArrests` data, and discover that 20 of the 200 values have been randomly corrupted and marked as missing. Unfortunately, the statistical learning methods that we have seen in this book cannot handle missing values. How should we proceed?

We could remove the rows that contain missing observations and perform our data analysis on the complete rows. But this seems wasteful, and depending on the fraction missing, unrealistic. Alternatively, if x_{ij} is missing, then we could replace it by the mean of the j th column (using the non-missing entries to compute the mean). Although this is a common and convenient strategy, often we can do better by exploiting the correlation between the variables.

In this section we show how principal components can be used to *impute* the missing values, through a process known as *matrix completion*. The completed matrix can then be used in a statistical learning method, such as linear regression or LDA.

This approach for imputing missing data is appropriate if the missingness is random. For example, it is suitable if a patient's weight is missing because the battery of the electronic scale was flat at the time of his exam. By contrast, if the weight is missing because the patient was too heavy to climb on the scale, then this is not missing at random; the missingness is

impute
imputation
matrix
completion

missing at
random

informative, and the approach described here for handling missing data is not suitable.

Sometimes data is missing by necessity. For example, if we form a matrix of the ratings (on a scale from 1 to 5) that n customers have given to the entire Netflix catalog of p movies, then most of the matrix will be missing, since no customer will have seen and rated more than a tiny fraction of the catalog. If we can impute the missing values well, then we will have an idea of what each customer will think of movies they have not yet seen. Hence matrix completion can be used to power *recommender systems*.

recommender
systems

Principal Components with Missing Values

In Section 12.2.2, we showed that the first M principal component score and loading vectors provide the “best” approximation to the data matrix \mathbf{X} , in the sense of (12.6). Suppose that some of the observations x_{ij} are missing. We now show how one can both impute the missing values and solve the principal component problem at the same time. We return to a modified form of the optimization problem (12.6),

$$\underset{\mathbf{A} \in \mathbb{R}^{n \times M}, \mathbf{B} \in \mathbb{R}^{p \times M}}{\text{minimize}} \left\{ \sum_{(i,j) \in \mathcal{O}} \left(x_{ij} - \sum_{m=1}^M a_{im} b_{jm} \right)^2 \right\}, \quad (12.12)$$

where \mathcal{O} is the set of all *observed* pairs of indices (i, j) , a subset of the possible $n \times p$ pairs.

Once we solve this problem:

- we can estimate a missing observation x_{ij} using $\hat{x}_{ij} = \sum_{m=1}^M \hat{a}_{im} \hat{b}_{jm}$, where \hat{a}_{im} and \hat{b}_{jm} are the (i, m) and (j, m) elements, respectively, of the matrices $\hat{\mathbf{A}}$ and $\hat{\mathbf{B}}$ that solve (12.12); and
- we can (approximately) recover the M principal component scores and loadings, as we did when the data were complete.

It turns out that solving (12.12) exactly is difficult, unlike in the case of complete data: the eigen decomposition no longer applies. But the simple iterative approach in Algorithm 12.1, which is demonstrated in Section 12.5.2, typically provides a good solution.⁵⁶

We illustrate Algorithm 12.1 on the **USArrests** data. There are $p = 4$ variables and $n = 50$ observations (states). We first standardized the data so each variable has mean zero and standard deviation one. We then randomly selected 20 of the 50 states, and then for each of these we randomly set one of the four variables to be missing. Thus, 10% of the elements of the data matrix were missing. We applied Algorithm 12.1 with $M = 1$ principal component. Figure 12.5 shows that the recovery of the missing elements

⁵⁶This algorithm is referred to as “Hard-Impute” in Mazumder, Hastie, and Tibshirani (2010) “Spectral regularization algorithms for learning large incomplete matrices”, published in *Journal of Machine Learning Research*, pages 2287–2322.

⁶Each iteration of Step 2 of this algorithm decreases the objective (12.14). However, the algorithm is not guaranteed to achieve the global optimum of (12.12).

Algorithm 12.1 Iterative Algorithm for Matrix Completion

1. Create a complete data matrix $\tilde{\mathbf{X}}$ of dimension $n \times p$ of which the (i, j) element equals

$$\tilde{x}_{ij} = \begin{cases} x_{ij} & \text{if } (i, j) \in \mathcal{O} \\ \bar{x}_j & \text{if } (i, j) \notin \mathcal{O}, \end{cases}$$

where \bar{x}_j is the average of the observed values for the j th variable in the incomplete data matrix \mathbf{X} . Here, \mathcal{O} indexes the observations that are observed in \mathbf{X} .

2. Repeat steps (a)–(c) until the objective (12.14) fails to decrease:

- (a) Solve

$$\underset{\mathbf{A} \in \mathbb{R}^{n \times M}, \mathbf{B} \in \mathbb{R}^{p \times M}}{\text{minimize}} \left\{ \sum_{j=1}^p \sum_{i=1}^n \left(\tilde{x}_{ij} - \sum_{m=1}^M a_{im} b_{jm} \right)^2 \right\} \quad (12.13)$$

by computing the principal components of $\tilde{\mathbf{X}}$.

- (b) For each element $(i, j) \notin \mathcal{O}$, set $\tilde{x}_{ij} \leftarrow \sum_{m=1}^M \hat{a}_{im} \hat{b}_{jm}$.
- (c) Compute the objective

$$\sum_{(i,j) \in \mathcal{O}} \left(x_{ij} - \sum_{m=1}^M \hat{a}_{im} \hat{b}_{jm} \right)^2. \quad (12.14)$$

3. Return the estimated missing entries \tilde{x}_{ij} , $(i, j) \notin \mathcal{O}$.
-

is pretty accurate. Over 100 random runs of this experiment, the average correlation between the true and imputed values of the missing elements is 0.63, with a standard deviation of 0.11. Is this good performance? To answer this question, we can compare this correlation to what we would have gotten if we had estimated these 20 values using the *complete* data — that is, if we had simply computed $\hat{x}_{ij} = z_{i1}\phi_{j1}$, where z_{i1} and ϕ_{j1} are elements of the first principal component score and loading vectors of the complete data.⁷ Using the complete data in this way results in an average correlation of 0.79 between the true and estimated values for these 20 elements, with a standard deviation of 0.08. Thus, our imputation method does worse than the method that uses all of the data (0.63 ± 0.11 versus 0.79 ± 0.08), but its performance is still pretty good. (And of course, the method that uses all of the data cannot be applied in a real-world setting with missing data.)

Figure 12.6 further indicates that Algorithm 12.1 performs fairly well on this dataset.

⁷This is an unattainable gold standard, in the sense that with missing data, we of course cannot compute the principal components of the complete data.

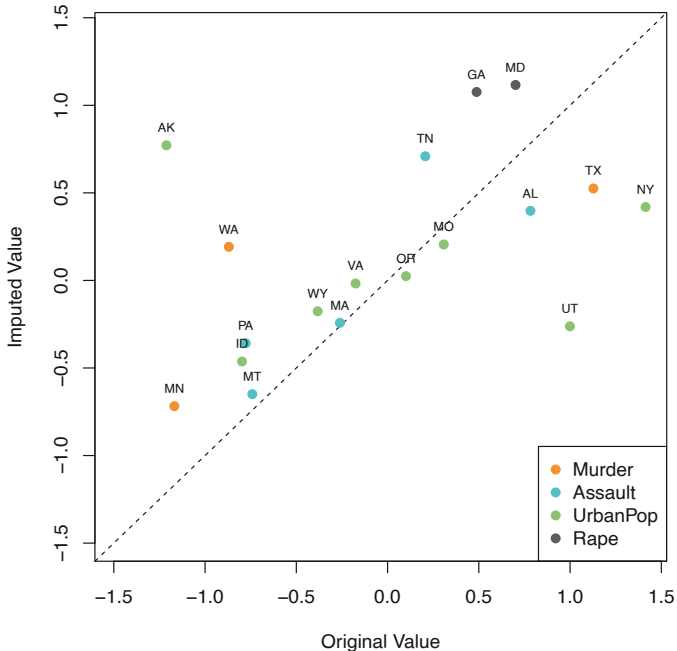


FIGURE 12.5. Missing value imputation on the `USArrests` data. Twenty values (10% of the total number of matrix elements) were artificially set to be missing, and then imputed via Algorithm 12.1 with $M = 1$. The figure displays the true value x_{ij} and the imputed value \hat{x}_{ij} for all twenty missing values. For each of the twenty missing values, the color indicates the variable, and the label indicates the state. The correlation between the true and imputed values is around 0.63.

We close with a few observations:

- The `USArrests` data has only four variables, which is on the low end for methods like Algorithm 12.1 to work well. For this reason, for this demonstration we randomly set at most one variable per state to be missing, and only used $M = 1$ principal component.
- In general, in order to apply Algorithm 12.1, we must select M , the number of principal components to use for the imputation. One approach is to randomly leave out a few additional elements from the matrix, and select M based on how well those known values are recovered. This is closely related to the validation-set approach seen in Chapter 5.

Recommender Systems

Digital streaming services like Netflix and Amazon use data about the content that a customer has viewed in the past, as well as data from other customers, to suggest other content for the customer. As a concrete example, some years back, Netflix had customers rate each movie that they had seen with a score from 1–5. This resulted in a very big $n \times p$ matrix for which the (i, j) element is the rating given by the i th customer to the

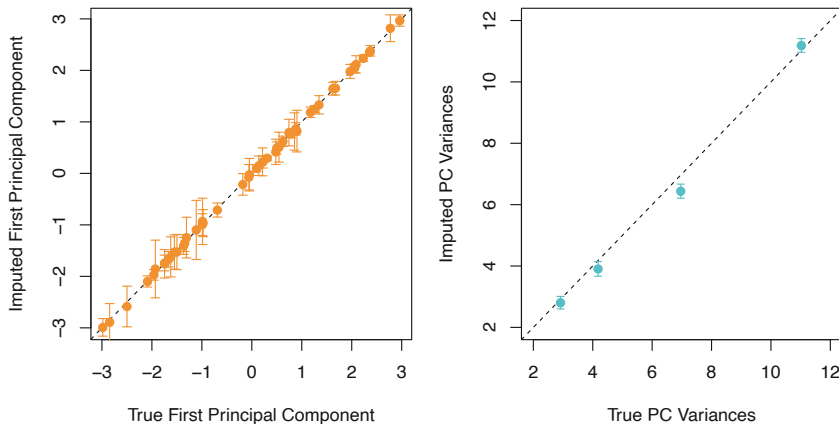


FIGURE 12.6. As described in the text, in each of 100 trials, we left out 20 elements of the USArrests dataset. In each trial, we applied Algorithm 12.1 with $M = 1$ to impute the missing elements and compute the principal components. Left: For each of the 50 states, the imputed first principal component scores (averaged over 100 trials, and displayed with a standard deviation bar) are plotted against the first principal component scores computed using all the data. Right: The imputed principal component loadings (averaged over 100 trials, and displayed with a standard deviation bar) are plotted against the true principal component loadings.

j th movie. One specific early example of this matrix had $n = 480,189$ customers and $p = 17,770$ movies. However, on average each customer had seen around 200 movies, so 99% of the matrix had missing elements. Table 12.2 illustrates the setup.

In order to suggest a movie that a particular customer might like, Netflix needed a way to impute the missing values of this data matrix. The key idea is as follows: the set of movies that the i th customer has seen will overlap with those that other customers have seen. Furthermore, some of those other customers will have similar movie preferences to the i th customer. Thus, it should be possible to use similar customers' ratings of movies that the i th customer has not seen to predict whether the i th customer will like those movies.

More concretely, by applying Algorithm 12.1, we can predict the i th customer's rating for the j th movie using $\hat{x}_{ij} = \sum_{m=1}^M \hat{a}_{im} \hat{b}_{jm}$. Furthermore, we can interpret the M components in terms of "cliques" and "genres":

- \hat{a}_{im} represents the strength with which the i th user belongs to the m th clique, where a *clique* is a group of customers that enjoys movies of the m th genre;
- \hat{b}_{jm} represents the strength with which the j th movie belongs to the m th *genre*.

Examples of genres include Romance, Western, and Action.

Principal component models similar to Algorithm 12.1 are at the heart of many recommender systems. Although the data matrices involved are

	Jerry Maguire	Oceans	Road to Perdition	A Fortunate Man	Catch Me If You Can	Driving Miss Daisy	The Two Popes	The Laundromat	Code 8	The Social Network	...
Customer 1	•	•	•	•	4	•	•	•	•	•	...
Customer 2	•	•	3	•	•	•	3	•	•	3	...
Customer 3	•	2	•	4	•	•	•	•	2	•	...
Customer 4	3	•	•	•	•	•	•	•	•	•	...
Customer 5	5	1	•	•	4	•	•	•	•	•	...
Customer 6	•	•	•	•	•	2	4	•	•	•	...
Customer 7	•	•	5	•	•	•	•	3	•	•	...
Customer 8	•	•	•	•	•	•	•	•	•	•	...
Customer 9	3	•	•	•	5	•	•	1	•	•	...
:	:	:	:	:	:	:	:	:	:	:	...

TABLE 12.2. Excerpt of the Netflix movie rating data. The movies are rated from 1 (worst) to 5 (best). The symbol • represents a missing value: a movie that was not rated by the corresponding customer.

typically massive, algorithms have been developed that can exploit the high level of missingness in order to perform efficient computations.

12.4 Clustering Methods

Clustering refers to a very broad set of techniques for finding *subgroups*, or *clusters*, in a data set. When we cluster the observations of a data set, we seek to partition them into distinct groups so that the observations within each group are quite similar to each other, while observations in different groups are quite different from each other. Of course, to make this concrete, we must define what it means for two or more observations to be *similar* or *different*. Indeed, this is often a domain-specific consideration that must be made based on knowledge of the data being studied.

clustering

For instance, suppose that we have a set of n observations, each with p features. The n observations could correspond to tissue samples for patients with breast cancer, and the p features could correspond to measurements collected for each tissue sample; these could be clinical measurements, such as tumor stage or grade, or they could be gene expression measurements. We may have a reason to believe that there is some heterogeneity among the n tissue samples; for instance, perhaps there are a few different *unknown* subtypes of breast cancer. Clustering could be used to find these subgroups. This is an unsupervised problem because we are trying to discover structure—in this case, distinct clusters—on the basis of a data set. The goal in supervised problems, on the other hand, is to try to predict some outcome vector such as survival time or response to drug treatment.

Both clustering and PCA seek to simplify the data via a small number of summaries, but their mechanisms are different:

- PCA looks to find a low-dimensional representation of the observations that explain a good fraction of the variance;
- Clustering looks to find homogeneous subgroups among the observations.

Another application of clustering arises in marketing. We may have access to a large number of measurements (e.g. median household income, occupation, distance from nearest urban area, and so forth) for a large number of people. Our goal is to perform *market segmentation* by identifying subgroups of people who might be more receptive to a particular form of advertising, or more likely to purchase a particular product. The task of performing market segmentation amounts to clustering the people in the data set.

Since clustering is popular in many fields, there exist a great number of clustering methods. In this section we focus on perhaps the two best-known clustering approaches: *K-means clustering* and *hierarchical clustering*. In *K-means clustering*, we seek to partition the observations into a pre-specified number of clusters. On the other hand, in hierarchical clustering, we do not know in advance how many clusters we want; in fact, we end up with a tree-like visual representation of the observations, called a *dendrogram*, that allows us to view at once the clusterings obtained for each possible number of clusters, from 1 to n . There are advantages and disadvantages to each of these clustering approaches, which we highlight in this chapter.

K-means clustering
hierarchical clustering
dendrogram

In general, we can cluster observations on the basis of the features in order to identify subgroups among the observations, or we can cluster features on the basis of the observations in order to discover subgroups among the features. In what follows, for simplicity we will discuss clustering observations on the basis of the features, though the converse can be performed by simply transposing the data matrix.

12.4.1 K-Means Clustering

K-means clustering is a simple and elegant approach for partitioning a data set into K distinct, non-overlapping clusters. To perform *K-means clustering*, we must first specify the desired number of clusters K ; then the *K-means* algorithm will assign each observation to exactly one of the K clusters. Figure 12.7 shows the results obtained from performing *K-means clustering* on a simulated example consisting of 150 observations in two dimensions, using three different values of K .

The *K-means* clustering procedure results from a simple and intuitive mathematical problem. We begin by defining some notation. Let C_1, \dots, C_K denote sets containing the indices of the observations in each cluster. These sets satisfy two properties:

1. $C_1 \cup C_2 \cup \dots \cup C_K = \{1, \dots, n\}$. In other words, each observation belongs to at least one of the K clusters.
2. $C_k \cap C_{k'} = \emptyset$ for all $k \neq k'$. In other words, the clusters are non-overlapping: no observation belongs to more than one cluster.

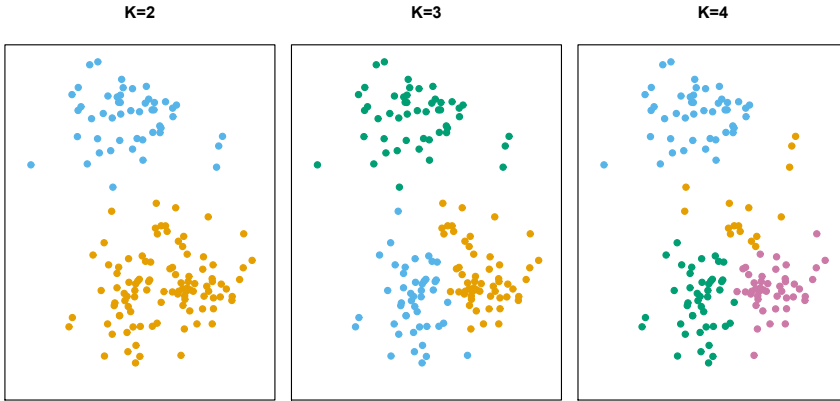


FIGURE 12.7. A simulated data set with 150 observations in two-dimensional space. Panels show the results of applying K -means clustering with different values of K , the number of clusters. The color of each observation indicates the cluster to which it was assigned using the K -means clustering algorithm. Note that there is no ordering of the clusters, so the cluster coloring is arbitrary. These cluster labels were not used in clustering; instead, they are the outputs of the clustering procedure.

For instance, if the i th observation is in the k th cluster, then $i \in C_k$. The idea behind K -means clustering is that a *good* clustering is one for which the *within-cluster variation* is as small as possible. The within-cluster variation for cluster C_k is a measure $W(C_k)$ of the amount by which the observations within a cluster differ from each other. Hence we want to solve the problem

$$\underset{C_1, \dots, C_K}{\text{minimize}} \left\{ \sum_{k=1}^K W(C_k) \right\}. \quad (12.15)$$

In words, this formula says that we want to partition the observations into K clusters such that the total within-cluster variation, summed over all K clusters, is as small as possible.

Solving (12.15) seems like a reasonable idea, but in order to make it actionable we need to define the within-cluster variation. There are many possible ways to define this concept, but by far the most common choice involves *squared Euclidean distance*. That is, we define

$$W(C_k) = \frac{1}{|C_k|} \sum_{i, i' \in C_k} \sum_{j=1}^p (x_{ij} - x_{i'j})^2, \quad (12.16)$$

where $|C_k|$ denotes the number of observations in the k th cluster. In other words, the within-cluster variation for the k th cluster is the sum of all of the pairwise squared Euclidean distances between the observations in the k th cluster, divided by the total number of observations in the k th cluster. Combining (12.15) and (12.16) gives the optimization problem that defines

K -means clustering,

$$\underset{C_1, \dots, C_K}{\text{minimize}} \left\{ \sum_{k=1}^K \frac{1}{|C_k|} \sum_{i, i' \in C_k} \sum_{j=1}^p (x_{ij} - x_{i'j})^2 \right\}. \quad (12.17)$$

Now, we would like to find an algorithm to solve (12.17)—that is, a method to partition the observations into K clusters such that the objective of (12.17) is minimized. This is in fact a very difficult problem to solve precisely, since there are almost K^n ways to partition n observations into K clusters. This is a huge number unless K and n are tiny! Fortunately, a very simple algorithm can be shown to provide a local optimum—a *pretty good solution*—to the K -means optimization problem (12.17). This approach is laid out in Algorithm 12.2.

Algorithm 12.2 *K*-Means Clustering

1. Randomly assign a number, from 1 to K , to each of the observations. These serve as initial cluster assignments for the observations.
 2. Iterate until the cluster assignments stop changing:
 - (a) For each of the K clusters, compute the cluster *centroid*. The k th cluster centroid is the vector of the p feature means for the observations in the k th cluster.
 - (b) Assign each observation to the cluster whose centroid is closest (where *closest* is defined using Euclidean distance).
-

Algorithm 12.2 is guaranteed to decrease the value of the objective (12.17) at each step. To understand why, the following identity is illuminating:

$$\frac{1}{|C_k|} \sum_{i, i' \in C_k} \sum_{j=1}^p (x_{ij} - x_{i'j})^2 = 2 \sum_{i \in C_k} \sum_{j=1}^p (x_{ij} - \bar{x}_{kj})^2, \quad (12.18)$$

where $\bar{x}_{kj} = \frac{1}{|C_k|} \sum_{i \in C_k} x_{ij}$ is the mean for feature j in cluster C_k . In Step 2(a) the cluster means for each feature are the constants that minimize the sum-of-squared deviations, and in Step 2(b), reallocating the observations can only improve (12.18). This means that as the algorithm is run, the clustering obtained will continually improve until the result no longer changes; the objective of (12.17) will never increase. When the result no longer changes, a *local optimum* has been reached. Figure 12.8 shows the progression of the algorithm on the toy example from Figure 12.7. K -means clustering derives its name from the fact that in Step 2(a), the cluster centroids are computed as the mean of the observations assigned to each cluster.

Because the K -means algorithm finds a local rather than a global optimum, the results obtained will depend on the initial (random) cluster assignment of each observation in Step 1 of Algorithm 12.2. For this reason, it is important to run the algorithm multiple times from different random

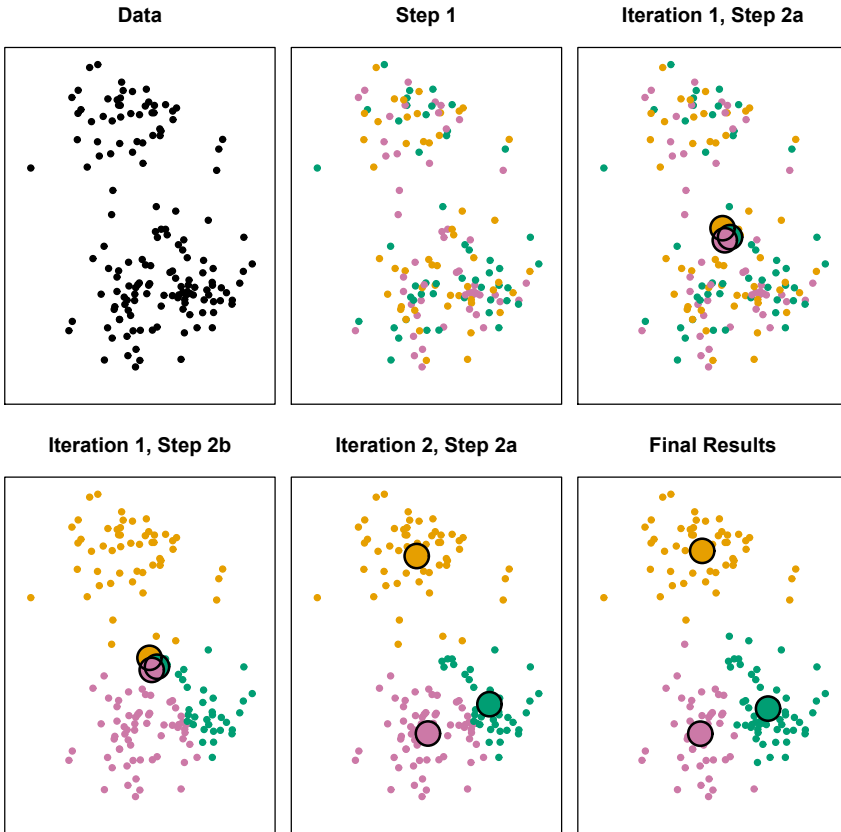


FIGURE 12.8. The progress of the K -means algorithm on the example of Figure 12.7 with $K=3$. Top left: the observations are shown. Top center: in Step 1 of the algorithm, each observation is randomly assigned to a cluster. Top right: in Step 2(a), the cluster centroids are computed. These are shown as large colored disks. Initially the centroids are almost completely overlapping because the initial cluster assignments were chosen at random. Bottom left: in Step 2(b), each observation is assigned to the nearest centroid. Bottom center: Step 2(a) is once again performed, leading to new cluster centroids. Bottom right: the results obtained after ten iterations.

initial configurations. Then one selects the *best* solution, i.e. that for which the objective (12.17) is smallest. Figure 12.9 shows the local optima obtained by running K -means clustering six times using six different initial cluster assignments, using the toy data from Figure 12.7. In this case, the best clustering is the one with an objective value of 235.8.

As we have seen, to perform K -means clustering, we must decide how many clusters we expect in the data. The problem of selecting K is far from simple. This issue, along with other practical considerations that arise in performing K -means clustering, is addressed in Section 12.4.3.



FIGURE 12.9. K -means clustering performed six times on the data from Figure 12.7 with $K = 3$, each time with a different random assignment of the observations in Step 1 of the K -means algorithm. Above each plot is the value of the objective (12.17). Three different local optima were obtained, one of which resulted in a smaller value of the objective and provides better separation between the clusters. Those labeled in red all achieved the same best solution, with an objective value of 235.8.

12.4.2 Hierarchical Clustering

One potential disadvantage of K -means clustering is that it requires us to pre-specify the number of clusters K . *Hierarchical clustering* is an alternative approach which does not require that we commit to a particular choice of K . Hierarchical clustering has an added advantage over K -means clustering in that it results in an attractive tree-based representation of the observations, called a *dendrogram*.

In this section, we describe *bottom-up* or *agglomerative* clustering. This is the most common type of hierarchical clustering, and refers to the fact that a dendrogram (generally depicted as an upside-down tree; see Figure 12.11) is built starting from the leaves and combining clusters up to the trunk. We will begin with a discussion of how to interpret a dendrogram

bottom-up
agglomerative

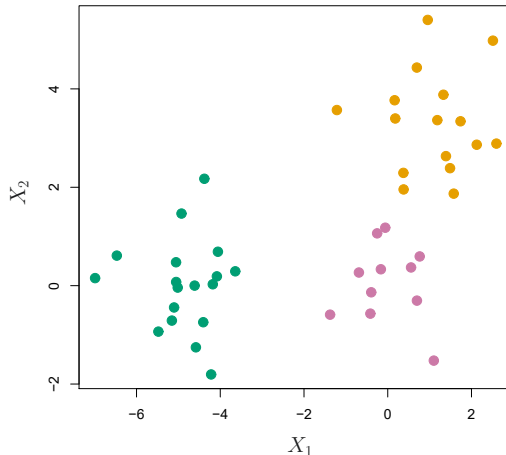


FIGURE 12.10. Forty-five observations generated in two-dimensional space. In reality there are three distinct classes, shown in separate colors. However, we will treat these class labels as unknown and will seek to cluster the observations in order to discover the classes from the data.

and then discuss how hierarchical clustering is actually performed—that is, how the dendrogram is built.

Interpreting a Dendrogram

We begin with the simulated data set shown in Figure 12.10, consisting of 45 observations in two-dimensional space. The data were generated from a three-class model; the true class labels for each observation are shown in distinct colors. However, suppose that the data were observed without the class labels, and that we wanted to perform hierarchical clustering of the data. Hierarchical clustering (with complete linkage, to be discussed later) yields the result shown in the left-hand panel of Figure 12.11. How can we interpret this dendrogram?

In the left-hand panel of Figure 12.11, each *leaf* of the dendrogram represents one of the 45 observations in Figure 12.10. However, as we move up the tree, some leaves begin to *fuse* into branches. These correspond to observations that are similar to each other. As we move higher up the tree, branches themselves fuse, either with leaves or other branches. The earlier (lower in the tree) fusions occur, the more similar the groups of observations are to each other. On the other hand, observations that fuse later (near the top of the tree) can be quite different. In fact, this statement can be made precise: for any two observations, we can look for the point in the tree where branches containing those two observations are first fused. The height of this fusion, as measured on the vertical axis, indicates how different the two observations are. Thus, observations that fuse at the very bottom of the tree are quite similar to each other, whereas observations that fuse close to the top of the tree will tend to be quite different.

This highlights a very important point in interpreting dendograms that is often misunderstood. Consider the left-hand panel of Figure 12.12, which shows a simple dendrogram obtained from hierarchically clustering nine

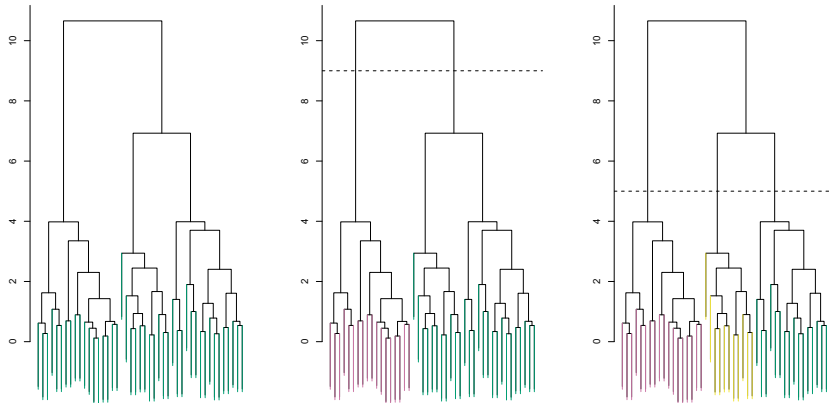


FIGURE 12.11. Left: *dendrogram obtained from hierarchically clustering the data from Figure 12.10 with complete linkage and Euclidean distance.* Center: *the dendrogram from the left-hand panel, cut at a height of nine (indicated by the dashed line).* This cut results in two distinct clusters, shown in different colors. Right: *the dendrogram from the left-hand panel, now cut at a height of five.* This cut results in three distinct clusters, shown in different colors. Note that the colors were not used in clustering, but are simply used for display purposes in this figure.

observations. One can see that observations 5 and 7 are quite similar to each other, since they fuse at the lowest point on the dendrogram. Observations 1 and 6 are also quite similar to each other. However, it is tempting but incorrect to conclude from the figure that observations 9 and 2 are quite similar to each other on the basis that they are located near each other on the dendrogram. In fact, based on the information contained in the dendrogram, observation 9 is no more similar to observation 2 than it is to observations 8, 5, and 7. (This can be seen from the right-hand panel of Figure 12.12, in which the raw data are displayed.) To put it mathematically, there are 2^{n-1} possible reorderings of the dendrogram, where n is the number of leaves. This is because at each of the $n - 1$ points where fusions occur, the positions of the two fused branches could be swapped without affecting the meaning of the dendrogram. Therefore, we cannot draw conclusions about the similarity of two observations based on their proximity along the *horizontal axis*. Rather, we draw conclusions about the similarity of two observations based on the location on the *vertical axis* where branches containing those two observations first are fused.

Now that we understand how to interpret the left-hand panel of Figure 12.11, we can move on to the issue of identifying clusters on the basis of a dendrogram. In order to do this, we make a horizontal cut across the dendrogram, as shown in the center and right-hand panels of Figure 12.11. The distinct sets of observations beneath the cut can be interpreted as clusters. In the center panel of Figure 12.11, cutting the dendrogram at a height of nine results in two clusters, shown in distinct colors. In the right-hand panel, cutting the dendrogram at a height of five results in three clusters. Further cuts can be made as one descends the dendrogram in order to obtain any number of clusters, between 1 (corresponding to no cut) and n

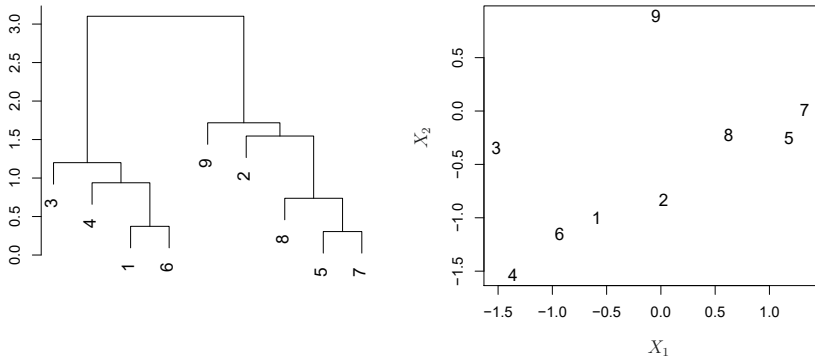


FIGURE 12.12. An illustration of how to properly interpret a dendrogram with nine observations in two-dimensional space. Left: a dendrogram generated using Euclidean distance and complete linkage. Observations 5 and 7 are quite similar to each other, as are observations 1 and 6. However, observation 9 is no more similar to observation 2 than it is to observations 8, 5, and 7, even though observations 9 and 2 are close together in terms of horizontal distance. This is because observations 2, 8, 5, and 7 all fuse with observation 9 at the same height, approximately 1.8. Right: the raw data used to generate the dendrogram can be used to confirm that indeed, observation 9 is no more similar to observation 2 than it is to observations 8, 5, and 7.

(corresponding to a cut at height 0, so that each observation is in its own cluster). In other words, the height of the cut to the dendrogram serves the same role as the K in K -means clustering: it controls the number of clusters obtained.

Figure 12.11 therefore highlights a very attractive aspect of hierarchical clustering: one single dendrogram can be used to obtain any number of clusters. In practice, people often look at the dendrogram and select by eye a sensible number of clusters, based on the heights of the fusion and the number of clusters desired. In the case of Figure 12.11, one might choose to select either two or three clusters. However, often the choice of where to cut the dendrogram is not so clear.

The term *hierarchical* refers to the fact that clusters obtained by cutting the dendrogram at a given height are necessarily nested within the clusters obtained by cutting the dendrogram at any greater height. However, on an arbitrary data set, this assumption of hierarchical structure might be unrealistic. For instance, suppose that our observations correspond to a group of men and women, evenly split among Americans, Japanese, and French. We can imagine a scenario in which the best division into two groups might split these people by gender, and the best division into three groups might split them by nationality. In this case, the true clusters are not nested, in the sense that the best division into three groups does not result from taking the best division into two groups and splitting up one of those groups. Consequently, this situation could not be well-represented by hierarchical clustering. Due to situations such as this one, hierarchical clustering can sometimes yield *worse* (i.e. less accurate) results than K -means clustering for a given number of clusters.

Algorithm 12.3 *Hierarchical Clustering*

-
1. Begin with n observations and a measure (such as Euclidean distance) of all the $\binom{n}{2} = n(n - 1)/2$ pairwise dissimilarities. Treat each observation as its own cluster.
 2. For $i = n, n - 1, \dots, 2$:
 - (a) Examine all pairwise inter-cluster dissimilarities among the i clusters and identify the pair of clusters that are least dissimilar (that is, most similar). Fuse these two clusters. The dissimilarity between these two clusters indicates the height in the dendrogram at which the fusion should be placed.
 - (b) Compute the new pairwise inter-cluster dissimilarities among the $i - 1$ remaining clusters.
-

The Hierarchical Clustering Algorithm

The hierarchical clustering dendrogram is obtained via an extremely simple algorithm. We begin by defining some sort of *dissimilarity* measure between each pair of observations. Most often, Euclidean distance is used; we will discuss the choice of dissimilarity measure later in this chapter. The algorithm proceeds iteratively. Starting out at the bottom of the dendrogram, each of the n observations is treated as its own cluster. The two clusters that are most similar to each other are then *fused* so that there now are $n - 1$ clusters. Next the two clusters that are most similar to each other are fused again, so that there now are $n - 2$ clusters. The algorithm proceeds in this fashion until all of the observations belong to one single cluster, and the dendrogram is complete. Figure 12.13 depicts the first few steps of the algorithm, for the data from Figure 12.12. To summarize, the hierarchical clustering algorithm is given in Algorithm 12.3.

This algorithm seems simple enough, but one issue has not been addressed. Consider the bottom right panel in Figure 12.13. How did we determine that the cluster $\{5, 7\}$ should be fused with the cluster $\{8\}$? We have a concept of the dissimilarity between pairs of observations, but how do we define the dissimilarity between two clusters if one or both of the clusters contains multiple observations? The concept of dissimilarity between a pair of observations needs to be extended to a pair of *groups of observations*. This extension is achieved by developing the notion of *linkage*, which defines the dissimilarity between two groups of observations. The four most common types of linkage—*complete*, *average*, *single*, and *centroid*—are briefly described in Table 12.3. Average, complete, and single linkage are most popular among statisticians. Average and complete linkage are generally preferred over single linkage, as they tend to yield more balanced dendograms. Centroid linkage is often used in genomics, but suffers from a major drawback in that an *inversion* can occur, whereby two clusters are fused at a height *below* either of the individual clusters in the dendrogram. This can lead to difficulties in visualization as well as in interpretation of the dendrogram. The dissimilarities computed in Step 2(b)

linkage

inversion

<i>Linkage</i>	<i>Description</i>
Complete	Maximal intercluster dissimilarity. Compute all pairwise dissimilarities between the observations in cluster A and the observations in cluster B, and record the <i>largest</i> of these dissimilarities.
Single	Minimal intercluster dissimilarity. Compute all pairwise dissimilarities between the observations in cluster A and the observations in cluster B, and record the <i>smallest</i> of these dissimilarities. Single linkage can result in extended, trailing clusters in which single observations are fused one-at-a-time.
Average	Mean intercluster dissimilarity. Compute all pairwise dissimilarities between the observations in cluster A and the observations in cluster B, and record the <i>average</i> of these dissimilarities.
Centroid	Dissimilarity between the centroid for cluster A (a mean vector of length p) and the centroid for cluster B. Centroid linkage can result in undesirable <i>inversions</i> .

TABLE 12.3. A summary of the four most commonly-used types of linkage in hierarchical clustering.

of the hierarchical clustering algorithm will depend on the type of linkage used, as well as on the choice of dissimilarity measure. Hence, the resulting dendrogram typically depends quite strongly on the type of linkage used, as is shown in Figure 12.14.

Choice of Dissimilarity Measure

Thus far, the examples in this chapter have used Euclidean distance as the dissimilarity measure. But sometimes other dissimilarity measures might be preferred. For example, *correlation-based distance* considers two observations to be similar if their features are highly correlated, even though the observed values may be far apart in terms of Euclidean distance. This is an unusual use of correlation, which is normally computed between variables; here it is computed between the observation profiles for each pair of observations. Figure 12.15 illustrates the difference between Euclidean and correlation-based distance. Correlation-based distance focuses on the shapes of observation profiles rather than their magnitudes.

The choice of dissimilarity measure is very important, as it has a strong effect on the resulting dendrogram. In general, careful attention should be paid to the type of data being clustered and the scientific question at hand. These considerations should determine what type of dissimilarity measure is used for hierarchical clustering.

For instance, consider an online retailer interested in clustering shoppers based on their past shopping histories. The goal is to identify subgroups of *similar* shoppers, so that shoppers within each subgroup can be shown items and advertisements that are particularly likely to interest them. Suppose the data takes the form of a matrix where the rows are the shoppers and the columns are the items available for purchase; the elements of the data matrix indicate the number of times a given shopper has purchased a

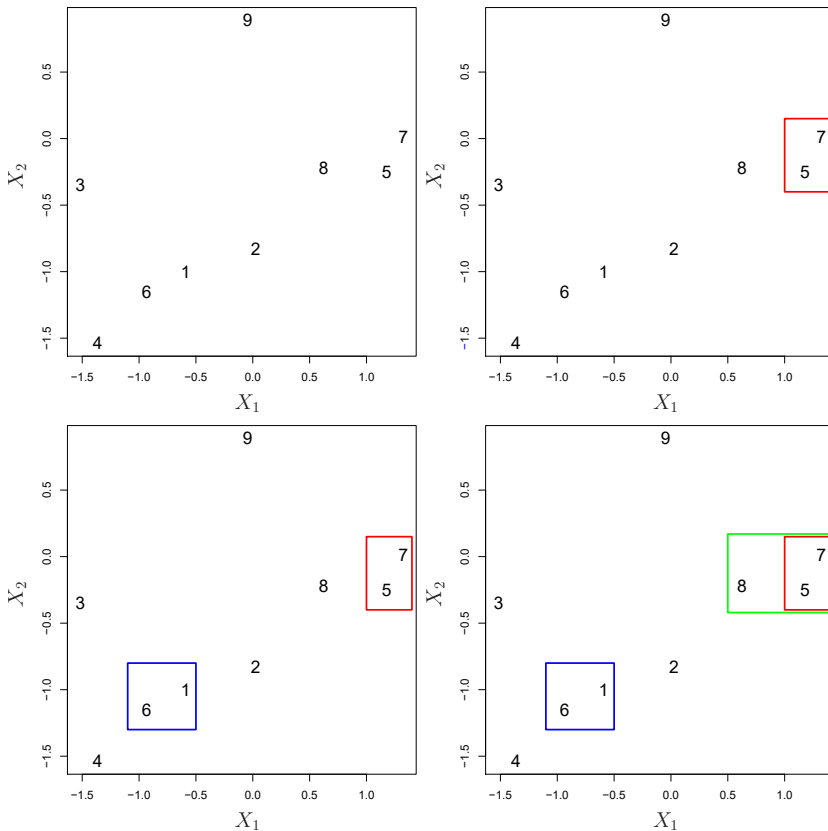


FIGURE 12.13. An illustration of the first few steps of the hierarchical clustering algorithm, using the data from Figure 12.12, with complete linkage and Euclidean distance. Top Left: initially, there are nine distinct clusters, $\{1\}, \{2\}, \dots, \{9\}$. Top Right: the two clusters that are closest together, $\{5\}$ and $\{7\}$, are fused into a single cluster. Bottom Left: the two clusters that are closest together, $\{6\}$ and $\{1\}$, are fused into a single cluster. Bottom Right: the two clusters that are closest together using complete linkage, $\{8\}$ and the cluster $\{5, 7\}$, are fused into a single cluster.

given item (i.e. a 0 if the shopper has never purchased this item, a 1 if the shopper has purchased it once, etc.) What type of dissimilarity measure should be used to cluster the shoppers? If Euclidean distance is used, then shoppers who have bought very few items overall (i.e. infrequent users of the online shopping site) will be clustered together. This may not be desirable. On the other hand, if correlation-based distance is used, then shoppers with similar preferences (e.g. shoppers who have bought items A and B but never items C or D) will be clustered together, even if some shoppers with these preferences are higher-volume shoppers than others. Therefore, for this application, correlation-based distance may be a better choice.

In addition to carefully selecting the dissimilarity measure used, one must also consider whether or not the variables should be scaled to have standard deviation one before the dissimilarity between the observations is computed. To illustrate this point, we continue with the online shopping ex-

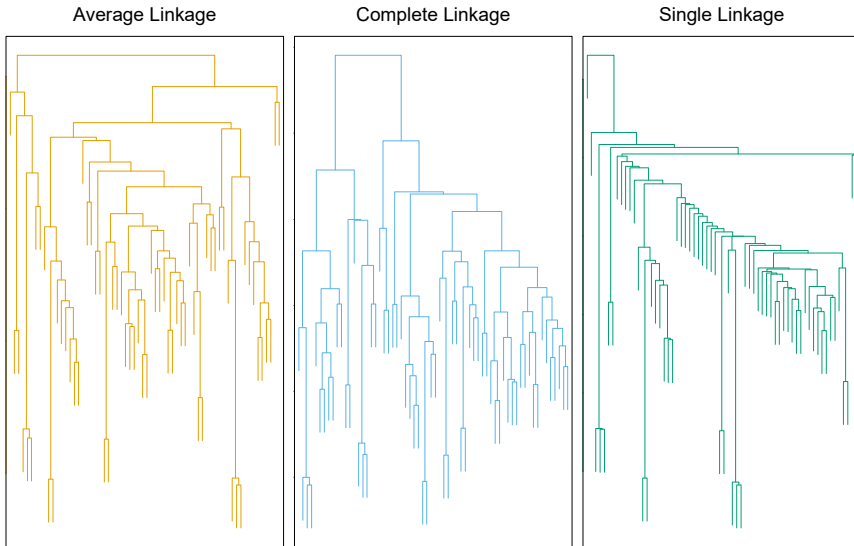


FIGURE 12.14. Average, complete, and single linkage applied to an example data set. Average and complete linkage tend to yield more balanced clusters.

ample just described. Some items may be purchased more frequently than others; for instance, a shopper might buy ten pairs of socks a year, but a computer very rarely. High-frequency purchases like socks therefore tend to have a much larger effect on the inter-shopper dissimilarities, and hence on the clustering ultimately obtained, than rare purchases like computers. This may not be desirable. If the variables are scaled to have standard deviation one before the inter-observation dissimilarities are computed, then each variable will in effect be given equal importance in the hierarchical clustering performed. We might also want to scale the variables to have standard deviation one if they are measured on different scales; otherwise, the choice of units (e.g. centimeters versus kilometers) for a particular variable will greatly affect the dissimilarity measure obtained. It should come as no surprise that whether or not it is a good decision to scale the variables before computing the dissimilarity measure depends on the application at hand. An example is shown in Figure 12.16. We note that the issue of whether or not to scale the variables before performing clustering applies to K -means clustering as well.

12.4.3 Practical Issues in Clustering

Clustering can be a very useful tool for data analysis in the unsupervised setting. However, there are a number of issues that arise in performing clustering. We describe some of these issues here.

Small Decisions with Big Consequences

In order to perform clustering, some decisions must be made.

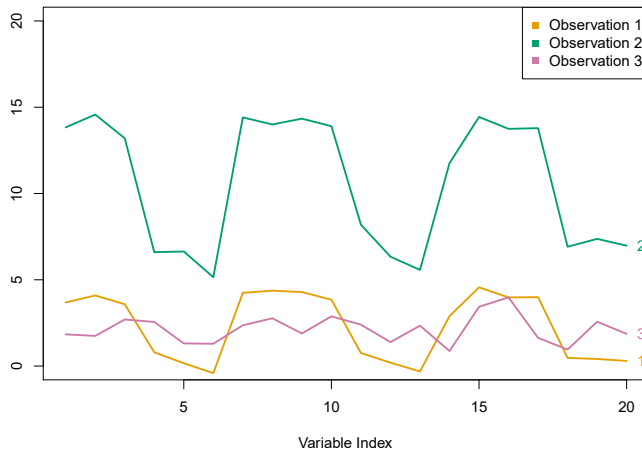


FIGURE 12.15. Three observations with measurements on 20 variables are shown. Observations 1 and 3 have similar values for each variable and so there is a small Euclidean distance between them. But they are very weakly correlated, so they have a large correlation-based distance. On the other hand, observations 1 and 2 have quite different values for each variable, and so there is a large Euclidean distance between them. But they are highly correlated, so there is a small correlation-based distance between them.

- Should the observations or features first be standardized in some way? For instance, maybe the variables should be scaled to have standard deviation one.
- In the case of hierarchical clustering,
 - What dissimilarity measure should be used?
 - What type of linkage should be used?
 - Where should we cut the dendrogram in order to obtain clusters?
- In the case of K -means clustering, how many clusters should we look for in the data?

Each of these decisions can have a strong impact on the results obtained. In practice, we try several different choices, and look for the one with the most useful or interpretable solution. With these methods, there is no single right answer—any solution that exposes some interesting aspects of the data should be considered.

Validating the Clusters Obtained

Any time clustering is performed on a data set we will find clusters. But we really want to know whether the clusters that have been found represent true subgroups in the data, or whether they are simply a result of *clustering the noise*. For instance, if we were to obtain an independent set of observations, then would those observations also display the same set of clusters? This is a hard question to answer. There exist a number of techniques for assigning a p-value to a cluster in order to assess whether there is more

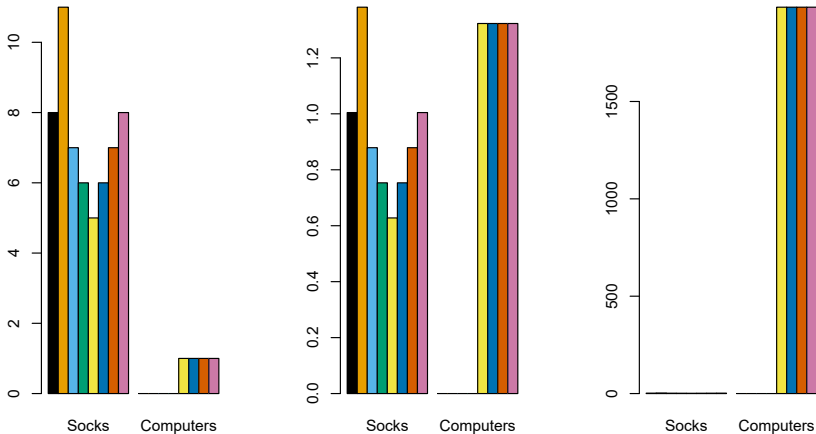


FIGURE 12.16. An eclectic online retailer sells two items: socks and computers. Left: the number of pairs of socks, and computers, purchased by eight online shoppers is displayed. Each shopper is shown in a different color. If inter-observation dissimilarities are computed using Euclidean distance on the raw variables, then the number of socks purchased by an individual will drive the dissimilarities obtained, and the number of computers purchased will have little effect. This might be undesirable, since (1) computers are more expensive than socks and so the online retailer may be more interested in encouraging shoppers to buy computers than socks, and (2) a large difference in the number of socks purchased by two shoppers may be less informative about the shoppers' overall shopping preferences than a small difference in the number of computers purchased. Center: the same data are shown, after scaling each variable by its standard deviation. Now the two products will have a comparable effect on the inter-observation dissimilarities obtained. Right: the same data are displayed, but now the y-axis represents the number of dollars spent by each online shopper on socks and on computers. Since computers are much more expensive than socks, now computer purchase history will drive the inter-observation dissimilarities obtained.

evidence for the cluster than one would expect due to chance. However, there has been no consensus on a single best approach. More details can be found in ESL.⁸

Other Considerations in Clustering

Both K -means and hierarchical clustering will assign each observation to a cluster. However, sometimes this might not be appropriate. For instance, suppose that most of the observations truly belong to a small number of (unknown) subgroups, and a small subset of the observations are quite different from each other and from all other observations. Then since K -means and hierarchical clustering force *every* observation into a cluster, the clusters found may be heavily distorted due to the presence of outliers that do not belong to any cluster. Mixture models are an attractive approach for accommodating the presence of such outliers. These amount to a *soft* version of K -means clustering, and are described in ESL.

⁸ESL: *The Elements of Statistical Learning* by Hastie, Tibshirani and Friedman.

In addition, clustering methods generally are not very robust to perturbations to the data. For instance, suppose that we cluster n observations, and then cluster the observations again after removing a subset of the n observations at random. One would hope that the two sets of clusters obtained would be quite similar, but often this is not the case!

A Tempered Approach to Interpreting the Results of Clustering

We have described some of the issues associated with clustering. However, clustering can be a very useful and valid statistical tool if used properly. We mentioned that small decisions in how clustering is performed, such as how the data are standardized and what type of linkage is used, can have a large effect on the results. Therefore, we recommend performing clustering with different choices of these parameters, and looking at the full set of results in order to see what patterns consistently emerge. Since clustering can be non-robust, we recommend clustering subsets of the data in order to get a sense of the robustness of the clusters obtained. Most importantly, we must be careful about how the results of a clustering analysis are reported. These results should not be taken as the absolute truth about a data set. Rather, they should constitute a starting point for the development of a scientific hypothesis and further study, preferably on an independent data set.

12.5 Lab: Unsupervised Learning

In this lab we demonstrate PCA and clustering on several datasets. As in other labs, we import some of our libraries at this top level. This makes the code more readable, as scanning the first few lines of the notebook tell us what libraries are used in this notebook.

```
In [1]: import numpy as np
import pandas as pd
import matplotlib.pyplot as plt
from statsmodels.datasets import get_rdataset
from sklearn.decomposition import PCA
from sklearn.preprocessing import StandardScaler
from ISLP import load_data
```

We also collect the new imports needed for this lab.

```
In [2]: from sklearn.cluster import \
    (KMeans,
     AgglomerativeClustering)
from scipy.cluster.hierarchy import \
    (dendrogram,
     cut_tree)
from ISLP.cluster import compute_linkage
```

12.5.1 Principal Components Analysis

In this lab, we perform PCA on **USArrests**, a data set in the **R** computing environment. We retrieve the data using `get_rdataset()`, which can fetch

```
get_
rdataset()
```

```
In [58]: hc_pca = HClust(n_clusters=None,
                      distance_threshold=0,
                      linkage='complete'
                     ).fit(nci_scores[:, :5])
linkage_pca = compute_linkage(hc_pca)
fig, ax = plt.subplots(figsize=(8, 8))
dendrogram(linkage_pca,
            labels=np.asarray(nci_labs),
            leaf_font_size=10,
            ax=ax,
            **cargs)
ax.set_title("Hier. Clust. on First Five Score Vectors")
pca_labels = pd.Series(cut_tree(linkage_pca,
                                 n_clusters=4).reshape(-1),
                       name='Complete-PCA')
pd.crosstab(nci_labs['label'], pca_labels)
```

12.6 Exercises

Conceptual

1. This problem involves the K -means clustering algorithm.

 - (a) Prove (12.18).
 - (b) On the basis of this identity, argue that the K -means clustering algorithm (Algorithm 12.2) decreases the objective (12.17) at each iteration.
2. Suppose that we have four observations, for which we compute a dissimilarity matrix, given by

$$\begin{bmatrix} & 0.3 & 0.4 & 0.7 \\ 0.3 & & 0.5 & 0.8 \\ 0.4 & 0.5 & & 0.45 \\ 0.7 & 0.8 & 0.45 & \end{bmatrix}.$$

For instance, the dissimilarity between the first and second observations is 0.3, and the dissimilarity between the second and fourth observations is 0.8.

- (a) On the basis of this dissimilarity matrix, sketch the dendrogram that results from hierarchically clustering these four observations using complete linkage. Be sure to indicate on the plot the height at which each fusion occurs, as well as the observations corresponding to each leaf in the dendrogram.
- (b) Repeat (a), this time using single linkage clustering.
- (c) Suppose that we cut the dendrogram obtained in (a) such that two clusters result. Which observations are in each cluster?
- (d) Suppose that we cut the dendrogram obtained in (b) such that two clusters result. Which observations are in each cluster?

- (e) It is mentioned in this chapter that at each fusion in the dendrogram, the position of the two clusters being fused can be swapped without changing the meaning of the dendrogram. Draw a dendrogram that is equivalent to the dendrogram in (a), for which two or more of the leaves are repositioned, but for which the meaning of the dendrogram is the same.
3. In this problem, you will perform K -means clustering manually, with $K = 2$, on a small example with $n = 6$ observations and $p = 2$ features. The observations are as follows.
- | Obs. | X_1 | X_2 |
|------|-------|-------|
| 1 | 1 | 4 |
| 2 | 1 | 3 |
| 3 | 0 | 4 |
| 4 | 5 | 1 |
| 5 | 6 | 2 |
| 6 | 4 | 0 |
- (a) Plot the observations.
 (b) Randomly assign a cluster label to each observation. You can use the `np.random.choice()` function to do this. Report the cluster labels for each observation.
 (c) Compute the centroid for each cluster.
 (d) Assign each observation to the centroid to which it is closest, in terms of Euclidean distance. Report the cluster labels for each observation.
 (e) Repeat (c) and (d) until the answers obtained stop changing.
 (f) In your plot from (a), color the observations according to the cluster labels obtained.
4. Suppose that for a particular data set, we perform hierarchical clustering using single linkage and using complete linkage. We obtain two dendograms.
- (a) At a certain point on the single linkage dendrogram, the clusters $\{1, 2, 3\}$ and $\{4, 5\}$ fuse. On the complete linkage dendrogram, the clusters $\{1, 2, 3\}$ and $\{4, 5\}$ also fuse at a certain point. Which fusion will occur higher on the tree, or will they fuse at the same height, or is there not enough information to tell?
 (b) At a certain point on the single linkage dendrogram, the clusters $\{5\}$ and $\{6\}$ fuse. On the complete linkage dendrogram, the clusters $\{5\}$ and $\{6\}$ also fuse at a certain point. Which fusion will occur higher on the tree, or will they fuse at the same height, or is there not enough information to tell?
5. In words, describe the results that you would expect if you performed K -means clustering of the eight shoppers in Figure 12.16, on the basis of their sock and computer purchases, with $K = 2$. Give three answers, one for each of the variable scalings displayed. Explain.

6. We saw in Section 12.2.2 that the principal component loading and score vectors provide an approximation to a matrix, in the sense of (12.5). Specifically, the principal component score and loading vectors solve the optimization problem given in (12.6).

Now, suppose that the M principal component score vectors z_{im} , $m = 1, \dots, M$, are known. Using (12.6), explain that each of the first M principal component loading vectors ϕ_{jm} , $m = 1, \dots, M$, can be obtained by performing p separate least squares linear regressions. In each regression, the principal component score vectors are the predictors, and one of the features of the data matrix is the response.

Applied

7. In this chapter, we mentioned the use of correlation-based distance and Euclidean distance as dissimilarity measures for hierarchical clustering. It turns out that these two measures are almost equivalent: if each observation has been centered to have mean zero and standard deviation one, and if we let r_{ij} denote the correlation between the i th and j th observations, then the quantity $1 - r_{ij}$ is proportional to the squared Euclidean distance between the i th and j th observations.

On the `USArrests` data, show that this proportionality holds.

Hint: The Euclidean distance can be calculated using the `pairwise_distances()` function from the `sklearn.metrics` module, and correlations can be calculated using the `np.corrcoef()` function.

`pairwise_distances()`

8. In Section 12.2.3, a formula for calculating PVE was given in Equation 12.10. We also saw that the PVE can be obtained using the `explained_variance_ratio_` attribute of a fitted `PCA()` estimator.

On the `USArrests` data, calculate PVE in two ways:

- Using the `explained_variance_ratio_` output of the fitted `PCA()` estimator, as was done in Section 12.2.3.
- By applying Equation 12.10 directly. The loadings are stored as the `components_` attribute of the fitted `PCA()` estimator. Use those loadings in Equation 12.10 to obtain the PVE.

These two approaches should give the same results.

Hint: You will only obtain the same results in (a) and (b) if the same data is used in both cases. For instance, if in (a) you performed `PCA()` using centered and scaled variables, then you must center and scale the variables before applying Equation 12.10 in (b).

9. Consider the `USArrests` data. We will now perform hierarchical clustering on the states.
- Using hierarchical clustering with complete linkage and Euclidean distance, cluster the states.
 - Cut the dendrogram at a height that results in three distinct clusters. Which states belong to which clusters?

- (c) Hierarchically cluster the states using complete linkage and Euclidean distance, *after scaling the variables to have standard deviation one*.
- (d) What effect does scaling the variables have on the hierarchical clustering obtained? In your opinion, should the variables be scaled before the inter-observation dissimilarities are computed? Provide a justification for your answer.
10. In this problem, you will generate simulated data, and then perform PCA and K -means clustering on the data.
- Generate a simulated data set with 20 observations in each of three classes (i.e. 60 observations total), and 50 variables.
Hint: There are a number of functions in Python that you can use to generate data. One example is the `normal()` method of the `random()` function in `numpy`; the `uniform()` method is another option. Be sure to add a mean shift to the observations in each class so that there are three distinct classes.
 - Perform PCA on the 60 observations and plot the first two principal component score vectors. Use a different color to indicate the observations in each of the three classes. If the three classes appear separated in this plot, then continue on to part (c). If not, then return to part (a) and modify the simulation so that there is greater separation between the three classes. Do not continue to part (c) until the three classes show at least some separation in the first two principal component score vectors.
 - Perform K -means clustering of the observations with $K = 3$. How well do the clusters that you obtained in K -means clustering compare to the true class labels?
Hint: You can use the `pd.crosstab()` function in Python to compare the true class labels to the class labels obtained by clustering. Be careful how you interpret the results: K -means clustering will arbitrarily number the clusters, so you cannot simply check whether the true class labels and clustering labels are the same.
 - Perform K -means clustering with $K = 2$. Describe your results.
 - Now perform K -means clustering with $K = 4$, and describe your results.
 - Now perform K -means clustering with $K = 3$ on the first two principal component score vectors, rather than on the raw data. That is, perform K -means clustering on the 60×2 matrix of which the first column is the first principal component score vector, and the second column is the second principal component score vector. Comment on the results.
 - Using the `StandardScaler()` estimator, perform K -means clustering with $K = 3$ on the data *after scaling each variable to have standard deviation one*. How do these results compare to those obtained in (b)? Explain.

11. Write a `Python` function to perform matrix completion as in Algorithm 12.1, and as outlined in Section 12.5.2. In each iteration, the function should keep track of the relative error, as well as the iteration count. Iterations should continue until the relative error is small enough or until some maximum number of iterations is reached (set a default value for this maximum number). Furthermore, there should be an option to print out the progress in each iteration.

Test your function on the `Boston` data. First, standardize the features to have mean zero and standard deviation one using the `StandardScaler()` function. Run an experiment where you randomly leave out an increasing (and nested) number of observations from 5% to 30%, in steps of 5%. Apply Algorithm 12.1 with $M = 1, 2, \dots, 8$. Display the approximation error as a function of the fraction of observations that are missing, and the value of M , averaged over 10 repetitions of the experiment.

12. In Section 12.5.2, Algorithm 12.1 was implemented using the `svd()` function from the `np.linalg` module. However, given the connection between the `svd()` function and the `PCA()` estimator highlighted in the lab, we could have instead implemented the algorithm using `PCA()`.

Write a function to implement Algorithm 12.1 that makes use of `PCA()` rather than `svd()`.

13. On the book website, www.statlearning.com, there is a gene expression data set (`Ch12Ex13.csv`) that consists of 40 tissue samples with measurements on 1,000 genes. The first 20 samples are from healthy patients, while the second 20 are from a diseased group.

- (a) Load in the data using `pd.read_csv()`. You will need to select `header = None`.
- (b) Apply hierarchical clustering to the samples using correlation-based distance, and plot the dendrogram. Do the genes separate the samples into the two groups? Do your results depend on the type of linkage used?
- (c) Your collaborator wants to know which genes differ the most across the two groups. Suggest a way to answer this question, and apply it here.